

APRIL 1978

# analytical chemistry



TRACE ORGANIC ANALYSIS



# NEW X-Y RECORDER

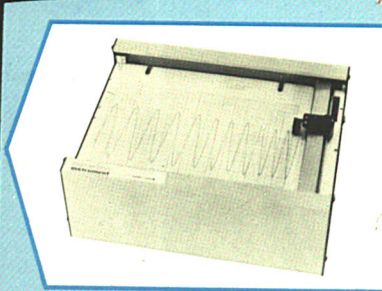
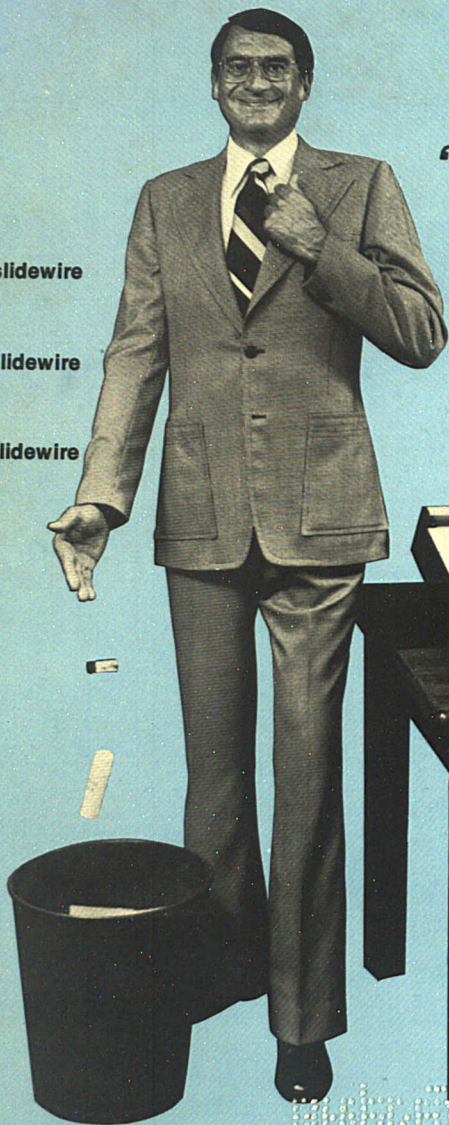
**MORE RELIABLE  
LESS EXPENSIVE  
BECAUSE...**

## **"THE POT IS NOT"**

A capacitance  
feedback transducer  
replaces the  
potentiometer  
and slidewire -

neatly eliminating  
the most troublesome  
components in X-Y  
servo systems

- ★ No more slidewire  
cleanser
- ★ No more slidewire  
lubricant
- ★ No more slidewire



Prices start at \$895.\*

Send today for complete information on  
the Series 100 - a new concept in low  
cost X-Y recorders.

**houston  
instrument**

**THE  
RECORDED  
COMPANY**

DIVISION OF BAUSCH & LOMB

ONE HOUSTON SQUARE (at 8500 Cameron Road) AUSTIN, TEXAS 78753  
(512) 837-2620 TWX 910-874-2022 cable HOINCO

TELECOPIER  
EUROPEAN OFFICE Rochesterlaan 6 8240 Gistel Belgium  
Phone 059/277445 Telex Bausch 81399

CIRCLE 95 ON READER SERVICE CARD

\* U.S. Domestic Price only

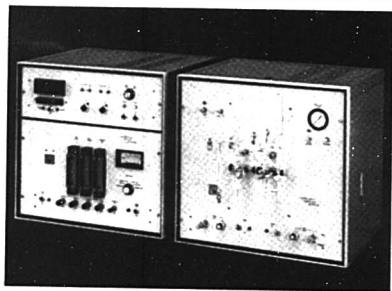
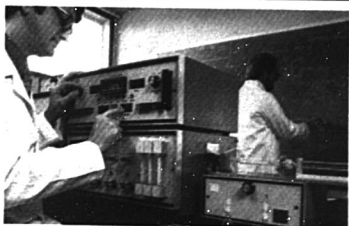
Visit us at the  
FACEB Show,  
booth B-32



# Even Better Ways of Doing What Dohrmann Does Best

## Measuring traces of nitrogen, sulfur, and halides

Dohrmann microcoulometric systems are leaders in the field for *fast, accurate and sensitive* determinations of traces of N, S, and Cl in solids, liquids and gases at the ppm level. Dohrmann's ongoing development of sampling accessories and methodology make this technique a powerful analytical tool in any laboratory. For details, call your local Dohrmann salesman or Doug Jones toll-free at (800) 538-7708.



## Analyzing water for ppb organic carbon

Dohrmann has added the DC-54 ultra-low-level organic carbon analyzer to its well established line of versatile TOC instruments. The DC-54 brings *speed, convenience and precision* to low-level TOC analysis: purgeables to  $\pm 1$  ppb, non-purgeables to  $\pm 10$  ppb.

If your TOC requirement runs from drinking to waste water, remember: **Dohrmann does it all.** For details on Dohrmann TOC analyzers, call your local Dohrmann salesman or Leon Hiam toll-free at (800) 538-7708.

## The DN-10 Total Nitrogen Analyzer

Using oxidative pyrolysis and chemiluminescence detection, the DN-10 offers even greater *convenience* when measuring traces of nitrogen in organics. It's a proven, reliable performer for rapid, routine, low level analysis of nitrogen in feedstocks, light oils, and other petroleum products. For details, call your local Dohrmann salesman or Doug Jones toll-free at (800) 538-7708.

For literature on all products described above, write or circle the reader service number below.



ENVIROTECH



CIRCLE 50 ON READER SERVICE CARD

DOHRMANN

3240 Scott Boulevard  
Santa Clara, California 95050

**CALL TOLL FREE  
(800) 538-7708**

In Alaska, California,  
Hawaii, Puerto Rico, call  
collect (408) 249-6000



# If you like our filter papers for paper chromatography, you'll love our chromatography papers for paper chromatography.

Whatman Chromatography Papers are made specifically for paper chromatography and electrophoresis. Manufacturing methods, materials — specially selected alpha cotton cellulose — and quality control procedures ensure characteristics essential to excellence in these applications.

Whatman Chromatography Papers are made and tested for very high purity, the best achievable uniformity and consistency, evenness of fiber distribution, freedom from "formation" and control of the microstruc-

ture of the fiber. All this results in high resolution, consistent, predictable and reproducible  $R_f$  values, high uniformity of spot or band shape and area.

In short, in excellent chromatographic results.

There are eight Whatman grades specifically manufactured for partition chromatography and electrophoresis. Plus ion exchange papers, and both silica gel loaded and silicone treated papers. Not to mention Glass Microfibre® grades.

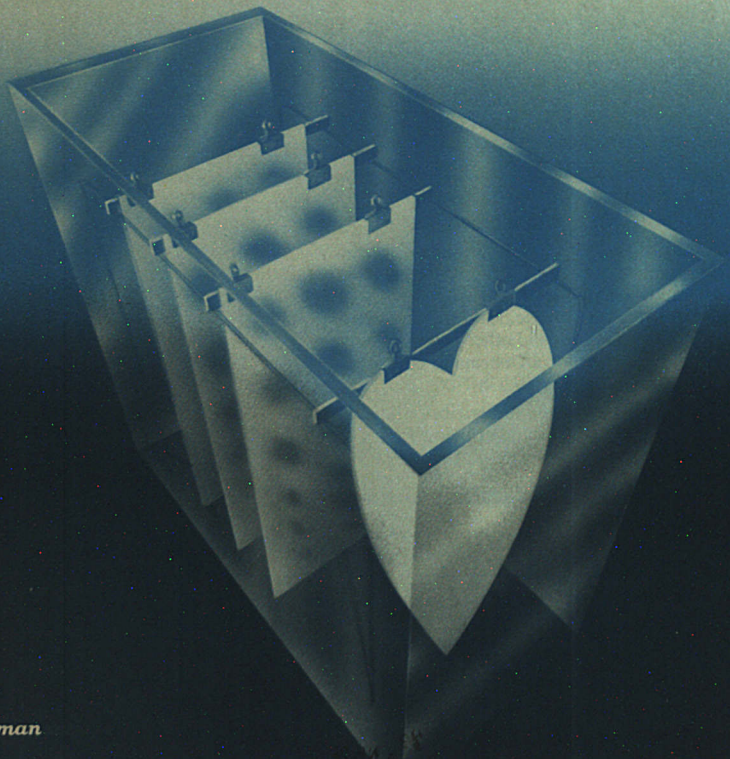
Like our filter papers, Whatman Chromatography Papers are available from your local laboratory supply dealer.

® Registered trademark of Balston Ltd.

A new "Handbook of Paper Chromatography" will be available shortly. For your free copy write:

**Whatman Inc.** ■ 9 Bridewell Place,  
Clifton, New Jersey 07014 ■ Tel. (201)  
777-4825.

CIRCLE 234 ON READER SERVICE CARD



**Whatman**



© Copyright 1978  
 by the American Chemical Society



Permission of the American Chemical Society is granted for libraries and other users to make reprographic copies for use beyond that permitted by Sections 107 or 108 of the U.S. Copyright Law, provided that, for all articles bearing an article code, the copying organization pay the stated per-copy fee through the Copyright Clearance Center, Inc. For further information, write to Office of the Director, Books and Journals Division, ACS, 1155 16th St. N.W., Washington, D.C. 20036.

Published monthly with review issue added in April and Laboratory Guide in August by the American Chemical Society, from 20th and Northampton Sts., Easton, Pa. 18042 Executive and Editorial headquarters, American Chemical Society, 1155 16th St. N.W., Washington, D.C. 20036 (202) 872-4600. Second class postage paid at Washington, D.C., and at additional mailing offices.

**1978 Subscription prices—including surface postage**

	1 yr	2 yr	3 yr
<b>MEMBERS:</b>			
Domestic	\$10.00	\$18.00	\$25.00
Foreign	19.00	36.00	52.00
<b>NONMEMBERS—PERSONAL:</b>			
Domestic	14.00	26.00	38.00
Foreign	23.00	44.00	65.00
<b>INSTITUTIONAL:</b>			
Domestic	14.00	26.00	38.00
Canada	23.00	44.00	65.00
Other foreign	29.00	54.00	77.00

Airmail and air freight rates are available from Membership & Subscription Services, ACS, P.O. 3337, Columbus, Ohio 43210 (614) 421-7230.

New and renewal subscriptions should be sent with payment to the Office of the Controller at the ACS Washington address.

Subscription service inquiries and changes of address (include both old and new addresses with ZIP code and recent mailing label) should be directed to the ACS Columbus address noted above. Please allow six weeks for change of address to become effective.

Claims for missing numbers will not be allowed if loss was due to failure of notice of change of address to be received in the time specified. If claim is dated (a) North America: more than 90 days beyond issue date; (b) all other foreign: more than one year beyond issue date; or if the reason given is "missing from files".

Microfilm subscriptions are available at the same prices but are mailed first class domestic and airmail foreign. Inquiries and payments to Microform Program, ACS Washington address.

Single issues, current year, \$3.00 except review issue and Labguide, \$4.00; back issues and volumes; microfilm editions from volume 1 to present; write or call Special Issues Sales, ACS Washington address (202) 872-4365.

Advertising Management: Centcom, Ltd., 25 Sylvan Road South, Westport, Conn. 06880 (203) 226-7131

# analytical chemistry

## CONTENTS

### REPORT

H. S. Hertz, W. E. May, S. A. Wise, and S. N. Chesler assess the current state-of-the-art of trace organic analysis and discuss the problems associated with performing these analyses **428 A**

### INSTRUMENTATION

Charles L. Wilkins or the University of Nebraska discusses the analytical advances and the future role in analysis of ion cyclotron resonance mass spectrometry **493 A**

### NEWS

"Chromatography and Ancillary Methods" is the subject of the 31st Summer Symposium of the ACS Division of Analytical Chemistry, June 26-28, 1978, University of Colorado, Boulder, Colo. The Optical Society of America names award winners **439 A**

### BOOKS

Books on chromatography, qualitative analysis, trace analysis of atmospheric samples, and solvent extraction are reviewed by James M. Bobbit, Stanley T. Marcus, E. W. Brethauer, and A. S. Kertes **479 A**

### EDITORS' COLUMN

Government funding for basic research will be emphasized in fiscal year 1979 **490 A**

### EDITORIAL

The proton microprobe serves as an excellent example of a new approach to sensitive elemental analysis **545**

Technical Contents/Briefs	412 A
Reader Survey	422 A
Letters	424 A
Call for Papers	446 A
Meetings	446 A
Short Courses	446 A
New Products	466 A
Manufacturers' Literature	473 A
Advertising Index	502 A
Author Index	IBC
Future Articles	IBC



The cover, based on this month's REPORT, illustrates the separation, isolation, and identification of trace organic substances



# Briefs

## Optimization of Reverse-Phase Liquid Chromatographic Separation of Weak Organic Acids 546

The effect of aqueous carrier solvent pH on the HPLC separation of several benzoic acids is presented.

Stanley N. Deming\* and Michael L. H. Tuross, Department of Chemistry, University of Houston, Houston, Tex. 77004  
*Anal. Chem.*, 50 (1978)

## Analysis of Carotenoid and Porphyrin Pigments of Geochemical Interest by High-Performance Liquid Chromatography 549

The identification of constituents and fingerprinting of petroporphyrin distributions in crude oil are possible.

S. K. Hajibrahim, P. J. C. Tibbets, C. D. Watts, J. R. Maxwell, and G. Eglinton, Organic Geochemistry Unit, School of Chemistry, University of Bristol, Cantock's Close, Bristol BS8 1TS, England, and H. Colin and G. Guichon, Laboratoire de Chimie Analytique Physique, Ecole Polytechnique, 91128 Palaiseau Cedex, France  
*Anal. Chem.*, 50 (1978)

## Determination of Benzodiazepine Anticonvulsants in Plasma by High-Performance Liquid Chromatography 554

A new internal standard and rapid HPLC method are introduced for quantitation of diazepam, nordiazepam, and clonazepam. Relative standard deviations for daily and long-term reproducibility studies are 4% and 6%, respectively.

Robert J. Perchalski\* and B. J. Wilder, Research and Neurology Services, Veterans Administration Hospital, and Department of Neurology, College of Medicine, University of Florida, Gainesville, Fla. 32610  
*Anal. Chem.*, 50 (1978)

## Microdetermination of Molecular Species of Oligo- and Polyunsaturated Diacylglycerols by Gas Chromatography-Mass Spectrometry of Their *tert*-Butyl Dimethylsilyl Ethers 557

Due to a prominent M - 57 ion, the tertiary-butyl dimethylsilyl ethers are preferred over the trimethylsilyl ether derivatives for the GC/MS determination of polyunsaturated diacylglycerols.

J. J. Myher, A. Kuksis, L. Marai, and S. K. F. Yeung, Banting and Best Department of Medical Research, University of Toronto, Toronto, Canada M5G 1L6  
*Anal. Chem.*, 50 (1978)

## Determination of Ruthenium in Automobile Exhaust Emissions by Negative Ion Chemical Ionization Mass Spectrometry 562

A method for preparing platinum bis(1,1,1-trifluoro-2,4-pentanedionate) is reported together with the analysis of ruthenium on membrane filters by negative ion chemical ionization mass spectrometry.

S. R. Prescott and T. H. Risby, Department of Chemistry, The Pennsylvania State University, University Park, Pa. 16802  
*Anal. Chem.*, 50 (1978)

## Determination of the Leachability of Solids 564

The leaching of radiotracers from cylindrical homogeneous solids is followed experimentally and interpreted by a well-fitting model based on diffusion theory.

O. U. Anders, J. F. Bartel, and S. J. Altschuler, The Dow Chemical Company, Midland, Mich. 48640  
*Anal. Chem.*, 50 (1978)

## Interferometric Concentration Determination of Dextran after Gel Chromatography 569

Errors due to the optical activity and the molecular weight dependence of the refractive index increment of dextran are negligible; however, errors caused by an absorbing sample solution or the nonlinear response of the instrument must be taken into account.

Lars Hagel, Pharmacia AB, Box 181, S-751 04 Uppsala, Sweden  
*Anal. Chem.*, 50 (1978)

## X-ray Photoelectron Spectroscopy of Alkylamine-Silanes Bound to Metal Oxide Electrodes 576

ESCA results are presented for SnO<sub>2</sub>, RuO<sub>2</sub>, TiO<sub>2</sub>, and Pt/PtO<sub>2</sub> oxide electrodes silanized with trialkoxyalkylaminesilanes.

P. R. Moses, Larry M. Wier, John C. Lennox, H. O. Finklea, J. R. Lenhard, and Royce W. Murray, Kenan Laboratories of Chemistry, University of North Carolina, Chapel Hill, N.C. 27514  
*Anal. Chem.*, 50 (1978)

## Analysis of Commercial Sodium Tripolyphosphates by Phosphorus-31 Fourier Transform Nuclear Magnetic Resonance Spectrometry 585

The accuracy (within 2%) and precision of the method are assessed and found to be satisfactory.

Stanley A. Sojka\* and Roger A. Wolfe, Hooker Chemicals and Plastics Corporation, Research Center, Grand Island Complex, M.P.O. Box 8, Niagara Falls, N.Y. 14302  
*Anal. Chem.*, 50 (1978)

## Microcomputer Assisted, Single Beam, Photoacoustic Spectrometer System for the Study of Solids 587

Spectra of Ho<sub>2</sub>O<sub>3</sub>, Er<sub>2</sub>O<sub>3</sub>, and UF<sub>4</sub> are presented. Sample size is generally 5 mg with resolution approximately 15 nm.

Harry E. Eaton\* and James D. Stuart, Chemistry Department, U-60, University of Connecticut, Storrs, Conn. 06268  
*Anal. Chem.*, 50 (1978)

## Practical Solutions to Matrix Effects in X-ray Fluorescence Analysis by Mathematical Methods 592

Interrelations between different equations used in x-ray fluorescence analysis are described, enabling the calculation of major oxide concentrations in fused glass specimens.

M. T. Hauka\* and I. L. Thomas, School of Earth Sciences, Department of Geology, University of Melbourne, Parkville, Victoria 3052, Australia  
*Anal. Chem.*, 50 (1978)

\* Corresponding author.



## ORION introduces a new pH electrode that won't get thirsty.

How about a combination pH electrode that's more convenient to use because you don't have to fill it—that you don't have to worry about breaking—a rugged electrode that will cost you less than you're now paying.

This electrode never needs to be filled with KCl—it comes with a lifetime charge of gelled electrolyte in a sealed chamber.

ORION's model 91-05 electrode just won't break in normal laboratory use—it has a tough epoxy outer body that protects the glass sensing element from damage.

You'll get the stable, drift-free readings you'd expect from the more expensive all-glass pH electrodes—but at a \$36 each list price. (If your facility buys electrodes in quantity, the list price drops to \$30.60 each, in cases of 24 electrodes.)

The model 91-05 combination pH electrode comes with a 30-inch long cable terminated with a standard U.S. connector that fits ORION, Corning, and Beckman pH meters. It's available off-the-shelf from most leading laboratory supply distributors.

### ORION RESEARCH

380 PUTNAM AVE., CAMBRIDGE, MA 02139  
(800) 225-1480

CIRCLE 156 ON READER SERVICE CARD

ANALYTICAL CHEMISTRY, VOL. 50, NO. 4, APRIL 1978 • 413 A



# Briefs

## Two-Phase Buffer Systems: Theoretical Considerations

597

Theoretical considerations and advantages over classical (monophase) buffer systems are described. The proposed extraction mechanism of action of these buffers is experimentally confirmed.

**Tomislav J. Janjić\*** and **Emil B. Milosavljević**, Chemical Institute, Faculty of Sciences, University of Belgrade, P.O. Box 550, 11001 Belgrade, Yugoslavia  
*Anal. Chem.*, 50 (1978)

## Enrichment of Anions of Weak Acids by Donnan Dialysis

601

A receiver pH which is less than the pK of the weak acid permits enrichment independent of sample pH. In 30 min, 7-fold enrichments are obtained.

**James A. Cox\*** and **Kuo-Hsien Cheng**, Department of Chemistry and Biochemistry, Southern Illinois University, Carbondale, Ill. 62901  
*Anal. Chem.*, 50 (1978)

## Simultaneous Multielement Determination by Atomic Emission with an Echelle Spectrometer Interfaced by Image Dissector and Silicon Vidicon Tubes

602

Results for multielement samples of alkali and alkaline earth and of transition metals are comparable in most respects to single element data obtained with conventional optics and detectors with the same plasma.

**Hugo L. Felkel, Jr.**, and **Harry L. Pardue\***, Department of Chemistry, Purdue University, West Lafayette, Ind. 47907  
*Anal. Chem.*, 50 (1978)

## Room-Temperature Phosphorescence of the Phthalic Acid Isomers, *p*-Aminobenzoic Acid, and Terephthalamide Adsorbed on Silica Gel

610

The mode of interaction of the compounds with the silica gel surface appears to be mainly hydrogen bonding.

**Charles D. Ford** and **Robert J. Hurtubise\***, Chemistry Department, University of Wyoming, Laramie, Wyo. 82071  
*Anal. Chem.*, 50 (1978)

## Solvent Enhancement Effects in Thin-Layer Phosphorimetry

613

Modification of a spectrofluorimeter sample compartment permits the determination of ng amounts of phosphorescent materials at 77 K on flexible chromatographic media. Phosphorescence is enhanced by spraying the media with organic solvents.

**J. N. Miller\***, **D. L. Philipps**, and **D. Thorburn Burns**, Department of Chemistry, Loughborough University, Loughborough, Leicestershire LE11 3TU, U.K., and **J. W. Bridges**, Department of Biochemistry, University of Surrey, Guildford, Surrey, GU2 5XH, U.K.  
*Anal. Chem.*, 50 (1978)

## Comparison of Different Experimental Configurations in Pulsed Laser Induced Molecular Fluorescence

616

A nitrogen pumped dye laser, cavity dumped argon ion laser, and externally pulse-picked mode-locked argon ion laser are compared as excitation sources for fluorimetry.

**J. H. Richardson\*** and **S. M. George**, Lawrence Livermore Laboratory, General Chemistry Division, University of California, Livermore, Calif. 94550  
*Anal. Chem.*, 50 (1978)

## Automated Three-Dimensional Plotter for Fluorescence Measurements

620

The method delineates all of the fluorescence spectral parameters for each peak in such a way that a "stereofingerprint" of fluorescent mixtures is produced for unique characterization of closely related compounds.

**Joon H. Rho\***, Clinical Pharmacology, Department of Medicine, Schools of Medicine and Pharmacy, University of Southern California, Los Angeles, Calif. 90033, and **J. L. Stuart**, J. Stuart Enterprises, Grass Valley, Calif. 95945  
*Anal. Chem.*, 50 (1978)

## Atomic Fluorescence Spectrometry with a Wavelength-Modulated Continuous Wave Dye Laser

625

A new wavelength-modulated CW dye laser gives improved limits of detection compared to amplitude modulation in the atomic fluorescence determination of barium.

**David A. Goff** and **Edward S. Yeung\***, Ames Laboratory—U.S. Department of Energy and Department of Chemistry, Iowa State University Ames, Iowa 50011  
*Anal. Chem.*, 50 (1978)

## Theory of Atom Vapor Transport from a Moving Point Source in Flame Spectrometry

628

The atom distribution of an analyte in an analytical flame is evaluated by using a moving point source model.

**Kuang-Pang Li**, Department of Chemistry, University of Florida, Gainesville, Fla. 32611  
*Anal. Chem.*, 50 (1978)

## Band-Broadening Phenomena in Microcapillary Tubes under the Conditions of Liquid Chromatography

632

Measurements carried out with a nonretained solute in microcapillaries of various diameters indicate that the plate height values are considerably better than predicted from the theory.

**Takao Tsuda** and **Milos Novotny\***, Department of Chemistry, Indiana University, Bloomington, Ind. 47401  
*Anal. Chem.*, 50 (1978)

## Improved Detectability of Barbiturates in High Performance Liquid Chromatography by Post-Column Ionization

635

The enhanced ultraviolet absorptivity of barbiturate anions is investigated as a means of improving the sensitivity of HPLC for 5,5-dialkylbarbiturates.

**C. Randall Clark\*** and **Jen-Lee Chan**, School of Pharmacy, Auburn University, Auburn, Ala. 36830  
*Anal. Chem.*, 50 (1978)

## Quantitative Determination of D- and L-Amino Acids by Reaction with *tert*-Butyloxycarbonyl-L-leucine N-Hydroxysuccinimide Ester and Chromatographic Separation as L,D and L,L Dipeptides

637

Ion exchange chromatographic separation allows the detection and quantitation of 0.1% of the opposite enantiomer in an amino acid.

**A. R. Mitchell**, **S. B. H. Kent**, **I. C. Chu**, and **R. B. Merrifield\***, The Rockefeller University, New York, N.Y. 10021  
*Anal. Chem.*, 50 (1978)

$C_2H_2$   
 $NH_3$   
 $Ar$   
 $AsH_3$   
 $BCl_3$   
 $H_2S$   
 $C_4H_4$   
 $CO_2$   
 $CO$   
 $Cl_2$   
 $D_2$   
 $(CH_3)_2NH$   
 $C_2H_6$   
 $C_2H_5Cl$   
 $C_2H_4$   
 $C_2H_4O$   
 $F_2$   
 $HBr$   
 $HCl$   
 $HF$   
 $H_2Se$   
 $C_4H_{10}$   
 $SiH_4$   
 $Kr$   
 $CH_4$   
 $CH_3Br$   
 $CH_3Cl$   
 $CH_3SH$   
 $(CN)_2$   
 $CH_3NH_2$   
 $Ne$   
 $NO$   
 $N_2$   
 $NO_2(N_2O_4)$

**Plus  
many more  
gases**

# Only Matheson has a full range of gases...and the delivery systems to control them

Matheson supplies more than 90 gases in a large variety of purities...enough to meet every requirement.

Some of these gases present real storage and handling problems. Matheson experience provides its customers with delivery systems specially designed for the safe use of these gases in lab or plant.

Matheson can stock these gases...all of them...at 13 different plants in the U.S., Canada and Europe. These are Matheson owned plants, and they are dedicated to Specialty Gases...our only business.

When you need gases, come to Matheson. We supply more gases in more sizes with more technology for their proper use than does any other specialty gas supplier. Fifty years of service to the scientific community makes us the first in specialty gases.



Lyndhurst, N.J. 07071

East Rutherford, N.J. 07073 / Morrow, Georgia 30260  
 Gloucester, Massachusetts 01930 / Joliet, Illinois 60434  
 La Porte, Texas 77571 / Cucamonga, California 91730  
 Newark, California 94560 / Bridgeport, N.J. 08014  
 Duxbury, Maryland 21227 / Whiteby, Ontario, Canada L1N 5B9  
 Edmonton, Alberta, Canada T5B 4K6 / B 2411 Oevel, Belgium  
 6056 Heusenstamm, West Germany



# Briefs

## Cyanuric Chloride as a General Linking Agent for Modified Electrodes: Attachment of Redox Groups to Pyrolytic Graphite 640

ESCA and electrochemical studies are presented for the use of cyanuric chloride as a covalent linking agent for the attachment of redox groups to pyrolytic graphite electrodes.

Alexander M. Yacynych and Theodore Kuwana,\* Department of Chemistry, The Ohio State University, Columbus, Ohio 43210  
*Anal. Chem.*, 50 (1978)

## Simultaneous Determination of Reversible Potential and Rate Constant for a First-Order EC Reaction by Potential Dependent Chronoamperometry 645

Simplex optimization of current vs. time transients to theoretical expressions allows determination of reversible  $E_{1/2}$  and EC rate constant with accuracy comparable to other electrochemical methods.

Hung-Yuan Cheng and Richard L. McCreery,\* Department of Chemistry, The Ohio State University, Columbus, Ohio 43210  
*Anal. Chem.*, 50 (1978)

## Volatilization of Arsenic(III, V), Antimony(III, V), and Selenium(IV, VI) from Mixtures of Hydrogen Fluoride and Perchloric Acid Solution: Application of Silicate Analysis 649

The results lead to a recommended procedure for the dissolution of siliceous materials in which As, Sb, or Se are to be determined.

Sixto Bajo, Swiss Federal Institute for Reactor Research, 5303 Würenlingen, Switzerland  
*Anal. Chem.*, 50 (1978)

## Comparison of Three Techniques for the Measurement of Depleted Uranium in Soils 652

Instrumental epithermal neutron activation analysis is shown to be an effective method as compared to the fluorometric and delayed neutron assay techniques.

Ernest S. Gladney,\* Walter K. Hensley, and Michael M. Minor, University of California, Los Alamos Scientific Laboratory, P.O. Box 1663, Los Alamos, N.M. 87545  
*Anal. Chem.*, 50 (1978)

## Correspondence

## Construction of pH Gradients in Flow-Injection Analysis and Their Potential Use for Multielement Analysis in a Single Sample Bolus 654

D. Betteridge\* and Bernard Fields, Chemistry Department, University College of Swansea, Swansea SA2 8PP, U.K.  
*Anal. Chem.*, 50 (1978)

## Gas Chromatographic Determination and Purification of Carbon Diselenide 656

J. R. Marquart, Department of Chemistry, Mercer University, Macon Ga. 31207 and R. L. Belford,\* School of Chemical Sciences, University of Illinois, Urbana, Ill. 61801  
*Anal. Chem.*, 50 (1978)

## Autoclave Digestion Procedure for the Determination of Total Iron Content of Waters 658

Joan Crowther, Ontario Ministry of the Environment, Laboratory Services Branch, Water Quality Section, Box 213, Rexdale, Ontario, Canada M9W 5L1  
*Anal. Chem.*, 50 (1978)

## On-Line Coupling of a Micro Liquid Chromatograph and Mass Spectrometer through a Jet Separator 659

Tsugio Takeuchi,\* Yukio Hirata, and Yoshio Okumura, Department of Synthetic Chemistry, Faculty of Engineering, Nagoya University, Nagoya, Japan  
*Anal. Chem.*, 50 (1978)

## Aids for Analytical Chemists

### Separation of Perfluorinated Hydrocarbons by Gas-Solid Chromatography 661

Ronald R. Shields,\* IBM Systems Products Division, East Fishkill Facility, Hopewell Junction, N.Y. 12533 and John A. Nieman, IBM System Products Division, Poughkeepsie, N.Y. 12602  
*Anal. Chem.*, 50 (1978)

### Removal of Soluble Organic Matter from Rock Samples with a Flow-Through Extraction Cell 663

Mattias Radke, Hans G. Sittardt, and Dietrich H. Welte,\* Programmgruppe für Erdöl und Organische Geochemie der Kernforschungsanlage Jülich GmbH, D-5170 Jülich, West Germany  
*Anal. Chem.*, 50 (1978)

### Computer Interfaceable Potentiostat 665

Basil H. Vassos\* and Guillermo Martinez, Chemistry Department, University of Puerto Rico, Rio Piedras, Puerto Rico 00931  
*Anal. Chem.*, 50 (1978)

### Technique for the Prevention of Column Contamination in Pyrolysis Gas-Liquid Chromatography 668

Annabel Mitchell and Manuel Needleman,\* Victorian College of Pharmacy, 381 Royal Parade, Parkville, Victoria, Australia, 3052  
*Anal. Chem.*, 50 (1978)

### Gas Chromatographic Determination of Dissolved Hydrogen and Oxygen in Photolysis of Water 669

Steven J. Valenty, General Electric Corporate Research and Development, Schenectady, N.Y. 12301  
*Anal. Chem.*, 50 (1978)

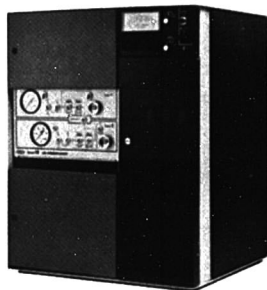
### Separation of Rhodium-103m from Ruthenium-103 by Solvent Extraction 670

Jih-Hung Chiu, Robert R. Landolt,\* and Wayne V. Kessler, Bionucleonics Department, Purdue University, West Lafayette, Ind. 47907  
*Anal. Chem.*, 50 (1978)

# An Award Winning Analytical Technique

## ION CHROMATOGRAPHY

1977  
I-R 100 AWARD  
PITTSBURGH  
APPLIED ANALYTICAL  
CHEMISTRY AWARD  
AND  
VAALER AWARD  
WINNER



Ion Chromatography (IC) analyzes ions in solution. IC is generally applicable to the separation and ppm-ppb detection of: **INORGANIC ANIONS, ORGANIC ACIDS, ORGANIC PHOSPHATES, AMMONIA, AMINES, QUATERNARY AMMONIUM SALTS, ALKALI METALS, ALKALI EARTH METALS.**

Due to the fact that IC analyzers separate the ions in a sample and detect them from 1% to trace level makes IC most appropriate in the following areas: (1) analysis in complicated matrices; (2) analysis of more than one ion simultaneously in a sample; (3) analysis of ions at low concentration in a large concentration of other ions; (4) analysis of trace (ppb) levels of ions; (5) the analysis of several samples of a given type, then several of a different type, etc.; and (6) automated analysis.

### NEW APPLICATIONS

### APPLICATION AREAS

#### AIR POLLUTION

Analysis of ambient aerosol filter extracts for nitrate and sulfate, sulfuric acid ( $\text{SO}_3$ ) in stack gas, sulfite and sulfate in FGD scrubber liquors and trace ions in rain water.

#### WATER POLLUTION

Ion characterization of waste effluents, routine ion analysis of ground waters, nitrate-N and phosphate-P in hatchery and bio-pond water, chloride, sulfate and oxalate in paper mill effluent.

#### ELEMENTAL ANALYSIS

Trace level and interference free analysis of organic fluorine, chlorine, bromine, iodine, sulfur and phosphorus after Schoniger oxidation.

#### SOIL ANALYSIS

Direct anion analysis of KCl, ammonium acetate and ammonium fluoride, sulfuric acid or bicarbonate soil extracts

#### BRINE ANALYSIS

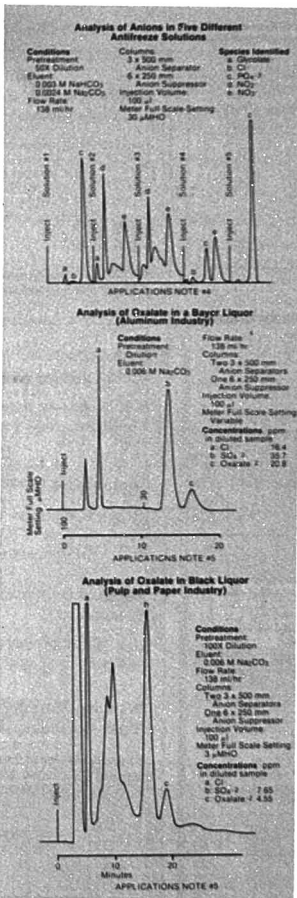
Direct analysis of chlorate, sulfate, calcium and magnesium in 25% brine and 50% caustic solutions; phosphate, bromide, nitrate, sulfate, calcium and magnesium in 2% brine.

#### POWER PRODUCTION

Trace ion analysis in boiler, boiler feed and cooling tower waters.

#### QUALITY CONTROL

Fluoride, chloride, sulfate and chromate in plating bath process water, trace ions in electronic device process water, glycolate in surfactants, monomethylamine in ethylenedichloride, thiocetic, thiolactic and thioglycolic acid in water, tetra-ethylammonium and tetra-N-butylammonium bromide in water, monomethylamine, dimethylamine and trimethylamine in water, mono and dibutyl phosphate in water and halides and sulfate in foods and food additives.



### UPCOMING EVENTS

#### Shows

##### IN EUROPE

**Analytica**, Munich  
April 18-22  
Representative: Biotronik

**IM 78**, Stockholm  
April 24-28  
Representative: Instrument AB Lambda

##### IN THE U.S.

**American Water Resources Symposium**  
San Francisco  
June 12-14, 1978

**NEW APPLICATIONS INFORMATION**  
Look for our full page Ad in the June and August issues of **ANALYTICAL CHEMISTRY** (in the briefs section) and the May, July and September issues of **AMERICAN LABORATORY** (next to the return card). Each month we will be featuring two or three new applications as well as a current schedule of seminars and road trips.

For information regarding applications of IC, circle the appropriate number or call the Dionex applications laboratory to discuss your particular application.

AIR POLLUTION 51  
WATER POLLUTION 52  
ELEMENTAL ANALYSIS 53  
SOIL ANALYSIS 54  
BRINE ANALYSIS 55  
POWER PRODUCTION 56  
QUALITY CONTROL 57  
NEW APPLICATIONS 58

**DIONEX**

#### Dionex Corporation

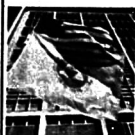
In the US contact: 1228 Titan Way, Sunnyvale, CA 94086, 408-737-0700

In Europe contact: 77 Tudor Drive, Yateley, NR, Camberley, Surrey GU17 7DB England, 01-464-7632



# A Century of Chemistry

The Role of Chemists and the American Chemical Society



Herman Skolnik,  
Chairman, Editorial  
Board  
Kenneth M. Reese,  
Editor

An illuminating  
portrait of the  
life and times  
of the world's  
largest scientific  
society devoted  
to a single  
discipline.

The book portrays the growth and activities of the ACS in the context of a century that saw two World Wars, the Great Depression, the Cold War, the Space Race, the environmental movement, and numerous scientific and engineering advances.

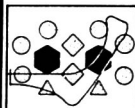
The volume traces the development of chemical science and technology in the framework of the 27 technical divisions of the Society. It includes a compact, 100-year record of ACS people and events.

**Part One: Historical Perspectives, Chemical Education, Professionalism, Publications, Impact of Government, Public Affairs, Intersociety Relations, Governance, Headquarters Staff and Operations, ACS Divisions and their Disciplines. Part Two: The Record—a list of past presidents, chairmen, members of the board of directors, editors, award winners, and more.**

468 pages (1976) \$15.00 clothbound  
LC 76-6126 ISBN 0-8412-0307-5

**Special Issues Sales**  
**American Chemical Society**  
1155 Sixteenth St., N.W.  
Washington, D.C. 20036

## Electrochemical Studies of Biological Systems



ACS  
Symposium  
Series No. 38

Donald T. Sawyer,  
Editor  
University of  
California

A symposium  
sponsored by the  
Division of  
Analytical  
Chemistry of the  
American Chemical  
Society.

The twelve papers in this significant new collection provide a representative cross section of the kinds of electrochemical methods used to characterize biological systems, as well as the kinds of biological problems that are being studied by such methods.

### CONTENTS

vitamin B<sub>12</sub> and related cobalamins •  
bioelectrochemical modelling of  
cytochrome c • potentials of metal ion  
complexes in complex •  
metalloporphyrins in aprotic solvents  
• N-bridged dimer in nonaqueous  
media • reduction of nitrogenase  
substrates • manganese (II) and -(III)  
8-quinolinol complexes • interfacial  
behavior of purines • coulometric  
titration of biocomponents • rotating  
ring disk enzyme electrode • left  
ventricle/aorta simulator • EDTA and  
NTA in phytoplankton media

216 pages (1977) clothbound \$15.50  
LC 76-30831 ISBN 0-8412-0361-X

Order from:  
SIS/American Chemical Society  
1155 16th St., N.W./Wash., D.C. 20036

## Briefs

### Serial Dilution Pipet for Generating Instrument Calibration Standards

671

Daniel S. Berry, Searle Diagnostics, Inc., 2000 Nuclear Drive, Des Plaines, Ill. 60018  
*Anal. Chem.*, 50 (1978)

### Preparation and Characterization of Glass Beads for Use in Thermionic Gas Chromatographic Detectors

672

J. A. Lubkowitz, B. P. Semonian, Javier Galobardes, and L. B. Rogers,\* Department of Chemistry, University of Georgia, Athens, Ga. 30602  
*Anal. Chem.*, 50 (1978)

### Microprocessor-Based, Linear Response Time Low-Pass Filter

676

T. C. O'Haver, Department of Chemistry, University of Maryland, College Park, Md. 20742  
*Anal. Chem.*, 50 (1978)

### Metaborate Digestion Procedure for Inductively Coupled Plasma-Optical Emission Spectrometry

679

Jan-Ola Burman, Christer Pontér, and Kurt Boström,\* Department of Economic Geology, University of Luleå, 951 87 Luleå, Sweden  
*Anal. Chem.*, 50 (1978)

### Size, Shape, and Position of a Spectrophotometer Light Beam

680

Stephen D. Rains, Bausch & Lomb Incorporated, Analytical Systems Division, 820 Linden Avenue, Rochester, N.Y. 14625  
*Anal. Chem.*, 50 (1978)

### Evaluation of the Dynamic Performance of Selected Ion Monitoring Mass Spectrometers

681

D. E. Matthews, K. B. Denson, and J. M. Hayes,\* Departments of Chemistry and Geology, Indiana University, Bloomington, Ind. 47401  
*Anal. Chem.*, 50 (1978)

### Photometric Detection of Oxygen

684

Zbigniew Mielniczuk, Christopher G. Flinn, and Walter A. Aue,\* 5637 Life Sciences Building, Dalhousie University, Halifax, N.S., Canada  
*Anal. Chem.*, 50 (1978)

### Modified Nebulizer for Inductively Coupled Plasma Spectrometry

686

D. L. Donohue\* and J. A. Carter, Oak Ridge National Laboratory, Oak Ridge, Tenn. 37830  
*Anal. Chem.*, 50 (1978)

### Dropping Mercury Electrode for Polarography in Glass-Corroding Media

687

Hugues Menard\* and Francine LeBlond-Routhier, Department of Chemistry, University of Sherbrooke, Sherbrooke, Quebec, Canada J1K 2R1  
*Anal. Chem.*, 50 (1978)

# Save energy.

Spending up to 20 complicated hours on moisture determination is just wasting our energy.

When this speedy Ohaus Moisture Determination Balance can complete most jobs in 15 to 20 minutes.

And deliver results that correlate very closely with the Oven Test. Results that read out directly... as you see above... in both weight and % moisture.

All you do is place a sample in the pan, set the correct time and temperature,



and turn it on.

Everything's automatic. And precise. With Ohaus features like polished agate bearings and these precision ground knives.

Then, when it's finished, the Ohaus Moisture Determination Balance shuts itself off and rings a bell. Service that's not only fast, it's actually polite.



We'll gladly show you all our features... just contact Ohaus Scale Corporation, 29 Hanover Road, Florham Park, N.J. 07932.

CIRCLE 157 ON READER SERVICE CARD



**Measuring up since 1907**



# Introducing The Model 303 Static Mercury Drop Electrode Module...

# See what you've been missing!

- Higher Sensitivity
- Greater Convenience
- Lower Cost

- **HIGHER SENSITIVITY**

*The name of the game!* The new 303 Static Mercury Drop Electrode Module gets you down to concentration levels that you were probably only guessing at before. With the 303 electrode, baseline distortions at ppb concentrations are drastically lowered and drop sizes are much larger. This means you'll get improved detection limits for both differential pulse polarography and stripping voltammetry (using the same static drop).

*Hang in there!* You get higher sensitivity with the 303 because each mercury droplet, rather than growing continually as in the conventional approach, is caused to remain stationary at the optimum size over the course of each current measurement. This is a great way to overcome the baseline distortion caused by the differential capacitance curve.

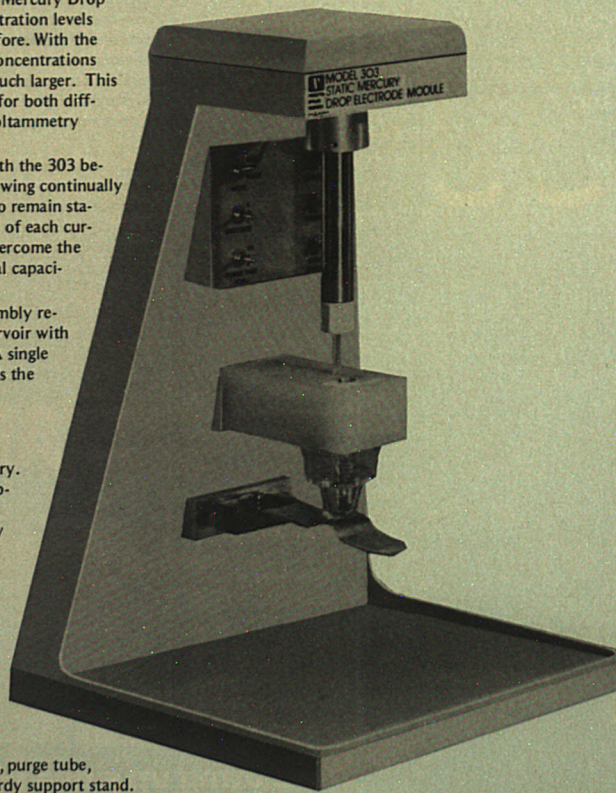
*And talk about simplicity!* There's no assembly required of the operator. Simply fill the reservoir with mercury and start running your analyses. A single moving part within the 303 Module controls the extrusion of each mercury drop.

- **GREATER CONVENIENCE**

*Simple switchover!* Use the Model 303 for either polarography or stripping voltammetry. Convert from one mode to the other by flipping a single panel switch. No other adjustments are necessary since the same capillary serves both techniques. And you'll appreciate the additional controls for purge, purge times, drop size, drop extrusion and drop dislodge.

- **LOWER COST**

*Now that's progress!* The Model 303 costs less than the two previous electrode assemblies you needed for doing polarography and stripping voltammetry. The 303 Module includes the mercury electrode, reference and counter electrodes, purge tube, cell bottoms, electronics package and a sturdy support stand.

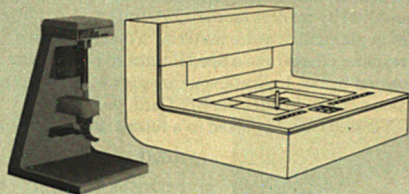




# See how it's used...

## A GREAT INSTRUMENT MADE BETTER... THE MODEL 374-3 MICROPROCESSOR-BASED ANALYZER SYSTEM

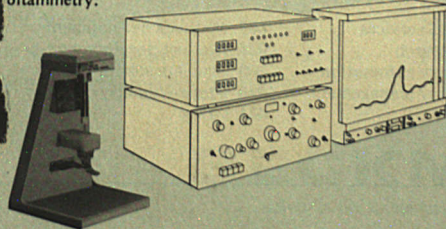
When your samples demand the utmost in voltammetric sensitivity and capability we've got it. The 374-3 combines the new Model 303 Static Mercury Drop Electrode Module with the popular Model 374 microprocessor-based polarographic analyzer to yield a truly unique approach to ultra-high sensitive voltammetry. The increased drop area of the 303 Module, the greatly reduced background current and the baseline storage feature of the microprocessor-based analyzer all combine to create the most favorable signal-to-noise ratio available in any commercial polarographic instrument.



A simple but elegant approach is used to create reproducible stationary mercury drops within the 374-3 System. A single vertically moving part controls the extrusion of each drop. Drops formed in this manner are stable for as long as you want. All set-up, scan, data reduction, calculation and symbolization steps are monitored and controlled for you by the built-in 16-bit microprocessor. Blank and sample scans are stored in separate 750 point memories within the 374-3 to give you automatic blank subtraction during the data reduction and calculation stages. And for your methods development work you'll appreciate the 22 override switches which provide a high degree of analytical flexibility.

## AN ECONOMICAL, HIGHLY SENSITIVE PACKAGE... THE MODEL 174 POLAROGRAPHIC ANALYZER SYSTEM

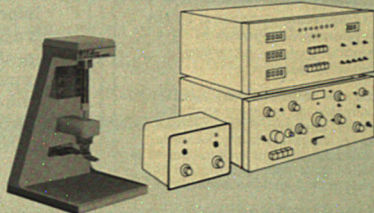
This system combines the new 303 Module with the versatile Model 174A Polarographic Analyzer, the 315A Automated Electroanalysis Controller and the 9002A X-Y recorder—a complete package for polarography and stripping voltammetry.



Circle 180 For information only

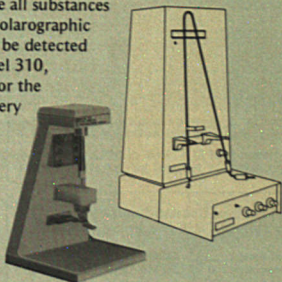
## ANALYZE IT CONTINUOUSLY WITH... THE MODEL 318 AUTOMATED BATCH SAMPLER INTERFACE

Now you can apply automated voltammetry to the analysis of process streams, reservoirs, holding tanks, plating baths and the like with our new Model 318 Automated Batch Sampler Interface. The 318 incorporates an electronic control package and a cell that is automatically refilled at regularly timed intervals with aliquots of the solution to be analyzed. The 318, shown here with the new Model 303 Static Mercury Drop Electrode Module, can be used with the 174A Polarographic Analyzer/315A Automated Electroanalysis Controller combination or with the 374-1 and 374-3 Polarographic Analyzers.



## A UNION OF TWO POWERFUL TECHNIQUES... THE MODEL 310 POLAROGRAPHIC LIQUID CHROMATOGRAPHY DETECTOR

The Model 310 Detector employs the new PARC Model 303 Static Mercury Drop Electrode Module to achieve ppb-level sensitivities for pharmaceuticals, pesticides, vitamins, metals, additives, pollutants and many other compounds. Typically 10 ng. ascorbic acid can be measured with little difficulty. The 310 Detector incorporates a specially-designed cell in which the LC eluate is led up and around the static mercury droplet. Since all substances that exhibit polarographic responses can be detected with the Model 310, applications for the detector are very broad.



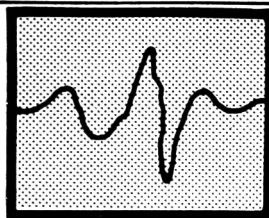
For more information on these new products, contact:  
Princeton Applied Research Corporation, P.O. Box 2565,  
Princeton, NJ 08540; or phone 609/452-2111.



**PRINCETON APPLIED RESEARCH**

AN **EG&G** COMPANY

Circle 181 Salesman Please Call



## Chemometrics: Theory and Application

ACS Symposium Series No. 52

Bruce R. Kowalski, Editor  
University of Washington

A symposium sponsored by the  
Division of Computers in  
Chemistry of the American  
Chemical Society.

This new collection constitutes an  
invaluable aid for every analytical  
chemist, instrument designer, and  
builder interested in the search for  
better measurement system control as  
well as up-to-date optimization and  
measurement analysis methods.

Increased use of chemical  
measurements, combined with the  
proliferation of computers in chemical  
laboratories, has prompted a drive for  
new and improved methods to design  
and control experiments and to analyze  
the wealth of data that can be generated.

The results of this research effort are  
discussed in 12 chapters covering the  
development and application of new  
mathematical and statistical analysis  
methods to extract useful chemical  
information from chemical  
measurements.

### CONTENTS

Optimization Methodology in Chemistry •  
ARTHUR and Experimental Data Analysis •  
Abstract Factor Analysis • Target-  
Transformation Factor Analysis •  
Application of Factor Analysis to the Study of  
Rain Chemistry • Electron Spin Resonance of  
Spin Labels • Stirred-Pool Controlled-  
Potential Chronocoulometry • Application of  
Nonlinear Regression Analysis to Chemical  
Data • Structure-Activity Studies •  
Enthalpy-Entropy Compensation • How to  
Avoid Lying with Statistics • SIMCA: A  
Method for Analyzing Chemical Data in  
Terms of Similarity and Analogy

288 pages (1977) \$21.00 clothbound  
LC 77-9088 ISBN 0-8412-0379-2

SIS/American Chemical Society  
1155 16th St., N.W./Wash., D.C. 20036

Please send \_\_\_\_\_ copies of SS 52  
Chemometrics at \$21.00 per copy.

☐ Check enclosed for \$ \_\_\_\_\_. ☐ Bill me.  
Postpaid in U.S. and Canada, plus 40 cents  
elsewhere.

Name \_\_\_\_\_

Address \_\_\_\_\_

City \_\_\_\_\_

State \_\_\_\_\_

Zip \_\_\_\_\_

# analytical chemistry

## Reader Survey

Information supplied by readers on their interests and activities  
aids a publication in planning feature material. To help us learn  
more about our readers, please take a few minutes to provide the  
information requested below. Indicate your answers by circling the  
appropriate numbers on the Reader Service Card, page 463 A.

Reader survey results will be reported in a future issue of the  
JOURNAL.

### A. This copy of ANALYTICAL CHEMISTRY is

- 301 My own  
302 Pass-along copy

### B. My employer's business is

- 303 Academic  
304 Industry  
305 Government  
306 Other

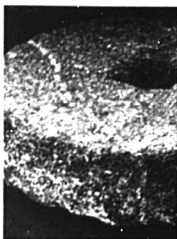
### C. Fields of Interest

- |                            |                             |
|----------------------------|-----------------------------|
| 307 Air analysis           | 320 Nonferrous metallurgy   |
| 308 Biological/medical     | 321 Oceanography            |
| 309 Clinical chemistry     | 322 Organic analysis        |
| 310 Coatings/paints        | 323 Pesticides              |
| 311 Drugs/cosmetics        | 324 Petroleum               |
| 312 Electrical/electronics | 325 Polymers/rubber         |
| 313 Fertilizers            | 326 Pulp/paper/wood         |
| 314 Food                   | 327 Soaps/cleaners          |
| 315 Forensic science       | 328 Solid and gaseous fuels |
| 316 Ferrous metallurgy     | 329 Textiles                |
| 317 Geochemistry           | 330 Toxicology              |
| 318 Inorganic analysis     | 331 Water analysis          |
| 319 Materials science      | 332 Other                   |

### D. Activities

- |                           |                             |
|---------------------------|-----------------------------|
| 333 Analytical services   | 337 Methods development     |
| 334 Basic research        | 338 Product development     |
| 335 Laboratory automation | 339 Problem solving         |
| 336 Laboratory management | 340 Process/quality control |
|                           | 341 Other                   |





**"Just like the wheel,  
and contrary to popular opinion, a good scientific instrument must  
be reinvented periodically."**

In the case of the very latest Beckman digital pH meter—our new 3560—reinvention meant incorporating a very special feature: Auto Read.

Now, with just the push of a button, all the guesswork is taken out of variations in electrode response. Solid-state logic determines exactly the right time to take your reading. And when the sample has fully stabilized, you are signaled by the read indicator light.

That's just about "foolproof" pH analysis, but only the beginning of the 3560's capability.

Along with Auto Read, you get built-in digital temperature readout for double duty from the same instrument.

Then there's recorder zero to expand any portion of the scale, a 15-volt power supply for accessories like our multiple electrode selector, printer output, and a broad range of features that add up to

unmatched automated pH performance.

Why not order that performance for your lab. We think it can make your work



**New 3560 Digital pH Meter features Auto  
Read for foolproof answers.**

roll along a lot faster and smoother. For full information, contact Scientific Instruments Division, Beckman Instruments, Inc., P.O. Box C-19600, Irvine, CA 92713.

**Innovation in pH since 1935.**

**BECKMAN®**

CIRCLE 28 ON READER SERVICE CARD

ANALYTICAL CHEMISTRY, VOL. 50, NO. 4, APRIL 1978 • 423 A

## Letters

### Nomenclature for Size-Exclusion Chromatography

**Sir:** One of the four separation modes in liquid chromatography, "steric exclusion", is a column fractionation method based on the molecular sieve effect. There are many names used for this chromatography: Gel Filtration Chromatography (GFC), Gel Permeation Chromatography (GPC), Molecular Sieve Chromatography, Gel Chromatography, Liquid Exclusion Chromatography, and Size-Exclusion Chromatography. The great variety of names applied to the same separation mode causes confusion. Part of this confusion stems from the origin of the chromatography.

Most gel filtration experiments have been carried out in aqueous solutions, with hydrophilic gels as bed materials. The term "GFC" is commonly employed today in the field of bio-

chemistry and clinical chemistry, while the term "GPC" is generally accepted in the field of polymer science for the measurement of molecular weight distributions with polystyrene gel in organic media. However, newly developed packing materials such as deactivated porous glass and silica have enabled the separation and the desalting of peptides and the determination of the molecular weight distribution of polymers in the same columns with different solvent media. The use of GFC or GPC, without further qualification, to describe this chromatographic system can be confusing and misleading.

Though no comprehensive and completely satisfactory theory for separation mechanisms has yet emerged, most experts agree that these separations are primarily based on the difference in size of solutes in solution and that the larger molecules, excluded from all or a portion of the pores of

gels by means of their physical size, elute before the smaller ones, regardless of the types of solutes, the mobile phases, and gels. The term "size exclusion" is a concise word for expressing this separation mode in analogy with the terms "adsorption", "partition", and "ion exchange", which express the other three separation modes.

This chromatography cannot be classified as "filtration". The term "permeation" represents neither the separation mechanism nor the separation mode. Since in liquid chromatography every solute must permeate into the pores of packing materials, those that cannot permeate into the pores are not separated. Strictly speaking, every chromatography is permeation chromatography. Porous glass can be used for this technique as packing materials, so that the nomenclature Gel (Permeation, Filtration) Chromatography is not in agreement with this chromatography in the strict sense of

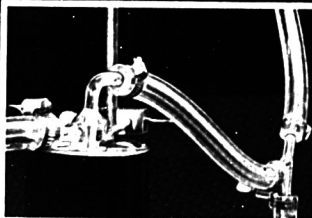
# TYGON<sup>®</sup> VACUUM TUBING

outlasts rubber in vacuum applications, and is more economical in many popular sizes. Tygon vacuum tubing is clear, so blockage is immediately visible, and because it has a low vapor pressure, test results are not affected.

Make your lab "Totally Tygon". See your lab supply house or call toll-free 800-321-9634 (except Ohio).

**NORTON** PLASTICS AND SYNTHETICS DIVISION

PO BOX 350 AKRON, OHIO 44309 TEL: (216) 633-3224



Tygon vacuum tubing withstands full vacuum at room temperature and 27 inches of mercury at 140°F.

CIRCLE 149 ON READER SERVICE CARD

Now from J.T. Baker As a  
'Baker Analyzed'® Reagent

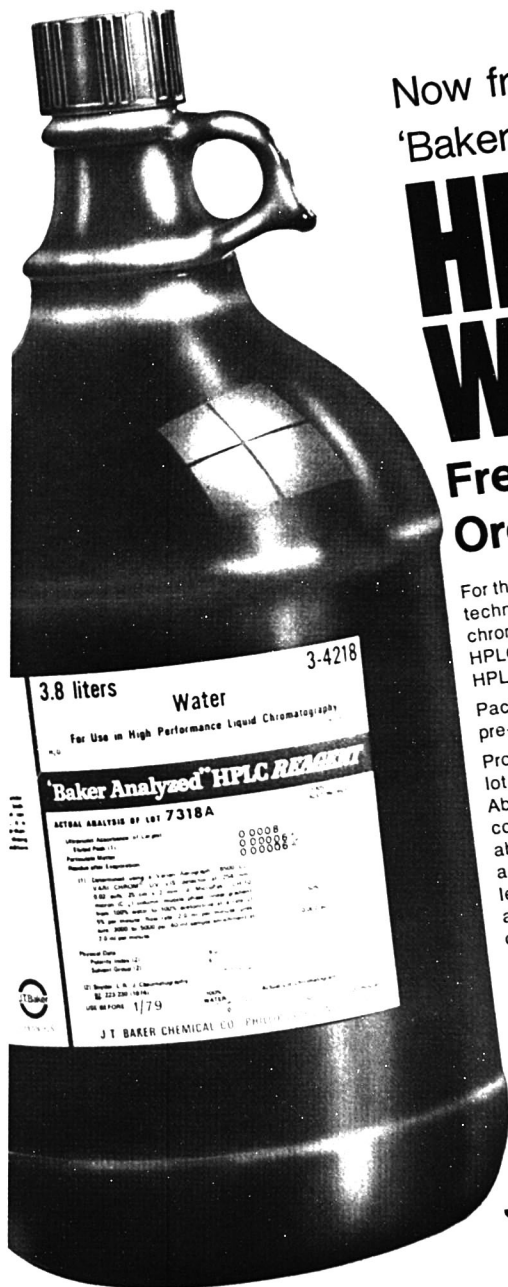
# HPLC Water

Free from  
Organic Impurities . . .

For the chromatographer engaged in the rapidly advancing technique of reverse-phase high performance liquid chromatography, J. T. Baker now introduces the first HPLC organics-free water suitable for use in virtually all HPLC applications.

Packaged under nitrogen in a 3.8-liter (1 gallon) pre-cleaned amber bottle, the product is ready to use. Proof of Purity . . . just examine the label . . . the actual lot chromatogram shows no significant impurity peaks. Absorbances caused by organic impurities are controlled by specification to less than 0.005 absorbance units (for a detector range of 0.02 au) and are typically below 0.002 absorbance units or less. J. T. Baker's water for HPLC is now available through more than 120 J. T. Baker distributor locations in the United States and Canada as product 3-4218.

Place an order today and evaluate  
J. T. Baker's efforts to help you.



3.8 liters Water 3-4218  
For Use in High Performance Liquid Chromatography

**'Baker Analyzed' HPLC REAGENT**

ACTUAL ANALYSIS OF LOT 7318A

Chromatogram: 100% pure water  
Absorbance: 0.0008  
0.0008  
0.0008

Residual after Evaporation:  
(1) Distillation residue: 0.0008  
(2) 100% water: 0.0008  
(3) 100% water: 0.0008  
(4) 100% water: 0.0008  
(5) 100% water: 0.0008  
(6) 100% water: 0.0008  
(7) 100% water: 0.0008  
(8) 100% water: 0.0008  
(9) 100% water: 0.0008  
(10) 100% water: 0.0008

Physical Data:  
Density: 1.000  
Viscosity: 0.010

(1) Supplier: J. T. Baker  
(2) Supplier: J. T. Baker  
(3) Supplier: J. T. Baker  
(4) Supplier: J. T. Baker  
(5) Supplier: J. T. Baker  
(6) Supplier: J. T. Baker  
(7) Supplier: J. T. Baker  
(8) Supplier: J. T. Baker  
(9) Supplier: J. T. Baker  
(10) Supplier: J. T. Baker

J. T. BAKER CHEMICAL CO. PHILLIPSBURG, NJ 08865

**J.T. Baker Chemical Co.**  
Phillipsburg, NJ 08865  
or call 201-859-2151



CIRCLE 25 ON READER SERVICE CARD



# SMI... first with innovations in plasma spectrometry



SMI is widely recognized and respected as both a leader in atomic analysis and innovator of plasma-emission measurement techniques that have become accepted in numerous laboratories and industries worldwide.

As a result of its continuing research and development efforts, SMI has evolved a new generation of low-cost plasma-emission spectrometers that combine the most desirable features of atomic-absorption and atomic-emission analyses, but provide greater capabilities than either.

These new total-measurement systems, called Spectraspan III and Spectraspan IV, are compact, bench-top units that operate on safe, inert argon, and are designed for both quantitative and qualitative analysis. The systems offer a hardware flexibility and operating versatility that ensure consistently superior data, and the high productivity demanded by today's analytical requirements.



Spectraspan IV performs automatic quantitative analysis of most elements on a sequential basis from major to trace concentrations including many of the so-called difficult elements. Rapid, comprehensive qualitative analysis is also available. Operating efficiency of the Spectraspan IV is improved through the use of a built-in INTEL microprocessor.

The most attractive feature, however, is the price which further reflects SMI's innovativeness. While Spectraspan IV offers far more potential, **it is priced competitively with atomic absorption units.**

Spectraspan III, the most versatile plasma-emission spectrometer, incorporates the same unique features as Spectraspan IV **plus** the ability to perform **simultaneous quantitative analysis of up to 20 different elements.** And the system price is also surprisingly modest.

If you want to increase your capabilities without increasing costs, do it with a Spectraspan III or Spectraspan IV system. Call SMI today for details. SMI is the innovative company that has more plasma-emission spectrometers in use by satisfied customers throughout the world than any other manufacturer.

# SMI

**SPECTRAMETRICS INCORPORATED**  
204 ANDOVER STREET, ANDOVER, MA 01810  
(617) 475-7015

CIRCLE 190 ON READER SERVICE CARD

## Letters

the word. The term "exclusion" includes steric exclusion as well as ion exclusion which belongs to a different technique.

It seems reasonable to assume that several proposed theories such as steric exclusion and restricted diffusion take each part of "size exclusion" mechanisms. This situation is similar to the fact that several adsorption or partition mechanisms are proposed for "Adsorption" or "Partition" Chromatography. To the end that we can use the consolidated terminology for the techniques, I propose that the term "Size Exclusion Chromatography (SEC)" be used to describe this chromatography instead of GPC, GFC, Gel Chromatography, and other related names.

Sadao Mori

Department of Industrial Chemistry  
Faculty of Engineering  
Mie University  
Tsu, Mie 514, Japan

## Graphite Furnace AA

Sir: I would like to clarify a point raised by Ralph Sturgeon in his INSTRUMENTATION article, "Factors Affecting Atomization and Measurement in Graphite Furnace Atomic Absorption Spectrometry" [ANAL. CHEM., 49, 1255A (1977)]. On page 1260 A he states, "It is the inseparability of the rate of heating of the atomizer and the maximum temperature which it attains that presents a major problem with commercial ET (electro-thermal) atomizers employing three-stage heating programs." He reiterates this throughout the text.

This problem has been recognised and eliminated by at least one manufacturer of commercial atomizers. The Varian CRA-90, which was released in January 1976 and described [B. R. Culver and D. E. Schrader, *Amer. Lab.*, 8 (3), 59 (1976)] in March 1976, allows independent selection of the heating rate and the maximum temperature. A ramp rate of up to 800 °C/s, a hold temperature of up to 3000 °C, and a hold time of up to 5 s may be independently selected for the atomization stage. I hope this letter will prevent your readers from gaining the mistaken impression that there is no commercial graphite furnace with the desirable characteristics specified by Dr. Sturgeon.

P. R. Liddell

Varian Techtron Pty. Ltd.  
679/687 Springvale Road  
Mulgrave, Vic., Australia 3170

## Micromeritics 7000B, The **PERFORMANCE** Liquid Chromatograph



### Simplified Methods Development Analytical or Research HPLC

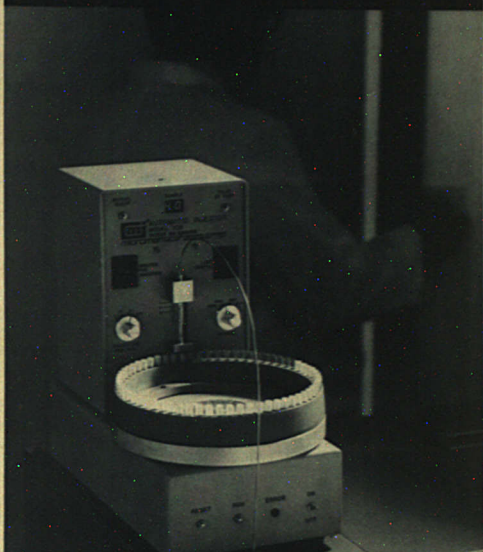
- Patented flow multiplexing compensates for differences in solvent compressibility to provide a constant pulseless flow solvent delivery system.
- Gradient and isocratic systems available with or without microprocessor control.
- Worldwide service, sales and applications support.
- Applications-oriented design allows operator to change columns, modes, solvents, and solvent conditions in minutes.

For more information, contact Micromeritics Instrument Corporation, Telephone (404) 448-8282 or write 5680 Goshen Springs Road, Norcross, Georgia 30093.

 **micromeritics**  
instrument corporation

CIRCLE 145 ON READER SERVICE CARD

## Micromeritics: Automatic Injector For Unattended HPLC



### Up to 64 samples Up to 192 injections Automatically

#### Micromeritics' Model 725 Automatic Injector for HPLC

- Microprocessor operation controls injections per sample, injection time, rinse between samples and automatic shutdown.
- Positive flow design requires only 0.75 ml of sample, allows precise, reproducible sample volumes.
- Adaptable to any HPLC solvent delivery system—can be externally controlled by computing integrator.

For more information, contact Micromeritics Instrument Corporation, Telephone (404) 448-8282 or write 5680 Goshen Springs Road, Norcross, Georgia 30093.

 **micromeritics**  
instrument corporation

CIRCLE 146 ON READER SERVICE CARD



# TRACE ORGANIC ANALYSIS

Until recently the major emphasis in trace analysis has been in the determination of inorganic substances.

However, we are now coming to realize that many of our most pressing problems require competence in trace organic analysis. These analyses are needed to protect our health and our environment, and to ensure the purity and nutritional value of our food. Recent Federal legislation recognizing these needs includes: the Federal Water Pollution Control Act (1972), the Federal Environmental Pesticide Control Act (1972), the Safe Drinking Water Act (1974), the Food Nutritional Labeling Act (1975), the Toxic Substances Control Act (1976), the Medical Devices Amendment (1976), and the pending refinements to the Clinical Laboratory Improvement Act (1967). The enforcement of such legislation is ultimately based on the ability of analysts to accurately identify and quantify trace levels of organic substances in diverse matrices.

When compared to trace inorganic analysis, the current state-of-the-art of trace organic analysis appears inadequate. One has to bear in mind, however, that trace inorganic analyses are usually limited to a finite number of elements, whereas the number of organic compounds of analytical interest is essentially infinite. A number of difficulties in trace organic analysis have limited the achievement of accuracy in this area. Lewis (1) and Beyermann (2) have discussed some of these problems. The purpose of this report is to assess the current state-of-the-art of trace organic analysis and to discuss the problems associated with performing such analyses. The first section, which discusses the difficulties in achieving accuracy, is intended as an overview for the analytical chemist.

Analysts actually involved in trace organic analysis will find the interlaboratory comparison studies in the second section, which deals with the current state-of-the-art, of more interest. Analysts unfamiliar with trace organic analysis will probably find that the discussion of the current state-of-the-art reveals a somewhat disturbing picture. This report is intended to make the analytical chemist, and chemists utilizing the results of organic analyses, aware of the limitations of these analyses and of the need for research to improve such measurements.

## Difficulties in Achieving Accuracy in Trace Organic Analysis

An accurate measurement system is one that produces precise numerical values that are free of, or corrected for, all systematic errors (3). The achievement of accuracy must be the major consideration in trace organic analysis. While true accuracy has not been realized in trace organic analysis of natural samples, studies of the intercomparability of laboratory data (relative precision) do exist. Relative determinations, although useful for monitoring changes in levels or identifying particularly high or low values, suffer from two serious disadvantages. First, these relative values are often method dependent; thus, values determined by one method may bear little absolute resemblance to those determined by another. Secondly, relative values do not suffice when absolute values are required. For example, legislated environmental standards are generally expressed in absolute quantities; therefore, unless analytical methods can be validated for accuracy, regulatory decisions will be based on values derived from methods of de-



H. S. Hertz, W. E. May, S. A. Wise, and S. N. Chesler

Institute for Materials Research, Analytical Chemistry Division  
National Bureau of Standards, Washington, D.C. 20234

batable quality. A notable exception to standards based on absolute values is the High Volume Method for the measurement of suspended particles in the atmosphere (4). This method requires no "true value"; instead, decisions are based on the response from a specific method written as part of the regulation.

Accuracy can be achieved only by identifying all sources of systematic error and by then removing or correcting for their effects. The typical trace organic analytical scheme consists of several distinct operations, namely: *collection, storage, extraction, concentration, isolation, identification, and quantitation*. Each of these individual steps possesses potential sources of error which will now be described.

**Collection.** The collection of the sample is often ignored as a significant source of error. This is a serious fallacy, however, since there are two potential sources of error that can occur in the sample collection. To assure meaningful results, the subsample selected must be representative of the system as a whole. An analysis of a nonrepresentative sample is by definition an inaccurate measurement. Sample contamination due to careless collection and handling is the second source of error. At trace levels almost any surface with which the sample comes in contact becomes a possible source of contamination, e.g., extractables from plastic containers, residues on glass or metal collection devices, etc.

**Storage.** Chemical processes that occur in the sample during storage, between the time of sample collection and analysis, can invalidate the analytical results. Organic compounds are susceptible to processes such as photo-

decomposition, adsorption, vaporization loss, thermal decomposition, microbial action, and chemical reaction; consequently, the choice of sample container and the conditions under which the sample is stored are of critical importance. Samples being held for extended periods prior to organic analysis should generally be stored in darkness in glass containers and maintained at subzero ( $^{\circ}\text{C}$ ) temperatures, since these conditions tend to inhibit the processes listed above. At trace levels the loss of analyte due to adsorption can result in serious inaccuracies. Adsorptive losses to the walls of storage vessels have been recently investigated in this laboratory. Experiments with polynuclear aromatic hydrocarbons (PAH's) in stirred aqueous solutions at the 1 ppb level indicated that losses of ~80% occurred after only 4 h and that losses increased to ~95% after 40 h. The use of freeze-drying for sample preservation results in the loss of volatile organic compounds.

**Extraction.** Extractions are commonly used to remove the analyte components from the sample matrix. Unfortunately, a large number of non-analyte components are also extracted from the sample matrix. Organic solvents have been traditionally used as extracting agents, although some recent methods utilize an inert gas (5-7). To assure accurate results, the extraction efficiency for the removal of each organic compound from the sample matrix must be determined. This is a difficult task (often impossible) in the case of environmental analyses where hundreds of organic compounds are frequently analyzed simultaneously. It is incorrect to assume (as is commonly done) an extraction efficiency of 100% for the removal of organic

compounds from matrices such as biological tissue, sediment, or food products. Even after extraction, unforeseen chemical reactions involving some of the extracted species may occur. Adsorptive loss of the analyte can also introduce errors during the extraction step. Another major source of error in trace organic analysis is the existence of impurities in the extracting solvent. Thus, solvents of high purity are a prerequisite for accuracy. Extraction procedures are rarely so selective that nonanalyte organic compounds are not also extracted; therefore, a sample cleanup is usually required to isolate the components of interest. These cleanup procedures generally involve column liquid chromatography (LC) or thin-layer chromatography (TLC).

**Concentration.** After extraction and chromatographic cleanup, the compounds are usually contained in a large volume of solvent requiring concentration prior to analysis. This sample concentration is usually accomplished by evaporation of the solvent and often results in severe and nonreproducible loss of the volatile components. These losses are difficult to prevent; however, they can be minimized by use of gentle evaporation procedures and/or a specialized evaporation apparatus, such as a Kuderna-Danish concentrator (8). With this apparatus, solutions can be concentrated from several hundred milliliters to a few milliliters in one step with only minimal losses of the volatile compounds. Further concentration to ~50  $\mu\text{L}$  is possible with a micro-Kuderna-Danish concentrator. Alternatively, the use of organophilic resins, such as XAD-2 (Rohm and Haas, Philadelphia, Pa. 19105) and TENAX-GC (Applied Science Laboratories, State College, Pa. 16801), for removal and

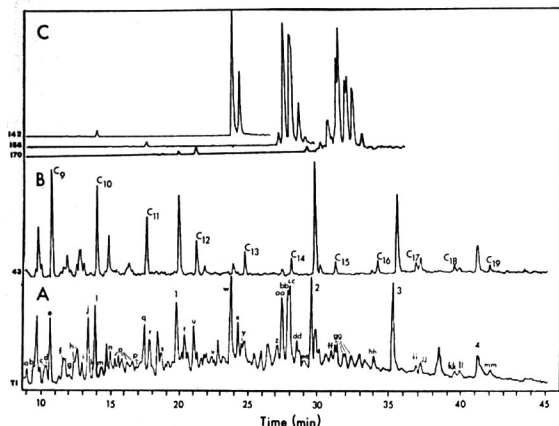


**Figure 1.** GC/MS analysis of petroleum hydrocarbon-containing sediment (A) Total ion chromatogram, (B)  $m/e$  43 mass chromatogram, (C) composite  $m/e$  142, 156, and 170 mass chromatograms indicating presence of  $C_1$ -,  $C_2$ -, and  $C_3$ -naphthalenes, respectively

**Table I. Identification of Peaks in Figure 1A<sup>a</sup>**

a	$C_2$ -cyclohexane	t	$C_2$ -decalin
b	$C_2$ - $\phi$	u	$n$ - $C_{12}$
c	$C_2$ - $\phi$	v	$C_6$ -cyclohexane
d	$C_3$ -thiophene	w	$C_1$ -naphthalene
e	$n$ - $C_9$	x	$C_1$ -naphthalene
f	$C_3$ -cyclohexane	y	$n$ - $C_{13}$
g	Propyl- $\phi$	z	Ethyl-naphthalene
h	$C_3$ - $\phi$	aa	$C_2$ -naphthalene
i	$C_3$ - $\phi$	bb	$n$ - $C_{14}$ & $C_2$ -naphthalene
j	$C_3$ - $\phi$ & $C_4$ -thiophene	cc	$C_2$ -naphthalene
k	$C_4$ -thiophene	dd	$C_2$ -naphthalene
l	$n$ - $C_{10}$	ee	Ethyl-naphthalene?
m	$C_3$ - $\phi$	ff	$n$ - $C_{15}$
n	$C_4$ -cyclohexane	gg	$C_3$ -naphthalene
o	$C_4$ - $\phi$	hh	$n$ - $C_{16}$
p	$C_5$ -thiophene?	ii	$n$ - $C_{17}$
q	$n$ - $C_{11}$	jj	Pristane
r	$C_4$ - $\phi$	kk	$n$ - $C_{18}$
s	$C_5$ -cyclohexane	ll	Phytane
		mm	$n$ - $C_{19}$

<sup>a</sup>  $C_x$  = alkane containing  $x$  carbon atoms.  $C_y$ - $\phi$  = benzene substituted with  $x$  carbon atoms (e.g.,  $C_3$ - $\phi$  could be trimethyl-, propyl-, isopropylbenzene, etc.). Peaks labeled 1, 2, 3, 4 are internal standards (methyl- $C_{11}$ , methyl- $C_{14}$ , methyl- $C_{16}$ , and methyl- $C_{18}$ , respectively). Identifications followed by "?" are not definite due to incompletely resolved spectra.

concentration of sample components minimizes volatilization losses (5-7). In either case, impurities present in the solvent are magnified by the concentration step, again emphasizing the need for pure extraction solvents.

**Isolation.** After the extraction and the concentration steps, the analyst can still have a multitude of organic compounds that must be separated for identification and quantitation. The isolation of individual components is generally accomplished using gas chromatography (GC), high-performance liquid chromatography (HPLC), or thin-layer chromatography (TLC). These chromatographic techniques can also introduce systematic errors due to irreversible adsorption, decomposition, chemical reaction, or incomplete separation (insufficient resolution).

**Identification.** After the chromatographic separation the analyst is confronted with the identification of the individual compounds. Identifications may be difficult not only because of the large number of organic species that may be present, but also because the compounds of interest may be substances for which the chemical nature is unknown, such as metabolites and decomposition products of drugs and pesticides. In addition, suitable, pure standards to allow positive identification are often unavailable. Should the substance of interest be a specific isomer of a compound, differentiating among several isomers can

be a formidable task. Obviously, if a compound cannot be identified, the concept of accuracy for that particular analysis has little or no meaning.

**Quantitation.** The final step in the analysis, quantitation, usually involves the electronic manipulation of a signal arising from the presence of the organic compound in the detector of an analytical instrument. Since errors in this measurement process are not readily apparent (i.e., hidden inside of a black box), they are often neglected. To ensure accuracy, detectors must be calibrated using appropriate chemical standards, and measurement algorithms must be verified.

The measurement of and correction for all systematic errors in the analytical procedure is a tedious and often impossible process. One way to circumvent much of this problem is by the use of an internal standard that should be added to the sample as soon as possible in the analytical scheme. The internal standard is assumed to be susceptible to the same systematic errors during the analytical scheme as the compound being determined. By measuring the relative signals for the internal standard and for the unknown organic compound, the concentration of the unknown can be calculated. This supposition is valid only if the internal standard exhibits all the chemical and physical properties of the organic compound being determined and is present in approximately the same concentration as the com-

pound of interest. However, internal standards are never liable to exactly the same systematic errors as the compound being determined. These errors are minimized in the case where the internal standard differs only in its isotopic composition (e.g.,  $^{13}CH_4$  as an internal standard for the determination of  $^{12}CH_4$ ). Even an isotopic internal standard (called an isotope diluent) cannot accurately mimic the behavior of the organic unknown unless the diluent is associated with the sample matrix in exactly the same manner as the compound to be determined and no isotope effect is observed. This is the crux of the problem in achieving accuracy in trace organic analysis. One can use an isotopically labeled internal standard, but the question of whether the internal standard is bound in the matrix exactly as the compound of interest is the ultimate limit on accuracy in trace organic analysis. (This problem is obviated in inorganic analyses by the use of digestion procedures that completely destroy the matrix prior to elemental analysis.)

#### Current State-of-the-Art

In chemical analyses, accuracy is a measure of how close a determined value comes to the "true value". Currently, in trace organic analysis an important consideration is often whether or not the correct analyte was measured. In the determination of organic compounds present at trace levels in

"real world" matrices, accurate qualitative results are often as difficult to obtain as accurate quantitative results. Several of the state-of-the-art techniques utilized in qualitative and quantitative measurement of trace-level organic compounds are discussed below.

**Compound Identification.** A number of different techniques are currently used for compound identification. A common method for identification is comparison of the chromatographic retention time (retention volume in LC,  $R_f$  in TLC) of a standard with that of the unknown under identical chromatographic conditions. However, incorrect identification may result using this method, since several compounds may coelute. Greater confidence with respect to qualitative accuracy can be achieved by utilizing: selectivity in the isolation and cleanup step, chromatography on two or more columns (or systems) utilizing different separation mechanisms, and highly selective chromatographic detectors. If more definitive qualitative information is necessary or if a standard for comparison is unavailable, more sophisticated means of identification are required. Spectroscopic analysis provides detailed information about an organic compound. Infrared (IR) and nuclear magnetic resonance spectroscopy (NMR) are widely used in qualitative organic analysis. However, even with Fourier transform systems to enhance signal-to-noise ratios, detectability limits still preclude the use of these spectroscopic techniques for most trace analyses. Ultraviolet spectroscopy (UV) has sufficient sensitivity, but it is only of limited value in deducing the molecular structure of an unknown compound.

The mass spectrometer provides sufficient sensitivity for trace analysis, and it is easily interfaced to a gas chromatograph. Gas chromatography/mass spectrometry (GC/MS) can provide qualitative information with nanogram amounts of single compounds present in the sample. Combined gas chromatography/mass spectrometry is currently the most powerful technique for the identification of trace levels of organic compounds. In addition to providing a mass spectrum of each peak eluting from the GC, GC/MS data can be plotted in the form of mass chromatograms as an additional interpretive aid. Such computer-generated, mass-specific gas chromatograms can be used in locating particular compounds or classes of compounds containing an indicative mass in their mass spectra. These capabilities of the GC/MS technique are illustrated in Figure 1 for a sediment sample with a low-level petroleum hydrocarbon burden. The total ion

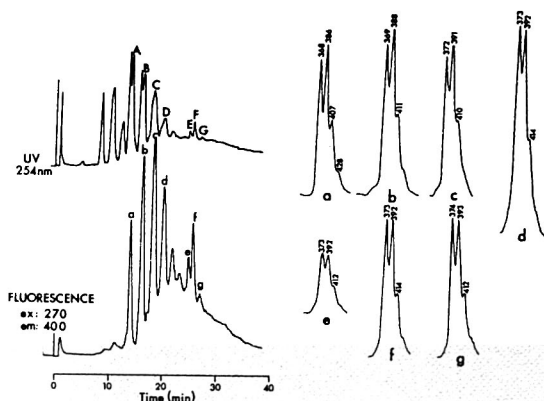


Figure 2. Left: liquid chromatograms of a sediment extract using UV and fluorescence detection. Right: fluorescence emission spectra obtained on peaks a (chrysene) and b-g (alkylated chrysenes), with wavelengths (nm) of maxima indicated

chromatogram (reconstructed gas chromatogram) for the sediment sample is presented in Figure 1A (peaks identified in Table I). A peak at mass 43 (or more correctly mass-to-charge ratio,  $m/e$ , 43) is indicative of aliphatic hydrocarbons. In Figure 1B the mass chromatogram for  $m/e$  43 helps to identify the homologous series, which could not have been otherwise visually identified in the complex chromatogram. By plotting mass chromatograms at other  $m/e$  ratios, additional components can be resolved easily from the complex chromatogram. An example is shown in Figure 1C which contains the composite mass chromatograms for  $m/e$  142, 156, and 170, the molecular ions indicating the presence of  $C_{11}$ ,  $C_{12}$ , and  $C_{13}$ -substituted naphthalenes, respectively. A detailed description of the use of the mass spectrometer as a GC detector is presented in a recent review by Fenselau (9). Several laboratories are now developing liquid chromatography/mass spectrometry instrumentation (10-12). The combination of LC and MS opens up new horizons in trace organic analysis for the identification of polar, less volatile, or thermally labile compounds.

For certain classes of compounds, fluorescence emission spectroscopy has also proved to be a powerful qualitative tool. We have employed an HPLC/fluorescence technique to analyze trace levels ( $\mu\text{g/kg}$ ) of polynuclear aromatic hydrocarbons (PAH's) in marine sediments and tissue extracts. Fluorescence spectroscopy offers se-

lectivity since it is possible to vary both the excitation wavelength and the wavelength at which the emission is observed, thus providing additional spectrometric information. Fluorescence excitation and emission spectra provide useful qualitative information. The qualitative capabilities of HPLC with fluorescence detection are illustrated in Figure 2. The liquid chromatograms in Figure 2 were recorded simultaneously by ultraviolet (UV) absorption and fluorescence emission. Fluorescence emission spectra obtained for each peak and chromatographic retention data were the basis for tentative compound identification.

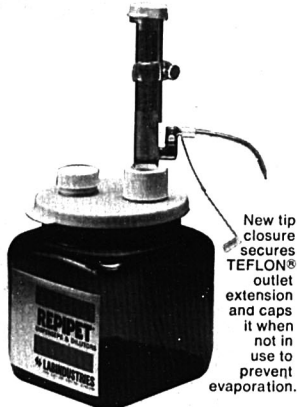
In addition to fluorescence emission spectroscopy, there are several other promising approaches to selectivity in HPLC detection. A detailed discussion of some of these newer liquid chromatographic detection techniques has been presented in a recent review by Wise and May (13). Selective detectors for gas chromatography have been discussed by David (14). Each of the identification techniques discussed above has advantages and limitations; therefore, a combination of techniques is often required to achieve positive identification of organic compounds.

**Analyte Quantitation.** Most trace organic analyses involve a chromatographic technique for the final quantitative determination. Gas chromatography is still the most widely used technique in trace organic analysis. However, recent advances in HPLC



# Known for quality

## L/I REPIPET® Reagent Dispensers



For more than 16 years Labindustries has been the quality leader in reagent dispensers. The workmanship, precision, dependability and unique features of REPIPET® reagent dispensers put them in a class by themselves.

Our most popular models are the space-saving Low Silhouette instruments. The low profile is ideal for storage anywhere. An innovative two-opening, wide mouthed bottle is a welcome convenience, and the square bottle offers solid support. The Teflon® inlet tube reaches to the bottom of the container. As with all REPIPET reagent dispensers, L/I guarantees 1% accuracy and 0.1% reproducibility, at full scale.

Because of PYREX® glass construction, any reagent except HF may be dispensed . . . including concentrated acids, concentrated alkalies and chlorinated hydrocarbons.

L/I stocks Low Silhouette REPIPET reagent dispensers in 0.5, 1, 5, 10, 20, and 50 ml sizes. Prices start at \$79.50.

Do you have our catalog? Contact:

### LABINDUSTRIES

620 Hearst Avenue, Berkeley, CA 94710  
Phone (415) 843-0220

**Table II. Chromatographic Analysis of  $\mu\text{g/g}$ -Level Solutions**

Sample	Method	No. of labs reporting	NDS av rel error for 5 compounds, %	All labs combined av rel error for 5 compounds, %
1st Hexane solution of PAH's	LC	4	1.8	9.8
	GC	6	2.2	11.0
2nd Hexane solution of PAH's	LC	4	2.1	12.3
	GC	6	2.0	10.4
Aqueous solution of phenols	LC	4	1.8	12.2
	GC	6	3.5	16.3

technology have made HPLC comparable to GC in speed, convenience, and efficiency (15). GC and HPLC complement each other in that each technique is better suited for different classes of compounds.

To begin assessing the accuracy currently obtainable in trace organic analyses, we have conducted a series of collaborative studies on samples containing environmentally significant molecules. Pure specimens of the compounds selected for analysis were sent to the participating laboratories. In addition, each laboratory received a solution containing all of these compounds at concentrations ranging from 1 to 100  $\mu\text{g/mL}$ . At these concentrations there is sufficient sample present in a few microliters of solution to permit direct instrumental analysis. These studies were thus assessing the accuracy and precision currently achieved in the final step (the quantitative measurement step) of the analytical scheme presented above. The first study involved a solution of five polynuclear aromatic hydrocarbons (PAH's) in hexane. The second study

was similar to the first, but the compounds were present at different concentrations. In a third study aqueous solutions containing five phenols were analyzed. Table II contains a summary of the results obtained in the three studies. Between the first and second study there was a meeting of representatives of the participating laboratories to discuss the results, methods used, and problems encountered with the first sample. This discussion of methods and problems did not improve the overall results for the second PAH study.

Table III contains, in somewhat more detail, a summary of the results obtained in the study on phenols. The intralaboratory relative standard deviation for a single compound for these analyses varied between  $\pm 0.2$  and  $\pm 6\%$ , but the overall interlaboratory relative standard deviation was greater than  $\pm 20\%$  for three of the five phenolic compounds. Tables II and III indicate that a substantial error is often introduced in the step that organic analysts take for granted: the chromatographic quantitation.

**Table III. Study of Quantitative Analysis of Phenols in Water**

	Phenol	p-Cresol	o-Cresol	2-Naphthol	2,4,6-Trimethylphenol
No. of labs reporting	10	9	9	9	10
Gravimetric value ( $\mu\text{g/g}$ )	21.0	54.3	34.3	71.4	38.8
Av value reported	18.6	49.0	32.1	66.9	37.4
Max value reported	26.0	57.5	36.0	106.3	56.1
Min value reported	11.7	35.5	25.7	12.9	17.0
SD	$\pm 4.4$ (24%) <sup>a</sup>	$\pm 7.2$ (15%)	$\pm 3.5$ (11%)	$\pm 24.2$ (36%)	$\pm 10.8$ (29%)
% Deviation of av from gravimetric value	-11%	-10%	-6%	-6%	-4%

<sup>a</sup> Numbers in parentheses represent relative standard deviations.

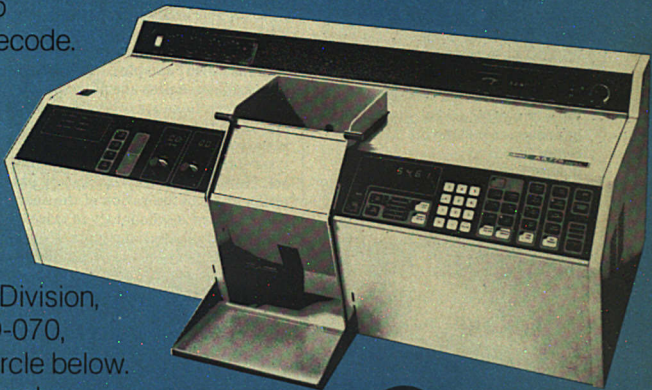
# Heralding Varian's AA-775... Sophisticated, Accurate, Simple.

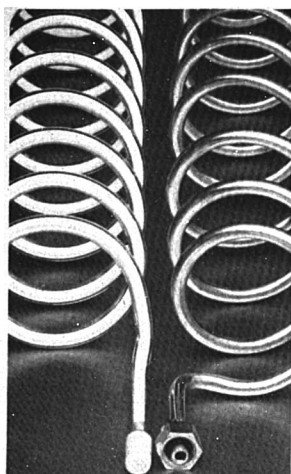
**Sophisticated.** Microprocessor calibration, integration, peaks, emission, statistics—even standard additions by regression. Then it divides by the sample weight. Four-lamp turret. Superbly automatic gas control. New high-performance monochromator. No compromises. Sophisticated.

**Accurate.** The best, most accurate curve corrector in the business (Pat App). Up to five standards. Calibration on the mean, not just on one reading. Peak height and area on the same peak, statistics on both. Elegant. Accurate.

**Simple.** Designed by users, not just microprocessor engineers. Touch-buttons with flashing lights that say 'push me'. Detects and corrects operator errors. Obvious operation, even for the beginner. No computer language to decode. No 'where was I' when you come back from that phone conversation. Obvious. Simple.

Maybe this really is the perfect AA instrument. Write Varian Instrument Division, 611 Hansen Way, Box D-070, Palo Alto, CA94303 or circle below. Circle 196 for product literature. Circle 197 for a Varian representative to call.





## These Super Pak™ 20M columns are packed with features for your GC success.

- Higher efficiency — 850-1000 theoretical plates/ft.
  - Wider operating range — 25-260°C. temperature stability
  - QC verified on each shipment for exceptional reproducibility
- Write or call for our helpful applications bulletin on Super Pak 20M columns and packing.

### Analabs®

A unit of Foxboro Analytical Division,  
80 Republic Drive, North Haven, CT 06473  
(203) 288-8463

**FOXBORO**

Trademark of Analabs, Inc.

CIRCLE 6 ON READER SERVICE CARD

**Table IV. 1973 AOAC Collaborative Assays of Vitamin A**

Sample	Av IU/lb	Range IU/lb	Coeff var, %	No. of labs *
Breakfast cereal	36 000	24 800-42 000	13	21 (20)
Feed (trace carotenoids)	19 000	15 700-21 300	8	21 (18)
Feed (normal carotenoids)	6 800	4 100-8 500	15	21 (17)
Feed (trace carotenoids)	6 800	5 100-8 800	13	21 (16)
Liquid feed supplement	17 200	12 400-21 200	12	19 (17)
Beverage powder	29 600	25 100-36 300	10	16 (15)

\* Values in parentheses represent number of laboratories whose results were used in calculating the data listed; the remainder were outside statistical limits.

The second stage in assessing the accuracy obtainable in trace organic analysis is the analysis of spiked natural samples. Table IV contains a summary of the results of a 1973 Association of Official Analytical Chemists (AOAC) collaborative study in which vitamin A was added to six different food products and assayed by standard methods in several laboratories (16). Interlaboratory averages, overall ranges, coefficients of variation, and the number of laboratories reporting data are listed. The interlaboratory coefficients of variation were considered acceptable for vitamin A analysis, and the averages were reasonably close to the amounts of vitamin A added. The results reported, however, do not represent all laboratories that participated, since data from some laboratories were eliminated as outliers in the statistical evaluation (see Table IV). Furthermore, the wide ranges of results indicate the difficulty experienced in achieving accurate trace organic analyses.

The third and final stage of assessing the current state-of-the-art of trace organic analysis is through interlaboratory comparison on natural ("real-world") samples. In the analysis of "real-world" samples, it is currently impossible to assess absolute accuracy, since extractions are often incomplete and since the matrix cannot be completely destroyed to release the analytes totally as in trace element analyses. However, the interlaboratory precision gives an indication of the need for improved methodology in trace organic analysis. Partial results of a collaborative study on a natural sample are summarized in Table V (17). Laboratories were supplied an oyster tissue homogenate and were asked to analyze for organochlorine compounds. Homogeneity studies of the samples, carried out at the International Laboratory of Marine Radioactivity, showed less than ±15% relative standard deviations for all compounds. Thus, the range of values reported in Table V is not the result of sample inhomogeneity but indicates that the state-of-the-art of trace organic analy-

**Table V. Organochlorine Compound Concentrations in Oyster Tissue Homogenate [Values Reported in ng/g (ppb) Dry Weight]**

	α BHC *	γ BHC *	Dieldrin
No. labs reporting	10	21	14
Av value	10	22	15
Max value	66	139	52
Min value	0.15	0.93	0.5
SD	±20 (200%) <sup>b</sup>	±32 (140%)	±13 (87%)

\* BHC = 1,2,3,4,5,6-hexachlorocyclohexane.

<sup>b</sup> Numbers in parentheses represent relative standard deviations.

sis of "real-world" samples, such as this oyster homogenate, requires considerable improvement.

### Conclusions

To perform accurate and precise analytical measurements, there are two prerequisites: suitable analytical methods and standards for quality control or calibration purposes. In most current problem areas in trace organic analysis, methods are still inadequate, and primary trace level standards in "real-world" matrices are nonexistent. A major goal of trace organic analysis at the National Bureau of Standards is the development of appropriate Standard Reference Materials (SRM's) for trace level organics in natural matrices. Cali (3, 18) recently discussed SRM's and the requirements for certification of such materials. The definition of an SRM requires the use of one of three modes of measurement to assure the accuracy of the value(s) of the SRM property(ies). These modes are: (a) definitive methods, (b) reference methods, or (c) two or more independent and reliable methods. The current state-of-the-art of trace organic analysis does not permit the issuance of an SRM based on this definition. Definitive methods in this area do not exist.

# the Varian CDS-111...a powerful chromatography data system that is easy to use

The CDS-111 efficiently uses the capabilities of advanced microprocessor technology to save the chemist's time and to make it easier to quantitate analysis results.

## Simple controls

The controls are simple and straightforward, easier to use than many hand calculators. Four switches and a small keyboard provide complete control. For example, to run a typical analysis, from injection through calculations and printed report, all you need to do is: press the "start" button, make your injection when the "ready" light comes on and, after the last peak elutes, press the compute button to get your complete report. It's that simple on the outside because the CDS-111 does so much more on the inside.

## Presets handle most chromatograms

For most chromatograms you don't have to program the CDS-111 at all. It has been preset at the factory so that the critical peak measuring parameters are automatically set up when you switch on the power. The presets provide initial monitoring and adjustment to instrument signal noise, detection and processing of peaks, automatic updating of peak measuring parameters if peaks become broader, perpendicular and tangent peak separation, trapezoidal baseline correction and reporting of area percent... all automatically!

## It's easy to set and change parameters to handle unusual chromatograms

Whenever you encounter an unusually complex analysis, it is easy to override the automatic preset parameters and manually set exactly the values that you need.

## It speaks the language of chemistry

The CDS-111 doesn't speak abstract computerese. It speaks the language of chemistry. For example, if there is no reference peak at a time when a reference peak is expected the CDS-111 doesn't vaguely say "error" and leave you guessing; it says "NORP." It is specific and understandable.

And the CDS-111 is really helpful when recalculation is required. It not only tells you if an error has occurred, it tells you what the error is so that you can easily correct it and recalculate, in most cases, without having to reinject.

## "Must" peak gives extra protection

To detect errors and provide extra protection for the system, the first reference peak can be designated as a "must" peak. Then, in each analysis, the "must" peak must occur within a prescribed time window and be within prescribed size limits. If the "must" peak fails to meet either of these criteria, an error is detected, a message is printed and the alarm count is incremented. If the alarm count reaches a significant level the CDS-111 can terminate the analysis. The "must" peak can detect faults or errors in all system components. It will detect incorrect flow rates, wrong detector, wrong sample, a deteriorating column, a plugged or leaking syringe, anything that causes the "must" peak to fail to meet its criteria.

## It has a nine-method memory

Once a method is set up, the CDS-111 will store it for instant call up. The CDS-111 will hold up to nine complete analytical methods in memory, each programmed to optimize a specific analysis and automatically control the entire chromatography system—chromatograph, automatic sampler, valving and external devices—in automatic, closed loop operation.

As a result, you don't have to reprogram every time you run a different sample. You can simply call up the method file that you set up and stored the first time you ran the analysis.

## The CDS-111 makes chromatography automation available to every lab

It interfaces simply with both gas and liquid chromatographs. Two different basic models are available, so you can choose a system that best meets your particular needs and budget.

To have a Varian technical representative contact you circle **Reader Service No. 1.**

For more information circle **Reader Service No. 2.**

Varian Instrument Division, 611 Hansen Way, Box D-070, Palo Alto, California 94303



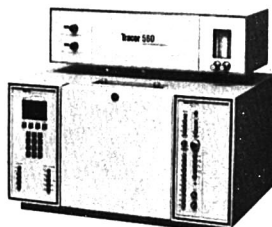
*The CDS-111 is priced to provide more performance per dollar than any other chromatography data system available today.*





# NEW 700A HALL™

## Electrolytic Conductivity Detector



The Model 700A HALL™ Electrolytic Conductivity Detector utilizes a new microreactor and bipolar pulse circuitry to provide *increased sensitivity* up to two orders of magnitude over other conductivity detectors. Improved capability for the *specific* detection of Halogen, Nitrogen or Sulfur containing compounds is now available in a single compact unit.

- ☐ Most Specific —  
N:HC, > 10<sup>6</sup>  
Cl:HC, > 10<sup>6</sup>  
S:HC, to 10<sup>5</sup>
- ☐ Most Sensitivity —  
1-4 x 10<sup>-12</sup>g N/sec  
2-5 x 10<sup>-13</sup>g Cl/sec  
1-4 x 10<sup>-12</sup>g S/sec
- ☐ The proven conductivity detector available only from Tracor.
- ☐ Designed for easy plug-in installation in any Tracor 560 G.C.

## Tracor Instruments

Tracor, Inc.  
6500 Tracor Lane  
Austin, Texas 78721  
Telephone 512-926 2800  
Telex 77-6414

In addition, a major obstacle to the development of an organic SRM is the lack of a means of matrix-free analysis. At present the analyst involved in trace organic analysis must satisfy himself with assuring the accuracy of his measurements on "synthetic" samples and with improving the precision of his measurements on "real-world" samples through the use of internal standards and careful monitoring of the analytical system blanks.

The intricacies of trace organic analysis are only now beginning to intrigue the analytical chemist. It is anticipated that the next decade will bring the challenges of trace analysis to the organic analyst, in the same fashion as the last decade saw these challenges being met in inorganic trace analysis. To provide a forum for an exchange of ideas and problems in Trace organic analysis, the National Bureau of Standards is sponsoring its Ninth Materials Research Symposium on April 10-13, 1978. The topic of the symposium is "Trace Organic Analysis: A New Frontier in Analytical Chemistry".

### Acknowledgment

The authors gratefully acknowledge R. S. Schaffer and W. H. Kirchhoff for critical reading of the manuscript.

### References

- (1) R. G. Lewis, in "Accuracy in Trace Analysis: Sampling, Sample Handling, Analysis", NBS Special Publ. 422, p 9, GPO, Washington, D.C., 1976.
- (2) K. Beyermann, *Angew. Chem. Int. Ed.*, 13, 224 (1974).
- (3) J. P. Cali and W. P. Reed, NBS Special Publ. 422, p 41, GPO, Washington, D.C., 1976.

- (4) "National Primary and Secondary Ambient Air Quality Standards", *Fed. Register*, 36, No. 8A (1971).
- (5) A. Zlatkis, H. Lichtenstein, and A. Tishbee, *Chromatographia*, 6, 67 (1973).
- (6) W. E. May, S. N. Chesler, S. P. Cram, B. H. Gump, H. S. Hertz, D. P. Enagnio, and S. M. Dyszel, *J. Chromatogr. Sci.*, 13, 535 (1975).
- (7) T. A. Bellar and J. J. Lichtenberg, *Water Treat. Exam.*, 23, 34 (1974).
- (8) F. A. Gunther, R. C. Blinn, M. J. Kolbezen, J. H. Barkley, W. D. Harris, and H. S. Simon, *Anal. Chem.*, 23, 1835 (1951).
- (9) C. Fenselau, *ibid.*, 49, 563A (1977).
- (10) R. P. W. Scott, C. G. Scott, M. Monroe, and J. Hess, Jr., *J. Chromatogr.*, 99, 395 (1974).
- (11) P. J. Arpino, B. G. Dawkins, and F. W. McLafferty, *J. Chromatogr. Sci.*, 12, 574 (1974).
- (12) E. C. Horning, D. C. Carroll, I. Dzidic, K. D. Haegele, M. G. Horning, and R. N. Stillwell, *ibid.*, p 725.
- (13) S. A. Wise and W. E. May, *Res. Dev.*, 28, 54 (1977).
- (14) D. J. David, "Gas Chromatographic Detectors", Wiley-Interscience, New York, N.Y., 1974.
- (15) R. E. Majors, *J. Chromatogr. Sci.*, 15, 334 (1977).
- (16) Reprinted from E. DeRitter, *Cereal Foods World*, 20, 34 (1975) with permission of American Assoc. of Cereal Chemistry, Inc.
- (17) Printed with permission of D. Elder, from Progress Report No. 1, "Intercalibration of Organochlorine Compound Measurements in Marine Environmental Samples", International Laboratory of Marine Radioactivity, Monaco.
- (18) J. P. Cali, *Anal. Chem.*, 48, 802A (1977).

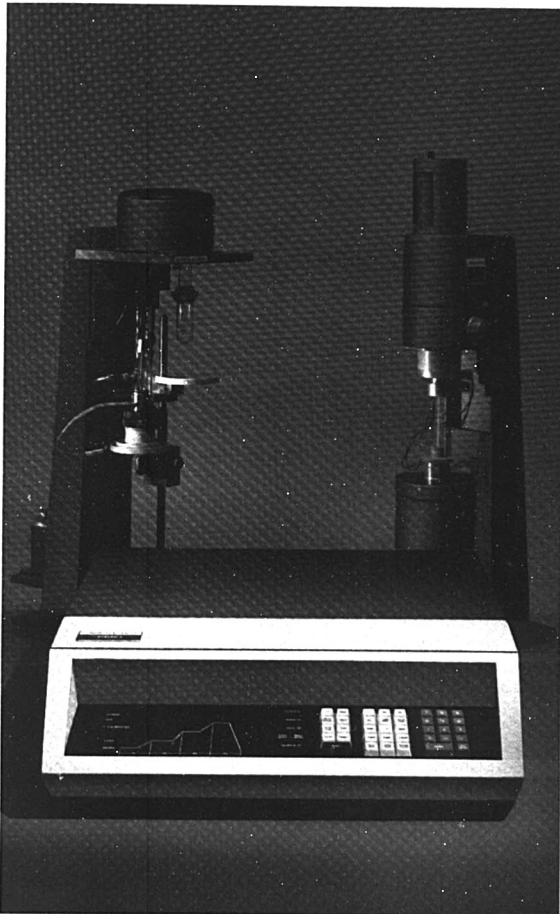
Some of the research reported herein was supported by the Division of Biomedical and Environmental Research of the Energy Research Development Administration. Identification of any commercial product does not imply endorsement by the National Bureau of Standards, nor does it imply that the particular product is necessarily the best available for that purpose.



From left to right: Willie E. May, Stephen N. Chesler, Stephen A. Wise, and Harry S. Hertz. The authors are research chemists in the Trace Organic Analysis Group of the Analytical Chemistry Division at the National Bureau of Standards. Their current research interests are in the area of environmental analytical chemistry, with special emphasis on toxic organic compounds related to offshore oil development, coal liquefaction, and oil shale processing. Research in these areas currently focuses on development of improved instrumentation and methodology for trace organic analysis in organic mass spectrometry, liquid chromatography, and gas chromatography.

CIRCLE 208 ON READER SERVICE CARD

# MORE THAN A TEMPERATURE PROGRAMMER: NEW SYSTEM 4 SIMPLIFIES ROUTINE THERMAL ANALYSIS



The System 4 program controller with the TGS-2 thermogravimetric analyzer (left) and the TMS-2 thermomechanical analyzer (right).

The new Perkin-Elmer System 4 micro-processor program controller reduces your thermomechanical or thermogravimetric analyses to a matter of pushing buttons. With a few key strokes, in a routine procedure, you can create — store — recall — and control *complete methods*. Yet the System 4 is attractively priced.

#### **Stored parameters simplify methods.**

A method on the System 4 stores parameters that specify the temperature program, recorder T-axis scaling and marking — and even purge-gas switchover.

Program set-up is quick and easy. The System 4 contains *built-in* programs for standard analyses, and a fully-automated *temperature calibration* routine.

**Make up your own programs.** It also gives you a choice of nine programs that you define yourself. Temperature program rates from 0.1 to 320 degrees C/minute are available. You can specify sample pre-conditioning and other completely-automated multiple-step analyses. Even complex analyses can be performed simply and reproducibly.

**Everything on display that you need to know.** Throughout an analysis, a four-digit, lighted display tells sample temperature to 0.1 degree C. A visual program ramp gives you the current status of the analysis. Parameter pushbuttons that light when depressed guide you through the set-up routine. This makes instrument set-up simple — with no chance for mistakes.

**Compare it with others.** To compare the System 4 point-by-point with any other instrument of its kind, write today for Paper No. L-550, to Perkin-Elmer Corporation, Main Avenue, M.S. 12, Norwalk, CT 06856. Or phone (203) 762-4131.

**PERKIN-ELMER**  
Expanding the world of analytical chemistry.



## New from Philips: Atomic Absorption programmed for your applications.

**Introducing the Pye Unicam SP2900 double-beam AA spectrophotometer with powerful Data Center.**

This versatile Atomic Absorption system features a microprocessor-based Data Center offering the user unprecedented flexibility. With the program cards provided, you can easily tailor system performance to meet your own individual operating requirements.

Data Center's program cards offer a wide variety of different curve corrections and calibrations. The SP2900 provides simultaneous high accuracy background correction over a wider absorbance range. Data Center does the

calculations, thus allowing you to do the chemistry!

You'll find that the SP2900 system offers a new level of precision, sensitivity and detection limits, all of which are backed up with fully-published specifications.

Beyond its pace-setting performance, there are many more reasons to see the SP2900 in action: Every Pye Unicam Atomic

Absorption system is backed by comprehensive applications, sales and service assistance throughout North America and overseas.

Invest a few minutes of your time to request our Atomic Absorption information package, or see a demonstration of this powerful system. We think you'll find it programmed for *your* applications.



### **Philips Electronic Instruments, Inc.**

A North American Philips Company

85 McKee Drive, Mahwah, N.J. 07430

Telephone (201) 529-3800

International — Contact Pye Unicam Ltd.  
York Street, Cambridge, England CB1 2PX  
Telephone, Cambridge (0223) 58866  
Telex 817331



**Electronic  
Instruments**

# PHILIPS

CIRCLE 162 ON READER SERVICE CARD



# Chromatography and Ancillary Methods

## 31st Annual Summer Symposium on Analytical Chemistry

University of Colorado  
Boulder, Colo.  
June 26–28, 1978

"Chromatography and Ancillary Methods" is the subject of the 1978 Summer Symposium of the ACS Division of Analytical Chemistry. The symposium will be held June 26–28, 1978, on the campus of the University of Colorado at Boulder. The symposium program has been arranged by Harold McNair of Virginia Polytechnic Institute and William Hines of Phillips Petroleum Co. Local arrangements are being made by Robert Sievers of the University of Colorado. The symposium is sponsored annually by the ACS Division of Analytical Chemistry and ANALYTICAL CHEMISTRY.

### About the University of Colorado

The University of Colorado at Boulder is nestled against the front range of the Rocky Mountains in beautiful physical surroundings. The university has a total student population of 21 000. The Chemistry Department has 36 faculty members and 131 graduate students. The analytical chemistry faculty consists of John Birks (atmospheric chemistry, kinetics of reactions of stratospheric significance, analytical spectroscopy), Robert Sievers (GC/MS, metal chelates, water and air pollution chemistry), and Harold Walton (liquid chromatography, ion exchange). Other faculty members, Robert Shapiro, Eldon Ferguson, and Will Castleman, also have research programs in analytical and environmental chemistry. The Chemistry Department faculty will be glad to discuss the research or teaching program of the university with interested attendees.

### Travel

For participants traveling by air, Boulder is approximately 27 miles northwest of Denver's Stapleton International Airport. As the eighth busiest airport in the U.S., Stapleton is served by frequent flights from every region, and Mexico and Canada as well. Bus service from the Denver airport to Boulder is available at intervals throughout the day. Taxi fare from the airport to Boulder is approximately \$28.

### Housing and Symposium Arrangements

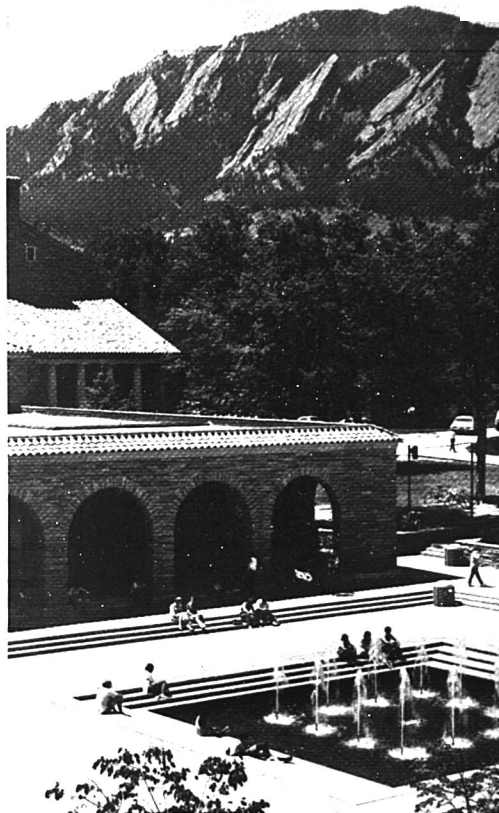
Upon arrival in Boulder, participants with reservations in university housing should register at the Hallett Hall desk. Although dormitory rooms are not air-conditioned, Boulder is more than a mile above sea level, and the air is usually cool and dry in June.

Rates for housing and meals, per person, will be \$56.56 for single occupancy and \$41.04 for double. The rates include lodging Sunday through Tuesday night and the following meals: breakfast and lunch on Monday; breakfast, lunch, and a western mountain cookout on Tuesday; and breakfast and lunch on Wednesday. No refunds will be made for missed

meals. Double rooms are equipped with two beds. There are no private baths, but bath and shower rooms are conveniently located on each floor. Daily maid service and all linens are provided. Meals will be served in Kirtledge Residence Halls, located close to Hallett Hall.

**Housing payment is due upon arrival and should not be made in advance.** Credit cards will not be accepted. Participants may check in anytime after noon on Sunday. Early arrivals must be approved by the manager of Hallett Hall, the Bureau of Conferences and Institutes, Room 217, Academy Building, 970 Aurora Ave., Boulder, Colo. 80302.

Although Boulder has several motels, June is a popular tourist month, and reservations should be made well in advance. The closest motels/hotels are located about one mile from Duane Physics Building Auditorium



View from the Chemistry Dept. at the University of Colorado

where the scientific sessions will be held. The dormitory is about three blocks from Duane Physics Building.

If special facilities are required for handicapped participants, please contact Professor Sievers so that arrangements can be made.

#### For Commuters Only

Tickets are available at the front desk of Kittredge Residence Halls for the Tuesday western mountain cook-out at a cost of \$5.05 per person. Tickets must be picked up prior to 1:00 p.m. on Monday, June 26. A limited number of individual meal tickets will be available at the front desk of Kittredge just prior to each meal. They may be purchased at \$2.15 for breakfast, \$4.10 for lunch, and \$4.15 for dinner.

#### Registration

The symposium fee of \$40 includes admission to all sessions, symposium materials, refreshment breaks, and university services. It does not include housing, meals, or the tours. All par-

ticipants are urged to send the registration form together with a check for \$40 made payable to the University of Colorado, before May 31, 1978. Advance registration is imperative to ensure that space will be available. After arrival, badges and conference materials should be picked up in the lobby of Hallett Hall on Sunday evening between 7:00 and 9:00 p.m. or on Monday morning in Duane Physics Room 030G between 7:30 and 8:30 a.m.

#### Tours

As an experiment this year, the scientific sessions are being held in the mornings and evenings to allow attendees to participate in informal conversations while enjoying the beautiful outdoor surroundings. Hiking, tennis, and other sports activities, as well as various tours are available during the afternoons.

The following tours are being planned: Central City (old restored mining town), Rocky Mountain National Park, National Center for Atmospheric Research, Air Force Academy and Garden of the Gods (Colorado Springs), and Georgetown (old mining town) and Vail (overnight—leave Wednesday afternoon, return Thursday). Please indicate your interest in these tours by checking the appropriate boxes on the registration form. Further information will be furnished upon request.

#### Monday Morning, June 26

##### Chromatography and Ancillary Techniques

F. W. Karasek, *Presiding*

8:20 Opening Remarks. R. E. Sievers, U of Colorado

8:30 New Selective Detectors for Gas Chromatography. W. A. Aue, Dalhousie U, Canada

9:30 Rapid Analysis of Complex Mixtures of Organic Compounds Extracted from Airborne Particulate Matter. F. W. Karasek, U of Waterloo, Canada

10:15 Application of Special Techniques of Gas Chromatography to Water Pollution Analysis. F. E. Onuska, Canada Centre for Inland Waters

10:45 Characterization of Isomeric Compounds via Gas and Plasma Chromatography. D. F. Hagen, 3M Research Center

11:15 Panel Discussion. Aue, Karasek, Onuska, Hagen

#### Monday Evening

##### GC/MS

E. Bonelli, *Presiding*

7:00 Digital Gas Chromatography-Mass Spectrometry. R. Board, Hewlett-Packard

7:30 Direct Injection LC/MS/COM Progress Using a Quadrupole Mass Spectrometer. J. Henion, Cornell U

8:00 Discussion

8:30 Some Analytical Applications of Crossed-Beam LC/MS. M. J. McAdams, C. K. Blakely, M. L. Vestal, U of Houston

9:00 Pollutant Analysis via Negative Ion Chemical Ionization. D. Beggs, Hewlett-Packard

9:30 Discussion

#### Tuesday Morning, June 27

##### Capillary GC Columns

S. Cram, *Presiding*

8:30 High-Efficiency, High-Resolution Capillary GC; Current Sta-

### Registration Form 31st Annual Analytical Summer Symposium

on

#### Chromatography and Ancillary Methods

June 26-28, 1978

Sponsored by the

#### ACS Division of Analytical Chemistry and ANALYTICAL CHEMISTRY

University of Colorado, Boulder, Colo. 80309

Name (please print): \_\_\_\_\_ Telephone: \_\_\_\_\_

Mailing address: \_\_\_\_\_

Professional affiliation: \_\_\_\_\_

Name(s) of accompanying guest(s): \_\_\_\_\_

(please indicate ages and sex of children and whether doubles or singles will be required)

☐ Enclosed is \$40 registration fee

#### Housing Reservation:

The rates include lodging Sunday through Tuesday night and the following meals: breakfast and lunch on Monday; breakfast, lunch, and a western mountain cookout on Tuesday; breakfast and lunch on Wednesday.

☐ Single \$56.56 ☐ Double \$41.04, Name of roommate, if preference: \_\_\_\_\_

I need ☐ do not need ☐ transportation to the Flagstaff cookout.

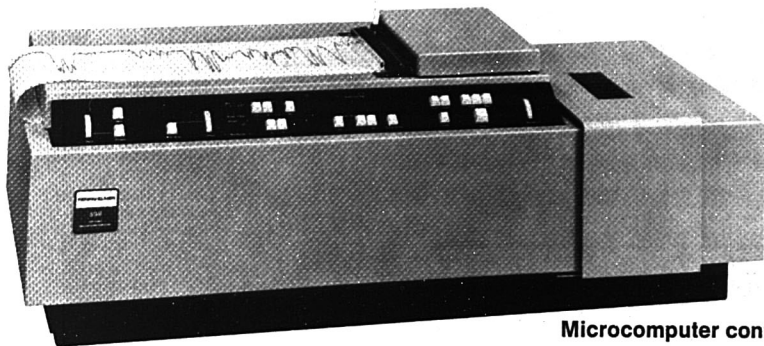
**DO NOT SEND MONEY IN ADVANCE FOR UNIVERSITY HOUSING OR MEALS**

I am interested in guided tours of: Central City ☐ Rocky Mountain National Park ☐ National Center for Atmospheric Research ☐ Georgetown and Vail ☐ Air Force Academy ☐

Please return this form by May 31, 1978, with check for \$40 made payable to the University of Colorado to: Bureau of Conferences and Institutes, Room 217, Academy Building, 970 Aurora Ave., Boulder, Colo. 80302

For general information contact: Robert E. Sievers, Dept. of Chemistry, University of Colorado, Boulder, Colo. 80309 (303-492-8083)

# EFFORTLESS INFRAREDS



## Microcomputer controlled

It's almost impossible to get a bad spectrum with our new X99 series of infrared spectrophotometers. And it's almost unnecessary for the operator to do any work.

The X99 spectrophotometers are the first medium priced IR instruments with microcomputers and integrated scan controls.

### Quick and easy

With the microcomputer controlling the recorder and optical systems, you can display the monochromator frequency continuously to 0.1  $\text{cm}^{-1}$  on the digital readout.

And with the integrated scan controls, you select a single parameter (scan time, slit setting or relative noise) and the instrument automatically sets the other two. The only other

requirement is to set the gain, using Perkin-Elmer's simple Auto-Chek® system.

The X99 instruments also give you resolution to 0.5  $\text{cm}^{-1}$ . Ordinate scale expansion is continuously variable in both linear absorbance and percent transmission, in discrete steps from 0.1 to 10X. You can quantify directly on the chart, get more information from microsamples, or reveal spectral information at low transmission values. Abscissa expansion is standard to 20X in discrete steps.

### Choose from three models

The Model 599 has a range of 4000 to 200  $\text{cm}^{-1}$ ; Model 399, 4000 to 400  $\text{cm}^{-1}$ ; Model 299, 4000 to 600  $\text{cm}^{-1}$ . To eliminate excess time and data, the 599's microcomputer lets you cut off scans at 600 or 400 by

simply setting a switch.

Regardless of the model you choose, you can set to any wave-number in less than 45 seconds or obtain a survey scan in only 3 minutes. They all have built-in service diagnostics — the microcomputer can check abscissa circuits and monitor recorder and optical moving parts.

Find out how simple and accurate infrared can be with the new X99 series. Call your Perkin-Elmer representative or write Perkin-Elmer Corp., Mail Station 12, Main Ave., Norwalk, CT 06856.

*Perkin-Elmer also offers the industry's largest line of infrared accessories. Ask for our accessories catalog L-396.*

## PERKIN-ELMER

CIRCLE 173 ON READER SERVICE CARD



**if you have a  
cleaning problem  
RBS-35<sup>®</sup> Concentrate  
can't solve...you've got a problem!**

The notoriously stubborn • silicone greases • oils • tars • blood • partially carbonized food residues • Apiezon<sup>®</sup> oils and greases • polymer resins • tenacious precipitates • cedar wood oils and Canada Balsam are mere routine for RBS-35.

RBS-35 rinses completely from a wide range of materials leaving them residue free. The effectiveness of RBS-35 in the removal of radioisotopic contamination is unequalled. In addition, RBS-35 is gentle to skin and harmless to clothing. There simply is no other cleaning product which offers you the safety, economy and performance of RBS-35.

Why not put RBS-35 to work on your cleaning problem today?

27952 RBS-35 Concentrate \$26.50/gal  
27950 RBS-35 Concentrate \$5.50/gal  
27954 RBS-35 Concentrate (220 kg) \$847/drum

PIERCE Eurochemie B.V., Rotterdam, Holland  
PIERCE & Warriner (UK) Ltd., Chester, Cheshire CH 14 4F England  
Lab Supply PIERCE, N.Z. Ltd., Auckland 10, New Zealand

**PIERCE**  
**CHEMICAL COMPANY**  
Box 117, Rockford, Illinois 61105

CIRCLE 172 ON READER SERVICE CARD

**bev-a-line<sup>®</sup> V HT  
lined tubing instead of TFE**

**• at temperatures to 180° F • at savings of 50% or more**

Now you can get the chemical resistivity of TFE in BEV-A-LINE V HT... a translucent, flexible lined tubing. Tasteless, odorless and autoclavable... BEV-A-LINE V HT revolutionizes purity and economy standards for brewery and distilling processes, Class VI reagent manufacture, laboratory, drug and chemical processing and many other applications requiring a high level of chemical resistance in a flexible high purity system.

BEV-A-LINE V HT contains no VCM and no plasticizer... lined for safe contact with food, drugs and beverages... tough outer shell provides improved characteristics for translucent, flexible, abrasion resistant tubing... tubing will not stress-crack... pliability is retained even after prolonged contact with alcohol.

BEV-A-LINE V HT  
the economical alternative to TFE



Call or write for literature:

**THERMOPLASTIC SCIENTIFICS, INC.**

A TPI Affiliate

57 Stirling Rd., Warren, N.J. 07060

N.J. (201) 647-1000 • N.Y. (212) 267-6220 • TWX 710-997-9583

CIRCLE 210 ON READER SERVICE CARD

**News**

tus and Future Trends. M. Novotny, U of Indiana

9:30 Discussion

10:00 Wide Bore Glass Capillary Columns for Isolation and Identification. J. Walrad, International Flavors and Fragrances

11:00 Development of Capillary GC Methods: Separation, Quantitation, and Troubleshooting. S. Cram, Varian

11:45 Discussion

**Tuesday Evening**

**General**

W. Hines, *Presiding*

7:00 Construction of High-Resolution HPLC Columns. R.P.W. Scott, Hoffman-La Roche

7:30 Anion-Exchange Separation and Radiometric Determination of Neptunium in Plutonium. J. D. Navratil, R. C. Nelson, R. A. Nixon, Rockwell Intl.

8:00 Discussion

8:30 Determination of Chlordiazepoxide and Its Metabolites in Plasma by HPLC. N. Strojny, C. Puglisi, J.A.F. de Silva, Hoffman-La Roche

9:00 Examination of Protein Isolates by HPLC. R. Barford, P. Magidman, W. Damert, H. Rothbait, USDA

9:30 Mass, NMR, and Raman Spectroscopy of Octyl-decyl-sulfide, Disulfide, and Tetra-sulfide. A. W. Schwab, USDA

10:00 Discussion

**Wednesday Morning, June 28**

**HPLC**

H. McNair, *Presiding*

8:30 Current Status of HPLC. H. McNair, VPI&SU

9:00 Simultaneous Multicomponent Detection in LC. L. Klatt, ORNL

9:30 Discussion

10:00 Liquid Chromatography on Porous Polymer Gels. H. F. Walton, T. Hanai, U of Colorado

10:30 Trace Analysis of Fluorescent Substances in Biological Fluids by HPLC. R. Majors, Varian

11:00 Combined TLC-Spectroscopy Techniques for Analysis of Microsamples. Haleem J. Issaq, NCI Frederick Cancer Research Center

11:30 Optimizing Reversed-Phase Sorbents for Analytical and Preparative HPLC. M. Gurkin, MCB

12:00 End of Symposium

**"An excellent,  
well laid-out  
gas catalog."**

Joe Arce  
Rockwell International  
Rancho Palos Verdes,  
California



Use reader service number for your free copy.

CIRCLE 18 ON READER SERVICE CARD

## ULTRAPURE chemicals

When you simply can't tolerate  
impurities or uncertainties in  
your reagents

Over 100 of the purest reagents and chemicals available anywhere in the world. Every product is accompanied by a detailed **Certificate of Analysis** of the actual lot supplied. In terms of spectrochemically detectable impurities, **ULTREX** products are typically 99.995% to 99.99995% pure. And the extremely low content of all impurities (often at the parts per billion level) satisfies the most rigid use requirements.

Whenever your requirements for purity and product definition are stringent, **ULTREX** ultrapures can indeed insure against loss of time, effort, and other expenses.

Consider **ULTREX** when you just can't afford to gamble with impurities or uncertainties.

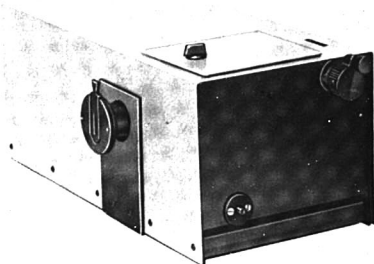
**ULTREX®**

Write for new **ULTREX** ultrapure  
Reagent brochure.

J. T. Baker Chemical Co.  
Phillipsburg, N.J. 08865  
201 859-5411



CIRCLE 27 ON READER SERVICE CARD



## Who put all those wonderful specifications in one little monochromator?

Who but **Jarrell-Ash**, for over half-a-century a leader in monochromator engineering. J-A's newest 1/4-meter, the Mark X, brings you more great features than ever:

■ Dramatically improved focal-plane accessibility. Lets you use the latest **multi-element arrays** (Vidicon, Pyrocon, charge-coupled devices, etc.) as well as photomultipliers. Incomparably versatile!

■ New optical design that **intrinsically** eliminates re-entry spectra at all wavelengths.

■ Superb infrared as well as visible and UV capability.

■ Choice of 10 quick-change pre-aligned gratings — a 175nm-40μ range. With remarkable dispersion (e.g., 3.0nm/mm with our 1200g/mm grating).

■ Finest resolution in its field. Better than 0.6nm with 1200 g/mm grating). On our parabolic-mirror model Mark X, it's 0.3nm!

■ Minimal scattered light. At 500nm, it's less than 0.05%!

■ A beautiful selection of accessories to make your lab life easier. Like digital Omni-Drive (1-200nm/minute) . . . quantum photometer . . . filter wheels to expedite fluorescence, phosphorescence, luminescence, polarization and photometry studies . . . and much more.

Use Mark X as a heavy-duty monochromator or as a spectrograph. In instruction or research. It's all in a handsome little package with a handsome little price. Not \$2500, not \$2000, but — thanks to volume production — a little over \$1000.

Incidentally, we call it a quarter-meter. Actually we've made it 275mm for greater dispersion, improved focal plane. The extra 25mm are on the house.

*The monochromator people*



**Jarrell-Ash**

590 Lincoln St.  
Waltham MA 02154  
(617) 890-4300

A Division of Fisher Scientific Company  
CIRCLE 75 ON READER SERVICE CARD

## Optical Society of America Names Award Winners



Peter Fellgett



Harold H. Hopkins

The Optical Society of America announces winners of three awards to be presented by the Society during 1978.

The winner of the 1977 R. W. Wood Prize is Peter Fellgett whose discovery of the multiplex advantage has led to the modern renaissance of Fourier transform spectrometry. He is professor and head of the Department of Cybernetics at the University of Reading in the United Kingdom. The award will be presented at the Eleventh Congress of the International Commission for Optics, September 10-17, 1978, in Madrid, Spain.

The 1978 Frederick Ives Medal will be presented to Harold H. Hopkins, professor of applied optics at the University of Reading. Professor Hopkins is recognized for his many outstanding contributions to the field of optics, including aberration theory, optical design, image evaluation, coherence theory, interferometry, and fiber optics. Presentation of the medal will take place at the annual fall meeting of the Society, October 31-November 3, 1978, in San Francisco.

Eli Yablonovitch of the Division of Applied Sciences of Harvard University will be the recipient of the Adolph Lomb Medal for 1978. Dr. Yablonovitch is honored for his pioneering work in laser physics, including the understanding of the optical breakdown strength in laser window materials, the development of ultrashort CO<sub>2</sub> laser pulses, and the identification of laser plasma heating processes. Presentation will be at the 1978 fall meeting of the Society.



Eli Yablonovitch

## Nobel Hall of Science

A "Nobel Hall of Science" honoring the accomplishments of American Nobel laureates in chemistry, physics, and medicine was opened at Chicago's Museum of Science and Industry on January 30, 1978. The Nobel Hall, the first such exhibit in the world, attempts to further public understanding of the nature and importance of basic research. The exhibit contains photographs, slides, models, a film, and historic artifacts of the 110 Americans who have received the Nobel Prize in the sciences through 1976. It also shows how the new knowledge gained from their basic discoveries has been applied to society. Included in the exhibit is a slide program about the life and work of Alfred Nobel, the Swedish scientist who invented dynamite and established the Nobel prize program.

The exhibit is made possible by a grant from the National Science Foundation under its Public Understanding of Science Program, as well as a grant from the Nobel Foundation, the Chicago Community Trust, and other organizations.

## Electrons Can Make PCB's Water Soluble

In research conducted by chemical engineers at the Massachusetts Institute of Technology, high-speed electron bombardment has been shown to alter the composition of polychlorinated biphenyls (PCB's)—compounds known for bioaccumulation and subsequent toxic effects. This finding raises hopes that the use of high-speed electrons (electrons accelerated to almost the speed of light) may be the answer to the treatment of industrial wastewater highly contaminated with PCB's and other trace organics.

The discovery was made as the team, headed by Edward W. Merrill, explored the effect of electron bombardment on sewage sludge. According to Dr. Merrill, an easily attainable level of electron bombardment—about 10 krad—was sufficient to degrade PCB's present in laboratory water samples. Dr. Merrill postulates that when high-speed electrons hit the water molecules, the molecules are split into highly reactive hydrogen and hydroxyl radicals. The hydroxyl radicals then attack the PCB's in water and convert them into molecules with a hydroxyl functional group, which renders the molecules water soluble. PCB's degrade extremely slowly in the environment and accumulate in body

because they are thousands of times more soluble in fatty tissues than in water. In their experiment, the water samples with PCB's were analyzed before and after electron bombardment by high-performance liquid chromatography. The HPLC analysis showed that more than 90% of the PCB's initially present disappeared after doses of less than 10 krad.

## Save Helium Now

Helium, a rare gas widely used for its inertness and its unique ability to remain liquid at temperatures close to absolute zero, is "a vital nonrenewable resource". That is the conclusion of the National Research Council's committee, which just completed a four-month assessment of possible helium-conservation policies for the U.S. Bureau of Mines. Foremost on the committee's list of recommended actions was the call for an immediate halt to all venting of helium separated from natural gas. Natural gas producers are currently venting helium separated from the other components of natural gas into the atmosphere, rather than storing it. Helium occurs naturally in the earth's atmosphere at only about 5 ppm. However, it is found in all natural gas, particularly in U.S.-produced gas, which contains 0.3-0.4% helium. Extensively utilized in chromatography as a carrier gas, helium is also used for purging and pressurizing, in leak detection, heat transfer, and in controlled atmospheres and breathing tests. The superconductivity of helium at near absolute zero temperatures also finds applications in developing technologies such as fusion reactors, high-temperature gas turbines, laser-based missile defense systems, and superconducting magnets. These potential uses, coupled with the ever-declining natural gas reserves, could cause an insufficiency in helium supplies in 20-30 years, just as the truly significant demands for the element would be emerging.

## Literature Searching via Communications Satellite

The day when the scientific community can obtain full texts of journal articles by communications satellite may be nearing. The January issue of *Physics Today* [published by the American Institute of Physics (AIP)] reports that an experimental project entitled "Assessment of Data Base Searching via Communications Satel-



# We made a good recorder better...

Introducing Model SRG-2 single pen and Model DSRG-2 dual pen potentiometric recorders. The latest in the Sargent-Welch family of recorders designed with the chemist in mind.

Both include linear and logarithmic operation. Log conversion is completely electronic—no gears to change. And the log range is expandable from  $\frac{1}{2}$  to 3 full cycles.

Ten spans from 1 mV to 1000 mV, calibrated or variable expansion in each span, and 9

chart speeds offer maximum flexibility.

Signals are traced by a disposable, fiber tip pen on metric chart paper with a 24 cm scale graduated -2 to 100.

Other features such as automatic gain control, zero adjust up and down scale and fast pen response combined with years of experience designing and building recorders result in unsurpassed versatility and dependability.

Optional accessories include

an event marker and new electronic integrator.

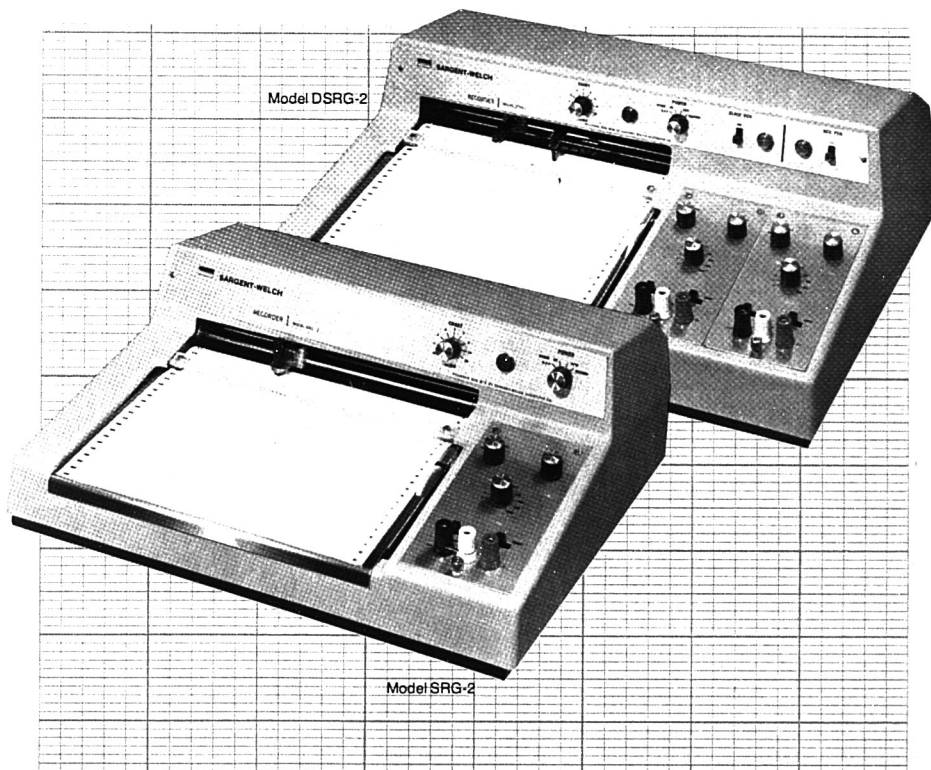
To learn more about how we made a good recorder better, call or write today.

Sargent-Welch Scientific Company  
7300 North Linder Avenue  
Skokie, Illinois 60076  
(312) 677-0600



**SARGENT-WELCH**

## Single and dual pen, linear/log, strip chart recorders



Anaheim/Birmingham/Chicago/Cincinnati/Cleveland/Dallas/Denver/Detroit/Springfield, N.J./Toronto/Montreal  
CIRCLE 189 ON READER SERVICE CARD

lite" is underway at AIP, with the financial support of the National Science Foundation. According to the report, the project is designed to evaluate the remote searching of a computerized file of abstracts of journal articles and also the ability to transmit the full text to the user almost instantly.

Participating in this test project are NASA's Goddard Space Flight Center, Ames Research Center, Lewis Research Center, and California Institute of Technology's Jet Propulsion Laboratory. Using a communications "link-up" between computer terminals routed through the geosynchronous Communications Technology Satellite, scientists at the participating laboratories examine AIP's data base, consisting of abstracts from all AIP and member society journals published over the past several years. Upon finding an abstract of interest, the user flashes AIP, where copies of the requested material can be sent by facsimile transmitter at the rate of one page every 30–90 seconds. After a year of actual operation, the timeliness and economic advantages of the system will be evaluated.

## GC/MS Methods for Analysis of Drugs of Abuse

As part of the efforts by the National Institute of Drug Abuse to help accelerate drug abuse research, Battelle's Columbus Laboratories is conducting a program on the validation of new analytical methods based on integrated GC/MS systems. These systems with the unique separation capabilities of GC and identification potential of MS will be used to determine the amount of drugs of abuse in plasma and urine.

Under the program, various laboratories in the U.S. with GC/MS instruments will be selected as possible participants and will be provided with biological samples containing specific drugs. The identity of the drugs will be disclosed to the laboratories, but only Battelle will know the concentration. The laboratories will then analyze the sample by methods also provided by Battelle in rough draft form. When the methods are perfected finally, they will be collected in eight booklets and published by the National Institute of Drug Abuse. In the booklet, drugs will be grouped according to structure and methods. The institute will disseminate the booklets to numerous toxicology, clinical, forensic, and other laboratories in the country.

## Call for Papers

### 27th Annual Denver Conference on

**Applications of X-ray Analysis**  
University of Denver, University Park Campus. Aug. 1–4. Papers on x-ray analysis with particular emphasis on x-ray powder diffraction and x-ray fluorescence are invited. Prospective authors should submit extended abstracts (approximately two pages, single spaced) not later than April 21, 1978, to: C. O. Ruud, Denver Research Institute, University of Denver, Denver, Colo. 80208.

## Meetings

*The following meeting is newly listed in ANALYTICAL CHEMISTRY. The 1978 meetings listed earlier appear in the March issue*

■ **Occupational Health & Safety Regulation Seminar.** Apr. 10–11. Capital Hilton Hotel, Washington, D.C. Contact: Nancy McNeerney, Government Institutes, Inc., 4733 Bethesda Ave., N.W., Washington, D.C. 20014. 301-656-1090

## Short Courses

**ACS Courses.** For more information, contact: Department of Educational Activities, American Chemical Society, 1155 Sixteenth St., N.W., Washington, D.C. 20036. 202-872-4508

**Carbon-13 NMR Spectroscopy**  
Philadelphia. Apr. 20–22. George C. Levy and Paul Ellis. \$255, ACS members; \$305, nonmembers

### Maintenance & Troubleshooting Chromatographic Systems Workshop

Houston, Tex. Apr. 21–22. John Q. Walker, M. T. Jackson, and M.P.T. Bradley. \$225, ACS members; \$265, nonmembers

**Toxicology for Chemists**  
Washington, D.C. May 2–4. Joseph Borzelleca and Frederick Sperling. \$395, ACS members; \$465, nonmembers

### Gas Chromatography–Mass Spectrometry

New York City. May 18–19. J. Throck Watson and O. David Sparkman. \$195, ACS members; \$235, nonmembers

**Creative Problem Solving**  
New York City. May 18–19. Moshe Rubinstein. \$195, ACS members; \$235, nonmembers

**Capillary Gas Chromatography**  
Washington, D.C. May 19–20. Milos Novotny and Stuart Cram. \$245, ACS members; \$295, nonmembers

**Laboratory Safety—Recognition and Management of Hazards**  
New York City. May 22–24. Norman Steere and Maurice Golden. \$275, ACS members; \$325, nonmembers

**Gas Chromatography, Theory and Practice**  
Blacksburg, Va. June 6–9. Harold M. McNair. \$395, ACS members; \$455, nonmembers

**Microprocessors and Minicomputers**  
Blacksburg, Va. June 11–16. Raymond Dessy. \$455, ACS members; \$515, nonmembers

**High-Pressure Liquid Chromatography Workshop**  
Boston. June 24–25. David Freeman. \$245, ACS members; \$295, nonmembers

**Microprocessors**  
Milwaukee, Wis. Apr. 10–15. \$375. Contact: Dept. of Engineering & Applied Science, U. of Wisconsin-Extension, 432 North Lake St., Madison, Wis. 53706

**Microchemical Analysis**  
Chicago. Apr. 24. \$450. Contact: McCrone Research Institute, 2508 S. Michigan Ave., Chicago, Ill. 60616

**Instrumental Surface Analysis**  
Academic Center, East Brunswick, N.J. Apr. 24–26. Cedric J. Powell. \$470. Contact: The Center for Professional Advancement, P.O. Box H, East Brunswick, N.J. 08816

**Transmission Electron Microscopy**  
Academic Center, East Brunswick, N.J. May 9–11. John R. Nichols and Joseph F. Gennaro. \$410. Contact: The Center for Professional Advancement, P.O. Box H, East Brunswick, N.J. 08816

**Acoustic Microscopy**  
Chicago. May 14–16. \$450. Contact: Sonoscan, Inc., 720 Foster Ave., Bensenville, Ill. 60106. 312-766-7088

# New HP 1084B

The original Hewlett-Packard 1084A processor-controlled liquid chromatograph introduced new standards of precision, automation and reliability, and freed the chromatographer from a lot of tedious manual intervention.

The new 1084B liquid chromatograph combines all the original innovations with a new automatically controlled variable wavelength UV/visible detector and a new expanded software package.

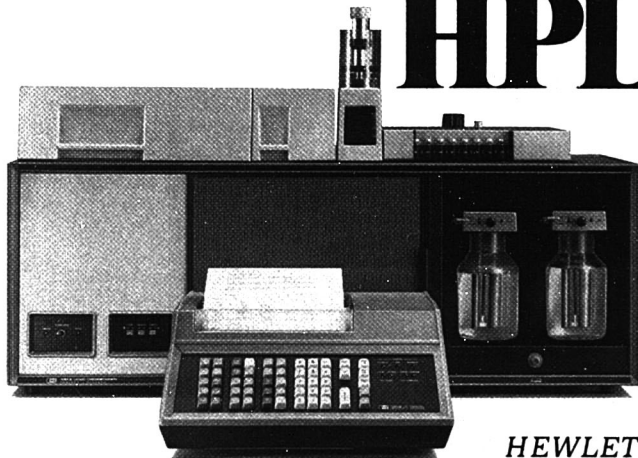
These advances, together with the recently introduced automatic sampling system, provide new modes of operation which enable HPLC method development, routine analysis and trace analysis to be performed with far greater precision and efficiency.

**Pre-programmed variable wavelength detection.** Now you can have fast, pre-programmed wavelength changes during an analysis, allowing individual sample components to be detected at their optimum wavelength. A scanning capability aids your method development and helps to confirm qualitative identification.

**Pre-programmed parameter changes.** The new software package allows you to change separation parameters, wavelength sequences, calibration factors and calculation procedures between runs, automatically. An automatic sampling system holds up to 60 samples.

**HP 1084A can be upgraded.** If you already use an HP 1084A and wish to have these enhanced capabilities, rest assured your equipment can be quickly upgraded on site. Why not write for details?

## HP: innovators in HPLC



HEWLETT  PACKARD



## Compare Chromatograms.

Let the chromatograms tell the story. Glenco's HPLC System I has the same high resolution and precise reproducibility of other HPLC systems—at a much lower cost.

Modular in design, the HPLC System I can be assembled to suit your needs and has all the features:

- Exclusive sample injection system (patent no. 4022065)
  - Pulse-free liquid delivery system—5000 psi
  - Complete choice of detectors
  - Programmable gradient system
- Write for our new catalog.



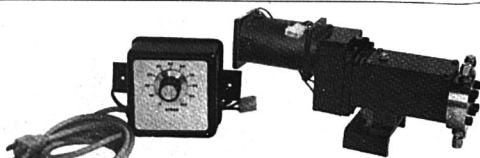
**Glenco Scientific Inc.**

The total LC supplier since 1962

2802 White Oak Drive • Houston, Texas 77007 • 713/861-9123



CIRCLE 84 ON READER SERVICE CARD



## OUR SMALL-SPACE METERING PUMP IS BIG ON ACCURACY.

Our Series 20 Chem/Meter hydraulic diaphragm metering pump will give you repetitive accuracy within  $\pm 1\%$  or better.

Measuring only  $9\frac{1}{2}'' \times 4\frac{1}{2}'' \times 3\frac{1}{2}''$ , it's designed for steady, continuous feeding of clear fluids. How? The programmed cam drive produces a constant velocity discharge—when the full displacement of two plungers working  $180^\circ$  apart are combined in a common manifold, a steady flow is established. And it provides capacities to 4.9 and 16.0 ML/min—with pressures to 1000 psig.

The series 20 Chem/Meter's wetted parts are made of corrosive resistant stainless steel with sapphire ball-seats and teflon diaphragms. With its totally enclosed, no-seal leakproof design and remote capacity control, its features make it ideal for applications such as chromatography columns, laboratory apparatus and industrial wet process analytical equipment.

To get all the details on why our little Chem/Meter is a big performer, write Chem/pump Division, Crane Co., Warrington, Pa. 18976.

**CRANE**

**CHEMPUMP**

CIRCLE 33 ON READER SERVICE CARD

## News

### Electroanalytical Chemistry

Academic Center, East Brunswick, N.J. May 15-18. Galen W. Ewing and Michael W. Miller. \$410 for 3 days; \$530 for 4 days. *Contact:* The Center for Professional Advancement, P.O. Box H, East Brunswick, N.J. 08816

### Finite Element Analysis

Milwaukee, Wis. May 15-19. \$395. *Contact:* Dept. of Engineering & Applied Science, U. of Wisconsin-Extension, 432 N. Lake St., Madison, Wis. 53706

### Design of Optical Systems

Madison, Wis. May 15-19. \$395. *Contact:* Dept. of Engineering & Applied Science, U. of Wisconsin-Extension, 432 N. Lake St., Madison, Wis. 53706

### Carbon-13 NMR Workshop

Kent State U., Kent, Ohio. May 17-19. \$150. *Contact:* Registrar,  $^{13}\text{C}$  NMR Workshops, Varian Associates, Box D-070, 611 Hansen Way, Palo Alto, Calif. 94303

### Applications of HPLC

Chase-Park Plaza Hotel, St. Louis, Mo. May 19-20. Sponsored by American Oil Chemists' Society. \$80, AOCS members; \$125, nonmembers; \$50, students. *Contact:* HPLC Short Course, American Oil Chemists' Society, 508 S. Sixth St., Champaign, Ill. 61820

### Computers for the Laboratory

Academic Center, East Brunswick, N.J. May 22-24. George Cohen and Joseph Liscouski. \$410. *Contact:* The Center for Professional Advancement, P.O. Box H, East Brunswick, N.J. 08816

### Minicomputers in Structural Analysis

Madison, Wis. May 31-June 2. \$225. *Contact:* Dept. of Engineering & Applied Science, U. of Wisconsin-Extension, 432 N. Lake St., Madison, Wis. 53706

### Statistical Experimental Design

Madison, Wis. June 5-9. \$350. *Contact:* Dept. of Engineering & Applied Science, U. of Wisconsin-Extension, 432 N. Lake St., Madison, Wis. 53706

### Atomic Absorption Spectroscopy

Occidental College, Los Angeles. June 12-14. \$225. *Contact:* C. David West, Dept. of Chemistry, Occidental College, 1600 Campus Rd., Los Angeles, Calif. 90041. 213-259-2761

(Continued on page 452 A)



**Jarrell-Ash  
Coast-to-Coast Seminars in  
Plasma Spectrometry**

Please reserve a place for me at the  
session to be held

DATE \_\_\_\_\_ CITY \_\_\_\_\_

and rush me all the details as to location,  
hours, speakers, etc.

NAME \_\_\_\_\_

TITLE \_\_\_\_\_

ORGANIZATION \_\_\_\_\_

ADDRESS \_\_\_\_\_

CITY \_\_\_\_\_ STATE \_\_\_\_\_ ZIP \_\_\_\_\_

PHONE (AREA CODE/NUMBER) \_\_\_\_\_

**Jarrell-Ash  
Coast-to-Coast Seminars in  
Plasma Spectrometry**

Please reserve a place for me at the  
session to be held

DATE \_\_\_\_\_ CITY \_\_\_\_\_

and rush me all the details as to location,  
hours, speakers, etc.

NAME \_\_\_\_\_

TITLE \_\_\_\_\_

ORGANIZATION \_\_\_\_\_

ADDRESS \_\_\_\_\_

CITY \_\_\_\_\_ STATE \_\_\_\_\_ ZIP \_\_\_\_\_

PHONE (AREA CODE/NUMBER) \_\_\_\_\_



**First Class**  
Permit No. 3902  
Pittsburgh, Pa.

**BUSINESS REPLY MAIL**

No Postage Stamp Necessary if Mailed in United States

Postage will Be Paid By

**Jarrell-Ash**

A Division of Fisher Scientific Company  
590 Lincoln Street Waltham, MA  
02154

ATTN: Ms. Linda Thomasino  
Plasma Seminars Coordinator



**First Class**  
Permit No. 3902  
Pittsburgh, Pa.

**BUSINESS REPLY MAIL**

No Postage Stamp Necessary if Mailed in United States

Postage will Be Paid By

**Jarrell-Ash**

A Division of Fisher Scientific Company  
590 Lincoln Street Waltham, MA  
02154

ATTN: Ms. Linda Thomasino  
Plasma Seminars Coordinator

# East & West, Jarrell-Ash carries the word on plasma spectrometry

## 12-city seminar series starts May 8.

### EAST

May 8	Washington DC
May 10	Atlanta
May 12	Houston
May 15	St. Louis
May 17	Chicago
May 19	Cincinnati

### WEST

May 8	Phoenix
May 10	Los Angeles
May 12	San Francisco
May 15	Seattle
May 17	Salt Lake City
May 19	Denver

Plasma spectrometry is **news**. It matches atomic absorption in sensitivity. But brings remarkable multi-element **capacity** to the field. There's nothing like it for high-workload performance.

That's why Jarrell-Ash invites you to a special seminar conducted by our plasma specialists in cities coast-to-coast. **See schedule at left.**

Each session covers everything you want to know about plasma spectrometry.

☐ Fundamentals of the inductively-coupled argon plasma (ICAP) source. What it is. How it works. What it does.

☐ Simultaneous multi-element trace-metal analysis in water, wastewater, air, soils, food, beverages, petroleum, biologicals.

☐ ICAP instrumentation (like the dramatically new computer-based direct-reading Plasma AtomComp).

☐ Accessories for accurate analysis even in the most severe background situations. (Like the **Spectrum-**

**Shifter** background correction system. And the **N+1 Channel** for dual-an-element capability.)

☐ State-of-the-art data-management systems for ICAP instruments.

☐ PLUS a look at the role of atomic absorption in expediting small-to-normal workloads. (Especially high-speed high-resolution flameless-AA systems.)

Plan now to attend. Enrollment limited. Use special Jarrell-Ash card bound into this journal for reservation and other details on the seminar in **your city**. Mail today!



Leaders in  
Plasma Spectrometry

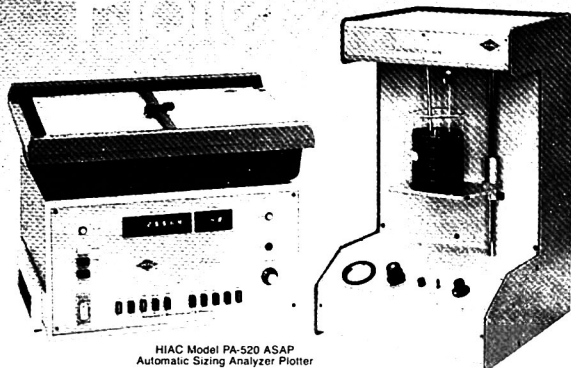
**Jarrell-Ash**

A DIVISION OF FISHER SCIENTIFIC COMPANY

590 Lincoln Street  
Waltham, Massachusetts 02154  
(617) 890-4300

CIRCLE 76 ON READER SERVICE CARD

# Automatic Sizing Analyzer Plotter



HIAC Model PA-520 ASAP  
Automatic Sizing Analyzer Plotter

**Measures particle size/volume (weight) distributions with pushbutton simplicity—delivers X-Y plots in 40 seconds!**

Just put in the sample, insert a chart and press a button. In less than a minute ASAP measures particle size and computes, in its microprocessor, particle size and volume (weight) distributions. 11" x 17" X-Y plots are automatically delivered in your choice of any or all of six different modes of data presentation, cumulative or differential.

**NON-ELECTROLYTIC HIAC\* PRINCIPLE/** You don't have to use electrically conductive carrier fluids. You can use water, alcohol, oil, solvents—almost any liquid—even viscous fluids, with HIAC accessories. Standard sensors cover from 1 micron through 1000 microns!

**HIGH RESOLUTION PRECISION/** ASAP can analyze up to one million particles per sample, with an accuracy traceable to NBS certified materials. Wide-range sensors analyze broad size distributions quickly, easily.

**DIVERSE APPLICATIONS/** Include powdered materials of all kinds—pigments, pharmaceuticals, metals, abrasives, ceramics, sediments, fillers, cement, ash, toners, food products. Liquid applications include emulsions, synthetic fibers, resins, agricultural chemicals, catalysts. Research and Development or Quality Control, ASAP can analyze your material quickly, accurately and easily.

## GET A FREE DEMONSTRATION—ASAP!

In your lab on your material—  
or send a sample for free analysis  
in our Applications Laboratory.

**PACIFIC  
SCIENTIFIC™**



HIAC INSTRUMENTS DIVISION

P.O. Box 3007, 4719 Brooks St., Montclair, Calif. 91763 Phone: (714) 621-3965

CIRCLE 171 ON READER SERVICE CARD

## News

### Environmental Monitoring

Madison, Wis. June 12-16. \$350. *Contact:* Dept. of Engineering & Applied Science, U. of Wisconsin-Extension, 432 N. Lake St., Madison, Wis. 53706

### Minicomputer Interfacing

Madison, Wis. June 13-15. \$285. *Contact:* Dept. of Engineering & Applied Science, U. of Wisconsin-Extension, 432 N. Lake St., Madison, Wis. 53706

### Polymer Microscopy

Chicago, June 19. \$450. *Contact:* McCrone Research Institute, 2508 S. Michigan Ave., Chicago, Ill. 60616

### Liquid Chromatography

Occidental College, Los Angeles, June 19-21. \$225. *Contact:* C. David West, Dept. of Chemistry, Occidental College, 1600 Campus Rd., Los Angeles, Calif. 90041. 213-259-2761

### Carbon-13 NMR Workshop

Rutgers U., New Brunswick, N.J. June 20-22. \$150. *Contact:* Registrar, <sup>13</sup>C NMR Workshops, Varian Associates, Box D-070, 611 Hansen Way, Palo Alto, Calif. 94303

## For Your Information

**Finnigan Corp.**, a leading manufacturer of GC/MS systems, has organized a new division dedicated to a wide range of instructional training and research services. The Finnigan Institute located in Cincinnati, Ohio, is scheduled to be in full operation by April 1, 1978. Among the courses to be offered are: **laboratory classes in basic GC/MS theory and practice; advanced GC/MS techniques; and basic and advanced mass spectral interpretation.** Also, courses in environmental analysis, forensic/toxicology, biomedical/pharmacology, and analytical methodologies are scheduled. Don C. DeJong, professor of chemistry at the University of Montreal for the past seven years, has been named president. Perkin-Elmer, another major instrument manufacturer, has agreed to participate in the institute. Perkin-Elmer will provide expertise in liquid chromatography, gas chromatography, and spectrophotometry.

The Scientific Apparatus Makers Association (SAMA) announces the availability of the following three revised standards: "Guidelines for the Purity and Handling of Gases Used



# AMINCO

Analytical  
Instrumentation

***A Fluorescence, UV-VIS, or HPLC Instrument to Fit Your Needs!***



## DW-2a™ UV-VIS Recording Spectrophotometer

An ideal instrument for spectrometric analysis of solutions, turbid samples, or solids. Highest sensitivity is 0.005A full scale. Differences as small as 0.0005A are easily read. Single or double beam operation from 200 to 825nm (1100nm with infrared accessory). Many accessories available.

Circle No. 7 for more information

## Fluoro- Colorimeter



A highly sensitive filter fluorometer used also for colorimetry, turbidimetry, and nephelometry. Ideal for assaying a progression of samples of unknown concentration with great efficiency and high sensitivity.

Circle No. 8 for more information

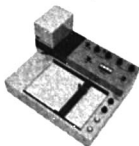
## Fluoro- Monitor™ Fluorometric Analyzer



For fluorescence detection in HPLC flow systems. The sensitivity, flexibility, and temperature stability make this an ideal low cost instrument for detecting HPLC effluents that fluoresce.

Circle No. 9 for more information

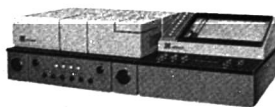
## Hem-O-Scan™ Oxygen Dissociation Analyzer



Produces oxygen dissociation curves in approximately 20 minutes from only 2 microliters of sample. As sample equilibrates with varying oxygen partial pressures, a continuous curve is simultaneously recorded on an X-Y recorder.

Circle No. 10 for more information

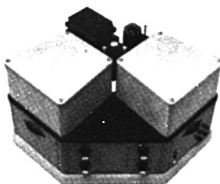
Circle No. 17 to have Sales Representative Call



## SPF-1000™ Corrected-Spectra Spectrofluorometer

Sophisticated instrument for working at the forefront of fluorescence research. Perform almost every measurement desired of a spectrofluorometer including quantum efficiencies, corrected phosphorescence spectra, corrected spectra, and differential fluorescence.

Circle No. 11 for more information



## AMINCO-BOWMAN® Spectrophotofluorometers

Grating-type spectrofluorometers ideal for research and routine applications in analytical, clinical, biomedical, and industrial specialties. Features precise and reproducible scanning speeds, sealed lamp housing and stabilization of the lamp arc movements. Ellipsoidal Light Condensing System, Ratio, and Photon-Counting models are also available.

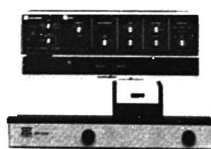
Circle No. 12 for more information

## Chem-Glow® photometer



For measurement of bioluminescence or chemiluminescence activity. Provides sensitive, linear, and reproducible results when measuring low light levels.

Circle No. 13 for more information



## SPF-500™ Spectrofluorometer

Has the features, flexibility, and ease-of-operation needed for today's fluorescence research applications. A uniquely designed xenon lamp gives you an intense excitation source and improved instrument sensitivity. Automatically performs all scaling functions and decimal point positioning without operator intervention. Digital readouts for quick and accurate readings. Available in Ratio, Corrected-Spectra, and Differential models.

Circle No. 14 for more information



## SPF-125™ Spectrophotofluorometer

For non-scanning or scanning fluorometric analysis, using grating separation of wavelength. Each monochromator has 1.5 to 44nm spectral band-pass at 6 slit positions. Standard 85 watt mercury lamp, xenon lamp optional.

Circle No. 15 for more information



## Aminco HPLC System

Applies high resolution fluorometric determination techniques to HPLC effluents that fluoresce. Fluorescence detector standard, optional detectors include: electrochemical, UV, ninhydrin, and colorimetric. Unattended, 24 hours/day operation with automatic sample injection and temperature programming.

Circle No. 16 for more information

See us at the FASEB, FEDERATION OF AMERICAN SOCIETIES FOR EXPERIMENTAL BIOLOGY, Meeting.

**AMERICAN INSTRUMENT COMPANY**  
DIVISION OF TRAVENOL LABORATORIES, INC.  
Silver Spring, Maryland 20910-Phone: 301-589-1727

# AMINCO®

©1977, Travencol Laboratories, Inc.

# High Speed Spectroscopy

## 1024 Spectral Channels Simultaneously

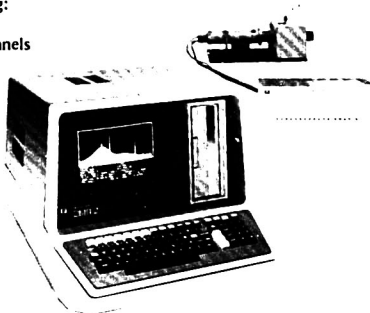
From The Princeton Applied Research OMA®

If your single channel technique is slowing you down, maybe it's time you joined the switch to the multi-channel approach.

OMA's (Optical Multichannel Analyzers) feature the following:

- Up to 1024 parallel channels
  - Spectral coverage from UV to thermal IR
  - Vidicon or Self-scanned Diode Array Detectors
  - Time resolved spectroscopy to 40 nanosecond resolution
  - Microcomputer data handling
- and much more.

Write or call for our OMA brochures: Princeton Applied Research Corp., P.O. Box 2565, Princeton, NJ 08540 609/452-2111



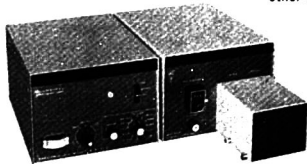
PRINCETON APPLIED RESEARCH

AN EG&G COMPANY

Circle #164 for Additional Information Only. Circle #165 have Salesman contact me.

## The only thing variable about the SF 770 Spectroflow Monitor for liquid chromatography ...is the wavelength!

- It consistently offers highest sensitivity with low noise and baseline drift.
- It classically follows Beer's law in its measurements.
- It routinely includes an automatic gain control and zero suppression.
- It equally interfaces with all Liquid Chromatography systems.
- It inconspicuously takes up very little room.
- It uniquely incorporates a double-beam design.
- It invariably is an honest instrument, not relying on gimmicks to achieve unrealistic specs.
- It indubitably is preferred by more liquid chromatographers than all other models combined.



Call or write now!

24 BOOKER STREET, WESTWOOD, NEW JERSEY 07675  
(201) 664-7263

**SCHOEFFEL**  
INSTRUMENT CORPORATION

CIRCLE 191 ON READER SERVICE CARD

## News

in Atomic Absorption Spectroscopy", "Glass pH & Reference Electrodes Evaluation & Calibration", and "Sizes for Laboratory Glassware". Single copies are available free of charge from: SAMA, 1140 Connecticut Ave., N.W., Washington, D.C. 20036, 202-223-1360. SAMA is a trade association representing over 200 of the leading manufacturers and distributors of scientific instruments, related apparatus, and chemicals.

Awards totaling \$4200 are being offered to U.S. and Canadian authors of papers on applications and techniques of electrofocusing in biochemistry by LKB Instruments, Inc., a company specializing in the development of instruments for electrofocusing. The awards will be presented at ELECTROFOCUS/78, which is being organized by the company. Anyone wishing to enter the contest is invited to submit original research papers not later than May 10, 1978. For more information contact: J. Ball, LKB Instruments, Inc., 12221 Parklawn Dr., Rockville, Md. 20852, 301-882-2510.

Marcel Dekker, Inc., the New York City-based publisher of scientific literature, has initiated two new scholarly journals—*Journal of Liquid Chromatography* and *Drug and Chemical Toxicology*. The former, edited by Jack Cazes of Waters Associates, Milford, Mass., will be published every two months, six issues per volume for \$48 per volume. The publisher promises to provide a forum for all phases of liquid chromatography from analytical and preparative articles to papers dealing with liquid chromatography as a science in itself. Papers in thin-layer chromatography and all modes of liquid column chromatography will also be welcomed. The first issue published in January 1978 contains eight papers. For more information contact: Marcel Dekker, Inc., 270 Madison Ave., New York, N.Y. 10016.

Schoeffel Instrument Corp., a leading manufacturer of detectors for gas chromatography, has entered into an agreement with Kratos, a California-based corporation. Under the agreement, Schoeffel Instrument will operate as a divisional entity of Kratos. Kratos is a high technology manufacturer of mass spectrometers, electron microscopes, and computer displays.

The Foxboro Co. of Foxboro, Mass., has formed a new analytical division to provide a broad range of ana-

# HERE'S HOW TO HANDLE PLUNGER PROBLEMS.

This syringe was designed to solve the problem of bending plungers. If you've been having that problem, this Hamilton 800 Syringe is your answer. It has a strong metal stem which travels through the handle and acts as a sturdy guide for the smaller plunger. The stem threads onto the plunger, stabilizing it and helping to prevent the plunger from bending.

It is really comfortable to hold and convenient to use a syringe with a handle. The weight balances nicely in your hand and allows you to hold the syringe without the heat of your body affecting the sample.

The flange in the handle contains a friction ring that gives you an adjustable drag on the stem-plunger, providing resistance against high pressure.

These syringes are essentially the tried and true Hamilton 700 Series Syringes, with accurate delivery to  $\pm 1\%$ . We've just added the handle to make them more convenient and versatile.

If you damage the glass, needle or plunger, you don't have to throw the whole syringe away. Just replace the syringe assembly.

The glass barrel threads into the handle to give you a solid connection. It's easy to make replacements.

The syringe with a handle. It comes in 5  $\mu$ l and 10  $\mu$ l capacities. (801N illustrated)

For more information and literature on our 800 Series Syringes, write to John Nadolny, Hamilton Co., P.O. Box 10030, Reno, Nevada 89510.

**HAMILTON**

CIRCLE 98 ON READER SERVICE CARD



# In Fraction Collecting, there are probably three names to know.

## Buchler is one of them.

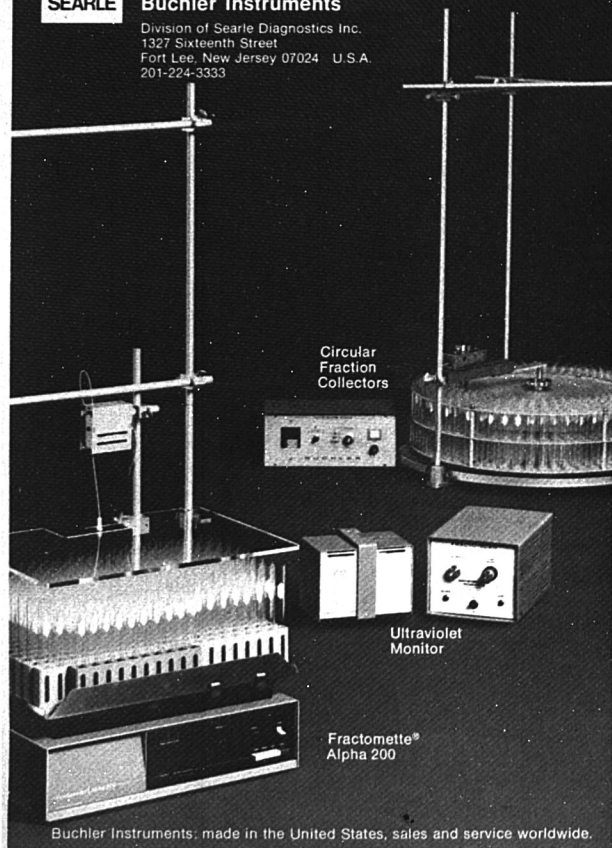
Buchler's Fractomette® Alpha 200 gives you more features as standard. Its low base price includes: automatic shutdown after preset number of tubes—up to a full 200; automatic flow interruption upon tube shift; heavy, rigid plastic dust cover; and much more... including Buchler's exclusive lift-off platform and patented overflow shutoff system. Reliability is enhanced by solid-state pull-out electronics and a dependable, easy-to-read L.E.D. digital display.

The Alpha 200 is big in value but small in size; it takes only 1½ square feet of space and was designed with cold-room use in mind. We have other circular and linear Fraction Collectors up to 400 tubes, as well as the Fracto-Scan™ for reliable UV monitoring. All are available through leading laboratory supply houses.

SEARLE

### Buchler Instruments

Division of Searle Diagnostics Inc.  
1327 Sixteenth Street  
Fort Lee, New Jersey 07024 U.S.A.  
201-224-3333



Buchler Instruments, made in the United States, sales and service worldwide.

CIRCLE 24 ON READER SERVICE CARD

## News

lytical instrumentation for both on-stream composition measurements and quantitative analysis in production control laboratories. The new division will offer existing Foxboro analytical equipment based on electrochemistry and gas chromatography as well as the infrared analytical devices of Foxboro/Wilks, Inc. (formerly Wilks Scientific Corp.), a recently acquired Foxboro subsidiary. These devices include on-stream infrared analyzers, portable and stationary toxic vapor monitors, and quantitative infrared spectrometers for control laboratories. The new division is headquartered in Burlington, Mass.

The Research & Development/Water Management Division of The Carborundum Co., Niagara Falls, N.Y., has been awarded a \$540 448 contract by the U.S. Environmental Protection Agency for analysis of industrial effluents for trace levels of organic compounds by GC/MS. The samples to be analyzed were taken from a variety of industrial sites throughout the country in conjunction with EPA's program to evaluate the best available technologies economically achievable for industrial waste treatment.

The proceedings of the second annual Toxic Substances Control Conference, held in Washington, D.C., December 8-9, 1977, are now being offered by the conference sponsor. The conference, attended by over 500 business representatives, dealt with public health, scientific, and regulatory aspects of toxic chemicals. Copies are available from: Government Institutes, 4733 Bethesda Ave., N.W., Washington, D.C., at \$25 per copy for paperbound.

Instruments SA, Inc., has added an applications laboratory to offer services in the areas of Raman spectroscopy and molecular microprobe techniques. The new laboratory is headed by Fran Adar, formerly of the University of Pennsylvania Solid State and Biophysics Department. As part of this service, the lab will do evaluation of samples and appraise the applicability of Raman and microprobe techniques to specific areas of investigation. The molecular microprobe service will also be made available on both a service lab basis and for basic joint research. For more information contact: Roy Grayzel, Instruments SA, Inc., 173 Essex Ave., Metuchen, N.J. 08840, 201-494-8660.



# SIEMENS

## The matchless investment in X-ray analysis is the system with unmatched features.

The most cost-effective automated sequential spectrometer on the market is also the most complete, offering a combination of benefits that are not available elsewhere.

The 4 KW output generator, for example, is powerful enough to operate two tubes at the same time. This parallel operation means that you can expand your system economically—without buying a second generator. Siemens also offers an ultra-stable generator with  $\pm .005\%$  stability.

The SRS 200, specially designed for automation, can be controlled by the computer of your choice or with our floppy-disk oriented computer. Either way, our software packages are available for sophisticated data manipulation, including the latest

correction methods. The computer also controls the filter and aperture changer and the X-ray tube power setting.

Other features include the detector pulse spectroscopy for initial setup and observation of the

pulse height selector, the 80-position sample changer for increased throughput, and an X-ray tube that can be changed in less than 5 minutes.

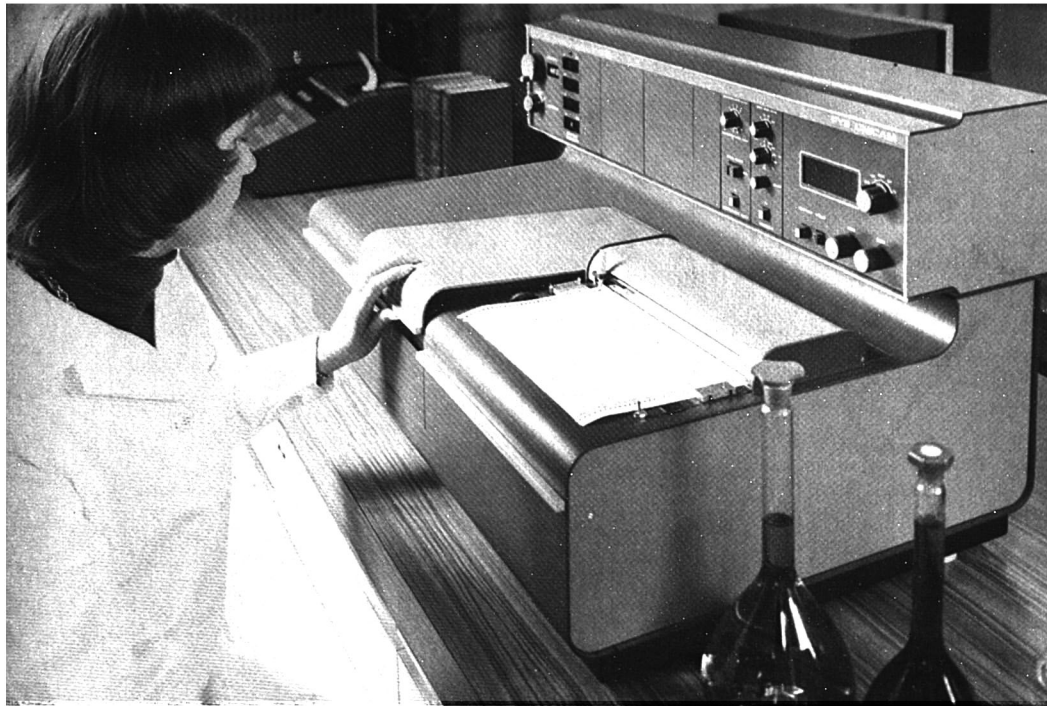
For complete information on the X-ray analyzer that gives you more when you analyze your investment, write or call: Mr. Pedro Arredondo.

**Siemens Corporation**  
Analytical Systems Division  
1 Computer Drive, Cherry Hill  
N.J. 08002, (609) 424-9212



## Siemens SRS-200.

CIRCLE 188 ON READER SERVICE CARD



## Get more UV-VIS spectrophotometer than your budget allows!

**Now from Philips, the Pye Unicam SP8-100 high performance spectrophotometer.**

You'll be most pleasantly surprised when you see the features packed into the SP8-100 . . . and learn how affordable it is. Get our brochure and compare this system with any other.

The SP8-100 is built by Pye Unicam, a leader in UV-VIS spectrophotometry, and is backed by Philips, a world leader in high technology systems. Our applications specialists and accessories

will help you get the most from your studies, including:

- reaction rate analysis
- color measurements
- fluorescence

- densitometry
- column monitoring
- turbid samples
- automated measurements

Stretch your budget . . . and your capabilities . . . with the Pye Unicam SP8-100.

**Philips Electronic Instruments, Inc.**

A North American Philips Company.

85 McKee Drive, Mahwah, N.J. 07430  
Telephone (201) 529-3800  
International — Contact Pye Unicam Ltd.  
York Street, Cambridge, England CB1 2PX  
Telephone, Cambridge (0223) 58866  
Telex 817331



Call, write or use the reader reply service for your copy of the SP8-100 brochure.



**Electronic Instruments**

# PHILIPS

CIRCLE 161 ON READER SERVICE CARD



Safe control to temperature extremes — hot or cold — with great precision. HAAKE Thermal Liquid Baths with external circulation offer quality performance and operational comfort. Advanced DAS IC control technology now available with automatic compensation for changes in thermal load, environmental temperature and line voltage fluctuations. HAAKE, your complete source for Laboratory Liquid Temperature Control.

Pictured: F3C-17"x15"x9"



# HAAKE

Temperature Control Equipment Division

HAAKE INC. 244 Saddle River Road, Saddle Brook, New Jersey 07662 (201) 843-7070

CIRCLE 99 ON READER SERVICE CARD

See us at FASEB, Booth # S-17 & 18.



# Only Beckman backs up a full UV line with a full 37 years of UV experience.



And that's why all our instruments from the workhorse 25 to the state-of-the-art 5270 offer exceptional reliability and performance.

They feature, too, genuine human engineering factors, the kind that simplify the acquisition of superior quality answers, and are only learned from years of hands-

---

**Model 24/25** Considered by many to be the standard for a high performance workhorse, the 24/25 series offers a unique *common optics* system and double beam capability at a single beam price. Minimal controls, formatted chart paper, digital

CIRCLE 36 ON READER SERVICE CARD

---

**Model 34/35** The new series 34/35 instruments offers a broad range of convenience, performance, and precision design features previously unavailable on medium-priced units. A *common optics* system with a common beam aperture, a program-

CIRCLE 37 ON READER SERVICE CARD

---

**Model 3600** The new 3600 features a high performance holographic grating monochromator teamed with common optics, programmable or fixed slits, automatic source change, and an advanced recorder. Pushbutton selection of 11 chart speeds.

CIRCLE 38 ON READER SERVICE CARD

---

**Model 5230** The 5230 is a complete research grade instrument designed with a classical superstructure for long-term optical stability and overall ruggedness and reliability. Exceptional quality supporting hardware includes an innovative holo-

CIRCLE 39 ON READER SERVICE CARD

---

**Model 5270** No short form list of performance characteristics can sum up the 5270. It is, for many researchers in biomedicine and chemistry, simply the best UV instrument that has ever been made. And you might say that excellence was 37 years

CIRCLE 40 ON READER SERVICE CARD



on field experience. As for breadth of applications, that's where experience can be critical. Since 1941 and the first DU,<sup>4</sup> we've developed over 40 major accessory systems to specialize an instrument (at a minimum cost) for a specific application.

Today, the Beckman tradition of UV innovation continues with special capabili-

ties for such applications as: Gel Scanning. Scatter Transmission. Kinetic Monitoring. Wavelength Programming. Column Monitoring. Reflectance Measurement—Specular and Diffuse. And Dissolution Monitoring to meet the most stringent government standards.

In short, whatever your budget or

whatever your application, the Beckman UV team can help. Check out the instruments below to find the one that meets your needs exactly. Then for more information contact Scientific Instruments Division, Beckman Instruments, Inc., P.O. Box C-19600, Irvine, CA 92713. **Innovation in UV since 1941.**

---

readout, and a long record for stable performance all work to make the 24/25's simple to operate, fast and precise.

---

mable slit system, automatic absorbance overrange detection, 0-3 absorbance range, *k Factor*, fast scanning speeds, expanded scales, and time constant selection are just some of the 34/35's attributes.

---

5 scan speeds, and 7 ordinate spans directly calibrated in absorbance provide a variety of convenient formats. Other capabilities include: Readout in absorbance, concentration, or percent transmission with first and second derivative recording, multi-

wave length programming, 0-3 absorbance range, and 4 Time Constant Selection.

---

graphic grating, true ratio recording capability, servo-operated slits, stepper motor drive, and computer compatible digital output to provide truly excellent performance for the instrument dollar.

---

in the making. Of course, if you can't put one in your lab on tomorrow's budget, we'd like you to remember that all Beckman Instruments share in the DU heritage and our 37 year commitment to UV analysis.

**BECKMAN®**

# A new concept in laboratory tube furnaces

## New 55000 Series tube furnaces

Lindberg's new Moldatherm® lab tube furnaces. They're ultra-light weight. Faster performing. Exceptionally economical to operate.

Moldatherm is the reason. This unique Lindberg® development combines ceramic fiber insulation and heating elements in one ultra-light weight composite. Its low thermal mass results in rapid heat-up and cooling rates. Enables you to save electrical energy and valuable lab time. There's no other tube furnace like it. Anywhere.

Used with Lindberg's new 58000 Series electronic control consoles, models of this furnace can heat to 1100 C from a cold start in less than 30 minutes. Much faster than conventional furnaces.

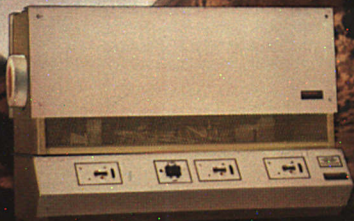
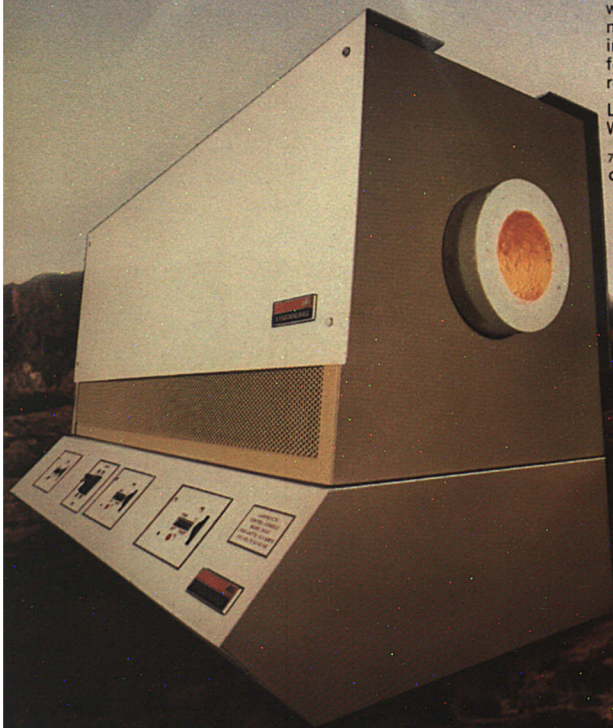
## New 58000 Series control consoles

Provide  $\pm 5$  C straight line control accuracy and solid state reliability in a portable modular design. Null fired triac output won't interfere with other sensitive equipment. And 100-1100 C digital setpoint range gives you maximum process flexibility. Available in your choice of single-zone or three zone control models. Used with the Moldatherm tube furnace, these control consoles will meet your less critical high-temperature needs at a surprisingly low cost. For more information, just contact Lindberg — your source for precision heating to meet every laboratory requirement.

Lindberg, Sola Basic Industries, 304 Hart Street, Watertown, WI 53094; 414-261-7000.

7L30

CIRCLE 128 ON READER SERVICE CARD



... the hottest heat source under the sun

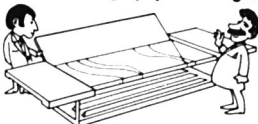
SOLA BASIC **SB**

**LINDBERG**

# NEW for TLC SB/CD CHAMBER

(SHORT-BED/CONTINUOUS DEVELOPMENT)

Another **INNOVATIVE** Product  
for Chromatography from Regis



## REGIS SB/CD CHAMBER

**Tom:** Got a new TLC tank? What's it good for?

**Frank:** Gives me better separations; plus saves me lots of time in selecting the optimum solvent system.

**Tom:** How can a tank do that?

**Frank:** It allows me to exploit the change in selectivity you get by reducing the polarity of the solvent. Then, with a few solvent experiments I can separate close R<sub>f</sub> spots.

**Tom:** But doesn't lowering the polarity of the solvents reduce the R<sub>f</sub>?

**Frank:** That's where the SB/CD Chamber makes the difference. It allows for continuous development of the plate which means a constant flow of solvent. And, because it's a short-bed development the solvent velocity is very high.

**Tom:** How do your results compare with conventional TLC?

**Frank:** Actually, they are better. Spots don't travel as far to get separated so they're sharper, less diffused. Lots of separations in a very small plate area. This tank does make a difference.

The Regis SB/CD Chamber is a new, unique, powerful tool for TLC. Solvent selectivity power — ability to separate close R<sub>f</sub> spots — which is realized by reducing polarity is well-known. Until now, there has never been a practical way to utilize it. Benefits to the chromatographer: simplified solvent searches, better separations, and sensitivity enhancement.

**203200 SB/CD Chamber \$85.00**

For Free Technical Bulletin

Call or Write **312-967-0000**  
**TWX REGIS 910-223-0808**

**REGIS CHEMICAL COMPANY**  
8210 Austin, Morton Grove, Illinois 60053

CIRCLE 174 ON READER SERVICE CARD



**PRESS IT OR GRIND IT**  
**or MIX IT SIEVE IT DIGEST IT ARC IT PHOTOGRAPH IT...**

Request our Spectrochemistry Catalog

**SPEX**

INDUSTRIES INC

P.O. BOX 798 METUCHEN N.J. 08840 (201) 549-7144

**SPEX**  
SUPPLIES IT\*

**\*SAMPLE PREPARATION AND HANDLING EQUIPMENT**

CIRCLE 187 ON READER SERVICE CARD

**FIRST CLASS**  
**Permit No. 25682**  
**Philadelphia, Pa.**  
**19101**

## BUSINESS REPLY CARD

No postage stamp necessary if mailed in the United States

POSTAGE WILL BE PAID BY

## ANALYTICAL CHEMISTRY

**P. O. Box #8660**

**Philadelphia, Pennsylvania 19101**

Analytical Chemistry

APRIL 1978

Valid through  
August 1978

NEW PRODUCTS, CHEMICALS, LITERATURE: 401 402 403 404 405 406 407 408 409 410 411 412 413 414 415  
416 417 418 419 420 421 422 423 424 425 426 427 428 429 430 431 432 433 434 435 436 437 438 439 440 441 442  
443 444 445 446 447 448 449 450 451 452 453 454 455 456 457 458 459 460 461 462 463 464 465 466 467 468 469  
470 471 472 473 474 475 476 477 478 479 480 481 482 483 484 485 486 487 488 489 490 491 492 493 494 495 496

ADVERTISED PRODUCTS: 1 2 3 4 5 6 7 8 9 10 11 12 13 14 15 16 17 18 19  
20 21 22 23 24 25 26 27 28 29 30 31 32 33 34 35 36 37 38 39 40 41 42 43 44 45 46  
47 48 49 50 51 52 53 54 55 56 57 58 59 60 61 62 63 64 65 66 67 68 69 70 71 72 73  
74 75 76 77 78 79 80 81 82 83 84 85 86 87 88 89 90 91 92 93 94 95 96 97 98 99 100  
101 102 103 104 105 106 107 108 109 110 111 112 113 114 115 116 117 118 119 120 121 122 123 124 125 126 127  
128 129 130 131 132 133 134 135 136 137 138 139 140 141 142 143 144 145 146 147 148 149 150 151 152 153 154  
155 156 157 158 159 160 161 162 163 164 165 166 167 168 169 170 171 172 173 174 175 176 177 178 179 180 181  
182 183 184 185 186 187 188 189 190 191 192 193 194 195 196 197 198 199 200 201 202 203 204 205 206 207 208  
209 210 211 212 213 214 215 216 217 218 219 220 221 222 223 224 225 226 227 228 229 230 231 232 233 234 235  
236 237 238 239 240 241 242 243 244 245 246 247 248 249 250 251 252 253 254 255 256 257 258 259 260 261 262

READER 301 302 303 304 305 306 307 308 309 310 311 312 313 314 315 316 317 318 319 320 321 322 323  
SURVEY: 324 325 326 327 328 329 330 331 332 333 334 335 336 337 338 339 340 341 342 343 344 345 346

Name \_\_\_\_\_ Position \_\_\_\_\_

Company \_\_\_\_\_

Street \_\_\_\_\_ City \_\_\_\_\_

State \_\_\_\_\_ Zip \_\_\_\_\_ Telephone \_\_\_\_\_

# USE . . .

these postage paid reply cards for free data  
on all products advertised in this issue.

Analytical Chemistry

APRIL 1978

Valid through  
August 1978

NEW PRODUCTS, CHEMICALS, LITERATURE: 401 402 403 404 405 406 407 408 409 410 411 412 413 414 415  
416 417 418 419 420 421 422 423 424 425 426 427 428 429 430 431 432 433 434 435 436 437 438 439 440 441 442  
443 444 445 446 447 448 449 450 451 452 453 454 455 456 457 458 459 460 461 462 463 464 465 466 467 468 469  
470 471 472 473 474 475 476 477 478 479 480 481 482 483 484 485 486 487 488 489 490 491 492 493 494 495 496

ADVERTISED PRODUCTS: 1 2 3 4 5 6 7 8 9 10 11 12 13 14 15 16 17 18 19  
20 21 22 23 24 25 26 27 28 29 30 31 32 33 34 35 36 37 38 39 40 41 42 43 44 45 46  
47 48 49 50 51 52 53 54 55 56 57 58 59 60 61 62 63 64 65 66 67 68 69 70 71 72 73  
74 75 76 77 78 79 80 81 82 83 84 85 86 87 88 89 90 91 92 93 94 95 96 97 98 99 100  
101 102 103 104 105 106 107 108 109 110 111 112 113 114 115 116 117 118 119 120 121 122 123 124 125 126 127  
128 129 130 131 132 133 134 135 136 137 138 139 140 141 142 143 144 145 146 147 148 149 150 151 152 153 154  
155 156 157 158 159 160 161 162 163 164 165 166 167 168 169 170 171 172 173 174 175 176 177 178 179 180 181  
182 183 184 185 186 187 188 189 190 191 192 193 194 195 196 197 198 199 200 201 202 203 204 205 206 207 208  
209 210 211 212 213 214 215 216 217 218 219 220 221 222 223 224 225 226 227 228 229 230 231 232 233 234 235  
236 237 238 239 240 241 242 243 244 245 246 247 248 249 250 251 252 253 254 255 256 257 258 259 260 261 262

READER 301 302 303 304 305 306 307 308 309 310 311 312 313 314 315 316 317 318 319 320 321 322 323  
SURVEY: 324 325 326 327 328 329 330 331 332 333 334 335 336 337 338 339 340 341 342 343 344 345 346

Name \_\_\_\_\_ Position \_\_\_\_\_

Company \_\_\_\_\_

Street \_\_\_\_\_ City \_\_\_\_\_

State \_\_\_\_\_ Telephone \_\_\_\_\_

## BUSINESS REPLY CARD

No postage stamp necessary if mailed in the United States

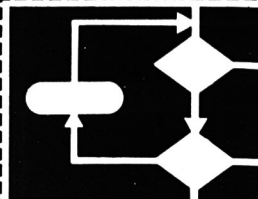
POSTAGE WILL BE PAID BY

# ANALYTICAL CHEMISTRY

P. O. Box #8660

Philadelphia, Pennsylvania 19101

FIRST CLASS  
Permit No. 25682  
Philadelphia, Pa.  
19101



## Algorithms for Chemical Computations

ACS Symposium Series No. 46

Ralph E. Christoffersen, Editor  
The University of Kansas

A symposium sponsored by the  
Division of Computers in Chemistry of  
the American Chemical Society.

This multidisciplinary collection of  
state-of-the-art papers assesses  
significant developments in algorithms  
for several important areas of  
chemistry and pinpoints places where  
currently available algorithms are  
inadequate.

Leading experts not only evaluate the  
tremendous opportunities for progress  
in chemical research that algorithms  
provide but also analyze the  
substantial difficulties that algorithms  
may present.

Topics covered include those of  
particular interest to scientists doing  
significant amounts of computing in  
the fields of quantum chemistry,  
scattering, computer handling of  
chemical information, and solid state  
theory.

### CONTENTS

Graph Algorithms in Chemical Computation •  
Algorithm Design in Computational Quantum  
Chemistry • Rational Selection of Algorithms for  
Molecular Scattering Calculations • Molecular  
Dynamics and Transition State Theory • New  
Computing Techniques for Molecular Structure  
Studies by X-ray Crystallography • Algorithms in  
the Computer Handling of Chemical Information

151 pages (1977) Clothbound \$12.75  
LC 77-5030 ISBN 0-8412-0371-7

SIS/American Chemical Society  
1155 16th St., N.W./Wash., D.C. 20036

Please send \_\_\_\_\_ copies of *SS 46 Algorithms  
for Chemical Computations* at \$12.75 per copy.

☐ Check enclosed for \$\_\_\_\_\_. ☐ Bill me.  
Postpaid in U.S. and Canada, plus 40 cents  
elsewhere.

Name \_\_\_\_\_  
Address \_\_\_\_\_  
City \_\_\_\_\_ State \_\_\_\_\_ Zip \_\_\_\_\_



# "With Graphics I can see at a glance what used to take hours to uncover."

## Problem: Data reduction can be the weakest link in your analytical chain.

Every time you have to analyze spectral data from lists of numbers, you not only lose a world of time, you risk not recognizing important spectral patterns.

## Solution: Tektronix Interactive Graphics can replace manual operations with precise, instant visual displays.

Tektronix Graphics Terminals let you keep to waveform display throughout your processing. You can manipulate data at will—

without tedious and time-consuming manual translation.

### You can see Graphic results immediately.

You can integrate and scale, correct baselines, perform mathematical transforms, and command camera-ready hard copy all with unequalled interactivity and simplicity.

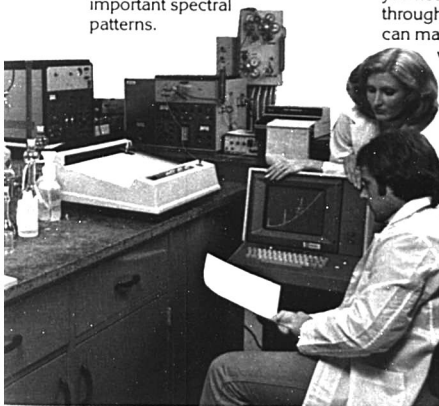


You can get clean, sharp, hard copies from the 4631 Hard Copy unit; local storage with the 4923 Digital Cartridge Tape Recorder; and multicolor plots from the 4662 Interactive Digital Plotter, shown left.

## Keeping your eyes on the display keeps your mind on the solution.

Tektronix Graphics is priced right to begin with, and more than pays for itself in performance. And because it's from Tektronix, you know it's got the reliability that's been respected by research for years.

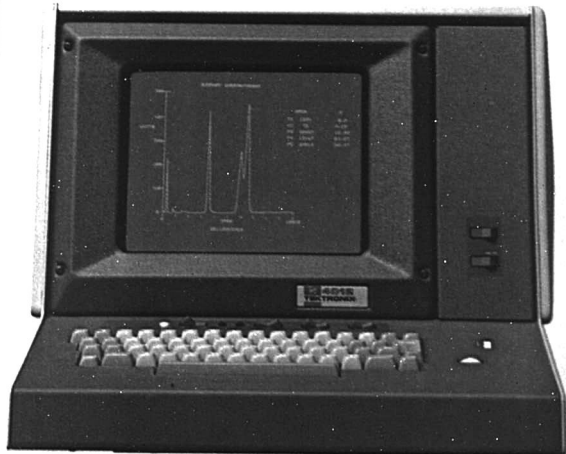
To get the whole Graphics story, talk to your Tektronix Sales Engineer, or write Tektronix.



Tektronix, Inc.  
Information Display Group  
P.O. Box 500  
Beaverton, OR 97077  
Tektronix Datatek N.V.  
P.O. Box 159, Badhoevedorp,  
The Netherlands

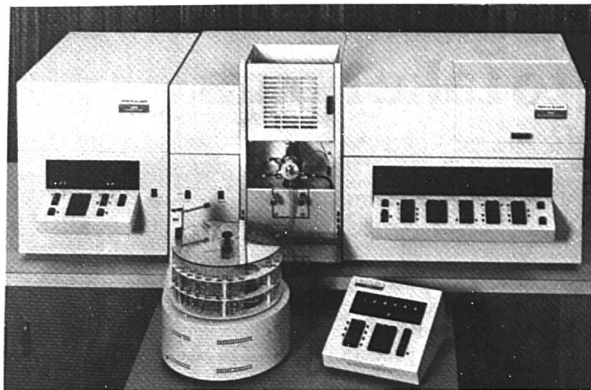
Copyright © 1977, Tektronix, Inc.  
All rights reserved.  
OEM Information Available

CIRCLE 209 ON READER SERVICE CARD



**Tektronix**  
COMMITTED TO EXCELLENCE

## New Products



**Model 5000 atomic absorption spectrophotometer** is fully automated and capable of sequential multielement analysis. Up to six elements in 50 samples can be determined in as short as 40 min. Features include a magnetic card reader to enter all operating conditions, a digitally controlled burner and gas control system, a six-lamp turret, background correction in both the UV and VIS ranges, and a programmable auto sampler. Wavelength, slit width, electrical parameters, gas choice and flow, and calibration are all microcomputer controlled and can be programmed into the spectrophotometer memory. Perkin-Elmer Corp. 401

### Fraction Collector

The fraction collector features a mobile delivery head and stationary test tubes to provide high mechanical reliability. The delivery head is mounted below all electrical and mechanical components to prevent contamination by accidental spillage. The collector has a capacity of 120 tubes and accepts 100 X 16 mm tubes or 4-mL autoanalyzer cups. The delivery head, attached to an endless toothed belt, stops at each tube for an adjustable period of 5 s to 90 min. Electrothermal Ltd. 410

### UV Detector for HPLC

**SpectroMonitor III** is a variable wavelength HPLC detector covering the most widely used UV range between 190 and 350 nm. Features include a removable 10-mm dual-path flow cell, a high-reliability dual silicon detector cell, eight selectable absorbance ranges from 0.01 to 1.28 AU, three selectable response times from 0.5 to 5.0 s, and automatic starting for the deuterium source lamp. Laboratory Data Control 416

For more information on listed items, circle the appropriate numbers on one of our Readers' Service Cards

### Autosampler

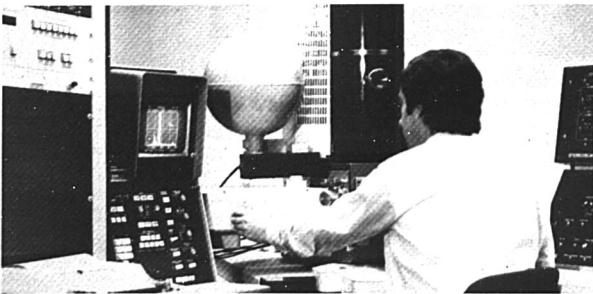
**Model AS-50 autosampler** is compatible with all P-E atomic absorption spectrophotometers. The AS-50 automatically presents up to 50 samples for analysis and activates the "read" cycle of instruments with signal integration capabilities. All control and logic functions are microcomputer controlled. Each sample container holds 15 mL. Perkin-Elmer Corp. 408

### Capillary Inlet for GC/MS

The capillary inlet accessory is designed for use with the 321 digital GC/MS system. With the accessory the 321 can use any type of high-resolution gas chromatographic column including WCOT, SCOT, or micropacked. The combined flow of the column and makeup gas through the specially designed column outlet connection results in 1 atm pressure at the column end, preventing pump-out of column liquid phase. Chromatographic resolution is maintained through the jet separator inlet under all column conditions. The 321 system is capable of detecting a few hundred picograms of material for complete sample identification. Du Pont Co. 412

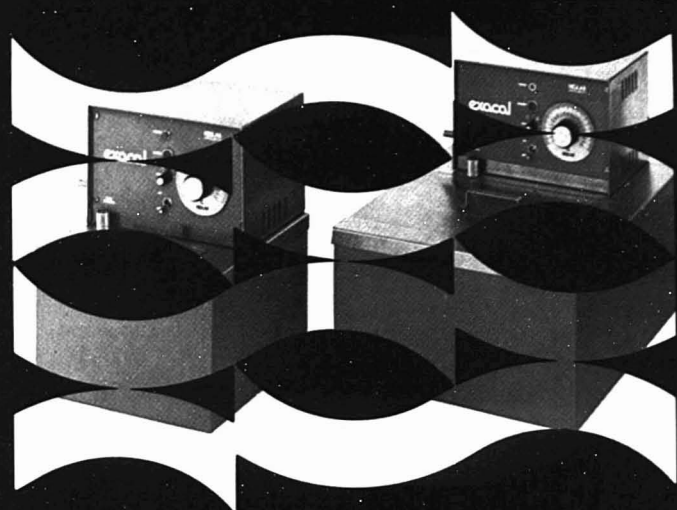
### UV Monitors

The UV-2 dual-path monitor has a 20- $\mu$ L cell that simultaneously monitors a sample through two different path-lengths (20 and 1 mm). This allows quantitation of very large peaks and very small peaks simultaneously, eliminating scale expansion interpretation problems. It can measure 254 and 280 nm simultaneously, with a choice of absorbance or transmittance output. The fused quartz cell has a uniform dimension of 1 mm. The UV-1 is a single-pathlength, single-wavelength UV monitor. Most specifications are identical to the UV-2, but the UV-1 operates with either a 3- or 10-mm cell and at either 280 or 254 nm. Pharmacia Fine Chemicals 417



**WEDAX 2 x-ray spectrometer system** integrates both wavelength and solid-state energy-dispersive x-ray spectrometry techniques with specimen stage automation. The result is an accurate, quantitative microanalytical system that can be added to a scanning electron microscope. With the addition of WEDAX 2, an SEM can provide quantitative analytical data on all elements from boron through uranium. Analyses are made with ZAF corrections applied to reduce raw data into quantified results. The system is provided in modular format. Cambridge Instrument Co., Inc. 402

**LOOK INTO THE LEADER  
IN TEMPERATURE CONTROLLED BATHS**



**NESLAB**

For the finest in temperature control systems, look into the company that pioneered the EXACAL BATH CIRCULATORS. With a temperature range from  $-100^{\circ}\text{C}$  to  $+300^{\circ}\text{C}$  NESLAB products represent the highest quality in IMMERSION COOLERS, RECIRCULATING EXCHANGERS and BATH CIRCULATORS. NESLAB also offers the technical advice of our chemists and engineers to help you solve your heating and cooling problems.



Call the leader — toll free

**1-800-258-0830**

In N.H. call collect 603-436-9444

**NESLAB**

**the name in circulation**

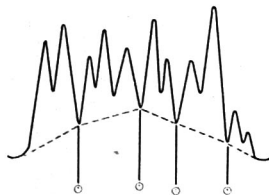


NESLAB INSTRUMENTS, INC. 871 ISLINGTON STREET, PORTSMOUTH, N.H. 03801 U.S.A. (603) 436-9444

CIRCLE 150 ON READER SERVICE CARD

## can your integrator do this?

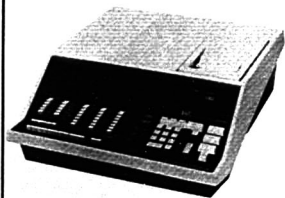
Baseline Forced  
by Timed Event  
(Nearest Valley)



## the SUPERGRATOR can!

Unlike other programmable computing integrators, the Supergrators allow you to force any valley to be identified as baseline, eliminating the effect of an underlying component under other components.

Timed events forcing the nearest valley to be called a baseline is only one of the dozens of reasons the Supergrators should be in your lab. Why not call CSI today for a demonstration?



**COLUMBIA SCIENTIFIC  
INDUSTRIES CORP.**

P.O. Box 9908, Austin, Texas 78766  
(512) 258-5191, TWX 910-874-1364  
Outside Texas call Toll Free  
(800) 531-5003

CIRCLE 34 ON READER SERVICE CARD



Edited by E.D. Meier 2nd Edition

In the five years since the first edition was published, *Hazards in the Chemical Laboratory* has become established as a vital handbook in all types of laboratory environment. However, over this period many developments have taken place which justify changes in scope and emphasis.

This second edition contains completely new chapters on Reactive Chemical Hazards, and Chemical Hazards and Toxicology. The authors of the chapters in the original volume have also brought their contributions up-to-date in the light of changing attitudes and legislative changes that are in progress. The section dealing with hazardous chemicals has been greatly expanded so as to provide detailed information on the properties, warning phrases, injunctions, toxic effects, hazardous reactions, first aid treatments, fire hazards and spillage disposal procedures for all common laboratory chemicals, together with short notes on the hazardous properties and reactions of several hundred other less common chemicals.

### Brief contents

Introduction; Health and Safety at Work etc. Act 1974; Planning for Safety; Fire Protection; Reactive Chemical Hazards; Chemical Hazards and Toxicology; Medical Services and First Aid; Hazardous Chemicals; Safety in Hospital Biochemistry Laboratories; Precautions Against Radiations.

**480 pages (1977) ISBN 0-85186-699-9 hardback \$15.75**

Distributed by The American Chemical Society  
Published by The Chemical Society

**SIS/American Chemical Society**  
1155 16th St., N.W./Wash., D.C. 20036

Please send \_\_\_\_\_ copies of *Hazards in the Chemical Laboratory*, 2nd Edition at \$15.75 per copy.

☐ Check enclosed for \$ \_\_\_\_\_. ☐ Bill me.  
Postpaid in U.S. and Canada, plus 40 cents elsewhere.

Name \_\_\_\_\_

Address \_\_\_\_\_

City \_\_\_\_\_

State \_\_\_\_\_

Zip \_\_\_\_\_

## New Products

### Digital Colorimeter

Type 22 digital colorimeter can be used for all general colorimetric determinations and is especially valuable as a teaching aid because of its simple operation and variety of applications. Features include digital display calibrated in percent transmittance, front panel control to select any one of eight narrow band filters with wavelength peaks centered at 350, 420, 460, 490, 530, 610, and 660 nm, and a tungsten lamp light source. Chemtrix, Inc. **418**

### Hydrogen Generator

Model 8325 produces ultrahigh purity (10 ppb impurity) hydrogen from distilled water for flame ionization gas chromatography. Pressure can be precisely regulated at any flow setting. The hydrogen generator is rated at 150 mm/min STP at any pressure up to 60 psig. The hydrogen is generated by dissociating water with electricity and diffusing the hydrogen through a palladium alloy membrane. Matheson **413**

### Display Module

Model 1340A CRT display module is designed to be easily integrated into instrument or system consoles and can be purchased with or without controls and power supply. The compact module supplies resolution, viewing area, and brightness suitable for applications such as spectrum, network, and vibration analysis. Spot size is less than 0.46 mm at center screen, and line resolution is about 25 lines/cm. The CRT can write directly from analog circuits or from digital memory on a refreshed basis. \$1000. Hewlett-Packard Co. **415**

### High-Pressure Liquid Chromatography Cell

The cell is designed for use in Beckman DB and Cary 118 spectrophotometers and features an 8-ml. lightpath volume, path length of 10 mm, and an aperture diameter of 1.0 mm. The cell window is made of UV grade fused quartz and the body formed of 316 stainless steel with flow connections to the cell via two 0.062-in. diameter stainless steel tubes. Inlet flow is split into two streams that enter the optical path by flowing across the window, then combine and leave by a central port. Precision Cells Inc. **420**

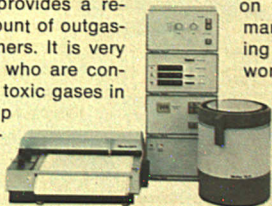
For more information on listed items, circle the appropriate numbers on one of our Readers' Service Cards





## Will the outgassing from the polymer be excessive?

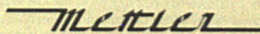
A Mettler thermal analysis system provides a reliable method for measuring the amount of outgassing of volatile materials from polymers. It is very useful to automotive manufacturers, who are concerned with the emission of possibly toxic gases in automobile interiors. Or it can help any user of plastic to verify the quality of materials received from suppliers. — Mettler helps solve problems in analytical laboratories and



on the production floors of industry. We market a variety of weighing and measuring instruments. All of them made with world-renowned Mettler craftsmanship. All of them backed by a worldwide team of highly-competent service specialists who can be there whenever you need them.

Mettler — instruments and people you can depend on.

## Depend on Mettler for the answer.

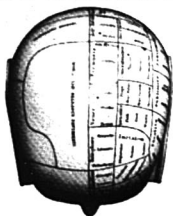


Electronic balances and weighing systems · Thermoanalytical instruments · Automatic titration systems · Laboratory automation

Mettler Instrumente AG, CH-8606 Greifensee-Zürich, Switzerland · Mettler-Waagen GmbH, D-63 Giessen 2, Postfach 2840, BRD  
Mettler Instrumenten B.V., Postbus 68, Arnhem, Holland · Mettler Instrument Corporation, Box 100, Princeton, N.J. 08540, USA

CIRCLE 143 ON READER SERVICE CARD

# MAGISCAN a special kind of freedom



Now  
there is  
a TV Image  
Analysis System  
that is totally flexible  
and allows decision processes  
of the brain to interact with a  
powerful and flexible mini  
computer.



Break away from the limitations  
of hard-wired  
modules and  
discover a  
special kind  
of freedom  
through  
MAGISCAN  
software.  
Magiscan -  
today's instrument that  
anticipate's tomorrow's problems...



## Joyce-Loebl

A Vickers Company

World Leaders in Image Analysis  
Marquisway, Team Valley, Gateshead NE11 1QW England  
Tel: 0632 822111 Telex: 53257

CIRCLE 114 ON READER SERVICE CARD

## New Products

### Gel Permeation Columns

MicroPak gel permeation columns are packed with microparticle, cross-linked TSK gels and have efficiencies in excess of 20 000 plates/m. Particles are spherical and 8-10  $\mu\text{m}$  in diameter, and each gel has a distinct pore size with a specific molecular exclusion limit. The range of pore sizes offered permits analysis and characterization of samples varying from homologous series with molecular weights less than 100, to large polymers and accompanying additives with molecular weights approaching one million. Varian Instrument Div. **407**

### UV-VIS Spectrophotometer

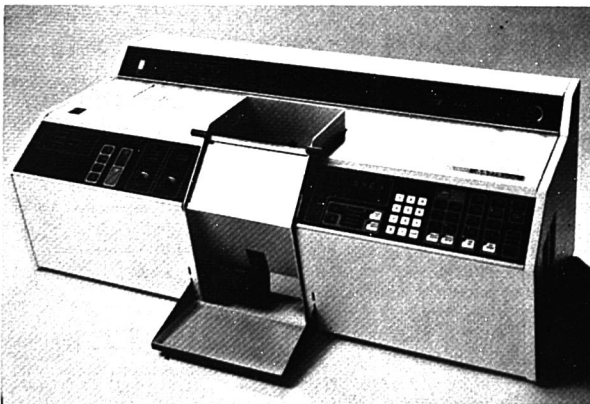
The Spectracomp 601 programmable spectrophotometer features a 190-850-nm range, auto source change, automatic baseline correction, 4-position sample and reference programmable cuvette holder with magnetic stirring, and temperature-controlled sample compartment. Other features include -3.5 to 3.5 A absorbance range; outputs to incremental plotter, TTY; and built-in alphanumeric printer, keyboard, and 32-character display for instrument interaction. Carlo Erba Strumentazione, P.O. Box 4342, 20100 Milano, Italy **409**

### Automatic Sample Injection Valve

This electropneumatically actuated automatic valve modifies amino acid analyzers and other liquid chromatographs for round-the-clock operation. It is rated for eluent pressures up to 70 atm (1000 lb/in.<sup>2</sup>), and the variable-volume loop-type stainless steel rotary valve can accommodate as many as 15 samples. An integrated circuit control module provides digital indication of valve position and shuts down the chromatograph after the last sample has been analyzed. Durrum Chemical Corp. **411**

### Multisampler

The Multisampler accessory is designed for use with the P-E Models 580, 283/281, X99 Series, and X97 Series infrared spectrophotometers. It fits into the sample slide of the spectrophotometer and is contained completely within the sample compartment. Samples are changed automatically upon command from the spectrophotometer. Fully automated sampling is possible for up to 30 consecutive samples in the form of KBr pellets or as polymer films. The accessory will not accept liquid samples. Perkin-Elmer Corp. **414**



AA 775 Series atomic absorption spectrophotometer features full microprocessor control for data collection, fast double beaming, background correction and absorbance conversion, and simplified execution of advanced data handling routines. These and other routines can be called for by single-function touch keys on the instrument control panel. The double-beam optical system ensures drift-free operation and includes a new 0.33-m Czerny-Turner monochromator with a high-dispersion 1800-line/mm grating and seven selectable slit widths. The automatic gas control system provides keyboard control of flame selection, ignition, and shut down. Accessories to complement the AA 775 include the CRA 90 carbon rod atomizer, the ADS 53 automatic sample dispenser, the DP 38 alphanumeric printer, and the M51 automatic sample changer. Varian Instrument Div. **403**



# THE LECO® EC-12 CARBON DETERMINATOR

**AUTOMATIC  
DIRECT READING  
AND  
AFFORDABLE**



Contact LECO® for information or a demonstration.



LECO CORPORATION 3000 Lakeview Ave. St. Joseph, MI 49085, U.S.A. Phone: (616) 983-5531

CIRCLE 126 ON READER SERVICE CARD

ANALYTICAL CHEMISTRY, VOL. 50, NO. 4, APRIL 1978 • 471 A

# Reliable. Fast and Easy. MCI automatic analyzer.

Incorporates coulometry principle applied to Karl Fischer titration. Operation is full-automatic. Measuring time is shortened. Accuracy is within 5 $\mu$ g for 10 $\mu$ g–1mg H<sub>2</sub>O and within 0.5% for 1–30mg H<sub>2</sub>O. Wide-range applications include measurement of ultra-trace water content in liquids, solids and gases. Range: 10 $\mu$ g–30mg H<sub>2</sub>O. An optional water vaporizer for speedy and accurate measurement of water content in plastics, grain, etc.

Printer (optional)



CA-02 Moisture Meter with Printer

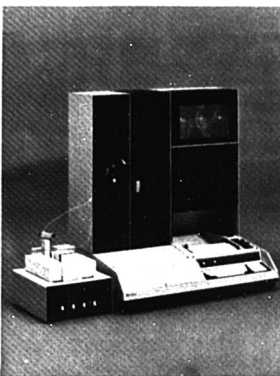


MITSUBISHI CHEMICAL INDUSTRIES LIMITED

Instruments Dept., Mitsubishi Bldg., 5-2, Marunouchi 2-chome, Chiyoda-ku, Tokyo, 100 Japan. Telex: J24901 Cable Address: KASEICO TOKYO

CIRCLE 144 ON READER SERVICE CARD

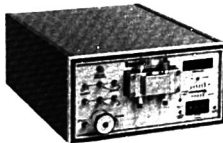
## New Products



The liquid chromatography autosampler is designed for use with the SP8000 high-pressure liquid chromatograph. The autosampler is microprocessor controlled by the SP8000. It holds up to 210 samples in multiple test tube racks. Each tube may be covered by a thin plastic cap to prevent evaporation and release of toxic vapors. A sipper needle pierces the cap as each tube is brought to the sampling position, and a peristaltic pump transports the sample to the injector loop of the chromatograph. Spectra-Physics 404

new

## Liquid Chromatography Instruments from Tracor

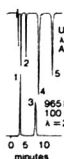


Tracor Model 950 Pump

CIRCLE 206 ON READER SERVICE CARD

- Flow rates from .01 to 40 ml/min.
- Pressures to 10,000 psi (to 10 ml/min)
- Compressibility auto-compensation
- Overpressure control
- Constant flow or constant speed
- Easy priming
- Pressure relief valve
- Moderate price

Pesticides with  
Aromatic Hydrocarbons



UV Detector  
 $\lambda = 254$  nm  
 $A = 0.32$

Tracor Model 965  
Photo-conductivity  
Detector

- 1 Benzene — 12  $\mu$ g plus
- 2 Dichlorobenzene — 200 ng
- 3 Naphthalene — 1  $\mu$ g
- 4 Phenanthrene — 0.8  $\mu$ g
- 5 Pyrene — 1  $\mu$ g



The FIRST halogen specific detector for  
Liquid Chromatography

CIRCLE 207 ON READER SERVICE CARD

Tracor Instruments

Tracor, Inc. 6500 Tracor Lane Austin, Texas 78721 Telephone 512-926 2800

## Spectroscopy Amplifier

Model 572 single-NIM-width nuclear spectroscopy amplifier features a built-in pulse-pileup rejector and gated baseline restorer that includes automatic threshold control. The pulse-pileup rejector significantly reduces background throughout the selected energy range and minimizes spectrum distortion at high count rates. Newly developed active filter pulse-shaping networks result in symmetrical outputs over a wide range of time constants. Excellent dc stability eliminates spectrum broadening caused by dc drift, and enables the user to get the best possible performance out of any modern detector. EG&G Ortec 419

## High-Frequency Lock-in Amplifier

Model 5202 100 kHz to 50 MHz lock-in amplifier is a powerful tool for the extraction of low-level signals from background noise. Features include megahertz range performance, microvolt level sensitivity, two-phase operation, high dynamic reserve, dual-channel output zero expansion and time constant, calibrated phase shifter, and a tracking reference channel. Princeton Applied Research Corp. 421



# Manufacturers' Literature

**Oscilloscopes.** Describes five new dual-trace oscilloscopes, Models OS 4000, OS 3300B, OS 1100, OS 260, and OS 245A. 4 pp. Gould Inc., Instruments Div. **425**

**Electronic Balances.** Features four Ainsworth top-loading electronic balances with single touch-bar for instant tare and instant sample readout on LED display. 8 pp. Fisher Scientific Co. **426**

**IR Optical Components.** Standard components available include wave plates, stacked plate polarizers, dispersive prisms, precision beam splitters, windows, and partial reflectors. Interactive Radiation, Inc. **427**

**Nuclear Electronic Modules.** Presents a full range of amplifiers, preamplifiers, analyzers, power supplies, ratemeters, scalars, timers, and many other NIM's. The Harshaw Chemical Co. **428**

**Liquid Scintillation Counting.** Provides information on an automatic quench compensation technique developed for use on the LS-8000 Series instruments. 14 pp. Beckman Instruments, Inc. **429**

**Iodine-125.** Safe handling guide includes sections on proper assay techniques, regulatory limits, methods of detection, and recommended handling procedures. 12 pp. Products brochure features Iodine-125 in a variety of concentrations as well as related kits and standards. 12 pp. New England Nuclear **430**

**Monochromators.** Describes the QPM 30 and QPM 30S quartz prism monochromators incorporating a modified Littrow mount with 60° quartz prism. 4 pp. Schoeffel Instrument Corp. **431**

**UV-VIS Spectrophotometers.** Provides a description of design and performance and a collection of five two-page data sheets on the 57-Series high performance UV-VIS spectrophotometers. Perkin-Elmer Corp. **432**

**Image Processing.** This introduction to computer-assisted image processing and analysis covers image enhancement, information extraction, and quantitative restoration in a wide variety of applications. 13 pp. Optronics International **435**

**Potentiostat and Waveform Generator.** Model MP-1026A 50W potentiostat is a combination high-voltage potentiostat, programmable power supply, and oper-

ational amplifier. The Model MP-1505 waveform generator is designed to operate in conjunction with the potentiostat by generating voltage ramps that are reproduced at the output of the potentiostat. 2 pp. Pacific Photometric Instruments **434**

**Ultracentrifuge Methods for Lipoprotein Research.** Explains the medical significance of elevated blood levels of cholesterol, types of lipoproteins, and how ultracentrifugation aids research. 12 pp. Beckman Instruments, Inc. **433**

**Automated Determination of Benzene.** Describes the determination of benzene adsorbed on charcoal tubes by an HP 5830/40A gas chromatograph equipped with an automatic liquid sampler. 4 pp. Hewlett-Packard Co. **436**

**UV-VIS Spectrophotometer.** Features the Model 200 double-beam instrument with digital ordinate display, recorder readout, three time constants, and continuously variable bandpass. 8 pp. Perkin-Elmer Corp. **437**

**Gas-Chrom Newsletter.** January issue features articles on the Meth-Prep II esterification reagent, the aflatoxin assay minicolumn, and guaranteed drug packings. 8 pp. Applied Science Laboratories, Inc. **438**

**Automatic Sample Dispenser.** Describes the ASD-53 and its use with the CRA-90 carbon rod atomizer in atomic absorption spectrometry. 8 pp. Varian Instrument Div. **439**

**Sample Vials.** Features a broad line of vials and accessories including auto-sampler vials, polypropylene Cryule vials, and sample storage vials and cases. 4 pp. Wheaton Scientific **440**

**Energy-Dispersive X-ray Fluorescence Spectrometry.** Two application notes describe the analysis of limestone and dolomite and the elemental analysis of oil by energy-dispersive x-ray fluorescence. EG&G Ortec **441**

**Moisture Determination Balance.** Describes the operation and applications of the Models 6010 with capacity of 10 g and the 6100 with capacity of 100 g. 6 pp. Ohaus Scale Corp. **450**

For more information on listed items, circle the appropriate numbers on one of our Readers' Service Cards



Pedersen builds strip chart recorders so accurate, flexible, easy to operate, free of trouble and easy to buy, we call them Workhorses. First, the single channel Model 27MR. Second, the 27MR with Integrator or Event Marker. Third, the 37MR Dual Channel Model. And fourth, exciting new recorders on the drawing boards. For particulars, write or call Svend Pedersen

From \$695.00

## Pedersen

Pedersen Instruments of Walnut Creek  
2772 Camino Diablo  
Walnut Creek, CA 94596  
(415) 937-3630

CIRCLE 163 ON READER SERVICE CARD

## Join the Barnes Special-of-the-Month Club and save on analytical accessories.

Each month in 1978 Barnes is featuring a special on IR analytical accessories. Offers include 10 and 20% discounts on transmission windows and cells, free gifts and useful application notes.

Each offer will be effective for one month only. To know about them in advance, join the Barnes Special-of-the-Month Club. Simply send us your name, title, organization. Clip out this ad and return it to us. We'll send you Barnes latest Infrared Analytical Accessories Catalog as well. You can't get the specials until Barnes gets your name, so act now! Write Barnes Engineering Co., 30 Commerce Rd., Stamford, Ct. 06904; or call us toll-free at (800) 243-3498.



Name \_\_\_\_\_

Title \_\_\_\_\_

Address \_\_\_\_\_

City/State/Zip \_\_\_\_\_

AC-4

CIRCLE 21 ON READER SERVICE CARD

## SEQUENTIAL PLASMA SPECTROANALYZER

Better than AA, the JY-38 high resolution spectroanalyzer, using an Inductively Coupled Plasma, offers unequalled speed, sensitivity and accuracy. Most elements, including B and P, can be analyzed in such materials as metals, alloys, coal, oils, rare earths, soils, ores, water pollutants, pharmaceuticals and biologicals.

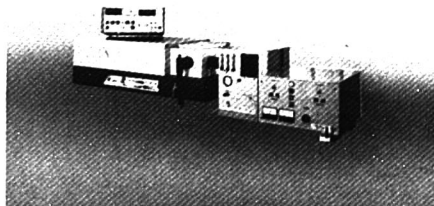
Advantages include holographic gratings permitting high accuracy. Repeatability in excess of 1%, dynamic range of  $10^5$  down to nanogram/ml. Send today for the details on the JY-38 and our JY-48 Simultaneous Spectroanalyzer.

Instruments SA, Inc., J-Y Optical Systems Division, 173 Essex Avenue, Metuchen, N.J. 08840. (201) 494-8660, Telex 844-516. In Europe, Jobin Yvon, Division d'Instruments SA, 16-18 Rue du Canal, 91160 Longjumeau, France, Tel. 909.34.93 Telex JOBYVON 842-692882.

**JOBIN  
YVON**



**Instruments SA, Inc.**  
J-Y Optical Systems Division



CIRCLE 111 ON READER SERVICE CARD

## Manufacturers' Literature

**Differential Scanning Calorimeter.** Discusses operation and applications of the Model DSC-2 which features improved subambient operation and automated data handling. 18 pp. Perkin-Elmer Corp. **442**

**Liquid Chromatography Bibliography.** Describes new service available listing newly published technical articles in liquid chromatography. 6 pp. Perkin-Elmer Corp. **444**

**Optical Emission Spectroscopy. The Spex Speaker, September 1977,** features an article on the inductively coupled plasma torch as a source for OES. 7 pp. Spex Industries, Inc. **445**

**Identification of Drugs of Abuse.** Describes the use of the CIRA 101 chromatographic infrared analyzer coupled with any standard dispersive infrared spectrometer in the analysis of mixtures of drugs of abuse. Sadler Research Laboratories, Inc. **446**

**X-ray Fluorescence Spectrometry.** Describes the Ultra-Trace system for non-destructive determination of elements present in concentrations below 1 ppm. 6 pp. Kevex Corp. **447**

**Gas Chromatography/Mass Spectrometry. Finnigan Spectra, January 1978,** features articles on chemical ionization in GC/MS, the use of internal standards in mass-fragmentography, and the study of large molecules by pyrolysis/MS. 8 pp. Finnigan Corp. **448**

**Preparing Your Laboratory for Atomic Absorption Spectrometry.** Provides detailed instructions regarding space and accessories required to operate P-E atomic absorption spectrophotometers. 9 pp. Perkin-Elmer Corp. **449**

**UV-VIS Application Literature.** Bulletins available describe  $T_m$  measurements of polynucleotides, a recently developed scatter transmission accessory for the Model 57 Series UV-VIS instruments, and limitations in photometric standards. Perkin-Elmer Corp. **443**

## Catalogs

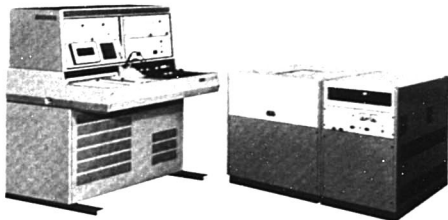
**Fume Hoods.** Uniflow fiberglass laboratory fume hoods include conventional, air by-pass, auxiliary air, and portable models. Hemco Corp. **457**

**Thermocouple Wire.** Lists full line of bare thermocouple wire, insulated thermocouple wire, and extension wire for use in temperature measurement applications. 8 pp. Nanmac Corp. **469**

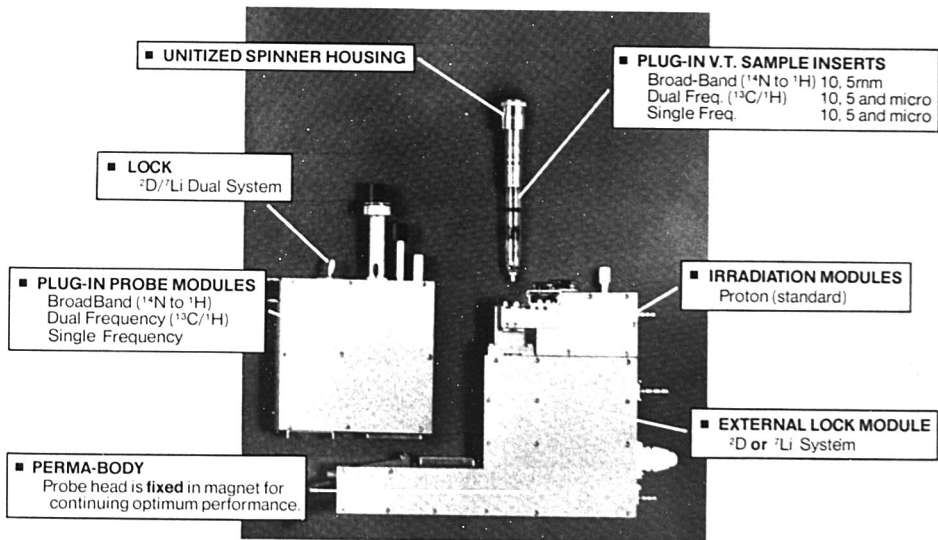
# The FX90Q

featuring the

## OMNI PROBE



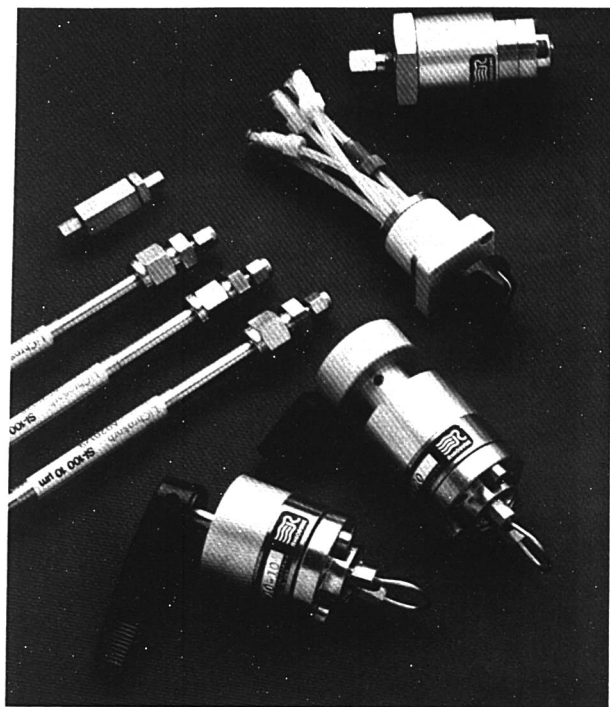
In the continuing development of the FX series, JEOL now offers a compact, 90 MHz, broad-band, FT NMR System at a cost comparable to the lower frequency systems. The "OMNI PROBE"™ system is designed to provide the highest performance throughout the **entire** observation range.



# JEOL

235 Birchwood Ave., Cranford, NJ 07016  
201-272-8820

CIRCLE 115 ON READER SERVICE CARD



## You can't get a good chromatogram without a great beginning. We make it happen!

### VALVES, WELL PACKED HPLC COLUMNS AND FILTERS

In a way, we're sort of the front-end company in high pressure liquid chromatography. Almost everything you need to make better chromatograms in the beginning is on our shelf. Here's our line to you:

**The 70-10 Sample Injection Valve.** For just \$290 you can get our 6-port sample injection valve with a removable sample loop and 7000 psi pressure rating. Size, 10  $\mu$ l to 2.0 ml.

**The 7120 Syringe Loading Sample Injector.** Fill loops conventionally or in the partial loop variable volume mode with only 0.5  $\mu$ l sample loss.

**Teflon Rotary Valves.** For about half the cost you'd expect to pay, we offer three, four and six way valves in 0.8 mm and 1.5 mm bores at \$70 to \$87. Features zero dead volume, chemical inertness and 300 psi rating.

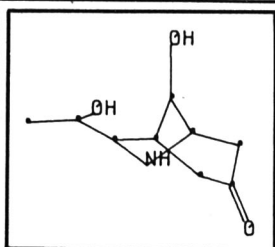
**HPLC Columns.** Here are the columns with guaranteed peak symmetry and minimum plates per meter to doubly assure optimum column performance. Six columns currently available priced from \$180 to \$240.

**The Column Inlet Filter.** It only costs a few dollars, but it can save you a boatload of trouble. Place this low dead volume filter between the injection valve and column to protect column inlet frits from plugging. Price, \$40.

**The Model 7037 Pressure Relief Valve.** Protect your set-up against damage from over pressure (2000 to 7000 psi setting range).

**Write or call for more information.**  
Address Rheodyne, Inc. 2809 Tenth Street, Berkeley, CA 94710. Phone (415) 548-5374.

  
**RHEODYNE**  
THE LC CONNECTION COMPANY  
CIRCLE 176 ON READER SERVICE CARD



## Computer-Assisted Structure Elucidation

ACS Symposium Series No. 54

Dennis H. Smith, Editor  
Stanford University School of Medicine

A symposium sponsored by the  
Division of Chemical Information  
of the American Chemical Society.

An up-to-date report on the growing use of computers to assist in the identification of complex unknown molecular structures in the laboratory.

The collection covers such diverse methodologies as library search techniques, pattern recognition, artificial intelligence programs, automated interpretation of chemical data, structure generation, and ranking of candidate structures based on prediction of chemical or spectroscopic behavior.

### CONTENTS

Structure Identification of Unknown Mass Spectra •  
Components of Complex Mixtures by GC-MS •  
NIH-EPA Chemical Information System •  
Determination of the Secondary Structure of Globular Proteins •  
Automatically Acquired  $^{13}\text{C}$  NMR Rules •  
Computerized Structural Predictions from  $^{13}\text{C}$  NMR Spectra •  
Interactive Structure Elucidation •  
CHEMICS: A Computer Program System for Structure Elucidation of Organic Compounds •  
Computer Assistance for the Structural Chemist

151 pages (1977) clothbound \$15.50  
LC 77-24427 ISBN 0-8412-0384-9

**SIS/American Chemical Society**  
1155 16th St., N.W./Wash., D.C. 20036

Please send \_\_\_\_\_ copies of SS 54  
Computer-Assisted Structure Elucidation at \$15.50

☐ Check enclosed for \$\_\_\_\_\_. ☐ Bill me.  
Postpaid in U.S. and Canada, plus 40 cents elsewhere.

Name \_\_\_\_\_  
Address \_\_\_\_\_  
City \_\_\_\_\_ State \_\_\_\_\_ Zip \_\_\_\_\_



**Laboratory Instruments and Supplies.** Includes information on atomic absorption systems, blood gas instrumentation, chemistry analyzers, electrolyte and related instrumentation, electrophoresis system, electrodes and probes, and expendable supplies. 20 pp. Instrumentation Laboratory Inc. 453

**Research Chemicals.** Lists nearly 400 high-purity intermediates including butanediamines, ethylenediamines, hexanediamines, aliphatic amines, polyamines, propanediamines, oximes, aldimines, nitrosamines, and hydroxyamines. 23 pp. The Ames Laboratories, Inc. 454

**Electron Microscopy and Electrophoresis Supplies.** Includes immunochemicals, laser dyes, polymer standards, histology/cytology supplies, and over 7000 reagents. 216 pp. Polysciences, Inc. 456

**Laboratory Instruments.** Includes information on filter fluorometers, spectrofluorometers, spectrophotometers, flame photometers, and a wide variety of accessories. 48 pp. Turner Associates 459

**Electronic Test Instrumentation.** Gives complete descriptions and specifications for oscilloscopes, laboratory grade strip and X-Y recorders, power supplies, signal and function generators, counters, multimeters, and associated accessories. 32 pp. Heath/Schlumberger Instruments 455

**Biomedical Supplies.** Lists over 1000 items including pipettors and tips, filter paper, membrane filters, dialysis membranes, liquid scintillation vials, and micro columns for isolation of drug metabolites and separation of steroids. 33 pp. California Scientific 458

**Lipid Handbook.** Features chemical structures and physical and chemical properties of fatty acids, esters, glycerides, phospholipids, glycolipids, tocopherols, steroids, bile acids, and selected carbohydrates. 98 pp. Supelco, Inc. 460

**Medical Products.** Contains complete line of medical products and services including products for blood gas analysis, electrolytes, radioimmunoassay, hematology, electrophoresis, and densitometry. 40 pp. Corning Medical, Corning Glass Works 470

**Books.** Describes 170 books on all phases of energy, air pollution control, water analysis and treatment, waste treatment and disposal, trace elements, and includes biochemistry, chemistry,

chemical engineering, food and agriculture, physics, electricity, particle analysis, engineering, and optics. 80 pp. Ann Arbor Science 461

**Electrochemical Instrumentation.** Details all the Metrohm products available for potentiometric measurements including titrators, pH meters, polarographic analyzers, and accessory systems. 52 pp. Brinkmann Instruments Inc. 463

**Syringes and Chromatography Accessories.** Features complete line of Unimetrics' micro syringes and liquid chromatography accessories and columns. 41 pp. Bradford Scientific, Inc. 462

**Radiochemicals.** Features over 1000  $^{14}\text{C}$ ,  $^3\text{H}$ ,  $^{32}\text{P}$ ,  $^{125}\text{I}$ , and  $^{35}\text{S}$  labeled chemicals as well as amino acid kits, radionuclides, and radioactive standards. 132 pp. New England Nuclear 466

**The Diagnostics Division of Abbott Laboratories is seeking several Biochemical Scientists to participate in one of the fastest growing and most dynamic divisions of our health care firm.**

*Candidates having the following qualifications are invited to apply:*

## Biochemist/Immunologist

A PhD in Immunology, Biochemistry or a related science coupled with at least 2-5 years experience in a research/development laboratory that involved enzymology, serology, endocrinology, virology, protein chemistry, radioactivity or infectious disease work will be required. Candidates should also have a background in purification of antigens and antibodies plus a working knowledge of diagnostic test systems, sophisticated lab equipment and instruments. Demonstrated ability to direct broad based projects with significant autonomy is preferred.

## Manager/Diagnostics Research & Development

We seek an individual with a PhD in Biochemistry, Immunology or a related science coupled with at least 2-5 years managerial experience in a research/development laboratory. Preferred candidate should have experience with in vitro diagnostic products and be strongly motivated. A demonstrated record of leadership, technical and organizational skills will be required.

## Biochemists/Diagnostic Applications

A PhD or equivalent in a biochemical science with at least 2 years of industrial experience which includes practical knowledge of immunological assay systems, GMP and general industrial development/manufacturing requirements will be required. The individuals we seek will be responsible for providing technical support to production of current products and the introduction of new products. Demonstrated ability to interact with both R & D and Operations functions is preferred. Previous clinical laboratory or project management experience and good communications skills are desired.

*We will look for a strong track record of accomplishment in the above areas as indicated by publications, patents, and independent research experience. The persons we seek will be highly motivated, capable of independent work, and will possess the ability to manage complete projects.*

*If qualified and interested in an advancement oriented career, send a resume with salary history, in complete confidence, to:*

**ABBOTT**  
NORTH CHICAGO, ILL. 60064

Maria Marciano  
Corporate Placement

*Abbott is an Affirmative Action Employer*

CIRCLE 3 ON READER SERVICE CARD

# Swagelok®

## Tube Fittings (1/16" to 1")

### Install them. Forget them.

Swagelok® Tube Fittings make their seal and grip the tubing in a patented way that allows you to forget tubing connections as a source of trouble in your system. They offer the industry's widest choice of standard sizes, shapes and materials to meet your needs exactly. *And they're locally available, off the shelf, from your Full Service Distributor.*



Patented

CRAWFORD FITTING COMPANY  
29500 Solon Road, Solon, Ohio 44139  
Crawford Fittings (Canada), Ltd., Ontario

CIRCLE 32 ON READER SERVICE CARD

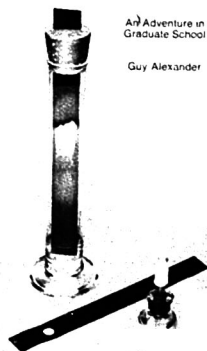
# Ion-Exchange Resins and Chromatography

**Chromatography: An Adventure in Graduate School.** Guy Alexander. 163 pages. American Chemical Society, 1155 Sixteenth St., N.W., Washington, D.C. 20036. 1977. \$7.50 (\$4.50, paper-bound)

Reviewed by James M. Bobbit, Dept. of Chemistry, University of Connecticut, Storrs, Conn. 06268

In this book, Professor Alexander has presented a reminiscence of his graduate school experience and, as a part of this experience, has attempted to present an overview or an introduction to ion-exchange resins and chromatography. The reminiscence is quite successful, although I felt that there was a little *too much* chemistry at times. However, as a technical book, it is less successful, and the main title "Chromatography" implying such is most unfortunate. Actually, the book is more devoted to ion-exchange resins than it is to chromatography.

## CHROMATOGRAPHY



As a reminiscence of Professor Alexander's experience as a graduate student at the University of Wisconsin just before and just after World War II, the book was a delight to read. Rarely does one find a scientist, at least a chemist, writing dialog and writing it so successfully. The trauma of being married and in graduate school at a great university with all of the tensions and pleasures attendant

is beautifully presented. The author has managed to describe accurately the fascination and enthusiasm that many of us, this reviewer included, felt when we first encountered chromatography and ion-exchange resins and realized what fabulous things one could do with these concepts and materials.

The overview and introduction of chromatography are presented through the medium of a seminar, at least partially mythical, given by another graduate student named Jim. Such a seminar would have some historical interest, but is not an effective method for presenting technical material. Besides, the bell rang, and the "seminar" was over just when it started to become interesting. The introduction to ion-exchange resins and their use in chromatography is exceptionally well presented and was in fact the subject of the author's thesis (specifically, the separation of rhenium and molybdenum salts by ion-exchange chromatography). In the Appendix, discussions of some gas chromatography theory and distillation column theory including the ubiquitous "theoretical plate" concept are given. The actual description of gas chromatography in the text is given in such a cursory fashion that the theoretical discussion seems almost pointless. The description of distillation column theory as a key to chromatography is not often found and is most useful. Thin-layer chromatography is mentioned only as thin-film chromatography and is discussed as it existed about 20 years ago.

In summary, the book is interesting as a reminiscence but would not be a very useful technical book.

**Introduction to Semimicro Qualitative Analysis, 5th Ed.** C. H. Sorum and J. J. Lagowski. x + 309 pages. Prentice-Hall, Inc., Englewood Cliffs, N.J. 07632. 1977. \$8.95

Reviewed by Stanley T. Marcus, Dept. of Chemistry, Cornell University, Ithaca, N.Y. 14853

As in previous editions, this well-known book is divided into two parts, the first of which is concerned with the theory, i.e., the underlying facts and principles and the logic behind qualitative analysis. The second part consists of the systematic procedures

using the traditional  $H_2S$ -based analytical scheme. Except for a few very minor changes, such as verifying zinc using diphenylthiocarbazon paper instead of using  $K_4Fe(CN)_6$ , Part II has been left as it was, a thoroughly tested set of procedures. Part I, on the other hand, has been almost completely rewritten, and it has been expanded considerably (from 86 to 137 pages).

Surprisingly, in the revision of Part I, a number of important topics, such as the relationship between ionic strength and activity to molar solubility and solubility product, were eliminated. The new edition states without qualification, "The entire sample of an ionic substance exists as ions in solution."

The section on chemical kinetics has been expanded and updated considerably. Except for the fact that the topic of inhibitors is introduced without adequate explanation, the presentation is straightforward. The treatment of free energy and equilibrium, on the other hand, is very weak, and at times, misleading. It states, for example, "The relationship between the equilibrium constant for a reaction and the free energy of the system is given by...  $G = -RT \ln K$ ."

Topics given more thorough treatment in this edition include acid and bases, stepwise ionization, hydrolysis, buffers, solubility, and colloids. Unfortunately, neither the Bronsted-Lowry nor the Lewis acid-base systems are utilized. It was somewhat distressing to see the unqualified use of the symbol " $NH_4OH$ " for aqueous ammonia. The expanded discussion of colloids represents a distinct improvement, in that colloid formation is a frequent source of frustration to students in qualitative analysis.

Another topic given more thorough coverage is bonding in complex compounds. The discussion of crystal field theory is generally straightforward, but it contains several careless errors. An energy diagram (page 97) is mislabeled, for example, and it is suggested that crystal field stabilization energy results from a gain, rather than a lowering, energy of the  $t_{2g}$  orbitals in an octahedral field compared with their energy in a spherical field.

In general, I think the revision represents an improvement over the previous editions, but I feel it could have been written with more care. In any

## ANALYSIS OF FOOD AND BEVERAGES

### Headspace Techniques

Edited by GEORGE CHARALAMBOUS

*Proceedings of a symposium organized by the Food Sub-division of the Agricultural and Food Chemistry Division of the American Chemical Society at the 174th national meeting, Chicago, Aug. 27-Sept. 2, 1977.*

CONTENTS: S. G. Wyllie et al., Headspace Sampling: Use and Abuse. H. Maarse and J. Schaefer, Quantitative Headspace Analysis: Total and Specific Group Analysis. F. Z. Saleeb and T. W. Schenz, A Technique for the Determination of Volatile Organic Compounds under Equilibrium and Non-Equilibrium Conditions. A. L. Boyko et al., Porous Polymer Trapping for GC/MS Analysis of Vegetable Flavors. D. A. Withycombe et al., Isolation of Trace Volatile Constituents of Hydrolyzed Vegetable Protein via Porous Polymer Headspace Entrapment. I. Klimes and D. Lamparsky, Headspace Techniques Utilized for the Detection of Volatile Flavor Compounds of the Vanilla Bean. O. G. Vitzthum and P. Werkhoff, Aroma Analysis of Coffee, Tea, and Cocoa by Headspace Techniques. E. D. Lund and H. L. Dinsmore, Determination of Citrus Volatiles by Headspace Analysis. J. T. Hoff et al., Flavor Profiling of Beer Using Statistical Treatments of GLC Headspace Data. A. C. Noble, Sensory and Instrumental Evaluation of Wine Aroma. H. Akiyama et al., Sake Flavor and Its Improvement Using Metabolic Mutants of Yeast. R. ter Heide et al., Concentration and Identification of Trace Constituents in Alcoholic Beverages. D. A. Mackay and M. M. Hussein, Headspace Techniques in Mouth Odor Analysis. J. A. Singleton and H. E. Pattee, Headspace Techniques Used in the Analysis of Volatile Components from Lipoxygenase Catalyzed Reactions.

1978, 416 pp., \$21.00/£13.65 ISBN: 0-12-169050-4

## GAS CHROMATOGRAPHY WITH GLASS CAPILLARY COLUMNS

By WALTER JENNINGS

CONTENTS: Introduction. The Glass Capillary Column. Column Coating, Inlet Systems. Column Installation. Measuring Column Efficiency. Treatment of Retention Data. Temperature Programming and Carrier Flow Considerations. Column Stability. Column Selection. Sample Preparation. Analysis of Materials of Restricted Volatility. Applications of Glass Capillary Gas Chromatography. Appendix I. Nomenclature. Appendix II. Liquid Phases. Appendix III. Porous Polymer Data. Appendix IV. Silylation and Derivatization Reactions.

1978, 200 pp., \$16.50/£11.70 ISBN: 0-12-384350-2

## pH MEASUREMENTS

By C. CLARK WESTCOTT

*pH Measurements* provides a basic, practical source of information about the principles, equipment and technique of this operation. Based on the author's experience with pH measurement for over a decade, this simplified guide is geared to laboratory applications for problem solving, training personnel, and obtaining accurate results. Chapters cover the theory of pH, characteristics, care, and performance of pH equipment and standard solutions, the use of proper technique in difficult applications, and troubleshooting, with examples drawn from everyday laboratory and field experience.

1978, 192 pp., \$16.00/£10.40 ISBN: 0-12-745150-1

Send payment with order and save postage plus 50¢ handling charge.

Prices are subject to change without notice.

## ACADEMIC PRESS, INC.

A Subsidiary of Harcourt Brace Jovanovich, Publishers  
111 FIFTH AVENUE, NEW YORK, N.Y. 10003  
24-28 OVAL ROAD, LONDON NW1 7DX  
CIRCLE 4 ON READER SERVICE CARD

## Books

case, the portion of the book likely to be used to the greatest extent is Part II, which remains very clear and error free.

**Trace Analysis of Atmospheric Samples.** Eikuo Oikawa. viii + 158 pages. Halsted Press, 605 Third Ave., New York, N.Y. 10016. 1977. \$22.50

Reviewed by E. W. Bretthauer, U.S. Environmental Protection Agency, Environmental Monitoring and Support Laboratory, P.O. Box 15027, Las Vegas, Nev. 89114

This book is intended to describe the most recent methods for sample collection and analysis of metals in atmospheric particulates. The book was reviewed for use (1) as a reference book for the professional environmental analyst and (2) the student who desires a primer for background information. The sampling and the sample pretreatment sections meet the latter requirement but are far too brief and incomplete for a reference book, i.e., sample siting criteria are contained in one short paragraph without references. In practice, the professional environmental analyst would need much more information to adequately conduct atmospheric particulate sampling of metals. The analytical section was found inadequate for either purpose. The major deficiencies in the analytical section are as follows.

1. Much of the information is out-of-date. For example, the described NASN method for emission spectroscopy analyses of air filters is approximately 10 years out-of-date. Many improvements have been made to the described NASN method and have been available in the literature for some time.

2. The author's greater familiarity with atomic absorption analysis appears to unfairly bias him against the other analytical techniques. For example, he states that optical emission is an expensive analytical technique for single sample analysis. In reality, single sample analysis by optical emission spectroscopy may be less expensive than comparable analyses by atomic absorption, depending on the number of elements analyzed in a sample. The author also states that atomic absorption analysis always provides lower detection limits than emission spectrometry with the exception of vanadium. Actually, the detection levels of the modern inductively coupled argon plasma optical emission spectrometer in most cases are equal to detection levels obtained by conventional atomic absorption.

3. Some of the information on ana-



# INTRODUCING I-DARSS

## Unparalleled sensitivity for rapid UV, VIS, near-IR spectroscopy.

Tracor Northern's new Intensified Diode Array Rapid Scan Spectrometer system combines the most recent advances in image intensification, fiber optics, and detector array development to provide the highest sensitivity, widest dynamic range, and lowest noise of any optical spectroscopy system available. I-DARSS enables you to perform previously impossible low-level spectral measurements, even of rapidly changing phenomena such as encountered in pulsed laser measurements. Consider these features:

**Simultaneous detection in up to 1024 channels.** I-DARSS simultaneously acquires information for all wavelengths imaged.

**Single photoelectron detection.** Maximum sensitivity

is up to 4 times greater than needed to detect single photoelectrons.

**Broad spectral coverage.** Advanced UV scintillator-extended ERMA response for the highest quantum efficiency available from 200-900 nm.

**Detector resolution of up to 25 line pairs/mm.** Your application's resolution

requirements can be met by interfacing the detector to the spectrometer of your choice, with twice the simultaneous spectral coverage of any other system.

**Dynamic range > 4000:1.**

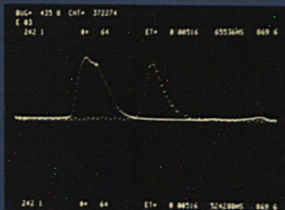
Thermoelectric cooling of the detector provides low noise and extended signal integration.

**Versatile signal averaging capability.** Detector exposure times and repetitive scans are adjustable over a wide range, giving you the highest S/N for your application.

**Modular, microcomputer-based TN-1710 signal analyzer** provides convenient firmware control of data acquisition, processing, and display. Accessories include floppy disk for mass storage of spectra and operating programs.

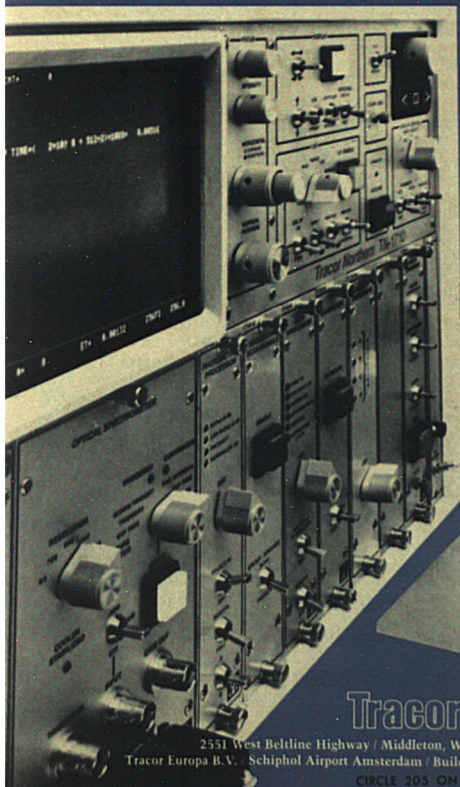
I-DARSS has the sensitivity to meet your spectral measurement needs with the highest speed and the lowest noise. Some applications are luminescence, fluorescence, and Raman spectroscopy, and chemical kinetics measurement.

Contact us for assistance in applying I-DARSS to your application or for a demonstration.



5-millisecond molecular fluorescence spectrum. Spectra can be expanded and overlapped for comparison. In addition to spectral data, all measurement parameters are displayed.

Modular TN-1710 microcomputer-based signal analyzer



TN-1223 Intensified DARSS detector

TN-1150 Holographic grating spectrograph

## Tracor Northern

2531 West Beltline Highway / Middleton, Wisconsin 53562 / (608) 831-6511 / TWX-910-280-2521  
Tracor Europa B.V. / Schiphol Airport Amsterdam / Building 106, The Netherlands / Telephone (020) 41 1865 / Telex 13695

CIRCLE 205 ON READER SERVICE CARD

lytical techniques is incorrect. For example, x-ray fluorescence, described as an absolute method, is certainly not. Appropriate standards are always necessary for calibration. The author's statement that x-ray fluorescence has an accuracy of 2-3% obviously is not correct. Poor syntax may be responsible for some of the incorrect material.

4. Many references that should be cited are not and many cited are out-of-date.

The editing of the book is very poor. There are numerous typographical errors. Many instances of poor syntax (e.g., standard adding in place of standard addition) are noted throughout.

**Solvent Extraction Chemistry: Fundamentals and Applications.** Tatsuya Sekone and Yuko Hasegawa. xii + 919 pages. Marcel Dekker, Inc., 270 Madison Ave., New York, N.Y. 10016. 1977. \$75

*Reviewed by A. S. Kertes, Dept. of Inorganic and Analytical Chemistry, The Hebrew University, Jerusalem, Israel*

According to the Contents, the book is divided into two parts, Fundamentals and Applications. In reality, however, it consists of three almost equal parts, with the third constituting 292 pages of references.

The Fundamentals part, of which I am rather critical, begins with an introductory chapter describing the development of the solvent extraction technique in the inorganic and analytical chemistry fields. It gives a rather fragmentary listing of review articles and monographs that have appeared up to 1972, the last year covered by the book. With the exception of one monograph, no mention is made of the extensive list of Russian books published in the field, several of which have been translated into English. I will mention just three I consider important: Fomin: "Chemistry of Extraction Processes" (English translation 1962), Shmidt: "Amine Extraction" (English translation 1971), and a very useful bibliography for the period 1945-1967, compiled by Bargeev et al.: "Extraction of Inorganic Compounds" (1971), containing some 10 000 entries. Also missing from the list is a 600-page monograph, "Recent Advances in Liquid-Liquid Extraction", edited by Hanson, published in 1971, and since translated into German and Russian. Numerous books, monographs, and conference proceedings have appeared since 1972, and it is unfortunate that the list of refer-

ences to this introductory chapter was not brought up-to-date when the camera-ready typed pages were proofread.

Chapter 2 could easily have been omitted. Its 50 pages deal with the description of aqueous solutions, properties of liquids, aqueous and organic, and basic partition equilibria. Many general chemistry textbooks published in the last decade provide a more systematic, and if needed, a more detailed treatment of these topics. Rather disturbing are unsound statements such as that on page 14 comparing the molecular weight of water and liquid hydrogen fluoride at room temperature, or that on page 46 suggesting that the synonym for inert solvent is aprotic solvent. Chapter 3, entitled "Statistical Treatment of Liquid-Liquid Distribution Equilibria", is probably the weakest part of the book. The expression "statistical treatment", repeatedly used in the text, is completely misleading. On some 30 pages the authors elaborate the simplest possible sets of mass-action law equilibria for two-phase systems. This is what they term "statistical analysis". Any practicing analytical chemist, even if he has never used solvent extraction as a tool, should be familiar with such basic solution chemistry concepts as distribution ratio, association, dissociation, formation of metal chelates, and mixed ligand complexes. At the level presented, all these are textbook items.

In Chapter 4, "Solvent Extraction Systems", the material is arranged in what I think is a reasonable classification of the major types of solvent extraction processes—but not more than that. There is no in-depth description of the fundamental chemistry involved, and there is an unnecessary amount of repetition. The same primitive set of equations (4.47, 4.57, 4.61, 4.67, etc.) is presented in a number of places, but in the very same context.

Part II, Applications, has two chapters. Chapter 6 deals with the use of solvent extraction as a tool for the determination of thermodynamic activity of solvent, solute, the equilibrium constants of association and dissociation reactions, and complex formation. It is my considered opinion that the recommendations concerning the usefulness of the method in deriving numerical equilibrium data are overly optimistic and frequently thermodynamically unjustified, as for example, the assumptions needed for the determination of solute and solvent activities (pages 314-19).

Chapter 7, "Application of Solvent Extraction to Analytical and Inorganic

Chemistry", is a constructive part of the volume. On some 280 pages of text, with 7300 references listed on 250 pages, this chapter is in effect an enormous bibliographic text, similar in style to that appearing annually in *ANALYTICAL CHEMISTRY Reviews*. The text is interspersed with many tabulations of numerical extraction data, unfortunately, representing an uncritical compilation. The coverage is exceedingly broad, including journals that are not readily available, and the reader will welcome the extensive list of references. The chapter's weakness is the virtual absence of any critical evaluation of the analytical methods cited, and the reader is left alone in deciding the relative merits of the various extractants used for any particular compound.

I can recommend this book as a reference source and believe the authors have succeeded in providing a well-ordered bibliography. As such, it is valuable to practicing analytical chemists, provided they can afford the price. However, I do not think I can recommend it as a textbook. It is not a comprehensive text for a graduate course in analytical, solution, or separation chemistry, as the title might suggest.

## New Books

**Toxic and Hazardous Industrial Chemicals Safety Manual.** 580 pages. Lab Safety Supply Co., P.O. Box 1363, Janesville, Wis. 53545. \$75

Toxicity and hazard data are given for over 700 industrial chemicals that pose danger to workers. Toxicity data include answers to questions such as: What are the acute and chronic symptoms of exposure? What is the toxic dose? Will it cause cancer? The hazard data provide information on flammability and reactivity, as well as specific instructions for extinguishing fires and emergency first-aid procedures. The manual also provides handling and storage instructions.

## Continuing Series

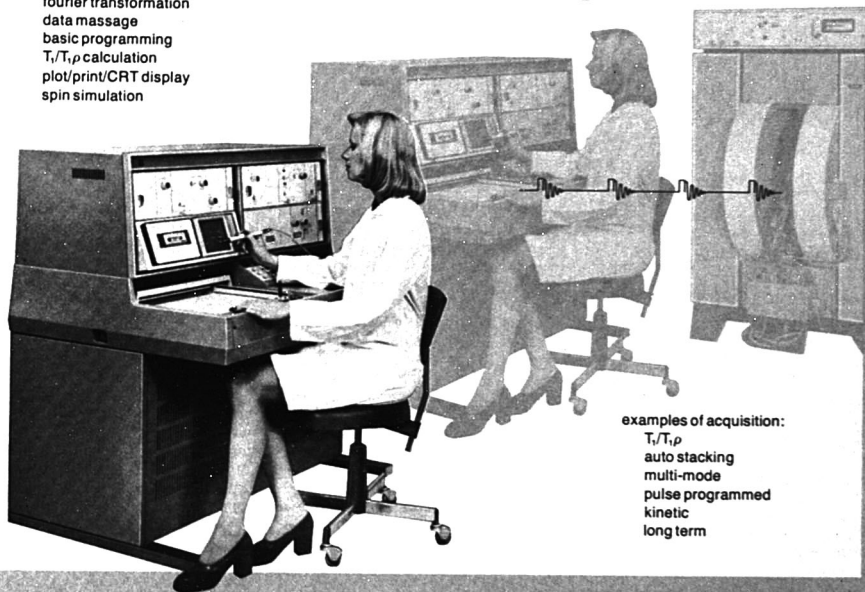
**Annual Reports on NMR Spectroscopy, Vol. 7.** G. A. Webb, Ed. ix + 300 pages. Academic Press Inc., 111 Fifth Ave., New York, N.Y. 10003. 1977. \$31.25

This is the first volume by G. A. Webb, who took over the editorship of this long-standing series on NMR

# While you're working in the foreground\*... your FX is working in the background\*

**examples:**

fourier transformation  
data massage  
basic programming  
 $T_1/T_2$  calculation  
plot/print/CRT display  
spin simulation



**examples of acquisition:**

$T_1/T_2$   
auto stacking  
multi-mode  
pulse programmed  
kinetic  
long term

**\* Foreground/Background system**

# JEOL

235 Birchwood Ave., Cranford, NJ 07016  
201-272-8820

**The FX60Q, FX90Q & FX100 features:**

- (DQD) DIGITAL Quadrature Detection System
- Multi-Frequency TUNEABLE Probe observation
- Dual Frequency probes
- 4-channel DIGITAL phase shifters (DPS)
- Comprehensive auto-stacking system
- Foreground/Background system
- Computer based pulse programmer with
  - Multiple Pulse Sequence Generator
- CPU Expandable to 65K words (MOS)
- 2-channel 12 bit AD/DA
- $T_1/\rho$  spin locking system
- Disc storage systems
- Multi-Mode HOMO/HETERO decoupling capabilities
- Programmable Variable Temperature Unit
- Simplex Y/Curvature gradient controller

\*

CIRCLE 112 ON READER SERVICE CARD





2, 3, and 4-way models

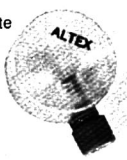
Every inert component you need to quickly construct any liquid or gas flow system.

- ☐ CHEMICALLY INERT
- ☐ ZERO DEAD VOLUME
- ☐ LEAK TIGHT TO 500 PSI
- ☐ MATE PERFECTLY WITH GLASS-METAL-PLASTIC



Compatible with other micro-plumbing components, the ALTEX system includes: Tees and Crosses, Luer Adapters, Couplings, Stainless-steel and Glass Tube Adapters, Plugs, Pipe Connectors, TEFLON Tubing and Flanging Tool.

Also... a complete line of Liquid Chromatography Columns and Sample Injection Valves.



COMPLETE CATALOG on request

**RAININ**  
INSTRUMENT CO. INC.

94 Lincoln Street • Brighton, MA 02135  
1-800-225-4590 • TELEX 94-0887  
CIRCLE 177 ON READER SERVICE CARD

## Books

from Eric Mooney. Under its new editorship, the emphasis of the series is on the review of nuclei other than proton, rather than the general review of NMR. Volume 7 contains three review chapters, the first two of which update previous chapters by the same authors in Volume 5B. In Chapter 1, R. Fields devotes his fluorine-19 NMR review to fluoroalkyl and fluoroaryl derivatives of transition metals. M. Witanowsky and his coworkers cover in Chapter 2 all of the nitrogen NMR literature that appeared between 1972 and 1976. Chapter 3 on spin-spin coupling interactions between carbon and first row nuclei is contributed by Roderick E. Wasylishen.

**Analysis of Drugs and Metabolites by Gas Chromatography-Mass Spectrometry, Vol. 3.** Benjamin J. Gudzinowicz and Michael J. Gudzinowicz. x + 268 pages. Marcel Dekker, Inc., 270 Madison Ave., New York, N.Y. 10016. 1977. \$29.75

The purpose of the series is to compile the various GC and GC/MS procedures from existing literature. In Volume 3 the literature is surveyed, in approximate chronological order, through 1975 for the analysis of antipsychotic, antiemetic, and antidepressant drugs and their metabolites. The book is intended for the analyst who is thoroughly familiar with the principles of GC and GC/MS; thus, the emphasis is on the specific application of these techniques. Some procedures are reviewed in sufficient detail to allow duplication without further reference. Chapter 1 covers procedures for drugs such as phenothiazine, butyrophenone, and thioxanthene derivatives that are antipsychotic and antiemetic drugs. Chapter 2 covers procedures for antidepressant drugs, which include monoamine oxidase inhibitors, tricyclic antidepressants, and several related compounds. The book is a good quality photo-offset copy of typewritten text.

**Residue Reviews, Vol. 66.** Francis A. Gunther, Ed. vii + 212 pages. Springer-Verlag New York Inc., 175 Fifth Ave., New York, N.Y. 10010. 1977. \$22.80

Of the five review articles concerned with residues of pesticides and PCB's, two are specifically devoted to analytical methods. A short chapter on advances in tin compound analysis provides a brief review of the chemistry of commonly used organotin compounds and a discussion on various analytical methodologies available for the deter-

mination of total tin and organotin compounds. The other analytical chapter is on recent advances in PCB analysis. The extraction of PCB's from environmental samples and the eventual determination by gas chromatographic methods are the topics of this chapter.

## ASTM Publications

*The following are available from the American Society for Testing and Materials, 1916 Race St., Philadelphia, Pa. 19103 (U.S., Canada, and Mexico add 3% shipping charges. Other countries add 5%)*

**Part 12 of 1977 Annual Book of ASTM Standards on Chemical Analysis of Metals, and Sampling and Analysis of Metal Bearing Ores.** 874 pages. 1977. \$28

Part 12 contains all ASTM standard specifications, test methods, practices, and definitions pertaining to the chemical analysis of metals and ores as well as the sampling of metal bearing ores. Of the 81 standards, 20 have been designated as American National Standards.

**Part 26 of 1977 Annual Book of ASTM Standards on Gaseous Fuels, Coal and Coke, and Atmospheric Analysis.** 856 pages. 1977. \$28

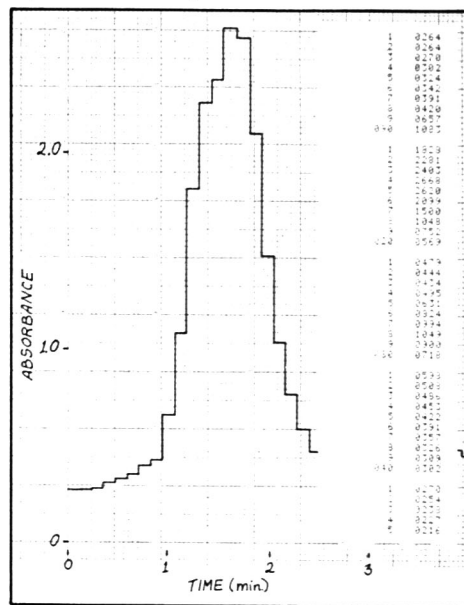
Among the new standards in Part 26 are: test for chromium in workplace atmospheres, test for tin in workplace atmospheres, calculating calorific value and specific gravity of gaseous fuels, test for nitrogen oxides in the atmosphere by the Griess-Saltzman reaction, and test for relative humidity by wet- and dry-bulb psychrometer. Contents include: coal and coke; gaseous fuels; sampling and analysis of atmosphere; specifications, sampling and measurement, and methods of testing and analysis.

**Manual on Hydrocarbon Analysis.** Third Ed. 640 pages. Paperbound. 1977. \$26

The third edition contains 37 ASTM standard test methods for determination of such physical parameters as specific gravity, melting/freezing points, viscosity, and refractivity. The analytical techniques used are solvency tests, correlative methods, liquid chromatographic and gas chromatographic methods, spectrometric methods, chemical methods, and other miscellaneous methods.



The recording shows the absorbance of fractions collected by molecular gel filtration from a separation of high and low molecular weight proteins. These were collected in a cold room and read at 280nm. The tape lists the absorbance value of every fraction and identifies each sample by its position on the transport.

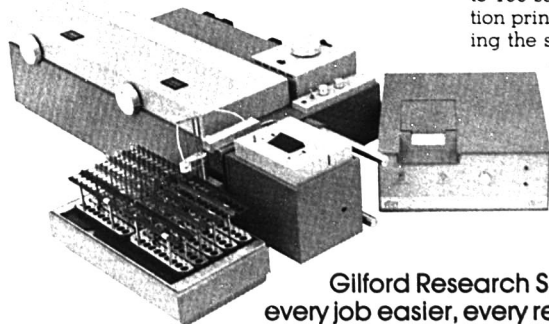


#### Retention of Sample

Sample return is standard: after samples are measured, you can discard them, return selected samples manually, or with the optional Sample Transport, return them all automatically.

#### Building Blocks Relieve the Budget

With the Rapid Sampler accessory alone, you read absorbance or concentration directly from the LED display. Use our Thermal Printer to provide a permanent record of results and to avoid transcription errors. Choose the Automatic Sample Transport for unattended processing of up to 100 samples, complete with sample identification printed out. Add the Thermocuvette, providing the same high-productivity sampling plus electronic control of sample temperature at 25, 30, 32, and 37°C...with automatic regulation to within  $\pm 0.05^\circ\text{C}$ .



**Gilford Research Spectrophotometers:**  
every job easier, every result more accurate.

**gilford**  
INSTRUMENT

Oberlin, Ohio 44074  
(216) 774-1041 Telex: 98-0456  
Paris (Malakoff), France  
Düsseldorf, W. Germany  
Teddington, Middx., England  
Toronto (Mississauga), Canada

CIRCLE 85 ON READER SERVICE CARD

## Gilford's Sample Processing System: when you need the accuracy of a research spectrophotometer with the productivity of an automatic analyzer.

#### More Measurements per Hour

Whether you base it on our Model 250 Spectrophotometer or the Series 252 updates on DU® or DU2® monochromators, the Gilford Sample Processing System is a real time-saver...up to 300 manual measurements per hour, as many as 500 per hour with the available Automatic Sample Transport.

#### Greater Accuracy, Fewer Reruns

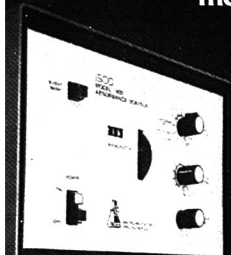
The precise sampling system aspirates the same amount of sample time after time. Combined with the NBS-traceable accuracy of the Gilford photometer, you get consistent high-quality results...hundreds per hour, with carryover of less than 1%.

#### Economy in Sample Size

Pickup volume is adjustable, with a minimum of 700  $\mu\text{l}$  for the standard aspirating cuvette; with the optional ultramicrocuvette, it's 350  $\mu\text{l}$ .

\* Registered trademark of Beckman Instruments, Fullerton CA

**ISCO's new tunable  
monitor detects  
sugars to  
cytochromes**



**...and  
everything  
in between**

Continuously variable wavelength selection from 190 to 620 nm lets you match wavelengths to the absorption characteristics of a wide variety of compounds.

In fact, with its ability to detect in the UV below 254 nm, the Model 1800 enables you to analyze many samples not usually thought of as UV-detectable—amino acids and certain carbohydrates, for example.

Detector sensitivity can be maximized by choosing the optimum wavelength for a particular compound to be analyzed. Or, selectivity can be increased by using a wavelength at which interfering solvents or impurities do not absorb.

A 10 mm pathlength flow cell and an exceptionally fast response speed allow you to separate small, sharp peaks easily. In addition, the high-performance, small-volume cell is temperature equilibrated to minimize instrument noise.

Reliable measurements are enhanced by low baseline drift, achieved with unique reference-compensated optics that combine high energy throughput with stability.

Controls are simple. Wavelength, range, and baseline are the only adjustments necessary. An event marker is provided to record injections. And of course, the Model 1800 connects easily to any ISCO recorder, fraction collector, or pump to give you an integrated liquid chromatography system.

For more information on ISCO absorbance monitors and other instruments, send for your free catalog today. Or dial direct, toll free: (800) 228-4250 (continental U.S.A. except Nebraska). Instrumentation Specialties Company, P.O. Box 5347, Lincoln, Nebraska 68505.



**Instruments with a difference**  
CIRCLE 110 ON READER SERVICE CARD

# polarimetry simplified

## the autopol series by rudolph research

Only two controls are needed to operate the Autopol, power and reset, all other functions are completely automatic. Rudolph's automatic polarimeters and saccharimeters offer wide range, high precision design and construction at a reasonable price.

Send for more information today. Call or write Rudolph Research, 40 Pier Lane, Fairfield, N.J. 07006 201/227-6810.



**RUDOLPH RESEARCH**  
the Polarimetry experts

CIRCLE 179 ON READER SERVICE CARD

## GFS CHEMICALS

### PERCHLORIC ACID ?

WHERE ELSE BUT FROM THE  
**GFS CHEMICALS' CATALOG**  
THAT LISTS MORE THAN  
475 OTHER CHEMICALS  
AND REAGENTS ...AND

**LOOKS LIKE THIS !**



Contact us to circle  
Reader Service Card for  
YOUR 50th ANNIVERSARY  
GENERAL CATALOG  
...it's FREE



"ANALYTICAL CHEMICALS SINCE 1928"

**G. FREDERICK SMITH  
CHEMICAL COMPANY**

867 McKinley Ave.  
Columbus, Ohio 43223

FOR PROMPT SHIPMENT  
**614 224-5343**

CIRCLE 193 ON READER SERVICE CARD

Liquid  
chromatographers  
will love  
this  
!



## Variable wavelength detection made really simple.

**The advanced new SpectroMonitor III** piles up advantage after advantage over all other variable UV detectors.

**Simplicity.** Reduced to a single module, the SpectroMonitor III is more compact than anything on the market.

**Automatic start.** Starts as easy as turning on a light switch.

**Easy inspection.** The cell and all liquid connections are easily removed from the front for inspection and servicing.

**Silicon UV photo detector.** Low noise, long term stability.

**Simplicity of optics.** Same proven simple

optics with true dual beam for long term stability.

**Wavelength coverage 195-350 nm.** Broad range covers majority of industrial and clinical applications.

**Price \$2895.** A variable UV at the price you'd expect to pay for a fixed wavelength detector!

Liquid  
chromatography  
by



**LABORATORY DATA CONTROL**

Division of Milton Roy Co.

P.O. Box 10235, Riviera Beach, FL 33404

305/844-5241.

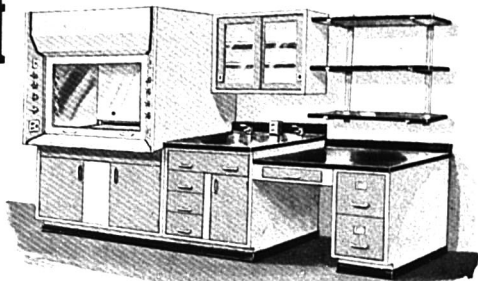
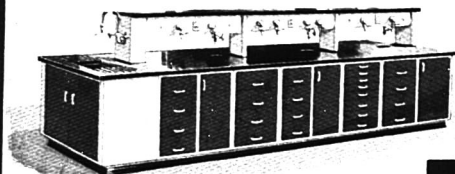
Telex 513479

CIRCLE 125 ON READER SERVICE CARD

# Quick Shipment

## Laboratory Furniture, Fume Hoods and Other Laboratory Equipment

Do you have an immediate requirement for metal laboratory furniture and equipment? If so, Kewaunee's "quick-shipment" line eliminates the need to look elsewhere. A wide selection of metal laboratory base cabinets, storage cases, service fittings and other specialized laboratory equipment is offered in this line. Customized work tops in several different materials are also available.



Kewaunee "stocks" fifteen (15) Laboratory Fume Hood models (4 ft., 5 ft. and 6 ft. lengths of five different types) to meet most laboratory requirements. In addition, Auxiliary Air Chambers, Filter Housings and Filters, and Direct and V-Belt Drive Exhaust and Auxiliary Fans are available in the line.

Want more information? Call or write for a copy of our No. KM-6 catalog, or contact your local Kewaunee representative.



**kewaunee**

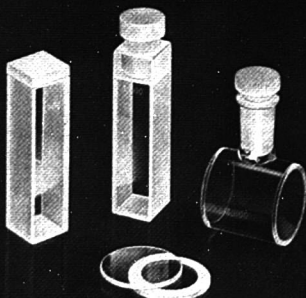
Kewaunee Scientific Equipment Corp.  
Metal Furniture Division  
Adrian, Michigan 49221

Phone: 517/263-5731

CIRCLE 116 ON READER SERVICE CARD

**HELLMA**

...tomorrow's designs today!



QS<sup>®</sup> QH<sup>®</sup> QS<sup>®</sup> OF<sup>®</sup> QU<sup>®</sup> QI<sup>®</sup>

Hellma—the largest assortment of highest precision glass and quartz cells.

Standard • Flow-through • Constant-temperature Anaerobic • Special Designs

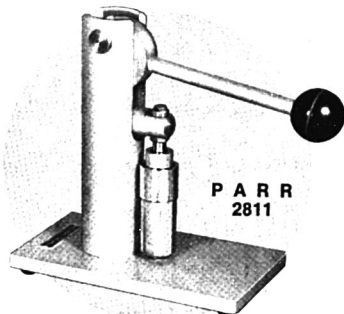
Also available—ULTRAVIOLET LIGHT SOURCES  
Deuterium Lamps • Mercury Vapor Lamps  
Hollow Cathode Lamps • Power Supplies

**HELLMA**  
CELLS, INC.

Write for literature  
Box 544  
Borough Hall Station  
Jamaica, New York 11424  
Phone (212) 544-9534

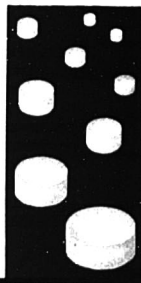
CIRCLE 94 ON READER SERVICE CARD

## PELLET PRESS



PARR  
2811

The convenient and inexpensive way to make pellets, tablets or wafers for any investigative or test purpose. Produces pellets quickly and easily in any of six different diameters up to one-half inch maximum using interchangeable punch and die sets. For details, write or phone: Parr Instrument Company, Moline, Ill. 61265. 309/762-7716



CIRCLE 166 ON READER SERVICE CARD



# The Bausch & Lomb SPECTRONIC® 21 Spectrophotometer

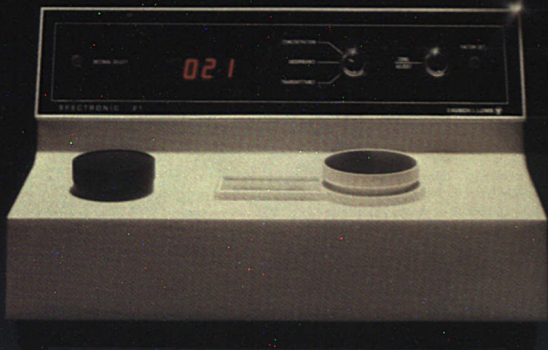
In the next century, testing will require the highest degree of simplicity and reliability. You will need a spectrophotometer that delivers a continuous wavelength of 200nm to 1000nm for uninterrupted testing. One that has an automatic 0%T feature to eliminate readjustment between tests. And one that has impeccable quality to assure fast output and accurate results.


But you don't have to wait that long. The Bausch & Lomb SPECTRONIC 21 Spectrophotometer lives up to these tests now. What's more, it is available in four different models, visible and UV-visible in meter and digital.

It is the greatest spectrophotometer value available today. And because it's from Bausch & Lomb, it will live up to the test of tomorrow.

Contact your nearest Bausch & Lomb distributor, or any of our offices listed below.

## Up to the test of the 21st century

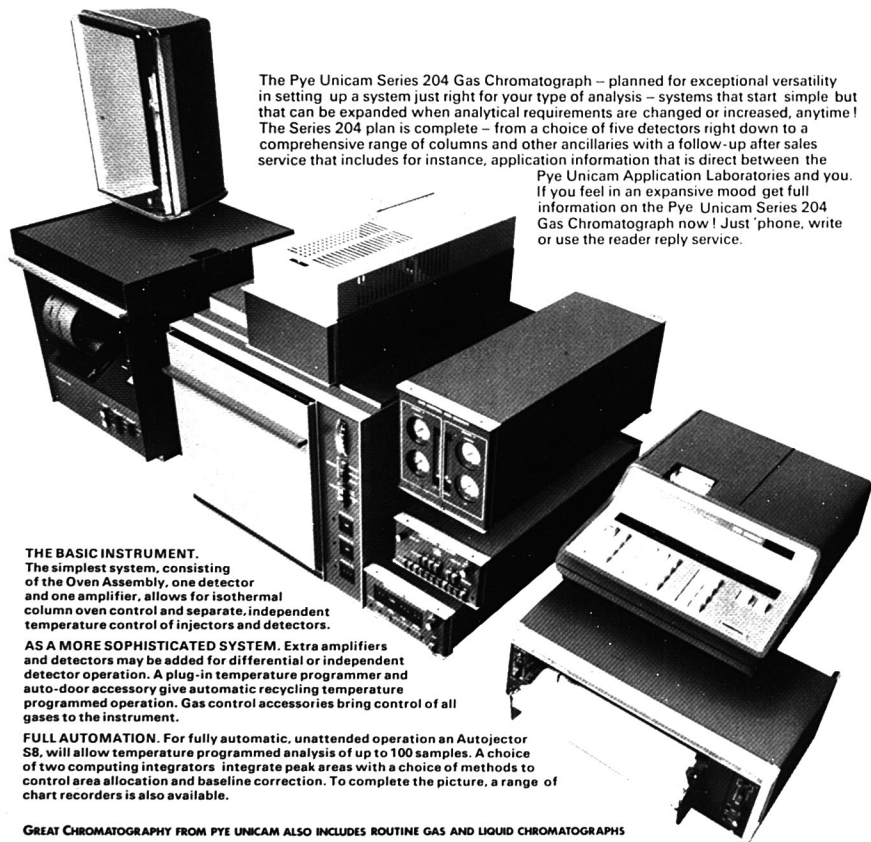


**BAUSCH & LOMB** 

Analytical Systems Division, 7 rue des Chantiers, 78000 Versailles, France  
Bausch & Lomb Belgium N.V., Analytical Systems Division, Rochesterlaan 6,  
8240 Gistel, Belgium/Bausch & Lomb GmbH, Analytical Systems Division,  
Munchener Strasse 72, 8043 Unterföhring, Germany.

CIRCLE 29 ON READER SERVICE CARD

# The 204 Chromatograph expansion plan



The Pye Unicam Series 204 Gas Chromatograph – planned for exceptional versatility in setting up a system just right for your type of analysis – systems that start simple but that can be expanded when analytical requirements are changed or increased, anytime! The Series 204 plan is complete – from a choice of five detectors right down to a comprehensive range of columns and other ancillaries with a follow-up after sales service that includes for instance, application information that is direct between the

Pye Unicam Application Laboratories and you. If you feel in an expansive mood get full information on the Pye Unicam Series 204 Gas Chromatograph now! Just phone, write or use the reader reply service.

#### THE BASIC INSTRUMENT.

The simplest system, consisting of the Oven Assembly, one detector and one amplifier, allows for isothermal column oven control and separate, independent temperature control of injectors and detectors.

**AS A MORE SOPHISTICATED SYSTEM.** Extra amplifiers and detectors may be added for differential or independent detector operation. A plug-in temperature programmer and auto-door accessory give automatic recycling temperature programmed operation. Gas control accessories bring control of all gases to the instrument.

**FULL AUTOMATION.** For fully automatic, unattended operation an Autoinjector S8, will allow temperature programmed analysis of up to 100 samples. A choice of two computing integrators integrate peak areas with a choice of methods to control area allocation and baseline correction. To complete the picture, a range of chart recorders is also available.

GREAT CHROMATOGRAPHY FROM PYE UNICAM ALSO INCLUDES ROUTINE GAS AND LIQUID CHROMATOGRAPHS



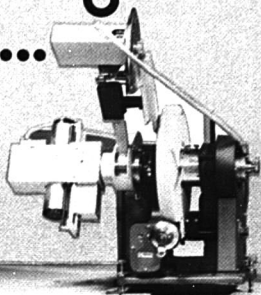
A member of the Pye of Cambridge Group

## Pye Unicam Ltd

York Street, Cambridge, England CB1 2PX  
Cambridge (0223) 58866. Telex: 817331

CIRCLE 167 ON READER SERVICE CARD

# If diffraction problems are holding you up...



## PHILIPS APD 10 AUTOMATIC POWDER DIFFRACTOMETRY SYSTEM

- Automatic data processing – more information per analysis, cheaper, faster and with less risk of operator error.
- Operates unattended, analyses up to 35 samples continuously.
- Cuts measurement time through use of new, high-intensity tubes.
- Stores up to 99 different measurement programmes – facilitates rapid adaptation to needs of varying analyses.
- Easy to operate – plain-language instructions via teletypewriter keyboard.
- Fortran programming package available for special user programmes.
- Peak search-match on mini-file gives plain language data output of compound analyses.

# PHILIPS

## ...we'll hand you the answer

CIRCLE 160 ON READER SERVICE CARD

To: Philips Industries, Scientific & Analytical Equipment Dept.,  
Lelyweg 1, Almelo, The Netherlands.

Name \_\_\_\_\_  
Company \_\_\_\_\_  
Address \_\_\_\_\_  
Tel. \_\_\_\_\_

APD 10

# IT'S JUST A MATTER OF TIME

**You have a choice.**  
**You can spend hours checking**  
**out tables of contents, looking**  
**for articles of special interest**  
**in your field—the ones you**  
**must read—or . . .**  
**. . . you can accomplish the**  
**same result in a matter of**  
**minutes—by using the**  
**ACS SINGLE ARTICLE**  
**ANNOUNCEMENT.**

Here's how it works: In the ACS SINGLE ARTICLE ANNOUNCEMENT you'll find the contents pages from the latest issues of all 18 ACS primary journals. Chances are good you'll see several articles that can help you in your work. Just send your order to ACS. We'll see to it that you get the material in a hurry. And the price is low.

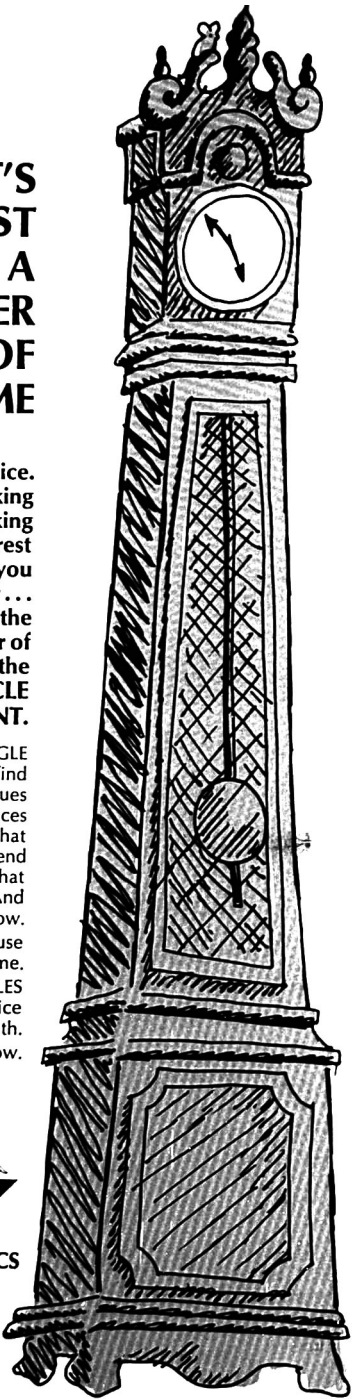
Every issue includes an easy-to-use order form to save you even more time.

The ACS SINGLE ARTICLES ANNOUNCEMENT is published twice a month.

Mail the coupon now.



**Another service of ACS**



## 18 Participating Journals

- Accounts of Chemical Research
- Analytical Chemistry
- Biochemistry
- Chemical Reviews
- Chemical Technology
- Environmental Science & Technology
- I&EC Fundamentals
- I&EC Process Design and Development
- I&EC Product Research and Development
- Inorganic Chemistry
- Journal of Agricultural and Food Chemistry
- Journal of the American Chemical Society
- Journal of Chemical Information and Computer Sciences
- Journal of Chemical and Engineering Data
- Journal of Medicinal Chemistry
- The Journal of Organic Chemistry
- The Journal of Physical Chemistry
- Macromolecules

## SINGLE ARTICLE ANNOUNCEMENT 1978

**American Chemical Society**  
 1155 Sixteenth Street, N.W.  
 Washington, D.C. 20036

Yes—I wish to receive the ACS SINGLE ARTICLE ANNOUNCEMENT at the one-year rate checked below:

		<b>U.S.</b>	<b>All Other Countries</b>
ACS Member*	<input type="checkbox"/> \$12.00	<input type="checkbox"/> \$17.00	
Nonmember	<input type="checkbox"/> \$24.00	<input type="checkbox"/> \$29.00	
<input type="checkbox"/> Payment enclosed <input type="checkbox"/> Bill me <input type="checkbox"/> Bill company <input type="checkbox"/> I am an ACS member <input type="checkbox"/> I am not an ACS member			

*Air freight rates available on request.*

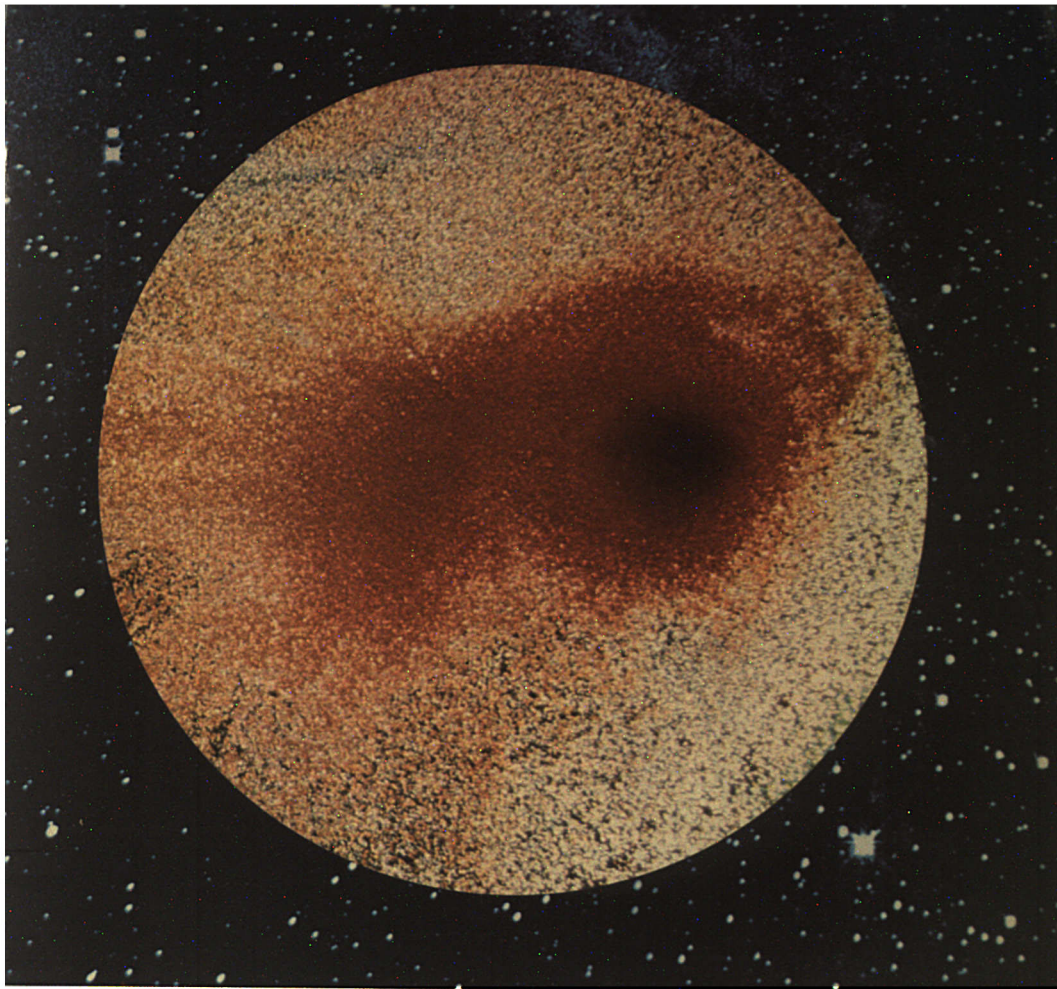
Name	Position		
<input type="checkbox"/> Home <input type="checkbox"/> Business (Specific title please)			
Address			
City	State/Country	Zip	

**Journal subscriptions start in January '78.**

Allow 90 days for your first copy to be mailed.

\*NOTE: Subscriptions at ACS member rates are for personal use only.





Photomicrograph by John Delly, McCrone Research Institute

FOR THE CREATIVE CHEMIST:

## **EASTMAN ORGANIC DYES, STAINS, AND INDICATORS.**

What might be a close-up of a lunar landscape is a photomicrograph of EASTMAN Organic Chemical 1757, Acridine Orange, taken by John Delly of McCrone Research Institute. It demonstrates one small, creative aspect of chemistry.

For practical, everyday applications in your lab, start with one of our many organics and

add your imagination. Your dealer in EASTMAN Organic Chemicals offers many pH, absorption, chelometric, colorimetric, and fluorometric indicators; biological dyes and stains; buffers, cyanine dyes, and spectral sensitizers; organic laser dyes; and phthalocyanine-type compounds. Plus Eastman reagents for electrophoresis, liquid scintillation counting, and protein

chemistry. See your dealer for fast, reliable service, and a free reminder that chemistry is creative.

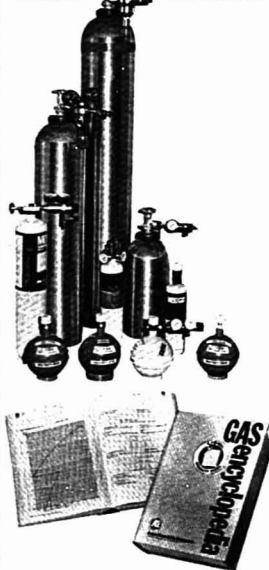
For complete details on dyes, stains, and indicators, send for free technical literature, JJ-196 and JJ-281. Write Eastman Organic Chemicals, Eastman Kodak Company, Dept. 412L, Rochester, N.Y. 14650.



Take a close look at EASTMAN Organic Chemicals. Dealers handling EASTMAN Organic Chemicals: American Scientific & Chemical, Bio Clinical Laboratories, Brand-Nu Laboratories, Inc., Bryant Laboratory, Inc., Cusrom Chemical Laboratories, Inc., Fisher Scientific, GAC Laboratories, Inc., Labproducts, Inc., Midland Scientific, Inc., North-Strang, Inc., Preiser Scientific, Sargent-Welch, Scientific Products, Scientific & Industrial Sales & Service, Inc., VWR Scientific Inc., Ward's Natural Science Establishment, Inc.

CIRCLE 63 ON READER SERVICE CARD

# LIF-O-GEN® SPECIALTY GASES The Highest Quality & Technology Costs ~~100~~ No More



Lif-O-Gen®, an affiliate, shares the expertise and vast technology of L'Air Liquide, the world leader in the industrial and medical gas field. We have a wide range of specialty gases and services.

## LIF-O-GEN® OFFERS

- The most precise gravimetric mixing equipment.
- The most modern micro-process control laboratory.
- A wide range of refillable aluminum and disposable steel cylinders.
- Lif-O-Gen® Gas Encyclopedia, most complete and advanced encyclopedia of its kind in the world.

For information, call or write Lif-O-Gen®  
Specialty Gases  
P.O. Box 149, Woods Road, Cambridge,  
Maryland 21613  
Telephone: 301-228-6400 TWX. 710-865-9652



**LIF-O-GEN®**  
American Life  
Support Corp.

A Subsidiary of Liquid Air Corp.  
of North America  
© Copyright 1978

## Editors' Column

### Government Spending for Science

The fiscal year 1979 budget announced by President Carter emphasizes "basic" in science and technology. Monies earmarked for research and development (R+D), however, are not exactly plentiful. The zero-based budget Carter proposed increases proposed total federal spending 8.2% while funding for R+D activities would rise only 6.1% to \$27.9 billion out of a total \$500.2 billion budget. Basic research funding increases 10.9% to \$3.65 billion. The greater increase in funding of basic research reflects the conclusions of experts that although science is in good condition at present there are problems to be faced:

- There are not enough young scientists doing basic research, partially because the tenure system tends to lock out new PhD's from university jobs.
- There are fewer first-class research centers because the quality of once excellent science departments is declining.
- Equipment is becoming obsolete because the country is beginning to lag in scientific instrumentation.
- There are more conservative research proposals advanced probably because of the lack of available money for nonconventional studies.

Increased funding for basic research has to mean a decrease elsewhere. Budget proposals suggest a decrease in demonstration projects or applications. However, specifics are not spelled out in each government agency's budget, and Congress or uncooperative agencies could ruin the budget philosophy that permits greater spending for basic research.

Out of total research support of \$829.2 million, the National Science Foundation (NSF) proposes 91% for basic research. The NSF budget shows an increase of \$22.3 million to \$268.3 million for Mathematical and Physical Sciences and Engineering (MPE). The MPE budget includes \$47.7 million for chemistry, \$18.1 million for computer research, and \$64.5 million for materials research. In these areas, MPE will provide strong support for high-quality research projects aimed at enriching our knowledge of materials, laws, and phenomena and will increase emphasis in computer research in nonnumeric computing and intelligent systems and research equipment. MPE will also broaden research on miniaturization necessary to further

developments in integrated circuits, magnetic memory systems, and optical communications systems and will provide for critically needed modernization and replacement of instruments at the Materials Research Laboratories.

Among the other government agencies concerned with science, the National Institutes of Health is pleased with the back to basics budget philosophy even though the increase in their budget will be negated by inflation. The National Aeronautics and Space Administration wanted major budget emphasis placed on space applications and aeronautical research and technology and less emphasis on space sciences. However, in the final proposed budget the largest percentage increase went to space sciences. At the Environmental Protection Agency, the first agency to use zero-based budget techniques, the result is a diminished emphasis of programs of lesser importance with obvious greater emphasis on those programs that are more important, e.g., a 97% funding increase for the implementation of the Toxic Substances Control Act. The National Bureau of Standards (NBS) is expected to get substantially more money, a budget increase of 20% to \$66 million. The increase is for an expanded effort to establish standards and for maintenance of NBS' basic science and engineering capability.

In other government/science economic activities, Richard A. Atkinson, director of NSF, announced that funding of university/industry cooperative research, aimed at both basic and applied investigations, will be given special attention in the competition for research support. Dr. Atkinson said that "while academic and industrial scientists working apart have been very productive, we believe that the special perspectives on research of scientists in both fields working together will act to produce beneficial results to the economy and speed solution of current and future societal needs". These cooperative efforts will require active participation by both university and industry. It is expected that an industrial firm or group of firms would contribute funds, personnel, or services reflecting their interest in the research. Jointly prepared proposals from cooperating institutions will compete with regular proposals, but cooperative projects would be a factor in the award decision process.

A. A. Husovsky

CIRCLE 214 ON READER SERVICE CARD

## INDICATING DESICCANT

*changes from blue when dry  
to rose-red when exhausted*

Indicating DRIERITE is a chemical drying agent for the efficient and rapid drying of air and gases in systems where visual indication of active desiccant is desired.

In use, the color changes sharply to a rose-red as the margin between the exhausted and active desiccant progresses through the tube or column.

It is available in 8 Mesh, the standard granule size, and in 20-40, 10-20, 6 and 4 Mesh.

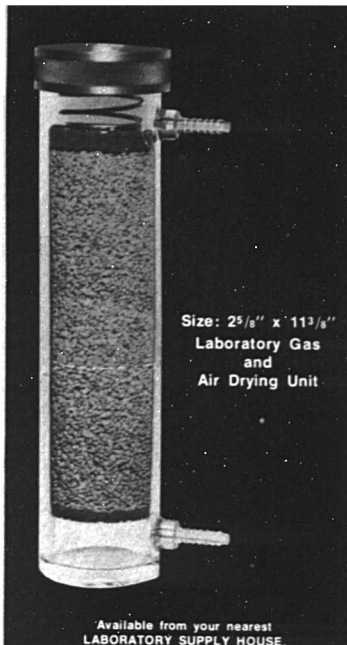
Impregnated with cobalt chloride, Indicating DRIERITE retains the high efficiency of Regular DRIERITE, anhydrous calcium sulfate, plus the added advantage of the color change for indication. It dries air and gases to a terminal dryness of 0.005 milligram per liter of gas.

Regeneration reverses the color change and makes possible repeated use after heating at 375-450°F while spread one granule deep for one hour.

Regular white DRIERITE (non-indicating) is available in the above mentioned sizes and also in 200 Mesh.

DRIERITE is a product of

W.A. Hammond Drierite Co., Xenia, Ohio 45385.



Size: 2 5/8" x 11 3/8"  
Laboratory Gas  
and  
Air Drying Unit

Available from your nearest  
LABORATORY SUPPLY HOUSE

CIRCLE 97 ON READER SERVICE CARD

## TSI Makes Generators for PARTICLE RESEARCH

TSI's particle generators are used in basic research; toxicology; inhalation studies; medical research; light scattering studies; calibration of impactors, cyclones and optical instruments in a 0.01 - 40  $\mu$ m range. For instance, TSI offers the Model 3050 for generating extremely uniform particle size... the Model 3076 for ultrafine droplets with constant output... the automatic, fluidized bed Model 3400 for complete dispersion of powder or dust. Or the Model 3071 Electrostatic Classifier for generating uniform particle size in the 0.01 to 0.3  $\mu$ m range.

For more information about TSI's family of particle research instruments, contact:

TSI Incorporated  
P.O. Box 3394  
St. Paul, MN 55165 USA  
612/483-0900 Telex 297-482



CIRCLE 203 ON READER SERVICE CARD

## Safe dry and clean up to 1100°C (2012°F)

*Fluidized baths are excellent  
for laboratory tests*

Compare with

An oil bath: fluidized bath is  
**safe**, works over wider temperature, **eliminates fumes**/  
odor and need for expensive oil

An oven: fluidized bath provides  
**better temperature uniformity**,  
more rapid heating, improved  
accessibility

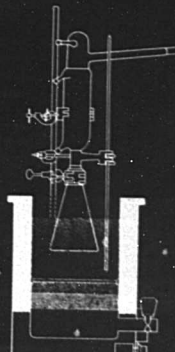
A heating mantle: fluidized  
bath accepts wide variety of  
lab vessels, gives **higher heat  
transfer rates**

Ideal for numerous lab applications  
Many standard units. Also  
specials

### Techn

## ORIGINATORS OF THE HIGH TEMP ERATURE LAB FLUIDIZED BATH

Techn Inc 3700 Brunswick Pike Princeton NJ 08540 609 452-9275



CIRCLE 204 ON READER SERVICE CARD



Introducing

# The Model 4202 Dual-Channel Signal Averager

No matter what you call your experiment—

• AUGER • ESCA • NMR • ESR • EPR • ION DETECTION • CYCLIC VOLTAMMETRY • MICROWAVE SPECTROSCOPY • MOLECULAR BEAM STUDIES • IR SPECTROSCOPY • TIME OF FLIGHT MASS SPECTROSCOPY • KINETICS

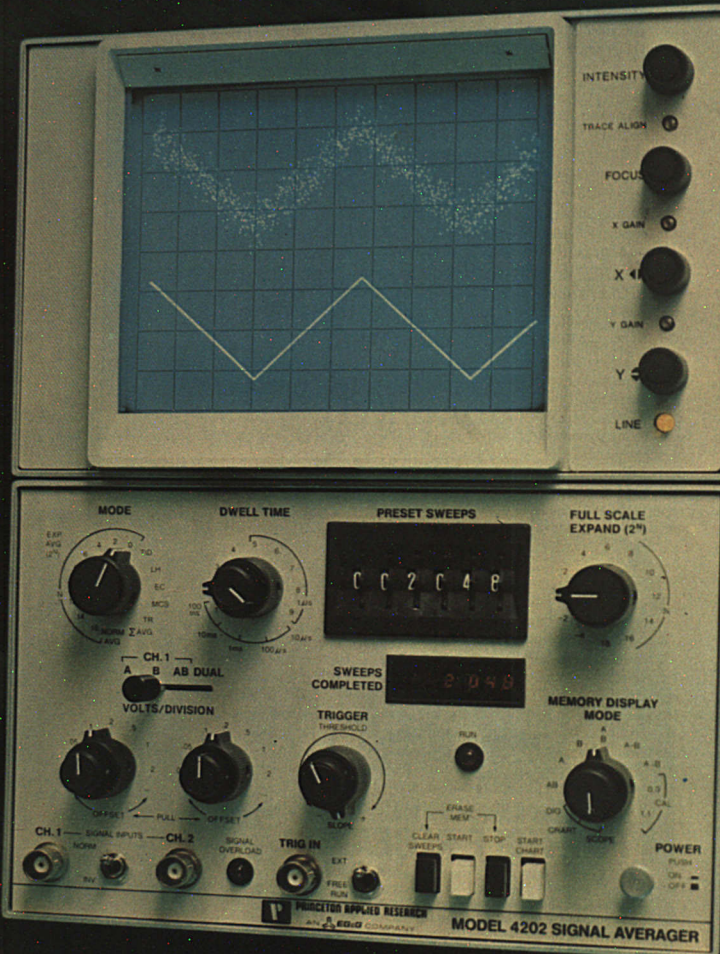
ask PARC about their NEW Model 4202.

You'll get all these outstanding features!

- Dual Input signal channels for processing two simultaneous signals.
- 3 switch selectable averaging modes (Linear Summation, Exponential, Normalized) —choose the one that best fits your type of signal.
- Huge memory of 2048 28-bit words—lets you average for hours without memory overflow.
- Variable Sampling Rates ( $5 \mu\text{s}$  to .9 s) to accommodate slow and fast signals.
- Division & Subtraction of curves stored in separate memory halves for data normalization and baseline (blank) subtraction.
- Analog & Digital outputs for X-Y plotters and computer peripherals.
- Transient Capture
- 4 Histogram Modes: Multi-channel Scaling, Time Interval Distribution, Event Correlation & Latency Histogram.

Low Cost—the Model 4202's domestic price is \$5495 including vertically-mounted CRT. A rack-mounted version including side-mounted CRT is \$5595. You can purchase the Model 4202 without CRT for a low \$4495.

Write to Princeton Applied Research Corporation, P.O. Box 2565, Princeton, NJ 08540; or phone 609/452-2111 to arrange a demonstration or additional information.



**Princeton Applied Research Corporation**

AN **EG&G** COMPANY

Circle #169 Additional Information  
Circle #170 Have a Salesman Contact Me.



# Fourier Transform Mass Spectrometry

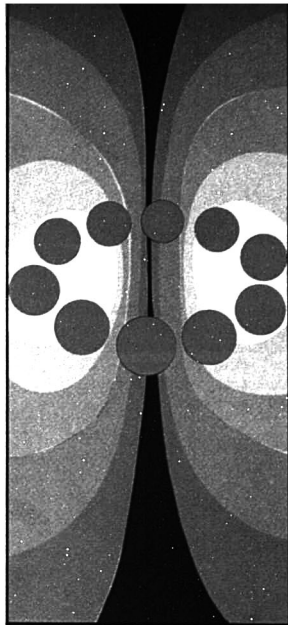
Charles L. Wilkins

Department of Chemistry  
University of Nebraska  
Lincoln, Neb. 68588

Less than 10 years ago, it was possible for Henis to accurately observe in a review article in this JOURNAL (1), "Indeed ion mass spectrometers are more limited with respect to mass range and resolution than are other types of mass spectrometers." A little more than two years afterward, we suggested in an instrumentation article (2), "Ion cyclotron resonance spectrometry is becoming established as an important analytical technique in its own right and a useful complement to conventional mass spectrometry." In both reviews, which sought to focus on the analytical potential of ICR, the emphasis of the discussions was primarily how the unique capabilities of the method for studying ion-molecule reactions could be used to advantage in an analytical chemistry context. We reported some results from our laboratory which established that certain operational enhancements were realizable by adding a digital computer to the ICR mass spectrometer system, and rather conservatively suggested that the application of computer-assisted experimental techniques would assist in ICR's transition from a physical chemist's research instrument to an analytical tool. During the intervening years, some truly exciting developments in ICR mass spectrometry have taken place. The purpose of this article is to assess the analytical implications of these advances and to attempt to project the future role of ion cyclotron resonance in analysis.

## Principles

Several of the earlier reviews (1-4) and an excellent new book by Lehman and Bursey (5) outline in detail the fundamental principles governing ion cyclotron resonance spectrometry. Accordingly, only a brief qualitative description of the basic phenomena will be included here. ICR spectrometry's unique properties derive from the be-



havior displayed by ions placed in a strong magnetic field. Such ions travel in circular paths perpendicular to the applied magnetic field. If no energy is added or lost by such an ion, the force exerted on it by the field is counterbalanced by the centrifugal force of its motion. Thus, Equation 1 can be written

$$mv^2/r = eBv \quad (1)$$

where  $m$  is the mass of the ion  $e$ , the charge;  $B$  the magnetic field strength;  $v$  its velocity; and  $r$  the radius of its path. When this equation is rearranged, the ratio of velocity to radius is, at a fixed magnetic field strength, a constant dependent upon only the mass and charge of the ion. The angular frequency  $\omega_c$  in rad/s defined in Equation 2 is therefore

$$\omega_c = v/r = eB/m \quad (2)$$

a characteristic and different ion cyclotron frequency for each ion with the same charge, but different mass. In its various forms, ion cyclotron resonance mass spectrometry consists of taking advantage of the properties of this fundamental phenomenon to detect and "count" ions present in the spectrometer cell after they have been generated in a suitable source region.

## Instrumentation

It will be helpful in understanding the newest advances to consider the development of ICR instrumentation along with the factors that prove lim-

## Instrumentation

iting with each of the successive designs. The first application of ICR in mass spectrometry was that of Hipple, Sommer, and Thomas in 1949 (6, 7). However, these investigators used the method primarily for gas analysis at masses below 50 and did not develop it as a general mass spectrometric technique. In their instrument, called the omegatron, after ions were generated in the cell they were excited with a radiofrequency radiation. Under these conditions, for any ion with  $\omega_c/2\pi$  equal to the imposed radiofrequency, absorption of energy will occur, the ion will be accelerated, and its path changed from a circular one (with respect to the axis of the cell) to an Archimedes spiral. As a result, an ion collector placed in the appropriate position can collect ions in resonance, whereas those not in resonance are not collected. With such a design, each ion can alternately be brought into resonance by either varying the magnetic field or the oscillating electric field frequency, resulting in a mass spectrum. A difficulty of this design is that stray ions can also be collected at the collector electrode, causing errors impossible to correct. One additional feature incorporated in the omegatron was provision of means for applying a trapping voltage, to prolong ion residence times.

The first commercial ICR instrument (introduced by Varian Associates in 1966 and removed from production a few years later) used a drift cell in which a marginal oscillator detected instantaneous power absorption of sample ions as they drifted through the analyzer region. In this 2.5 cm-square by 8.6 cm-long three-section cell, ions were first formed in a source region, then drifted into an analyzer region where they were irradiated and detected, and finally collected at a total ion collector. Its major shortcoming was its limited ion trapping capability (in the range 1 to sev-

eral milliseconds) and its low resolution and restrictive upper mass range limit (ca. unit resolution at  $m/e = 200$ ). A theoretical resolution limit for this kind of cell is determined by the ion drift time through the analyzer section. Comisarow and Marshall have derived an equation describing resolution in the zero pressure limit, using the linewidth at half peak height to define resolution (8). In Equation 3,  $e$  is the charge in multiples of elementary charge,  $B$  the magnetic field in kilogauss,  $m$  the mass in amu, and  $T$  is given in milliseconds. Notice particularly that resolution is a linear function of detection time (i.e., the longer ions can be seen, the higher the resolution).

$$m/m_{50\%} = eBT/5.769 \times 10^{-4} \text{ m} \quad (3)$$

Because of the short residence (and hence, detection) times, the next major development effort was aimed at prolonging those times. Clever trapped ion cell designs by McMahon and Beauchamp (9) and McIver (10), which allow ion "storage" for periods on the order of a second or more, resulted. Nevertheless, resolution achievable in the trapped-cell mode with conventional instruments is not significantly greater than that obtained with the original drift cell design, although the mass range has been extended as high as 500 with unit resolution. Operation of the single section trapped cell is generally in the pulsed mode, where the temporal behavior of single ions is usually observed for the purpose of kinetic studies. If an entire spectrum were to be collected with this cell, measurement would normally be done, as with the drift cell, at a fixed radiofrequency while scanning the magnetic field. This mode of producing spectra limits the speed with which measurements can be made, because of the difficulty in making rapid changes in the magnetic field strength.

For the conventional ICR spectrometers described, other designs can lead to improved mass range and mass measurement accuracy, but slow scan rates and low resolution will probably continue to limit the generality of their analytical capabilities. It is primarily because of these limitations that researchers interested in expanding the general-purpose analytical utility of ICR mass spectrometry have turned to investigations of Fourier transform approaches.

## Fourier Transform MS

Within the past several years, analytical chemistry has been a primary beneficiary of the minicomputer technology revolution. Dramatic advances in the state-of-the-art of digital electronics have allowed such analysis methods as Fourier transform infrared and nuclear magnetic resonance spectrometry to become not only practical, but commonplace. Previous instru-

ment scanning modes. As a result, when a time domain signal is sampled at  $N$  equal intervals, signal-to-noise ratio is enhanced by a factor  $\sqrt{N}$ . In the infrared spectral case, the advantage becomes one-half this factor because the half-silvered mirrors used in interferometers reject half the incident radiation. This time advantage, called the Fellgett advantage (18), permits spectroscopists to complete a spectrum in  $1/N$  of the time

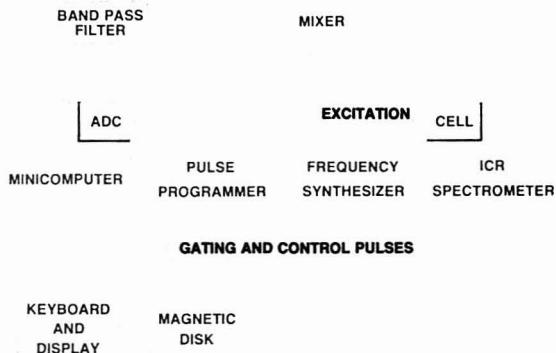


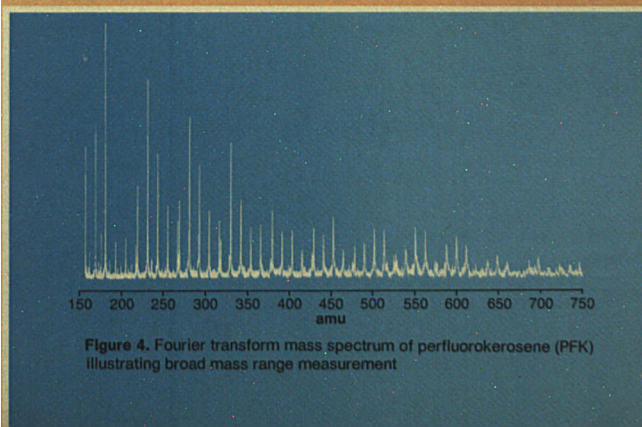
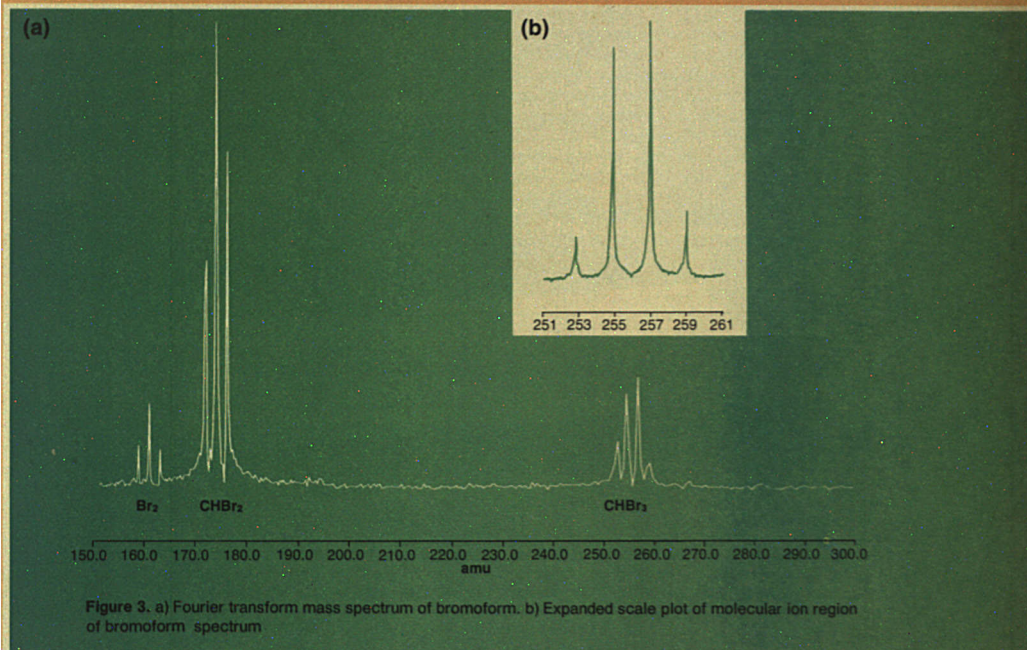
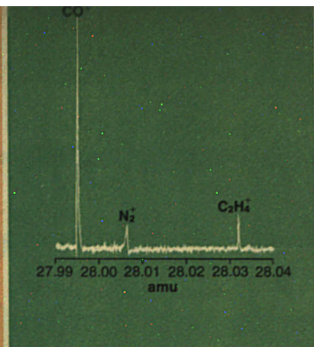
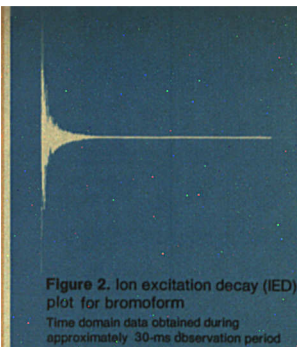
Figure 1. Block diagram of Fourier transform ion cyclotron resonance mass spectrometer system

mentation articles have lucidly detailed the principles and advantages of both Fourier and Hadamard transform spectroscopy methods (11-16), most recently in the comprehensive discussion of Marshall and Comisarow (17). It is not, then, surprising that such techniques would suggest themselves for possible application to ICR spectrometry. Although complete discussions of the principles involved are included in the references cited above, the qualitative aspects of the use of time domain measurements, and their transformation to the frequency domain will be outlined here.

Briefly, the primary contribution of Fourier transform methods in both infrared spectrometry and nuclear magnetic resonance spectrometry is the fact that, in such experiments, measurements can be made in a fraction of the time required by conventional frequency (or, for NMR, mag-

netic field) scanning modes. As a result, when a time domain signal is sampled at  $N$  equal intervals, signal-to-noise ratio is enhanced by a factor  $\sqrt{N}$ . In the infrared spectral case, the advantage becomes one-half this factor because the half-silvered mirrors used in interferometers reject half the incident radiation. This time advantage, called the Fellgett advantage (18), permits spectroscopists to complete a spectrum in  $1/N$  of the time

required for a frequency domain measurement and obtain the same signal-to-noise ratio, or alternatively, to achieve increased sensitivity in the same total measurement time. NMR spectrometry and ion cyclotron resonance, at least superficially, have much in common, with the primary difference being the nature of the phenomena observed and the absolute frequencies involved. In the NMR experiment, a brief radiofrequency pulse (typically from 1 to 50  $\mu$ s for  $^{13}\text{C}$  and  $^1\text{H}$  NMR) is used to excite simultaneously the nuclei absorbing over a frequency range of 10 kHz or less (12). Subsequently, the free induction decay of the ensemble of excited nuclei is observed, and the resulting time domain sequence (each point of which contains information regarding all portions of the frequency range covered) is subjected to a Fourier transformation that converts it to





# COMPARE YOUR IDEA OF A WORKHORSE RECORDER TO OURS.

The rugged Gould 105 General Purpose Strip Chart Recorder delivers such reliable performance, with so many unexpected features, that it goes beyond the traditional definition of a workhorse unit.

Die-cast to handle the day-to-day rigors industrial analytical instrumentation must face, the 105 still offers you a full complement of features you might not expect on such a competitively priced recorder.

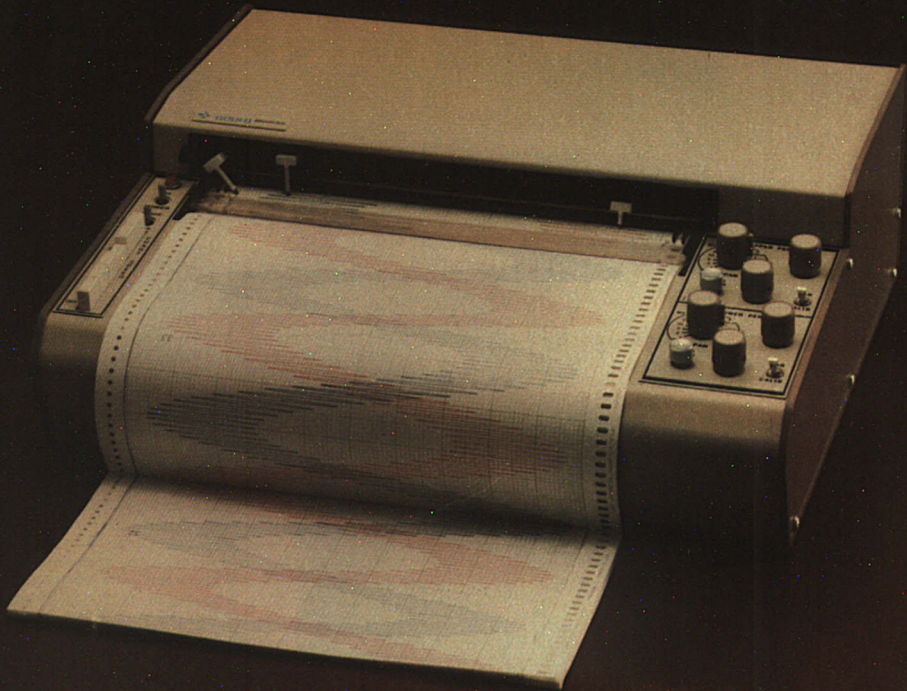
Full scale linearity is 99.9%. Rectilinear data presentation is available in either single or dual 10-in. channels. Response time (10% to 90% full scale) is less than 350 ms.

The Model 105 uses disposable felt tip pens avail-

able in four colors. It easily takes Z-fold or roll paper without modification. Chart speeds range from 1 in./hr. to 20 in./min. It even makes chart annotation simpler with a flatbed, "write-on" design and event marking standard.

And of course you have the Gould/Brush sales and service organization should you ever need us. Check Gould's 105 — a workhorse of a recorder with a tradition of thoroughbreds.

For more information contact, Gould Inc., Instruments Division, 3631 Perkins Ave., Cleveland, Ohio 44114. Or Gould Alco S.A., 57 rue St. Sauveur, 91160, Ballainvilliers, France. **For brochure, call toll free (800) 325-6400, Ext. 77.** In Missouri: (800) 342-6600.



**GOULD**

CIRCLE 86 ON READER SERVICE CARD



the frequency representation preferred by spectroscopists. Relaxation of the nuclei as a function of time is the phenomenon monitored in this case. As mentioned earlier, in an ion cyclotron resonance spectrometer, ions (rather than nuclei) absorb radio-frequency energy at frequencies (typically between 0 and 1 MHz) characteristic of their  $m/e$  ratios if magnetic field is held constant. As in the NMR experiment, it was found convenient in the earlier instruments, particularly those employing the three-section drift cell mentioned earlier, to operate at fixed frequency and to scan magnetic field, alternately bringing ions of each mass into resonance at that frequency to obtain a spectrum.

Continuing the analogy, it is also possible to visualize an experiment for ICR superficially identical to that carried out in Fourier NMR. First, ions are generated, then the ions (rather than nuclei) are subjected to irradiation over a broad frequency range, and the time dependent behavior of the ensemble of excited ions is observed. Fourier transformation of the time domain data thus obtained yields a mass spectrum, rather than an NMR spectrum, but it too is simply the frequency domain representation of the time-intensity data collected during the data acquisition period. Here, however, the principal phenomenon observed is, rather than de-excitation from nuclear excited states (the relaxation process in NMR), the decay of ions back to thermal energies as a result of momentum loss through collisional processes. One very important consequence of this difference in the relaxation processes involved (intra- vs. intermolecular) is the possibility that resolution for Fourier ICR, in contrast to NMR, can be improved by using more dilute samples. Another important difference is the bandwidth for the ICR experiment can be as much as 1 MHz in contrast to the 10 kHz or less involved in Fourier carbon NMR.

Comisarow and Marshall, working at the University of British Columbia, have verified the feasibility of Fourier transform ion cyclotron resonance and described their results in a series of communications beginning in 1974 (8, 17, 19-25). Examples of actual spectral measurements they reported in 1975 (23) include a spectrum of tris(perfluoroheptyl)azine that clearly shows the molecular ion at  $m/e = 1885$ ; an ultrahigh-resolution spectrum of a mixture of CO, N<sub>2</sub>, and ethylene in the  $m/e = 28$  region where  $m/m_{\text{CO}} = 250\,000$ , and a spectrum of perfluorokerosene (obtained in 10 segments) extending from  $m/e = 69$  to  $m/e = 605$ . These encouraging results obtained with a prototype instrument

suggested the enormous potential of FT-ICR for analytical applications. As a result, several groups have begun actively pursuing such development. Most recently, McIver has advocated (and demonstrated) a technique whereby instead of temporally separating ion excitation and detection as in the Comisarow and Marshall formulation of the Fourier transform experiment, detection is begun simultaneously with irradiation (26). His experiment is carried out on a somewhat slower time scale and uses a new capacitance bridge detector of his own design which appears to be promising. Both approaches utilize a frequency synthesizer as the excitation source and incorporate minicomputers as integral parts of the spectrometer system. Figure 1 shows a block diagram of a Fourier ion cyclotron resonance mass spectrometer, and Figures 2-5 are representative examples of recent spectra recorded with a contemporary prototype instrument.

### Analytical Prospects for FT-ICR

It is clear at this point that the transition of ICR to a general analytical tool may well be possible using Fourier transform methods. Because of the potential high sensitivity of ICR and the latitude it permits in choice of reagent ions (for ion-molecule reaction and chemical ionization studies), it may well compete with conventional high-resolution and chemical ionization mass spectrometers. The high sensitivity arises because the residence times possible in an ICR spectrometer make ion-molecule reactions observable at pressures from five to six orders of magnitude lower than in a conventional source. As a result, only small quantities of samples need to be used, and partial pressures of  $10^{-7}$  to  $10^{-8}$  torr are adequate for ionization of nonvolatile materials. Another source of high sensitivity is the 100% ion collection efficiency realized in ICR spectrometers, in contrast to the thousandfold worse efficiency of sector instruments. Of course, the use of electron multipliers (not possible in FT-ICR) allows the sector instruments to recapture part of the sensitivity lost due to inefficiency. One example of the suggested high sensitivity is McIver's experimental observation that sample consumption rates of about 1 ng/s are adequate for producing identifiable ICR signals (27).

Let us return briefly to Comisarow and Marshall's work: At the 1975 "Annual Conference on Mass Spectrometry and Allied Topics" (23), they projected a Fourier ICR mass spectrometer would have the capability of producing mass spectra up to 10 000 times faster than a conventional ICR

instrument or to be up to 100 times as sensitive. Concurrently, such an instrument would have the capability of yielding high-resolution mass spectra (routine resolution 10 000 up to  $m/e = 1000$ ) calibrated throughout the mass range and would retain all the capabilities of conventional ICR spectrometers. These predictions, together with the experimental data thus far obtained using prototype instruments, suggest a number of exciting analytical possibilities.

### The Future

It could be that Fourier ICR will have some of the impact on mass spectrometry that Fourier NMR has had on nuclear magnetic resonance spectrometry. In particular, it may ultimately provide the means for achieving another order of magnitude in trace analysis sensitivity for organic materials over that obtainable today with state-of-the-art conventional mass spectrometers. Furthermore, the expected capability of obtaining an entire spectrum over a moderate mass range [for example, from a minimum mass of 125 amu, with a resolution of 10 000 ( $m/m_{25\%}$ )] using a 14 000 gauss magnetic field and a few hundred milliseconds data acquisition time, will certainly have major impact on the practice of gas chromatography/mass spectrometry, should it prove possible to successfully interface the ICR spectrometer to a gas chromatograph in a way that permits FT-ICR. These kinds of analytical advances have yet to be demonstrated, although the evidence is clear that there is a very reasonable chance that they will come within the next two or three years.

Judgment should be reserved until the experimental results are in, but it does appear that analytical ion cyclotron resonance spectrometry is on the threshold of assuming its role as an analytical method of major importance.

### Acknowledgment

It is a pleasure to acknowledge the valuable and critical contributions to this article by my colleague Michael L. Gross. The spectra in Figures 2-5 were provided by Nicolet Technology Corp., Mountain View, Calif. 94041.

### References

- (1) J.M.S. Henis, *Anal. Chem.*, **41** (10), 22A (1969).
- (2) M. L. Gross and C. L. Wilkins, *ibid.*, **43** (14), 65A (1971).
- (3) J. D. Baldeschwieler, *Science*, **159**, 263 (1968).
- (4) J. D. Baldeschwieler and S. S. Woodgate, *Acc. Chem. Res.*, **4**, 114 (1971).
- (5) T. A. Lehman and M. M. Bursey, "Ion Cyclotron Resonance Spectrometry", Wiley-Interscience, New York, N.Y., 1976.



**Don't inventory  
all those grades of a solvent  
when **ONE** from B&J  
will do the job ... better**

- Fewer bottles mean greater safety – fewer hazards.
- Fewer bottles mean less storage space – more lab space.
- Fewer bottles mean lower inventory costs.

You get the best when you order high purity solvents from Burdick & Jackson Laboratories, Inc. All solvents are available in either gallons or quarts.

Send for BJ-25.



**BURDICK  
& JACKSON  
LABORATORIES, INC.**

MUSKEGON, MICHIGAN 49442

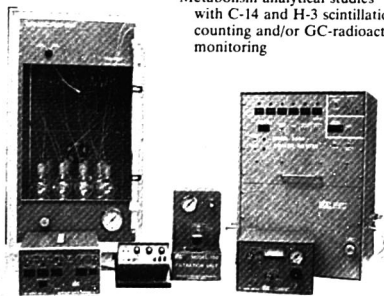
(616) 726-3171

CIRCLE 26 ON READER SERVICE CARD

## **Analytical services, analytical instruments. We do both.**

### **Analytical Services**

Pesticide residues  
Trace organic pollutants  
Trace metals  
Aquatic toxicology  
Amino acid and other  
nutritional analyses  
Drug residues  
Methods development  
Metabolism analytical studies  
with C-14 and H-3 scintillation  
counting and/or GC-radioactive  
monitoring



### **Analytical Instruments**

GPC 1001 Autoprep - auto residue  
cleanup  
150 Filtration Unit - crude  
fiber without asbestos  
250 GC-Vent - precolumn venting  
of solvent packed or capillary  
350B Aquatic Dispenser - flow  
through aquatic toxicology  
450 Precision Calibrator -  
calibrate recorders, integra-  
tors, etc.



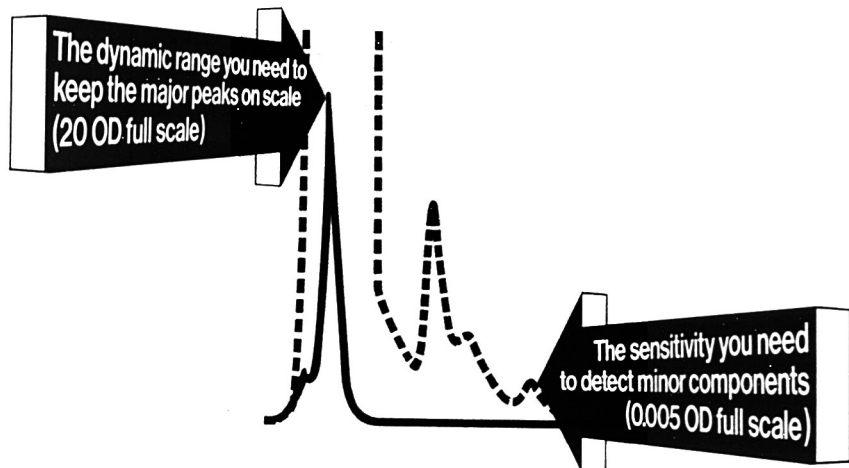
**Analytical BioChemistry Laboratories, Inc.**  
7200 East ABC Lane - P.O. Box 1097  
Columbia, MO 65201 Phone 314/474-8579

Germany, Belgium and Netherlands:  
N. Foss Electric A/S GMBH  
2000 Hamburg 19 Postfach 7718  
Phone 8590 16/19

Italy:  
Foss Electric (Italia) SPA  
Via Tito Livio  
35042 Este 38, Italy  
Phone (0429) 4770

CIRCLE 5 ON READER SERVICE CARD

# Now you can have it both ways!



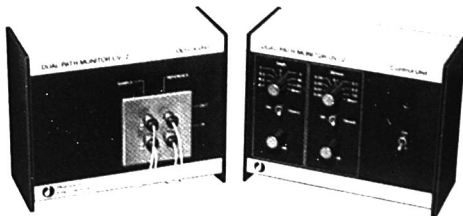
## Pharmacia Dual Path Monitor UV-2

has a unique flow cell with two optical path-lengths for new versatility in UV-monitoring.

- Monitor absorbance quantitatively up to 20 OD units full scale with a sensitivity of 0.005 OD units full scale at the same time, in the same run.
- Monitor at 254 nm and/or 280 nm with two completely independent measuring systems.

The Dual Path Monitor UV-2 has all the other features you expect of a high performance monitor: stability, cold room operation convenience and compact design. For less-demanding applications you can choose the Pharmacia Single Path Monitor UV-1 with a choice of 3 mm or 10 mm flow cell and operation at 254 nm or 280 nm.

Find out more about the practical advantages of column monitoring with the UV-2 and UV-1 Monitors. Ask about the Pharmacia Recorders too.

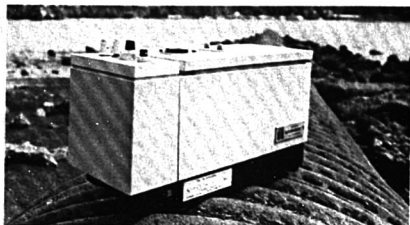


**Pharmacia Fine Chemicals**  
Division of Pharmacia, Inc.  
Piscataway, New Jersey 08854  
Phone (201) 469-1222

 **Pharmacia  
Fine Chemicals**

CIRCLE 168 ON READER SERVICE CARD

## The *Auto Analyzer*\* is the standard



and **ALPKEM**  
rebuilds the standard.

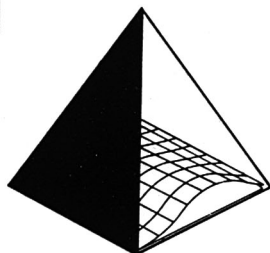
- \* Rebuilt AutoAnalyzer instruments
- \* Full line of accessories & supplies
- \* Applications Engineering

### ALPKEM Corporation

1234 S.E. Union Ave., Portland, OR 97214  
503 - 233-3626 or 800 - 547-5535

\*Trademark Technicon Corp.

CIRCLE 19 ON READER SERVICE CARD



## Validation of the Measurement Process

ACS Symposium Series No. 63

James R. DeVoe, *Editor*  
Institute for Materials Research,  
National Bureau of Standards

A symposium sponsored by the Division  
of Analytical Chemistry of the American  
Chemical Society.

The minicomputer is broadening the  
scope of the analytical chemist by  
emphasizing microprocessors and digital  
computers in day-to-day data analysis. It  
permits the analytical chemist to establish

a higher degree of statistical control,  
implement computational techniques to  
validate the measurement process, and  
control experimental parameters to  
facilitate data collection and  
computational fine-tuning.

This book focuses on the strategy for  
optimizing experimental parameters in  
chemical analysis and minimizing  
components of variation with respect to  
the variable size simplex, Poisson  
probability distribution, and acceptability  
limits.

### CONTENTS

Statistical Control of Measurement Processes •  
Testing Basic Assumptions in the Measurement  
Process • Systematic Error in Chemical  
Analysis • Role of Reference Materials and  
Reference Methods in the Measurement  
Process • Optimization of Experimental  
Parameters in Chemical Analysis •  
Components of Variation in Chemical Analysis

207 pages (1977) clothbound \$20.00  
LC 77-15555 ISBN 0-8412-0396-2

SIS/American Chemical Society  
1155 16th St., N.W./Wash., D.C. 20036

Please send \_\_\_\_\_ copies of SS 63 *Validation of  
the Measurement Process* at \$20.00 per copy

☐ Check enclosed for \$ \_\_\_\_\_ ☐ Bill me.  
Postpaid in U.S. and Canada, plus 75 cents elsewhere.

Name \_\_\_\_\_

Address \_\_\_\_\_

City \_\_\_\_\_

State \_\_\_\_\_

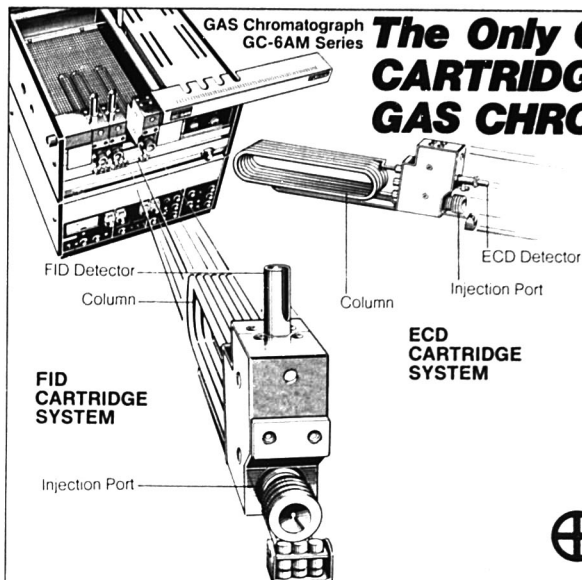
Zip \_\_\_\_\_

- (6) J. Hipple, H. Sommer, and H. Thomas,  
*Phys. Rev.*, **76**, 1877 (1949).
- (7) H. Sommer, H. Thomas, and J. Hipple,  
*ibid.*, **82**, 697 (1951).
- (8) M. B. Comisarow and A. G. Marshall,  
*J. Chem. Phys.*, **64**, 110 (1976).
- (9) T. B. McMahon and J. L. Beauchamp,  
*Rev. Sci. Instrum.*, **43**, 509 (1972).
- (10) R. T. McIver, Jr., *ibid.*, **41**, 555 (1970).
- (11) M. J. D. Low, *Anal. Chem.*, **41** (6), 97A  
(1969).
- (12) T. C. Farrar, *ibid.*, **42** (4), 109A  
(1970).
- (13) G. Horlick, *ibid.*, **43** (8), 61A (1971).
- (14) J. A. Decker, Jr., *ibid.*, **44** (2), 127A  
(1972).
- (15) M. Margoshes, *ibid.*, **43** (4), 101A  
(1971).
- (16) A. J. Senzel, Ed., "Instrumentation  
in Analytical Chemistry", American  
Chemical Society, Washington, D.C.,  
1973. Refs. 2 and 11-15 included in this  
text.
- (17) A. G. Marshall and M. B. Comisarow,  
*Anal. Chem.*, **47**, 491A (1975).
- (18) P. Felgett, *J. Phys. Radium*, **19**, 187  
(1958).
- (19) M. B. Comisarow and A. G. Marshall,  
*Chem. Phys. Lett.*, **25**, 282 (1974).
- (20) M. Comisarow and A. G. Marshall,  
"Annual Conference on Mass Spectrom-  
etry and Allied Topics", Philadelphia,  
Pa., May 1974.
- (21) M. B. Comisarow and A. G. Marshall,  
*Chem. Phys. Lett.*, **26**, 489 (1974).
- (22) M. B. Comisarow and A. G. Marshall,  
*Can. J. Chem.*, **52**, 1997 (1974).
- (23) M. B. Comisarow and A. G. Marshall,  
"Annual Conference on Mass Spectrom-  
etry and Allied Topics", Houston, Tex.,  
May 1975.
- (24) M. B. Comisarow and A. G. Marshall,  
*J. Chem. Phys.*, **62**, 293 (1975).
- (25) M. B. Comisarow, *Adv. Mass Spec-*  
*trum.*, **7**, in press.
- (26) R. T. McIver, Jr., and R. L. Hunter,  
"Annual Conference on Mass Spectrom-  
etry and Allied Topics", Washington,  
D.C., May 1977.
- (27) M. L. Gross, University of Nebraska,  
private communication.



Charles L. Wilkins is professor of  
chemistry at the University of Ne-  
braska. His research interests include  
pattern recognition techniques, labo-  
ratory computer interfacing, and nu-  
clear magnetic resonance and mass  
spectrometry.





GAS Chromatograph  
GC-6AM Series

## The Only One---- CARTRIDGE SYSTEM GAS CHROMATOGRAPH\*

The Shimadzu Cartridge System Gas Chromatograph comprises all the modules required for fast, accurate analysis. No worries about cross contamination between samples. Possibility of several applied flow systems.

### Main cartridge systems are:

- FID cartridge system
- ECD cartridge system
- TCD cartridge system (factory installed)
- Backflush cartridge system
- Precut cartridge system
- Column conditioning cartridge system
- Capillary column cartridge system

**\*U.S. PATENT 4044593**



**SHIMADZU**  
SCIENTIFIC INSTRUMENTS, INC.  
9147 Red Branch Road, Columbia, Md. 21045  
**SHIMADZU**  
SEISAKUSHO LTD KYOTO JAPAN

**THERE'S NO NEED TO COOL THE COLUMN, INJECTION PORT AND DETECTOR, EVEN TO CHANGE THE ENTIRE ANALYSIS SYSTEM!**

CIRCLE 192 ON READER SERVICE CARD

## NEW \*THREAD-TITE™ & MINIVIALS

**SAVE**  
BUY MINIVIALS DIRECT  
FROM MANUFACTURER

**SAVE up to 25%**

Quantity discounts available  
Send for list of sizes,  
related accessories,  
and prices!



### \*THREAD-TITE™ MINI-VIALS



- Threaded  $\frac{1}{8}$  outer joint provides positive pressure and vacuum connections to glassware assemblies.
- Compatible with  $\frac{1}{8}$  14/20 glassware.
- Syringe penetrable closures.

\*Patent pending

### \*THREAD-TITE™ MICRO SYSTEMS



- Fractional distillation
- Reflux
- Freeze drying
- Derivatization
- Radiosyntheses
- Extraction
- Concentration

Available  
in organic kits  
for both Micro and  
Semi-Micro scale.

## RELIANCE GLASS WORKS, INC.

17 Gateway Rd. Dept. AC-48 Bensenville, IL 60106 (312) 766-1816

CIRCLE 175 ON READER SERVICE CARD

# LABORATORY SERVICE CENTER

In addition to our regular line of Fine Organics • Reagents  
Special Intermediates • Indicators and Biochemicals  
**WE ARE NOW OFFERING:**

o, m, & p-Fluoroanilines • Fluoroanisoles • Fluorobenzaldehydes  
Fluorobenzoic Acids • Fluoronitrobenzenes • Fluorophenols  
Fluorophenylacetoneitriles and Fluorotoluenes  
plus many other fluorinated compounds.

Please send your specific inquiries

Tel.: 516-273-0900 Write for our Products List of over 3,000 chemicals TWX: 510-227-6230

**EASTERN CHEMICAL**

Division of GUARDIAN CHEMICAL CORP.

BOX 2500 K

HAUPPAUGE, N. Y. 11787

## ANALYTICAL SERVICES



## LAB SAFETY

Send for 1978 Catalog  
LAB SAFETY SUPPLY CO.  
P.O. Box 1422, Janesville, WI 53545

## Microparticle Standards

Large assortment of well-characterized microspheres and micro-powders for analytical, research, and testing applications. Range of diameters from .05 to 500 microns (µm). Size and other physical properties are listed for each product. Materials include polystyrene, glass, pollens, minerals, many others. Write or telephone for Data File 45.



Duke Scientific Corporation  
445 Sherman Avenue  
Palo Alto, CA 94306  
Phone (415) 328-2400

## Oxygen 18

15 years' experience in synthesizing  
LABELLED COMPOUNDS



19 Ox Bow Lane  
Summit, N. J. 07901  
201-273-0440

NEW  
LABORATORY  
AVAILABLE

## PROJECT ENGINEER

To assume complete responsibility for development and design of laboratory equipment and scientific apparatus. Must be inquisitive, creative and work with minimum supervision. We are a small but growing company with high quality products in liquid handling, pumping, dispensing. BSME required with knowledge of simple motor control circuitry and about 5 years experience in related field with significant product achievements.

George Fried, VP Engineering  
**MANOSTAT CORPORATION**  
519 Eighth Avenue  
New York, NY 10018  
212-594-6262

## USE LABORATORY SERVICE CENTER

## INDEX TO ADVERTISERS IN THIS ISSUE

CIRCLE INQUIRY NO.	ADVERTISERS	PAGE NO.	CIRCLE INQUIRY NO.	ADVERTISERS	PAGE NO.
3	Abbott	477A	64	Extranuclear Laboratories, Inc. And Associates	504A
4	Bentley, Barnes & Lynn, Inc.	480A	75	Fisher Scientific Company	443A, 449A, 450A, 451A
18	Academic Press Flamm Advertising Alroco Industrial Gases Hammond Farrell Inc. Alpkem Corporation	443A 000A	85	Tech-Ad Associates Gifford Instrument Laboratories, Inc.	485A
7-17	American Instrument Company Industrial Advertising Associates	453A	84	Glenco Scientific	448A
6	Analabs	434A	86	Boone Advertising, Inc.	496A
5	Shepherd, Tibbalt, Galog Associates	499A	88	Gould Incorporated	496A
25, 27	Analytical Biochemistry Laboratories Carol Watts Creative Services	425A, 443A	99	Carr Liggett Advertising, Inc.	459A
21	J. T. Baker Chemical Company	474A	98	Haake	455A
29	Naimark & Barba, Inc.	474A	98	Hamilton Company	455A
28, 36-40	Barnes Engineering Company Jarman, Spitzer & Felix, Inc.	488B	97	Measler & Emerson, Inc.	491A
23	Bausch & Lomb	488B	94	W. A. Hammond Drierite Company	488A
23	Beckman Instruments, Inc.	423A, 460A-461A	96	Hellma International, Inc.	447A
24	N W Ayer ADH International	0BC	96	Miller Advertising Agency	447A
24	Brinkman Instruments, Inc.	456A	95	Hewlett-Packard S.A.	447A
26	Blatt Advertising, Inc.	456A	95	Dorland Advertising Limited	IFC
26	Buchler Instruments	499A	111	Cooley & Shillinglaw, Inc.	474A
34	Fletcher-Walker-Gesell, Inc.	468A	110	Instrument SA, Inc., J-Y Optical Systems Div.	474A
33	Burdick & Jackson Laboratories, Inc.	468A	110	Kathy Wyatt & Associates	486A
32	Studio 5 Advertising	468A	112, 115	ISCO	475A, 483A
50	Columbia Scientific Industries	468A	114	Farnaux Associates Advertising	470A
51-58	Columbia Advertising Associates	478A	116	Weinrich Associates, Inc.	488A
63	Crane Company	409A	127	Joyce-Loeb Advertising	487A
	Doremus Updown	417A	126	S & M E Winship	487A
	Crawford Filling Company	489A		Kwaunee Scientific Equipment Corporation	487A
	Falls Advertising Company			Fahlgren & Ferriss, Inc.	432A
	Dohmann			Labindustries	487A
	Fred Schott & Associates			Fred Schott & Associates	487A
	Durum Instrument Corporation			Laboratory Data Control	487A
	Eastman Kodak Company			Kelisher, Bamberger, Terry	487A
	Rumrill-Hoyt, Inc.			Leco Corporation	471A

# INDEX TO ADVERTISERS IN THIS ISSUE

CIRCLE INQUIRY NO.	ADVERTISERS	PAGE NO.
128	Lindberg Fensholt Incorporated	462A
141	Matheson Kenyon Hoag Associates	415A
139-140	MC/B Manufacturing Chemists, Inc. Liebel & Company Advertising	472B, 472C
143	Mettler Harris D. McKinney, Inc.	469A
145, 146	Micromeritics Instrument Corporation Adgraphics	427A
144	Mitsubishi Chemical Industries Ltd. Global Advertising Co., Ltd.	472A
150	Neslab Instruments, Inc. The Ramphastos Agency	467A
149	Norton Plastics & Synthetics Division Northlich, Stolley of Akron, Inc.	424A
157	Ohaus Scale Corporation Michel-Cather, Inc.	419A
156	Orion Research, Inc. OBC Advertising	413A
171	Pacific Scientific Allen, Dorsey & Hatfield, Inc.	452A
166	Parr Instrument Company F. Willard Hills Advertising	488A
163	Pedersen Instruments Benjamin Paul Harold Advertising	473A
159, 173	Perkin-Elmer Corporation Marquardt & Roche, Inc. Advertising	437A, 441A
168	Pharmacia Fine Chemicals Cummins, MacFail & Nutry, Inc.	499A
161, 162	Phillips Electronic Instruments, Inc. Shepherd, Tibball, Galog Associates	438A, 458A
160	Philips Industries C. J. Nicholl & Associates Ltd.	488D
172	Pierce Chemical Company Pierce Ad Graphics	442A
164-165, 169-170, 180-181	Princeton Applied Research Corporation The Message Center	420A-421A, 454A, 492A
167	Pye Unicam Ltd.	488C
177	Rainin Instrument Company, Inc. Robert J. Allen	484A
174	Regis Chemical Company Dick Loew & Associates Advertising	463A
175	Reliance Glass Company MG Creative Arts	501A
176	Rheodyne Bonfield Associates, Inc.	476A
179	Rudolf Research Kathy Wyatt & Associates	486A
189	Sargent-Welch Polytech Advertising	445A
191	Schoffel Instrument Corporation Tel-Mark, Inc.	454A
192	Shimadzu Seisakusho Ltd. General Advertising Agency, Inc.	501A
188	Siemens Hanson Fassler, Kolody, Inc.	457A
193	G. Frederick Smith Chemical Company Andrew Show Advertising	486A
190	Spectrametrics S. Gunnar Myrbeck & Co., Inc.	426A
187	SPEX Industries Seymour Nussenbaum	463A
204	Technic, Incorporated Brunswick Advertising	491A
209	Tektronix-IDP Young, Wain & Roehr, Inc.	465A
210	Thermoplastic Processes, Inc. Gilbert, Whitney & Johns, Inc.	442A
206, 207, 208	Tracor Analytical Instruments Aim Advertising Agency	436A, 472A
205	Tracor Northern, Inc. Aitchnew Energetics	481A

CIRCLE INQUIRY NO.	ADVERTISERS	PAGE NO.
203	TSI Inc. Visual-Media Inc.	491A
214	U.S. Divers Company International Communications	490A
1-2, 196-197	Varian Moran, Lanig & Duncan Advertising	433A, 435A
234	Whatman, Inc. J. S. Lanza & Associates	410A

\* See ad in ACS Laboratory Guide

\*\* Company so marked has advertisement in the foreign regional edition only

Advertising Management for the American Chemical Society Publications

## CENTCOM, LTD.

Thomas N. J. Koerwer, President; James A. Byrne, Vice President; Clay S. Holden, Vice President; Benjamin W. Jones, Vice President; Robert L. Voepel, Vice President; C. Douglas Wallach, Vice President, 25 Sylvan Rd. South, Westport, Connecticut 06880 (Area Code 203) 226-7131

## ADVERTISING SALES MANAGER

James A. Byrne

## SALES REPRESENTATIVES

Atlanta, GA ... Robert E. Keichner, CENTCOM, Ltd. Telephone: 203-226-7131  
 Boston, MA ... Don Davis, CENTCOM, LTD. Telephone 203-226-7131  
 Chicago ... Thomas Hanley, CENTCOM, LTD., 540 Frontage Rd., Northfield, Ill. 60093. 312-441-6383.  
 Cleveland ... James Pecoy, CENTCOM, LTD., Suite 205, 18615 Detroit Ave., Lakewood, Ohio 44107. 216 228-8050.  
 Houston ... Robert LaPointe, CENTCOM, LTD., 415-692-0949.  
 Denver ... Clay S. Holden, CENTCOM LTD., 213-776-0552.  
 Los Angeles 90045 ... Clay S. Holden, CENTCOM, LTD., Newton Pacific Center, 3142 Pacific Coast Highway, Suite 200, Torrance, CA 90505, 213-325-1903  
 New York 10017 ... Don Davis, Richard L. Going, CENTCOM LTD., 60 East 42nd St., 212-972-9660  
 Philadelphia ... Richard L. Going, CENTCOM LTD., GSB Building, Suite 510 1 Belmont Avenue Bala Cynwyd, Pa. 19004. Telephone: 215-667-9666  
 San Francisco, CA ... Robert LaPointe, CENTCOM, LTD., Room 235, 1499 Bayshore Highway, Burlingame, CA 94010. Telephone: (415) 692-0949  
 Westport 06880 ... Don Davis, CENTCOM, LTD., 25 Sylvan Rd. So., 203-226-7131.  
 Manchester, England ... Jill E. Loney, Technomedia Ltd., 216, Longhurst Lane, Melior, Stockport, SK6 5PW. Telephone: 061-427-5860  
 Reading, England ... Malcolm Thiele, Technomedia Ltd., Wood Cottage, Shurlock Row, Reading, RG10 0OE. Telephone 073-581-302  
 Tokyo, Japan ... Haruo Moribayashi, International Media Representatives Ltd., 1, Shiba-Kotohiracho, Minato-ku Tokyo. Telephone: 502-0656  
 Verviers, Belgium ... Andre Jamar, Etablissements Andre Jamar, 1 Rue Mallard, 4800 Verviers. Telephone (087) 22-53-85.

## PRODUCTION DEPARTMENT

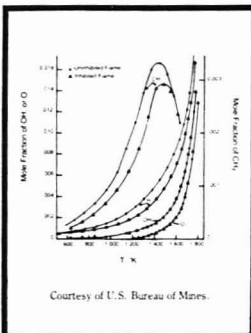
Production Director  
Joseph P. Stenza

Advertising Production Assistant  
Barbara Auferheide

# How in the world can four metal rods make for safe coal mines and warm homes?

The immediacy of the energy crisis has led to the rediscovery of this country's greatest natural resource . . . coal. Billions of tons are in reserve; enough potential energy to last far into the future. But can the hazards of mining be overcome? Can coal be consumed safely without harming the environment? Some interesting studies are underway to determine solutions to both problems.

In the coal mine, the threat of a fire or explosion is ever-present. Investigations of flames by direct examination of radical formations are pinpointing flame propagation mechanisms. The study of changes in radical concentrations, as influenced by flame temperature and the presence of various chemicals, provides valuable information for controlling mine environments. Now, effective retardants can be developed for the prevention and quick suppression of mine fires.



Fuel for thought.

As a solid mineral, coal is impractical for large scale use. Modern homes, utilities and factories are no longer equipped to burn it, and distribution would be costly. Additionally, poor quality coals, burned in open fires, release high levels of sulphur dioxide into the atmosphere. Potential solutions to these problems call for conversion of coal into a pollutant-free form. Studies in coal gasification, liquification and hydrogenation are designed to find the most amenable varieties of coal and the chemical additives which might enhance the conversion and clean-up processes.

In both studies, the prime investigatory tool is mass spectrometry. Extranuclear Laboratories manufactures mass spectrometers of modular component design to serve these and other specific applications. Such innovative techniques as molecular beam modulation permit the examination and identification of not only stable chemicals but neutrals, radicals and ions as well. In coal gasification, powdered coal is heated in the absence of air to 1700° F and radicals such as H, OH, O, and SO quantitatively measured as functions of temperature, coal type, and additive concentrations.

**Modulated molecular beam mass spectrometry**, as demonstrated by EMBA II, has applications in plasma and flame analysis, high temperature dissociation, radical-molecule interaction and many other areas. The unique property of the technique is its ability to monitor the chemically unstable species formed by dynamic systems . . . a subject untouched by conventional mass spectrometry.

**And the four metal rods? They're the heart of our quadrupole mass spectrometer systems.**



**Extranuclear Laboratories, Inc.**  
P.O. Box 11512 / Pittsburgh, Pennsylvania 15238 (412) 782-3884  
Telex: 812-316 Extralab Pgh

CIRCLE 64 ON READER SERVICE CARD



Use this card to receive  
your own monthly copy of

1978

## ANALYTICAL CHEMISTRY

Start my subscription as follows:

	U. S.	Can.**	Foreign**
ACS Members*	<input type="checkbox"/> \$10.00	<input type="checkbox"/> \$19.00	<input type="checkbox"/> \$19.00
Nonmembers (Personal)	<input type="checkbox"/> \$14.00	<input type="checkbox"/> \$23.00	<input type="checkbox"/> \$23.00
Institutional	<input type="checkbox"/> \$14.00	<input type="checkbox"/> \$23.00	<input type="checkbox"/> \$29.00

☐ Bill me ☐ Bill Company ☐ Payment enclosed  
(Make payable: American Chemical Society)

Name \_\_\_\_\_

Position \_\_\_\_\_

Your Employer \_\_\_\_\_

Address ☐ Home  
☐ Business \_\_\_\_\_

City \_\_\_\_\_ State \_\_\_\_\_ ZIP \_\_\_\_\_

Employer's business ☐ Manufacturing ☐ Academic  
☐ Government ☐ Other

If manufacturer, type of products produced \_\_\_\_\_

\*Subscriptions at ACS member rates are for personal use only

\*\*Payment must be made in U. S. Currency, by international money order, UNESCO coupons, U. S. bank draft, or through your book dealer

Allow 60 days for your first copy to be put in the mail 9998-G

**Mail this postage-free card today**

Use this card to receive  
your own monthly copy of

1978

## ANALYTICAL CHEMISTRY

Start my subscription as follows:

	U. S.	Can.**	Foreign**
ACS Members*	<input type="checkbox"/> \$10.00	<input type="checkbox"/> \$19.00	<input type="checkbox"/> \$19.00
Nonmembers (Personal)	<input type="checkbox"/> \$14.00	<input type="checkbox"/> \$23.00	<input type="checkbox"/> \$23.00
Institutional	<input type="checkbox"/> \$14.00	<input type="checkbox"/> \$23.00	<input type="checkbox"/> \$29.00

☐ Bill me ☐ Bill Company ☐ Payment enclosed  
(Make payable: American Chemical Society)

Name \_\_\_\_\_

Position \_\_\_\_\_

Your Employer \_\_\_\_\_

Address ☐ Home  
☐ Business \_\_\_\_\_

City \_\_\_\_\_ State \_\_\_\_\_ ZIP \_\_\_\_\_

Employer's business ☐ Manufacturing ☐ Academic  
☐ Government ☐ Other

If manufacturer, type of products produced \_\_\_\_\_

\*Subscriptions at ACS member rates are for personal use only

\*\*Payment must be made in U. S. Currency, by international money order, UNESCO coupons, U. S. bank draft, or through your book dealer

Allow 60 days for your first copy to be put in the mail 9998-G

**Mail this postage-free card today**

**FIRST CLASS**  
Permit No. 1411-R  
Washington, D. C.

**BUSINESS REPLY MAIL**

No postage stamp necessary if mailed in the United States

Postage will be paid by

**AMERICAN CHEMICAL SOCIETY**  
**1155 Sixteenth Street, N. W.**  
**Washington, D. C. 20036**

*ATTN: G. HEBRON*

**FIRST CLASS**  
Permit No. 1411-R  
Washington, D. C.

**BUSINESS REPLY MAIL**

No postage stamp necessary if mailed in the United States

Postage will be paid by

**AMERICAN CHEMICAL SOCIETY**  
**1155 Sixteenth Street, N. W.**  
**Washington, D. C. 20036**

*ATTN: G. HEBRON*

Editor: **Herbert A. Laitinen**

EDITORIAL HEADQUARTERS

1155 Sixteenth St., N.W.  
Washington, D.C. 20036  
Phone: 202-872-4570 Teletype: 710-8220151

Managing Editor: Josephine M. Petruzzl

Associate Editor: Andrew A. Husevsky

Associate Editor, Easton: Elizabeth R. Rule

Assistant Editors: Barbara Cassatt, Nancy J.

Oddenino, Deborah C. Stewart

Production Manager: Leroy L. Corcoran

Art Director: John V. Sinnott

Designer: Alan Kahan

Artist: Diane Reich

**Advisory Board:** Donald H. Anderson, Peter Carr, Velmer Fassel, David Firestone, Kurt F. J. Heinrich, Philip F. Kane, Barry L. Karger, J. Jack Kirkland, Lynn L. Lewis, Marvin Margoshes, Harry B. Mark, Jr., J. W. Mitchell, Harry L. Pardue, Garry A. Rechnitz, W. D. Shults

**Instrumentation Advisory Panel:** Gary D. Christian, Catherine Fenselau, Nathan Gochman, Gary M. Hieftje, Gary Horlick, Peter J. Kissinger, James N. Little, C. David Miller, Sidney L. Phillips

**Contributing Editor:** Claude A. Lucchesi  
Department of Chemistry, Northwestern  
University, Evanston, Ill. 60201

Published by the  
**AMERICAN CHEMICAL SOCIETY**  
1155 16th Street, N.W.  
Washington, D.C. 20036

**Books and Journals Division**

Director: D. H. Michael Bowen

Editorial: Charles R. Bertsch

Magazine and Production: Bacil Guiley

Research and Development: Seldon W.  
Terrant

Circulation Development: Marion Gurfein

Manuscript requirements are published in the January 1978 issue, page 189. Manuscripts for publication (4 copies) should be submitted to ANALYTICAL CHEMISTRY at the ACS Washington address.

The American Chemical Society and its editors assume no responsibility for the statements and opinions advanced by contributors. Views expressed in the editorials are those of the editors and do not necessarily represent the official position of the American Chemical Society.

## The Proton Microprobe

The announcement of the proton microprobe [*Science*, **199**, 765 (1978)] by two groups in Heidelberg marks the addition of still another approach to sensitive elemental analysis with high spatial resolution. As with every new analytical development, the method needs evaluation as to its place in the framework of modern methodology.

It is essentially a refinement of particle induced x-ray emission (PIXE) by focusing a proton beam to a spot size of  $2 \times 2$  micrometers. As such, it is a potential competitor to other probe methods such as the electron microprobe, ion microprobe mass spectrometer, and laser mass spectrometer. In comparison with the latter two methods, the proton microprobe offers the advantage of being a nondestructive method. In comparison with the electron microprobe, it is one to two orders of magnitude higher in sensitivity for trace elements. This increased sensitivity was demonstrated by analyzing grains of lunar minerals for trace elements. Several trace elements undetected by the electron microprobe were proved to be present.

As always, the advantages of a new method need to be weighed against its disadvantages. Apart from the obvious problems of instrumental complexity and expense, there are inherent differences in principle that need consideration. The relatively large penetration depths (20 to 70 micrometers) of the 0.5 to 4 MeV proton beam increase the background due to bremsstrahlung and characteristic x-rays from the sample backing. What is more important, the analytical sample is defined by the cross section of the beam and its penetration depth. The response from different regions of the sample varies with depth because of loss of proton energy with consequent change in x-ray yield. Thus, for quantitative results to be obtained for trace elements, the nature of the matrix and its physical form must be taken into account. There are, of course, competing trace analytical methods for *average* composition (e.g., neutron activation analysis), so the whole point of considering a probe approach is the need for spatial resolution.

In summary, the proton microprobe serves as an excellent example of a new approach which offers advantages for specific applications at the expense of disadvantages that need to be considered by the analytical chemist in deciding whether it should be added to the existing capability of an analytical facility.



# Optimization of Reverse-Phase Liquid Chromatographic Separation of Weak Organic Acids

Stanley N. Deming\* and Michael L. H. Turoff

Department of Chemistry, University of Houston, Houston, Texas 77004

The effect of aqueous carrier solvent pH upon the high performance reverse-phase liquid chromatographic separation of several benzoic acids is studied. A semiempirical optimization strategy is demonstrated: retention times of the weak acids of interest are measured at three or more values of pH in an appropriate buffer, models are fit to the data, and the model parameters are used to construct window diagrams from which the optimum pH can be estimated.

It has long been suggested that liquid chromatography should be a more versatile analytical tool than gas chromatography, in part because of the larger number of variable factors associated with the mobile liquid phase—e.g., in reverse-phase liquid chromatography, it is possible to vary pH, ionic strength, polarity, counterion concentration, etc. (1). To date, however, there have been few studies suggesting a systematic means of adjusting these factors to provide optimum liquid chromatographic performance. We present here a strategy for selecting a value of one of these factors, pH, to achieve optimum resolution of simple organic acids in reverse-phase chromatographic systems.

## THEORY

The optimization of chromatographic resolution is especially difficult because of the existence of multiple optima (2). The intentional variation of system conditions (e.g., temperature or pH) can often cause peaks to "cross" one another. Conditions for which two or more peaks of interest are eclipsed clearly represent minimum performance from the system (no separation). Conditions for which all peaks are separated from each other represent maximum performance. In chromatographic systems, there are often many sets of conditions that give rise to local maxima. The problem, then, is to predict the location in factor space of these local maxima and to choose the best (or global) maximum, often within certain constraints such as maximum allowable analysis time. Once this desirable region of factor space has been approximately located, local optimization procedures can be used to find the exact location of the maximum (3).

Laub and Purnell have presented a series of papers (4–7) in which "window diagrams" are used to locate optima in gas chromatographic systems for which the composition of a mixed stationary phase is a variable factor. We have found the concept of window diagrams to be equally useful for locating optima in reverse-phase liquid chromatographic systems for which pH is a variable factor. The following derivation is similar to those of Horvath et al. (8) and Pietrzyk and Chu (9).

Given a small amount of weak acid HA that dissociates to give conjugate base A<sup>-</sup> in a solution buffered by a more concentrated weak acid HB and its conjugate base B<sup>-</sup> (see

Figure 1), it can be shown that

$$\frac{[A^-]}{[HA]} = \left( \frac{K_{HA}}{K_{HB}} \right) \left( \frac{[B^-]}{[HB]} \right) = Kr \quad (1)$$

where  $K_{HA}$  and  $K_{HB}$  are the acid dissociation constants of HA and HB,  $K = K_{HA}/K_{HB}$ , and  $r = ([B^-]/[HB])$ . In a reverse-phase system, species HA and A<sup>-</sup> will each have individual affinities for both the aqueous (polar, mobile) phase and the organic (nonpolar, stationary) phase. At extreme values of pH where either HA or A<sup>-</sup> predominate, the relative affinities for the stationary phase are indicated by the retention times  $t_{HA}$  and  $t_{A^-}$ . Because the equilibrium between HA and A<sup>-</sup> is very fast with respect to the separation process, at intermediate values of pH the retention time  $t$  of the single observed peak might be expected to be a weighted average of the individual retention times

$$t = t_{HA} \left( \frac{[HA]}{[HA] + [A^-]} \right) + t_{A^-} \left( \frac{[A^-]}{[HA] + [A^-]} \right) = \frac{t_{HA} + t_{A^-} Kr}{1 + Kr} \quad (2)$$

The parameters  $t_{HA}$ ,  $t_{A^-}$ , and  $K$  can be estimated from experimental data obtained by measuring  $t$  for at least three different values of  $r$ . Different weak acids would be expected to give different sets of values for these three parameters because of their different affinities for the mobile and stationary phases, and because of their different acid dissociation constants.

## EXPERIMENTAL

**Chromatograph.** All separations were carried out using a Model 6000A pump (Waters Associates, Milford, Mass. 01757), a U6K injector (Waters), a Model SP8200 detector (Spectra Physics, Santa Clara, Calif. 95051) operated at 254 nm, and a Model 281 strip chart recorder (Soltec, Encino, Calif. 91316). A 10-cm section of 2-mm i.d. Bondapak C<sub>18</sub>/Corasil (Waters) was used as a precolumn to a 30-cm × 4-mm i.d.  $\mu$ C<sub>18</sub> Bondapak high efficiency column. A flow rate of 2.0 mL min<sup>-1</sup> was used throughout the study. Injection volumes were 5  $\mu$ L or less. The time equivalent of the void volume (1.65 min) was measured by noting the small change in detector signal after injecting a water sample.

**Solvents.** Nine buffer solutions were prepared as shown in Table I using 1.00 M acetic acid (HAc, Mallinckrodt Chemical Works, St. Louis, Mo. 63147), 1.00 M NaOH (Fisher Scientific Co., Fairlawn, N.J. 07410), and 1.00 M NaCl (Fisher) to provide a set of solvents for which the ionic strength was essentially constant (0.06 M) as the  $r$  value ranged from 0.111 to 9.00.

**Weak Acids.** Solutions of five weak organic acids—benzoic acid, 2-aminobenzoic acid, 4-aminobenzoic acid, 4-hydroxybenzoic acid, and 1,4-benzenedicarboxylic acid—were prepared by dissolving 50 mg of the weak acid in 10 mL distilled water and filtering through a 0.45  $\mu$ m filter (type GA-6, Gelman, Ann Arbor, Mich. 48106). A mixture of all five weak acids was prepared by combining appropriate amounts of the individual solutions.



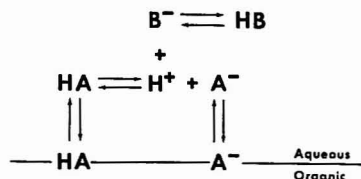


Figure 1. Equilibria involved in the reverse-phase liquid chromatographic separation of weak acids

Table I. Solvent Composition

Solvent	mL 1.00 M HAC <sup>a</sup>	mL 1.00 M NaOH <sup>a</sup>	mL 1.00 M NaCl <sup>a</sup>	$r^b$
1	30.00	3.00	27.00	0.111
2	30.00	6.00	24.00	0.250
3	30.00	9.00	21.00	0.429
4	30.00	12.00	18.00	0.667
5	30.00	15.00	15.00	1.00
6	30.00	18.00	12.00	1.50
7	30.00	21.00	9.00	2.33
8	30.00	24.00	6.00	4.00
9	30.00	27.00	3.00	9.00

<sup>a</sup> In 0.500 liters of solution. <sup>b</sup>  $([\text{B}^-]/[\text{HB}])$ ; see text.

Calculations. The parameters of Equation 2 were fit to the data for each of the weak acids using a simplex nonlinear least-squares program similar to that described by O'Neill (10).

## RESULTS

Table II contains observed retention times for each of the five weak acids at each of the different solvent compositions. Replicates were carried out at  $r = 0.111, 1.00$ , and  $9.00$ . Using these experimental data, the parameters of Equation 2 were fit for each weak acid. The results are presented in Table III. Figure 2 shows calculated and observed retention times as a function of  $\log(r)$  (equivalent to an offset pH scale, where  $\log(r) = 0$  corresponds to  $\text{pK}_{\text{HB}}$ ).

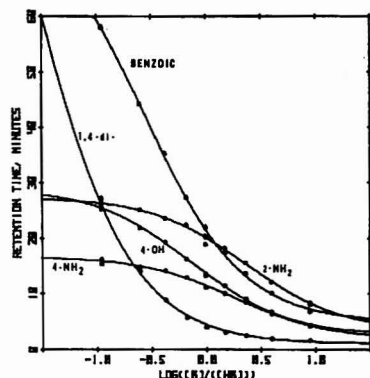


Figure 2. Retention time vs.  $\log(r)$  for five weak acids. Solid lines are predicted behavior, dots are observed behavior

The relative net retention of two compounds X and Y is defined as  $(t_X - t_Y)/(t_Y - t_V)$ , where  $t_X$  and  $t_Y$  are the observed (uncorrected) retention times of X and Y, and  $t_V$  is the time equivalent of the void volume. If the relative net retention is calculated to be less than unity, the reciprocal is taken; thus, relative retention is always greater than or equal to unity.

Figure 3 is a window diagram (4) showing relative net retention for all ten pairs of the five weak acids as a function of  $\log(r)$ . Those conditions giving a relative retention of unity for a pair of components represent minimum performance from the system (eclipsed peaks). Those conditions giving relative retentions greater than unity give improved separation for that pair. The tops of the "windows" indicate conditions for which the relative retentions of two pairs are equal—each of the two pairs is equally well separated. The tops of the windows thus represent conditions giving the best separation for the worst separated pairs—all other pairs will be better separated. In Figure 3, the best conditions occur at  $r = 0.54$ .

Table II. Retention Times of Weak Acids

$r$	Experiment	Retention time, min				
		Benzoic acid	2-Amino-benzoic acid	4-Amino-benzoic acid	4-Hydroxy-benzoic acid	1,4-Benzenedicarboxylic acid
0.111	3	58.10	26.50	16.25	25.25	25.30
	7	58.20	25.80	15.40	25.60	27.27
0.250	10	44.30	25.15	14.85	21.95	14.15
	4	35.40	23.65	14.15	19.40	8.88
0.667	12	27.40	22.45	12.90	16.35	5.74
	6	22.15	20.35	11.15	13.60	4.05
1.00	11	20.50	19.05	11.15	13.30	3.99
	5	17.55	18.40	10.05	11.45	3.10
2.33	8	13.70	16.70	8.50	9.10	2.51
	1	10.15	12.15	6.40	6.75	1.97
4.00	2	7.00	8.42	4.29	4.42	1.68
	9	6.86	8.11	4.26	4.32	1.70

Table III. Calculated Parameters

Weak acid	$t_{\text{HA}}$ , min	$t_{\text{A}^-}$ , min	$K$	$10^4 \times K_{\text{HA}}^a$	$10^4 \times K_{\text{HA}}^b$ , lit.
Benzoic	77.73	4.84	3.320	6.5	6.3
2-Aminobenzoic	27.25	3.19	0.414	0.81	1.0
4-Aminobenzoic	16.72	1.76	0.549	1.1	1.2
4-Hydroxybenzoic	28.79	2.48	1.344	2.6	2.9
1,4-Benzenedicarboxylic	130.0	1.00	36.77	71.7	15.0

<sup>a</sup> Calculated using  $K_{\text{HB}} = 1.95 \times 10^{-4}$ . <sup>b</sup> Reference 13.

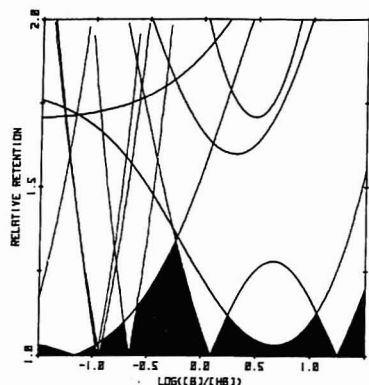


Figure 3. Window diagram for all ten pairs of five weak acids

An optimum solvent was prepared containing 30.00 mL 1.00 M HAc, 10.50 mL 1.00 M NaOH, and 19.50 mL 1.00 M NaCl in 0.500 L and was used to separate a mixture of the five weak acids.

Figure 4 shows chromatograms obtained at  $r = 9.00$ , 0.111, and 0.54. In chromatogram A (higher pH), 4-aminobenzoic acid and 4-hydroxybenzoic acid are eclipsed (see Figure 2); in chromatogram B (lower pH), 2-aminobenzoic acid, 4-hydroxybenzoic acid, and 1,4-benzenedicarboxylic acid elute together; chromatogram C (optimum pH) shows baseline separation of all peaks.

### DISCUSSION

At low values of  $r$  (relatively acidic conditions), the benzoic acids are protonated (uncharged) and have a greater affinity for the stationary nonpolar phase; their retention times are relatively long (see Figure 2). At higher values of  $r$  (relatively basic conditions), the acids are unprotonated (negatively charged) and have a greater affinity for the mobile polar phase; their retention times are relatively short. This behavior has been observed previously for other weak acids and bases (e.g., 8, 9, 11, 12).

Because  $K = K_{HA}/K_{HB}$ , values of  $K_{HA}$  can be calculated from the estimated values of  $K$  and a known value of  $K_{HB}$ . Table III compares values of  $K_{HA}$  estimated in this study with values from the literature. The agreement is good except for 1,4-benzenedicarboxylic acid. (However, as can be seen in Figure 2, data for 1,4-benzenedicarboxylic acid correspond to predominantly ionized conditions for the acid. The estimates

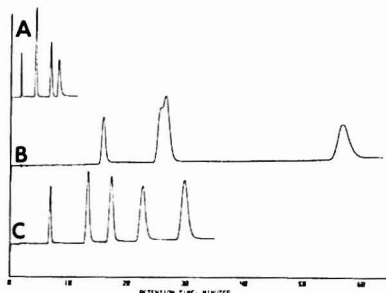


Figure 4. Chromatograms of mixture of five weak acids. Chromatogram A:  $r = 9.00$ . Chromatogram B:  $r = 0.111$ . Chromatogram C:  $r = 0.54$

of  $t_{HA}$  and  $K$  are subject to significant uncertainty. Thus, the calculated value of  $K_{HA}$  for 1,4-benzenedicarboxylic acid is an imprecise estimate, and the discrepancy between calculated and literature values of  $K_{HA}$  is not highly significant from a statistical point of view.)

### CONCLUSION

A semiempirical optimization strategy has been demonstrated: retention times of the weak acids of interest are measured at three or more values of  $r$  in an appropriate buffer, models are fit to the data, and the model parameters are used to construct window diagrams from which optimum chromatographic conditions can be estimated.

### LITERATURE CITED

- (1) J. J. Kirkland, "Modern Practice of Liquid Chromatography", Wiley, New York, N.Y., 1971, p. 162.
- (2) S. L. Morgan and S. N. Deming, *Sep. Purif. Methods*, **5**, 333 (1976).
- (3) S. L. Morgan and S. N. Deming, *J. Chromatogr.*, **112**, 267 (1975).
- (4) R. J. Laub and J. H. Purnell, *J. Chromatogr.*, **112**, 71 (1975).
- (5) R. J. Laub and J. H. Purnell, *Anal. Chem.*, **48**, 799 (1976).
- (6) R. J. Laub and J. H. Purnell, *Anal. Chem.*, **48**, 1720 (1976).
- (7) R. J. Laub, J. H. Purnell, and P. S. Williams, *J. Chromatogr.*, **134**, 249 (1977).
- (8) C. Horvath, W. Melander, and I. Molnar, *Anal. Chem.*, **49**, 142 (1977).
- (9) D. J. Pietrzyk and C. H. Chu, *Anal. Chem.*, **49**, 860 (1977).
- (10) R. O'Neill, *Appl. Statist.*, **20**, 338 (1971).
- (11) R. A. Hartwick and P. R. Brown, *J. Chromatogr.*, **126**, 679 (1976).
- (12) I. Molnar and C. Horvath, *Clin. Chem. (Winston-Salem, N.C.)*, **22**, 1497 (1976).
- (13) R. T. Morrison and R. N. Boyd, "Organic Chemistry", Allyn and Bacon, Boston, 1959, pp. 454, 677.

RECEIVED for review October 27, 1977. Accepted January 9, 1978. Financial support of Grant E-644 from the Robert A. Welch Foundation is gratefully acknowledged.

# Analysis of Carotenoid and Porphyrin Pigments of Geochemical Interest by High-Performance Liquid Chromatography

S. K. Hajibrahim, P. J. C. Tibbetts, C. D. Watts, J. R. Maxwell, and G. Eglinton

*Organic Geochemistry Unit, School of Chemistry, University of Bristol, Cantock's Close, Bristol BS8 1TS, England*

H. Collin and G. Gulochon\*

*Laboratoire de Chimie Analytique Physique, Ecole Polytechnique, 91128 Palaiseau Cedex, France*

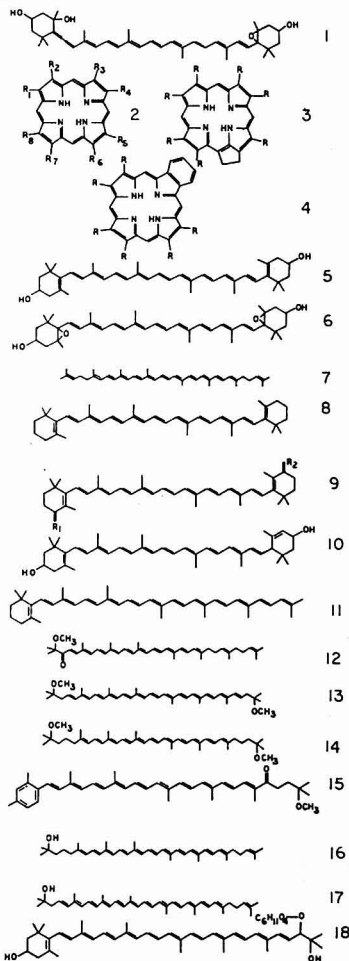
High-performance liquid chromatography (HPLC) is shown to be a powerful tool in the analysis of carotenoid and porphyrin pigments. Columns packed with 5- $\mu\text{m}$  irregular silica gel particles by a high density and high constant pressure method allow efficient separation of mixtures of total nonsaponifiable carotenoids from recent sedimentary situations. Good reproducibility of retention times (within 2%) is achieved in the gradient elution mode. However, attention must be paid to reequilibration of the column after each injection by washing with the less polar solvent for a minimum of 15 min (for carotenoids) or of 30 min (for porphyrins). HPLC appears to be useful in "fingerprinting" petroporphyrin distributions in crude oil.

The majority of applications of HPLC to pigment analysis have been concerned with aromatic compounds, particularly quinones (1) and azo dyes (2) and there are no reports of the analysis of porphyrin or carotenoid pigments in samples of geological interest. The technique has been applied in the analysis of biological porphyrins and of chlorophyll derivatives (3). Resolution of a synthetic coproporphyrin mixture has been achieved by recycling on 10- $\mu\text{m}$  Porasil columns (4); ten recycles on two 30 cm  $\times$  4 mm i.d. columns connected in series were necessary to obtain separation of the isomers coproporphyrin III and IV as their tetramethyl esters. There is only one report of the analysis of carotenoids by HPLC; in this case magnesium oxide and zinc carbonate were used for the separation of citrus fruit carotenes and xanthophylls, respectively (5). Resolution of *cis-trans* isomers was obtained, but retention times for polar carotenoids were long (e.g. ca. 4.5 h for neoxanthin, 1. Structures are shown Chart I).

In general, mixtures of pigments of geochemical origin are more complex than those found in organisms, as a result of the wide diversity of inputs contributing to forming sediments and of the diagenetic changes which subsequently occur; also they are normally present in lower concentrations. Porphyrin mixtures extracted from petroleum (petroporphyrins) typically contain (6) series of nickel and vanadyl complexes of alkyl-substituted petroporphyrins of two major skeletal types—etio (2, R = H or alkyl) and desoxophylloerythroio—(DPEP, 3, R = H or alkyl) and a minor type—rhodo (tentatively assigned as 4; the alkyl substituents contain from ca. 6 to ca. 19 carbon atoms, although the actual sites of substitution and the exact nature of the substituents have not been fully determined (6). In addition, structural isomers are known to occur in petroleum (7–10). In sedimentary situations, carotenoid mixtures containing up to 12 major components and a large number of minor components are frequently obtained (11).

Neither porphyrins nor carotenoids can be analyzed directly by gas-liquid chromatography, as a result of their involatility and/or thermal instability. An analytical technique with high resolving power and sensitivity is therefore required for the separation of these compounds. The present study reports the application of HPLC to the analysis of carotenoid mixtures

Chart I



isolated from a recent lacustrine sediment and from an algal mat, and of metallo- and demetallated-petroporphyrin mixtures isolated from crude oil. The separations obtained on columns containing 10- $\mu\text{m}$  spherical and 5- $\mu\text{m}$  irregular

silica particles packed by different slurry methods are compared.

### EXPERIMENTAL

**Isolation of Carotenoids.** The sediment sample from Grasmere (an oligotrophic lake, English Lake District) was obtained from the deepest part of the lake using a Gilson mud sampler (12). The core was sectioned in situ and the sections were transported to the laboratory in isopropanol and were stored in a deep freeze ( $-20^{\circ}\text{C}$ ) prior to extraction. The algal mat sample was collected from Baja California, Mexico, using a scoop. The top 3–4 cm layer was stored (ca. 7 days) in isopropanol at  $0^{\circ}\text{C}$  and then at  $-20^{\circ}\text{C}$ . Both samples were extracted with isopropanol/hexane (4/1) and detailed procedures for the isolation of total carotenoid nonsaponifiable fractions are listed by Watts et al. (11). Small aliquots of these fractions were examined by HPLC; for comparison with the HPLC data, the remainder of each fraction was further separated by preparative-scale thin-layer chromatography (TLC) to isolate individual components for identification by UV/VIS spectrophotometry and mass spectrometry (detailed procedures given in Ref. 11).

**Isolation of Petroporphyrin Concentrates.** Petroporphyrin concentrates were obtained from Boscan (well No. 9K3) crude oil (Eocene, W. Venezuela); details of the distributions obtained by probe mass spectrometry of the same oil have been reported (9, 10). Concentrates were also obtained in the same way from Kuwait (Cretaceous) crude oil.

**Metallopetroporphyrins.** To Boscan crude (1 g) in toluene (3 mL) was added anhydrous MeOH ( $5 \times 6$  mL) and the mixture was sonicated (ca. 3 min); centrifugation (ca. 3000 rpm, 5 min) afforded an upper layer (wine-red) containing the crude metallopetroporphyrins which was removed by pipet and filtered through pre-washed (MeOH) cotton wool.

**Demetallated Petroporphyrins.** The metals were removed from the metallopetroporphyrin concentrate by treatment with methane sulfonic acid and the free bases were recovered as outlined previously (8).

**High-Pressure Liquid Chromatography.** HPLC analyses were mainly carried out using silica columns (stainless steel, 24 cm  $\times$  4.6 mm i.d.) and gradient elution. The equipment comprises two solvent delivery pumps (Waters Associates M6000D), a solvent programmer (Waters M660), and a spectrophotometer (Varian Variscan L635M) with Varian flow cells (8  $\mu\text{L}$ ) as detector. Solutions of samples were introduced into the column, using the stop-flow technique, from a 10- $\mu\text{L}$  syringe via a septum inlet port. Redistilled solvents (laboratory reagent) were employed as mobile phase.

Two packing methods were used. In the first, spherical silica particles (10  $\mu\text{m}$ , Spherisorb, Phase-Sep Ltd.) were packed as a slurry in methanol (2.5 g in 25 mL), the slurry being introduced to a precolumn attached to the main column. The pre-column was connected to one of the Waters pumps and the slurry pumped (9 mL/min) into the column; after 10 min, the flow rate of methanol was decreased (2.5 mL/min) and pumping was continued (1 h). The column was conditioned by pumping acetone for 20 min with a flow rate of 2.5 mL/min, then a linear gradient of acetone in hexane (100 to 0% over 20 min) and finally hexane (2.5 mL/min; 10 min). The second method was the balanced density method described by Martin et al. (13). Either irregular (5  $\mu\text{m}$ , Partisil, Whatman) or spherical silica particles (10  $\mu\text{m}$ , Spherisorb, Phase-Sep Ltd.) were packed as a balanced density slurry in a 1,2-dibromomethane/benzene mixture. The correct density of the mixture was obtained by slurring the particles in 1,2-dibromomethane and by adding benzene dropwise until no appreciable sedimentation of particles was observed after centrifugation at 2000 rpm (30 s). The empty column was first fitted with a cylinder which was connected to the pump (Orlita S600) through a two-way valve. The valve was closed and the pressure allowed to build up to 450 atm by increasing the volume of the pump chamber. The slurry was then forced into the column by opening the valve. During the packing procedure, the pressure remained constant at 450 atm except for the first few tenths of a second when the flow-rate was higher than 100  $\text{cm}^3/\text{min}$  and the pressure fell sharply. The high initial flow is necessary to ensure a large linear velocity of packing. Thus the pump has to be capable of delivering high flow rates and consequently capable

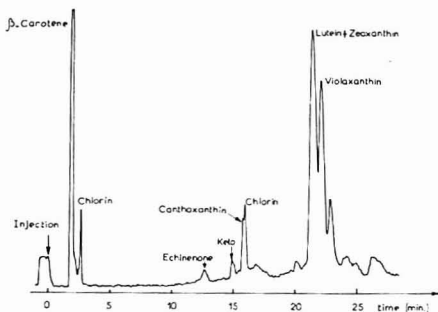


**Figure 1.** HPLC record of total nonsaponifiable carotenoids from Grasmere sediment (core section: 17–40 cm). Conditions: 10- $\mu\text{m}$  spherical silica packed by methanol slurry, column 30 cm  $\times$  1.8 mm i.d., solvent gradient 2–50% acetone in hexane (concave) over 20 min, flow rate 1 mL/min, detector 451 nm

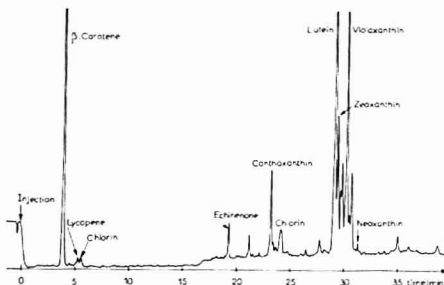


**Figure 2.** HPLC record of total nonsaponifiable carotenoids from Grasmere sediment (core section 17–40 cm). Conditions: 5- $\mu\text{m}$  irregular silica particles, packed by balanced density, column 24 cm  $\times$  4.6 mm i.d., solvent gradient 1–75% acetone in hexane (concave) over 30 min, flow rate 1 mL/min, detector 451 nm (each peak labeled "chlorin" represents a different compound of the chlorin type)

of being operated at high pressures. With the Orlita S600 Model, flow rates larger than several liters per minute can be generated at pressures larger than 12000 psi.

### RESULTS AND DISCUSSION

**Carotenoids.** The distributions of total nonsaponifiable carotenoids from Grasmere sediment (17–40 cm from sediment/water interface) are shown in Figures 1 and 2. With the exception of zeaxanthin, 5, and violaxanthin, 6, components were assigned initially by coinjection with authentic standards. Identities were confirmed by TLC with the standards, by preparative-scale TLC, and by comparison of mass and UV/VIS spectra with those of the standards (11). Lycopene, 7, and neoxanthin, 1, were present in insufficient concentrations to obtain a mass spectrum from the appropriate TLC fraction. Zeaxanthin, 5, was identified in the same way as the other components but was not coeluted. Violaxanthin, 6, was tentatively assigned by comparison of the HPLC distribution with that from a higher plant leaf known to contain this component as a major carotenoid. Chlorins were assigned by monitoring the column effluent at 410 nm; these are dihydroporphyrin pigments present in the nonsaponifiable carotenoid fraction.

Resolution of carotenoids with different functional groups was readily accomplished by the 10- $\mu\text{m}$  column packed by the methanol-slurry method (Figure 1). Thus, hydrocarbons ( $\beta$ -carotene, 8, mono-keto (echinenone, 9,  $\text{R}^1 = \text{O}$ ,  $\text{R}^2 = \text{H}_2$ ),



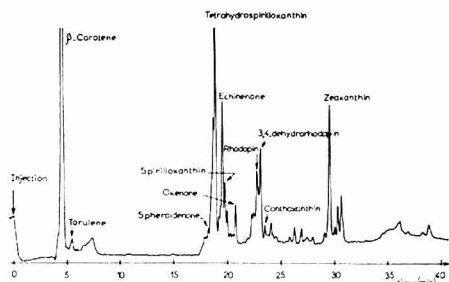


Figure 3. HPLC record of total nonsaponifiable carotenoids from Baja algal mat. Conditions as for Figure 2 (each peak labeled "chlorin" represents a different compound of the chlorin type)

diketo-(canthaxanthin, 9,  $R^1 = R^2 = O$ ), dihydroxy-(lutein, 10, and zeaxanthin, 5,) carotenoids were separated to baseline under the conditions used. Only partial resolution of lutein/zeaxanthin from violaxanthin, 6, which differ by the presence of two epoxy groups in the latter, was obtained and no resolution of the double-bond positional isomers, lutein and zeaxanthin, was observed. The orders of elution are similar to those obtained from TLC analysis of the same mixture on Silica Gel G layers ( $CH_2Cl_2/EtOAc$ ; 80/20 as developer). A significant improvement in resolution was observed, however, with the 5- $\mu m$  irregular silica column packed by the balanced density method (Figure 2). Not only was separation according to functionality obtained, but there was partial resolution of the isomers lutein, 10, and zeaxanthin, 5, as of other unidentified polar carotenoids. This increased resolution is accounted for by several factors which improve the efficiency. First, the column packed with 5- $\mu m$  particles has a larger diameter (4.6 mm) than the 10- $\mu m$  particle columns (1.8 mm), which increases efficiency in two ways: a. Larger bore columns generally yield more plates (for the same particle diameter and constant solvent velocity). b. At constant flow-rate ( $1 \text{ cm}^3/\text{min}$  in Figures 1 and 2), the reduced velocity ( $v$ ) is 13 times smaller for the 5- $\mu m$  particles column and is close to  $v_{opt}$  (where the column works at maximum efficiency). Second, it is obvious that for similarly packed columns operated at the same  $v$ , a 30-cm long column packed with 10- $\mu m$  particles will be less efficient than a 24-cm long one made of 5- $\mu m$  particles. Third, it is expected that the high pressure packing technique is better than the constant flow one. Note also that the packing materials do not come from the same manufacturer (Spherisorb for the 10- $\mu m$  particles and Partisil for the 5- $\mu m$  ones).

Although similar resolution has been obtained with zinc carbonate as adsorbent (5), elution times were far higher (ca. 3 h for violaxanthin compared to ca. 32 min under the conditions used herein) and peak widths of several minutes were obtained.

The algal mat showed a more complex mixture on the 5- $\mu m$  irregular silica column; of these  $\beta$ -carotene, 8; torulene, 11; spheroidenone, 12; echinenone (9,  $R^1 = O$ ,  $R^2 = H_2$ ); spirilloxanthin, 13; canthaxanthin (9,  $R^1 = R^2 = O$ ); and zeaxanthin, 5, were initially assigned by coinjection with authentic standards as above. Tentative assignment of tetrahydrospirilloxanthin, 14, and assignment of okenone, 15; rhodopin, 16; 3,4-dehydrorhodopin, 17, in Figure 3 was based on the relative abundance of these components recognized from comparison of their UV/VIS and mass spectra with those of literature examples (14). Thus, resolution of bicyclic ( $\beta$ -carotene, 8) and monocyclic (torulene, 11) carotenes was achieved as well as resolution of components differing by only

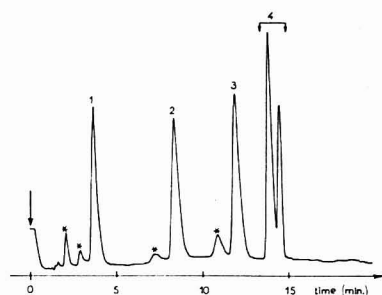


Figure 4. HPLC record of selected alkyl porphyrins. Conditions: 10- $\mu m$  silica (Spherisorb S 10) packed by constant flow-rate method using methanol slurry, column  $24 \text{ cm} \times 4.6 \text{ mm i.d.}$ , solvent gradient 2–50%  $CHCl_3$  in hexane (linear) over 20 min, flow rate  $1.8 \text{ mL/min}$ , detector  $400 \text{ nm} \times 1.0 \text{ AUFS}$ . Peak identity: (1) Ni-eto I; (2) octaethylporphyrin; (3) etio I; (4) VO-DPEP type mixture ( $m/e$  527 and 541)

a degree of unsaturation (i.e., rhodopin, 16, and dehydro-rhodopin, 17).

The characteristic blue green algal carotenoid, myxoxanthophyll, 18, was shown to be present by co-chromatography on TLC of the tetraacetate with a standard and by comparison of its UV/VIS spectrum with that of a standard. Its HPLC behavior was not investigated under the conditions used.

The other, unidentified peaks observed in Figures 2 and 3 could be either different compounds or geometrical isomers of the assigned components, since coinjection is carried out in all cases with the authentic all-trans isomers.

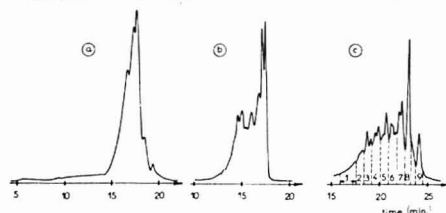
The carotenoid distributions in both situations provide further evidence that these pigments, because of the characteristic occurrence of certain of them in different types of organisms, can be used to provide qualitative information about different inputs to sediments. The carotenoids present in the algal mat demonstrate contributions of organic matter from blue green algae, purple photosynthetic bacteria, and from fungi, with little or no contribution from higher plants or green algae (11). Similarly, the Grasmere sediment, which is oligotrophic, contrasts with samples from two nearby eutrophic lake sediments in showing, as expected, no blue green algal input in the form of myxoxanthophyll (11).

**Reference Porphyrins.** The Ni complex of etioporphyrin-I (2,  $R^1 = R^3 = R^5 = R^7 = CH_3$ ;  $R^2 = R^4 = R^6 = R^8 = CH_2CH_3$ ), octaethylporphyrin (2,  $R = C_2H_5$ ), and etioporphyrin-I were chromatographed with a vanadyl-DPEP mixture (containing two major components with molecular ions corresponding to  $m/e$  527 and 541) to establish suitable conditions for optimum separation. The distribution obtained (Figure 4) on the 10- $\mu m$  silica column packed by the methanol slurry method shows that the nickel complex is readily separated from the vanadyl complexes. In addition, the elution order indicates that separation must be partly related to polarity differences, with the least polar component eluting first and the polar vanadyl complexes eluting last.

**Boscan 9K3 Metal-Free Petroporphyrins.** The metal-free petroporphyrins isolated from Boscan 9K3 revealed poor resolution of the components under identical conditions (Figure 5a). A significant improvement was achieved on 10- $\mu m$  spherical silica packed by the balanced density method (Figure 5b). Further resolution was obtained on the 5- $\mu m$  irregular silica particles packed by the same method (Figure 5c). In order to obtain an indication of the chromatographic behavior of the petroporphyrins on the 5- $\mu m$  silica, nine fractions were collected (cf. Figure 5c) and analyzed by

Table I. Visible Light Absorption Data and Mass Spectrometric Data for Boscan 9K3 Petroporphyrin Fractions Trapped from HPLC over 5- $\mu$ m Irregular Silica

Fraction <sup>a</sup>	Type of VIS spectrum	Molecular ions (M/E)					
		Etio range	Max.	DPEP range	Max.	Rhodo range	Max.
1	Etio	492-548	506	n.d. <sup>b</sup>	—	470-568	498
2	Etio	436-450	436	n.d.	—	n.d.	—
3	Etio	450-506 <sup>c</sup>	464	n.d.	—	n.d.	—
4	Etio	464-534 <sup>c</sup>	478	n.d.	—	n.d.	—
5	DPEP	422-464	450	n.d.	—	n.d.	—
6	DPEP	422-478	464	448-490 <sup>c</sup>	462	n.d.	—
7	DPEP	422-450	450	490-546	518	n.d.	—
8	DPEP	n.d.	—	448-476 <sup>c</sup>	448	n.d.	—
9	DPEP	n.d.	—	476-532	504	n.d.	—
Unfractionated total	DPEP	n.d.	—	462, 490, 504	490	n.d.	—
				476-490	476	n.d.	—
				462-476	462	n.d.	—
				406-546	476	n.d.	—

<sup>a</sup> As Figure 5 c. <sup>b</sup> n.d., not detected. <sup>c</sup> Major.

example, for a given petroporphyrin mixture, the retention times are reproducible within 2% for consecutive runs provided that the chromatographic conditions (including amount of sample injected) are kept constant. However, significant variations in reproducibility (up to 4%) were observed for the first few peaks when the sample amount injected and/or the column reequilibration time were altered. These may be explained by association of the porphyrins in solution or on the surface of the silica particles (15). Most probably, however, this effect comes from overloading of the column at the beginning, resulting in nonlinear isotherms.

It was hoped that reverse-phase LC (e.g.,  $\mu$ Bondapak/C18 column, Waters Associates) could offer a better alternative to LC on silica for the separation of the series of alkyl petroporphyrins. However, this was not the case as evidenced by the smaller number of peaks which could be obtained using the C18 column (Figure 6). Unlike silica, all the peaks from the C18 column showed multiple petroporphyrin  $M^+$  ions in their mass spectra.

The usefulness of HPLC on 5- $\mu$ m irregular silica as a "fingerprinting" technique for petroporphyrins is very promising, as indicated by the different distributions obtained for Boscan and Kuwait crudes (Figure 6).

**Boscan 9K3 Metallopetroporphyrins.** Figure 7 shows the distribution of the metallopetroporphyrins from Boscan 9K3 crude. The method provides a rapid, sensitive, and convenient separation of total nickel from total vanadyl complexes. Thus, collection of the two fractions (Figure 7) and examination by mass and UV/VIS spectrometry showed that nickel complexes were isolated completely in fraction I, whereas only vanadyl complexes were present in fraction II.

### CONCLUSION

HPLC using silica gel columns is a powerful technique for the separation of mixtures of carotenoids and porphyrins and thereby "fingerprinting" the distributions of these compounds in nature. As could be predicted, better results are obtained when using columns packed with 5- $\mu$ m particles rather than 10- $\mu$ m particles, although such columns are more difficult to pack and of shorter working life. A constant high pressure (up to 6000-7000 psi) packing method associated with a precise, balanced-density slurry provided more efficient columns than a constant flow-rate method operated with a methanol slurry.

With columns of 24 cm packed with 5- $\mu$ m irregular particles, the times of analysis in the gradient mode are very short; it is possible to complete the separation of complex mixtures containing closely related isomers within 25 min. Retention

times are reproducible, provided care is taken to use solvents of high quality and constant composition, to achieve the proper reproducibility of the gradient profile, to avoid local overloading and to reequilibrate the column between injections. Reequilibration is carried out by washing (15 min for carotenoids, 30 min for porphyrins) the column with the less polar solvent used in the gradient elution for each pigment class.

### ACKNOWLEDGMENT

We thank K. Owen (Esso Oil Company, U.K.) for providing the Kuwait oil sample, K. Smith (University of Liverpool) and A. H. Jackson (University College, Cardiff) for authentic etio-I and octaethyletioporphyrin samples, respectively, A. Treibs (University of Munich) for the Ni-etio-I and VO-DPEP samples. S.K.H. and P.J.C.T. are especially grateful to G. Johnston (Waters Associates, U.K.) for helpful advice and assistance.

### LITERATURE CITED

- (1) S. H. Byrne, J. A. Schmit, and P. E. Johnson, *J. Chromatogr. Sci.*, **9**, 592 (1971).
- (2) R. J. Pasarelli and E. S. Jacobs, *J. Chromatogr. Sci.*, **13**, 153 (1975).
- (3) N. Evans, D. E. Games, A. M. Jackson, and S. A. Matlin, *J. Chromatogr.*, **115**, 325 (1975).
- (4) A. R. Batterby, D. G. Buckley, G. L. Hodgson, R. E. Markwell, and E. McDonald in "High Pressure Liquid Chromatography in Clinical Chemistry", Dixon, Gray, and Lim, Ed., Academic Press, London, 1976, p. 63.
- (5) I. Stewart and T. A. Wheaton, *J. Chromatogr.*, **55**, 325 (1971).
- (6) E. W. Baker, in "Organic Geochemistry, Methods and Results", Eglinton and Murphy, Ed., Springer-Verlag, Berlin, 1969, p. 464.
- (7) M. Blumer and M. Rudrum, *J. Inst. Pet.*, **58**, 99 (1970).
- (8) Y. I. A. Alturki, G. Eglinton, and C. T. Pillinger, in "Advances in Organic Geochemistry", 1971, Gaertner and Wehner, Ed., Pergamon Press, Braunschweig, 1972, p. 135.
- (9) B. Didyk, Ph.D. Thesis, University of Bristol, 1975.
- (10) B. Didyk, Y. I. A. Alturki, C. T. Pillinger, and G. Eglinton, *Chem. Geol.*, **15**, 193 (1975).
- (11) C. D. Watts, J. R. Maxwell, and H. Kjosens, in "Advances in Organic Geochemistry 1975", Campos and Goni, Ed., Enadisma, Madrid, 1977, p. 371.
- (12) T. T. Macan, in "Biological Studies of the English Lakes", Longman, London, 1970.
- (13) M. Martin, C. Eon, and G. Guiochon, *Res./Dev.*, **28**, 24 (April 1975).
- (14) W. Vetter, G. Englert, N. Rigassi, and U. Schwieter, in "Carotenoids", Isler, Ed., Birkhauser, Basel, 1971, p. 189.
- (15) J. E. Falk, Ed., "Porphyrins and Metalloporphyrins", Elsevier, Amsterdam, 1964, p. 189.

RECEIVED for review June 17, 1977. Accepted October 21, 1977. The Natural Environment Research Council (GR/3/2420) provided the HPLC system. W. K. Seifert and the management of Chevron Oil Field Research Co. and Hoffmann-La Roche provided financial aid to S.K.H. and P.J.C.T., respectively.

# Determination of Benzodiazepine Anticonvulsants in Plasma by High-Performance Liquid Chromatography

Robert J. Perchalski\* and B. J. Wilder

Research and Neurology Services, Veterans Administration Hospital, and Department of Neurology, College of Medicine, University of Florida, Gainesville, Florida 32610

A sensitive, specific high-pressure liquid chromatographic procedure for determination of the major benzodiazepine anticonvulsants is described. 4,5-Dihydrodiazepam hydrochloride is easily synthesized and used as internal standard. After a single extraction from alkaline plasma, diazepam, nordiazepam, and clonazepam can be quantitated to a lower limit of 5–10 ng/sample. Relative standard deviations for daily and long-term reproducibility studies were 4% and equal to or less than 6%, respectively. Preliminary studies indicate that the method can easily be adapted to allow analysis of other benzodiazepines.

The pharmacokinetics, metabolism, and possible mechanisms of action of a number of the more significant benzodiazepines have been discussed in detail (1). Two extensive reviews (2, 3) published in 1974 indicated that the most popular method of analysis for these drugs was gas-liquid chromatography with electron-capture detection. De Silva et al. (4) recently published a comprehensive, optimized study of this methodology in which procedures were given for analysis of biological samples containing any single benzodiazepine and its metabolites. Although procedures were optimized for specific groups of drugs, the two primary anticonvulsants, diazepam and clonazepam, required different methods of protein precipitation and postextraction handling. This inconvenience prompted us to investigate high-performance liquid chromatography (HPLC) as an alternative method for monitoring these benzodiazepines in the clinical and toxicological situation.

Scott and Bommer (5) described an HPLC method for analysis of some benzodiazepines and applied it to analysis of animal urine. The chromatography was limited by the state of the art at that time, but the authors showed the potential of liquid chromatography for separation, identification, and quantitation of benzodiazepines in metabolite studies. More recently, Bugge (6) and Vree et al. (7) reported analyses of diazepam and nordiazepam and of flunitrazepam, respectively. The mobile phase employed by Bugge is relatively nonspecific and barely gives baseline resolution of diazepam and nordiazepam. The procedure is long, and no internal standard is used. Vree and co-workers use diazepam as an internal standard, so this procedure is not immediately applicable to routine analysis of human samples, since diazepam is a commonly prescribed drug. Both methods employ UV detection at 230 nm, which at the present time requires a variable wavelength detector. The expense of this instrument precludes its use in a dedicated routine application. Harzer and Barchet (8) reported on conditions for analyzing several benzodiazepines and their respective benzophenones, using a reverse phase system. In their analysis of whole blood, 5–10 mL of sample were used. Limits of detection were not given for drugs carried through the extraction.

In this study, we report a rapid (single extraction), sensitive, and selective method, incorporating an easily synthesized internal standard and UV detection at 254 nm, for the determination of diazepam, clonazepam, and nordiazepam in

plasma or whole blood. Some other applications that require little or no modification of the technique are also suggested.

## EXPERIMENTAL

**Apparatus.** The liquid chromatograph consisted of an ISCO Model 384 gradient pump with a Model UA-5 absorbance monitor (Instrumentation Specialties Company, Lincoln, Neb.). The optical unit was set up to observe the difference between the mobile phase entering the column and that flowing out of the column at a wavelength of 254 nm. The column was 250 mm × 4.6 mm i.d., packed with a 5-μm totally porous silica gel (Partisil-5, Reeve Angel, Liquid Chromatography Division, Clifton, N.J.). Samples were injected with a six-port sampling valve having a 20-μL sample loop (Valco Instruments Company, Houston, Tex.).

**Reagents.** All chemicals were analytical reagent grade. Clonazepam and diazepam (Applied Science Laboratories, Inc., State College, Pa.) were used as received. Metabolites of clonazepam were made by catalytic hydrogenation of the parent drug over 5% palladium on carbon in ethanol and by acetylation of the resulting 7-aminoclonazepam with acetic anhydride to obtain 7-acetamidoclonazepam. The internal standard, 4,5-dihydrodiazepam, was made by catalytic hydrogenation of diazepam over platinum oxide in glacial acetic acid according to the method of Sternbach and Reeder (9). Diazepam (100 mg) was dissolved in 1 mL of glacial acetic acid in a 5-mL Reacti-Vial closed with a Tuf-Bond disk (Teflon bonded to silicone) (Pierce Chemical Company, Rockford, Ill.). Two 1.5-mm ( $1/16$ -inch) diameter holes were bored through the disk and fitted with 1.5-mm o.d. × 0.3-mm i.d. Teflon tubing to allow introduction (tube extends to bottom of vial) and venting of hydrogen gas. Platinum oxide (10 mg) was added, the vial closed, and hydrogen gas bubbled through the solution for 30 min. A sample of the reaction mix taken at that time, evaporated under vacuum, dissolved in mobile phase, and analyzed by HPLC with UV detection at 254 nm showed 96% conversion of diazepam to the 4,5-dihydro derivative, 2% unreacted starting material, and two minor products which eluted after 4,5-dihydrodiazepam. The entire solution was centrifuged to separate out the platinum black, and the supernatant was evaporated to a light brown oil under vacuum. Aqueous 1 M HCl (2 mL) was added to the residue, and the material was allowed to digest in an 85 °C water bath for 30 min. During that time, the oily residue was converted to an off-white precipitate in a yellow solution. Addition of 1.5–2 mL of methanol to the hot solution was sufficient to just dissolve the precipitate, and the hydrochloride salt crystallized as light yellow needles. A second recrystallization from fresh 1 M HCl:methanol (1:1) also gave light yellow needles. The free amine was extremely difficult to recrystallize, and all samples contained a small amount of diazepam impurity. The salt decomposed between 180 and 250 °C. Analysis of part of the residue by dissolution in mobile phase and injection into the liquid chromatograph indicated loss of HCl to give the free secondary amine and partial reconversion to diazepam. Structures of the clonazepam metabolites and 4,5-dihydrodiazepam were verified by mass spectrometry after purification by semipreparative HPLC.

The mobile phase used for quantitation of diazepam, clonazepam, and nordiazepam was cyclopentane:chloroform:acetonitrile:methanol (29:55:5:10:0.05). Flow rate was 60 mL/h at a pressure of 6.67 MPa (967 psi).

The internal standard stock solution was made by dissolving about 1 mg of 4,5-dihydrodiazepam hydrochloride (0.887 g base/g salt) in 1 M HCl:methanol (1:9) and diluting to 10 mL. The working internal standard solution was made by adding 0.300 mL



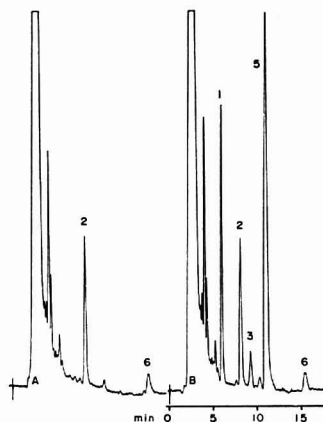


**Figure 1.** Extractions of drug-free plasma (A) and drug-free plasma spiked with diazepam (1), clonazepam (3), and nordiazepam (5) at concentrations of 172 ng/mL, 53 ng/mL, and 461 ng/mL, respectively. 4,5-Dihydrodiazepam (2) was added as in Procedure. A small amount of caffeine (6) was present. Column: 250 mm  $\times$  4.6 mm Partisil (5  $\mu$ m). Mobile phase: cyclopentane:chloroform:acetonitrile:methanol (29:55:5:15.0:0.5) at 60 mL/h

of internal standard stock solution to 50 mL of 0.1 M ascorbic acid:methanol (9:1).

The stock drug standard was made by dissolving diazepam, clonazepam, and nordiazepam (3 mg, 1 mg, and 9 mg, respectively) in methanol and diluting to 10 mL. The working drug standard was made by adding 0.300 mL of the stock solution to methanol and diluting to 20 mL with methanol. All standards were stored in silanized amber bottles with Teflon-lined screw caps. Methanolic standards were refrigerated. Plasma standards were made by evaporating 5–100  $\mu$ L of the methanolic standard in an extraction tube, adding 1.00 mL of drug-free plasma to the residue, and extracting.

**Procedure.** To 1.00 mL of plasma in a 16- $\times$ 125-mm culture tube with Teflon-lined screw cap, add 0.50 mL of the working internal standard solution, 0.5 mL of glycine buffer (2.0 mol/L, pH 10.5) and 5 mL of benzene:dichloromethane (9:1). After shaking the mixture for 10 min and centrifuging, transfer the organic layer to a 5-mL Reacti-Vial, and evaporate to dryness at 55  $^{\circ}$ C under a stream of nitrogen. Dissolve the residue immediately in 70  $\mu$ L of mobile phase, and within 3 days inject approximately one third of the extract (20  $\mu$ L) into the liquid chromatograph. Quantitate by peak height ratio.

## RESULTS AND DISCUSSION

**Extraction.** Various buffers and extracting solvents were evaluated to optimize recovery of all drugs and at the same time keep interferences to a minimum. Concentrated buffers tended to minimize interferences, and the 2 M glycine buffer (pH 10.5) used by Wad and Hanifi (10) for the TLC determinations of diazepam and its metabolites was superior to similar phosphate and borate buffers. Diazepam and nordiazepam are easily extracted by nonpolar solvents (i.e., cyclopentane); however, concurrent extraction of clonazepam requires a solvent of higher strength. The benzene:dichloromethane (9:1) solvent of De Silva et al. (4) gave good recovery of all drugs without introducing significant interferences.

**Stability.** Peak height ratios of extracted drugs are constant for at least 3 days if the residue from extraction is dissolved in mobile phase shortly after evaporation of the solvent. A decrease in peak height of the internal standard was repeatedly observed if the residue was allowed to remain

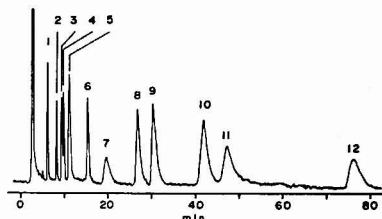


**Figure 2.** Chromatogram of drug standards run under same conditions as in Figure 1. Peaks represent diazepam (1), 4,5-dihydrodiazepam (2), clonazepam (3), nitrazepam (4), nordiazepam (5), caffeine (6), carbamazepine (7), demoxepam (8), 7-chloro-4,5-epoxy-2-methylamino-5-phenyl-3H-1,4-benzodiazepine (tentative) (9), 7-amino-clonazepam (10), chlordiazepoxide (11), and 7-acetamidoclonazepam (12)

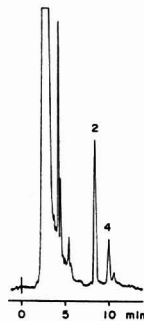


**Figure 3.** Extraction of drug-free plasma spiked with 44.1 ng/mL of nitrazepam (4). Internal standard (2) was added as in the procedure. Chromatographic conditions were as in Figure 1

dry overnight. It was not necessary to silanize or to use any special cleaning procedures on the extraction tubes or Mini-vials; however, the methanolic standards were more stable if stored in silanized bottles. It is possible that the benzene:acetone:methanol (80:15:5) solvent used by De Silva et al. (4) for making up standards may eliminate the need for silanizing storage vessels.

**Reproducibility.** Short-term reproducibility of the method was determined by extracting ten replicates of a drug-free plasma sample, spiked with diazepam, clonazepam, and nordiazepam at concentrations of 255 ng/mL, 109 ng/mL, and 780 ng/mL, respectively. Relative standard deviations were 4% for all three drugs. Long-term reproducibility was evaluated over a 30-day period (nine determinations) at two different concentrations of each drug. One set of samples contained 98 ng/mL, 42 ng/mL, and 300 ng/mL of diazepam, clonazepam, and nordiazepam, respectively. The other set contained 294 ng/mL, 126 ng/mL, and 900 ng/mL, respectively. Relative standard deviations of the set containing low levels of the drugs were 4%, 6%, and 6% for diazepam, clonazepam, and nordiazepam, respectively; and 4%, 5%, and 3.3%, respectively, for the set containing high levels. The range of slopes of analytical curves run at the beginning and end of this period was within 4% of the mean slope for each drug.

**Recovery.** Recovery of each drug was evaluated by calculating concentrations of drugs carried through the extraction by using analytical curves derived from samples to which various concentrations of the three drugs were added after transfer of the organic phase. Equal quantities of the internal

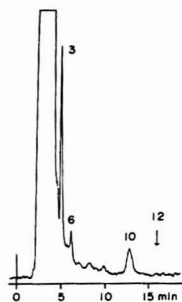


Figure 4. Extraction of 2 mL plasma from a patient taking 13 mg/day of clonazepam. Chromatogram shows clonazepam (3), caffeine (6), 7-aminoclonazepam (10), and expected position of 7-acetamidoclonazepam (12). Column: 250 mm  $\times$  4.6 mm Partisil PAC (alkylnitrile)-10  $\mu$ m. Mobile phase: chloroform:acetonitrile:methanol (60:39:1) at 60 mL/h.

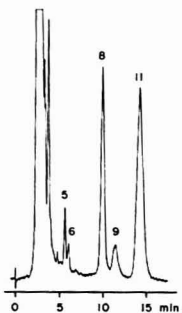


Figure 5. Extraction of 1 mL whole blood from medical examiner subject suspected of taking chlordiazepoxide. Peaks are nordiazepam (5), caffeine (6), demoxepam (8), 7-chloro-4,5-epoxy-2-methylamino-5-phenyl-3H-1,4-benzodiazepine (tentative) (9), and chlordiazepoxide (11). Chromatographic conditions were the same as those in Figure 4.

standard (as the free base) were added to all tubes after transfer of the organic phase. Four replicates, spiked with 138 ng/mL, 42.4 ng/mL, and 268 ng/mL of diazepam, clonazepam, and nordiazepam, respectively, were extracted. Recoveries were  $92.9 \pm 3.3\%$ ,  $89.6 \pm 5.2\%$ , and  $93.6 \pm 3.8\%$ , respectively. Lower limits of quantitation are 5 ng/mL for diazepam and 10 ng/mL for clonazepam and nordiazepam. The lower limit of detection for clonazepam is 3.1 ng injected with detector noise equal to  $1.0 \times 10^{-4}$  absorbance unit. Therapeutic concentrations are 200–500 ng/mL, 600–1500 ng/mL, and 40–100 ng/mL for diazepam, nordiazepam, and clonazepam, respectively.

**Interferences.** The chromatograms in Figure 1 show extraction of drug-free plasma (A) and drug-free plasma spiked with 172 ng/mL, 53 ng/mL, and 461 ng/mL of diazepam, clonazepam, and nordiazepam, respectively (B). This procedure has been in use for the past 5 months, and plasma from patients on common anticonvulsant medications contains no interfering peaks. In some plasma, including some drug-free plasma, a large peak is present which elutes immediately before diazepam. Although it does not interfere, it may be mistakenly identified as diazepam in samples that do not contain this drug. A major metabolite of carbamazepine, probably the epoxide, elutes just before nordiazepam. Again, this peak does not interfere with clonazepam or nordiazepam. An interference that has been noted in only one medical

examiner specimen (not from an epileptic patient) has been identified by mass spectral analysis as phenacetin. This compound elutes at the same time as 4,5-dihydrodiazepam. The short half-life of this drug (1–3 h), and the availability of alternative analgesic medication should make this a minor problem for epileptic patients on benzodiazepine therapy. If the drug must be used, it should not be taken for at least 24 h before sampling for benzodiazepine analysis. During the initial development of this method, a reverse phase system was also evaluated. Carbamazepine could not be resolved in a reasonable time from clonazepam with water:methanol or water:acetonitrile mobile phases.

**Other Applications.** Numerous other possible applications of this basic method have been indicated, primarily during analysis and identification of unknown compounds present in medical examiner samples. Figure 2 shows the elution pattern of the drugs of interest, along with the internal standard and some related compounds that are easily extracted by this method. This figure was included only to show the chromatographic relationship of related and coextractable substances, and not to suggest that these conditions provide an optimized assay for all components. Caffeine and carbamazepine were included because the former is found in almost all samples and the latter is a common anticonvulsant. An extraction of a plasma sample spiked with 44.1 ng/mL of nitrazepam is shown in Figure 3.

To determine whether this method was applicable to quantitation of the clonazepam metabolites, a 250-mm  $\times$  4.6-mm i.d. column packed with a 10- $\mu$ m alkyl nitrile bonded-phase packing (Partisil 10/25 PAC, Reeve-Angel) was used with chloroform:acetonitrile:methanol (60:39:1) as mobile phase at 60 mL/h. Figure 4 shows an extraction of 2 mL of plasma from a patient on a continual dose of 13 mg of clonazepam/day. The clonazepam level in this sample was 90.1 ng/mL. The 7-acetamido metabolite was not detected.

A medical examiner sample from a person suspected of taking chlordiazepoxide (Librium) was extracted according to the procedure and chromatographed under the conditions used for clonazepam metabolites. The resulting chromatogram is shown in Figure 5. Chlordiazepoxide was quantitated by comparison of peak areas of extracted standards with that of the unknown and found to be about 600 ng/mL. With inclusion of a suitable internal standard, a simple, rapid analysis of chlordiazepoxide and its principal metabolite, demoxepam, is possible. The component that elutes after demoxepam has been tentatively identified by mass spectral and UV absorption studies as the 4,5-epoxide of chlordiazepoxide. This compound has been reported in chemical studies of chlordiazepoxide (11), but has never been found as a metabolite, probably because of its easy reconversion to chlordiazepoxide with heat or in dilute acid.

The proposed method for diazepam, clonazepam, and nordiazepam is rapid, sensitive, and easily applied to routine therapeutic monitoring of epileptic patients on benzodiazepine therapy. The required instrumentation is less expensive and easier to maintain than the more commonly used electron capture gas chromatograph and is more practical for dedicated clinical analysis than the liquid chromatograph with a variable wavelength detector. The method can be applied directly to the determination of nitrazepam and, with a simple change of column and mobile phase, to the determination of chlordiazepoxide and demoxepam. Manipulation of the mobile phase within these two basic systems should allow analysis of many of the other less commonly used benzodiazepines.

#### ACKNOWLEDGMENT

Thanks are due to J. L. Templeton and B. D. Andresen for mass spectral data and to R. M. Thomas and D. M. Mitchell for technical assistance.

## LITERATURE CITED

- (1) S. Garrattini, E. Mussini, and L. O. Randall, Ed., "The Benzodiazepines", Raven Press, New York, N.Y., 1973.
- (2) J. M. Clifford and W. F. Smyth, *Analyst (London)*, **99**, 241 (1974).
- (3) D. M. Hailey, *J. Chromatogr.*, **98**, 527 (1974).
- (4) J. A. F. De Silva, I. Bekersky, C. V. Bugli, M. A. Brooks, and R. E. Weinfeld, *Anal. Chem.*, **48**, 10 (1976).
- (5) C. G. Scott and P. Bommer, *J. Chromatogr. Sci.*, **8**, 446 (1970).
- (6) A. Bugge, *J. Chromatogr.*, **128**, 111 (1976).
- (7) T. B. Vree, B. Lenseleink, E. van der Kleijn, and G. M. M. Nijhuis, *J. Chromatogr.*, **143**, 530 (1977).
- (8) K. Harzer and R. Barchet, *J. Chromatogr.*, **132**, 83 (1977).
- (9) L. H. Sternbach and E. Reeder, *J. Org. Chem.*, **26**, 4936 (1961).
- (10) N. T. Wad and E. J. Hanifi, *J. Chromatogr.*, **143**, 214 (1977).
- (11) L. H. Sternbach, B. A. Koechlin, and E. Reeder, *J. Org. Chem.*, **27**, 4671 (1962).

RECEIVED November 15, 1977. Accepted January 12, 1978.  
This work was supported by the Medical Research Service of the Veterans Administration, the Epilepsy Research Foundation of Florida, Inc., and the College of Pharmacy Mass Spectrometry Facility of the University of Florida.

## Microdetermination of Molecular Species of Oligo- and Polyunsaturated Diacylglycerols by Gas Chromatography-Mass Spectrometry of Their *tert*-Butyl Dimethylsilyl Ethers

J. J. Myher, A. Kuksis,\* L. Maral, and S. K. F. Yeung

Banting and Best Department of Medical Research, University of Toronto, Toronto, Canada M5G 1L6

Gas chromatography-mass spectrometry (GC/MS) was used to determine the molecular association and positional distribution of fatty acids in submicrogram quantities of diacylglycerols following their conversion into the *tert*-butyl dimethylsilyl (*t*-BDMS) ethers. The abundant  $M - 57$  ion provided the molecular weights for both saturated and unsaturated species. The 1,3 isomers were identified by the  $M - \text{acyloxymethylene}$  fragments which are absent in the *sn*-1,2- and *sn*-2,3-diacylglycerols. The abundance ratio of the ions due to losses of the acyloxy radical ( $M - \text{RCOO}$ ) from position 1 (or 3) and position 2 indicated the proportions of the reverse isomers, e. g. *sn*-1-palmitoyl, 2-stearoyl, and *sn*-1-stearoyl 2-palmitoylglycerols.

The early methods of complete determination of the molecular species of diacylglycerols were based on combined application of argentation thin-layer chromatography ( $\text{AgNO}_3$ -TLC), gas-liquid chromatography (GLC), and enzymatic degradation (1, 2). These techniques, although extensively applied in research (3), are laborious and time consuming, and require more material than conveniently prepared from such natural sources as cell membranes and lipoproteins.

The potential usefulness of mass spectrometry for a rapid analysis of minute amounts of molecular species of diacylglycerols has been recognized (4, 5) since the introduction of GC/MS methods to the investigation of the structure of complex glycerolipids, but the relative unavailability of the instruments prevented progress in the methodology or its widespread utilization in assessment of natural mixtures of diacylglycerols. Current GC/MS analyses of diacylglycerols utilize trimethylsilyl (TMS) ethers (6-8), which are unstable and cannot be purified before analysis, or acetates (9-11), which do not yield sufficiently characteristic spectra for polyunsaturates.

The present study demonstrates that the *t*-BDMS ethers of diacylglycerols possess many of the mass spectrometric properties of the TMS ethers along with a prominent  $M - 57$  fragment, which can be utilized for accurate measurement of molecular weight. The *t*-BDMS ethers are stable to moisture and can be isolated from the reaction mixture and purified

prior to analysis, as previously shown for the corresponding derivatives of simple alcohols (12, 13).

### EXPERIMENTAL

**Standards.** Synthetic mono- and diacid *sn*-1,2-diacylglycerols of 16 and 18 carbon fatty acids were purchased from Applied Science Laboratories (State College, Pa.) and Supelco (Bellefonte, Pa.). The reverse isomers of *rac*-1-palmitoyl 2-stearoyl and *rac*-1-stearoyl 2-palmitoyl glycerols were prepared in the laboratory by Grignard degradation of *rac*-1-palmitoyl 2-stearoyl 3-palmitoyl glycerol and *rac*-1-stearoyl 2-palmitoyl 3-stearoylglycerol as previously described (11). The triacylglycerols were prepared by acylation with the acid chlorides of the corresponding 1,3-diacylglycerols.

Mono-, di-, tri-, tetra-, and hexaenoic *sn*-1,2-diacylglycerols of natural origin were isolated by argentation TLC of the *t*-BDMS ethers of *sn*-1,2-diacylglycerols derived from egg yolk and rat liver phosphatidylcholines by hydrolysis with phospholipase C (14). The  $\text{AgNO}_3$ -TLC fractions contained largely mixtures of palmitoyl and stearoyl oleates, linoleates, arachidonates, and docosahexaenoates, respectively, but dioleoyl, oleoyl linoleoyl, dilinoleoyl, and oleoyl arachidonoyl species were also present.

**Preparation of 1,2-(2,3)- and 1,3-Dipalmitoyl-*sn*-glycerol- $d_2$ .** Glycerol- $d_2$  (20 mg) was reacted for 4 h at 80 °C with palmitoyl chloride (120 mg) in benzene (0.5 mL) containing a catalytic amount of dry pyridine (30 mg). The mixture was extracted with  $\text{CHCl}_3/\text{MeOH}$  (2:1, v/v) and washed with water. Analysis of the products by GLC (15) indicated the presence of mono-, di-, and tripalmitoyl-glycerols. The 1,2(2,3)- and 1,3-dipalmitoyl-*sn*-glycerols- $d_2$  were isolated from the mixture by TLC on borate impregnated silica gel using  $\text{CHCl}_3/\text{acetone}$  (96:4, v/v) as the developing solvent (16). The diacylglycerols were converted into their respective *t*-BDMS ethers and purified by TLC on silica gel H as described below.

**Preparation of *t*-BDMS Ethers.** The *t*-BDMS ethers of diacylglycerols were prepared by a modification of the method described by Corey and Venkateswarlu (12) for prostaglandins. A mixture of 0.5 mg diacylglycerol and 150  $\mu\text{L}$  *tert*-butyldimethylchlorosilane/imidazole reagent (Applied Science Laboratories) is heated at 80 °C for 20 min. After cooling, the reaction mixture is thoroughly mixed with 5 mL of light petroleum spirit (bp 30-40 °C) and washed three times with 0.5 mL of water. The petroleum extract is then dried over  $\text{Na}_2\text{SO}_4$  and taken to dryness under a stream of nitrogen. No isomerization of mono- or diacylglycerols was observed to take place during derivatization as determined by GLC. The *t*-BDMS ethers of acyglycerols are suitable for TLC and  $\text{AgNO}_3$ -TLC. The *t*-BDMS ethers can be stored in petroleum ether at -20 °C for protection of double bonds.

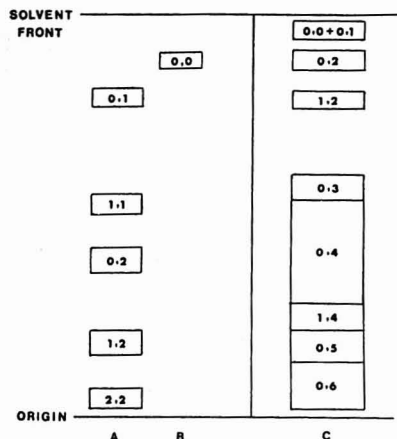


Figure 1. Separation of diacylglycerols as *t*-BDMS ethers on silica gel H impregnated with 20%  $\text{AgNO}_3$ : (A) corn oil *rac*-1,2-diacylglycerols developed in  $\text{CHCl}_3/\text{MeOH}$  (99:1, v/v); (B) standard *rac*-1,2-dipalmitoylglycerol developed in  $\text{CHCl}_3/\text{MeOH}$  (99:1, v/v); (C) *sn*-1,2-diacylglycerols derived from rat liver lecithins developed in  $\text{CHCl}_3/\text{MeOH}$  (98:2, v/v).

There was no breakdown of the ethers observed over several months of storage.

**TLC and  $\text{AgNO}_3$ -TLC.** The *t*-BDMS ethers of diacylglycerols were isolated by TLC on silica gel H using conventional equipment and benzene (or toluene):diethyl ether 97:3 as developing solvent. The diacylglycerol ethers ( $R_f = 0.65$ ) were clearly resolved from the *t*-BDMS esters of free fatty acids ( $R_f = 0.76$ ) and the *t*-BDMS ethers of monoacylglycerols ( $R_f = 0.76$ ), free cholesterol ( $R_f = 0.76$ ), triacylglycerols ( $R_f = 0.50$ ), as well as from the *t*-BDMS ethers of the tertiary alcohols ( $R_f = 0.25$ ) generated during Grignard reaction ( $\text{EtMgBr}$ ). Any alkyl acyl- or alkenyl acylglycerols present in the diacylglycerol mixtures prepared from natural glycerophospholipids were found to migrate ahead of the diacylglycerols as described previously for the diacylglycerol acetates (17), and were recovered separately.

The *t*-BDMS ethers of diacylglycerols were resolved according to degree of unsaturation by  $\text{AgNO}_3$ -TLC (20%  $\text{AgNO}_3$ ) using conventional equipment and chloroform-methanol 99:1 as the developing solvent for complete resolution of saturates, monoenes, dienes, and partial resolution of polyenes. The polyenes were resolved further following elution and rechromatography with

chloroform-methanol 98:2 as the developing solvent. Complete resolution was obtained for various trienes, tetraenes, pentaenes, and hexaenes. The various lipid subfractions were recovered with chloroform-methanol 2:1. One  $\mu\text{L}$  of a solution containing  $5 \mu\text{g}/\mu\text{L}$  of diacylglycerol was injected into the GC/MS system.

**GLC AND GC/MS.** Carbon number resolution of the *t*-BDMS ethers of diacylglycerols was obtained on stainless steel columns ( $18 \times 0.125$  in. o.d.) packed with 3% OV-1 on Gas Chrom Q (100-120 mesh) and installed in a Beckman GC-4 gas chromatograph. The column oven was temperature-programmed from 240-340  $^\circ\text{C}$  at 12  $^\circ\text{C}/\text{min}$  with the injector heater at 300  $^\circ\text{C}$  and the detector heater at 350  $^\circ\text{C}$  as previously described (15). Nitrogen was the carrier gas. The *t*-BDMS ethers were admitted to the mass spectrometer from a glass column ( $36 \times 0.125$  in. i.d.) packed with 3% OV-1 on Gas Chrom Q (100-120 mesh) and installed in a Varian 2400 gas chromatograph, using temperature programming from 290-320  $^\circ\text{C}$  at 4  $^\circ\text{C}/\text{min}$  and helium as the carrier gas. Mass spectrometry of the GLC peaks was made by repetitive scanning at 4 s/decade at a resolution of 800-1000. The instrument was a Varian MAT CH-5 single focusing mass spectrometer coupled to a Varian 620i computer. The mass spectrometer was coupled to the gas chromatograph by means of a Watson-Biemann glass frit molecular separator, as previously described (18). The mass spectrometer was operated at an ionization voltage of 70 eV, an accelerating voltage of 3000 V, electron emission energy of 100  $\mu\text{A}$ , and an ion source temperature of 310  $^\circ\text{C}$ . The mass spectra were corrected for background using Module SUB.

**Evaluation of Mass Spectra.** The molecular species of the diacylglycerols were identified from the GLC elution time and the total mass spectra of the *t*-BDMS ethers. The *sn*-1,2-(2,3)-diacylglycerols were eluted earlier than the 1,3-diacylglycerol ethers. In addition, the unsaturated diacylglycerols were eluted somewhat ahead of the corresponding saturated diacylglycerols. The mass spectra provided the exact pairing of the fatty acids in the diacylglycerol molecules and the relative proportions of the species in each GLC peak. This was accomplished by means of characteristic ion ratios as established in the study.

## RESULTS AND DISCUSSION

**Chromatographic Properties of *t*-BDMS Ethers of Diacylglycerols.** The *t*-BDMS ethers were found to be fully stable to the developing or elution solvents and to water or dilute aqueous ammonia used during recovery of the fractions from TLC and  $\text{AgNO}_3$ -TLC plates. The *t*-BDMS ethers possessed excellent TLC properties as indicated by the absence of tailing, compact bands, and completeness of resolution from other neutral lipids present in natural mixtures. Compact and well resolved bands were also obtained for the *t*-BDMS ethers on the  $\text{AgNO}_3$ -TLC plates, which in many respects resembled those of the diacylglycerol acetates. No resolution was obtained for the *rac*-1,2- and 1,3-diacylglycerols on either plain

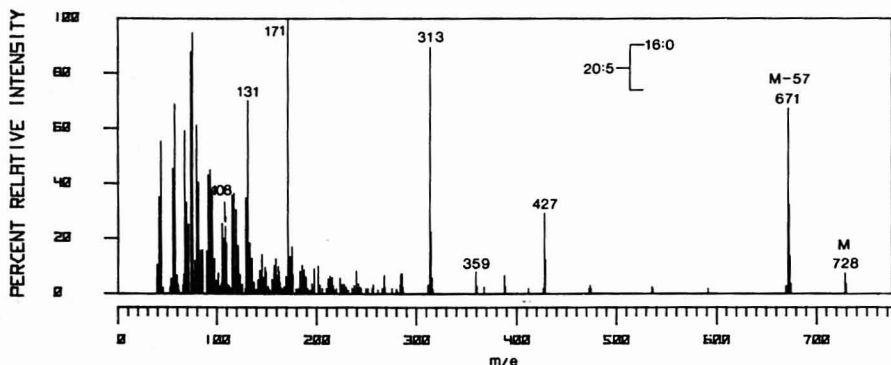


Figure 2. GC/MS spectrum of the *t*-BDMS ether of 1-palmitoyl-2-eicosapentaenoic-*sn*-glycerol



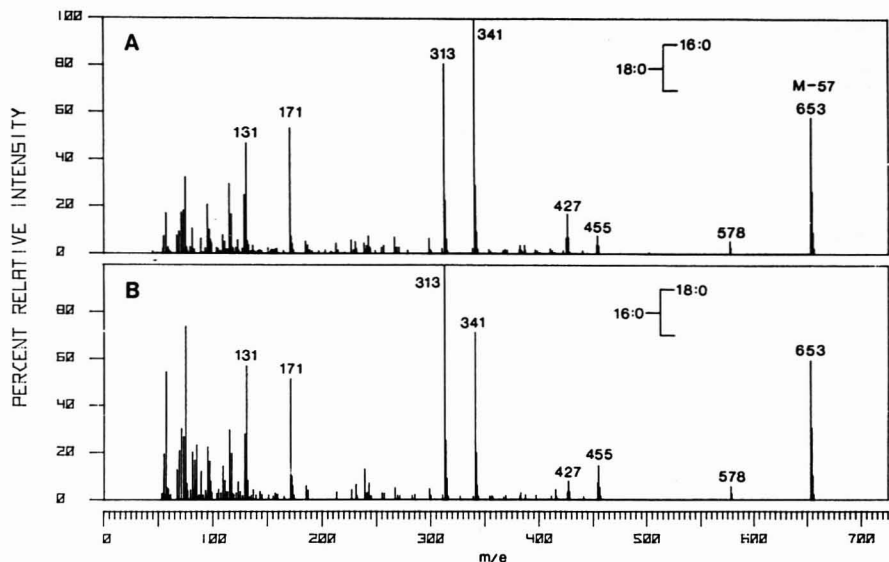


Figure 3. GC/MS spectra of the *t*-BDMS ethers of reverse isomers of *rac*-1,2-diacylglycerols: (A) 1-palmitoyl-2-stearoyl-*rac*-glycerol; (B) 1-stearoyl-2-palmitoyl-*rac*-glycerol

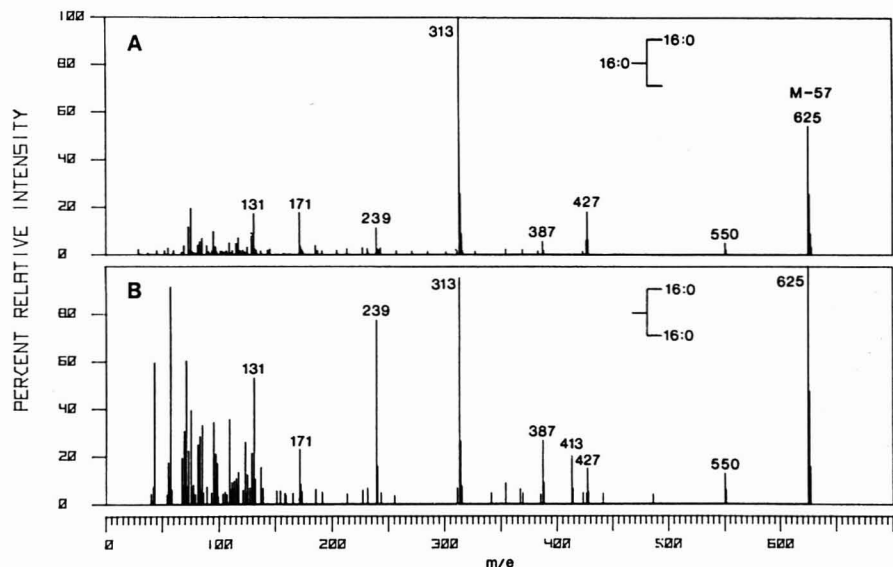


Figure 4. GC/MS spectra of the *t*-BDMS ethers of *rac*-1,2- and 1,3-diacylglycerols: (A) 1,2-dipalmitoyl-*rac*-glycerol; (B) 1,3-dipalmitoyl-*rac*-glycerol

silica gel plates or on plates made from silica gel impregnated with  $\text{AgNO}_3$ .

Figure 1 illustrates the separations obtained for the *t*-BDMS ethers of the saturated and unsaturated diacylglycerols derived from corn oil triacylglycerols and rat liver phosphatidylcholine. Major bands are seen for the mono-, di-, tri-, tetra-, penta-,

and hexaenoic species, as already reported for the corresponding acetates (19).

The *t*-BDMS ethers of diacylglycerols also possess excellent GLC properties but are eluted from nonpolar columns about two methylene units later than the corresponding TMS derivatives or acetyl derivatives, both of which overlap

Table I. Relative Abundances Obtained by GC/MS for the Major Ions Found in the Mass Spectra of the *t*-BDMS Ethers of Some Diacylglycerols

Ion type, <i>m/e</i>	Position 1: 16:0 <sup>a</sup> Position 2: 16:0	Relative abundance					
		16:0 16:0	16:0 18:0	18:0 16:0	16:0 18:1	16:0 18:2	
M		-	-	-	-	-	
M - 57	100	73	48	63	62	76	
M - 132	14	7	5	7	6	4	
M - R <sub>1</sub> COO <sup>b</sup>			8	9	5	4	
	16	23					
M - R <sub>2</sub> COO <sup>b</sup>			16	15	32	15	
M - R <sub>1</sub> COOCH <sub>2</sub>	24	-	-	-	-	-	
R <sub>1</sub> CO + 2 × 74	27	8	6	5	5	5	
R <sub>2</sub> CO + 2 × 74			1	3	3	3	
R <sub>1</sub> CO + 74	96	100	88	70	100	100	
R <sub>2</sub> CO + 74			100	100	88	72	
R <sub>1</sub> CO	84	20	10	6	7	7	
R <sub>2</sub> CO			5	12	12	16	
R <sub>1</sub> CO-1	-	-	-	-	3	5	
171	28	25	51	56	75	89	
131	75	24	55	61	46	62	

Ion type, <i>m/e</i>	Position 1: 16:0 Position 2: 20:3 ω 6	Relative abundance			
		16:0 20:4	18:1 20:4	16:0 20:5	16:0 22:6
M	1.5	4	5	6	4
M - 57	55	35	47	64	43
M - 132	2	1	-	-	-
M - R <sub>1</sub> COO <sup>b</sup>	-	-	2	3	2
M - R <sub>2</sub> COO <sup>b</sup>	18	25	30	34	36
M - R <sub>1</sub> COOCH <sub>2</sub>	7	-	-	-	-
R <sub>1</sub> CO + 2 × 74	-	5	8	7	5
R <sub>2</sub> CO + 2 × 74	-	-	-	-	-
R <sub>1</sub> CO + 74	100	87	72	88	74
R <sub>2</sub> CO + 74	30	10	12	10	8
R <sub>1</sub> CO	7	6	5	7	8
R <sub>2</sub> CO	12	8	10	8	7
R <sub>1</sub> CO-1	6	11	12	8	6
171	77	100	100	100	100
131	52	68	66	65	35

<sup>a</sup> 1,3-Dipalmitoyl glycerol. All other diacylglycerols are the 1,2 isomers. <sup>b</sup> R<sub>1</sub> and R<sub>2</sub> designate the hydrocarbon portions of the fatty acids substituted at the 1 and 2 positions respectively.

completely with the free parent diacylglycerols (20). The 1,3-diacylglycerol ethers are retained longer than the ethers of the X-1,2-diacylglycerols, giving a separation factor of 1.07 on a 6-ft long 3% OV-1 column. The unsaturated diacylglycerols are eluted slightly ahead of their saturated homologues, but the separation factor is not sufficiently high for practical resolution.

**GC/MS Properties.** The advantages of the *t*-BDMS ethers for the GC/MS of diacylglycerols are highlighted by the mass spectra obtained for the polyunsaturated species. Figure 2 gives the mass spectrum recorded for 1-palmitoyl-2-eicosapentaenoyl-*sn*-glycerol. Many of the fragments are similar to those reported for the diacylglycerol TMS ethers (4, 8), but the most important feature is the high abundance peak corresponding to (M - 57)<sup>+</sup> that is also characteristic of the *t*-BDMS spectra of steroids and prostaglandins (13) and of free fatty acids (21). The high intensity of the (M - 57)<sup>+</sup> ion allows the ready determination of carbon number and degree of unsaturation even for species containing docosahexaenoic acid (22:6). Species representing 0.5% of the total have been detected via M - 57 ions when 10 μg of a complex mixture of diacylglycerol *t*-BDMS ether was injected into the GC/MS system. The other important ions in the over 200 *m/e* region have only one fatty acid residue remaining.

Ions result from the loss of RCOO and RCOOH moieties. In the case of the disaturated species (Figure 3A) the frag-

ments due to losses of the RCOO radicals (*m/e* 427 and 455) are almost twice as abundant as the ions resulting from the losses of RCOOH groups (*m/e* 426 and 454). For mixed saturated-unsaturated 1,2-diacylglycerols (Figure 2), the ion resulting from the loss of the unsaturated RCOO radical (*m/e* 427) is 10–20 times more intense than the ion resulting from the loss of the unsaturated RCOOH group (*m/e* 426). On the other hand, the ions formed by losses of the saturated RCOO (*m/e* 473) and RCOOH (*m/e* 472) moieties have similar intensities. The total ion abundance of fragments formed by loss of RCOO and RCOOH from the 2 position is greater than that due to the corresponding losses from the 1 position. The latter ions also decrease in intensity as the acyl function in position 2 increases in unsaturation.

Also of interest in the spectra of 1-palmitoyl-2-eicosapentaenoyl-*sn*-glycerol is the ion at *m/e* 108. In common with the spectra of fatty acid methyl esters (22), an enhanced intensity at *m/e* 108 is indicative of ω 3 polyunsaturation. Similarly an enhanced intensity at *m/e* 150 is indicative of ω 6 polyunsaturation of a component fatty acid in the spectra of diacylglycerols. The ions at *m/e* 131 and 171 are abundant in the spectra of the *t*-BDMS ethers of all diacylglycerols. The most probable simple formulas of these ions are discussed below.

Figure 3 gives the mass spectra of the *t*-BDMS ethers of the reverse isomers of two saturated *rac*-1,2-diacylglycerols.

There is a difference in the spectra of the 1-palmitoyl-2-stearoyl (Figure 3A) and the 1-stearoyl-2-palmitoyl-*rac*-glycerol (Figure 3B), which is manifested in the abundance ratio of the ions due to losses of the acyloxy radicals from position 1 and position 2. For the above two reverse isomers, the ratios of  $m/e$  427 (loss of stearoyl) to that of  $m/e$  455 (loss of palmitoyl) are 2.0 and 0.6, respectively. There is also a smaller change in intensity ratio for the acyl + 74 ions at  $m/e$  313 and 341. Comparable differences between the mass spectra of these reverse isomers have been previously observed for the direct probe spectra of the TMS ethers, but the GC/MS spectra were claimed to be indistinguishable (4). The above method of determination of the reverse isomers of *sn*-1,2-diacylglycerols should be satisfactory for analysis of oligoenoic but not polyenoic diacylglycerols. In the latter, the yield of the *M* - acyloxy fragment falls off with increasing unsaturation. This problem can be overcome, however, by examining the appropriate molecular species of the diacylglycerols following  $\text{AgNO}_3$ -TLC separation and hydrogenation, provided the fatty chains in the 1 and 2 positions differ in their carbon number. As a result it is possible to estimate the reversed isomer content for all 16/18, 16/20, 18/20, 16/22, and 18/22 fatty carbon species.

Figure 4 compares the mass spectra of the *t*-BDMS ethers of *rac*-1,2-dipalmitoyl and 1,3-dipalmitoylglycerols. A comparison of these spectra with those of the glycerol- $d_5$  analogues was used to confirm the nature of the major ion fragments. The two spectra are distinguishable by the (*M* -  $\text{RCOOCH}_2$ )<sup>+</sup> fragment at  $m/e$  413 found only in the spectrum of the 1,3 isomer (Figure 4B). The absence of the corresponding fragment from the spectra of other *rac*-1,2- and *sn*-1,2-diacylglycerols was confirmed for all saturated derivatives examined. Also different are the relative intensities of the ions at  $m/e$  239 (acyl) and 387 (acyl + 2 × 74) which are much higher for the 1,3 isomer than for the 1,2(2,3) isomers. Since the mass of the (acyl + 2 × 74) ion is found 5 *m/e* units higher in the case of the glycerol- $d_5$  analogues,  $\text{RCOOCH}_2\text{CH}(\text{OH})\text{CH}_2\text{OSi}(\text{CH}_3)_2$  represents a probable structure for this ion. Since 99% of the (RCO + 74) ion intensity of 1,2(2,3)-dipalmitoylglycerol remains at  $m/e$  313, the major portion of this ion has the same rearranged structure,  $\text{RCOOSi}(\text{CH}_3)_2$ , as reported for the spectra of diacylglycerol TMS ethers (8). The (*M* - 57) and (*M* -  $\text{RCOO}$ ) and (*M* -  $\text{RCOOH}$ ) ions contain all five glycerol hydrogens and are shifted 5 *m/e* units higher in the spectrum of the glycerol- $d_5$  analogue. The major portion (93%) of the  $m/e$  171 ion contains four glycerol hydrogens and may be a mixture of  $\text{H}_2\text{CCH}_2\text{O}-t\text{-BDMS}$  and  $\text{H}_2\text{CCHCHO}-t\text{-BDMS}$  (8). The ion at  $m/e$  131 of 1,2(2,3)-dipalmitoylglycerol is split into 3 components in the spectrum of the glycerol- $d_5$  analogue: 25% has no glycerol hydrogen (*O*-*t*-BDMS), 20% has 4 glycerol hydrogens, and 55% has five glycerol hydrogens. Different spectra for the *sn*-1,2- and *sn*-1,3-diacylglycerols have previously been reported for the TMS ethers, while the spectra of the underivatized compounds were found to be indistinguishable (4). The mass spectra of the above derivatives of the *sn*-1,2- and *sn*-2,3-diacylglycerols are indistinguishable.

Table I summarizes the major abundances obtained by GC/MS for the *t*-BDMS ethers of the synthetic diacylglycerols and the natural diacylglycerols derived from rat liver phosphatidylcholines by hydrolysis with phospholipase C and argentation TLC.

**Applications.** The analysis of mixed acid diacylglycerols as the *t*-BDMS ethers by direct GC/MS is suitable for the determination of the molecular species of glycerophospholipids

in natural membranes and lipoproteins. The method is also applicable to the analysis of the diacylglycerol moieties of triacylglycerols derived from Grignard degradation or enzymic lipolysis. The main advantage of the GC/MS method is that the determination can be made rapidly on minute quantities of sample, as it eliminates the need for extensive preliminary fractionation.

If larger samples are available, the diacylglycerols can be profitably subjected to prefractionation and a more complete account obtained of trace components. An application of this procedure to the assessment of molecular species of rat liver phosphatidylcholines has yielded over 60 molecular species not including the reverse isomers. Previous analyses by combined application of  $\text{AgNO}_3$ -TLC and GLC methods had given a maximum of 30 species, the bulk of which had to be calculated by reiterated fitting (23). Likewise, the GC/MS method has given detailed accounts of the molecular species of the phosphatidylcholines of plasma lipoproteins, which could not be properly determined in the past because of the difficulty of preparing sufficient amounts of the lipoprotein fractions for detailed analysis of molecular species by conventional methods. Finally, the above procedure has been demonstrated to be satisfactory for the measurement of the deuterium content of molecular species of diacylglycerols generated during hepatic synthesis in the presence of deuterium oxide, provided the mixture is first fractionated by  $\text{AgNO}_3$ -TLC. Detailed studies in several of these areas have been made (24) and appropriate manuscripts are currently in preparation and will appear elsewhere.

## LITERATURE CITED

- (1) A. Kuksis and L. Marai, *Lipids*, **2**, 217 (1967).
- (2) O. Renkonen, *Adv. Lipid Res.*, **5**, 329 (1967).
- (3) E. J. Holub and A. Kuksis, *Metabolism of Molecular Species of Diacylglycerophospholipids*, *Adv. Lipid Res.*, **16** (1978), in press.
- (4) M. Barber, J. R. Chapman, and W. A. Wolstenholme, *J. Mass Spectrom. Ion Phys.*, **1**, 98 (1968).
- (5) G. Casparini, M. G. Horning, and E. C. Horning, *Anal. Lett.*, **1**, 481 (1968).
- (6) M. G. Horning, G. Casparini, and E. C. Horning, *J. Chromatogr. Sci.*, **7**, 267 (1969).
- (7) M. G. Horning, S. Murakami, and E. C. Horning, *Am. J. Clin. Nutr.*, **24**, 1086 (1971).
- (8) T. Curstedt, *Biochim. Biophys. Acta*, **360**, 12 (1974).
- (9) K. Hasegawa and T. Suzuki, *Lipids*, **8**, 631 (1973).
- (10) K. Hasegawa and T. Suzuki, *Lipids*, **10**, 66 (1975).
- (11) N. H. Morley, A. Kuksis, D. Buchnea, and J. J. Myher, *J. Biol. Chem.*, **250**, 3414 (1975).
- (12) E. J. Corey and A. Venkateswarku, *J. Am. Chem. Soc.*, **94**, 3190 (1972).
- (13) R. W. Kelly and P. L. Taylor, *Anal. Chem.*, **48**, 465 (1976).
- (14) O. Renkonen, *J. Am. Oil Chem. Soc.*, **42**, 298 (1965).
- (15) A. Kuksis, L. Marai, and J. J. Myher, *J. Am. Oil Chem. Soc.*, **50**, 193 (1973).
- (16) A. E. Thomas III, J. E. Scharoun, and H. Raiston, *J. Am. Oil Chem. Soc.*, **42**, 789 (1965).
- (17) O. Renkonen, "Progress in Thin-Layer Chromatography and Related Methods", Vol. II, A. Niederwieser and G. Pataki, Ed., Ann Arbor Science Publishers, Ann Arbor, Mich., 1971, p. 143.
- (18) J. J. Myher, L. Marai, and A. Kuksis, *J. Lipid Res.*, **15**, 586 (1974).
- (19) A. Kuksis, W. C. Breckenridge, L. Marai, and O. Stachnyk, *J. Am. Oil Chem. Soc.*, **45**, 537 (1968).
- (20) A. Kuksis, O. Stachnyk, and B. J. Holub, *J. Lipid Res.*, **10**, 660 (1969).
- (21) G. Philippou, D. A. Bigham, and R. F. Seamark, *Lipids*, **10**, 714 (1975).
- (22) J. J. Myher, L. Marai, and A. Kuksis, *Anal. Biochem.*, **82**, 188 (1974).
- (23) A. Kuksis, L. Marai, W. C. Breckenridge, D. A. Gornall, and O. Stachnyk, *Can. J. Physiol. Pharmacol.*, **46**, 511 (1968).
- (24) J. J. Myher, L. Marai, S. K. F. Yeung, and A. Kuksis, *Proc. Can. Fed. Biol. Sci.*, **20**, 133 (1977); Abs. No. 530.

RECEIVED for review September 19, 1977. Accepted January 3, 1978. The paper was reported in part at the 20th Annual Meeting of the Canadian Federation of Biological Societies, Calgary, Alberta, Canada, 1977. This research was supported by grants from the Medical Research Council of Canada and the Ontario Heart Foundation, Toronto, Ontario.

# Determination of Ruthenium in Automobile Exhaust Emissions by Negative Ion Chemical Ionization Mass Spectrometry

S. R. Prescott and T. H. Risby\*

Department of Chemistry, The Pennsylvania State University, University Park, Pennsylvania 16802

An analytical procedure is presented for the determination of ruthenium on membrane filters. Also the preparation of platinum bis(1,1,1-trifluoro-2,4-pentanedionate) is described and a discussion of the structure of this complex is included. The negative ion chemical ionization mass spectra of this chelate and the following complexes are reported: palladium bis(1,1,1-trifluoro-2,4-pentanedionate) and ruthenium tris(1,1,1-trifluoro-2,4-pentanedionate).

As a result of the use of platinum and palladium metals in catalytic converters in mobile sources manufactured after 1973, and the proposed use of ruthenium metal in converters in automobiles to be manufactured in the future, accurate and sensitive methods of analysis for these elements are required to monitor possible increases in environmental baseline levels. The need for an effective method of analysis was demonstrated at a Platinum Research Review Conference sponsored by the U.S. Environmental Protection Agency. At this conference it was reported that although the Los Angeles Catalyst Study has been on-line since June 1974, no measurements of the levels of platinum were possible since typical atmospheric ambient loadings were too low (1).

There are several methods of analysis which may be suitable for the monitoring of these elements in ambient air, water, or the biota although to date only a few studies have been reported. Flameless atomic absorption spectrometry has been used to determine platinum and palladium in biological tissues and fluids at levels of approximately 30 ppb (2, 3). Neutron activation analysis has quantitatively detected platinum and palladium in a wide variety of environmental and biological matrices in the nanogram range (3), and low level concentrations of platinum and palladium (picograms per cubic meter of air) have been measured with isotope dilution spark source mass spectrometry (4). To our knowledge, no investigations into the presence of ruthenium in water, air, or biota have been reported although a number of analytical chemistry techniques would appear to be suitable for such analyses (5).

These elements are currently receiving extensive investigation for another reason: at this present time the only toxicological data on ruthenium, platinum, and palladium (3, 6-8) available are related to forms of these elements which are not potentially environmentally significant. Therefore, before their impact may be ascertained, environmental baselines and toxicology must be measured.

Studies have shown that chemical ionization mass spectrometry is an attractive method of analysis for trace metals (9-11). A more recent study in our laboratory has demonstrated that  $\beta$ -diketonates which contain fluorine atoms have superior detection limits if negative ion chemical ionization mass spectrometry is used instead of the more conventional positive ion chemical ionization mass spectrometry (12). This increase in sensitivity toward negative ion formation is due to the increased electron capture cross section and/or electron affinity contributed by the fluorine atoms.

This present paper reports an analytical procedure for the determination of ruthenium in doped automobile exhaust

particle emissions trapped on membrane filters using a gas chromatography chemical ionization mass spectrometer system operated in the negative ion detection mode. The preparation of platinum bis(1,1,1-trifluoro-2,4-pentanedionate) together with a brief discussion of the structure of this complex will be reported. Finally, the negative ion chemical ionization mass spectra of this chelate and the following  $\beta$ -diketonates will be presented: palladium bis(1,1,1-trifluoro-2,4-pentanedionate) and ruthenium tris(1,1,1-trifluoro-2,4-pentanedionate).

## EXPERIMENTAL

**Instrumentation.** A gas chromatograph (Hewlett-Packard 402B) coupled to a chemical ionization mass spectrometer (Scientific Research Instruments Corporation Biospect System) which has been previously described (12) was used for the analyses. The initial mass spectra were obtained by placing solid samples directly onto the direct insertion probe; whereas for the analytical determinations of ruthenium, the samples were introduced through the gas chromatographic inlet. Methane served as both the reagent and carrier gas and spectra were recorded at a source pressure of 1.0 Torr. The gas chromatograph contained a 6-mm o.d., 3-mm i.d. glass column 55 cm long packed with 5% Dexil 300 on Supelcoport (100-120 mesh). The column was operated at 160 °C with a flow rate of 60 mL/min. The column effluent was split between atmosphere and the CI source in a ratio of 6:1. The gas chromatographic inlet consisted of a precision bore Pyrex capillary (0.2-mm i.d.) which was continuous from the column outlet to the source of the mass spectrometer. This interface was contained in an oven which was maintained at 180 °C.

The mass to charge ratios of the various peaks were determined by the mass marker which had been calibrated with methyl stearate and lutetium tris(2,2,7,7-tetramethyl-3,5-heptanedionate) (12). The proton magnetic resonances were measured with a Varian A60 NMR spectrometer and the infrared spectra of the potassium bromide disks were obtained using a Perkin-Elmer 621 IR spectrometer. The melting point of Pt(tfa)<sub>2</sub> was measured using a Thomas-Hoover melting point apparatus.

Neutron activation analysis was performed on the membrane filters using a 5-min irradiation at 1 MW followed by a 30-min decay. The samples were then counted for either 200, 800, or 4000-s intervals with a 36-cm<sup>2</sup> Ge(Li) detector. The 724.3 keV gamma ray of <sup>106</sup>Ru(*t*<sub>1/2</sub> = 4.5 h) was used for the analysis. Standards were prepared using known weights of RuO<sub>2</sub> (≈0.001 g).

**Chelate Preparation.** Palladium bis(1,1,1-trifluoro-2,4-pentanedionate) [Pd(tfa)<sub>2</sub>] (13) and ruthenium tris(1,1,1-trifluoro-2,4-pentanedionate) [Ru(tfa)<sub>3</sub>] (14) were prepared by methods which have been previously described. The chelates were purified by either recrystallization or reduced pressure sublimation.

Platinum bis(1,1,1-trifluoro-2,4-pentanedionate) [Pt(tfa)<sub>2</sub>] was prepared in the following manner: potassium tetrachloroplatinate was dissolved in water and the pH of the solution was adjusted to 8.5 by adding an aqueous solution of potassium hydroxide. The resulting solution was warmed to 60 °C and a slight excess of H(tfa) added. The solution was stirred for 2 h, after which time an equal volume of benzene was added, and the organic layer extracted. The solvent was evaporated and a yellowish residue remained which was washed with water and recrystallized from 2-methyl-2-propanol and water.

**Chemicals.** Reagent grade chemicals were used throughout except where otherwise specified and were obtained from the

following sources: 1,1,1-trifluoro-2,4-pentanedione (Pierce Chemical Co.), palladium chloride (K and K Laboratories, Inc.), ruthenium chloride (Research Organic/Inorganic Chemicals Corp.), and potassium tetrachloroplatinate (Strem Chemicals Inc.). The nitric and hydrochloric acids were ultrapure (Ultrax, Baker Chemical Co.).

**Analytical Procedure.** Prior to use, the heavy walled glass ampules were leached with *aqua regia* followed by washing with doubly distilled deionized water, acetone, and a solution of H(tfa) in toluene (10%). The fluoropore filters (Millipore Co 1  $\mu$ m) were rolled with Teflon coated forceps and placed into the ampules. A solution which consisted of 1.0 mL of HCl (11.0M) and a few drops of HNO<sub>3</sub> (16.0 M) was added to the ampules and they were placed in an oven at 50 °C for 1 h. The ampules were removed from the oven and 0.5 mL of HCl (1.1 M) was added along with 0.5 mL of H(tfa). The contents of the ampules were then refluxed in a heating mantle for 1 h. The refluxing was maintained by passing water through copper tubing (3-mm o.d.) coiled around the top of the ampule. After this time, the ampules were cooled and the resulting mixtures were neutralized to a pH of 6 with a solution of K<sub>2</sub>CO<sub>3</sub> (25% w/w) and 0.5 mL of toluene was added. The ampules were sealed and shaken for 30 min. The resulting toluene layers containing the Ru(tfa)<sub>3</sub> were transferred to sample vials, capped, and were ready for analysis. Blanks were prepared by following the same procedure with nontreated filters.

**Samples.** The samples consisted of 47-mm fluoropore filters which had been obtained from the Mobile Source Laboratory of the U.S. Environmental Protection Agency. The samples marked "Automobile Exhaust Only" were taken from the dynamometer warmup cycle using an uncontrolled (1972) vehicle operated on unleaded gasoline. The samples of "10.1  $\mu$ g Ru Automobile Exhaust" were collected by spotting the filters with RuCl<sub>3</sub> and the automobile exhaust pulled through at the same time as the "Automobile Exhaust Only" samples. Other samples consisted of spotting filters with known volumes of RuCl<sub>3</sub> in 9 M HCl and then wetting the filter with isopropanol to disperse and infuse the material.

## RESULTS AND DISCUSSION

The formation of a complex between platinum(II) and 1,1,1-trifluoro-2,4-pentanedione has been reported previously (15). However, this complex was reported to be bonded conventionally through the oxygen atoms on one ligand and through the methine carbon atom on the other. This complex is water soluble, but the Pt(tfa)<sub>2</sub> which is reported in this study is water insoluble and readily dissolved in a variety of organic solvents. The proton magnetic resonance spectrum of this complex shows signals at 2.1 and 6.0 ppm (8) with an integrated ratio of 3:1. These signals correspond to the presence of two identical methyl groups and methine proton resonances. Therefore, these data suggest the complex prepared contains two equivalent ligands.

The infrared spectrum of this complex shows two strong absorptions at 1590 and 1530 cm<sup>-1</sup>. H(tfa) exists as a mixture of keto and enol tautomers with the carbonyl stretches of the keto tautomer occurring at 1775 and 1745 cm<sup>-1</sup>, whereas the carbonyl stretches of the enol form are observed around 1600 cm<sup>-1</sup>. Thus it appears that the complex exists in the enolic form and is bonded through the oxygen. These observations are substantiated by the absorptions in the low frequency region of the infrared which consists of a broad band with a maximum at 437 cm<sup>-1</sup>. This absorption corresponds to the frequency of the platinum-oxygen vibration and no evidence of platinum-carbon stretching was observed (16). Therefore, in conclusion we feel that the Pt(tfa)<sub>2</sub> which is reported in this work is consistent with all other metal tfa complexes (13). A melting point of the complex was attempted, but the complex decomposed at 210 °C without melting completely.

**CI Mass Spectra.** The negative ion chemical ionization mass spectra of Pt(tfa)<sub>2</sub>, Pd(tfa)<sub>2</sub>, and Ru(tfa)<sub>3</sub> showed that the molecular parent ion was the major ion observed which is formed by resonance capture of low energy electrons. This

Table I. Formation Efficiency

Sample	Amount initially, $\mu$ g Ru	Formed, %
13	20	28 $\pm$ 1.1
14	20	29 $\pm$ 0.9
15	10	33 $\pm$ 0.1
16	10	34 $\pm$ 0.2
17	1.0	30 $\pm$ 0.3
18	1.0	32 $\pm$ 0.2
		Av 31 $\pm$ 0.5

observation was expected from an earlier study carried out in our laboratory (12). Apart from the molecular parent ion at 561 amu, the only other ion observed (<5% parent ion intensity) occurred at 153 amu and is attributed to the ligand, H(tfa).

**Analysis of the Membrane Filters.** Analytical procedures were investigated which were suitable for all these platinum group metals; however, after exhaustive studies it was found it was impossible to form a reproducible yield of Pt(tfa)<sub>2</sub>. Also it was found that it was impossible to form Ru(tfa)<sub>3</sub> using a sealed tube reaction under any conditions which is a rather surprising result. In the initial stages of this work, the membrane filters were treated with a mixture of 1.0 mL of HNO<sub>3</sub> and a few drops of HCl. When this procedure was used, very low amounts of Ru were extracted (<5%). An important aspect of ruthenium chemistry is the formation of nitric oxide complexes. Upon treatment with nitric acid, most ruthenium compounds will react preferentially with nitric oxide which will certainly inhibit the formation of Ru(tfa)<sub>3</sub>. To prevent the formation of nitric oxide complexes, the dissolution of the sample was accomplished by using 1.0 mL of HCl and 1 or 2 drops of HNO<sub>3</sub>. However, the chloride is volatile, so care must be taken to maintain a temperature below 50 °C to prevent loss of the sample. Ruthenium was introduced into the source of the mass spectrometer from the gas chromatograph, whereas the palladium and platinum chelates were introduced on a capillary tube via the heated solids probe. Divalent transition metal  $\beta$ -diketonates have problems associated with their gas chromatographic separation due to their tendencies toward oxidation, polymerization, or solvation (hydration) (17, 18). Therefore, it was decided to use the method of time resolved scans (19-23) for the analysis of divalent metals. Attempts to obtain quantitative measurements for the chelates Pd(tfa)<sub>2</sub> and Pt(tfa)<sub>2</sub> failed because of loss of the chelate when the solvent was removed prior to introduction into the mass spectrometer source.

The analysis of the Ru(tfa)<sub>3</sub> was performed using the technique of single ion monitoring. Known concentrations of Ru(tfa)<sub>3</sub> in toluene were injected into the gas chromatograph and mass chromatograms were obtained by scanning repeatedly across the mass window 555-565 amu which encompasses the molecular parent anion. The resulting areas of the mass chromatograms were measured and a calibration curve was plotted. The calibration curve for Ru(tfa)<sub>3</sub> was found to be linear from 100 ppb to 100 ppm with the minimum detectable amount of ruthenium, after taking into account the splitting ratio, being  $2.4 \times 10^{-13}$  g. This result represents the sensitivity of the CI technique and does not necessarily correspond to the minimum detectable amount of Ru in automobile exhaust. The results of the analyses of the various samples of ruthenium on membrane filters are shown in Tables I and II. Table I summarizes the efficiency of formation of Ru(tfa)<sub>3</sub> determined from a series of standards prepared in our laboratory. Knowing the amount of sample added to the filter, it was possible to calculate the efficiency of the formation of Ru(tfa)<sub>3</sub> by comparison of the measured



Table II. Determination of Ruthenium in Membrane Filters

Sample	Amt. initially, $\mu\text{g Ru}$	Amt found, $\mu\text{g Ru}$	
		NAA	CIMS
1 12 (as 1,10-phenanthroline)	-	-	-
2 12 (as 1,10-phenanthroline)	-	-	-
3 10	8.9 $\pm$ 0.09	9.2 $\pm$ 0.15	
4 10	8.6 $\pm$ 0.1	9.5 $\pm$ 0.26	
5 10 + Auto exhaust	8.0 $\pm$ 0.08	8.2 $\pm$ 0.47	
6 10 + Auto exhaust	8.7 $\pm$ 0.1	9.1 $\pm$ 0.29	
7 1.0	1.0 $\pm$ 0.1	0.97 $\pm$ 0.08	
8 1.0	1.1 $\pm$ 0.1	1.0 $\pm$ 0.1	
9 Auto exhaust only	not detected	not detected	
10 Auto exhaust only	not detected	not detected	
11 Blank filter	not detected	not detected	
12 Blank filter	not detected	not detected	

signal to the calculated signal from the calibration curve. From these measurements, it was established that the efficiency of formation was 31% with a relative standard deviation of ( $\pm 0.5\%$ ). Aliquots (0.8  $\mu\text{L}$ ) of the real sample solutions were injected into the gas chromatograph, and the resulting areas were recorded and measured. Knowing the formation efficiency, the amount of ruthenium on the filters was determined and is listed in Table II. Based on this developed methodology, the minimum detectable amount of ruthenium is on the order of 0.1  $\mu\text{g}$  contained on the membrane filter. Also shown is the amount of ruthenium contained on the membrane filters determined by neutron activation analysis. The precision of the CI technique is comparable to the precision obtained with neutron activation analysis as evidenced by the relative standard deviations of the two methods. The loss of ruthenium(III) as the 1,10-phenanthroline chloro complex may be due to the decomposition of the complex with the concomitant formation of ruthenium chloride which is volatile (24).

Currently further studies are being undertaken using other  $\beta$ -diketones in order to increase the extraction efficiency and thus increase the sensitivity of this technique. Also other ligand systems such as the tetradentate  $\beta$ -keto amines are being investigated to attempt to develop similar analytical procedures for platinum and palladium.

## Determination of the Leachability of Solids

O. U. Anders,\* J. F. Bartel, and S. J. Altschuler

The Dow Chemical Company, Midland, Michigan 48640

A novel method for measuring the leachability of homogeneous solids is reported using as examples radioactive tracers incorporated in plastics and concrete. Theoretical treatment of the data using simple diffusion theory is able to reduce the experimental information to a single "leachability constant" for the material and permits the calculation of the leaching behavior as a function of time for any size regular-shape object made of it.

The leachability of a material is frequently measured by experiments which either use Soxhlet extraction equipment

## ACKNOWLEDGMENT

We thank G. Wilkinson, R. E. Sievers, K. J. Eisentraut, P. C. Uden, and H. Veening for their advice on the analysis of ruthenium and J. E. Sigbsby for supplying the samples.

## LITERATURE CITED

- (1) C. E. Rodes, "Overview of the Los Angeles Catalyst Study", presented at the Platinum Research Review Conference, Quail Roost, N.C., December 1975.
- (2) A. F. LeRoy, W. S. Friauf, C. L. Litterst, T. E. Gram, A. M. Guarino, and R. L. Dedrick, "Platinum analysis in animal tissues and fluids", in Ref. 1.
- (3) A. H. Jones, *Anal. Chem.*, **48**, 1472 (1976).
- (4) D. A. Becker, P. D. LaFleur, and A. F. LeRoy, "Spontaneous determination of platinum, palladium and gold in biological and environmental materials", in Ref. 1.
- (5) J. A. Carter and W. R. Musick, "Platinum metals in air particulates near a catalytic converter test site as measured by isotope dilution spark source mass spectrometry", in Ref. 1.
- (6) J. J. Dulka, and T. H. Risby, *Anal. Chem.*, **48**, 640A (1976).
- (7) H. A. Schroeder, "The Poisons Around Us", Indiana University Press, Bloomington, Ind., 1974.
- (8) "Air Pollution Aspects", Litton Reports, P. B. 188074-PB188091, September 1969.
- (9) T. H. Risby, P. C. Jurs, F. W. Lampe, and A. L. Yergey, *Anal. Chem.*, **48**, 161 (1974).
- (10) Ref. 9, p. 726.
- (11) S. R. Prescott, J. E. Campana, P. C. Jurs, T. H. Risby, and A. L. Yergey, *Anal. Chem.*, **48**, 829 (1976).
- (12) J. E. Campana, S. R. Prescott, and T. H. Risby, *Anal. Chem.*, **49**, 1501 (1977).
- (13) R. W. Mosher and R. E. Sievers, "Gas chromatography of metal chelates", Pergamon Press, Elmsford, N.Y., 1965; References cited therein.
- (14) H. Veening, W. E. Bachman, and D. M. Wilkinson, *J. Gas Chromatogr.*, **5**, 248 (1967).
- (15) D. Gibson, J. Lewis, and C. Oldham, *J. Chem. Soc. A*, 1453 (1966).
- (16) R. D. Gillard, H. G. Wilver, and J. L. Wood, *Spectrochim. Acta*, **20**, 63 (1964).
- (17) J. P. Fackler, Jr., *Prog. Inorg. Chem.*, **7**, 361 (1966).
- (18) D. F. Groddon, *Coord. Chem. Rev.*, **4**, 1 (1969).
- (19) A. E. Jenkins and J. R. Major, *Talanta*, **14**, 777 (1967).
- (20) A. E. Jenkins, J. R. Major, and M. J. A. Reade, *Talanta*, **14**, 1213 (1968).
- (21) J. R. Major, M. J. A. Reade, and W. I. Stephen, *Talanta*, **14**, 373 (1968).
- (22) R. Belcher, J. R. Major, R. Perry, and W. I. Stephen, *Anal. Chim. Acta*, **43**, 451 (1968).
- (23) B. R. Kowalski, T. L. Isenhour, and R. E. Sievers, *Anal. Chem.*, **41**, 998 (1969).
- (24) T. D. Avokratova, "Analytical Chemistry of Ruthenium", Oldenbourg Press, Munich, 1963, pp 80-81.

RECEIVED for review September 14, 1977. Accepted January 9, 1978. Part of this work was presented at the Platinum Research Review Conference at Quail Roost, N.C., December 1975, sponsored by the U.S. Environmental Protection Agency. This work was supported by a grant sponsored by the U.S. Environmental Protection Agency (No. R803651010 and No. R803651020).

to ascertain zero concentration of the leachant at all times or involve immersion of the solid until an equilibrium concentration is reached in the liquid (1, 2).

Such experiments generally follow protocols specifying a certain specimen size and shape and are carried out at elevated temperatures to hasten the leaching process (3). These test protocols and their results stand by themselves and serve as yes-no criteria for quality control and legislation etc. (4). They do not yield insight into the leaching process nor do they represent the real world. In particular, they do not answer the often most important question: what is the amount of noxious substance leached from an object made of the tested material during the object's use time. For example, it is not

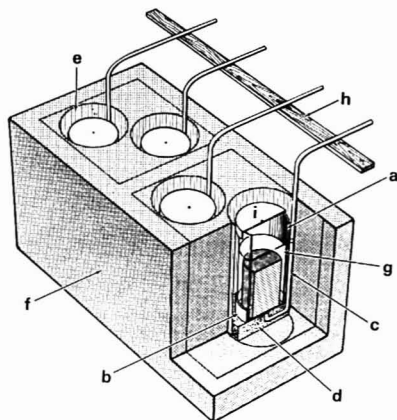


**Figure 1.** Schematic of leach test equipment: (a) Leaching vessel, (b) Rubber septum, (c) Thin plastic tubing, (d) Plastic foam support plug, (e) Drywell liner (empty beverage can) embedded in concrete, (f) Concrete building block, (g) Leaching liquid, (h) Loading board, (i) Cap with vent hole

important to know how much of a monomer can be leached from a specimen of plastic, but rather how much is leached into the soft drink while the liquid is in a bottle made of the material. And this quantity may be orders of magnitude different than the amount leached under extreme conditions.

It is the purpose of this report to introduce a new and inexpensive approach to leachability measurement which is both fast and applicable to ambient conditions and determines a "leachability parameter" specific for the material being tested. Its significance is readily interpreted by theory and can be extrapolated to arbitrary specimen size and shape as a function of time.

## EXPERIMENTAL

The experimental investigation addressed itself to the leaching of radioactive isotopes from cylinders prepared by the solidification of simulated rad-waste in plastics and concrete (5). The study included the solidification of true solutions as well as of suspensions or slurries of ion-exchange resins. The experiments were performed in multiples using different specimens cast from the same preparations by the same, or supposedly same, procedure.

The dimensions of the specimens were kept small to limit the amounts of radioactive material involved and to enhance the leaching process. The leaching was carried out with relatively small amounts of leachant in contact with the specimen in order to minimize dilution and render most of the leached radioactivity accessible to measurement in the counting aliquots.

The apparatus shown in Figure 1 consists of a leaching vessel made of plastic tubing (a) cut to the right length to contain the specimen and the leaching aliquot. This tubing is closed at the bottom with a septum (b) through which penetrates a 1-mm diameter plastic tubing, 1 or 2 ft long (c). This "vessel" is mounted on a plastic-foam plug (d) provided with a cut-in recess to receive the septum and guide the small tubing in a 180° turn.

The mounted vessel is inserted into a beverage can without lid (e) which in turn is cast into a concrete building block (f) using portland cement. Four such beverage cans can be mounted in one building block as seen in the figure.

An array of leaching vessels was constructed of these concrete blocks. Other concrete blocks served both as the supports and the biological shielding surrounding the radioactive experiments. The thin plastic tubings were brought out toward the front of the structure and lined up on a "loading board" (h) consisting of a wooden lath onto which the tubings were fastened and labeled with the number of the respective leaching vessel.

To initiate the experiments, the radioactive specimens were prepared, counted, weighed, and their dimensions measured with calipers. They were then placed into the leaching vessels. Each leaching vessel was covered with a cap (i) provided with a small vent hole, and the biological shielding was put into place.

The parallel experiments used both deionized water and a commercially available formulation simulating ocean water as leachants.

The leaching experiments were carried out in the following manner.

For each experiment a 10-mL plastic syringe was provided with a plastic tip such as used with 0.1-mL disposable pipets. The syringes were labeled and kept in sequence in an appropriate rack.

After loading each specimen, 10 mL of leach solvent was injected through the tube into the vessel by means of a dispensing pipet and immediately withdrawn with the syringe. This served as an initial rinse. A second 10-mL portion was then injected and left in contact with the specimen for the desired length of time.

After the leach interval, the leach solvent was withdrawn. Five milliliters of the solution was transferred to a counting vial while the rest was discarded. Quantitative recovery of the leach aliquot was thus not required.

In order to prepare for the subsequent leach interval, 10 mL of solvent was again injected into the vessel and immediately withdrawn and discarded. This operation assured the removal of any leachate remaining from the preceding time interval. A second charge of 10 mL of the leachant was then introduced into the vessel and remained there for the next leaching interval.

The experimental run described was carried out with 54 such leaching experiments performed simultaneously. From the theoretical considerations, it appeared that initial leaching would be significant. The leaching time intervals were thus kept short at first and followed each other in relatively rapid succession. In order to accomplish this, a rigid time schedule was followed for the initial phase of the experiments.

Leaching started with a 0.5-h interval which was followed by a 1.5-h interval and subsequently by 3-h, 6-h, 18-h, and 24-h leach intervals. After this, leaching times of 1 day were in order excepting weekends and holidays, when, after the initial week of operation, up to 96-h leach intervals were tolerated. It was assumed that the accumulation of dissolved material in the leach solution would not significantly affect the theoretical assumption of having zero-concentration leachant present at all times. The total amount of radioactivity present in the solutions for these experiments was kept to below 20% of the original radioactivity present in the specimen.

The run was subdivided into three sets so that 18 experiments in groups of six could be started together on one day. The second 18 followed the next day, and the third 18 were started the day after. In this way there was only one, and on the subsequent days two 0.5-h periods during which more than six leach changes had to be performed. This schedule permitted the operation to be carried out by one person.

The radioactivity of the 5-mL aliquots in the counting vials was crudely measured by holding them in front of a Geiger-tube laboratory monitor and comparing the approximate counting rates with that of a comparison standard. In case the aliquot exceeded this counting rate, a 1:5 dilution was prepared. The counting vials were then sealed and counted in a 3 in.  $\times$  3 in. well-type NaI(Tl) detector of a  $\gamma$ -ray spectrometer capable of handling up to 100 samples per counting run.

Many of the investigations were carried out using both  $^{137}\text{Cs}$  and  $^{60}\text{Co}$  tracers in the same specimens. In the present context, this was done merely to obtain twice as much data from the same experiments. The fact that different behavior of the tracers was observed in certain matrixes demonstrated the dependence of the leachability on the chemical nature of the species and the matrix material. A detailed study of this subject will have to wait for a later time.

$\gamma$ -Ray spectrometry was used to distinguish between the two isotopes, so that their individual leaching rates could be followed. In order to ensure consistency of the counting data, the measurements were carried out relative to standards which were used throughout the counting experiments. The counting data were obtained in units of these counting standards. The radioactivity originally present in the specimens was also determined relative

to these counting standards by counting both with a low-sensitivity Ge(Li)  $\gamma$  spectrometer. In this way the selection of the  $\gamma$ -spectrometer window widths was not critical from day to day and week to week.

One set of experiments was carried out with tritium as the radioactive species. The initial loading of the tritium-containing specimens was determined from their weights and the specific activity of the formulation from which they were prepared. A small piece of the plastic was weighed, burned in oxygen, and the resulting tritiated water was counted with a liquid-scintillation counter. The leach aliquots from the tritium-leaching experiments were similarly counted with the liquid-scintillation counter.

## DISCUSSION AND THEORY

An evaluation of the results of these leaching experiments was found possible with reference to simple diffusion theory (6-8). A mathematical model could be derived for the case of the leaching of homogeneous solids of regular shape, assuming no chemical interaction between leachant and the material being leached. It was assumed that diffusion through the matrix is the rate-limiting process.

The general diffusion equation:

$$\frac{\partial c}{\partial \theta} = k \nabla^2 c \quad (1)$$

describes the rate of change of concentration at a given location in the diffusion medium in terms of the size- and shape-dependent Laplacian operator and a diffusivity constant  $k$  characteristic of the material. Solutions of the general diffusion equation are thus shape- and size-dependent. They can be derived by various techniques well known to mathematicians.

To provide a needed base for the present discussion, the following equations are given which describe the diffusion behavior of simple bodies progressing from the "infinite slab", the "parallelepiped", the "sphere", and the "infinitely-long cylinder" to the cylinder of finite length.

For specific cases the integrals of the diffusion equation are conveniently presented in the form (9):

$$\frac{c - c_1}{c_0 - c_1} = \frac{\text{the difference between the concentration at a point and the concentration in the liquid at time } \theta}{\text{the initial uniform concentration in excess of the concentration of the leach liquid at time } \theta} \quad (2)$$

where  $c$  is the concentration of the leachable substance in the solid,  $c_0$  is the concentration in the initially homogeneous solid and  $c_1$  is the equilibrium concentration in the leachate at time  $\theta$ .

Equation 3 represents the leaching behavior of an infinite slab of thickness  $2a$ :

$$\frac{c - c_1}{c_0 - c_1} = \frac{4}{\pi} \left\{ \cos \frac{\pi x}{2a} \exp \left( -k\theta \left( \frac{\pi}{2a} \right)^2 \right) - \frac{1}{3} \cos \frac{3\pi x}{2a} \exp \left( -9k\theta \left( \frac{\pi}{2a} \right)^2 \right) + \frac{1}{5} \cos \frac{5\pi x}{2a} \exp \left( -25k\theta \left( \frac{\pi}{2a} \right)^2 \right) - \dots \right\} \quad (3)$$

Equation 4, in analogy to Equation 3, describes the parallelepiped.

$$\frac{c - c_1}{c_0 - c_1} = (\text{Series A}) (\text{Series B}) (\text{Series C}) \quad (4)$$

Series A is that given in Equation 3. In series B and C, the thickness  $2a$  is replaced with the corresponding thicknesses in the other two dimensions.

The equivalent equation describing the diffusion behavior of the sphere, Equation 5 contains a similar series:

$$\frac{c - c_1}{c_0 - c_1} = \frac{2r}{\pi r} \left\{ \sin \frac{\pi r}{r} \exp \left( -k\theta \left( \frac{\pi}{r} \right)^2 \right) - \frac{1}{2} \sin \frac{2\pi r}{r} \exp \left( -4k\theta \left( \frac{\pi}{r} \right)^2 \right) + \frac{1}{3} \sin \frac{3\pi r}{r} \exp \left( -9k\theta \left( \frac{\pi}{r} \right)^2 \right) - \dots \right\} \quad (5)$$

where  $r$  is the radius of the sphere.

Equation 6 describes the instantaneous concentration at a distance ( $r$ ) from the axis of an initially homogeneous, infinitely long cylinder of radius ( $r$ ) at the time  $\theta$  after the beginning of the diffusion process:

$$\frac{c - c_1}{c_0 - c_1} = 2 \left[ \frac{J_0 \left( \frac{R_1}{r} \right)}{R_2 J_1 \left( \frac{R_1}{r} \right)} \exp \left( -k\theta \left( \frac{R_1}{r} \right)^2 \right) + \frac{J_0 \left( \frac{R_2}{r} \right)}{R_2 J_1 \left( \frac{R_2}{r} \right)} \exp \left( -k\theta \left( \frac{R_2}{r} \right)^2 \right) + \dots \right] \quad (6)$$

The right side of this equation we will denote as "Series R", in which:

$$J_0(x) = 1 - \frac{x^2}{2^2} + \frac{x^4}{2^2 4^2} - \frac{x^6}{2^2 4^2 6^2} + \dots \quad (7)$$

and

$$-J_1(x) = \frac{d(J_0(x))}{dx} = - \left[ \frac{x}{2} - \frac{x^3}{2^2 4} + \frac{x^5}{2^2 4^2 6} - \dots \right] \quad (8)$$

For the finite cylinder of length ( $2a$ ) and radius ( $r$ ) the flow is described by:

$$\frac{c - c_1}{c_0 - c_1} = (\text{Series R}) (\text{Series A}) \quad (9)$$

Integration of these equations permits the determination of the total transport from the surface of the specimen into the surrounding liquid as a function of time. One can thus calculate both the leaching rate at a given time and the fraction of the unleached constituent still remaining in the solid.

For the present purpose, it is sufficient to be able to calculate the average residual concentration in the solid relative to the initial loading. The equations then take on the form (9, 10):

$$\frac{w - c_1}{c_0 - c_1} = \frac{\text{average concentration in excess of } c_1}{\text{initial uniform concentration in excess of } c_1} \quad (10)$$

where  $w - c_1$  is the average concentration of the leachable substance in the solid at some given time  $\theta$  in excess of the concentration in the leachate.

The corresponding equations are the following. For the slab:

$$\frac{w - c_1}{c_0 - c_1} = \frac{8}{\pi^2} \left[ \exp\left(-\left(\frac{k\theta}{a^2}\right)\left(\frac{\pi}{2}\right)^2\right) + \frac{1}{9} \exp\left(-9\left(\frac{k\theta}{a^2}\right)\left(\frac{\pi}{2}\right)^2\right) + \frac{1}{25} \exp\left(-25\left(\frac{k\theta}{a^2}\right)\left(\frac{\pi}{2}\right)^2\right) + \dots \right] \quad (11)$$

For the sphere:

$$\frac{w - c_1}{c_0 - c_1} = \frac{6}{\pi^2} \left[ \exp\left(-\left(\frac{k\theta}{r^2}\right)\pi^2\right) + \frac{1}{4} \exp\left(-4\left(\frac{k\theta}{r^2}\right)\pi^2\right) + \frac{1}{9} \exp\left(-9\left(\frac{k\theta}{r^2}\right)\pi^2\right) + \dots \right] \quad (12)$$

For the cylinder:

$$\frac{w - c_1}{c_0 - c_1} = 4 \left[ \frac{1}{R_1^2} \exp\left(-\left(\frac{k\theta}{R_1^2}\right)R_1^2\right) + \frac{1}{R_2^2} \exp\left(-\left(\frac{k\theta}{R_2^2}\right)R_2^2\right) + \dots \right] \quad (13)$$

and for the finite cylinder:

$$\frac{w - c_1}{c_0 - c_1} = 4 \left[ \frac{1}{R_1^2} \exp\left(-\left(\frac{k\theta}{R_1^2}\right)R_1^2\right) + \frac{1}{R_2^2} \exp\left(-\left(\frac{k\theta}{R_2^2}\right)R_2^2\right) + \dots \right] \times \frac{8}{\pi^2} \left[ \exp\left(-\left(\frac{k\theta}{a^2}\right)\left(\frac{\pi}{2}\right)^2\right) + \frac{1}{9} \exp\left(-9\left(\frac{k\theta}{a^2}\right)\left(\frac{\pi}{2}\right)^2\right) + \frac{1}{25} \exp\left(-25\left(\frac{k\theta}{a^2}\right)\left(\frac{\pi}{2}\right)^2\right) + \dots \right] \quad (14)$$

Equation 14 for the finite cylinder has two parts, one stemming from the equation of the infinite cylinder or radius ( $r$ ) the other from the slab of thickness ( $2a$ ). These dimensions are the size parameters for our cylinder. The equation contains as additional parameter the leachability (= diffusivity) constant  $k$  ( $\text{cm}^2 \text{s}^{-1}$ ) for the material. The terms  $R_1$ ,  $R_2$ , etc. represent the roots of the zero-order Bessel function of the first kind (11),  $J_0(r)$ , and  $\theta$  is the time elapsed since the beginning of the leaching process.

It was found that the two mathematical series making up Equation 14, each representing one of the simpler geometrical shapes that constitute the finite cylinder, converge very slowly for small values of  $k\theta/a^2$  or  $k\theta/r^2$ . For reasonable accuracy, calculations must thus consider a large number of terms in each series. This virtually requires that the calculations be carried out with a computer or programmable calculator. For the range of interest in this discussion, it is necessary to include between 100 and 200 terms of the series to arrive at meaningful leaching rates for the initial phases of the leaching process.

The Equations 11, 12, 13, and 14 give the average concentration of the leachable substance in the solid after a given time  $\theta$  as a fraction of the initial loading. The fraction leached during an interval of interest is thus computed as the difference of the fractions remaining in the solid at the beginning and the end of the leaching interval.

## RESULTS

The experimental data from several of the specimens investigated are presented as plots in Figures 2, 3, and 4. The theoretical curves were calculated with the aid of the described

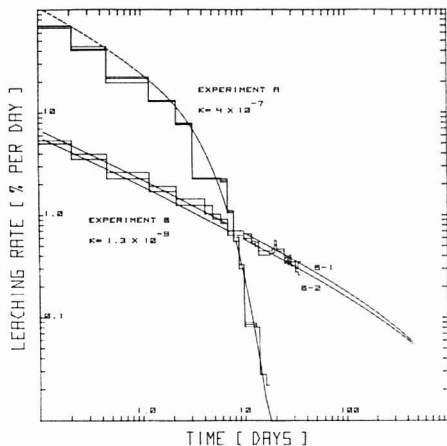


Figure 2. Experiment A:  $^{137}\text{Cs}$  leaching data of three cylinders, 5 cm long and 1.28-cm diameter made of a portland cement-simulated liquid rad-waste formulation. Deionized water used as leachant. Experiment B: Tritiated water leaching data from 5 cm long, 1.19-cm diameter and 1.42-cm diameter cylinders made of a plastic formulation. Deionized water used as leachant. The theoretical curves are calculated with an estimated leachability parameter,  $k$ , to fit the experimental data. B-1 and B-2 are calculated for the two sizes of cylinders used in experiment B, made of the same material for which  $k = 3 \times 10^{-9} \text{ cm}^2 \text{ s}^{-1}$ .

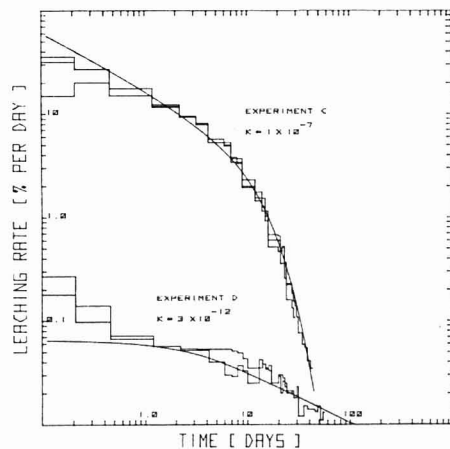


Figure 3. Experiment C: Leaching data of  $^{137}\text{Cs}$  from 5 cm long, 1.19-cm diameter cylinders made of a different type plastic formulation. Simulated ocean water used as leachant. Experiment D: Leaching data of  $^{60}\text{Co}$  from two cylinders made of yet another plastic formulation. Deionized water used as leachant.

model for the finite cylinder of the dimensions of the respective specimens and estimated "leachability constant" ( $k$ ) to fit the data.

The deionized-water leaching rates determined for  $^{137}\text{Cs}$  from three identical specimens made of a formulation of simulated rad-waste and portland cement are plotted in Figure 2 as "experiment A". The cylindrical specimens were 5 cm

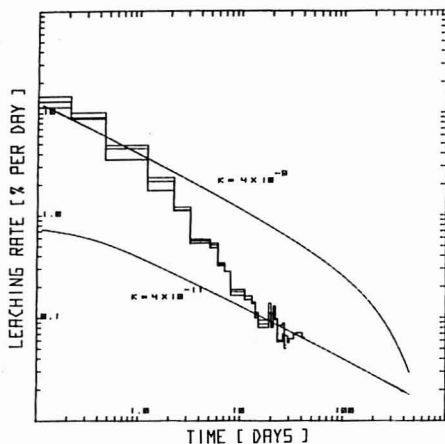


Figure 4. Ocean-water leaching rates of  $^{137}\text{Cs}$  from two cylinders 4.9 cm long and 1.18-cm diameter made of an inhomogeneous material containing ion-exchange beads

long and 1.28 cm in diameter. The resulting histogram is fit well by the model prediction using  $k = 4 \times 10^{-7} \text{ cm}^2 \text{ s}^{-1}$  as the leachability constant of the material.

The two histograms representing the data from "experiment B" are also plotted in Figure 2. The tracer, tritiated water, was solidified in a plastic formulation as two different-size ingots. Both were 5 cm long, one had a diameter of 1.19 cm, the other of 1.42 cm. As predicted by the model, the leaching rates obtained with deionized water for the smaller cylinder remained higher than those of the larger cylinder throughout the experiment. The theoretical curves, B-1 and B-2, calculated with  $k = 1.3 \times 10^{-9} \text{ cm}^2 \text{ s}^{-1}$  for the two sizes have about the same distance as the corresponding histograms.

In Figure 3 the results of "experiment C" are well matched by the model using  $k = 1 \times 10^{-7} \text{ cm}^2 \text{ s}^{-1}$  as the material parameter. This experiment involved the ocean-water leaching of  $^{137}\text{Cs}$  tracer from another plastic formulation.

The model also accommodated the much lower leaching rates found for  $^{60}\text{Co}$  leached by deionized water from yet another plastic formulation. The leachability constant in this case was only  $k = 3 \times 10^{-12} \text{ cm}^2 \text{ s}^{-1}$ .

The leachability parameter introduced here is a function of the matrix as well as of the leachant and the species being leached. For different leachable species present in the same solid, one would thus expect to obtain different values for the respective leachability constants.

It is apparent that the experimental results are generally in good agreement with the model. For each case studied, it is thus possible to describe the results by a single number,  $k$ , representing the material and with its aid calculate the expected leaching behavior as a function of time for any regular-shaped body made of the material.

Figure 5 is presented to facilitate the extrapolation of experimental data, obtained with small specimens in a few days, to the 55-gallon drum size ingots customary in radioactive-waste burial operations. The figure includes the expected leaching rates for materials of different "leachabilities" for times up to 1000 years. It also includes, as dotted curves, the predicted fractional amounts of leachable material left in the solid as a function of the leaching time.

Whenever nonhomogeneous leach specimens are investigated the leaching data obtained deviates from the theoretical

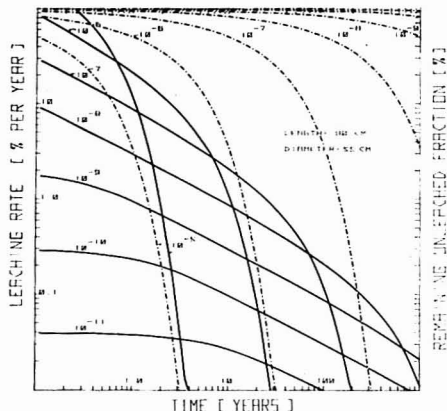


Figure 5. Calculated leaching rates for barrel-size cylindrical ingots of 90-cm height and 55-cm diameter as function of time for materials with different values of the leachability parameter  $k$  [ $\text{cm}^2 \text{ s}^{-1}$ ]. The dotted curves represent the fractional amounts of leachable material left in the solid as a function of leaching time

model. Figure 4 presents the data of a  $^{137}\text{Cs}$  leaching experiment using ingots made of ion-exchange resin beads solidified in a plastic matrix and ocean water as leachant. The surfaces of the two specimens were formed in part by exposed resin beads which showed an enhanced leaching rate relative to the average composite.

Porous materials and specimens with rough surfaces also exhibit initially higher leaching rates, since their surface-to-volume ratios are greater than for a regular body (cf. Figure 3, experiment D).

After the surface layer is depleted to some depth, the relative effects of the surface irregularities and micro-inhomogeneities are overcome or averaged out and the theoretical leaching curve is approached (Figure 4). Due to the higher surface-to-volume ratio, such irregularities are more pronounced in experiments using small ingots. They become less important as the size is increased.

The assumption that the diffusion across the solid-liquid interface is rapid relative to the diffusion in the solid is given its most severe test at the beginning of the leaching experiments with high- $k$  materials, where relatively high leaching rates are encountered. The effect of surface-diffusion limitation is thus seen only in Figure 3, experiment C for the  $k = 1 \times 10^{-7} \text{ cm}^2 \text{ s}^{-1}$  material during the first day of the run. The experimental data there definitely stayed below the prediction of the simple model.

In case a chemical interaction between the leachant and constituents of the solid causes changes which affect the characteristics of the material, i.e., the diffusivity etc. or causes the leachable material to precipitate and change chemically in the solid, we expect deviations from the model.

## CONCLUSION

The leachability of solidified low-level radioactive waste forms is one of the critical parameters determining the quality of the product and its acceptability for burial (12). The present work provides a simple procedure to measure this parameter in a few days of experimentation and supplies a mathematical model able to predict the leaching behavior of waste forms made of the material. As an extension of the reported approach, the method might find application in the quality assurance testing of materials used for beverage



containers etc. to measure and predict the amounts of noxious materials leached during their actual use.

### ACKNOWLEDGMENT

The writers are indebted to H. Filter, K. Roberson, and W. Strom for providing the molded radioactive specimens and to I. Takahashi for providing the tritium tracer and performing the tritium counting.

### LITERATURE CITED

- (1) "Technique of Organic Chemistry", Arnold Weissberger, Ed., Vol. III, Section IV, Interscience, New York, N.Y., 1950.
- (2) "Official Methods of Analysis", Section 21.010-21.015, 12th ed., 1975, Association of Official Analytical Chemists, P.O. Box 540, Benjamin Franklin Station, Washington, D.C. 20044.
- (3) J. E. Mendel, "A Review of Leaching Test Methods and the Leachability of Various Solid Media Containing Radioactive Wastes", Document BNWL-1765 (July 1973), Brookhaven National Laboratory, Upton, N.Y.
- (4) "FDA Guidelines for Chemistry and Technology Requirements of Indirect Food Additive Petitions", Bureau of Food and Drug Administration, Washington, D.C. (March 1976).
- (5) E. D. Hespe, Ed., "Leach Testing of Immobilized Radioactive Waste Solids, A Proposal for a Standard Method", International Atomic Energy Agency, *At. Energy Rev.*, 9 (1), 195-207 (1971).
- (6) P. G. Shewman, "Diffusion in Solids", McGraw Hill Book Co. New York, N.Y., 1963.
- (7) H. S. Carslaw and J. C. Jaeger, "Conduction of Heat in Solids", Oxford Press, London, 1959.
- (8) R. M. Barrer, "Diffusion In and Through Solids" The University Press, Cambridge, 1951.
- (9) A. B. Newman, *Trans. Am. Inst. Chem. Eng.*, 27 310 (1931).
- (10) E. L. Lederer, *Kolloid-Z.*, 44, 108 (1928).
- (11) "Royal Society Mathematical Tables", F. W. Oliver, Ed., Bessel Functions III, University Press, Cambridge, 1960.
- (12) H. W. Godbee and D. S. Joy, "Assessment of the Loss of Radioactive Isotopes from Waste Solids to the Environment", Document ORNL-TM-4333, Oak Ridge National Laboratory, Oak Ridge, Tenn.

RECEIVED for review June 6, 1977. Accepted January 5, 1978.

## Interferometric Concentration Determination of Dextran after Gel Chromatography

Lars Hagel<sup>1</sup>

Pharmacia AB, Box 181, S-751 04 Uppsala, Sweden

An interferometric method for the concentration analysis of dextran in column effluent, using the Multiref 901, has been investigated. The basic theory of the instrument as well as a theoretical interpretation of the expected sources of error is given. Whereas errors due to the optical activity and the molecular weight dependence of the refractive index increment of the sample are negligible, errors caused by an absorbing sample solution or the nonlinear response of the instrument can, if not corrected, reach a level of some per cent. The theoretical conclusions are verified experimentally. The physical interferometric method is compared to the chemical anthrone method for the analysis of dextran.

Dextran is a polysaccharide consisting of  $\alpha$ -D-glucose units mainly linked at the 1-6 positions. The glucose polymer is produced by biological synthesis using a nonpathogenic bacteria (e.g., *Leuconostoc mesenteroides*).

Dextran has found applications in numerous fields (1) and the most well known are as plasma expanders (e.g., Macrodex, Rheomacrodex) and in the production of chromatographic resins (e.g., Sephadex).

For use as a plasma expander, dextran is partly hydrolyzed and fractionated to yield molecules within a suitable weight range. The physiological properties of dextran are closely related to the molecular weight of the polymer (2). It is therefore essential that the molecular weight distribution of clinical dextran is well specified and controlled. The distribution analysis may today advantageously be performed by gel chromatographic techniques (3-5).

For the analysis of dextran in the column effluent chemical methods involving on-line determination (6, 7) as well as separate analysis of collected fractions (8, 9) have been described. The method currently used in this laboratory for the determination of dextran after gel chromatography is the well known reaction between carbohydrates and the sulfuric

acid-anthrone reagent (10, 11). This reaction, however, consumes large amounts of reagents and the corrosive waste products are unpleasant to handle.

Dextran can also be determined without prior hydrolysis of the polymer by a physical measurement. As an example, the specified relationship between concentration and refractive index can be utilized (12). In fact, refractometric devices are among the most common detectors used for concentration analysis of column effluents and have recently been applied in the determination of dextran in the molecular weight distribution analysis by gel chromatography (4, 13, 14). The instruments (i.e., Waters R-401 and Knauer 5100) used by these authors are based upon the measurement of the deflection of a beam, while some other instruments (e.g., LDC 1107) measure the intensity of the transmitted light as a function of refractive index. An interesting interferometric principle not utilized earlier in commercial detectors is presented in the Multiref 901 (15). In this instrument a difference in the refractive index between the sample and reference cells is transformed into a rotation of the plane of polarization of the measuring beam.

In most work using RI-detectors for the analysis of column effluent, it is anticipated that the instrument response is dependent on solute concentration only. This is not always the case, however (16), and it is therefore essential that the properties of the analyzed solution in relation to the measuring principle of the instrument are well known.

The aim of this investigation was to examine the theoretical and practical capability of the Multiref 901, primarily as a tool for the determination of dextran in column effluents, as compared to chemical methods of assay.

### THEORY

**Principle of the Multiref 901.** The principle of the instrument is based upon wave-front shearing of polarized light. A similar arrangement has been applied earlier in interference microscopes (17). Since the theory of interferometric concentration analysis using Multiref 901 has not been published elsewhere, it will, in order to simplify the following interpretation, be presented in detail below (18, 19).

<sup>1</sup> Present address, Institute of Chemistry, Analytical Department, Box 531, S-751 21 Uppsala, Sweden.

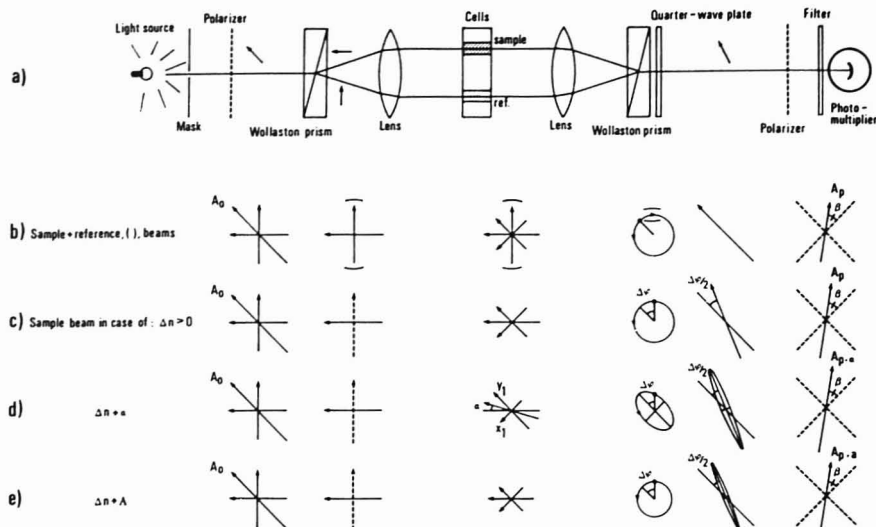


Figure 1. Lightpath in Multiref 901, 902. (a) Sample and reference beams as seen from above. (b) Sample and reference,  $(\perp)$ , beams as seen from the photomultiplier. (c) As in (b) when  $n_{\text{sample}} > n_{\text{reference}}$ . (d) As in (c) and in case of sample optical activity. (e) As in (c) and in case of sample absorbance.

The lightpath in the instrument is schematically illustrated in Figure 1. The light beam from an electric bulb is linearly polarized at  $-45^\circ$  to the horizontal plane. The beam is split by a Wollaston prism consisting of two parts having different refractive indexes for horizontally and vertically polarized light. These beams are focused on the cells where the beam passing through the sample cell is horizontally polarized. After passing the cells, the beams are focused on a second Wollaston prism followed by a quarter-wave plate having its fast axis at  $-45^\circ$  to the horizontal plane. A beam, linearly polarized in the fast axis plane will, after passage of the plate, lead another linearly polarized but orthogonal beam by a quarter of a wave length. Such a phase difference will result in a circularly polarized beam. Now, each of the beams focused on the Wollaston prism can be considered as consisting of two such perpendicular beams and the result, after the quarter-wave plate, is two circularly polarized beams with opposite rotations. These beams will interfere to yield the original linearly polarized beam (Figure 1b). The second polarizer is placed at an angle  $90-\beta$  to the first one to let 35% of the signal reach the photomultiplier. A filter transmitting 546 nm is placed in front of the photomultiplier.

If the sample cell contains a higher concentration of the solute than the reference cell, the refractive index will also generally be higher and the interfering beams will not be in phase (Figure 1c). The refractive index difference,  $\Delta n$ , and the phase difference,  $\Delta\varphi$ , are related by (20):

$$\Delta\varphi = \Delta n l (360/\lambda)^{-1} \text{ degrees} \quad (1)$$

where  $l$  = cell length and  $\lambda$  = wavelength of the light source in vacuum.

The circularly polarized beams will therefore interfere to yield a linearly polarized beam which has rotated  $\Delta\varphi/2$  degrees and the amplitude striking the photomultiplier,  $A_p$ , will be:

$$A_p = A_o \cos(90 - \beta - \Delta\varphi/2) = A_o \sin(\beta + \Delta\varphi/2) \quad (2)$$

**Sources of Error.** In the interferometric concentration analysis of dextran, some physical properties such as molecular weight dependence of refractive index increment, sample optical activity, and sample absorbance, as well as instrumental properties like nonlinear response can be expected to introduce errors. Whereas errors due to the optical activity of the sample influence only the interferometric principle, the other sources of error can be assumed to influence all concentration analysis based upon refractive index differences. Thus, nonlinear response can be noticed for Multiref 901, Waters R-401, and Knauer 5100 as stated by the manufacturers.

Since it is of utmost importance that the sources of error are known and corrected for if not negligible, a detailed deduction of the influence of the expected errors in interferometric concentration analysis is given below.

**Variation of the Refractive Index Increment with the Molecular Weight of the Sample.** For some polymers, for example polystyrenes in benzene, the refractive index increment ( $dn/dc$ ) varies with sample molecular weight and this dependence must be taken into account when calculating the absolute values of molecular weights from gel permeation data (16). For aqueous solutions of dextrans information about  $dn/dc$  at 546 nm is very scanty but at 436 nm, the following values of  $dn/dc$  ( $\text{cm}^3 \text{g}^{-1}$ ) have been given; for glucose, 0.147 (21), and for dextrans ( $M_w = 18 \times 10^3$ – $9.5 \times 10^6$ ) 0.151 (22). This deviation is small compared to that reported for polystyrenes in benzene where an increase in  $M_w$  from  $4 \times 10^3$ – $4 \times 10^6$  increases the refractive index increment by 11% (16). It may be concluded that the variation of refractive index increment with molecular weight for dextran does not introduce any significant error in interferometric concentration analysis.

**Error due to the Optical Activity of the Sample.** Dextran is an optically active substance and for this dextran the specific rotation,  $[\alpha]$ , at 546 nm and  $20^\circ \text{C}$  is  $23.5 \pm 0.1^\circ \text{cm}^2 \text{g}^{-1}$  (23). As  $[\alpha]$  varies with molecular weight (as shown by the values of  $[\alpha]_D$  for isomalto-oligosaccharides (24) and dextran (23)), it is

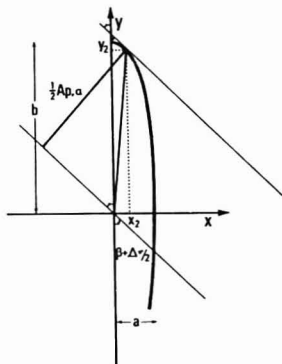


Figure 2. Construction of  $A_{p,\alpha}$  for an elliptically polarized ray

essential that the contribution from the optical activity to the rotation of the measuring beam is negligible. Since  $dn/dc = 0.1498 \pm 0.0003 \text{ cm}^3 \text{ g}^{-1}$  for dextran at 546 nm (25) and the highest acceptable value of  $\Delta\varphi/2$  is  $32.97^\circ$  (18), the maximal rotation due to sample optical activity is:

$$\alpha = [\alpha]c = [\alpha] \frac{\Delta\varphi}{360} \lambda \frac{dc}{dn} < 1.57 \times 10^{-3} \text{ degrees} \quad (3)$$

The relative error caused by the optical activity of the sample can be deduced in the following way (Figure 1d).

A rotation of  $\alpha$  degrees of the plane of polarization gives:

$$x_1 = \frac{1}{\sqrt{2}} A_o \sin(45 - \alpha) = \frac{1}{2} A_o (\cos \alpha - \sin \alpha) \quad (4a)$$

and

$$y_1 = \frac{1}{\sqrt{2}} A_o \cos(45 - \alpha) = \frac{1}{2} A_o (\cos \alpha + \sin \alpha) \quad (4b)$$

As a result, the sample beam will, after the quarter-wave plate, be elliptically not circularly polarized. The amplitude,  $A_e$ , of this ellipse at an angle  $\theta$  is given by:

$$\frac{x^2}{x_1^2} + \frac{y^2}{y_1^2} = 1 \Rightarrow \frac{(A_e \sin \theta)^2}{x_1^2} + \frac{(A_e \cos \theta)^2}{y_1^2} = 1 \Rightarrow$$

$$A_e = \frac{1}{2} A_o \cos 2\alpha (1 + \sin 2\alpha (2 \sin^2 \theta - 1))^{-1/2} \quad (5)$$

The sample and reference beams interact to give another elliptically polarized beam with the large axis,  $2b$ , at  $\theta = \Delta\varphi/2$  and the small axis,  $2a$ , at  $\theta = \Delta\varphi/2 + 90^\circ$ . The amplitude in the polarizer plane,  $A_{p,\alpha}$ , is deduced from the relations (Figure 2):

$$\frac{1}{2} A_{p,\alpha} = \left( x_2^2 + y_2^2 \right)^{1/2} \sin \left( \beta + \Delta\varphi/2 + \arctan \frac{x_2}{y_2} \right) \quad (6)$$

and

$$\cot(\beta + \Delta\varphi/2) = -\frac{d}{dx} \left( \left( b^2 - \frac{b^2}{a^2} x^2 \right)^{1/2} \right)_{x=x_2} \quad (7)$$

to give

$$A_{p,\alpha} = 2b \left[ \frac{1 + \frac{a^4}{b^4} \cot^2(\beta + \Delta\varphi/2)}{1 + \frac{a^2}{b^2} \cot^2(\beta + \Delta\varphi/2)} \right]^{1/2}$$

$$\sin \left[ \beta + \Delta\varphi/2 + \arctan \left( \frac{a^2}{b^2} \cot(\beta + \Delta\varphi/2) \right) \right] \quad (8)$$

where

$$\alpha = \frac{1}{4} A_o (1 - \cos 2\alpha (1 + \sin 2\alpha (2 \sin^2(\Delta\varphi/2 + 90^\circ) - 1))^{-1/2}) \quad (9)$$

and

$$b = \frac{1}{4} A_o (1 + \cos 2\alpha (1 + \sin 2\alpha (2 \sin^2(\Delta\varphi/2 - 1))^{-1/2})) \quad (10)$$

Now, when  $\alpha$  is small, the approximations:

$$a \approx \frac{1}{4} A_o (1 - \cos 2\alpha) \approx \frac{1}{2} A_o \alpha^2 \quad (11)$$

$$b \approx \frac{1}{4} A_o (1 + \cos 2\alpha) \approx \frac{1}{2} A_o (1 - \alpha^2) \quad (12)$$

$$\frac{a^2}{b^2} \cot(\beta + \Delta\varphi/2) \approx \alpha^4 \quad (13)$$

where  $\alpha_r = \alpha \pi/180$ , are valid. Thus,

$$A_{p,\alpha} \approx 2b \sin(\beta + \Delta\varphi/2) \approx A_o (1 - \alpha_r^2) \sin(\beta + \Delta\varphi/2) \quad (14)$$

The average counting rate of the photomultiplier and thus the signal is proportional to the square of the amplitude. This together with the adjustment of the output signal to zero for  $\sin^2 \beta = 0.35$  and Equations 2 and 14 gives the expression of the relative error at sample optical activity:

$$f_{rel} = \frac{(A_{p,\alpha}^2 - A_o^2 \sin^2 \beta) - (A_p^2 - A_o^2 \sin^2 \beta)}{A_p^2 - A_o^2 \sin^2 \beta} \approx$$

$$\frac{-2\alpha_r^2}{1 - \left( \frac{\sin \beta}{\sin(\beta + \Delta\varphi/2)} \right)^2} \quad (15)$$

In the measuring range of  $\Delta\varphi/2$  ( $0 < \Delta\varphi/2 < 32.97^\circ$ ) the relative error will approximately vary between  $-0.02\alpha_r$  and  $-3.33\alpha_r^2$  and is for  $\alpha_r < 1.57 \times 10^{-3} \times \pi/180$  less than  $3 \times 10^{-9}$ .

**Error due to Sample Absorbance.** The most serious error is introduced when the sample solution is absorbing at 546 nm. This reduces the amplitude of the circularly polarized beam,  $A_e$ , according to:

$$\frac{A_e^2}{\left( \frac{1}{2} A_o \right)^2} = \frac{P}{P_o} = 10^{-A} = A_c = \frac{1}{2} A_o \times 10^{-A/2} \quad (16)$$

where  $A$  is the absorbance of the solution and  $P_o$  and  $P$  are the powers of the incident and transmitted beam, respectively. The sample and reference beams interfere to yield an elliptically instead of linearly polarized beam (Figure 1e). This phenomenon is known as circular dichroism (26). Both the large

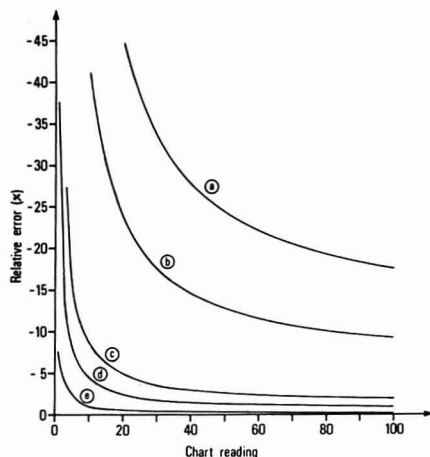


Figure 3. Relative error as a function of chart reading at sensitivity 100 for a sample absorbance of:  $a = 0.1$ ,  $b = 0.05$ ,  $c = 0.01$ ,  $d = 0.005$ , and  $e = 0.001$  as calculated from Equation 20

and small axis of this ellipse will contribute to the amplitude in the polarizer plane,  $A_{p,a}$ , as in Equation 8 but here,

$$a = \frac{1}{4} A_0 (1 - 10^{-A/2}) \quad (17)$$

and

$$b = \frac{1}{4} A_0 (1 + 10^{-A/2}) \quad (18)$$

Since  $a^2/b^2 \ll 1$  for  $A < 0.1$ , the amplitude is in this case reduced to:

$$A_{p,a} \approx 2b \sin(\beta + \Delta\varphi/2) \approx \frac{1}{2} A_0 (1 + 10^{-A/2}) \sin(\beta + \Delta\varphi/2) \quad (19)$$

The relative error caused by an absorbing sample solution is thus approximately,

$$f_{rel} \approx \frac{\frac{1}{4} (1 + 10^{-A/2})^2 - 1}{1 - \left( \frac{\sin \beta}{\sin(\beta + \Delta\varphi/2)} \right)^2} \quad (20)$$

The relative error as function of chart reading (100 = full scale) for  $0.001 < A < 0.1$  is shown in Figure 3. It can be concluded that the absorbance of the sample solution should not exceed 0.001 for a relative error of 1% on sensitivity 100 ( $\Delta n = 100 \times 10^{-6}$  RIU for full scale).

If the absorption of the sample solution is caused by the solute of interest (e.g., Blue Dextran 2000), application of the Lambert-Beer law and Equation 1 in Equation 20 gives:

$$f_{rel} \approx \frac{\frac{1}{4} (1 + 10^{-k\Delta\varphi/2})^2 - 1}{1 - \left( \frac{\sin \beta}{\sin(\beta + \Delta\varphi/2)} \right)^2} \quad (21)$$

where

$$k = \frac{1}{2} \epsilon \frac{dc}{dn} M^{-1} \times 10^3 \times \frac{1}{180} \times \lambda = 1.012 \times 10^{-3} \epsilon M^{-1}$$

Here  $\epsilon$  is the molar absorptivity at 546 nm and  $M$  is the molecular weight of the colored solute. The value of  $f_{rel}$  given by Equation 21 increases with increasing value of  $\Delta\varphi/2$  and the largest relative error is thus found for  $\Delta\varphi/2 = 32.97^\circ$ . For a relative error of less than 1%, the product  $\epsilon M^{-1}$  must be less than 0.08. The maximum relative error can also be read from chart reading 100 in Figure 3, showing that the absorbance of the solute should not exceed 0.005 for a relative error of less than 1% on sensitivity 100.

**Nonlinear Response.** With the Multiref 901, the signal reaching the detector is of sine-form. This signal is approximated to a linear function, thus introducing a systematic error. It is, however, possible to theoretically deduce formulas for the magnitude of this error and correct the results as follows.

In the calibration procedure, the sine wave from  $-\pi/2$  to  $\pi/2$  is adjusted to cover the calibration range from 0 to 100, i.e.,

$$\begin{aligned} \alpha &\rightarrow y; y = 50 \sin \alpha + 50 \\ -\pi/2 < \alpha < \pi/2, 0 < y < 100 \end{aligned} \quad (22)$$

The calibration range is thereafter mapped into each measuring range in the following way (18),

$$y \rightarrow x; \begin{cases} 35 \rightarrow 0 & \text{for all sensitivities} \\ 89.3 \rightarrow 100 & \text{for sensitivity 100} \\ 62.8 \rightarrow 100 & \text{for sensitivity 50} \\ 46.1 \rightarrow 100 & \text{for sensitivity 20} \\ 40.6 \rightarrow 100 & \text{for sensitivity 10} \end{cases}$$

i.e.,

$$y \rightarrow x; x = \frac{1}{a} (y - 35) \quad (23)$$

where  $a = 0.543, 0.278, 0.111$ , and  $0.056$  for sensitivity 100, 50, 20, and 10, respectively. Thus,

$$\begin{aligned} \alpha &\rightarrow x; x = \frac{1}{a} (50 \sin \alpha + 15) \Leftrightarrow \alpha = \\ &\arcsin(0.02ax - 0.3) \end{aligned} \quad (24)$$

The angle being measured is,

$$\alpha_{\text{sample}} - \alpha_{\text{reference}} = \arcsin(0.02ax - 0.3) + \arcsin 0.3 \quad (25)$$

The instrument is constructed to give  $\alpha = 65.93^\circ$  for  $\Delta n = 100 \times 10^{-6}$  (18) and if  $x$  should be a linear function of  $\alpha$  then:

$$\alpha = x \frac{\Delta n \times 10^6 \times 0.6593}{100} \quad (26)$$

and the relative error due to nonlinear response becomes:

$$f_{rel} = \frac{x \Delta n \times 10^6 \times 0.6593}{\arcsin(0.02ax - 0.3) + \arcsin 0.3} - 1 \quad (27)$$

The chart reading corrected for nonlinearity is,

$$x_{\text{corr}} = \frac{\arcsin(0.02ax - 0.3) + \arcsin 0.3}{\Delta n \times 0.6593 \times 10^4} \quad (28)$$

where  $a = 0.543, 0.278, 0.111$ , and  $0.056$  for sensitivity ( $\Delta n \times 10^6$ ) 100, 50, 20, 10, respectively. The calculated relative

Table I. Influence from Absorption on the Chart Reading of Dextran Solutions at Sensitivity 100 as Compared to the Theoretical Error

[Bromocresol green], $\mu\text{g mL}^{-1}$	0	7.09	28.36	56.72
[Dextran], ( $\mu\text{g mL}^{-1}$ )				
0	Chart reading <sup>a</sup>	-3.14	-11.77	-20.63
	$A_{546}$ (approx) <sup>b</sup>	0.022	0.088	0.168
70.0	Chart reading <sup>a</sup>	9.58	3.21	-2.5
	Rel. error, %	-11	-66	-126
	Rel. error, %	-19	-71	-127
350.0	Chart reading <sup>a</sup>	49.65	47.42	40.24
	Rel. error, %	-4	-19	-35
	Rel. error, %	-5	-21	-38
700.1	Chart reading <sup>a</sup>	99.65	97.13	84.46
	Rel. error, %	-2	-15	-29
	Rel. error, %	-4	-16	-28

<sup>a</sup> Corrected for nonlinear response and the contribution to  $\Delta n$  from bromocresol green. <sup>b</sup> As calculated from Equations 16 and 23. <sup>c</sup> As calculated from Equation 20.

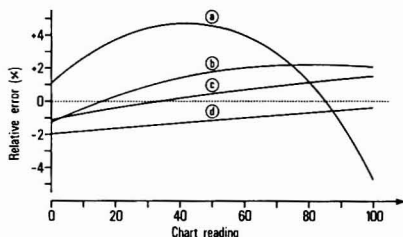


Figure 4. Relative error due to nonlinear response of the Multiref 901 at sensitivity: a = 100, b = 50, c = 20, and d = 10

error as function of chart reading is shown in Figure 4.

### EXPERIMENTAL

The sources of error were tested experimentally by suction of aqueous solutions of dextran through the detector (Multiref 901, 1-mm. cell, Optilab AB) with a pulse free pump (Labotron LDP 13, Kontron AB). For changing samples, a sampler (Sampletron Pb 1000, Stålprodukter, Uppsala) was used. The signal was registered by a recorder (Servograph Rec. 51, Radiometer). The influence of absorption of the sample solution was tested by adding bromocresol green to solutions of dextran to yield an absorbance of 0.02–0.2 as calculated by applying Equations 16 and 23 on the chart reading of solutions of bromocresol green.

The concentrations of dextran obtained by interferometry were then compared to those obtained by the anthrone method mentioned above. In these experiments, a chromatographic column (K16/70 or K16/40, Pharmacia Fine Chemicals) was packed with Sepharose CL-4B (Ph F C). The effluent from the column (0.3% sodium chloride + preservative) was connected to the detector (above) and the flow was adjusted to 20 mL/h by means of a peristaltic pump (P-3, Ph F C). After the pump, the effluent was sampled (1 mL/sample) and after dilution (1 → 3), analyzed for dextran with the anthrone method (11) (Figure 5). The fraction collector (FR 4, Stålprodukter, Uppsala) was synchronized to lag the detector by one fraction. The signal from the detector was registered as above. The continuous interferometric curves were evaluated using a desk calculator (HP 9100B) with an extended memory (HP 9101A) and equipped with a digitizer assembly (HP 9107A). The results were after correction for the nonlinear response typed by a typewriter (IBM).

### RESULTS

The response of Multiref 901 was found independent of molecular weight of dextran in the investigated range  $M_w = 2 \times 10^5$ – $2.4 \times 10^6$ .

The nonlinear response at sensitivity 100 is illustrated in Figure 6, where correction according to Equation 28 yields the expected linear relationship.

The experiment showing the influence of sample absorbance on the instrumental response is summarized in Table I. It

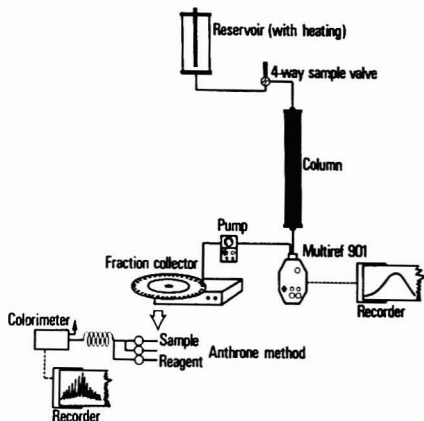


Figure 5. Experimental assembly for comparing the interferometric and chemical concentration analysis of dextran in column effluents

can be concluded that the magnitude of the relative error from an absorbing sample solution is accurately expressed by Equation 20 and that an absorbance of 0.001 causes a relative error of roughly 1% on sensitivity 100.

The comparison between the interferometric and chemical assay of dextran in column effluent is illustrated in Figure 7. Here the interferometric elution curve was quantified by relating the numerical mean height of the curve section corresponding to each fraction with the values obtained by the anthrone method. The correlation coefficient is 0.9991 and the residual standard deviation corresponding to 4  $\mu\text{g mL}^{-1}$  dextran can mainly be attributed to the known random error in the method for chemical analysis of dextran. From the slope, 0.9026, the refractive index increment of dextran can be calculated as:

$$\frac{dn}{dc} = \frac{dn}{dx} \times \frac{dx}{dc} \times \frac{1}{a} = \frac{50 \times 10^{-6}}{100} \times 0.9026 \times \frac{1}{2.954} = 0.1528 \text{ cm}^3 \text{ g}^{-1} \quad (29)$$

where  $x$  = chart reading and  $a$  = dilution factor. This is in agreement with earlier reported values of  $dn/dc$  for dextran in aqueous solutions at 546 nm, e.g., 0.154  $\text{cm}^3 \text{ g}^{-1}$  (22) and 0.1498  $\pm 0.0003 \text{ cm}^3 \text{ g}^{-1}$  (25).

The two methods agreed also when a more complicated mixture of dextrans ( $M_w = 516000 + 14700 + 2030$ ) was analyzed. Figure 8 shows the interferometric elution curve



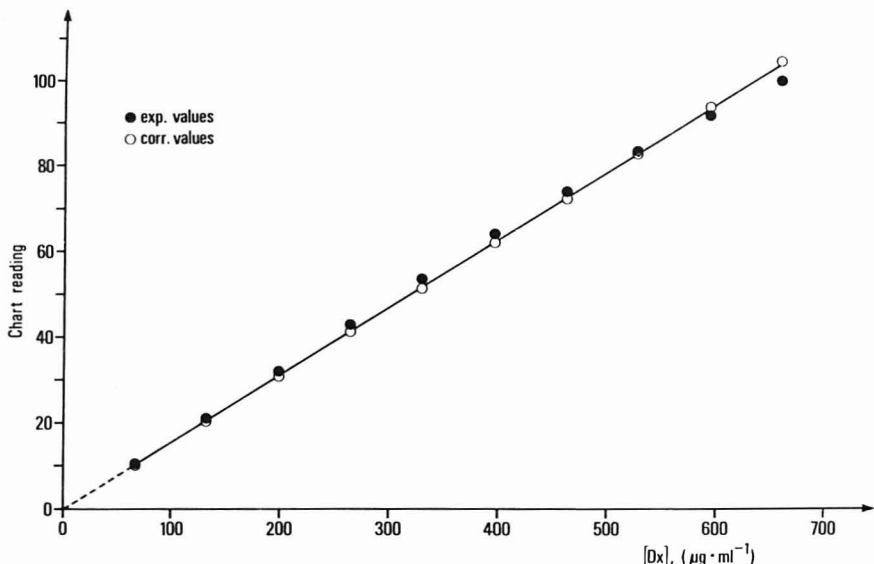


Figure 6. Nonlinear response of Multiref 901 at sensitivity 100. (●) = experimental values, (O) = values corrected according to Equation 28

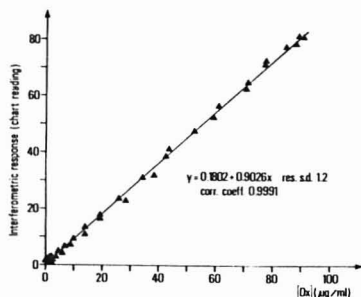


Figure 7. Correlation of corrected interferometric response and content of dextran according to the anthrone method

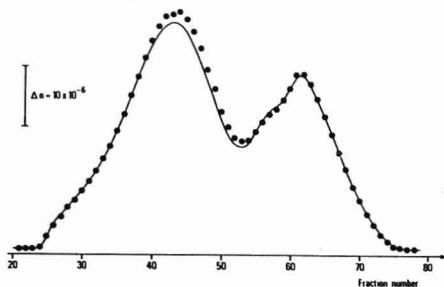


Figure 8. Interferometric chromatogram of dextran mixture ( $M_w = 516\,000 + 14\,700 + 2030$ ). (●) = chart reading corresponding to content of dextran according to the anthrone method (Column: K 16/40) and corresponding values from the collected fractions as calculated from the anthrone analyses and the value of  $dn/dc$

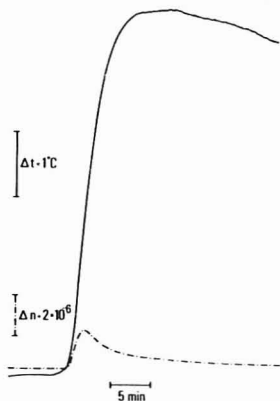


Figure 9. Effect of increase in temperature of sample solution, (—) on detector baseline, (---) at sensitivity 20

given by Ref. 25. Computations from such a run, utilizing equipment described elsewhere (5), gave  $M_w = 286\,000$  and  $M_n = 7\,200$  as calculated from the interferometric curve and  $M_w = 285\,000$  and  $M_n = 7900$  as calculated from the anthrone analysis.

## DISCUSSION

When soft gels are used for molecular weight distribution analysis, the flow rates used are often very low as compared to those used in GPC. Consequently, the time of analysis is rather long and this creates special demands on the baseline stability of the detector. Furthermore, when the samples being analyzed are heterogeneous giving broad peaks, detector sensitivity normally within the range  $20\text{--}50 \times 10^{-6}$  (RIU for full scale) is necessary. These are, besides the nonspecificity,

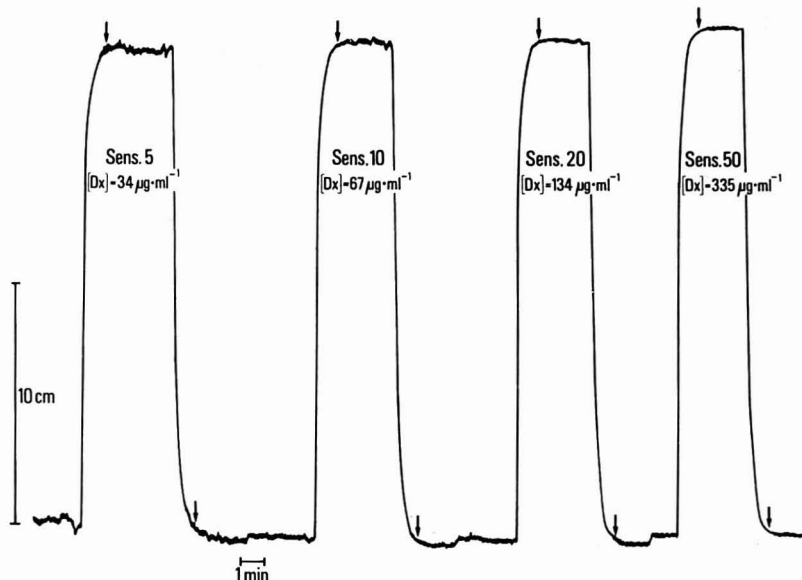


Figure 10. Use of Multiref 901 as a detector of discrete samples of dextran in distilled water

the major drawbacks of the methods based upon refractive index. These difficulties can, however, be overcome by decreasing the time of analysis employing a column packing which allows high flow rates, by increasing the sample concentration, or by working with an instrument especially designed to meet high demands. The advantages of a physical detection are the continuous information obtained from the on-line determination, the elimination of reagent costs and that the entire procedure can easily be automated. A step in this direction has been taken in this laboratory by introducing a motor valve (Labotron 002 540, Kontron AB), governed by a homemade electronic device, for automatic sample application. In this way, it is possible to apply four consecutive samples at present sample and eluting times (3 minutes and 6 hours, respectively). The curves obtained are quantified as earlier but the results are punched on a tape and evaluated by a data equipment for which the software has been elaborated earlier (5). The governing and data sampling can also be accomplished by a desk calculator, thus making the system completely automatic. The need for baseline stability resulted in that the manufacturer improved the instrument during this work to give a baseline drift (at static conditions) of less than  $10^{-7}$  per one degree change of the ambient temperature (providing that a high performance circulating water bath is used for thermostating the instrument) (18). This instrument model is called Multiref 902.

During operation, however, the ambient temperature not only affects the electronics but also the temperature of the column effluent. The efficiency of the heat exchanger preceding the cell was therefore tested by increasing the temperature of the sample solution (while the reference solution was trapped) and registering the variance of the baseline. The temperature of the sample solution was continuously measured at the sample inlet with a thermistor (YSI 410) coupled to a telethermometer (YSI 42 SC). As shown in Figure 9, the instrument seems to respond, not to the absolute temperature but to the temperature increment. The positive deflection

is however surprising, bearing in mind that  $dn/dT \approx -1 \times 10^{-4}$  per  $^{\circ}\text{C}$  (27), thus implying that some other (temperature related) influence is responsible for the effect. For slow temperature changes, corresponding to  $5^{\circ}$  per hour, no deflection of the baseline was found at sensitivity 20.

The arrangement of continuous detection of column effluents obviously requires one detector per column. In this investigation, the Multiref 901 was used also as a detector for discrete samples. This works well for samples containing dextran and water only (Figure 10) but when analyzing samples collected from the column effluent, the salt content of the eluate makes evaporation from the samples a critical factor.

#### ACKNOWLEDGMENT

The author express gratitude to Bengt Nygård and Kirsti Granath for very helpful discussions and comments in the preparation of this manuscript. The fruitful discussions with Leon Carlson are gratefully acknowledged. The author thanks Adolf Berggren and Rune Andersson for placing laboratory facilities at his disposal.

#### LITERATURE CITED

- (1) A. Jeanes, "Encyclopedia of Polymer Science and Technology", Vol. 4, H. F. Mark, N. G. Gaylord and N. M. Bikales, Ed., J. Wiley & Sons, New York, N.Y., 1966, p. 805.
- (2) W. Appel, *Med. Klin.*, **66**, 484 (1971).
- (3) G. Aronson and K. Granath, *Clin. Chim. Acta*, **37**, 309 (1972).
- (4) A. M. Basow and K. H. Ebert, *Infusionstherapie*, **2**, 261 (1975).
- (5) G. Nilsson and K. Nilsson, *J. Chromatogr.*, **101**, 137 (1974).
- (6) M. John, G. Trénel, and H. Dellweg, *J. Chromatogr.*, **42**, 476 (1969).
- (7) S. A. Barker, B. W. Hatt, and P. J. Somers, *Carbohydr. Res.*, **11**, 355 (1969).
- (8) Z. Dische, "Methods of Biochemical Analysis", Vol. 2, D. Gluck, Ed., Interscience, New York, N.Y., 1955, p. 319.
- (9) M. Dubois, K. A. Gilles, J. K. Hamilton, P. A. Rebers, and F. Smith, *Anal. Chem.*, **28**, 350 (1956).
- (10) T. A. Scott, Jr., and E. H. Melvin, *Anal. Chem.*, **25**, 1656 (1953).
- (11) J. R. Bart, *Anal. Biochem.*, **9**, 293 (1964).
- (12) A. J. Hale, "The Interference Microscope in Biological Research", E&S Livingstone LTD, Edinburgh, 1958, p. 82.
- (13) A. L. Spatarico and G. L. Beyer, *J. Appl. Polym. Sci.*, **19**, 2933 (1975).
- (14) H. Pitz, *Anaesthesist*, **24**, 500 (1975).

- (15) "Multitel 901, Instruction Manual", Optilab AB, Box 138, S-162 12 Vällingby 1, Sweden.
- (16) F. Candau, J. Francois and H. Benoit, *Polymer*, **15**, 626 (1974).
- (17) L. Carlson, *Histochemie*, **21**, 289 (1970).
- (18) L. Carlson, Optilab AB, Sweden, private communication, 1976.
- (19) F. S. Crawford Jr., "Waves", Berkeley Physics Course, Vol. 3, McGraw-Hill, New York, N.Y., 1968, pp 394-436.
- (20) W. Nebe, "Comprehensive Analytical Chemistry", Vol. 8, G. Svehla, Ed., Elsevier, Amsterdam, 1977, p 423.
- (21) I. Brandrup and E. H. Immergut, "Polymer Handbook", Interscience, New York, N.Y., 1966, p IV-302.
- (22) F. R. Sentil, N. N. Hellman, N. H. Ludwig, G. E. Babcock, R. Tobin, C. A. Glass, and B. L. Lamberts, *J. Polym. Sci.*, **17**, 527 (1955).
- (23) C. F. Snyder, H. S. Isbell, M. R. Dryden, and N. B. Holt, *J. Res. Natl. Bur. Stand.*, **53**, 3 (1954), RP 2525.

- (24) I. Brandrup and E. H. Immergut, "Polymer Handbook", Wiley-Interscience, New York, N.Y., 1975, p VI-47.
- (25) L.-O. Sundelöf and P. H. Norberg, unpublished work, Institute of Physical Chemistry, Uppsala, Sweden, 1964. (See also P. H. Norberg and L.-O. Sundelöf, *Makromol. Chem.*, **77**, 77 (1964).)
- (26) F. Daniels and R. A. Albery, "Physical Chemistry", J. Wiley & Sons Inc., New York, N.Y., 1967, p 690.
- (27) I. M. Kolthoff, E. B. Sandell, E. J. Meehan, and S. Bruckenstein, "Quantitative Chemical Analysis", Macmillan Company, London, 1969, p 1007.

RECEIVED for review September 12, 1977. Accepted December 1, 1977. The author is indebted to Pharmacia AB for their support of this work.

## X-ray Photoelectron Spectroscopy of Alkylamine-Silanes Bound to Metal Oxide Electrodes

P. R. Moses, Larry M. Wier,<sup>1</sup> John C. Lennox,<sup>2</sup> H. O. Finklea, J. R. Lenhard, and Royce W. Murray\*

Kenan Laboratories of Chemistry, University of North Carolina, Chapel Hill, North Carolina 27514

ESCA results are presented for  $\text{SnO}_2$ ,  $\text{RuO}_2$ ,  $\text{TiO}_2$ , and  $\text{Pt/PtO}$  oxide electrodes silanized with trialkoxyalkylamine-silanes. Observations include effects of reaction conditions, assay of the fraction of amine-like surface nitrogen, assay of N/Si surface atom ratios, O 1s spectra, and fluoride dopant depth profile in  $\text{SnO}_2$ . The silanized surfaces are amine-like but also exhibit other chemical features. The implications of various alkylamine-silane surface structures on electrochemical applications are discussed.

Trialkoxyalkylamine-silanes react with the surfaces of several metal oxides which are useful as electrodes in electrochemical experiments. These include highly doped  $\text{SnO}_2$  (1),  $\text{RuO}_2$  (2), and "PtO" electrochemically formed on Pt metal (Pt/PtO electrode) (3). Carbon electrodes also react with organosilanes (4). Binding of the alkylamine-silanes to these surfaces is a first step toward immobilizing various reagents on the chemically modified electrodes. Immobilization of several reversibly reduced redox reagents via amide bond formation on alkylamine-silanized  $\text{RuO}_2$ , Pt/PtO, and  $\text{SnO}_2$  electrodes has been described (2, 3, 5). Electron transfer reactions between immobilized redox reagents and the electrode surface may be sensitive to the connecting alkylamine-silane layer's structure, composition, and stereochemistry. We report here a number of experiments, principally using ESCA (Electron Spectroscopy for Chemical Analysis), directed at these aspects of the metal oxide/alkylamine-silane interface.

Our (1, 6) and others' (7) previous pictures of silanized metal oxide electrode surfaces were simplified versions of interfaces which are more complex in a variety of ways. The present study aims at furthering our understanding of the structure and composition of the metal oxide/alkylamine-silane interface. Parts of a model have been discussed (5, 8). The trialkoxyalkylamine-silanes employed are 3-(2-aminoethyl-

amino)propyltrimethoxysilane (*en* silane) and 3-amino-propyltriethoxysilane (*PrNH<sub>2</sub>* silane), and the metal oxide electrodes are  $\text{SnO}_2$ ,  $\text{RuO}_2$ ,  $\text{TiO}_2$ , and Pt/PtO. Continuing study of the alkylamine-silane and other silanized interfaces will doubtless in the future evoke additional understandings. In particular, we note that the four metal oxide surfaces have not been subjected with equal thoroughness to all different types of experiments discussed. In many respects the four metal oxides appear to behave similarly, but some intrinsic differences beyond those noted probably exist. Presumption of general similarity must be regarded for the present as a crude approximation.

The observations fall into four major categories: (i) effects of reaction conditions, (ii) assay of the fraction of surface nitrogen which reacts in a normal, "amine-like" manner, (iii) assay of bound silane composition through N/Si atom ratios, and (iv) O 1s ESCA spectra of the silanized surfaces. We also describe a depth profile of fluoride dopant in  $\text{SnO}_2$  electrodes, and a lack of success in achieving useful amidizations of alkylamine-silanized carbon electrodes (4).

Alkylamine-silanes are widely employed for the chemical modification of various silica and alumina surfaces used in bonded phase liquid chromatography (9-11), affinity chromatography (12), trace metal analysis (13, 14), immobilization of transition metal catalysts (15), and in adhesion technology (16), among others. While we have carried out few experiments on nonconducting oxides, our model appears consistent with what is known about alkylamine-silanized silica and alumina, and adds by inference some additional features.

### EXPERIMENTAL

**Metal Oxide Electrodes.**  $\text{TiO}_2$  was prepared in polycrystalline thin film form by chemical vapor deposition according to Bard (17) or by simply heating Ti metal in a Bunsen burner flame.  $\text{SnO}_2$  films on glass (commercially prepared) (1), spray-atomized  $\text{RuO}_2$  films on Ti (2) and Pt/PtO electrodes (3) were obtained as previously described.

**Chemicals.** The  $\text{PrNH}_2$  silane (3-amino-propyltriethoxysilane) and *en* silane (3-(2-aminoethylamino)propyltrimethoxysilane) (PCR Chemical Co.), earlier used as received, are now routinely vacuum distilled upon ESCA evidence of polymer contaminant. Nitrobenzoyl and fluorobenzoyl chlorides were from Aldrich. Benzene was dried over sodium.

<sup>1</sup>Present address, Department of Chemistry, Union College, Schenectady, N.Y. 12308.

<sup>2</sup>Present address, Department of Chemistry, University of Arkansas, Fayetteville, Ark. 72701.

ESCA. X-ray (Mg anode) photoelectron spectra were obtained with a DuPont 650B electron spectrometer (1). In later experiments the data acquisition and manipulation features of this instrument were modified with a microprocessor system to be described elsewhere (18). Typical vacuum level was  $1 \times 10^{-7}$  Torr. A C 1s contaminant line was reproducibly present. B.E. of other elements are referenced to the C 1s line taken as 285.0 eV. Sputtering experiments were typically carried out with 1.5 keV and 35 mA  $\text{Ar}^+$  beam current. As samples for electron spectroscopy were necessarily exposed to the atmosphere during the synthetic preparation, care was taken to avoid contaminant sources particularly of Si and N, and to check for these elements with control samples. Si remained a problem with  $\text{SnO}_2$  electrodes as discussed in the text. Possibly excepting Pt/PtO, the metal oxides do not tend to adsorb alkylamines (probable silane reagent contaminant) from benzene control solutions.

**Silanization Reaction Conditions.** Procedures identified previously as reaction Methods A, C, and D (1, 6) are: Method A involves prolonged reflux of the metal oxide electrode in a 10% silane solution in benzene or xylene. Method C carries out the reaction in a glove box (Vacuum Atmospheres) or in syringe cap vials in 1–5% silane solutions in benzene at room temperature for 5–60 min. Method D uses typically 1% silane in 6 °C benzene for periods ranging from 10 s to 10 min. Silanized samples are washed very thoroughly with dry benzene before removal from the reaction flask, to avoid contact of any silane-containing solvent with atmospheric moisture, and then with methanol in many cases. An additional silanization procedure (Method E) has undergone preliminary tests; in this method the sample is reacted with silane vapor in an apparatus maintaining the sample at ca. 60 °C for 12 h. We have little ESCA data on samples prepared by Method E, but silanization does occur on  $\text{RuO}_2$ , and amidization with 3,5-dinitrobenzoyl chloride yields the expected surface electrochemistry (2).

**Amidization Conditions.** Reaction of 3,5-dinitrobenzoyl chloride with silanized metal oxide samples has been carried out using a range of conditions. Typical solution concentration is 0.05 M in  $\text{CHCl}_3$  solvent, the reaction time ranges from 10–60 min, and temperature from room to ca. 60 °C. In some cases a catalyst base such as 2,6-lutidine or 1,8-dimethylaminonaphthalene is added, but care must be taken in the washing procedure that this nitrogen-containing material is adequately washed from the sample. The latter base, for instance, adsorbs rather strongly on  $\text{RuO}_2$  surfaces, and its use there is undesirable for experiments involving N 1s ESCA spectra.

## RESULTS

**Effects of Reaction Conditions.** Reaction conditions for metal oxide silanizations include the (i) pretreatment of the metal oxide surface, (ii) conditions under which the silane is contacted with the surface and excess rinsed from the surface, and (iii) conditions under which the freshly silanized surface is handled en route to subsequent measurements or chemical reactions with the alkylamine moiety. We will discuss each of these in turn.

**Pretreatment.** Pretreatment is known to be important for chemical modification of  $\text{SiO}_2$  surfaces. At room temperature only ca. 50% of the surface oxygens are thought to achieve a hydroxylated ( $-\text{SiOH}$ ) state (19, 20). Except under highly acidic, basic, or dehydrating conditions, infrared measurements on  $\text{TiO}_2$  (21), and  $\text{SnO}_2$  (22) powders indicate that the surface lattice oxygens are predominantly in a hydroxylated ( $-\text{MOH}$ ) state. Strongly dehydrating conditions are required to reduce O–H stretching intensities with generation, presumably of oxygen-bridged M–O–M sites. The  $-\text{MOH}$  site should constitute the reactive site for the alkoxysilane groups. Thus it is not greatly surprising that no influence of pretreatment, under conditions ranging from hot concentrated HCl to 450 °C drying followed by re-exposure to air, was discerned in previous (1) and ensuing studies of  $\text{SnO}_2$ .

Pretreatment conditions employed thus far for  $\text{RuO}_2$  and  $\text{TiO}_2$  films have been governed by considerations of producing

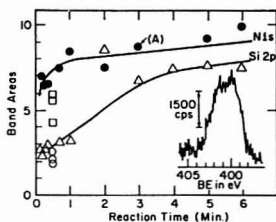


Figure 1. Reaction kinetics of *en* silane in 6 °C benzene with  $\text{SnO}_2$ . Reaction quenched with benzene rinse. (—●—)  $I_{\text{N}1s}$  for 1% silane solution, (—△—)  $I_{\text{Si}2p}$  for 0.1% solution, (O) for 0.001% solution; (—△—)  $I_{\text{Si}2p}$  for 1% solution. N 1s spectral inset for data point "A"

adherent and properly conducting or doped materials in the film preparation process itself. Exposure to laboratory air is permitted before silanization. These surfaces are reactive toward the silane reagents and we have no data suggesting that they are not extensively hydroxylated.

Pretreatment of the approximate monolayer of oxide on Pt/PtO electrodes has been restricted to low temperature oven drying (50 °C) to protect the layer. The silanization reaction is sensitive to the conditions of the electrochemical preparation of the oxide layer (4).

Overall, while detailed investigation of pretreatment effects is incomplete, we have not yet, except for perhaps Pt/PtO, discerned pretreatment to be as important a reaction condition variable as those described below.

**Silanization Reaction Conditions.** The significance of anhydrous reaction conditions for the silanization process has been emphasized (1). Growth of three-dimensional siloxane polymer can be substantially avoided under anhydrous conditions (6). Of the various reaction methods employed (see Experimental), the earliest (Method A) (1) is unnecessarily forcing for the metal oxides considered here. The room temperature Method C is convenient and is thought to yield a limiting coverage as "monolayer" to distinguish it from "multilayer" (as with siloxane polymer growth). We emphasize that this is a reaction site-limited coverage and may not be the same as a coverage limited by the molecular dimension of the alkylamine-silane. Molecular dimension-limited coverages are those typical in Langmuir-Blodgett experiments (23).

The very mild Method D was originally investigated as a strategy to achieve coverages less than the reaction site-limited value. Figure 1 shows N 1s and Si 2p ESCA band intensities on  $\text{SnO}_2$  surfaces reacted with 6 °C, 1% *en* silane solutions for various times. The time dependence of the two elements is different; we believe the N 1s data represent alkylamine-silane coverage more accurately. The Si 2p data will be discussed later. The N 1s band is a doublet due to free base and protonated amine ( $\text{N}$  and  $\text{NH}^+$ ) forms (1); relative  $\text{N}/\text{NH}^+$  intensity is not a function of reaction time. The Figure 1 data are total N 1s intensity, which rises quite rapidly to a gradually sloping plateau. For a 3–6 min reaction time, the N 1s intensity achieved is within 20% of the average intensity (1) for *en* silane reacted successfully with  $\text{SnO}_2$  using Method A.

The N 1s data of Figure 1 show that achieving less than limiting coverages of *en* silane on  $\text{SnO}_2$  using 1% silane solutions with Method D requires inconveniently short reaction times. Lowering the *en* silane concentration can be an effective tactic for a 30-s reaction period, as illustrated by Figure 1 for 0.1% and 0.001% solutions. The latter corresponds to about 25% coverage. The reproducibility of such low coverage experiments is not very good, and comparable experiments have not yet been conducted on the other metal oxides.

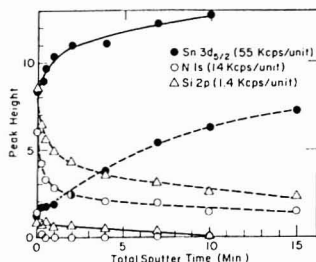


Figure 2. 1.5 keV  $\text{Ar}^+$  sputter of  $\text{SnO}_2/\text{en}$  electrodes prepared by Method D (—) and by a Method A experiment in which polymer formed (----)

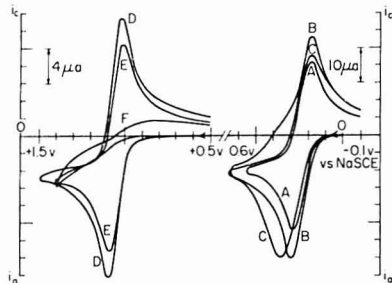


Figure 3. Cyclic voltammograms on  $\text{SnO}_2$  (Curves A, D),  $\text{SnO}_2/\text{en}$  prepared with Method D (Curves B, E), and  $\text{SnO}_2/\text{en}$  prepared with Method A (Curves C, F). Same electrode preparation as used for data of Figure 2 but different specimens. Curves A–C: ca. 2 mM ferrocyanide in 0.1 M KCl and pH 2.4, 0.5 M glycine buffer. 200 mV/s. Curves D–F: 1 mM  $\text{Ru}(\text{bpy})_3\text{ClO}_4$  in 0.18 M  $\text{H}_2\text{SO}_4$ , 0.1 M KCl. 200 mV/s

Electrodes with sub-monolayer silane coverage may be useful for study of steric aspects of redox couples (2, 24) immobilized on electrodes using alkylamine-silane chemistry.

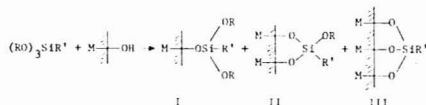
The incidence of poor electrode preparations in which siloxane polymer-forming misadventures occur is much higher with Method A than the milder Methods C and D. For example, in a comparison preparation of  $\text{SnO}_2/\text{en}$  electrodes using Methods A and D, the Method A electrode showed evidence of polymer formation by greatly reduced  $\text{Sn } 3d_{5/2}$  band intensity ( $I_{\text{silane}}/I_{\text{unreact}} = 0.09$  vs. 0.68 on the Method D electrode) and prolonged N 1s and Si 2p signals upon sputtering, as shown in Figure 2. On method D (and C) electrodes, N 1s disappears after a few seconds of sputtering, and Si 2p a little more slowly. Both bands were persistent on the polymer-coated Method A electrode, and Sn  $3d_{5/2}$  and O 1s intensity remained low after several minutes of erosion.

We presumed earlier (1) that electrochemical properties would be quite sensitive to siloxane polymer formation. Figure 3 compares cyclic voltammetry of aqueous ferrocyanide and  $\text{Ru}(\text{bpy})_3^{2+}$  on native  $\text{SnO}_2$  and on the Method A and D  $\text{SnO}_2/\text{en}$ . The reversibility of both electrode reactions on native  $\text{SnO}_2$  and Method D- $\text{SnO}_2/\text{en}$  is quite similar. The oxidation of  $\text{Ru}(\text{bpy})_3^{2+}$  on the polymer-bearing Method A- $\text{SnO}_2/\text{en}$  is poorly defined, very irreversible, with small currents, but the ferrocyanide reaction is only mildly irreversible (Curve C). The negatively charged  $\text{Fe}(\text{CN})_6^{4-}$  apparently readily penetrates the siloxane film, which at the solution pH employed should bear positive ammonium sites.  $\text{Ru}(\text{bpy})_3^{2+}$  tends to be excluded because of either its charge or larger size. This comparison shows that electrochemical

properties are not necessarily good criteria to distinguish polymer-coated from monolayer-coated electrodes.

Gleria and Memming (25) have reported abnormally small, nondiffusion controlled currents for aqueous  $\text{Ru}(\text{bpy})_3^{2+}$  oxidation at highly doped  $\text{SnO}_2$  in aqueous acid, interpreting this as  $\text{Ru}(\text{bpy})_3^{2+}$  adsorption on the  $\text{SnO}_2$  surface. In our experiments, we saw no evidence for adsorption by ESCA of  $\text{Ru}(\text{bpy})_3^{2+}$ -exposed  $\text{SnO}_2$ . Cyclic voltammetric  $i_p/v^{1/2}$  of aqueous  $\text{Ru}(\text{bpy})_3^{2+}$  solutions is constant over 5–500 mV/s sweep rate. The diffusion coefficient calculated from the  $i_p/v^{1/2}$  data has a normal value ( $6 \times 10^{-6} \text{ cm}^2/\text{s}$ ).

**Post-Silanization Treatment.** If the reaction of the three alkoxy silane functions present on  $\text{PrNH}_2$  and en silanes with the metal oxide surface is incomplete, "dangling" alkoxy silane groups may exist on the electrode surface after silanization is terminated. The fate of these dangling groups, as determined by handling of the silanized electrode, may influence the behavior of the alkylamine-silane/metal oxide interface in subsequent measurements or reactions of the amine sites. The reaction of the trialkoxyalkylamine-silane with hydroxylated metal oxide surface can be written



where Structures I, II, and III represent different degrees of coupling and R' is the alkylamine or some other group. Published descriptions of the relative proportions of these structures are both sparse and generally nonquantitative, as analysis for them is a difficult problem. In reactions of chloromethylsilanes with silica surfaces, Structure I is often presumed without justification other than probable bond strain in Structure III plus incomplete  $\text{SiO}_2$  surface hydroxylation. Residual Si-Cl has been detected after silica reaction with dimethyldichlorosilane (20). An average of two Al–O–Si bonds per silane (e.g., Structure II) was reported (26) after reaction of a trichlorosilane with alumina. After reaction of dimethyldichlorosilane with tin(IV) oxide gel, Harrison and Thornton (27) showed that the silanized material reacts with acetic acid vapor to yield infrared bands assignable to a silyl ester, which was hydrolyzed slowly by water with appearance of spectral features attributed to –SiOH groups. Examination of  $\text{SnO}_2$  films by inelastic tunneling spectrometry following reaction with triethoxyvinylsilane has produced evidence for dangling ethoxysilane groups (28). Similarly, Raman bands assigned to Si–Cl have been observed on  $\text{SnO}_2$  following reaction with 3-chloropropyltrichlorosilane (29). Thus some evidence exists for Structures I and II and for dangling reactive groups on silanized surfaces, but none for Structure III.

Accordingly, it seems reasonable to assume in silanizations of metal oxide electrodes with trialkoxyalkylamine-silanes that the surface products contain, or perhaps are predominantly, Structures I and II. Post-silanization handling of these surfaces can be in three modes. Assuming for the discussion Structure II, the post-silanization environment of the surface can be maintained in an anhydrous and aprotic state, to attempt to preserve the dangling alkoxy silane. Alternatively, the surface can be deliberately exposed to moisture, hydrolyzing the alkoxy silane group to an –SiOH function as in Structure IV



Thirdly, thermal curing can be used to attempt two-di-



Table I. Assay of Active Amine

## Acid-Base Assay

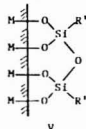
Expt	Electrode <sup>a</sup>	Treatment <sup>b</sup>	$I_{N\ 1s(400)}/I_{N\ 1s(401.5)}$ , %	Active amine <sup>d</sup> , %
I-1	SnO <sub>2</sub> /PrNH <sub>2</sub>	pH 10 wash 0.05 M HCl wash	76/24 58/42	16
I-2	SnO <sub>2</sub> /en	pH 10 wash 0.05 M HCl wash	72/28 41/59	31
I-3	RuO <sub>2</sub> /en	pH 10 wash 0.05 M HCl wash	61/37 39/63	26

## Amidization Assay

Expt	Electrode <sup>a</sup>	Treatment <sup>b</sup>	$I_{N\ 1s(400.5)}/I_{N\ 1s(Amine + amide)}$	$I_{F\ 1s(687)}/I_{F\ 1s(Amine + amide)}$	Active amine <sup>e</sup> , %
I-4	SnO <sub>2</sub> /PrNH <sub>2</sub>	4-(NO <sub>2</sub> )PhCOCl	0.20, 0.27		20, 27
I-5	SnO <sub>2</sub> /PrNH <sub>2</sub>	3,5-(NO <sub>2</sub> ) <sub>2</sub> PhCOCl	0.13		6
I-6	SnO <sub>2</sub> /PrNH <sub>2</sub>	4-FPhCOCl		0.53	22
I-7	SnO <sub>2</sub> /en	4-(NO <sub>2</sub> )PhCOCl	0.29		29
I-8	SnO <sub>2</sub> /en	3,5-(NO <sub>2</sub> ) <sub>2</sub> PhCOCl	0.96, 0.98, 1.00		48, 49, 50
I-9	SnO <sub>2</sub> /en	4-FPhCOCl		1.84	77
I-10	RuO <sub>2</sub> /PrNH <sub>2</sub> <sup>j</sup>	3,5-(NO <sub>2</sub> ) <sub>2</sub> PhCOOH <sup>i</sup>	1.48		74
I-11	RuO <sub>2</sub> /PrNH <sub>2</sub> <sup>j</sup>	3,5-(NO <sub>2</sub> ) <sub>2</sub> PhCOCl	0.42, 0.27, 0.33, 0.30		21, 13, 16, 15
I-11a	RuO <sub>2</sub> /PrNH <sub>2</sub> <sup>j</sup>	4-(NO <sub>2</sub> )PhCOCl	0.20		20
I-12	RuO <sub>2</sub> /en <sup>h</sup>	3,5-(NO <sub>2</sub> ) <sub>2</sub> PhCOCl	0.49, 0.53, 0.72, 1.35		24, 25, 36, 63
I-13	TiO <sub>2</sub> /en	3,5-(NO <sub>2</sub> ) <sub>2</sub> PhCOOH <sup>i</sup>	0.24		12
I-13a	TiO <sub>2</sub> /en	3-(NO <sub>2</sub> )PhCH <sub>2</sub> COOH <sup>i</sup>	0.21		21
I-14	Pt/PtO/en	3,5-(NO <sub>2</sub> ) <sub>2</sub> PhCOCl	0.45		(23) <sup>j</sup>
I-15	Pt/PtO/en	3,5-(NO <sub>2</sub> ) <sub>2</sub> PhCOOH <sup>i</sup>	0.45, 0.68		(23, 34) <sup>j</sup>

<sup>a</sup> Electrode/PrNH<sub>2</sub> and electrode/en denote surfaces reacted using Method C with 3-aminopropyltriethoxysilane and 3-(2-aminoethylamino)propyltrimethoxysilane, respectively. <sup>b</sup> ESCA data comparing acid and base treatment are on separate specimens to avoid possible beam damage effects. <sup>c</sup> Intensities are in % of total amine band area; actual B.E. in alkylamine-silane doublet are 399.3 eV and 400.6 eV for en and 400.3 eV and 401.9 eV for PrNH<sub>2</sub>. <sup>d</sup> Percentage of total nitrogen intensity shifted to higher B.E. by acid wash. <sup>e</sup> Percentage of total alkylamine-silane N 1s band (Amine + Amide) which yields tagged derivative. Nitro derivatives normalized according to number of nitro sites; fluoro derivative normalized with cross-section (30) ratio 0.42. <sup>f</sup> Data taken from figure in ref. 7, silanization reaction Method A. <sup>g</sup> Silanization Method D used. <sup>h</sup> Thermal curing post-silanization treatment. <sup>i</sup> Amidization using DCC coupling procedure. <sup>j</sup> Anhydrous post-silanization handling, reactions conducted in glove box. <sup>k</sup> Silanization Method E used. <sup>l</sup> See text.

mensional cross-linking of the surface, expelling H<sub>2</sub>O and/or ROH to yield siloxane bridges as in Structure V.



Consequences of these three modes of post-silanization handling have been observed in several experiments. RuO<sub>2</sub> and Pt/PtO surfaces after silanization with en silane react with nitrobenzoyl chlorides; the resulting surfaces exhibit electrochemical surface waves characteristic of the nitroaromatic moiety (2, 3). Differences in the electrochemical behavior were noted on the Pt/PtO surfaces depending on whether the freshly prepared Pt/PtO/en surface was exposed to moisture or not prior to the amidization step (3). This possibly is associated with reactivity of dangling -SiOH groups in the water-exposed samples. An analogous sensitivity of RuO<sub>2</sub>/en surfaces toward moisture was not observed (2) in the electrochemistry of nitroaromatics immobilized on the RuO<sub>2</sub>/en electrodes, which had been thermally cured, and which were thus probably in the less reactive Structure V. Effects of thermal curing are also found in tests of stability of RuO<sub>2</sub>/en surfaces toward hot (ca. 80 °C) water. Freshly silanized RuO<sub>2</sub>/en is stable in a variety of solvents, but a few minutes' exposure to hot water completely strips the alkylamine-silane as evidenced by disappearance of its N 1s spectrum. After curing at 85 °C (in vacuo) for 30 min, 50–60% of the N 1s band survives the hot water test. Involvement of Structure V is implied but not proven by this experiment; whether the hot water degradation is due to -RuOSi- bond

hydrolysis or dissolution of the outermost RuO<sub>2</sub> lattice is not known. In contrast to the result on RuO<sub>2</sub>/en, boiling a SnO<sub>2</sub>/en electrode for 2 h in water produced no alteration in the observed N 1s or Si 2p spectral intensities. Curing effects on SnO<sub>2</sub>/en have not been ascertained, and on Pt/PtO/en thermal curing incurs unacceptable and not further investigated increases in electrochemical background currents. These various observations show that the form of post-silanization handling is an experimental variable which merits detailed attention in electrode preparation.

**Analysis of Alkylamine-Silanized Metal Oxide Surfaces for Active Amine.** Since one intent of alkylamine-silanization is to immobilize amine sites on the metal oxide electrode as reagents for further molecular elaboration of the surface, analysis of the fraction of immobilized nitrogen which actually will react as amine is a relevant measurement. Using ESCA N 1s data, we have measured active amine as protonatable base, and as amide-forming functionality.

**Acid-Base Reactions of Immobilized Alkylamine-Silane.** The N 1s band observed on SnO<sub>2</sub> electrodes immediately after reaction with alkylamine-silane (Figure 1) and alkylpyridine-silane (1) is a doublet which from the observed binding energies and separation (400.3 and 401.9 eV for PrNH<sub>2</sub> and 399.3 and 400.6 eV for en silane) is reasonably interpreted as a mixture of free and protonated amine. Exposure to water or dilute base diminishes but does not eliminate the higher B.E. band (unexpected since a protonated alkylammonium site attached to the metal oxide surface only through the alkyl chain should be deprotonated by this treatment). Also, exposure to strong acid (0.05 M HCl) only partially converts the free base band into the higher B.E. form. These effects are reversible and occur with little change in total N 1s intensity.

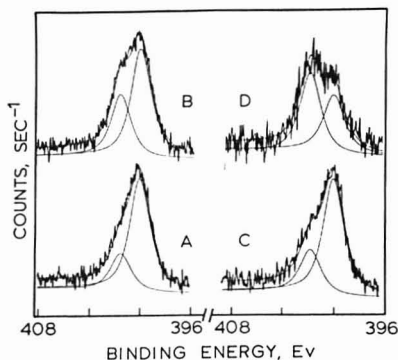


Figure 4. N 1s spectra for  $\text{SnO}_2/\text{PrNH}_2$  (Curves A, B) and  $\text{SnO}_2/\text{en}$  (Curves C, D) electrodes exposed to pH 10 aqueous base (lower) and to 0.05 M HCl (upper) resolved into protonated and free base spectral components. Different samples used for each experiment.

Figure 4 shows the N 1s doublet for  $\text{SnO}_2/\text{PrNH}_2$  and  $\text{SnO}_2/\text{en}$  surfaces exposed to aqueous acid and base, and Table I gives areas of the resolved bands (Experiments 1, 2). Taking the relative change in intensity of the higher binding energy band as a measure of active amine, the results indicate that only a small portion of the nitrogen on the  $\text{PrNH}_2$  silane surface is active base. A larger fraction is active on the  $\text{SnO}_2/\text{en}$  surface. On both surfaces a significant fraction of the nitrogen retains the higher binding energy even upon base wash.  $\text{RuO}_2/\text{en}$  behaves similarly (Experiment 3).

These results suggest three forms of nitrogen on alkylamine-silanized metal oxide: a form with free amine binding energy which resists protonation in acid (designated as [N] form), a form with ammonium binding energy which resists deprotonation (designated as [NH] form), and an active, reversibly protonated form (designated as [N/NH] form). Analysis of the data in this manner is subject to criticism as it neglects "transfer" effects (changes in the alkylamine-silane surface in going from an aqueous acid-base equilibrium to a dry state and thence into the vacuum of the electron spectrometer). For example, amine protonated while in contact with the aqueous acid is possibly deprotonated when dried or placed under vacuum, in which case the determined % [N/NH] form is too low and the actual % [N] form is lower than that measured (or non-existent). The lability of the acid-base reaction is a potential liability in the active amine assay. An active amine analysis in which the amine derivatization is more permanent, such as in an amide, is desirable.

**Amidization of Immobilized Alkylamine-Silane.** Amidization of an  $\text{en}$  or  $\text{PrNH}_2$  alkylamine-silanized surface with an acid chloride or with a carboxylic acid in the presence of a dehydrating agent such as  $N,N'$ -dicyclohexylcarbodiimide (DCC), produces little change in the overall appearance of the alkylamine-silane N 1s doublet. The amide and alkylamine nitrogens have similar binding energies (31). To determine the fraction of amide nitrogen in the unresolved amine + amide band, the amidizing reagent should contain a "tag" atom with distinctive binding energy. For instance, reaction of a  $\text{SnO}_2/\text{PrNH}_2$  surface with 3,5-dinitrobenzoyl chloride yields a nitro N 1s band at 406.5 eV, well resolved from the amine + amide band. The relative intensities of the two bands reflect the extent of amide formation. If the  $\text{SnO}_2/\text{PrNH}_2$  surface consists of 100% active amine, the band area of the nitro band would be  $2 \times$  that of the amine + amide band. A different element can alternatively be used for the tag atom, such as F or S. In this case a relative elemental sensitivity

factor becomes included in the active amine determination, which is thereby somewhat less reliable.

Results of such tag atom amidization assays for active amine are given in Table I. Examples of spectra have been reported previously (2, 3). Shake-up bands as observed for nitroanilines (32) or beam damage effects are not seen in the nitro tag spectra or in a spectrum of authentic *n*-propyl-3,5-dinitrobenzamide, which exhibits a stable nitro/amide N 1s band area ratio of 2/1 as expected.

The experiments on  $\text{SnO}_2$  employ several amide reagents since the initial work was done on this material. On a  $\text{SnO}_2/\text{PrNH}_2$  surface, Experiments 1-4, 5, and 6 show only 6-27% of the surface nitrogen amidized by the indicated reagents, in contrast with  $\text{SnO}_2/\text{en}$  where 50% amidization is obtained using 3,5-dinitrobenzoyl chloride (Experiment 1-8). Note that  $\text{en}$  silane contains two alkylamine functions, so if one assumes that amidization occurs predominantly at the terminal primary nitrogen, Experiment 1-8 results indicate 100% active primary amine for  $\text{en}$  silane as compared to 6-27% for  $\text{PrNH}_2$  silane. While the fraction of amine which is active on both  $\text{en}$  and  $\text{PrNH}_2$  silanized surfaces is actually dependent on experimental variables as discussed below, the key result is that a lower fraction of primary nitrogen undergoes amidization on  $\text{PrNH}_2$ -silanized surfaces.

Incomplete reactivity of surface nitrogen on  $\text{SnO}_2/\text{PrNH}_2$  and  $\text{SnO}_2/\text{en}$  surfaces can be interpreted in terms of hydrogen-bonding of amine, principally that in the  $\gamma$  position on the alkyl chain, to silanol (-SiOH) functions on the parent or neighbor silane which result from hydrolysis of uncoupled silane. (In most of these experiments, no special precautions were taken to maintain anhydrous post-silanization conditions.) Additionally hydrogen bonding could involve unsilanized metal hydroxyl (-MOH) sites. We suggest that the surface structures may be



where  $R = \text{H}$  for  $\text{PrNH}_2$  and  $R = -\text{CH}_2\text{CH}_2\text{NH}_2$  for  $\text{en}$  silane.

There is considerable precedent in previous silanization work conducted under both polymer forming and anhydrous conditions for this explanation of inactive amine. Hydrogen bonding of amine sites in alkylamine-silanes to silanol or other surface hydroxyls has been widely inferred (33-35). Infrared spectra demonstrate the adsorption of ammonia on silanol groups at silica (36). Kahn (37) obtained evidence for liquid crystal orientations at  $\text{PrNH}_2$ -silanized surfaces from which a parallel orientation of the alkylsilane chain, and hence cyclical bonding of the amine, is implied. Anderson et al. (38) observed a doublet N 1s ESCA band on a polymeric  $\text{PrNH}_2$  silane coating on silicon and attributed the higher binding energy nitrogen to ammonium sites caused by presence of silanol functions. The results in Table I and the postulated Structures VI and VII are consistent with this background, and demonstrate methodology for a more quantitative description of hydrogen bonding on alkylamine-silanized surfaces than has been previously accomplished.

Depending on steric and solvation effects, the stability of hydrogen bonded Structures VI and VII may vary throughout the surface population. In an amidization assay for active amine, therefore, the unbonded "normal" amine ([N/NH] form) population may be augmented by reaction of some more weakly bonded Structures VI and VII, in which case the active amine assay is not absolute but becomes an apparent and variable quantity which depends on the amidization reagent and the reaction conditions. There is some indication that this may be a considerable effect. For instance, assay results using the 4-nitrobenzoyl, 3,5-dinitrobenzoyl, and 4-fluoro-

benzoyl chlorides on  $\text{SnO}_2/\text{en}$  surfaces vary widely (Experiments I-7, 8, 9). The active amine assayed by 3,5-dinitrobenzoyl chloride on  $\text{RuO}_2/\text{PrNH}_2$  and  $\text{SnO}_2/\text{PrNH}_2$  is normally low (Experiments 4-6, 11), but one experiment using anhydrous post-silanization and DCC coupling conditions gave a high % active amine assay (Experiment I-10). Results on  $\text{RuO}_2/\text{en}$  surfaces (Experiment I-12) indicate a generally higher % active primary amine but are scattered since a range of 3,5-dinitrobenzoyl chloride reaction conditions was employed. Results on  $\text{Pt}/\text{PtO}/\text{en}$  are probably erroneously low due to interference from adsorbed amine impurity on this particular oxide. Finally, because of interference from direct adsorption of metal ions by the  $\text{SnO}_2$  oxide (1), we are unable to quantitate  $\text{SnO}_2/\text{en}$  reactivity toward metal ion coordination. Whether metal ions are effective in disrupting Structures VI and VII to form *en*-chelates, on these oxides or on silica (13), is a question specifically unanswered by the present data.

The amidization results generally substantiate the acid-base assay in terms of an unreactive amine population. The hydrogen bonded amines of Structures VI and VII represent the nonprotonatable [N] and nondeprotonatable [NH] forms, respectively, which should exhibit a binding energy difference similar to that between free base and protonated amine. The acid-base results for active amine are lower than those obtained by amidization so the acid-base conditions used are either less reactive at opening Structures VI and VII or do so less permanently (e.g., transfer effects).

Thus, binding of alkylamine-silane to  $\text{SnO}_2$  and  $\text{RuO}_2$  is thought to involve cyclical hydrogen-bonded structures whose specific reactivity depends both on silane and the assaying reagent. A larger fraction of amine can be induced to undergo amidization on *en* silane since its terminal primary amine site is less subject to hydrogen-bonding. For this reason the *en* silane is preferred over  $\text{PrNH}_2$  silane when high coverages of immobilized redox couples are sought on chemically modified electrodes (2, 3). Also, in the absence of assays such as above, it is risky to assume that reactivity of a surface immobilized chemical functionality is quantitatively the same as its solution counterpart. Perturbing interactions not present in the solution environment can disturb a quantitative parallel.

**Alkylamine-Silanized Glassy Carbon: Acid-Base Behavior and Unsuccessful Amidization.** Reaction of glassy carbon electrodes with  $\text{PrNH}_2$  and *en* silanes in warm dry benzene for ca. 1 h yields surfaces exhibiting N 1s and Si 2p bands more intense than typical background. These surfaces are stable to a variety of organic solvents and, provided they are first thermally cured, to hot water and dilute aqueous acid and base. However, contrary to our previous expectations (4), neither alkylamine-silanized carbon yields evidence of surface amidization using a variety of reagents at room temperature, including 4-nitrobenzoyl, 4-fluorobenzoic, and 3-bromopropionyl chlorides and 1,1'-ferrocenedicarboxylic acid (DCC procedure). The tag element ESCA band in each attempted amidization was not significantly different from a control (not silanized) electrode. Some loss of amine band intensity was usually noted after reaction. More forcing reaction conditions, e.g., base catalysis or elevated temperatures, resulted in cleavage of silane from the surface. Dithiocarbamate and Schiff base formations were also attempted without success. Alkylamine-silanized glassy carbon does not seem to provide useful coupling chemistry for the preparation of chemically modified carbon electrodes, at least not under monolayer coverage conditions. A different chemical approach is more successful (39).

Alkylamine-silanized glassy carbon does exhibit a protonated/free base amine N 1s doublet (4) similar to that observed on the metal oxide electrodes. Figure 5 illustrates

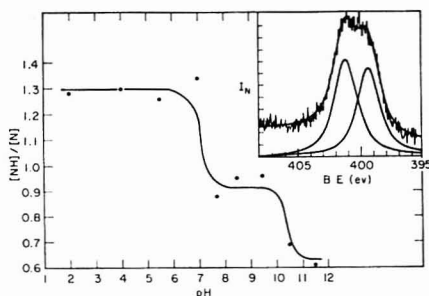


**Figure 5.** Ratio of protonated and free base ( $I_{\text{NH}}/I_{\text{N}}$ ) N 1s intensities on glassy carbon/en electrodes as a function of pH of aqueous buffer to which the surface was exposed. Inset shows resolving of two N 1s components. Different sample used for each pH point

resolution of this doublet. C/en surfaces were exposed to a series of buffer solutions, the surfaces blown dry with an air jet, and the  $I_{\text{NH}}/I_{\text{N}}$  intensity ratio measured. Discontinuities in  $I_{\text{NH}}/I_{\text{N}}$  occur (Figure 5) near the pK values (6.85 and 9.93) (40) of free ethylenediamine. The discontinuities appeared each of several times this experiment was repeated but varied as much as one pK unit. C/PrNH<sub>2</sub> surfaces, in contrast, exhibited no change in the  $I_{\text{NH}}/I_{\text{N}}$  ratio (0.75) over a similar pH range. These results are difficult to interpret cleanly, but could be rationalized in terms of a stable array of surface structures cyclized at the  $\gamma$ -amine site as in Structures VI and VII. The terminal amine of Structure VII in C/en would be more basic than that for Structure VII for the same reason that ordinary ethylenediamine exhibits two different pK values. Thus the titration of Figure 5 would correspond to neutralization of Structures VI and VII. Validity of this tentative model aside, the interesting aspect of Figure 5 is a suggestion that quantitative information on surface acid-base properties may be obtainable using a very primitive solution-to-vacuum transfer. The behavior of the buffer solution as a thin film of it dries on the surface during the transfer may be crucial.

The acid-base behavior of the C/en surface is difficult to reconcile with the lack of success in amidizing the apparent surface amine. It may be that the loss of N 1s intensity upon attempted amidization is associated with cleavage of the active amine form of the *en* silane from the surface under the reaction conditions. In view of this complication, further experiments like that in Figure 5 will focus on different substrates than carbon.

**Analysis of N/Si Surface Atom Ratios.** The structural integrity of alkylamine-silanes immobilized on the metal oxide surface is measurable using N/Si ESCA band intensities (area). Table II gives data. Comparing surfaces prepared by reaction with *en* silane,  $I_{\text{N}}/I_{\text{Si}}$  data differ between the various metal oxides. The  $I_{\text{N}}/I_{\text{Si}}$  ratios tend to be low on  $\text{SnO}_2/\text{en}$  surfaces, and to depend there on silanization reaction conditions.  $I_{\text{N}}/I_{\text{Si}}$  values on  $\text{SnO}_2/\text{en}$  surfaces prepared under the mildest conditions (Experiment II-2, 10 s) are comparable to  $I_{\text{N}}/I_{\text{Si}}$  data on  $\text{RuO}_2/\text{en}$  and  $\text{TiO}_2/\text{en}$  surfaces prepared using Method C (Experiments II-7, 8, 10).  $\text{SnO}_2/\text{en}$  surfaces prepared under the most forcing silanization conditions (Method A, Experiment II-1) exhibit the lowest  $I_{\text{N}}/I_{\text{Si}}$  ratios. Pt/PtO/en surfaces exhibit high  $I_{\text{N}}/I_{\text{Si}}$  ratios.

The quality of the  $I_{\text{N}}/I_{\text{Si}}$  data is of course influenced by background N 1s and Si 2p bands. Unreacted samples of  $\text{RuO}_2$  and  $\text{TiO}_2$  are typically free from significant N 1s or Si 2p blanks. On  $\text{SnO}_2$ , however, a Si 2p background appears at the same B.E. as the silane band, with erratically varying

Table II. N/Si Surface Atom Ratio from ESCA Band Intensities  
Alkylamine-Silanized Electrodes

Expt	Electrode	$I_N/I_{Si}^a$	Calcd N/Si <sup>b</sup>	N/Si in silane <sup>c</sup>	Silane N/Si/ Calcd N/Si
II-1	SnO <sub>2</sub> /en <sup>d</sup>	1.09 ± 0.38 (8)	0.60	2	3.33
II-2	SnO <sub>2</sub> /en <sup>d</sup>				
	(10 s)	2.95	1.62	2	1.23
	(20 s)	2.42	1.33	2	1.50
	(1 min)	2.64	1.45	2	1.38
	(3 min)	1.29	0.71	2	2.82
	(6 min)	1.33	0.73	2	2.74
II-3	SnO <sub>2</sub> /en <sup>f</sup>	1.34	0.74	2	2.70
II-4	SnO <sub>2</sub> /en <sup>g</sup>	1.93	1.06	2	1.89
II-5	RuO <sub>2</sub> /PrNH <sub>2</sub> <sup>h</sup>	1.46 ± 0.10 (4)	0.80	1	1.25
II-6	RuO <sub>2</sub> /PrNH <sub>2</sub> <sup>i</sup>	1.76 ± 0.09 (4)	0.97	1	1.03
II-7	RuO <sub>2</sub> /en <sup>h</sup>	2.52 ± 0.36 (2)	1.38	2	1.45
II-8	RuO <sub>2</sub> /en <sup>i</sup>	2.86	1.57	2	1.27
II-9	RuO <sub>2</sub> /triam <sup>h</sup>	5.77	3.17	3	0.95
II-10	TiO <sub>2</sub> /en <sup>h</sup>	3.42 ± 0.38 (3)	1.88	2	1.06
II-11	Pt/PtO/en <sup>h</sup>	7.0 ± 1.0 (6)	4.02	2	0.50
II-12	Pt/PtO/en <sup>i</sup>	2.70 ± 0.22 (2) <sup>j</sup>	1.55	2	1.29
Standard Materials					
Expt	Sample	$I_N/I_{Si}$	Calcd N/Si <sup>b</sup>	Actual N/Si	Actual/calcd
II-13	Si <sub>3</sub> N <sub>4</sub>	1.74 ± 0.16 (3)	0.96	1.33	1.39
II-14	PrNH <sub>2</sub> silane				
	polymer <sup>k</sup>	1.85	1.02	0.91 <sup>l</sup>	0.89
II-15	en silane				
	polymer <sup>k</sup>	2.78	1.53	1.54 <sup>l</sup>	1.01
II-16	triam silane				
	polymer <sup>k</sup>	4.55	2.50	3.06 <sup>l</sup>	1.22

<sup>a</sup> Band area ratios of N 1s at 401.5 ± 400 eV to Si 2p at 102 eV, except for Expts II-11, 12, which used Si 2s at 160 eV to avoid interference with a Pt band. Number of specimens in parentheses. <sup>b</sup> Band area ratio converted to atom ratio using sensitivity factor of N/Si of 1.82 to N 1s/Si 2p and 1.74 for N 1s/Si 2s. See text. <sup>c</sup> Stoichiometric atom ratio in the indicated pure silane. <sup>d</sup> Electrodes prepared using silanization Method A. <sup>e</sup> Silanization Method D; data from Figure 1. <sup>f</sup> Silanization Method D. <sup>g</sup> Silanization Method D followed by amidization with 4-(NO<sub>2</sub>)<sub>2</sub>PhCOCl. <sup>h</sup> Silanization Method C. <sup>i</sup> Silanization Method C followed by amidization with 3,5-(NO<sub>2</sub>)<sub>2</sub>PhCOOH (DCC). <sup>j</sup> Band area ratio of N 1s at 406 eV to Si 2s at 160 eV and assumption of 50% active amine. <sup>k</sup> Polymer samples prepared from silane by hydrolysis with water, drying, grinding to powder. <sup>l</sup> Polymer sample analysis by Galbraith Laboratories.

intensities (entirely absent on occasional samples and amounting to 50% of the band on a silanized SnO<sub>2</sub> surface in other instances). A background correction was not attempted because of this inconsistent behavior, and the SnO<sub>2</sub>/en  $I_N/I_{Si}$  are thus known to be low. It is not clear, however, that the Si background problem can account for the systematic variation of SnO<sub>2</sub>/en surfaces with silanization reaction conditions. Relative to RuO<sub>2</sub>/en and TiO<sub>2</sub>/en, then, except for the mild silanization reaction condition, the SnO<sub>2</sub>/en surfaces appear qualitatively Si-rich (or N-poor). On Pt/PtO surfaces, no difficulties exist with Si blanks as long as silicon-containing polishing materials are avoided in the Pt electrode resurfacing which follows each experiment. N 1s background bands are seen at ca. 400 eV from time to time but are not typically large enough to cause as high a  $I_N/I_{Si}$  as observed on Pt/PtO/en surfaces (Experiment II-11), which seem to be N-rich.

Conversion of  $I_N/I_{Si}$  data to N/Si atom ratios involves a relative ESCA elemental sensitivity factor

$$\frac{I_N}{I_{Si}} = \left[ \frac{\sigma_N \lambda_N \phi_N}{\sigma_{Si} \lambda_{Si} \phi_{Si}} \right] \frac{T_N C_N D_N}{T_{Si} C_{Si} D_{Si}} \quad (1)$$

where  $\sigma$  is photoionization cross-section for the N 1s and Si 2p(1/2+3/2) levels,  $\lambda$  are the escape depths for photoelectrons from these levels,  $\phi$  is the angular correlation factor for photoelectrons at the photon beam-sample-spectrometer acceptance angle,  $T$  is spectrometer efficiency for electrons of the given kinetic energies,  $C$  is an attenuation factor for adsorbed contaminant hydrocarbon layer on the sample, and  $D$  is atom density. Using computed and tabularized (30)

cross-sections  $\sigma_N/\sigma_{Si(2p)} = 2.06$ ;  $\phi_N/\phi_{Si(2p)}$  is calculable (41) (equals 1.107 for our spectrometer's 67° angle); and  $\lambda_N/\lambda_{Si}$  is estimable from the  $\lambda\lambda(KE)^{0.75}$  relationship which at KE ≥ 300 eV is a good approximation (42) to a more exact formulation (43) (equals 0.80 for N 1s/Si 2p). The term in brackets in Equation 1 is thus 1.82 for N 1s/Si 2p. The dispersion of our spectrometer's efficiency with kinetic energy, if any, is not documented. It employs a voltage retarding feature which at the extreme could yield a relation (44)  $T\lambda(KE)^{-1}$ , which would correspond to  $T_N/T_{Si} = 1.35$ . Attenuation by the contaminant is also an uncertain factor; if the film is assumed to be ca. 20 Å hydrocarbon, which is probably generous, a very rough calculation gives  $C_N/C_{Si} \sim 0.8$  (attenuation is larger for the lower KE N 1s photoelectrons). The last two factors tend to cancel one another, and if we then assume  $T_N C_N/T_{Si} C_{Si} \sim 1.0$ , the theoretical estimate for the N 1s/Si 2p sensitivity ratio is 1.82.

The N 1s/Si 2p sensitivity ratio was also evaluated with chemical standards. Several materials (not sputtered) are compared to the theoretical value in Table II. Prepared, analyzed (bulk) alkylamine siloxane polymers agree reasonably well with the theoretical value. Data for Si<sub>3</sub>N<sub>4</sub> agree less well. Previous (45, 46) sputter profiles of Si<sub>3</sub>N<sub>4</sub>, however, suggest that its unsputtered surfaces tend to be N-poor. Other available standards work likewise notes a problem with Si data (42). The 1.82 factor was adopted for conversion of  $I_N/I_{Si}$  in Table II to N/Si atom ratios, but the reader will note that use of a 1.31 factor from the Si<sub>3</sub>N<sub>4</sub> sample would not alter essential features of the following discussion.

Examining RuO<sub>2</sub> electrodes first, the calculated N/Si atom ratios on electrodes silanized with PrNH<sub>2</sub>, en, and triam

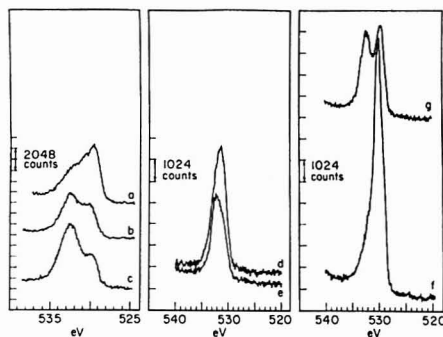
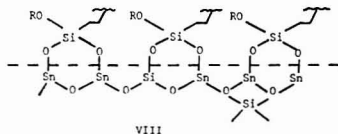


Figure 6. O 1s spectra on various metal oxides. Curve A:  $\text{RuO}_2$ ; Curve B:  $\text{RuO}_2/\text{en}$ ; Curve C:  $\text{RuO}_2/\text{PrNH}_2$ ; Curve D:  $\text{SnO}_2$ ; Curve E:  $\text{SnO}_2/\text{PrNH}_2$ ; Curve F:  $\text{TiO}_2$ ; Curve G:  $\text{TiO}_2/\text{en}$ .

silanes are in reasonable agreement with the ideal molecular ratios. The result for  $\text{TiO}_2/\text{en}$  is similar. Structural degradation of the alkylamine-silane does not appear to occur upon binding to these surfaces.

The N/Si atom ratio results for  $\text{SnO}_2/\text{en}$  surfaces, known to involve error from the Si background problem, suggest a nonideal N/Si surface stoichiometry, particularly for surfaces prepared under the more vigorous reaction conditions. Two explanations for silicon-richness on a silanized metal oxide surface can be offered. First, it is possible that the silane reagents contain deaminated trialkoxyalkylsilanes or these are produced by decomposition pathways in the reacting solution. Secondly, the silane reagent may penetrate the outermost, hydrated one or two atomic layers of the  $\text{SnO}_2$  lattice, nucleophilic attack by  $-\text{SnOH}$  on the alkylamine sidechain then occurring to expel that group with its amine nitrogen. The silicon would reside as silicate sites interspersed in the surface  $\text{SnO}_2$  lattice, as below



VIII

Both explanations for Si-richness are speculations.

The N/Si atom ratio on  $\text{Pt}/\text{PtO}/\text{en}$  shows that this surface is N-rich. The  $\text{Pt}/\text{PtO}$  surface differs from the other electrodes in that the oxide layer is an approximate monolayer rather than a bulk oxide (3). This oxide, or patches of exposed  $\text{Pt}^0$ , may chemisorb amine components from decomposed alkylaminesilane in the reacting solution. If so, the amine + amide N 1s band of Table I is enhanced on  $\text{Pt}/\text{PtO}$  and the active amine assay of Table I (Experiments I-14, 15) is thereby low. Electrochemical experience with the  $\text{Pt}/\text{PtO}/\text{en}$  surface suggests fairly high coverages in amidization reactions (3), and the portion of immobilized alkylamine-silane which reacts as active amine may be higher than that represented in Table I by 2X or more. If, for instance, we assume the reactivity of  $\text{en}$  silane on  $\text{Pt}/\text{PtO}/\text{en}$  is like that on  $\text{SnO}_2/\text{en}$  surfaces (e.g., 50% active amine), and then employ  $I_{\text{N}}/I_{\text{O}}$  data taken using the 406 eV nitro band on a silanized, amidized electrode (Experiment II-12), an atom ratio more in line with the results on  $\text{RuO}_2/\text{en}$  and  $\text{TiO}_2/\text{en}$  surfaces results. A better-substantiated quantitative picture of the alkylamine-silane stoichiometry on  $\text{Pt}/\text{PtO}/\text{en}$  surfaces than this is obviously

Table III. O 1s Binding Energies

Sample	O 1s B.E., eV <sup>a</sup>		Source
		Lattice	
$\text{SnO}_2$	sh	530.8	This work
	532 (sh)	530.5	(7)
	531.7 <sup>b</sup>	530.1	(47)
$\text{SnO}_2/\text{PrNH}_2$	531.8	sh	This work
$\text{SnO}_2/\text{en}$	~531.5	530.8	This work
$\text{SnO}_2/\text{PrNH}_2$	532	530.5 (sh)	(7)
$\text{RuO}_2$	~532	529.6	This work
$\text{RuO}_2$	530.5 (sh) <sup>c</sup>	529.4	(48)
$\text{RuO}_2/\text{PrNH}_2$ (or en)	532.1 ± 0.2	529.7 ± 0.2	This work
$\text{TiO}_2$	sh	530.0	This work
$\text{TiO}_2/\text{en}$	532.0 ± 0.3	529.8 ± 0.3	This work
Porous silica		532.8	This work
Glass		532.5	This work
Glass fibers		532.4	(55)
Glass		531.2, 529.4 <sup>d</sup>	(56)
NiO	531.2 <sup>b</sup>	529.4	(50)
CuO	531.6 <sup>b</sup>	529.7	(51)

<sup>a</sup> B.E. in this work referenced to C 1s (285 eV); B.E. by others referenced variously to Au, Ag, C 1s, and exact correspondence B.E. cannot be expected. <sup>b</sup> Interpreted variously as chemisorbed oxygen species or surface hydroxyl. <sup>c</sup> Hydrated sample; pure prepared sample has 531.5 band interpreted as  $\text{RuO}_2$  defect. <sup>d</sup> Interpreted as "non-bridging oxygen".

desirable but will require further experiments.

**Effect of Silanization on O 1s Spectra of Metal Oxides.** Each of the three bulk metal oxide electrodes exhibits a dominant O 1s band which is presumably the lattice -MOM-oxygen, and also a higher B.E. O 1s band which is poorly resolved from the main band for  $\text{SnO}_2$  (Figure 6, Curve D) but distinct for  $\text{RuO}_2$  and  $\text{TiO}_2$  (Curves A, F). The  $\text{SnO}_2$  shoulder has been observed by others (7, 47), and similar shoulders are common observations (48-54) on other metal oxides especially upon exposure to air and moisture. A collection of metal oxide O 1s data is given in Table III. The higher B.E. shoulder is usually interpreted as surface hydroxyl (7, 47, 50-54) although evidence for a different metal oxidation state was presented for  $\text{RuO}_2$  (48).

Reaction of the metal oxide electrodes with an organosilane produces a much more prominent higher B.E. O 1s band (Curves B, C, E, G, Figure 6). The B.E. of this band is approximately the same for  $\text{PrNH}_2$  and  $\text{en}$ -silanized surfaces, and on  $\text{RuO}_2$  and  $\text{TiO}_2$ , where accurate B.E. measurements were feasible. The intensity of the higher B.E. band roughly correlates with the intensity of the N 1s band of the alkylamine-silane and thus it is related to coverage achieved in the silanization reaction. It is particularly intense on samples bearing siloxane polymer. The lattice O 1s band exhibits no change in B.E. upon silanization but is lowered in intensity presumably because of photoelectron scattering by the overlying silane.

The higher B.E. O 1s band which appears upon silanization can be interpreted as -MOSi- oxygen, (although contributions from  $-\text{SiOH}$ ,  $-\text{SiOR}$ , or adsorbed water are also possibilities). The lattice O 1s band for  $-\text{SiOSi}-$  bound oxygen (as in silica) lies at higher B.E. (by 2-3 eV, see data in Table III) than the typical lattice oxygen in the more ionic metal oxides. The band on silanized metal oxide has an intermediate B.E.; compare 530.0 eV for  $\text{TiO}_2$  lattice O 1s and 532.5 eV for glass (our data) with the observed 532.0 eV on  $\text{TiO}_2/\text{en}$ . This would qualitatively be expected for -MOSi- oxygen. The -MOSi- band overlies or supplants by reaction the surface hydroxyl present on the metal oxide before silanization. In the case of  $\text{SnO}_2$ , care must be taken to avoid specimens with surface Si contaminant when examining the effects of silanization.



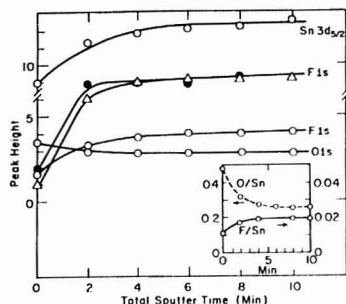


Figure 7. 1.5 eV  $\text{Ar}^+$  sputter profile for  $\text{SnO}_2$  (Specimen I,  $\bullet$ , and specimen II,  $\circ$ ) and  $\text{SnO}_2/\text{en}$  Method D, Specimen III,  $\Delta$ ) electrodes for O 1s, Sn 3d<sub>5/2</sub>, and F 1s. Sputter profiles are on arbitrary intensity scales different for each element; band intensity ratios in inset are actual band areas.

The O 1s spectral region has potential qualitative usefulness in study of silanization reactions. We regard quantitative interpretations of intensities as tenuous because of the metal hydroxyl feature and the presence of surface water, adsorption of which is conceivably enhanced by the presence of the silane.

**$\text{SnO}_2$  Dopant Concentration and Depth Profile.**  $\text{SnO}_2$ , an *n*-type semiconductor in pure form, is useful as a non-rectifying working electrode at positive potentials only when doped with high levels of appropriate carriers. The  $\text{SnO}_2$  electrodes employed here are fluoride doped; a F 1s band can be detected for this at B.E. 687 eV. The dopant concentration and depth profile are of interest. Figure 7 shows  $\text{Ar}^+$  sputter profiles for two native  $\text{SnO}_2$  and one silanized  $\text{SnO}_2$  electrodes. The variation of  $I_F$  with sputter time indicates that the outermost 10–20 Å of the  $\text{SnO}_2$  electrode is depleted in dopant. The degree of depletion varies with the electrode as does the interior level of dopant. There is no obvious dependence on the electrode having been subjected to silanization. Applying Equation 1 in the same manner as for N/Si, a relative sensitivity factor of 0.26 is used to convert the  $I_F/I_{\text{Sn}}$  band area ratios (Figure inset) for Specimen II at zero sputtering time (surface) and 10-min sputtering time (interior) to F/Sn atom ratios of 0.034 and 0.056, respectively. These are approximate values since  $I_F$  for Specimen I, for instance, was twice as large, and also the relative sensitivity factor was not compared to standards. Using 6.95 g/cm<sup>3</sup> for  $\text{SnO}_2$  density, carrier populations of  $9.4 \times 10^{20}$  and  $1.6 \times 10^{21}$  atoms/cm<sup>3</sup> are calculated for the  $\text{SnO}_2$  surface and bulk, respectively. The surface carrier population is sufficiently high that adverse electrochemical properties are not expected from the depletion effect, and importantly the depletion effect is not enhanced by the silanization reaction.

The dopant depletion for  $\text{SnO}_2$  is in contrast to Sn-doped  $\text{In}_2\text{O}_3$ , which according to Kuwana exhibits a higher Sn/In ratio at the surface of this electrode material than in its bulk (57).

Figure 7 also shows a variation of  $I_O/I_{\text{Sn}}$  (band areas) with  $\text{Ar}^+$  sputtering similar to a previous measurement (57). The F dopant depletion falls within the region of enhanced  $I_O/I_{\text{Sn}}$ , which we interpret as a layer of partially hydrated  $\text{SnO}_2$  lattice, for the following reasons. Using a relative O/Sn sensitivity factor 0.20 derived from Equation 1, the calculated O/Sn atom ratio for  $\text{SnO}_2$  electrodes varies typically from 2.4 prior to sputtering to about 1.4 after sputtering attains a constant  $I_O/I_{\text{Sn}}$ . (One sample gave an initial O/Sn ratio of 3.5, but the same final value.) These calculations, by themselves, suggest that while the outermost surface is hydrated, the  $\text{Ar}^+$  beam sputtering induces a chemical change in the  $\text{SnO}_2$  to a lower

oxide form and so the actual depth of lattice hydration is less than the profile of Figure 7 implies. The possibility of reduction during sputtering of  $\text{SnO}_2$  powder has been advanced (47). In an alternate interpretation, using an empirical relative O/Sn sensitivity factor 0.11 (58) with Figure 7 yields O/Sn atom ratios typically 4.3 before sputtering and 2.5 after. This calculation suggests even more extensive surface hydration and little or no  $\text{Ar}^+$  reduction effect. A sputtering experiment with 400 eV  $\text{Ar}^+$  was stated elsewhere not to cause reduction of  $\text{SnO}_2$  (59). Lastly, we have observed an example of metal ion chemisorption (60) to the same depths as the  $I_O/I_{\text{Sn}}$  variation. The evidence supports our interpretation of Figure 7 in terms of a hydration deeper than the outermost  $\text{SnO}_2$  lattice plane.

## DISCUSSION

For the most part, the above results show that the alkylamine-silanized surfaces exhibit expected and understandable properties, and the hope of chemical amine-like predictability of the modified metal oxide electrode surface is qualitatively realized. The alkylamine-silanized interface cannot, on the other hand, be considered as solely an amine-like surface; its chemistry is more complex than this. This is not surprising for a surface synthesized under conditions far from the atomically clean single crystal domain. Such chemical complexity will probably be common for other forms of electrode surface modification upon examination on a comparable level of detail.

The motivation for our study of the alkylamine-silanized interface is in its use as a connecting bridge for immobilization of redox reagents on electrode surfaces. We should consider how the present results relate to that application. The alkylamine-silane chain is not itself a good electron transport bridge between immobilized redox reagent and electrode. The length of a bonded *en* silane from metal to primary amine nitrogen is  $\sim 12$  Å in extended form and  $\sim 9$  Å in the hydrogen bonded Structure VII. Unless the activation barrier for electron transfer over such distance proves to be modest, flexible motions of the alkylamine-silane chain will play a role in the electron transfer process. The premise of the so-called "floppy model" (2, 24) is that such flexibility will exist in these modified surfaces. At least three factors are involved, the frequency of the motion, which will influence the pre-exponential kinetic factor (maximum value  $kT/h \sim 10^{13} \text{ s}^{-1}$ ) (61, 62), and the distance and geometry of redox reagent approach to metal oxide, which will influence  $\Delta G^\ddagger$ . Motions of the alkylamine-silane chain will be affected by Structures I–III, V, VI, and VII. Overall stability of the modified surface is enhanced by multiple  $-\text{MOSi}-$  bonds, and by cross-linking as in Structure V, but motional freedom of the amine site diminishes in the order of Structures I > II > III. We conjectured that I and II are more likely, but no quantitative analysis of this bonding problem is available. Structures VI and VII provide a shorter connecting bridge but also tend to restrain the approach distance. It would appear from the amidization data that the hydrogen-bonded structures may be prevalent in alkylamine-silanes with  $\gamma$ -amine sites. For purposes of modeling of electron-transfer events, then, combinations of Structures I and II with VI and VII probably present a good estimate of the average surface stereochemistry. A considerable complication in such modeling, however, is the possibility that very rapid electron transfer is to but a small population of sites possessing optimum alkylamine-silane chain flexibility. Subsequent lateral propagation of electron transfer to other more motionally restricted sites then might actually be the controlling mechanism. Quantitative modeling is unenlightening until such eventualities are evaluated.

Our interpretation of the ESCA results indicates that a variety of surface structures may exist within a single specimen

of alkylamine-silanized metal oxide electrode. We can draw from this the intimation that a redox reagent bound to the alkylamine-silane may find itself in a spectrum of slightly different chemical environments. The redox reagent may as a consequence exhibit a spectrum of formal electrochemical potentials, which in turn has the effect of broadening the electrochemical surface wave observed for the reagent. To what extent broadening we have observed in surface waves on alkylamine-silanized electrodes is due to this chemical heterogeneity as opposed to interactive effects within the chemically bound layer (62) or to both, remains to be resolved.

#### ACKNOWLEDGMENT

Assistance from D. N. Smith in ESCA bandfitting is gratefully acknowledged.

#### LITERATURE CITED

- (1) P. R. Moses, L. Wier, and R. W. Murray, *Anal. Chem.*, **47**, 1882 (1975).
- (2) P. R. Moses and R. W. Murray, *J. Electroanal. Chem.*, **77**, 393 (1977).
- (3) J. R. Lenhard and R. W. Murray, *J. Electroanal. Chem.*, **78**, 195 (1977).
- (4) A. Diaz, *J. Am. Chem. Soc.*, **99**, 5838 (1977); G. J. Leigh and C. J. Pickett, *J. Chem. Soc., Dalton Trans.*, 1797 (1977).
- (5) C. M. Elliott and R. W. Murray, *Anal. Chem.*, **48**, 1247 (1976).
- (6) P. R. Moses, J. C. Lennox, J. Lenhard, and R. W. Murray, 173rd National Meeting, American Chemical Society, New Orleans, La., March 1977.
- (7) D. F. Unterker, J. C. Lennox, L. M. Wier, P. R. Moses, and R. W. Murray, *J. Electroanal. Chem.*, **81**, 309 (1977).
- (8) M. Fujihira, T. Matsue, and T. Osa, *Chem. Lett.*, 875 (1976).
- (9) D. F. Unterker, P. R. Moses, L. M. Wier, C. M. Elliott, and R. W. Murray, 149th Electrochemical Society Meeting, Washington, D.C., May 1976.
- (10) E. Grushka, Ed., "Bonded Stationary Phases in Chromatography", Ann Arbor Science Publications, Ann Arbor, Mich., 1974.
- (11) C. H. Lochmuller and C. W. Amoss, *J. Chromatogr.*, **108**, 85 (1975).
- (12) E. Grushka and E. J. Kikla, Jr., *Anal. Chem.*, **48**, 1370 (1974).
- (13) H. H. Weetall, *Sop. Purif. Methods*, **2**, 199 (1973).
- (14) D. M. Hercules, L. E. Cox, S. Onisick, G. D. Nichols, and J. C. Carver, *Anal. Chem.*, **45**, 1973 (1973).
- (15) D. E. Leyden and G. H. Luttrell, *Anal. Chem.*, **47**, 1612 (1975).
- (16) R. L. Burwell, *Chem. Technol.*, 370 (1974).
- (17) E. P. Plueddemann, *Adhes. Age*, **18**, 36 (1975); *Chem. Abstr.*, **83**, 148735 (1975).
- (18) K. Hardee and A. J. Bard, *J. Electrochem. Soc.*, **122**, 739 (1975).
- (19) N. C. Reilly and W. S. Woodward, to be submitted for publication.
- (20) H. P. Boehm, "Chemical Identification of Surface Groups", *Adv. Catal.*, **16**, 179 (1966).
- (21) R. K. Gilpin and M. F. Burke, *Anal. Chem.*, **45**, 1383 (1973).
- (22) E. W. Thornton and P. G. Harrison, *J. Chem. Soc. Faraday Trans. 1*, **71**, 461 (1975).
- (23) D. J. C. Yates, *J. Phys. Chem.*, **65**, 746 (1961).
- (24) H. Kuhn, "Spectroscopy of Monolayer Assemblies", in "Physical Methods of Chemistry", A. Weissberger and B. Rossiter, Ed., Wiley, New York, N.Y., 1972, Part III, p. 577.
- (25) P. R. Moses and R. W. Murray, *J. Am. Chem. Soc.*, **98**, 1435 (1976).
- (26) M. Gieria and R. Menning, *Z. Phys. Chem. (Frankfurt am Main)*, **98**, 303 (1975).
- (27) A. A. Oswald, L. L. Murrell, and L. J. Boucher, *Am. Chem. Soc., Div. Pet. Chem., Abstr.*, 168th National Meeting, American Chemical Society, Los Angeles, Calif., 1974.
- (28) P. G. Harrison and E. W. Thornton, *J. Chem. Soc., Faraday Trans. 1*, **1310** (1976).
- (29) A. Diaz, *J. Am. Chem. Soc.*, **99**, 6780 (1977).
- (30) V. S. Srinivasan and W. J. Lamb, *Anal. Chem.*, **49**, 1639 (1977).
- (31) J. H. Scofield, Lawrence Livermore Laboratory Report No. UCR-L-51326, January 1973.
- (32) D. M. Hercules, *Anal. Chem.*, **42** (1), 20A (1970).
- (33) S. Pignataro and G. Distefano, *J. Electron Spectrosc. Relat. Phenom.*, **2**, 171 (1973).
- (34) H. F. Weetall and L. S. Hersh, *Biochim. Biophys. Acta*, **208**, 54 (1970).
- (35) L. Lee, *J. Colloid Interface Sci.*, **27**, 751 (1968).
- (36) E. P. Plueddemann, *J. Adhes.*, **2**, 184 (1970).
- (37) M. L. Hark, "Infrared Spectroscopy in Surface Chemistry", M. Dekker, New York, N.Y., 1967, p. 102.
- (38) F. J. Kahn, *Appl. Phys. Lett.*, **22**, 386 (1973).
- (39) H. R. Anderson, F. M. Fowkes, and F. H. Heischler, *J. Polym. Sci., Polym. Phys. Ed.*, **14**, 879 (1976).
- (40) J. C. Lennox and R. W. Murray, *J. Electroanal. Chem.*, **78**, 195 (1977).
- (41) J. N. Butler, "Ionic Equilibria", Addison Wesley, Reading, Mass., 1964, p. 466.
- (42) R. F. Reilman, A. Meezan, and S. T. Manson, *J. Electron Spectrosc. Relat. Phenom.*, **8**, 389 (1976).
- (43) C. D. Wagner, *Anal. Chem.*, **49**, 1282 (1977).
- (44) D. R. Penn, *J. Electron Spectrosc. Relat. Phenom.*, **9**, 29 (1976).
- (45) J. C. Helmer and N. H. Weichert, *Appl. Phys. Lett.*, **13**, 266 (1968).
- (46) J. S. Johansson, W. E. Spicer, and Y. E. Strauss, *Thin Solid Films*, **32**, 311 (1976).
- (47) P. H. Holloway and H. J. Stein, *J. Electrochem. Soc.*, **123**, 723 (1976).
- (48) A. W. C. Lin, N. R. Armstrong, and T. Kuwana, private communication, March 1977.
- (49) K. S. Kim and N. Winograd, *J. Catal.*, **35**, 66 (1974).
- (50) N. S. McIntyre and M. G. Cook, *Anal. Chem.*, **47**, 2208 (1975).
- (51) W. Dians and J. E. Lester, *Surf. Sci.*, **43**, 602 (1974).
- (52) T. Robert, M. Bartel, and G. Offergeld, *Surf. Sci.*, **33**, 123 (1972).
- (53) K. S. Kim, A. F. Gossman, and N. Winograd, *Anal. Chem.*, **48**, 197 (1974).
- (54) G. C. Allen, M. T. Curtis, A. J. Hooper, and P. M. Tucker, *J. Chem. Soc., Dalton Trans.*, 1525 (1974).
- (55) K. Kishi and S. Ikeda, *Bull. Chem. Soc. Jpn.*, **48**, 341 (1975).
- (56) J. P. Rynd and A. K. Rastogi, *Surf. Sci.*, **48**, 22 (1975).
- (57) S. R. Nagel, J. Tauc, and B. G. Bagley, *Solid State Commun.*, **20**, 245 (1976).
- (58) N. R. Armstrong, A. W. C. Lin, M. Fujihira, and T. Kuwana, *Anal. Chem.*, **48**, 741 (1976).
- (59) C. D. Wagner, *Anal. Chem.*, **44**, 1050 (1972).
- (60) K. S. Kim, W. E. Baitinger, J. W. Amy, and N. Winograd, *J. Electron Spectrosc. Relat. Phenom.*, **5**, 351 (1974).
- (61) L. Wier, unpublished results, University of North Carolina, 1976.
- (62) R. C. Baetzold and G. A. Somorjai, *J. Catal.*, **45**, 94 (1976).
- (63) F. C. Anson, U.S.-Japan Seminar, San Francisco, Calif., May 1977.

RECEIVED for review September 14, 1977. Accepted December 19, 1977. This paper is Part IX of a series on "Chemically Modified Electrodes". This research was assisted by the National Science Foundation under grants MPS75-07863, CHE76-24564, DMR72-03024 and by the Office of Naval Research.

## Analysis of Commercial Sodium Tripolyphosphates by Phosphorus-31 Fourier Transform Nuclear Magnetic Resonance Spectrometry

Stanley A. Soljka\* and Roger A. Wolfe

Hooker Chemicals and Plastics Corporation, Research Center, Grand Island Complex, M.P.O. Box 8, Niagara Falls, New York 14302

Commercial sodium tripolyphosphate samples were analyzed by phosphorus-31 Fourier transform nuclear magnetic resonance spectrometry. The accuracy and precision of the method were assessed and found to be satisfactory. Identification of phosphorus-containing species was possible. In some cases, the presence of high polyphosphates interfered with the analysis.

The Fourier transform (FT) approach (1) has added new

dimensions to <sup>31</sup>P NMR spectrometry. The time savings and sensitivity enhancement inherent in the FT approach have been realized in practice, and analytical applications are becoming increasingly apparent (2). Detection of organophosphorus compounds at the level of the parts-per-million range has been reported (3). This paper describes the use of <sup>31</sup>P FT NMR spectrometry to analyze commercial samples of sodium tripolyphosphate (4, 5), including the determination of accuracy and precision. The advantages of this approach over other analytical procedures, such as gel chromatography

Table I.  $^{31}\text{P}$  FT NMR Parameters for Phosphates<sup>a</sup>

Phosphate	$^{31}\text{P}$ , ppm <sup>b</sup>	$T_1$ , s
$\text{NaH}_2\text{PO}_4$	0.8	—
$\text{Na}_2\text{HPO}_4$	3.3	14.1
$\text{Na}_3\text{PO}_4$	5.7	—
$\text{Na}_4\text{P}_2\text{O}_7$	-5.3	3.3
$\text{Na}_5\text{P}_3\text{O}_{10}$	-21.0	23.1
$\text{Na}_6\text{P}_4\text{O}_{13}$	4.7 <sup>c</sup>	7.6
	-19.1 <sup>d</sup>	6.0
$\text{Na}_7\text{P}_5\text{O}_{16}$	-23.4	—

<sup>a</sup> Chemical shifts and  $T_1$  values are subject to sample conditions (e.g., pH, concentration). See Ref. 15. <sup>b</sup> In ppm relative to 85%  $\text{H}_3\text{PO}_4$ . <sup>c</sup> Doublet,  $J_{\text{PP}} = 19$  Hz. <sup>d</sup> Triplet,  $J_{\text{PP}} = 19$  Hz.

(6), paper chromatography (7), ion exchange chromatography (8), and colorimetry (9), are that it (1) enables identification of the phosphorus-containing constituents, (2) requires a short time for each analysis, and (3) requires simple sample preparation.

### EXPERIMENTAL

**Apparatus.** A Varian XL-100-12 NMR spectrometer was operated at 40.49 MHz with an internal deuterium field-frequency lock. The spectrometer was used in conjunction with a Nicolet TT-100 Fourier transform unit. A 30° pulse took 3.83  $\mu\text{s}$  and the time between pulses was 60 s. The sweep width was 1600 Hz and 8K computer points were used for time domain data accumulation. Proton decoupling was not used. Sixteen free induction decays were accumulated before Fourier transformation. Quadrature phase detection was used to detect signals. Chemical shifts are reported relative to 85%  $\text{H}_3\text{PO}_4$  which was contained in a concentric capillary. Negative chemical shifts are associated with signals to higher field strength than 85%  $\text{H}_3\text{PO}_4$  (to the right of 85%  $\text{H}_3\text{PO}_4$ ). The inversion-recovery pulse sequence was used to measure spin-lattice relaxation times ( $T_1$ ). A three-parameter exponential fit was used to obtain  $T_1$  from experimental data (10). The probe temperature was 26 °C.

**Sample Preparation.** Samples were made as concentrated as possible using  $\text{D}_2\text{O}$  as solvent. A standard mixture sample was made with known weights of four phosphates to test accuracy and precision. The standard phosphates were analytical grade and commercially available. Their purity was checked by  $^{31}\text{P}$  NMR spectrometry.

### RESULTS AND DISCUSSION

There are several problems to overcome in order to perform quantitative work by  $^{31}\text{P}$  NMR spectrometry. Proton decoupling can produce a nuclear Overhauser effect (NOE) (11, 12) which enhances signal intensities such that peak areas may no longer be proportional to the number of nuclei. Although there are various means of avoiding this possibility (13, 14), the measurements here did not use proton decoupling and, thus, the NOE did not exist.

Secondly, signal intensity decreases with increasing separation from the carrier frequency. This is because the irradiation power decreases with distance from the carrier frequency. This problem was surmounted by using a small sweep width and quadrature phase detection. Thus, all signals are within 600 Hz of the carrier frequency. With a 11.5  $\mu\text{s}$  90° pulse, there is no meaningful dropoff of rf power, even several kilohertz away from the carrier frequency.

Finally, the time between pulses must be chosen so that the magnetization is given sufficient time to return to equilibrium before the next pulse. This time is governed by the spin-lattice relaxation time ( $T_1$ ). This obstacle to obtaining quantitative results may be overcome by reducing all spin-lattice relaxation with the addition of a paramagnetic relaxant (2, 3, 5) or by using a small pulse flip angle and long pulse delay. Since these samples are highly concentrated, we chose to do the latter.

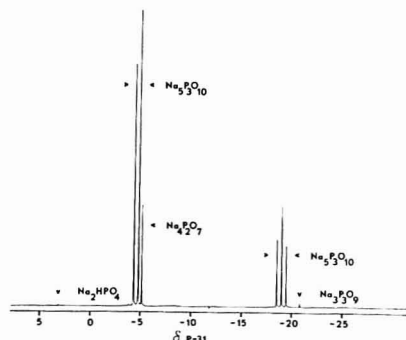


Figure 1.  $^{31}\text{P}$  FT NMR spectrum of a commercial sodium tripolyphosphate sample

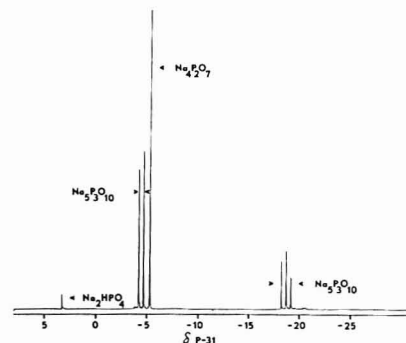


Figure 2.  $^{31}\text{P}$  FT NMR spectrum of a commercial sodium tripolyphosphate sample containing high polyphosphates

Table II. Statistical Data for  $^{31}\text{P}$  FT NMR Assay of Known Phosphate Sample

Phosphate	Av rel wt, %	Known wt, %	Rel % accuracy	Std dev, S
$\text{Na}_2\text{HPO}_4$	1.55	1.55	0	0.04
$\text{Na}_4\text{P}_2\text{O}_7$	12.81	13.03	1.69	0.63
$\text{Na}_5\text{P}_3\text{O}_{10}$	8.86	8.88	0.23	0.24
$\text{Na}_6\text{P}_4\text{O}_{13}$	76.75	76.54	0.27	0.73

It has been shown that the  $T_1$ 's, as well as the chemical shifts and coupling constants for these compounds may be sensitive to pH, concentration, temperature, and the nature of the counterion (15, 16). In the pH range of these samples ( $\text{pH} = 9.0 \pm 0.5$ ), the  $T_1$ 's should be relatively short (15).

In order to assist in determining adequate pulse conditions, the spin-lattice relaxation times of the phosphates were measured under typical sample conditions. Table I shows the  $^{31}\text{P}$  NMR chemical shifts and the  $T_1$  values for standard samples. Using a 30° pulse flip angle and a time between pulses of 60 s will enable sufficient magnetization to return to equilibrium so that quantitative peak area measurements can be made. Figure 1 shows the  $^{31}\text{P}$  FT NMR spectrum of a commercial tripoly sample. The signal-to-noise ratio was excellent while all signals are well separated and easily integrated.

The accuracy and precision of this quantitative method were assessed by performing six analyses on a known standard

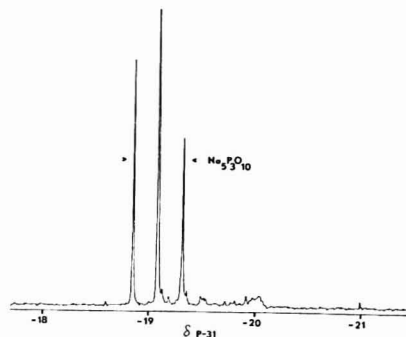


Figure 3. Scale expansion of spectrum in Figure 2 clearly showing numerous signals from high polyphosphates

mixture of  $\text{Na}_2\text{HPO}_4$ ,  $\text{Na}_4\text{P}_2\text{O}_7$ ,  $\text{Na}_3\text{P}_3\text{O}_{10}$ , and  $\text{Na}_5\text{P}_3\text{O}_{10}$ . Table II shows the average relative weight percent, the known weight percent, and the relative percentage accuracy. For an NMR method of analysis, both the accuracy and precision are outstanding.

The average relative weight percent may be taken as the average absolute weight percent since all the constituents of commercial tripoly samples so far analyzed contained phosphate, thus eliminating the necessity of adding an internal standard.

The presence of higher polyphosphates will interfere with this analysis. Figure 2 shows the  $^{31}\text{P}$  FT NMR spectrum of another commercial tripoly sample. The signals from  $\text{Na}_2\text{HPO}_4$ ,  $\text{Na}_4\text{P}_2\text{O}_7$ , and  $\text{Na}_5\text{P}_3\text{O}_{10}$  are clearly seen. However, upon scale expansion of the  $\text{Na}_5\text{P}_3\text{O}_{10}$  triplet region, as in Figure 3, numerous signals from higher polyphosphates can be detected (16). The analysis can still be performed, although the accuracy will be reduced.

#### LITERATURE CITED

- (1) T. C. Farrar and E. D. Becker, "Pulse and Fourier Transform NMR", Academic Press, New York, N.Y., 1971.
- (2) I. K. O'Neill and N. A. Pringuer, *Anal. Chem.*, **49**, 558 (1977).
- (3) T. W. Gurley and W. M. Ritchey, *Anal. Chem.*, **48**, 1137 (1976).
- (4) J. G. Colson and D. H. Marr, *Anal. Chem.*, **45**, 370 (1973).
- (5) T. W. Gurley and W. M. Ritchey, *Anal. Chem.*, **47**, 1444 (1975).
- (6) N. Yozu, K. Kouchiyama, T. Miyajima, and S. Ohashi, *Anal. Lett.*, **8**, 641 (1975).
- (7) R. H. Kolloff, *Anal. Chem.*, **33**, 373 (1961).
- (8) D. P. Lundgren and N. P. Loeb, *Anal. Chem.*, **33**, 366 (1961).
- (9) W. B. Chess and D. N. Bernhart, *Anal. Chem.*, **30**, 111 (1958).
- (10) J. Kowalewski, G. C. Levy, L. F. Johnson, and L. Palmer, *J. Magn. Reson.*, **26**, 533 (1977).
- (11) J. H. Noggle and R. E. Shimer, "The Nuclear Overhauser Effect", Academic Press, New York, N.Y., 1971.
- (12) P. L. Yeagle, W. C. Hutton, and R. B. Martin, *J. Am. Chem. Soc.*, **97**, 7175 (1975).
- (13) O. A. Gansow and W. Shitenhelm, *J. Am. Chem. Soc.*, **93**, 4294 (1971).
- (14) T. Glonek, *J. Am. Chem. Soc.*, **98**, 7090 (1976).
- (15) T. Glonek, P. J. Wang, and J. R. VanWazer, *J. Am. Chem. Soc.*, **98**, 7968 (1976).
- (16) T. Glonek, A. J. R. Costello, T. C. Myers, and J. R. VanWazer, *J. Phys. Chem.*, **79**, 1214 (1975).

RECEIVED for review August 10, 1977. Accepted January 3, 1978.

## Microcomputer Assisted, Single Beam, Photoacoustic Spectrometer System for the Study of Solids

Harry E. Eaton\* and James D. Stuart

Chemistry Department, U-60, University of Connecticut, Storrs, Connecticut 06268

A photoacoustic spectrometer system, for the study and analysis of solid materials, is described in detail. The system has been designed to make the photoacoustic technique available to most laboratories. Expensive, commercial, data acquisition units have been replaced by commonly available, inexpensive, and easily constructed components. The problems associated with the single beam mode of operation (i.e., source output correction, background compensation, and temporal variations) have been accounted for with the use of a microcomputer for data acquisition and reduction. Evaluation of the system is presented along with the spectra of  $\text{H}_2\text{O}_2$ ,  $\text{Er}_2\text{O}_3$ , and  $\text{UF}_4$ . Resolution is approximately 15 nm. Standard sample size is generally 5 mg while the lower limit of material necessary for an analysis is at the submilligram level—being both analyte and matrix dependent.

Photoacoustic spectrometry (PAS) has received attention lately as a tool for the investigation of the ultraviolet, visible, and infrared transmission properties of solid and semisolid materials which heretofore were inaccessible because of the physical nature. The technique has been used in the analysis

and study of, among others, thin-layer chromatography plates (1); semiconductor materials (2); low magnitude optical absorption coefficients (3–5); thermal diffusivity constants (6); fluorescence in solids (7–9); radiationless transitions (10, 11); qualitative identification of uranium tetrafluoride (12); biological systems (13–16); and excited states of a solid (17).

Articles in the literature have advanced theoretical expressions to explain signal generation (4, 5, 18, 19). The basis of the technique is the radiationless conversion of resonant, periodic, incident radiation into heat within the sample surface. The result is a periodic change in the kinetic energy of gas molecules in contact with the sample to produce pressure changes detectable as sound. For an incident wavelength, the magnitude of the sound is dependent on the optical absorption coefficient of the sample for that particular wavelength, the thermal diffusivity, and the sample thickness. By monitoring the magnitude of the sound vs. the incident radiation wavelength, a photoacoustic spectrum is produced which is analogous to a conventional absorption or transmission spectrum.

While literary descriptions of photoacoustic spectrometer systems have appeared for both single (20) and double beam instrumentation (21), experimentation connected with the

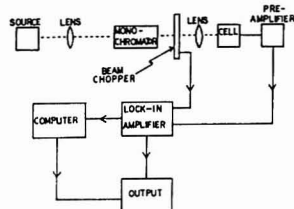


Figure 1. Diagram of photoacoustic spectrometer system

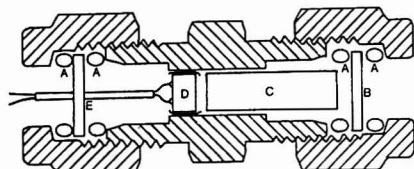


Figure 2. Photoacoustic detection cell. (A) silicon O-ring; (B) optical grade quartz window; (C) 1-cm diameter optical grade quartz spacer rod; (D) Radio Shack, Model 33-1055, electret microphone; (E) aluminum plate

technique has been said to be both sophisticated and relegated to well equipped laboratories (22, 23). Single beam instrumentation has been described recently as tedious and suffering from error due to temporal variation in the source which can be solved only by the double beam approach (24). We feel that the single beam instrument offers distinct advantages over the double beam with respect to expense and both to simplicity in construction and to operation. The microcomputer is becoming evermore commonplace in the laboratory; and, for the single beam design, it is the solution to spectral correction. In addition, the microcomputer provides for the capability of signal averaging to increase the signal to noise ratio, to store and update data, and to produce the difference between two spectra. We describe in this paper a detailed account of an inexpensive, easily constructed, single beam, microcomputer assisted, photoacoustic spectrometer system intended for general usage and which is designed to bring the technique within the scope of most laboratories.

### EXPERIMENTAL

**Apparatus.** The spectrometer system is schematically represented in Figure 1. The source is a 1000-W, high pressure, xenon lamp (Model 6117, Oriol Corp., Stamford Conn. 06902). The monochromator has a UV-VIS grating, 5-, 10-, or 20-nm bandpass slits,  $f/3.5$  efficiency, and a 20 nm/min clock motor drive (High Intensity Model 5, Bausch & Lomb Inc., Rochester, N.Y. 14602). The beam chopper is a home made device, involving a blade with 21 slots, driven by a 4.00-Hz constant speed motor to produce an 84-Hz signal. For the purposes of comparison and evaluation, the source, monochromator, and beam chopper system (10-nm bandpass slits and 84-Hz chopping frequency) produces at the sample surface within the PAS cell 0.11 mW of power at 200 nm, 8.5 mW of power at 480 nm, and 3.6 mW of power at 633 nm. This was determined by using the spectrometer system as an optical power meter and measuring the millivolt reading with a blackbody absorber in the PAS cell. Calibration was performed using the 633 nm line of a 1.8 mW helium-neon laser (Model 132, Spectra-Physics, Mountain View, Calif. 94042). A simple PAS cell can be fabricated from a  $1/2$ -in. brass union (Swagelok, Crawford Fitting Co., Solon, Ohio 44139) and is pictured in Figure 2. The leading edge of each male thread has been filed to produce a flat surface. Silicon O-rings are used to make an air tight seal. Radiation passes through the quartz window and strikes the sample which is attached with two-sided tape to the front surface of a solid quartz rod. The quartz rod is used to minimize the

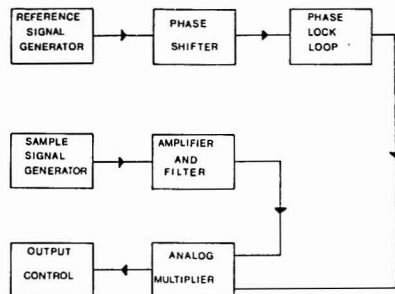


Figure 3. Diagram of electronic data acquisition unit

internal cell volume to approximately  $0.5 \text{ cm}^3$ . Sample size is generally 5 mg; i.e., that which is necessary to cover the end surface of the quartz spacer. The electret microphone, extracted from a Radio Shack hand-held microphone (Model 33-1055, Tandy Corp., Fort Worth, Texas 76107), fits snugly inside the union and is insulated electronically with Teflon gasket material. The leads for the microphone are fed through an aluminum plate to complete the seal of the PAS cell.

The necessary electronic equipment is easily assembled from common components. A diagram of the system is given in Figure 3 and Figure 4 provides the detailed electronic schematic. A lock-in amplifier incorporating a phase-lock loop (25) is used for signal acquisition. A cadmium sulfide photoconductive cell (Model 276-129, Radio Shack) is aimed directly at the source through the beam chopper and provides the necessary reference signal.

Our system employs a microcomputer (Model 8800b, MITS Altair, Albuquerque, N.M. 87106). The computer uses a CRT terminal (Model H 1000, Hazeltine Corp., Greenlawn, N.Y. 11740); a cassette tape recorder (Model 152, Audiotronics Corp., North Hollywood, Calif. 91609); a 10-bit analog to digital converter for input (Model 8701, Teledyne Semiconductor, Mountain View, Calif. 91609); a 10-bit digital to analog converter for output (Model AD 7530, Analog Devices, Inc., Norwood, Mass. 02062); and, a line printer for hard-copy (Model DMTP-6, Practical Automation Inc., Shelton, Conn. 06484). The system is programmed with 8k Basic (MITS Altair) and has 24k of static memory. Spectra are put out from the microcomputer through the digital to analog converter to a 10-inch mV recorder (Beckman Instruments Inc., Fullerton, Calif. 92634).

**Reagents.** Holmium oxide, erbium oxide, uranium tetrafluoride, and carbon black were purchased from Ventron Corp., Alfa Products, Danvers, Mass. 01923.

### RESULTS AND DISCUSSION

**Electronics.** In describing a PAS system for general use with the aim of making it available to most laboratories, it must be realized that while certain components can be constructed "in house", other components cannot be. In fact, this is the situation with the 1000-W xenon source, the monochromator, and the computing hardware. Items of the PAS system which can be assembled easily and inexpensively include the beam chopper, the PAS cell with microphone, the electronics unit, and the software.

Previously, signal acquisition has been accomplished through the use of commercial phase sensitive lock-in amplifiers. G. Horlick and K. R. Betty (26) have evaluated the phase-lock loop and analog multiplier as a means of tracking low level signals amid high background noise. This approach in conjunction with an additional preamplifier and two-stage filter (Figure 4) is successful in this application.

The reference signal is generated as an ac voltage at the output of OAI by the varying resistance of the CdS photocell. The two-stage phase shifter provides for  $0$ – $360^\circ$  phase adjustment between the reference and sample signals. The reference becomes a square wave out of the phase-lock loop



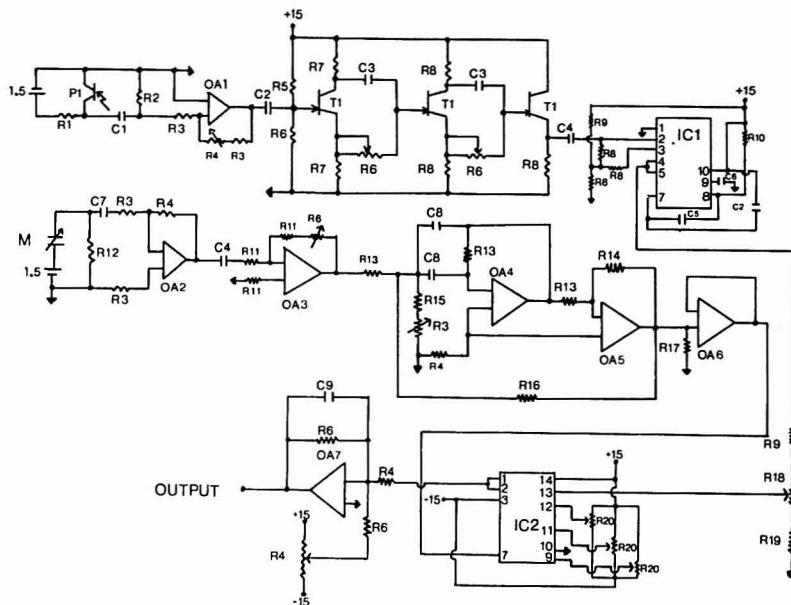


**Figure 4.** Schematic of electronic data acquisition unit.  $R_1 = 15 \text{ k}\Omega$ ,  $R_2 = 220 \text{ k}\Omega$ ,  $R_3 = 100 \text{ }\Omega$ ,  $R_4 = 100 \text{ k}\Omega$ ,  $R_5 = 6.8 \text{ M}\Omega$ ,  $R_6 = 1.0 \text{ M}\Omega$ ,  $R_7 = 2.2 \text{ k}\Omega$ ,  $R_8 = 4.7 \text{ k}\Omega$ ,  $R_9 = 10 \text{ k}\Omega$ ,  $R_{10} = 3 \text{ k}\Omega$ ,  $R_{11} = 1 \text{ k}\Omega$ ,  $R_{12} = 1.5 \text{ k}\Omega$ ,  $R_{13} = 120 \text{ k}\Omega$ ,  $R_{14} = 322 \text{ k}\Omega$ ,  $R_{15} = 550 \text{ }\Omega$ ,  $R_{16} = 148 \text{ k}\Omega$ ,  $R_{17} = 470 \text{ k}\Omega$ ,  $R_{18} = 5 \text{ k}\Omega$ ,  $R_{19} = 7.5 \text{ k}\Omega$ ,  $R_{20} = 20 \text{ k}\Omega$ ,  $C_1 = 0.1 \text{ }\mu\text{F}$ ,  $C_2 = 0.5 \text{ }\mu\text{F}$ ,  $C_3 = 0.01 \text{ }\mu\text{F}$ ,  $C_4 = 5.0 \text{ }\mu\text{F}$ ,  $C_5 = 0.001 \text{ }\mu\text{F}$ ,  $C_6 = 1.0 \text{ }\mu\text{F}$ ,  $C_7 = 10.0 \text{ }\mu\text{F}$ ,  $C_8 = 0.22 \text{ }\mu\text{F}$ ,  $C_9 = 1 \text{ or } 3 \text{ }\mu\text{F}$ . IC1 = Signetics 565 Phase Lock Loop, IC2 = AD 530 Multiplier-Analog Devices. OA1 through OA7 = Radio Shack 276-1741. P1 = Radio Shack 276-129. M = Radio Shack 33-1055 microphone. T1 = 2N3070

and subsequently an operand for the analog multiplier. The magnitude of the reference signal is not critical and needs only to be large enough to be acquired by the phase-lock loop ( $\sim 100 \text{ mV}$ ).

The sample signal is generated by the microphone, amplified 1000-fold, and presented as an ac voltage to OA3 for amplification. This variable amplification is useful to maximize the signal to noise ratio between different samples. The two-stage filter is tuned for 84 Hz and exhibits a  $Q$  of  $\sim 15$ . The multiplier, IC2, produces a time averaged signal that is positive in value for a sample signal of identical frequency to the reference, providing that the sample and reference signals have been properly phase aligned. The output of the multiplier is RC filtered (either 1- or 3-s time constant when using the 10-nm bandpass filter), the baseline is dc offset, and amplification to  $\pm 10 \text{ V}$  is necessary for computer input. For our microcomputer, a large input signal is required in order to minimize the finite reading error, 40 mV, caused by the computer 8-bit word length (e.g., 1 part in 256 error in a full scale  $\pm 10 \text{ V}$  analog to digital conversion).

Operation of the electronics unit at other frequencies is possible and is dependent on the tuning of the phase-lock loop and the two-stage filter. The phase-lock loop is tuned for 100 Hz, but has a lock-range of between 46.7 and 153.3 Hz. Further adjustment of the free running frequency,  $f_0$ , can be accomplished according to

$$f_0 = 1.2/4 R_{10} C_6 \quad (1)$$

where  $R_{10}$  and  $C_6$  are as listed in Figure 4 and the value of  $R_{10}$  should be kept between 2 and 20 k $\Omega$ . With a power supply voltage of  $\pm 15 \text{ V}$ , the lock-range is  $\pm 53\%$  of  $f_0$ . Tuning of the two-stage filter can be accomplished by adjusting the value

of the  $C_8$  capacitors such that the product of the capacitor value (in microfarads) and the chopping frequency (in Hertz) equals the numerical value of 18.5.

**Data Acquisition.** Both the output power of the xenon source and the throughput efficiency of the monochromator vary with the wavelength, so that it is necessary to correct any spectrum produced from a single beam instrument. Correction is accomplished by obtaining the signal ratio of the sample to a blackbody absorber at each wavelength. This can be effectively and rapidly accomplished by a microcomputer system. The microcomputer not only overcomes the correction difficulty but allows for the following additional options: averaging several spectra, thereby increasing the signal to noise ratio; storing and updating the reference and sample spectra; producing the difference between two sample spectra; and permanently storing the data on magnetic tape.

Since the blackbody spectrum cannot be recorded simultaneously with the sample spectrum, it is recorded separately and stored by the computer. Basic to this is the assumption that the source output remains constant over the time interval that the reference and sample spectra are acquired. We agree with Grey et al. (24) that the source output exhibits temporal fluctuations, but find that this can be dealt with. The noise of the source is composed of two components. The first is a small (1-3% relative) ac variation, perhaps due to the nature of the arc, which can be averaged by recording slowly and/or using a timing capacitor. Generally a 1-s time constant is sufficient to reduce the source and instrumental noise. The second is the small but absolute change in the relative, output magnitude of different spectral regions which occurs naturally with aging of the lamp. Our experience is that no more than an approximate relative change of 10% has occurred over 250



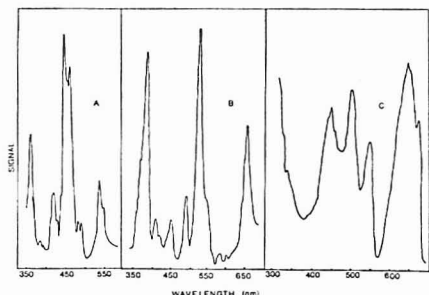


Figure 6. Photoacoustically generated spectra. (A)  $\text{H}_2\text{O}_2$ , (B)  $\text{Er}_2\text{O}_3$ , (C)  $\text{UO}_2\text{F}_2$ .

use. Signal averaging is accomplished by adding newly acquired data to old data present in the data array as indicated in subroutine A of Figure 5. The output subroutine allows for output of the blackbody or sample spectrum on either a chart recorder or a line printer. The blackbody spectrum is uncorrected while the sample spectrum is corrected by obtaining the ratio of it and the blackbody spectrum. The output rate to the chart recorder is 5 points per second and can also be adjusted in the software. The input data subroutine provides a means of loading data from magnetic tape, while the store data subroutine allows storage of the spectrum data array on magnetic tape. The exit or clear subroutine provides both a means to exit the program without losing the data stored in memory and to clear the blackbody and/or sample array prior to additional data input. A difference spectrum is produced by loading two sample spectra, then obtaining the point by point subtraction of one corrected spectrum from the other.

**System Evaluation.** Generally, for the purposes of evaluation, correction for source output irregularities should produce a constant value at each wavelength. This is to say that the response of the system should be constant valued if two identical samples are normalized with respect to each other. It is not possible to observe this directly with our system because of the nature of the computer since two identical inputs are dissimilar by 1 part per 256. This error would be amplified to +10 V because of the necessity to maximize the voltage to increase the resolution of the computer output. The spectrum output would not be constant valued in this case and in fact would be discontinuous ranging from 0 to +10 V. System evaluation for the effectiveness of source correction is achieved by examining the spectra of standard materials.

The spectra of holmium oxide, erbium oxide, and uranium tetrafluoride are presented in Figure 6. Holmium oxide was recorded using 5-nm bandpass slits, a 3-s time constant, a 20-nm/min scan rate and is the summation of four spectra. While the 446- and 460-nm bands are clearly distinguishable, the 453-nm band is poorly resolved. Increased resolution can be achieved by decreasing the scan rate to 10 nm/min, through substitution of a different clock motor in the drive of the monochromator, and by decreasing both the chopping rate of the beam chopper to 40 Hz and the bandpass slit width to 3 nm. For general usage, the resolution displayed in the erbium oxide spectrum (10-nm bandpass slits, 1-s time constant, 20 nm/min scan rate, and the summation of two spectra) is quite adequate due to the natural width seen in most ultraviolet-visible spectra. The uranium tetrafluoride spectrum is an example of good resolution of a multiple

banded spectrum having comparatively large absorption coefficients.

Linearity of the signal strength with component concentration and the limit of sample detection are sample dependent due primarily to the background contribution from the more abundant component present and to the magnitude of the absorption coefficient, respectively. Analysis (27) of binary mixtures of uranyl fluoride and uranium tetrafluoride shows a linear relationship between 1% and 90% uranyl fluoride by weight composition vs. the relative photoacoustic signal. This suggests that for a 5-mg sample size, the limit of detection is less than 50  $\mu\text{g}$  for uranyl fluoride and less than 500  $\mu\text{g}$  for uranium tetrafluoride.

## CONCLUSIONS

While the spectral source, monochromator, and computational hardware must be supplied, they are not uncommon laboratory items (costing—monochromator, \$1000; source, \$2700; and today's microcomputer, \$600 to \$5000). The microphone and electronic components described above can be purchased for under \$100 (microphone, \$10; synchronous motor, \$12; transistors, \$5; photodiode, \$2; operational amplifiers, \$15; phase lock loop, \$5; analog multiplier, \$35). This PAS system is for general usage; to encompass the largest number of applicants and applications. Variations of the scheme are certainly possible; e.g., redesign of the detector cell for gas or liquid analysis. The intent is both to present instrumentation and to demonstrate the simplicity of a technique which can provide not only information on the transmission properties (and sample thickness) of opaque solids but information, for the more theoretically inclined, on the nonradiative energy transitions which occur.

## ACKNOWLEDGMENT

The authors thank Douglas R. Anton for technical assistance with the computer software.

## LITERATURE CITED

- (1) A. Rosencwaig and S. S. Hall, *Anal. Chem.*, **47**, 548 (1975).
- (2) A. Rosencwaig, A. P. Ginsberg, and J. W. Koepke, *J. Inorg. Chem.*, **15**, 2540 (1976).
- (3) A. Hordvik and H. Schlossberg, *J. Appl. Opt.*, **16**, 101 (1977).
- (4) J. G. Parker, *J. Appl. Opt.*, **12**, 2974 (1973).
- (5) H. S. Bennett and R. A. Forman, *J. Appl. Opt.*, **15**, 2405 (1976).
- (6) M. J. Adams and G. F. Kirkbright, *Spectrosc. Lett.*, **9**, 255 (1976).
- (7) L. C. Aamodt and J. C. Murphy, *Bull. Am. Phys. Soc.*, **21**, 423 (1976).
- (8) W. Lahmann and H. J. Ludwig, *Chem. Phys. Lett.*, **45**, 177 (1977).
- (9) M. J. Adams, J. G. Highfield, and G. F. Kirkbright, *Anal. Chem.*, **49**, 1850 (1977).
- (10) L. D. Merkle and R. G. Powell, *Chem. Phys. Lett.*, **48**, 303 (1977).
- (11) M. B. Robin, *J. Luminiscence*, **12**, 131 (1976).
- (12) H. E. Eaton and J. D. Stuart, *Spectrosc. Lett.*, **10**, 847 (1977).
- (13) T. H. Maugh, *Science*, **188**, 38 (1975).
- (14) A. Rosencwaig, *Science*, **181**, 657 (1973).
- (15) M. J. Adams, B. C. Beadle, A. A. King, and G. F. Kirkbright, *Analyst (London)*, **101**, 553 (1976).
- (16) A. Rosencwaig and E. Pines, *Biochim. Biophys. Acta*, **493**, 10 (1977).
- (17) M. G. Rockley and J. P. Devlin, *Appl. Phys. Lett.*, **31**, 24 (1977).
- (18) A. Rosencwaig and A. Gershow, *J. Appl. Phys.*, **47**, 64 (1976).
- (19) M. J. Adams and G. F. Kirkbright, *Analyst (London)*, **102**, 281 (1977).
- (20) M. J. Adams, A. A. King, and G. F. Kirkbright, *Analyst (London)*, **101**, 73 (1976).
- (21) M. J. Adams, B. C. Beadle, and G. F. Kirkbright, *Analyst (London)*, **102**, 569 (1977).
- (22) D. M. Munroe and H. S. Reichard, *Am. Lab.*, **9**, 119 (1977).
- (23) F. W. Karasek, *Res./Dev.*, **28**, 38 (1977).
- (24) R. C. Grey, V. A. Fishman, and A. J. Bard, *Anal. Chem.*, **49**, 697 (1977).
- (25) H. V. Malmstadt, C. G. Enke, S. R. Couch, and G. Horlick, "Electronic Measurements for Scientists", W. A. Benjamin, Inc., Reading, Mass., 1974, p. 824.
- (26) G. Horlick and K. R. Berry, *Anal. Chem.*, **47**, 363 (1975).
- (27) H. E. Eaton and J. D. Stuart, unpublished work, the University of Connecticut, Storrs, Conn., 1977.

RECEIVED for review November 16, 1977. Accepted January 11, 1978. The support of this work by the University of Connecticut Research Foundation is gratefully acknowledged.

# Practical Solutions to Matrix Effects in X-ray Fluorescence Analysis by Mathematical Methods

M. T. Haukka\* and I. L. Thomas

School of Earth Sciences, Department of Geology, University of Melbourne, Parkville, Victoria 3052, Australia

**Interrelations between different equations used in x-ray fluorescence (XRF) analysis have been described, enabling the calculation of major oxide concentrations in fused glass specimens, either in the glass itself or on an ignited or unignited basis in the sample. Independent or dependent numerical changes of every factor in the equations have been investigated leading to useful applications. The benefits of these manipulations have been shown with practical examples.**

This article describes in detail different modifications for x-ray fluorescence (XRF) equations used mainly with fused preparation techniques to determine components' concentrations in specimens. The mathematical and physical meanings, and effects of every variable in the equations are probed. In accordance with these investigations, it is possible to generalize earlier specific calculation problems (1-8) encountered in XRF methods.

The purpose of this article is to promote a broader recognition that the determination of new influence coefficients or modification of existing  $\alpha$  factors for matrix correction is a relatively easy matter; and to encourage modification of existing sets of  $\alpha$  factors (or other constants) in certain ways, where this will enable a more effective use or a wider range of practical situations for their use.

## THEORETICAL DISCUSSION

**Evaluation of Equations.** The general practice in XRF analysis, to calculate concentrations, is to compare the measured element's x-ray intensity against the same line intensity in a known reference standard after multiplying by total matrix absorption factor. Mathematically this is expressed in the well known form:

$$C_i = \frac{I_{\text{spec}}}{I_{\text{ref}}} C_{i,\text{ref}} \sum_{j=1}^n \alpha_{ij} C_j \quad (1)$$

Symbols used are fully defined in Appendix I.

The numerical values of  $\alpha$  factors are proportional to each other in a similar way as absorptions of specimen components and they are in usual practice regarded to be independent constants, i.e., invariable in any concentration combinations. However, the  $\alpha$  factors can be normalized, i.e., multiplied by the same number in order to give the summated term the exact value one for some average specimen. At the same time, the Reference Standard is allotted the average specimen's total matrix absorption factor 1.00, although it need not be the average specimen used for normalization.

In many earlier papers (1-3) pure element or oxide has been selected to be Reference Standard and it has been used also as a normalizing average specimen, i.e., its total matrix absorption factor is one. The associated  $\alpha$  factors have been usually further modified by subtracting the value one from each  $\alpha$  factor, and to compensate the change in the total matrix absorption factor, it is necessary to add the same figure one as constant under the summation mark. This operation

is valid so long as  $\sum C_j = 1$ . In this way the "self absorption" factor  $\alpha_{ii}$  becomes zero and the measured element (oxide) does not contribute anything to the total matrix absorption factor, and there are usually positive and negative  $\alpha$  factors with small magnitude. This procedure has a favorable effect because small (or even big) errors in estimated concentrations do not cause excessively large errors in the summated term in Equation 1. By using fused specimens one can obtain positive and negative  $\alpha$  factors by subtracting from every element's  $\alpha$  factor the corresponding flux's  $\alpha$  factor (4). This method is beneficial only if flux's absorption is nearly equal ( $\alpha_{ij} \approx \alpha_{i,\text{sample}}$ ) to the sample's absorption. (See the derivation of equation in Appendix II.)

These manipulations need not be so rigid as described by earlier authors. As a normalizing specimen, it is best to use a composition which is really an average of the specimens analyzed, e.g., an average of basalt and granite in the geological laboratory. As Reference Standard it is best to use a composition giving count rates which are higher than count rates in the average specimen, but not so high to cause troubles with drifting energy peaks in the discriminator window. Zero  $\alpha_{ii}$  factor is useful only if the analyzed element is the most, or nearly the most, abundant element in a specimen. The analyst can easily subtract any constant numerical value from every normalized  $\alpha$  factor and add the same subtracted value as a constant term under the summation mark in Equation 1. This allows useful applications by eliminating any element's effects, one at a time, in the total matrix absorption term.

For instance, with rock analyses, it is useful to make  $\alpha_{i,\text{SiO}_2}$  zero, and at the same time it happens that the  $\alpha$  factors of the second most abundant oxide,  $\text{Al}_2\text{O}_3$ , are also nearly zero. If there is some element, e.g., fluorine or a still lighter element which is difficult or otherwise unnecessary to determine, its effect on the total matrix absorption is easy to eliminate by this method. This is also useful if there is only one element,  $j$ , which has the enhancing effect on the element  $i$  intensity (so that the additional term used by Rasberry and Heinrich (5) can be avoided).

If there are flux containing specimens, it is possible to modify Equation 1 by separating the flux absorption part to obtain Equation 2.

$$C_i (= \frac{M_i}{M_d} W_i) = \frac{I_{\text{spec}}}{I_{\text{ref}}} C_{i,\text{ref}} (\alpha_{if} \frac{M_f}{M_d} + \frac{M_s}{M_d} \sum_{j=1}^n \alpha_{ij} W_j) \quad (2)$$

$M_d/M_s$  is the dilution factor and  $W_j = (M_d/M_s) C_j$  applies to all Equations 2-4, allowing further modifications of those equations.

In order to obtain the concentrations in original and ignited samples, we must multiply every concentration  $C_i$  by the dilution factor  $M_d/M_s$ , or to simplify calculations, we can multiply both sides of Equation 2 by that factor to obtain Equation 3.

$$\frac{M_d}{M_s} C_i (= W_i) = \frac{I_{\text{spec}}}{I_{\text{ref}}} C_{i,\text{ref}} (\alpha_{if} \frac{M_f}{M_s} + \sum_{j=1}^n \alpha_{ij} W_j) \quad (3)$$

Table I. Concentration and Total Matrix Absorption Factor Calculations by Using Binary Component Fused Specimens

Weight fraction SiO <sub>2</sub>			Total matrix absorption factor for Si K $\alpha$		
Case A: 2 g LiBO <sub>2</sub> -flux + 0.6 g SiO <sub>2</sub> + 0.4 g Fe <sub>2</sub> O <sub>3</sub> ; basic $\alpha$ factors <sup>a</sup>					
Eq 2	0.6/3	= 0.20	0.2655 $\times$ 2/3	+ 0.308 $\times$ 0.20 + 0.745 $\times$ 0.1333	= 0.3379
Eq 3	3/1 $\times$ 0.6/3	= 0.60	0.2655 $\times$ 2/1	+ 0.308 $\times$ 0.60 + 0.745 $\times$ 0.40	= 1.0138
Eq 4	0.6/3	= 0.60	0.2655 $\times$ 2	+ 0.308 $\times$ 0.60 + 0.745 $\times$ 0.40	= 1.0138
Ratios 0.20:0.60:0.60 = 0.3379:1.0138:1.0138					
Case B: 2 g LiBO <sub>2</sub> -flux + 0.3 g SiO <sub>2</sub> + 0.1 g Fe <sub>2</sub> O <sub>3</sub> ; basic $\alpha$ factors					
Eq 2	0.3/2.4	= 0.125	0.2655 $\times$ 2/2.4	+ 0.308 $\times$ 0.125 + 0.745 $\times$ 0.0417	= 0.2908
Eq 3	2.4/0.4 $\times$ 0.3/2.4	= 0.75	0.2655 $\times$ 2/0.4	+ 0.308 $\times$ 0.75 + 0.745 $\times$ 0.25	= 1.7448
Eq 4	2.4 $\times$ 0.3/2.4	= 0.30	0.2655 $\times$ 2	+ 0.308 $\times$ 0.30 + 0.745 $\times$ 0.10 + 0.000 $\times$ 0.60	= 0.6979
Ratios 0.125:0.75:0.30 = 0.2908:1.7448:0.6979					
Case C: Disk as for Case B; modified $\alpha$ factors (modification: $k_{if,mod} = 1$ for Eq 4) <sup>b</sup>					
Eq 2	0.3/2.4	= 0.125	0.469 - 0.2035 $\times$ 2/2.4 + (-0.161)0.125 + 0.276 $\times$ 0.0417		= 0.2908
Eq 3	2.4/0.4 $\times$ 0.3/2.4	= 0.75	0.469 + 0.2655 $\times$ 2/0.4 + (-0.161)0.75 + 0.276 $\times$ 0.25		= 1.7448
Eq 4	2.4 $\times$ 0.3/2.4	= 0.30	0.469 + 0.2655 $\times$ 2 + (-0.161)0.30 + 0.276 $\times$ 0.10 + (-0.469)0.60		= 0.6979

<sup>a</sup> Basic  $\alpha$  factors from literature (9):  $k_{if} = 0.531$  and  $\alpha_{if} = k_{if}/M_f = 0.2655$ ;  $\alpha_{i, SiO_2} = 0.308$ ;  $\alpha_{i, Fe_2O_3} = 0.745$ . <sup>b</sup> Explanations for modified  $\alpha$  factors:  $k_{if,mod} - k_{if} = 0.469$ ;  $\alpha_{if,mod} = \alpha_{if} - 0.469 = -0.2035$  (applies only to Eq 2 because only here  $W_{flux}$  is needed to bring  $\Sigma W = 1.0$ );  $\alpha_{i, SiO_2, mod} = \alpha_{i, SiO_2} - 0.469 = -0.161$ ;  $\alpha_{i, Fe_2O_3, mod} = \alpha_{i, Fe_2O_3} - 0.469 = 0.276$ ;  $\alpha_{i, Loss, mod} = 0 - 0.469 = -0.469$ ;  $W_{Loss} = 1 - (M_S W_{SiO_2} + M_S W_{Fe_2O_3}) = 0.60$ .

<sup>a</sup> Basic  $\alpha$  factors from literature (9):  $k_{if} = 0.531$  and  $\alpha_{if} = k_{if}/M_f = 0.2655$ ;  $\alpha_{i, SiO_2} = 0.308$ ;  $\alpha_{i, Fe_2O_3} = 0.745$ . <sup>b</sup> Explanations for modified  $\alpha$  factors:  $k_{if,mod} = k_{if} = 0.469$ ;  $\alpha_{if,mod} = \alpha_{if} - 0.469 = -0.2035$  (applies only to Eq 2 because only here  $W_{flux}$  is needed to bring  $\Sigma W = 1.0$ );  $\alpha_{i, SiO_2, mod} = \alpha_{i, SiO_2} - 0.469 = -0.161$ ;  $\alpha_{i, Fe_2O_3, mod} = \alpha_{i, Fe_2O_3} - 0.469 = 0.276$ ;  $\alpha_{i, Loss, mod} = 0 - 0.469 = -0.469$ ;  $W_{Loss} = 1 - (M_s W_{SiO_2} + M_s W_{Fe_2O_3}) = 0.60$ .

By multiplying both sides in Equation 2 by  $M_d$ , we obtain Equation 4.

$$M_d C_i (= M_s W_j) = \frac{I_{spec}}{I_{ref}} C_{i,ref} (\alpha_{if} M_f + M_s \sum_{j=1}^n \alpha_{ij} W_j) \quad (4)$$

At first sight, this seems to be paradoxical but it is, however, the simplest, most useful, and most used equation for fused specimens. If  $M_f$  and  $M_s$  are constants and there is no ignition loss or gain, it behaves similarly to the earlier equations, and the flux absorption contribution is constant as it should be. But if there is ignition loss or gain or if the weight,  $M_s$ , is different from the standardized value, the flux absorption contribution should change in spite of constant  $M_f$ . (In practice it is best to weigh accurately dried flux and sample quickly to the range of  $\pm 5\%$  from standardized weights and feed these together with the fused glass weight and intensity values to computer which converts weighed  $M_s/M_f$  ratio to correspond to the constant standardized  $M_f$  weight and, of course, calculates ignition loss or gain and the final concentrations). From the mathematical point of view, we can thus see that the term  $\alpha_{if} M_f$  in Equation 4 is constant in all conditions, and in order to function properly  $\Sigma M_s W_j$  must contain also the ignition loss or gain, or the corresponding difference from the standardized weights if the  $M_s/M_f$  ratio is not the usual. After adding loss (positive) or gain (negative) values as weight fractions to the other oxide concentrations in the sample,  $\Sigma(M_s W_j + W_{loss})$  becomes 1.00.

If all  $\alpha$  factors are in original forms, i.e., their ratios to each other are the same as ratios of real oxides' absorptions at the wavelength of any measured line, Equation 4 retains also physical reality, even though the  $M_s/M_f$  ratio may not have the standardized constant value in the fused glass. When the standardized  $M_f$  weight is 2.0 g and sample is 1.0 g, and if  $M_d$  is 2.9 g, it means that the ignition loss is 10% (flux has no loss). We can imagine that this 10% ( $H_2O + CO_2$ ) leaves empty holes scattered evenly in the glass. This vacancy "mass" concentration has no absorption ability and accordingly its corresponding  $\alpha_{i,loss}$  factors are zero; only fills the gap in the  $\Sigma M_s W_j$  term in order to make it 1.0.

For Equation 4, we can modify  $\alpha$  factors as described earlier, for instance subtracting  $\alpha_{i, SiO_2}$  from all  $\alpha_{ij}$  factors and adding the same value as constant (which we can combine with the

other ("flux") constant  $\alpha_{if} M_f (= k_{if})$ . Also in this case loss (or gain) behaves like a real element or oxide component and we must subtract  $\alpha_{i, SiO_2}$  also from  $\alpha_{i,loss}$  values which were earlier zero.

Actually this "ghost" vacancy mass concentration is not so mysterious because it is analogous with the treatment in solid state physics of vacant positions in crystals as real particle components in mathematical calculations. Although in fused glass, escaped  $H_2O$  and  $CO_2$  molecules do not really leave any vacant positions, the counter does not see any differences between these cases because vacancies are filled in the same proportion as ions exist in the final fused glass, and the same physical reality still holds as described earlier. The change in glass volume between these imagined "hollow" and "solid" forms is not so great as to cause any difference in the geometry of the x-ray beam.

**Numerical Comparison between the Equations.** Table I shows in detail the interrelation between Equations 2-4 by using as examples binary component ( $SiO_2$ - $Fe_2O_3$ ) fused specimens. The ratio 1:2 (1 g sample + 2 g  $LiBO_2$ -flux) is the basic dilution used in calibration (9, 10). The counter sees the situation to be similar in spite of what equation is used and thus the factors  $I_{spec}/I_{ref}$  and  $C_{i,ref}$  are the same for all equations. Therefore they do not affect the ratios in concentration and total matrix absorption factor values between the equations mentioned, and we need not take those factors into consideration in this context, although we could well insert these measured intensity and calibrated Reference Standard concentration values into the equations.

**Background Determination.** Intensity measurement at peak position gives total intensity  $I_p$ . In order to obtain net intensity  $I_p - I_b$ , we can measure background on one or both sides of the peak or even determine background profile between both background positions (11). Measured background intensity is used generally for trace elements.

For major and minor elements, calculated background is used more often. It is considered that  $I_p - I_b$  and  $I_b$ , at the same wavelength, behave similarly with respect to the total matrix absorption factor although at longer wavelengths  $I_b$  is not so accurately inversely proportional to this quantity (12). Thus, after being multiplied by the total matrix absorption factor,  $I_b$  is a constant for all specimens and its numerical value



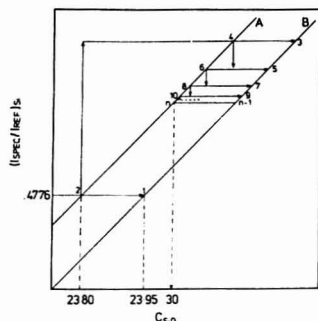


Figure 1. Graphical expression for nominal and background concentrations and for iteration process. Numerical examples represent Table II values, but the lines are not in actual proportion in order to make the figure clearer.

is the same as the background intensity for the average specimen, i.e., for the specimen where the total matrix absorption factor = 1.0. This constant can be subtracted directly from  $I_p$ , or  $I_b$  can be multiplied by the rest of Equations 1, 2, or 4 devoid of  $I_p$ . This gives a constant background the dimension of which is the same as the corresponding element's concentration. With Equation 3, we can not regard the background as a constant concentration, because, in that case, pure flux would give for any element's concentration an infinitely high value ( $M_i/M_j = \infty$ , and at the same time  $I_p \rightarrow 0$ ).

Figure 1 applies to Equation 4, where line A is the calibration line for  $\text{SiO}_2$  (intensities are dead time corrected and multiplied by the total matrix absorption factor). Line B goes through the origin and is parallel to line A, and it (B) gives the so-called nominal concentration percentage of each specimen. The distance between these parallel lines, in the direction of the X axis, is the constant background concentration. Line B gives also the nominal percentage for the Reference Standard, its value corresponding to the ordinate value 1.0. In order to make the figure clearer, the positions of the lines are not in actual proportion.

**Iteration Process.** In Equations 2-4,  $W_j$  values are not known initially. The main principle is to estimate the best possible concentration values and insert these into the place of  $W_j$  values in the equations, calculate concentrations (with background subtracted) for every component, and insert these better values again into the place of  $W_j$ . This iteration process continues so long as concentration values converge. If some elements' concentrations are determined independently beforehand, they are inserted directly into the equation and these  $W_j$  values are constants during the iteration. Considering  $M_i$  and  $M_j$  before the summation mark in Equations 2 and 4 and combining these with the  $W_j$  value, it is clear that the expressions for the concentration in both sides of the equations are identical.

Figure 1 shows graphically how iteration proceeds by using Equation 4 and background expressed as concentration, and subtracted each time. The example is a specimen containing 30%  $\text{SiO}_2 + 70\% \text{Al}_2\text{O}_3$  by using 1:2 dilution with  $\text{LiBO}_2$ -flux. Table II shows the same steps in an algebraic form.

The concentrations are converging whether or not we subtract the background in every cycle (Table II), but the final concentrations are slightly higher if we subtract the background only once after the first convergence (columns 3 and 4). If we continue iteration from this point by subtracting the background in every cycle, the concentrations will converge the second time and the final figures will be exactly the same

Table II. Successive Iterations for 30%  $\text{SiO}_2 + 70\% \text{Al}_2\text{O}_3$ . Concentrations are Weight Fractions

	Backgr. subtract. after every step		Backgr. was not subtracted	
	$\text{SiO}_2$	$\text{Al}_2\text{O}_3$	$\text{SiO}_2$	$\text{Al}_2\text{O}_3$
Intensity ratios $R_i$	0.4776	3.4134	0.4776	3.4134
Nominal %	0.2395	0.7595	0.2395	0.7595
Nominal % - backgr.	0.2380	0.7586		
Iteration steps				
1.	0.3067	0.6989	0.3086	0.7003
2.	0.2989	0.7012	0.3009	0.7029
3.	0.2988	0.6999	0.3009	0.7017
4.	0.2986	0.6996	0.3006	0.7014
5.	0.2985	0.6995	0.3006	0.7013
6.	0.2984	0.6995	0.3005	0.7013
7.	0.2984	0.6994	0.3005	0.7013
Backgr. subtracted finally			0.2990	0.7004

as if we had subtracted the background every time from the very beginning according to Figure 1.

Table II applies to a binary mixture where all other oxide concentrations are expected to be zero and, since they do not participate in the iteration process, they don't contribute anything to the total matrix absorption factor. However, in practice there is a bigger set of influence  $\alpha$  factors for computation (10-20 absorbers). If we subtract the background only once (in the final iteration cycle), we include all the background concentrations in the total matrix absorption factor calculation right until convergence, though we might have only a one-component specimen. This example is a further proof that we should subtract the background in every cycle according to Figure 1, to obtain immediately the best possible estimates of concentration.

If there are both positive and negative  $\alpha$  factors, convergence takes place more quickly, than if there were only positive  $\alpha$  factors.

**Interplay between Dead Time and  $\alpha_{ij}$  Factor.** Inspection of the earlier equations shows that at high concentrations even a small increase (decrease) in dead time or  $\alpha_{ij}$  factor increases (decreases) drastically the calculated concentration. More detailed inspection shows that both these factors have quite a parallel effect on concentration, i.e., a change in dead time can be completely compensated by the change of  $\alpha_{ij}$  factor or vice versa. Because the Reference Standard count rate also changes with dead time, it is necessary to compensate this change by changing the Reference Standard nominal percentage proportionately by the same amount in the same direction. In practice this operation may be useful to know, because different x-ray tubes and geometry of spectrometers give a different  $\alpha_{ij}$  factor owing to the high primary beam absorption contribution to  $\alpha_{ij}$  for heavy elements (9, 10).

For the  $\text{LiBO}_2$  fusion system, changing the dead time by a factor of 4 from 1.2 to 4.8  $\mu\text{s}$  (actual value 2.4  $\mu\text{s}$ ) is exactly balanced by changing, for instance, the  $\alpha_{\text{Si, Si}}$  factor from 0.357 to 0.211, and the  $\alpha_{\text{Fe, Fe}}$  factor from 1.274 to 0.788, with simultaneous Reference Standard % change from 48.959 to 52.716%, and from 7.361 to 7.634%, respectively.

## EXPERIMENTAL

The basis for the following calculations are  $\text{LiBO}_2$ -fused specimens and calculation of composition using Equation 4 and a set of  $\alpha$  factors published earlier (9).

Table III, line 1 shows computer calculated concentrations for our laboratory's basalt standard DCB-1 by using  $\alpha$  factors in the original form, i.e., all positive and  $\alpha_{\text{Li, Li}} = 0$ . In line 2,  $k_{ij} = 1.000$ , which has been obtained by subtracting  $(1 - \text{original } k_{ij})$  from all  $\alpha_{ij}$  factors, and by adding this constant to the original  $k_{ij}$  value giving the new  $k_{ij}$  value, 1.000. Lines 3 and 4 are the same as lines 1 and 2, except the fused glass has been ground and pelletized. Line 5 shows the concentrations, when  $\alpha_{\text{Si, Si}} = 0$ , i.e.,  $\alpha_{\text{Si, Si}}$  has

Table III. Concentration Comparison for Glass Disks and Powder Pellets by Using Basic and Modified  $\alpha$  Factors<sup>a</sup>

Type of $\alpha$ factors	SiO <sub>2</sub>	TiO <sub>2</sub>	Al <sub>2</sub> O <sub>3</sub>	Fe <sub>2</sub> O <sub>3</sub>	MnO	MgO	CaO	K <sub>2</sub> O	P <sub>2</sub> O <sub>5</sub>	Na <sub>2</sub> O	Total
1. $\alpha_{i,loss} = 0$	51.82	1.78	14.71	10.56	0.155	7.37	8.90	0.99	0.30	3.03	99.62
2. $k_{if} = 1$	+0.05	0.00	+0.01	+0.02	0.00	0.00	+0.01	0.00	0.00	0.00	+0.09
3. $\alpha_{i,loss} = 0$ (powdered)	-0.28	-0.05	-0.40	-0.36	-0.01	-0.18	-0.24	-0.03	0.00	-0.01	-1.56
4. $k_{if} = 1$ (powdered)	+0.19	-0.02	-0.28	-0.21	-0.01	-0.12	-0.11	-0.02	0.00	+0.01	-0.57
5. $\alpha_{i,SiO_2} = 0$	+0.01	0.00	0.00	+0.01	0.00	0.00	+0.01	0.00	0.00	+0.01	+0.04
6. $\alpha_{i,loss} = 0$ (SiO <sub>2</sub> > 2%)	+0.34	+0.02	+0.08	+0.13	0.00	+0.04	+0.11	+0.01	0.00	+0.02	+0.75
7. $\alpha_{i,SiO_2} = 0$ (SiO <sub>2</sub> > 2%)	-	0.00	0.00	0.00	0.00	0.00	0.00	0.00	0.00	0.00	0.00
8. $\alpha_{i,loss} = 0$ (Na <sub>2</sub> O = 0)	-2.35	-0.08	-0.66	-0.50	-0.01	-0.33	-0.42	-0.05	-0.01	-	-4.41
9. $\alpha_{i,SiO_2} = 0$ (Na <sub>2</sub> O = 0)	-0.67	+0.02	-0.22	+0.13	0.00	-0.12	+0.11	+0.01	0.00	-	-0.74
10. $\alpha_{i,loss} = 0$	67.55	0.617	14.73	4.29	0.065	1.56	2.89	4.01	0.17	3.15	99.03
11. $k_{if} = 1$	+0.13	0.00	+0.02	+0.01	0.00	0.00	+0.01	+0.01	0.00	0.00	+0.18
12. $\alpha_{i,loss} = 0$ (powdered)	-1.07	-0.02	-0.37	-0.16	0.00	-0.04	-0.09	-0.14	+0.01	-0.07	-1.95
13. $k_{if} = 1$ (powdered)	-0.18	-0.01	-0.21	-0.07	0.00	-0.02	-0.03	-0.07	+0.01	-0.04	-0.62
14. $\alpha_{i,loss} = 0$	-0.16	0.00	-0.13	-0.04	+0.01	-0.07	-0.02	0.00	+0.01	+0.01	-0.39
15. $k_{if} = 1$	+0.17	0.00	-0.06	-0.02	+0.01	-0.06	-0.01	+0.02	+0.01	+0.02	+0.08
16. $\alpha_{i,loss} = 0$ (powdered)	-1.10	-0.02	-0.40	-0.18	+0.01	-0.07	-0.11	-0.16	+0.01	+0.03	-1.99
17. $k_{if} = 1$ (powdered)	-0.06	0.00	-0.15	0.00	+0.01	-0.03	0.00	+0.01	0.00	+0.05	-0.17
18. $\alpha_{i,loss} = 0$ (powdered)	-7.69	-0.07	-1.21	-0.64	-0.01	0.00	-0.47	-0.54	+0.01	-0.17	-10.79
19. $k_{if} = 1$ (powdered)	-2.56	-0.01	-0.22	-0.20	+0.01	+0.13	-0.20	-0.16	+0.02	+0.03	-3.16

<sup>a</sup> Line 1: actual values of DCB-1 basalt standard, LOI = 0.1%. Line 10: actual values of CGD-1 granodiorite standard, LOI = 0.5%. Differences in absolute %, positive if greater than expected. Line 6: +0.34 for SiO<sub>2</sub> is additional difference after subtraction of simulated error, absolute %. Glasses (No. 3, 4, 12, 13, 16, and 17) have been ground in agate mortar and therefore SiO<sub>2</sub> contents are slightly too high.

been subtracted from all  $\alpha_{ij}$  factors, and added to the flux constant  $k_{if}$ . In lines 6 and 7,  $\alpha$  factors are identical to those in lines 1 and 5, but there is a simulated error (2% increase in dead time corrected counts for Si K $\alpha$  radiation). Also lines 8 and 9 correspond to lines 1 and 5, except Na<sub>2</sub>O has not been counted. Lines 10–13 correspond to the same conditions as lines 1–4, using granodiorite CGD-1 instead of DCB-1. Lines 14–17 correspond to lines 10–13, except dilution ratio for CGD-1 is 2.22. Lines 18 and 19 correspond to lines 16 and 17, but "dry mix", i.e. pelletized unfused flux + CGD-1 rock powder mixture was used.

### DISCUSSION

The theoretical section contains the derivations of different modifications for the basic Equation 1. Table I shows the meaning of these equations in practice, when original, basic ( $\alpha_{i,loss} = 0$ ) and modified  $\alpha$  factors are used. The determination of basic (all-positive)  $\alpha$  factors is presented in our earlier paper (9).

If the ignition loss, LOI, is not important to determine by weighing, and all the major components have been determined (either by XRF or independently) and included in the matrix calculation, it is best to use basic  $\alpha$  factors. LOI is simply obtained by difference from 100% in the final total; an obvious saving in preparation time. It is not so simple to determine LOI when  $\alpha_{i,loss} \neq 0$ .

If there is an error in one component's count rate (or one or more major components are not determined) and we use all positive  $\alpha$  factors, this single count rate error does not cause error only in that component, but it transfers the error (through faulty total matrix absorption factor) into other components' concentrations. This process continues further during iterations, causing a "snowballing effect". Although the concentration values converge, this phenomenon has a harmful effect as we see in Table III, specimens No. 6 and 8. The use of the modified  $\alpha$  factors reduces this "snowballing effect" ( $\alpha$  factors are positive and negative and nearer value 0), as we see in the specimens No. 7 and 9, where the input count rates are exactly the same as in No. 6 and 8, (the modifications  $k_{if} = 1$  or  $\alpha_{i,SiO_2} = 0$  for the set of  $\alpha$  factors are practically the same; compare No. 2 and 5).

This "snowballing effect" is still more striking, if there are errors in all count rates in the same direction, and  $\alpha_{i,loss} = 0$ . This is the case if we analyze flux-containing powder pellets by using standard calibration for corresponding glass disks. Because some oxides (Cr, Ti, Zr) at high concentrations

crystallize when such glass melts cool before pressing the disk, or some are volatile (As, Hg), it is necessary in the first case to cool the glass extremely quickly by some coolant (water, solid CO<sub>2</sub>, liquid nitrogen) to avoid crystallization (at high temperature Cr, Ti, Zr are soluble) then grind and pelletize it or, in the latter case, simply grind it with flux ("dry mix") and pelletize without fusing. By comparing the count rates of these powder pellets against those of the corresponding glass disks, we find that powder pellet values are lower. The benefits of the modified  $\alpha$  factors in this case are to be seen by comparing Table III specimens No. 3 and 4; 12 and 13; 16 and 17; 18 and 19. The specimens No. 4, 13, 17, and 19 are clearly usable; the errors introduced to any element oxide by increasing the calculated result by 0.6% relative for ground glasses, and 3% relative for dry mix, are not significant. Recalibration of the Reference Standard nominal percentages and the Background values can yield still better values from flux-containing powder pellets.

### CONCLUSIONS

This article is aimed at the proposition that  $\alpha$  factors—or matrix correction parameters in general—can be changed, to analytical advantage.

The way in which they can be changed has been given a general basis, and was illustrated by examples of calculations for geological samples.

The rationale behind the success of such "number juggling" has once again been on a general basis, and we think draws attention to the fact that all previous manipulations of  $\alpha$  factors, such as those of Lucas-Tooth and Pym (6), Traill and Lachance (7), Hughes (8), Rasberry and Heinrich (5), Norrish and Hutton (4), Tertian (3), and others, fit into a broad set of principles.

A major criticism of even the most empirical methods of matrix correction used by these authors, is that they have been too concerned with relating some part of the  $\alpha$  factor derivation to "theoretical fundamentals", and in some cases have sacrificed some of the benefits such as mathematical stability, more rapid iteration, or a null effect for the major absorber or the LOI, which can be arranged by judicious manipulation.

Finally, we express the hope that people involved in XRF analysis will use  $\alpha$ -factor correction instead of simply relying on calibration graphs (80% of XRF determinations use this

method (12)), and possibly even do some "number juggling" for themselves.

## APPENDIX I

### Symbols and Definitions Used

Sample	material (rock, mineral, etc.) to be analyzed.
Specimen	final preparation for XRF analysis is glass disk, resulting from fusion of sample with flux.
$C_i$	concentration of component $i$ in specimen (glass), weight fraction.
$I_{\text{spec}}$	X-ray intensity at analytical wavelength of element $i$ , for specimen.
$I_{\text{Ref}}$	X-ray intensity of Reference Standard.
$C_{i,\text{Ref}}$	nominal concentration of $i$ in Reference Standard (usually calibrated to give concentration on sample basis for unknown samples).
$W_j$	weight fraction of component $j$ in sample, volatile free basis in Equations 2-4.
$\alpha_{ij}$	experimental interelement influence coefficient of influencing (absorber) oxide $j$ on emitter $i$ ( $\alpha$ consists of secondary beam absorption and possible primary beam absorption and enhancement effects).
$\alpha_{if}$	influence coefficient of flux for emitter $i$ .
$k_{if}$	flux constant ( $= \alpha_{if} M_f$ ).
$M_s, M_f, M_d$	weights of sample, flux, and fused glass disk, all on volatile, LOI, free basis. ( $M_s$ can be on volatile containing basis in Equation 4, but in that case $W_j$ must be also on volatile containing basis in order to obtain the same numerical figure as $M_s W_j$ gives when the both factors are on volatile free basis).
$M_d/M_s$	dilution factor (so that $W_j = M_d/M_s \times C_j$ ).
$\mu_{i,\text{spec}}$	total matrix absorption factor of specimen (glass) at analytical wavelength of emitter $i$ (summed term in Equation 1, bracketed term in all other equations).
LOI	loss on ignition.

## APPENDIX II

The derivation of the expression where the actual influence coefficients are the differences between components' and flux's influence coefficients:

$$\left. \begin{aligned} \mu_{i,\text{spec}} &= \alpha_{if} \frac{M_f}{M_d} + \frac{M_s}{M_d} \sum_{j=1}^n \alpha_{ij} W_j \\ &= \alpha_{if} \frac{M_d - M_s}{M_d} + \frac{M_s}{M_d} \sum_{j=1}^n \alpha_{ij} W_j \\ &= \alpha_{ij} - \alpha_{if} \frac{M_s}{M_d} + \frac{M_s}{M_d} \sum_{j=1}^n \alpha_{ij} W_j \\ &= \alpha_{if} + \frac{M_s}{M_d} \sum_{j=1}^n (\alpha_{ij} - \alpha_{if}) W_j \end{aligned} \right\} \text{from Equation 2}$$

$$\mu_{i,\text{spec}} = \alpha_{if} M_d + M_s \sum_{j=1}^n (\alpha_{ij} - \alpha_{if}) W_j \quad \text{to Equation 4}$$

The same derivation could have been obtained by the general principle presented in the Theoretical section: adding  $\alpha_{if} M_s$  in Equation 4 to the flux constant  $\alpha_{if} M_f$  (because  $M_s + M_f = M_d$ ), and subtracting the same from  $M_s \alpha_{ij}$ .

In the last expression,  $M_s W_j$  includes also ignition loss or gain, and we have a Loss correction equal to  $-M_s \alpha_{ij}$ . This is the Loss correction factor of Norrish and Hutton (4), who also give the physical explanation for this type of modified matrix correction.

## ACKNOWLEDGMENT

We thank J. F. Lovering and A. Cundari in the Geology Department and M. A. Chaudhri in the Physics Department for their help and critical reading of the paper, and T. C. Hughes for the effective management of the XRF-XRD laboratory.

## LITERATURE CITED

- (1) G. R. Lachance, *Can. Spectrosc.*, **15**, 64 (1970).
- (2) D. A. Stephenson, *Anal. Chem.*, **43**, 310 (1971).
- (3) R. Tertian, *X-Ray Spectrom.*, **4**, 52 (1975).
- (4) K. Norrish and J. T. Hutton, *Geochim. Cosmochim. Acta*, **33**, 431 (1969).
- (5) S. D. Raspberry and K. F. J. Heinrich, *Anal. Chem.*, **46**, 81 (1974).
- (6) H. J. Lucas-Tooth and C. Pyne, *Adv. X-Ray Anal.*, **7**, 523 (1964).
- (7) R. J. Traill and G. R. Lachance, *Can. Spectrosc.*, **11**, 63 (1966).
- (8) H. Hughes, *Analyst (London)*, **97**, 161 (1972).
- (9) M. T. Haukka and I. L. Thomas, *X-Ray Spectrom.*, **6**, 204 (1977).
- (10) I. L. Thomas and M. T. Haukka, *Chem. Geol.*, **21**, 39 (1978).
- (11) B. W. Chappell, W. Compston, P. A. Arriens, and M. J. Vernon, *Geochim. Cosmochim. Acta*, **33**, 1002 (1969).
- (12) R. Jenkins, *Philips Scientific and Analytical Equipment Bulletin*, 79.177/FS27 (1969).

RECEIVED for review September 12, 1977. Accepted December 12, 1977.

# Two-Phase Buffer Systems: Theoretical Considerations

Tomislav J. Janjić\* and Emil B. Milosavljević

Chemical Institute, Faculty of Sciences, University of Belgrade, P.O. Box 550, 11001 Belgrade, Yugoslavia

In this paper, two-phase buffer systems are described. These systems are made of two phases: one is an aqueous (buffered) phase and the other is a less polar water-insoluble phase which serves only as the reservoir for one of the components of an acid-base pair. It is established that two-phase buffer systems have the following advantages over classical (monophase) systems: (1) With the same acid-base pair, the pH value at which the buffer capacity has its maximum can be varied with variation of experimental conditions; and (2) Acids and bases which are almost insoluble in water can also be used for preparing two-phase buffers. The extraction mechanism of action of such buffers proposed in the present paper has been experimentally confirmed.

So far, numerous monophase buffer systems have been described in the literature. They consist of an acid-base pair dissolved in a single phase, most frequently water. These buffers have their maximum buffer capacity at  $\text{pH} = \text{p}K_a$ , while their region of practical application ( $\beta > 0.19 C_{\text{tot}}$ ) lies within the limits  $\text{pH} = \text{p}K_a \pm 1$  (1). These limitations considerably hinder the selection of suitable acid-base pairs, especially since the very chemical nature of a buffer is frequently of decisive importance as regards to its applicability in a given case. For the above mentioned reasons, synthesis and application of acids with suitable  $\text{p}K_a$  values and other properties, as required for their use in the preparation of buffer solutions, is a problem of constant interest.

For some time we have been working on a different approach to this problem. We have been studying buffer systems consisting of two phases: a water (buffered) phase, and another, less polar, water insoluble phase, which serves only as the reservoir for one of the components of the acid-base pair used. In the less polar phase, only the charge-free component of the acid-base pair will be present in an appreciable concentration, whereas the charge-carrying component is retained in the more polar, water phase.

So far, few papers dealing with acid-base equilibria in two-phase systems, either liquid-liquid (2-4), liquid-resin exchanger (5), or liquid-solid (6-8), have been published. In these papers, buffer capacity of the investigated systems has not been considered.

Setnikar (9) has studied acid-base equilibria in systems containing the insoluble solid base as the second phase, and he has derived the functional dependence of buffer capacity on the fraction titrated for such systems. The time needed for equilibration of these heterogeneous systems is long, and the buffer curves are essentially different from those obtained for two-phase buffers described in the present paper.

Komar (10) has theoretically investigated differential titration of two monoprotic acids in an aqueous-organic solvent system, and he has derived the equation for calculating the buffer capacity at the pH value corresponding to the first equivalence point. On the basis of this equation, the possibility of such titrations is considered.

As can be seen from the foregoing, two-phase buffer systems proposed in the present paper have not been described in the literature as yet. This paper offers theoretical considerations

of such buffers and points to some of their advantages over classical (monophase) buffer systems.

## MATHEMATICAL CONSIDERATIONS

In deriving the relationships given below, it is assumed that the ionic strength of the solution is equal to zero, since in this case it may be written that:  $\text{pH} = -\log C_H$ .

Depending on whether the acid or base component of the acid-base pair is a nonelectrolyte, a distinction must be made between two types of two-phase buffer systems, the mathematical treatment of each differing somewhat.

**Buffer Type I (Molecular Acid/Anionic Base).** For this type of buffer, the following relationship holds:

$$K_a^{\text{app}} = \frac{C_H C_b}{C_a^{\text{app}}} \quad (1)$$

where  $K_a^{\text{app}}$  is the apparent acid dissociation constant,  $C_H$  is the concentration of hydronium ions in the water phase,  $C_b$  is the concentration of the anionic base in the water phase, and  $C_a^{\text{app}}$  is the apparent concentration of nonprotolyzed acid in the water layer. The apparent concentration of a component in the water phase is the concentration that would exist if the total amount of that component, in the entire system, were dissolved in the water phase alone.

From the mass balance equation it follows that

$$C_a^{\text{app}} = C_{\text{tot}}^{\text{app}} - C_b \quad (2)$$

where  $C_{\text{tot}}^{\text{app}}$  is the apparent total concentration of the acid-base pair.

Substituting in Equation 1  $C_{\text{tot}}^{\text{app}} - C_b$  for  $C_a^{\text{app}}$  and solving for  $C_b$ , we obtain

$$C_b = \frac{K_a^{\text{app}} C_{\text{tot}}^{\text{app}}}{K_a^{\text{app}} + C_H} \quad (3)$$

Differentiation,  $dC_b/dC_H$ , of Equation 3 and substitution of  $dC_H$  with  $-2.303 C_H \text{ dpH}$ , gives the following relationship for buffer capacity ( $\beta_{\text{Hb}}$ ):

$$\frac{dC_b}{\text{dpH}} = \beta_{\text{Hb}} = 2.303 \frac{K_a^{\text{app}} C_{\text{tot}}^{\text{app}} C_H}{(K_a^{\text{app}} + C_H)^2} \quad (4)$$

Substituting in Equation 1  $C_{\text{tot}}^{\text{app}} - C_a^{\text{app}}$  for  $C_b$  and solving the resulting equation for  $C_a^{\text{app}}$  we get

$$C_a^{\text{app}} = \frac{C_H C_{\text{tot}}^{\text{app}}}{K_a^{\text{app}} + C_H} \quad (5)$$

Multiplying Equation 3 by Equation 5 and dividing the product by  $C_{\text{tot}}^{\text{app}}$  we obtain

$$\frac{C_a^{\text{app}} C_b}{C_{\text{tot}}^{\text{app}}} = \frac{K_a^{\text{app}} C_{\text{tot}}^{\text{app}} C_H}{(K_a^{\text{app}} + C_H)^2} \quad (6)$$

From Equations 4 and 6, we arrive at the relationship

$$\beta_{\text{Hb}} = 2.303 \frac{C_a^{\text{app}} C_b}{C_{\text{tot}}^{\text{app}}} \quad (7)$$

For two-phase buffers containing a molecular acid the following relationship applies:

$$C_a^{app} = C_a \left( \frac{V_o}{V_w} (K_p)_a + 1 \right) \quad (8)$$

where  $C_a$  is the concentration of nonprotonated acid in the water phase,  $V_o$  and  $V_w$  are the equilibrium volumes of the organic and water phase, respectively, and  $(K_p)_a$  is the ratio of the concentration of the molecular acid in the organic phase to that in the water phase (partition coefficient).

From Equations 1 and 8 it follows that the apparent acid dissociation constant ( $K_a^{app}$ ) and acid dissociation constant, defined as  $K_a = (C_H C_b)/C_a$ , are interrelated by the following equation:

$$K_a^{app} = \frac{K_a}{\frac{V_o}{V_w} (K_p)_a + 1} \quad (9)$$

Taking the logarithm of the equation obtained, and multiplying it by -1, we get

$$pK_a^{app} = pK_a - p \left( \frac{V_o}{V_w} (K_p)_a + 1 \right) \quad (10)$$

**Buffer Type II (Cationic Acid/Molecular Base).** For this type of buffer, the following relationship holds:

$$K_a^{app} = \frac{C_H C_b^{app}}{C_a} \quad (11)$$

where  $C_a$  is the concentration of cationic acid in the water phase, and  $C_b^{app}$  is the apparent concentration of nonprotonated base in the water layer.

Further mathematical treatment, analogous to that for two-phase buffers of type I, gives the following equations:

$$\frac{dC_b^{app}}{dpH} = \beta_{Hb} = 2.303 \frac{K_a^{app} C_{tot}^{app} C_H}{(K_a^{app} + C_H)^2} \quad (12)$$

$$\beta_{Hb} = 2.303 \frac{C_a C_b^{app}}{C_{tot}^{app}} \quad (13)$$

$$pK_a^{app} = pK_a + p \left( \frac{V_o}{V_w} (K_p)_b + 1 \right) \quad (14)$$

where  $(K_p)_b$  is the partition coefficient of the molecular base between the organic solvent and water.

## DISCUSSION

Equations 4 and 12 are analogous with the corresponding equation for monophasic buffer systems which reads:

$$\frac{dC_b}{dpH} = \beta_{Hb} = 2.303 \frac{K_a C_{tot} C_H}{(K_a + C_H)^2} \quad (15)$$

where  $C_{tot}$  is the total concentration of the acid-base pair. It follows that the graphic representation of the function  $\beta_{Hb} = f(pH)$  will be also analogous for both monophasic and two-phase buffer systems. This plot for two-phase buffer systems has its maximum value,  $\beta_{Hb}^{max} = 0.58 C_{tot}^{app}$  (for monophasic buffers,  $\beta_{Hb}^{max} = 0.58 C_{tot}$ ).

Equation 7 shows that for two-phase buffers of type I, maximum buffer capacity will be attained when  $C_a^{app} = C_b$ , because the right-hand side of Equation 7 then reaches its maximum possible value. Likewise, from Equation 13, it may be seen that for two-phase buffers of type II, maximum buffer capacity will be attained when  $C_b^{app} = C_a$ . Furthermore, from Equations 1 and 11, it is derived that maximum buffer ca-

pacity for two-phase buffers, irrespective of the type to which they belong, will be at:

$$pH = pK_a^{app} \quad (16)$$

From the acid dissociation constant, phase volumes and partition coefficient of the molecular acid or base, it is possible, by Equation 10 or 14, to calculate the apparent acid dissociation constant and thereby also the pH value at which the buffer capacity will attain a maximum. It may be seen from Equations 10 and 14 that as the volume of the organic phase increases relative to that of the water phase, and/or as the partition coefficient increases, the pH value at which the buffer capacity reaches its maximum in buffers of type I shifts to higher pH values, whereas in buffers of type II it shifts to lower pH values. Here it should be stressed that the very nature of two-phase buffers implies that the water phase will be saturated with the organic solvent. Therefore, strictly speaking, measurement on a pH meter calibrated with a standard buffer solution in water gives pH(R) values (11). The mathematical treatment in question as well as the conclusions drawn from it, are completely valid only in the limiting case:

$$\lim pH(R) = pH$$

(concentration of organic solvent in water)  $\rightarrow 0$

For two-phase buffers where the fulfillment of this condition is approached, the obtained pH(R) values correspond fairly closely to the operationally defined pH values in water. If this is not the case, these systems should be considered as two-phase buffers with individual pH(R) scales. This, however, does not mean that such two-phase buffers are unusable in practice.

The mathematical treatment given in this paper is valid only in the simple case when the partition of the molecular component of the acid-base pair is not complicated by secondary reactions. If this is not the case (for example, if appreciable dimerization of the molecular acid occurs in the organic phase), a functional dependence of  $\beta_{Hb}$  on pH different from the one given by Equations 4 and 12 should be expected. A different functional dependence should also be expected if extraction of ion-pairs, containing as one of the constituents anionic base (buffers of type I) or cationic acid (buffers of type II), occurs in a significant amount. In that case, the assumption that the total amount of the charge carrying component of the acid-base pair remains in the water phase is not valid.

## EXPERIMENTAL CONFIRMATIONS

As is seen from mathematical considerations of two-phase buffer systems, we have assumed an extraction mechanism of action for such buffers. To prove the validity of the mechanism proposed we prepared a series of two-phase buffers by mixing 40.00 mL of 0.0975 M *n*-caproic acid in 1-octanol (the solubility of 1-octanol in water is 0.007 mol % at 25 °C (12)), (40.00 - A) mL of water and A mL of a standard sodium hydroxide solution. Prior to determination of the acid and base concentrations in the water phase and the acid concentration in the organic phase, we established that the pH values measured in emulsions of the well stirred two-phase buffers agreed, within the limits of experimental error, with pH values of the separated water layer of the buffer (a Radiometer PHM 62 pH meter with glass-calomel electrode assembly was used for measuring the pH values). The acid and base concentrations in the aqueous phase were determined by potentiometric titrations with standard sodium hydroxide or hydrochloric acid solution. The acid concentrations in the organic phase were determined by taking the water-emulsified aliquots of the organic phase and titrating them with standard sodium hydroxide solution.

On the basis of good accordance between the analytically found concentration of anionic base and the concentration of sodium hydroxide solution added to achieve partial neutralization of the acid, it may be concluded that extraction of ion pairs containing



Table I. Experimental Data Confirming the Validity of the Proposed Extraction Mechanism of Action of Two-Phase Buffers<sup>a</sup>

Total acid neutralized, %	$C_b$ , mol/L	$C_a$ , mol/L	$C_a^o$ , mol/L <sup>b</sup>	Activity coefficient, $f_z^c$	pH calculated <sup>d</sup>	pH measured	$V_o/V_w$ , mL/mL, from Eq. 17	$pK_a^{app}$ from Eq. 10
5	$5.065 \times 10^{-3}$	$8.876 \times 10^{-4}$	$8.913 \times 10^{-3}$	0.926	5.60	5.60	41.19/38.81	6.91
20	$2.029 \times 10^{-2}$	$7.823 \times 10^{-4}$	$7.480 \times 10^{-3}$	0.868	6.23	6.26	41.30/38.70	6.89
35	$3.525 \times 10^{-2}$	$5.917 \times 10^{-4}$	$6.102 \times 10^{-3}$	0.838	6.58	6.57	41.16/38.84	6.92
50	$4.984 \times 10^{-2}$	$4.814 \times 10^{-4}$	$4.704 \times 10^{-3}$	0.817	6.81	6.83	41.06/38.94	6.90
65	$6.526 \times 10^{-2}$	$3.410 \times 10^{-4}$	$3.302 \times 10^{-3}$	0.800	7.06	7.10	40.95/39.05	6.89
80	$7.978 \times 10^{-2}$	$2.258 \times 10^{-4}$	$1.899 \times 10^{-3}$	0.787	7.32	7.45	40.57/39.43	$(6.82)^e$

<sup>a</sup> The systems investigated were prepared by mixing 40.00 mL of 0.0975 M *n*-caproic acid in 1-octanol, (40.00 -  $A$ ) mL of water and  $A$  mL of a standard sodium hydroxide solution,  $t = 25 \pm 0.1^\circ\text{C}$ . <sup>b</sup>  $C_a^o$  = Concentration of *n*-caproic acid in the organic phase. <sup>c</sup> Calculated according to the Davies equation:  $-\log f_z = 0.509 z^2 / (\sqrt{I} (1 + \sqrt{I}) - 0.2 I)$ , where  $z$  is the charge of the ion and  $I$  is the ionic strength; ( $I = C_b$ ). <sup>d</sup> Calculated by the equation:  $\text{pH} = \text{p}K_a + \log C_b/z/C_a$ . <sup>e</sup> Rejected on the basis of  $Q_{o,w} = \text{test for } n = 6$ .

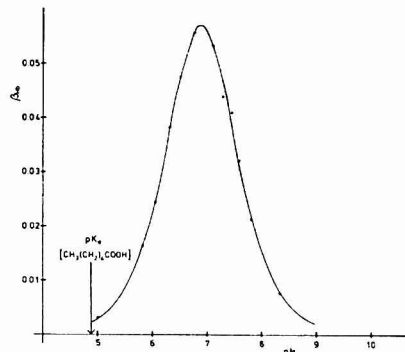


Figure 1. Buffer capacity as a function of the pH value of the solution for a two-phase buffer made up of 20.00 mL of 0.1000 M *n*-caproic acid in 1-octanol and 20.00 mL of water. Values determined experimentally are denoted by circles. Values calculated by Equation 4, using the mean  $pK_a^{app}$  value (6.90) from Table I, are represented by the unbroken line. The pH value corresponding to the maximum buffer capacity of the monophasic buffer in water is indicated by an arrow. All data are valid for  $I = 0$  and  $t = 25 \pm 0.1^\circ\text{C}$ .

the *n*-caproic anion does not occur in a significant amount.

The results obtained are summarized in Table I, from which it can be seen that there is high agreement between the measured pH values and those calculated from the acid and base concentrations found in the water layer. In order that the value of  $pK_a^{app}$  (which corresponds to the pH value at the maximum buffer capacity of the two-phase buffer) may be calculated from the results of the determinations presented above (Table I), it is necessary to know the equilibrium volumes of the phases. They can be calculated by the following equation:

$$T_o \left( \frac{V_o^i + \delta}{V_o^t} \right) + T_w \left( \frac{V_w^i - \delta}{V_w^t} \right) = \frac{Q_{tot} - V_{NaOH} M_{NaOH}}{Q_{tot} - V_{NaOH} M_{NaOH}} \quad (17)$$

where  $\delta$  is the increase in the organic phase volume, or the decrease in the water phase volume relative to the initial volumes of the phases,  $T_o$  is the amount of acid in the organic phase aliquot,  $V_o^i$  is the volume of the titrated organic phase aliquot,  $T_w$  is the amount of acid in the water layer aliquot,  $V_w^i$  is the volume of the titrated water aliquot,  $V_o^i$  and  $V_w^i$  are the initial volumes of the organic and water phase, respectively,  $Q_{tot}$  is the total amount of acid,  $V_{NaOH}$  is the volume, and  $M_{NaOH}$  is the molarity of the sodium hydroxide solution used for the preparation of the two-phase buffer (all the amounts are in moles, all the volumes are in liters). In the given experiments, no appreciable change in the total volume of the two phases has been observed, which represents the condition of applicability of Equation 17 for the calculation of the equilibrium phase volumes.

The dependence of buffer capacity on the pH value of the two-phase buffer investigated was determined by an analysis of the corresponding titration curve with the necessary corrections made for the salt effect and for the change in solution volume during titration. The time needed for establishing equilibrium in vigorously stirred two-phase buffers is short, and pH values could be measured almost immediately after the addition of a strong acid or base to the buffer.

The results of the experimental determination of the functional dependence of  $\beta_{HB}$  on pH are presented in Figure 1. From Figure 1, it may be seen that the values of the function  $\beta_{HB} = f(\text{pH})$  determined experimentally are in good agreement with those calculated theoretically by Equation 4. It may also be noticed that there is very high agreement between the experimentally determined pH value corresponding to the maximum value of  $\beta_{HB}$  (pH 6.89) and the  $pK_a^{app}$  values calculated by Equation 10 (see Table I). Finally, from Figure 1, it may be seen that the point

Table II. Most Important Characteristics of Some Two-Phase Buffers<sup>a</sup>

Acid (base) used	pK <sub>a</sub> (Ref.)	Buffer type	pH value corresponding to $\beta_{HB}^{\max}$ for two-phase buffer, pK <sub>a</sub> <sup>app</sup>	Shift in pH units, pK <sub>a</sub> <sup>app</sup> - pK <sub>a</sub>
Benzoic	4.20 (15)	I	6.12	1.92
p-Nitrophenol	7.15 (16)	I	9.13	1.98
n-Hexylamine	10.64 (17)	I	8.55	-2.09
N,N-Diethylaniline	6.61 (18) (at 22 °C)	II	3.52	-3.09

<sup>a</sup> The systems investigated were prepared by mixing 20.00 mL of 0.1000 M solution of the molecular acid (base) in 1-octanol and 20.00 mL of water. The systems were titrated with a standard sodium hydroxide (hydrochloric acid) solution. If not otherwise stated, all data are valid for  $I = 0$  and  $t = 25$  °C.

of maximum buffer capacity of the two-phase buffer under consideration has shifted by about 2 pH units with respect to a corresponding monophasic buffer in water, since the thermodynamic pK<sub>a</sub> value for *n*-caproic acid at 25 °C is 4.88 (13).

In Table II, the most important characteristics of some other two-phase buffer systems of type I and II are presented. In all investigated two-phase buffer systems with 1-octanol as the organic phase, the functional dependence  $\beta_{HB} = f(\text{pH})$  agrees well with the equations derived in this paper.

It may be concluded from the foregoing that the experimental evidence completely confirms the validity of the conclusions to which we arrived on the basis of our mathematical considerations of such simple systems.

In the course of our investigations of two-phase buffers of type I, we encountered cases when the functional dependence of  $\beta_{HB}$  on pH did not agree with Equation 4. This was the case with two-phase buffer systems containing *n*-caproic acid and the solvent pair toluene/water or cyclohexane/water. In both of these systems, buffer curves  $\beta_{HB} = f(\text{pH})$  were higher ( $\beta_{HB}^{\max} > 0.58 C_{\text{tot}}^{\text{app}}$ ) and asymmetrical (the right-hand side sloping more steeply than the left-hand side of the curve). Mathematically it can be proved that such buffer curves should be expected in cases of appreciable dimerization of the molecular acid in the organic phase.

#### EFFECT OF DILUTION ON pH VALUES OF TWO-PHASE BUFFERS

In addition to the factors cited in the literature which induce a change in pH value with dilution of monophasic buffers (14), the following factors are of significance in two-phase buffer systems:

(1) **Shift of Distribution Equilibrium.** On a twofold dilution of the water layer of a two-phase buffer the concentration of the ionic component of the acid-base pair reduces to nearly one half of the original value, whereas the concentration of the molecular component, in the cases where

$$\log \left( \frac{V_o}{V_w} (K_{p,a,b} + 1) \right) \geq 2$$

decreases only negligibly. This brings about a change in pH value of the water layer of about 0.3 pH unit, the shift in buffers of type I being to lower pH values and in those of type II to higher ones.

(2) **Decrease in Equilibrium Volume of Organic Phase Due to Dissolution of Organic Solvent in Water.** This factor induces a change in the pH value of the water layer in the same direction as a shift in the distribution equilibrium does. In the case of organic solvent with a very low solubility in water and if  $V_o/V_w$  ratio is not too low, it seems that the effect of this factor on pH value, after a twofold dilution of the water layer of two-phase buffer, is considerably smaller than that of factor 1.

It follows that two-phase buffers are very sensitive to dilution of the aqueous phase only. On dilution of both phases such that their ratio remains unchanged, it may be expected for factors 1 and 2 to have no effect. This is confirmed by

Table III. Effect of Dilution on pH Values of Two-Phase Buffers<sup>a</sup>

Total acid neutralized, %	pH value		
	of the buffer	of the buffer after 15.00 mL of water were added <sup>b</sup>	of the buffer after 15.00 mL of water and 15.00 mL of 1-octanol were added
25	6.34	6.00	6.31
50	6.85	6.52	6.82
75	7.35	7.02	7.33

<sup>a</sup> The systems investigated were prepared by mixing 15.00 mL of 0.1041 M *n*-caproic acid in 1-octanol, (15.00 - *B*) mL of water and *B* mL of a standard sodium hydroxide solution,  $t = 25 \pm 0.1$  °C. <sup>b</sup> The difference between the initial and equilibrium phase volumes is less than 3.5%.

experimental investigation of the effect of dilution on pH values in such buffers (Table III).

#### CONCLUSION

It may be concluded that for two-phase buffer systems, the pH value at which the buffer capacity has its maximum can be varied by changing the ratio of the phase volumes as well as by choosing an appropriate organic phase.

Investigations of new two-phase buffer systems and their applicability in analytical chemistry are in progress.

#### LITERATURE CITED

- (1) R. G. Bates, "Determination of pH: Theory and Practice", 2nd ed., Wiley-Interscience, New York, N.Y., 1973, p. 128.
- (2) J. A. Christensen, *Acta Chem. Scand.*, **16**, 2363 (1962).
- (3) D. Ratajewska and Z. Ratajewska, *Chem. Anal. (Warsaw)*, **16**, 1299 (1971).
- (4) D. Rysen, *Sven. Kern. Tidskr.*, **64**, 213 (1952).
- (5) F. F. Cantwell and D. J. Pietrzyk, *Anal. Chem.*, **46**, 344 (1974).
- (6) C. F. Hiskey and F. F. Cantwell, *J. Pharm. Sci.*, **57**, 2105 (1968).
- (7) D. Ratajewska and Z. Ratajewska, *Chem. Anal. (Warsaw)*, **16**, 913 (1971).
- (8) A. E. Mans and G. J. Verweke, *Recl. Trav. Chim. Pays-Bas*, **71**, 977 (1952).
- (9) I. Setnikar, *J. Pharm. Sci.*, **55**, 1190 (1966).
- (10) N. P. Komar, *Zavod. Lab.*, **34**, 513 (1968).
- (11) D. D. Cantwell and B. Dempsey, "Buffers for pH and Metal Ion Control", Chapman and Hall, London, 1974, p. 79.
- (12) G. L. Dorough, H. B. Glass, T. L. Gresham, G. B. Malone, and E. E. Reid, *J. Am. Chem. Soc.*, **63**, 3100 (1941).
- (13) J. F. J. Dippy, *J. Chem. Soc.*, 1222 (1938).
- (14) R. G. Bates, *Anal. Chem.*, **26**, 871 (1954).
- (15) F. G. Brockman and M. Kilpatrick, *J. Am. Chem. Soc.*, **56**, 1483 (1934).
- (16) R. A. Robinson and A. J. Biggs, *Trans. Faraday Soc.*, **51**, 901 (1955).
- (17) C. W. Hoer, M. R. McCorkle, and W. E. Ralston, *J. Am. Chem. Soc.*, **65**, 328 (1943).
- (18) H. F. Hall and M. R. Sprinkle, *J. Am. Chem. Soc.*, **54**, 3469 (1932).

RECEIVED for review May 17, 1977. Accepted December 12, 1977. This work was presented in part at the 20th Annual Meeting of the Serbian Chemical Society, Belgrade, January 17, 1977. The authors are grateful to the Serbian Republic Research Fund for financial support.

# Enrichment of Anions of Weak Acids by Donnan Dialysis

James A. Cox\* and Kuo-Hsien Cheng

Department of Chemistry and Biochemistry, Southern Illinois University, Carbondale, Illinois 62901

The rate of Donnan dialysis enrichment of weak acids was found to be influenced by the pH of the sample and of the receiver electrolyte; however, when the receiver pH is much less than the  $pK$  of the most acidic species, the transfer rate is independent of sample pH over a wide range. Under optimum conditions, the enrichment rate of several anions is identical. These results suggest that diffusion of the sample anion is not the rate-determining step in these enrichments and, further, that the rate of transfer across the membrane/receiver interface is especially important.

Donnan dialysis enrichment involves separation of a sample solution from a relatively high ionic strength receiver electrolyte by an anion-exchange membrane (1, 2). The approach to Donnan equilibrium results in transfer of ions of the appropriate charge sign from the sample to the receiver; thus, if the latter volume is smaller, enrichment of those ions is accomplished. Since the transfer rate is time independent (as long as the system is not near Donnan equilibrium) and is directly proportional to the concentration of the selected ion in the sample over a wide range of conditions (3), pre-concentrations for prescribed times result in linear relationships between readout and initial sample concentration when metal ions or anions of strong acids are subsequently determined in the receiver (3, 4).

Donnan dialysis of conjugate bases of weak acids presents a special problem because the distribution of these species according to charge is a function of pH, thereby possibly complicating the enrichment procedure. The present study was initiated to determine the factors which primarily influence their transfer rate and to establish conditions which would permit pre-concentrations in direct proportion to their initial sample concentration. Because of their general importance and polybasic nature,  $H_3PO_4$  and  $H_3AsO_4$  were selected as the major test species.

## EXPERIMENTAL

The anion-exchange membranes were Permapion P-1025 obtained from RAI Research Corporation, Hauppauge, Long Island, N.Y. They were successively rinsed in 0.1 F HCl,  $H_2O$ , 0.1 F NaOH,  $H_2O$ , 0.1 F  $KNO_3$  and 0.1 F  $KNO_3$  prior to use. The acid-base cycle was repeated three times; they were soaked at least 24 h in the 0.1 F  $KNO_3$  prior to use. When receiver electrolytes other than  $KNO_3$  were used, the latter two solutions of the sequence were altered accordingly.

The analytical methods employed in this work were the following: phosphate and arsenate, molybdenum blue method (5); chloride, differential pulse polarography; sulfate, chloranilate spectrophotometric method (6); pyruvate, linear scan voltammetry; chloroacetate, linear scan voltammetry.

The electrochemical experiments were performed with a PAR 170 system. Reagent grade chemicals and doubly deionized water were used throughout.

## RESULTS AND DISCUSSION

The primary difference between the Donnan dialysis behavior of anions which are conjugate bases of weak acids and previously studied ions is the effect of pH, the importance of which is demonstrated by the experiments summarized in

Table I. Influence of pH on the Donnan Dialysis Enrichment of Phosphate

Receiver pH	Sample pH	Enrichment factor <sup>a</sup>
1.5	2.0	2.8
1.5	3.0-10.0	$7.0 \pm 0.03$
3.5	4.0	6.3
5.2	4.0	4.9
5.2	6.9	3.9
5.2	9.2	3.3

<sup>a</sup> Ratio of receiver concentration after enrichment to the original sample concentration. Receiver: 2 mL of 0.1 M  $KNO_3$ , adjusted with  $HNO_3$  or  $KOH$ . Membrane: 4.9  $cm^2$  P-1025. Enrichment time, 30 min.

Table II. Effect of pH on the Donnan Dialysis Enrichment of Selected Weak Acids<sup>a</sup>

Acid, $pK$	Receiver pH	Sample pH	Enrichment factor
Chloroacetic (2.8)	1.5	4.0	6.8
	3.0	4.0	6.9
	5.6	4.0	5.4
Pyruvic (2.2)	1.5	4.2	7.0
	1.5	6.0	6.9
	3.0	4.2	6.8
Arsenic (2.6, 7.0, 11.5)	5.6	4.2	5.4
	1.5	1.3	0.4
	1.5	4.9	7.2
	1.5	9.0	7.0
	5.7	3.0	7.1
Sulfuric ( $pK_a$ , 1.9)	5.7	4.0	2.5
	1.5	4.0	2.9

<sup>a</sup> Conditions the same as reported in Table I.

Table I. The data indicate that if the receiver pH is much less than the  $pK$ (s), the rate of Donnan dialysis transfer, which establishes the enrichment factor, is independent of sample pH; it is also necessary that the sample not be so acidic that the major fraction of the weak acid system is a neutral species.

The hypothesis was substantiated by comparable studies with other weak acids (Table II). Except for the case of sulfate, the weak acids which were investigated all gave enrichment factors of about 7 for a 30-min pre-concentration into a pH 1.5 receiver. This fact, along with the observation that a very acidic receiver yields the greatest enrichment rate, suggests that the rate of transfer across the membrane/receiver boundary may be the rate-limiting step of a Donnan dialysis of weak acids with anion-exchange membranes. Otherwise, it would be required that the anions have similar diffusion coefficients in the membrane.

The relatively low enrichment rate for sulfate may be due to strong interaction with the fixed sites of the membrane. This interpretation is consistent with the results of experiments on the Donnan dialysis of samples of mixtures of weak acids. The results are summarized in Table III. Although the tabulated data are for pH 5.2 samples, the results were unchanged over the pH range 4-9. Mixtures which did not contain sulfate exhibited the same enrichment as the single-component cases in Table I and II. The decrease of the Donnan dialysis enrichment rate in the presence of sulfate (or bisulfate) could not be eliminated by changing the receiver

Table III. Donnan Dialysis Enrichment of Mixtures of Weak Acids

Test anion	Added anion	EF <sup>a</sup>
Phosphate	10 <sup>-5</sup> M sulfate	7.1
	10 <sup>-4</sup> M	6.7
	10 <sup>-3</sup> M	4.8
Pyruvate	10 <sup>-4</sup> M	6.3
	10 <sup>-3</sup> M	4.7
Phosphate	10 <sup>-4</sup> M pyruvate	7.2
	10 <sup>-4</sup> M acetate	7.2

<sup>a</sup> Enrichment factor of the test anion. Sample pH, 5.2; other conditions the same as Table I.

electrolyte pH or anion; for the latter, chloride, bromide, acetate, chloroacetate, nitrate, and citrate were used.

To establish which of the above observations are related to the weak acid nature of the investigated systems, selected experiments were repeated with chloride-containing samples. Using the conditions outlined in Table I, 10<sup>-4</sup>–10<sup>-5</sup> M Cl samples were enriched by a factor of 7.0 in 30 min, and the results were independent of sample pH over the investigated range of 2–9. Unlike the weak acid cases, variation of the receiver pH over the range 2–6 did not change the enrichment factor (7.02 ± 0.03, 8 points). With mixed samples, the enrichments of phosphate and chloride were mutually independent. In addition, the presence of sulfate does not influence the enrichment of chloride.

These results are generally consistent with the previous observations. Chloride would be expected to weakly associate

with the ion-exchange sites, so pH effects should be negligible. Likewise, the presence of competing anions should not alter the enrichment. That the enrichment factor for chloride is the same as those for weak acids when the latter are transferred into a low-pH solution supports a model for Donnan dialysis transfer in which the primary factor which determines the rate is the Donnan potential; with weak acids the primary rate can be decreased by the exchange reaction at the membrane/receiver interface but not by diffusion of the test species; i.e., the electric field gradient predominates over the diffusion gradient. Further study is in progress to substantiate and refine this model.

That conditions can be defined which permit Donnan dialysis of weak acids to be independent of sample pH is important. Applications to chemical analysis such as for matrix normalization and/or enrichment of trace samples are feasible.

#### LITERATURE CITED

- (1) R. M. Wallace, *Ind. Eng. Chem., Process Des. Dev.*, **6**, 423 (1967).
- (2) W. J. Blauvelt and T. J. Hauptert, *Anal. Chem.*, **38**, 1305 (1966).
- (3) G. L. Lundquist, G. Washington, and J. A. Cox, *Anal. Chem.*, **47**, 319 (1975).
- (4) J. A. Cox and J. E. DiNunzio, *Anal. Chem.*, **49**, 1272 (1977).
- (5) "Standard Methods for the Examination of Water and Wastewater", 13th ed., American Public Health Association, Inc., Washington, D.C., 1971.
- (6) R. J. Bertolacini and J. E. Barney, *Anal. Chem.*, **29**, 281 (1957).

RECEIVED for review November 21, 1977. Accepted January 16, 1978. This work was supported in part through the Water Resources Center, University of Illinois, Project A-087-ILL, in the OWRT Allotment Program.

## Simultaneous Multielement Determination by Atomic Emission with an Echelle Spectrometer Interfaced to Image Dissector and Silicon Vidicon Tubes

Hugo L. Felkel, Jr., and Harry L. Pardue\*

Department of Chemistry, Purdue University, West Lafayette, Indiana 47907

Silicon target vidicon and image dissector camera systems have been coupled to an echelle grating spectrometer for multielement determinations with a dc plasma excitation source. Spectral resolution expressed as full width at half height ranges from 0.4 to 0.9 Å for the vidicon system and 0.2 to 0.7 Å with the image dissector system, and wavelength calibration procedures permit locations of lines to be predicted to between 0.03 and 0.2 Å for both systems. Effects of peak height and peak area measurements on signal-to-noise ratios for both detectors are evaluated. Results for multielement samples of alkali and alkaline earth and of transition metals obtained with the echelle spectrometer/image dissector are comparable in most respects to single element data obtained with conventional optics and detectors with the same plasma. Some interelement effects associated with the dc plasma are discussed.

Numerous recent reports have discussed the application of imaging detectors for a variety of applications involving atomic spectrometry (1–10). One of the promising areas of applications is for the simultaneous determination of metallic

elements by atomic absorption and atomic emission spectrometry. Most applications in this area have been based on imaging detectors used with conventional optics that disperse spectra in only one dimension. These applications impose a severe tradeoff between spectral range and spectral resolution. Some recent reports have demonstrated the feasibility of using echelle grating spectrometers to take advantage of the two-dimensional character of some imaging detectors to obtain good resolution over spectral ranges of several hundred nanometers (1, 9–11). Applications reported to date have included both atomic emission and atomic absorption spectrometry.

In this paper we describe and compare results obtained with an image dissector and a silicon target vidicon tube used with an echelle grating spectrometer and a direct current plasma excitation source. Items included in the study are: useful spectral range and resolution, wavelength accuracy, effects on signal to noise of peak height and peak area measurements, some interelement effects in the dc plasma, comparisons of sensitivities in single- and multielement mixtures, comparisons of sensitivities and other characteristics of the detectors, and detection limits for several elements. The image dissector system is up to 25 times more sensitive than the silicon target

vidicon system and multielement results obtained with the dc plasma-echelle-image dissector system compare favorably with single element results reported previously with dc plasma excitation sources.

### EXPERIMENTAL

**Instrumentation.** The instrumental system consists of a dc plasma excitation source used with an echelle grating spectrometer interfaced to either a silicon target vidicon or an image dissector tube. Information related to the design and operation of the silicon target vidicon detector system has been reported previously (1) and is not discussed further here. Some features of the other components are discussed here.

**Optical System.** Experiments described in this paper were designed to evaluate performance characteristics of the two detectors under conditions such that both would cover the same spectral range, namely that from below 2000 to above 7700 Å. The modifications necessary to reduce the size of the image from the echelle grating spectrometer to that consistent with the size of the vidicon detector have been described previously (1). Because the image dissector tube has a larger image format, the cassegrainian mirror system (13.5-cm focal length at  $f/1.6$  for the vidicon) was replaced by a similar unit with a focal length of 20.0 cm at  $f/2.8$  (Nye Optical Co., Spring Valley, Calif. 92077) producing an image reduction factor of 3.9 for the image dissector compared with 5.8 for the silicon target vidicon. An entrance slit width of 200  $\mu$ m and height of 500  $\mu$ m was used throughout these experiments for both detectors.

**Plasma Source.** The excitation source used in this work is an argon supported, dc plasma source (Spectrametrics, Inc., Model 53000, Spectra Jet II). The argon flow rate to the cathode and anode electrodes (thoriated tungsten) was 1.6 L/min and the flow rate through the ceramic nebulizer was 3.1 L/min. The plasma is sustained by passing 7.5 A at 40-V dc between the two electrodes. The sample uptake rate for this plasma is about 2 mL/min with a nebulizer efficiency approaching 10%. The characterization of this plasma by Skogerboe and co-workers (12) suggests that the analyte experiences effective source temperatures of 6000–7000 K in the excitation region. The small volume of the excitation region of this plasma is particularly well suited for use with the echelle spectrometer because a rather short entrance slit height is used, providing for optimum signal-to-background ratios.

**Image Dissector.** A commercially available image dissector detector system (Model 658A, EMR Photoelectric, Princeton, N.J. 08540) employs the EMR Model 575E image dissector that has a sapphire window and a 43-mm diameter S-20 photocathode, providing a useful spectral response from 1800 to about 7500 Å. In this sensor, the photoelectrons generated by the optical image on the photocathode are magnetically focused onto a plate which has a 38- $\mu$ m circular aperture. The photoelectrons passing through this aperture are then multiplied by the 13-stage, Cu-Be, venetian blind electron multiplier, producing a current at the anode that is linearly related to the input photon flux. The voltage applied to the electron multiplier is approximately 2.4 kV, providing a current gain of about  $6 \times 10^5$ . The gain of the electron multiplier of the image dissector was maintained constant throughout these experiments. The dimensions of the aperture were chosen to provide the best intensity-resolution tradeoff for this particular application.

The entire electron image of the photocathode is deflected by two digitally-controlled magnetic fields, allowing any region of the photocathode to be addressed. The addressing accuracy of this system is rated by the manufacturer to be 3% of field with a repeatability of 0.1%; however, our data show that this is a rather conservative specification. Input to the sensor consists of 12-bit parallel binary X or Y position information, load X, load Y, and convert command lines. There are also two additional lines which are decoded to select one of four possible bandwidths in the video processor. The standard bandwidths available vary from 0.1 to 100 kHz in decade steps; however, we have modified the system to provide a bandwidth range of 10 Hz to 10 kHz. Since the image dissector is a nonintegrating detector, there is no need to erase or prime the detector between random access scans as for the silicon vidicon. This permits simpler software control than is required for the silicon vidicon (1). The analog signal corresponding to the intensity at each location is digitized by a 0–10

Table I. Spectral Resolution and Wavelength Prediction Error

Order <sup>a</sup>	$\lambda$ , Å	Resolution <sup>b</sup>		$\lambda$ prediction error, Å		
		Ex-pected	Found	$\lambda$	Vidicon	Image dissector
72 (Hg)	3125.66	0.18	0.20	2000	0.03	0.05
	3131.55					
62 (Hg)	3650.15	0.20	0.20	3000	0.05	0.07
	3654.84					
60 (Fe)	3737.13	0.23	0.25	4000	0.06	0.10
	3745.56					
39 (Hg)	5769.59	0.33	0.47	5000	0.08	0.12
	5790.65					
32 (Ne)	7024.05	0.42	0.74	6000	0.10	0.16
	7032.41			7000	0.11	0.18

<sup>a</sup> Mercury lines from mercury pen lamp, Mn lines from Mn hollow cathode lamp, Fe and Ne lines from Fe hollow cathode lamp.

<sup>b</sup> Resolution for image dissector only; see Ref. 1 for vidicon data.

V input, analog-to-digital converter (ADC-EH12B2, Datel Systems, Inc., Canton, Mass. 02021) which has a 4- $\mu$ s conversion time.

**Reagents.** The Ca and Li analyte solutions were prepared by dissolving reagent grade  $\text{CaCO}_3$  and  $\text{Li}_2\text{CO}_3$  in dilute HCl. Solutions containing Ba, Na, and K were prepared from the reagent grade chloride salts. The other analyte solutions were certified atomic absorption standards (Fisher Scientific Co., Fair Lawn, N.J. 07410) prepared from the metal (Mg, Ni, Mn, Mo, Co), the oxide (Cu, Cr), the chloride (Fe), or the carbonate (Sr) and contain dilute HCl,  $\text{HNO}_3$ , or aqua regia as the solvent.

The effect of phosphate and aluminum on the emission responses of the alkali and alkaline earth metals was studied by adding solutions of reagent grade  $\text{H}_3\text{PO}_4$  (85%),  $\text{Al}(\text{NO}_3)_3 \cdot 9\text{H}_2\text{O}$ , or  $\text{AlCl}_3$ .

### RESULTS AND DISCUSSION

Unless stated otherwise, uncertainties are quoted at the 95% confidence level and imprecision of ratios or other combinations of data are computed using standard propagation of error equations. Detection limits are quoted at the two standard deviation unit level.

**Resolution and Wavelength Prediction Errors.** Wavelength resolution data for the silicon vidicon have been presented earlier (1), and resolution data for the image dissector and wavelength prediction errors for both detectors as functions of wavelength are presented in Table I. The resolution of both systems was determined by measuring the full width at half maximum (FWHM) of several atomic lines from various hollow cathode lamps and a mercury pen lamp. The reciprocal linear dispersion (RLD) was also determined for each order in which spectral lines were measured. The values of FWHM and RLD are used to compute the theoretical and experimental resolutions as given by

$$\text{Theoretical resolution } (\text{\AA}) =$$

$$\text{Slit width } (\mu\text{m}) \times \text{RLD } (\text{\AA}/\text{DAC step})$$

$$\text{Experimental resolution } (\text{\AA}) =$$

$$\text{FWHM (DAC steps)} \times \text{RLD } (\text{\AA}/\text{DAC step})$$

The data in Table I show that for the image dissector there is good agreement between experimental and theoretical resolution up to about 6000 Å. The deviation of the resolution of the image dissector from theoretical at 7024.05 Å may be attributed to curvature of field in the reduced image of the spectral focal plane because the line is near the edge of the photocathode.

In order to evaluate the ability of each system to locate spectral lines, a preliminary wavelength calibration was carried out with the emission spectrum of a mercury pen lamp and



then the peak maxima of several atomic lines from an iron hollow cathode lamp were located. The root mean square (RMS) prediction error, which is the difference between the predicted and the observed location of a line, for the vidicon detector system was 1.4 DAC steps. Because it is known from system calibration data that one DAC increment corresponds to 0.0125 mm on the active surface of the vidicon, the absolute error in position prediction is 0.018 mm. For the image dissector, the RMS prediction error was 7.6 DAC steps, and because one DAC step for this system corresponds to 0.0055 mm on the photocathode, the absolute error in the predicted coordinate is 0.042 mm. Table I includes a comparison of the wavelength position prediction errors for the two detectors. These values were calculated by multiplying the absolute errors of the predicted positions by the RLD at each wavelength. These data show that wavelength prediction errors are well within the FWHM of a spectral line at all wavelengths for both systems. Because there are finite errors, an optimization routine is used with both detector systems to center the raster pattern around the peak maximum after its general location has been identified.

**Signal-to-Noise Characteristics.** Earlier work with the silicon vidicon system has shown that it has a background noise component that contributes a fixed uncertainty of about  $\pm 0.08$  nA at the 95% confidence level (1). That work also showed that increased sampling time could be used to improve the signal-to-noise ratio (S/N) for the silicon vidicon system. Experiments were performed in this study to evaluate the noise characteristics of the image dissector system.

To facilitate this and related studies, the bandwidth of the video processor was reduced to 10 Hz. Sampling theory suggests that as long as a signal is sampled at a frequency equal to or greater than twice the bandwidth, then the effective signal bandwidth is given by

$$\Delta f_s = 1/2\Delta t \quad (1a)$$

and the effective noise bandwidth is given by

$$\Delta f_N = \pi/4\Delta t \quad (1b)$$

Accordingly, as long as the modified video processor signal is sampled at a rate of 20 Hz or faster, the effective bandwidth is inversely proportional to the observation time. In all of our studies with the 10-Hz bandwidth, sampling rates were fast enough to satisfy this 20-Hz criterion.

To evaluate the effect of signal amplitude on detector noise, 12 lines from a multielement hollow cathode lamp were used to obtain signal amplitudes between 4 and 5000 nA. For each line, ten sets of 2048 points each were collected at a sampling rate of 2048 Hz, corresponding to a total sampling time of 10 s and an effective bandwidth of 0.05 Hz. The average of the 2048 points for each of the ten sets for each wavelength was computed, and these ten averages were used to compute the standard deviations of repeated measurements at each wavelength. A plot of the log of the standard deviation at each wavelength vs. the log of the signal amplitude between 4 and 5000 nA was linear with a slope of  $0.51 \pm 0.07$  and an intercept of  $-1.49 \pm 0.19$ . The slope confirms a shot noise limit for the image dissector system and the intercept corresponds to a noise of 0.032 nA, which when combined with the effective noise bandwidth of 0.079 Hz (Equation 1b with  $\Delta t = 10$  s), leads to equations of the form

$$N_r = 0.12\sqrt{I\Delta f_N} \quad (2a)$$

and

$$N_r = 0.10\sqrt{I/\Delta t} \quad (2b)$$

where  $N_r$  is the random component of the noise expressed as

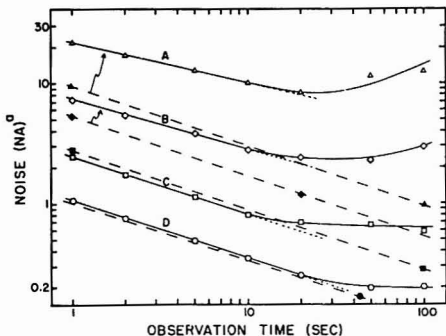


**Figure 1.** Effect of observation time on imprecision of measurements with the image dissector system. Noise expressed as standard deviation of ten runs with 2048 points per run (see text). Source: Mn hollow cathode lamp with Cu impurity. ( $\Delta$ ) Mn (4030.76 Å), 8930 nA; ( $\circ$ ) Cu (3247.54 Å), 2970 nA; ( $\square$ ) Cu (3273.96 Å), 774 nA; ( $\nabla$ ) Mn (3794.82 Å), 104 nA; ( $\blacktriangle$ ), ( $\blacktriangledown$ ), ( $\blacksquare$ ) Curves predicted using Equation 2b with  $I = 8930, 2790, 774$ , and 104 nA, respectively

nA,  $I$  is the current amplitude in nA,  $\Delta f_N$  is the noise bandwidth, and the uncertainty of the proportionality constant is  $\pm 0.04$  at the 95% confidence level. It is pertinent to subsequent discussions to note that only 1 of the 12 wavelengths used to evaluate the noise corresponded to a current above 2000 nA, and that point near 5000 nA was above the least-squares line by about one standard error unit.

Equation 2 suggests that the purely random components of the noise should vary in proportion to the square root of the effective bandwidth. To test this behavior for the image dissector system, ten measurements, each based upon the average of 2048 points, were collected over periods of time ranging from 1 to 100 s for each of four lines from a Mn hollow cathode lamp containing a Cu impurity. Standard deviations computed from the ten points for each line at each observation time are plotted as a function of the observation time in Figure 1. The solid lines associated with the linear regions of the data represent the least-squares fits of the data, the dashed extensions of the linear plots represent continuation of the regression lines, the curved extensions of these lines represent visual fits of the data, and the linear dashed lines represent the curves for each set of conditions predicted with Equation 2.

There is good agreement between expected and observed results at the shorter observation times for the lower currents represented by curves C and D. However, at longer observation times for the lower currents, there is poor agreement between predicted and observed data. The least-squares slopes for the linear portions of curves C and D are  $-0.48 \pm 0.01$  as expected for a random noise-limited system, and the slopes of curves A and B are  $-0.34 \pm 0.01$  and  $-0.41 \pm 0.04$ , respectively.

These data suggest that there is a nonrandom noise component associated with the observed signal, and the fact that the magnitude of the nonrandom component increases with signal amplitude suggests that it is associated with the hollow cathode lamp (13). Any nonrandom component would cause the imprecision in repeated measurements to tend to increase with observation time and this explains the deviations from the expected slopes of  $-0.5$  and the eventual increase in imprecision at the longer observation times for curves A and B. Although procedures described earlier (13) could be used to evaluate the coefficient for the nonrandom component, this was not done because the coefficients would apply only

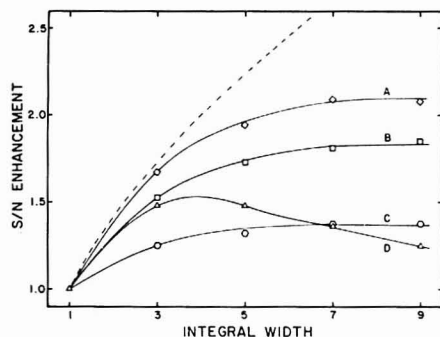


**Figure 2.** Ratios of S/N for summed signals to S/N for peak height signal vs. integral width. (A-C) Image dissector; (A) 32 averaging cycles; (B) 128 averaging cycles; (C) 1024 averaging cycles; (D) Vidicon, 32 averaging cycles. The S/N of the peak wavelength for the ten wavelengths interrogated varied from 50 to 150 with the vidicon for 32 averaging cycles and from 80 to 180 with the image dissector when 1024 averaging cycles were used.

for the hollow cathode lamp and its specific operating conditions. The magnitudes of the nonrandom component can be obtained easily as the difference between the shot noise-limited plots and the plots of experimental data.

The most important conclusion to be drawn from these data is that the image dissector system is shot noise-limited at low light levels for observation times extending at least to 20 s.

It has been suggested that peak area measurements of intensity can provide significant improvements in signal to noise ratios (S/N) in comparison with peak height measurements (14-16). Data that show effects of peak area measurements on the S/N are plotted in Figure 2 for the silicon vidicon and the image dissector. The abscissa represents the number of equally spaced points along the wavelength axis at which emission signals are summed to generate the integral; the ordinate represents the ratio of the S/N of the integral data to the S/N of the peak wavelength data. Each point on the curve represents the average of the relative S/N values obtained for 30 runs on each of ten different wavelengths from an iron hollow cathode lamp operated at 15 mA.

For the vidicon experiments, a shutter was used (1) to expose the detector to radiation from the hollow cathode lamp for 300 ms during each measurement cycle. Between exposures, the target was primed by 20 erase cycles of 10-ms duration. The spacing between points was 2 DAC steps corresponding to three points per peak half width. A total of 21 points was collected across each peak and data from 32 scans were averaged at each point. All of these operations correspond to 480 s per experiment.

The data for the vidicon shows that summing over a region slightly larger than the peak half width (3 points) produces the optimum enhancement in S/N. The decrease in enhancement with the inclusion of more data in the summation was expected because the vidicon is essentially amplifier noise-limited. The fixed amplifier background noise degrades the S/N when measurements are extended to the low amplitude "wings" of the peaks where noise adds in at a more rapid rate than signal. In the remainder of this work with the vidicon, we have used data corresponding to three points centered around the peak maximum.

The bandwidth of the image dissector video processor was 10 kHz and the scan time was 12.5 ms. The spacing between points was four DAC steps corresponding to four points per

half width. Twenty-five points were collected across each of ten peaks and data are reported in Figure 2 for averages of 32, 128, and 1024 scans (curves A-C, respectively). These operations correspond to 12, 48, and 284 s per experiment.

The data in Figure 1 show that for low signal amplitudes and short sampling times, the image dissector-hollow cathode lamp system is shot noise-limited. For a shot noise-limited system, the ratio of S/N values for summed data,  $(S/N)_s$ , to values for peak data,  $(S/N)_p$ , would be given by

$$\frac{(S/N)_s}{(S/N)_p} = \frac{\sqrt{n_p S_p + n_1 S_1 + n_2 S_2 + \dots + n_m S_m}}{\sqrt{n_p S_p}} \quad (3)$$

where  $n_p, n_1, n_2, \dots, n_m$  represent the number of points collected at each signal level,  $S_p, S_1, S_2, \dots, S_m$ . In the experiments described above,  $n_p = n_1 = n_2 = \dots = n_m$  so that Equation 3 reduces to

$$\frac{(S/N)_s}{(S/N)_p} = \frac{\sqrt{n_p (S_p + S_1 + S_2 + \dots + S_m)}}{\sqrt{n_p S_p}} \quad (4a)$$

$$\frac{(S/N)_s}{(S/N)_p} = \frac{\sqrt{S_p + S_1 + S_2 + \dots + S_m}}{\sqrt{S_p}} \quad (4b)$$

Therefore, the ratios of S/N values are expected to increase as different signals across a peak are summed together, but the rate of increase as the "integral width" is increased is expected to fall off both because of the square root function and because the signal amplitudes decrease as the integral width moves further from the peak.

If the system were purely shot noise-limited, then Equation 4b predicts that ratios of S/N values should be independent of  $n$  and the three curves (A-C) that represent different numbers of data points should be superimposed. However, the data in Figure 1 show that some component(s) in the system (probably the hollow cathode lamp) is introducing a nonrandom component to the noise at longer observation times. This nonrandom noise component would be expected to degrade the signal to noise enhancement at longer times, and that is what is observed in curves B and C that involve total observation times of 48 s and 384 s, respectively.

Although Figure 2 shows that data summed from different segments of a peak can provide improved S/N for the types of experiments described above, this does not necessarily represent the optimum expenditure of time for a shot noise-limited nonintegrating detector such as the image dissector. Because the image dissector is a nonintegrating detector, it cannot store information from one part of the image while another region is being interrogated. The signal-to-noise relationship for a shot noise-limited system involving multiple measurements can be represented as

$$\frac{S}{N} \propto \frac{\sqrt{n_p S_p + n_1 f_1 S_p + n_2 f_2 S_p + \dots + n_m f_m S_p}}{n_m f_m S_p} \quad (5)$$

where  $f_1, f_2, \dots, f_m$  represent the fractions the different signal amplitudes are of the peak signal amplitude ( $f_m = S_m/S_p$ ) and the other symbols were defined above. It is obvious that the S/N relationship will have its maximum value when all values of  $f$  are unity or when all available time is spent making repeated measurements at the peak maximum. The dashed curve in Figure 2 represents the response that would result for a shot noise-limited system when all data are collected at the peak maximum. The S/N enhancement is observed to be higher than for any other situation.

The analytical data reported below are based on peak height measurements and background measurements on each side of each peak. Each peak height and background datum is the average of 2048 repetitive measurements made during a 1-s

Table II. Effect of Rubidium, Phosphate, and Aluminum on Multielement Emission

Element, $\lambda^a$	ME/SE <sup>b</sup>	SE + Rb/SE <sup>c</sup>	ME + Rb/SE + Rb <sup>d</sup>	ME + PO <sub>4</sub> /ME <sup>e</sup>	ME + Al/ME <sup>f</sup>
Li (6103.64) I	1.06 ± 0.03	1.66 ± 0.11	1.04 ± 0.07	1.01 ± 0.08	0.98 ± 0.06
Na (5889.95) I	1.44 ± 0.15	2.33 ± 0.14	1.06 ± 0.06	0.99 ± 0.04	1.01 ± 0.07
Na (5895.92) I	1.43 ± 0.03	2.37 ± 0.16	1.04 ± 0.12	1.00 ± 0.04	1.01 ± 0.09
K (7698.98) I	1.37 ± 0.11	2.36 ± 0.25	1.04 ± 0.07	0.98 ± 0.06	0.99 ± 0.06
Mg (2795.53) II	1.40 ± 0.13	1.89 ± 0.09	1.06 ± 0.05	1.00 ± 0.08	1.03 ± 0.10
Mg (5183.62) I	1.35 ± 0.32	1.65 ± 0.33	1.05 ± 0.09	1.02 ± 0.06	1.02 ± 0.24
Ca (3933.67) II	1.53 ± 0.15	2.75 ± 0.16	1.02 ± 0.11	1.01 ± 0.04	0.99 ± 0.09
Ca (4226.73) I	1.55 ± 0.23	2.56 ± 0.28	0.98 ± 0.16	1.02 ± 0.08	0.72 ± 0.07
Sr (4077.71) II	1.86 ± 0.16	3.57 ± 0.15	1.01 ± 0.06	1.00 ± 0.02	1.00 ± 0.08
Sr (4215.52) II	1.82 ± 0.16	3.47 ± 0.23	1.07 ± 0.15	0.99 ± 0.06	0.98 ± 0.10
Sr (4607.33) I	1.75 ± 0.13	3.81 ± 0.22	0.98 ± 0.07	1.01 ± 0.04	0.66 ± 0.07
Ba (4554.04) II	1.71 ± 0.24	3.09 ± 0.41	1.07 ± 0.12	0.98 ± 0.04	0.99 ± 0.07
Cu (3247.54) I	1.06 ± 0.05	1.08 ± 0.06	1.05 ± 0.04		
Cr (4254.35) I	1.04 ± 0.06	1.90 ± 0.13	0.97 ± 0.04		
Mn (4030.76) I	1.01 ± 0.03	1.56 ± 0.06	1.05 ± 0.08		
Mo (3798.25) I	1.00 ± 0.03	0.95 ± 0.06	1.03 ± 0.06		
Co (3453.51) I	1.00 ± 0.02	1.11 ± 0.02	1.00 ± 0.02		
V (4379.24) I	1.03 ± 0.05	1.08 ± 0.04	1.02 ± 0.03		
Ni (3619.39) I	1.05 ± 0.04	1.05 ± 0.08	1.02 ± 0.02		
Fe (3737.13) I	1.00 ± 0.04	1.05 ± 0.03	1.03 ± 0.03		

<sup>a</sup> I denotes neutral species, II denotes singly charged species. <sup>b</sup> Intensity signal observed for multielement solution divided by the intensity signal for the single element solution. <sup>c</sup> Intensity signal observed for single element solution containing 1000 mg/L Rb divided by the intensity signal for the single element solution with no Rb present. <sup>d</sup> Intensity signal observed for multielement solution containing 1000 mg/L Rb divided by the intensity signal obtained for the single element solution containing 1000 mg/L Rb. <sup>e</sup> Intensity signal observed for multielement solution containing 0.25 mol/L H<sub>3</sub>PO<sub>4</sub> divided by the intensity signal for the multielement solution with no H<sub>3</sub>PO<sub>4</sub> present. <sup>f</sup> Intensity signal observed for the multielement solution containing 0.0054 mol/L AlCl<sub>3</sub> divided by the intensity signal for the multielement solution with no AlCl<sub>3</sub> present.

observation period with a video system bandwidth of 10 Hz.

**Plasma Characteristics.** The image dissector operating with a bandwidth of 10 Hz and an observation time of 2 s was used for all measurements reported in this section.

Initial experiments with the plasma source were conducted with single element solutions and with two different multielement solutions. One solution contained 5 mg/L (ppm) Ca; 10 mg/L Na, K, Sr, and Ba; 20 mg/L Mg; and 40 mg/L Li. The other solution contained 6 mg/L Cu, Cr, and Mo and 20 mg/L Ni, Co, Fe, V, and Mn. Each element was studied individually with the observation region in the plasma selected to give the maximum emission intensity for the particular element under investigation.

Although the primary goal of this work was to evaluate performance characteristics of the echelle spectrometer/imaging detector systems, preliminary experiments showed that some characteristics of the dc plasma source needed study because some significant interactions among different alkali and alkaline earth element responses were observed. These effects are illustrated by data in the second column in Table II where it is apparent that ratios of multielement responses to single element responses are statistically different from unity for all alkali and alkaline earth elements. These interelement effects caused serious nonlinearities in calibration curves for these elements in multielement solutions and it was necessary to resolve this problem before continuing with the multielement determinations.

The fact that the alkali and alkaline earth metals showed these interactions while the transition metals did not, suggested the possibility that the plasma was causing the alkali and alkaline earth metals to be highly ionized and that the presence of other ionizable elements would increase the partial pressure of electrons in the plasma so that equilibria would be shifted toward lower oxidation states and thereby enhance emission from these states. If this were the case, then a high concentration of an easily ionizable element should minimize interactions among small amounts of different elements in analytical mixtures. To test this hypothesis, the single- and multielement experiments were carried out in the presence

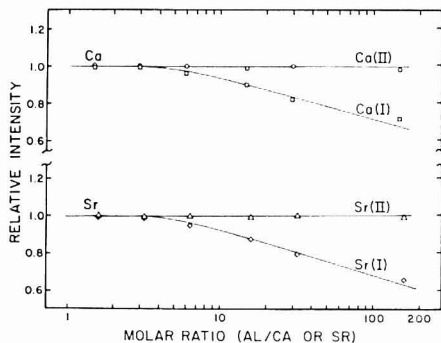


Figure 3. Effect of aluminum on calcium and strontium emission intensities. Ca II (3933.67 Å); Ca I (4226.73 Å); Sr II (4077.71 Å); Sr I (4607.33 Å). Solution contained 2 mg/L Ca; 4 mg/L Na, Ba, Sr; 8 mg/L Mg; 16 mg/L Li and K, and indicated amount of Al as AlCl<sub>3</sub> or Al(NO<sub>3</sub>)<sub>3</sub>.

of 1000 mg/L rubidium and the results are presented in the third and fourth columns of Table II. The high concentration of Rb is observed to enhance the responses of all of the alkali and alkaline earth metals as well as some of the transition elements. Most importantly from the point of view of this study, data in the fourth column show that the Rb serves its intended function of "buffering" out interactions among different elements in multielement solutions. Accordingly, all subsequent experiments with the dc plasma were carried out with solutions containing 1000 mg/L Rb.

Having noted the interactions among alkali and alkaline earth metals, we elected also to examine other interactions that are common in flame emission, namely effects of phosphate and aluminum on calcium emission. Response ratios for the alkali and alkaline earth elements in the presence and absence of phosphate and aluminum are included as the

Table III. Comparison of the Silicon Vidicon and the Image Dissector for the Simultaneous Determination of Li, Na, K, Mg, Ca, Sr, and Ba with a dc Plasma

Element ( $\lambda$ )	Silicon vidicon			Image dissector			Detection limit ratio (STV/ID)
	Back-ground std dev, nA <sup>a</sup>	Sensitivity, nA/mg/L <sup>b</sup>	Detection limit, mg/L <sup>c</sup>	Back-ground std dev, nA <sup>a</sup>	Sensitivity, nA/mg/L <sup>b</sup>	Detection limit, mg/L <sup>c</sup>	
Li (6103.64)	0.043	0.317 $\pm$ 0.003	0.271	0.081	8.2 $\pm$ 0.4	0.020	14
Na (5889.95)	0.051	3.75 $\pm$ 0.19	0.027	0.089	115 $\pm$ 3	0.0015	18
Na (5895.92)	0.058	1.90 $\pm$ 0.06	0.061	0.093	69 $\pm$ 2	0.0027	23
K (7698.98)	0.052	0.701 $\pm$ 0.007	0.148	0.064	3.28 $\pm$ 0.09	0.039	4
Mg (5183.62)	0.056	0.042 $\pm$ 0.002	2.667	0.105	1.08 $\pm$ 0.06	0.194	14
Mg (2795.53)	— <sup>d</sup>	—	—	0.063	33.5 $\pm$ 0.9	0.0038	—
Ca (3933.67)	0.047	4.13 $\pm$ 0.16	0.023	0.161	449 $\pm$ 11	0.00072	32
Ca (4226.73)	0.055	1.98 $\pm$ 0.02	0.066	0.098	122 $\pm$ 3	0.0016	35
Sr (4077.71)	0.052	2.64 $\pm$ 0.05	0.039	0.171	346 $\pm$ 5	0.00099	39
Sr (4215.52)	0.043	1.72 $\pm$ 0.04	0.050	0.161	127 $\pm$ 4	0.0025	20
Sr (4607.33)	0.057	0.91 $\pm$ 0.02	0.125	0.128	36.9 $\pm$ 0.9	0.0069	18
Ba (4554.04)	0.056	1.48 $\pm$ 0.06	0.076	0.112	75.1 $\pm$ 2.8	0.0030	25

<sup>a</sup> Based on six replicate measurements of the Rb blank. <sup>b</sup> Slope of the calibration plot based on three measurements at each concentration used. <sup>c</sup> Concentration producing a signal equal to twice the background standard deviation. <sup>d</sup> Glass faceplate prohibited measurements for this wavelength.

last two columns in Table II. There are no statistically significant effects of phosphate on any elements, and effects of aluminum are significant only for the Ca (4226.73) and Sr (4607.33) lines. To explore these effects further, measurements were made on Ca and Sr at several different aluminum concentrations and results are presented in Figure 3. The effects of aluminum on the Ca and Sr emissions were independent of whether  $\text{AlCl}_3$  or  $\text{Al}(\text{NO}_3)_3$  was used, an observation that is consistent with findings for an inductively coupled plasma (17). These data show that determinations of Ca and Sr with this dc plasma in the presence of aluminum are best based on the Ca (3933.67) and Sr (4077.71 or 4215.52) lines.

**Analytical Results.** Analytical data with the vidicon were obtained using a tube with a glass faceplate (No. 4532 A, RCA) which dictated that the comparison be made with the alkali and alkaline earth metals, because the strongest emission lines for these elements are in the visible region of the spectrum. This comparison of detectors is valid because the wavelength range was confined to a region in which the response of the vidicon with the glass faceplate is similar to that of the tube with a fused silica faceplate (1).

For the silicon vidicon, the target was primed between 200-ms exposures by 20 erase cycles of 10-ms duration each. Twenty-five points were acquired at each wavelength and the three points corresponding to the highest intensities were summed to produce a peak area that was then corrected for background by subtracting a weighted average of the first and last two data points for each wavelength. Thirty-two exposures were summed at each wavelength requiring approximately 13 s per run. For the image dissector, a 1-s observation time at a 10-Hz bandwidth was used providing a total analysis time of 12 s per run.

The observation region in the plasma was selected to provide the best compromise in the signal-to-background ratio observed for the largest possible number of wavelengths. The effect of this compromise on sensitivity is discussed in a later section.

Figure 4 represents plots of data from the image dissector for solutions containing Li, Na, K, Mg, Ca, Sr, and Ba. The solid lines represent the unweighted least-squares fits to the data sets. Each data point shown is the average of three replicate determinations. Although multiple wavelengths were observed for most of the elements, only the most intense line is shown here to avoid congestion. The slopes of the log-log plots range from  $0.983 \pm 0.027$  for Ba to  $1.022 \pm 0.036$  for Mg with standard errors of estimate of 0.014 and 0.018, re-

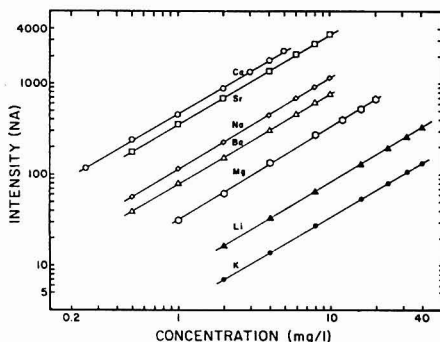


Figure 4. Linearity plots for the simultaneous determination of lithium, sodium, potassium, magnesium, calcium, strontium, and barium by atomic emission spectrometry. Ca (3933.67 Å); Sr (4077.71 Å); Na (5889.95 Å); Ba (4554.04 Å); Mg (2795.53 Å); Li (6103.64 Å); K (7698.98 Å).

spectively. Additionally, a linear analysis of the data showed that intercepts are not statistically different from zero. Standard errors of estimate ranged from 1.04 to 16.8 for K and Ca, respectively. The average relative standard deviation for the data obtained with both detectors is about 3.0%, as estimated from the slopes and confidence intervals listed in Table III, which is indicative of the precision of measurements obtainable with this plasma source.

The data in Table III suggest that for emission measurements, the detection limits for the image dissector system are lower than those for the silicon vidicon system by a factor of about 24. The decrease in the detection limit ratio at longer wavelengths ( $> 5000$  Å) results from a decrease in the luminous sensitivity of the image dissector relative to the silicon vidicon. The effect is quite apparent in the case of potassium.

Because the image dissector system exhibits a significant sensitivity advantage in relation to the silicon vidicon, the remainder of our attention in this study was devoted to the image dissector. Solutions containing varying amounts of Cu, Cr, Mo, Mn, Co, Ni, Fe, and V were examined using procedures described earlier in this section, and results of the study are summarized in Figure 5 and Table IV. Slopes of plots

Table IV. Comparison of Single Element and Multielement Sensitivities

Element ( $\lambda$ )	Single element sensitivity, nA/ppm <sup>a</sup>	Multielement sensitivity, nA/ppm <sup>b</sup>	Sensitivity ratio, SE/ME <sup>c</sup>
Li (6103.64)	9.6 $\pm$ 0.3	8.2 $\pm$ 0.4	1.17 $\pm$ 0.09
Na (5889.95)	166 $\pm$ 8	115 $\pm$ 3	1.44 $\pm$ 0.11
Na (5895.92)	92 $\pm$ 3	69 $\pm$ 2	1.34 $\pm$ 0.08
K (7698.98)	4.68 $\pm$ 0.21	3.28 $\pm$ 0.09	1.43 $\pm$ 0.10
Mg (2795.53)	41.4 $\pm$ 1.5	33.5 $\pm$ 0.9	1.24 $\pm$ 0.08
Mg (5183.62)	2.02 $\pm$ 0.09	1.08 $\pm$ 0.06	1.87 $\pm$ 0.19
Ca (3933.67)	493 $\pm$ 20	449 $\pm$ 8	1.10 $\pm$ 0.06
Ca (4226.73)	161 $\pm$ 5	122 $\pm$ 3	1.32 $\pm$ 0.07
Sr (4077.71)	360 $\pm$ 8	346 $\pm$ 5	1.04 $\pm$ 0.04
Sr (4215.52)	144 $\pm$ 5	127 $\pm$ 4	1.13 $\pm$ 0.07
Sr (4607.33)	46 $\pm$ 1	36.9 $\pm$ 0.9	1.25 $\pm$ 0.06
Ba (4554.04)	80 $\pm$ 2	75.1 $\pm$ 2.8	1.07 $\pm$ 0.07
Cu (3247.54)	41.2 $\pm$ 0.6	35.0 $\pm$ 0.3	1.17 $\pm$ 0.03
Cr (4354.35)	28.2 $\pm$ 0.4	26.4 $\pm$ 0.2	1.07 $\pm$ 0.02
Mn (4030.76)	16.3 $\pm$ 0.1	15.6 $\pm$ 0.4	1.04 $\pm$ 0.03
Mo (3798.25)	18.3 $\pm$ 0.1	17.8 $\pm$ 0.5	1.03 $\pm$ 0.03
Co (3453.51)	7.23 $\pm$ 0.09	6.93 $\pm$ 0.08	1.04 $\pm$ 0.02
V (4379.24)	3.44 $\pm$ 0.09	2.80 $\pm$ 0.07	1.23 $\pm$ 0.08
Ni (3619.32)	5.50 $\pm$ 0.04	5.63 $\pm$ 0.08	0.98 $\pm$ 0.02
Fe (3737.13)	3.20 $\pm$ 0.05	2.94 $\pm$ 0.07	1.09 $\pm$ 0.04

<sup>a</sup> Slope of calibration plot based on two replicate measurements at each concentration. <sup>b</sup> Slope of calibration plot based on three replicate measurements at each concentration. <sup>c</sup> Single element sensitivity divided by the multielement sensitivity.

Table V. Statistical Data for Simultaneous Determination of Cu, Cr, Mo, Mn, Co, Ni, Fe, and V with an Image Dissector and dc Plasma

Element ( $\lambda$ )	Background std dev, nA <sup>a</sup>	Sensitivity, nA/mg/L <sup>b</sup>	Detection limit, mg/L <sup>c</sup>	Intercept, nA	Linear correlation coefficient	log-log slope
Cu (3247.54)	0.086	35.0 $\pm$ 0.3	0.004	0.46 $\pm$ 2.5	0.9998	0.995 $\pm$ 0.010
Cr (4254.35)	0.071	26.4 $\pm$ 0.2	0.005	0.92 $\pm$ 3.4	0.9986	0.979 $\pm$ 0.024
Mo (3798.25)	0.090	17.8 $\pm$ 0.5	0.010	-4.3 $\pm$ 5.6	0.9990	1.013 $\pm$ 0.035
Mn (4030.76)	0.095	15.6 $\pm$ 0.4	0.012	3.4 $\pm$ 3.8	0.9994	1.023 $\pm$ 0.033
Co (3453.51)	0.093	6.93 $\pm$ 0.08	0.027	0.07 $\pm$ 2.9	0.9998	0.996 $\pm$ 0.019
Ni (3619.32)	0.122	5.63 $\pm$ 0.08	0.043	1.8 $\pm$ 3.9	0.9996	0.999 $\pm$ 0.021
Fe (3737.13)	0.107	2.94 $\pm$ 0.07	0.073	0.79 $\pm$ 2.8	0.9990	0.966 $\pm$ 0.043
V (4379.24)	0.047	2.80 $\pm$ 0.07	0.034	-3.2 $\pm$ 3.3	0.9993	0.976 $\pm$ 0.032

<sup>a</sup> Based on six replicate measurements of the Rb blank. <sup>b</sup> Slope of calibration plot based on three replicate measurements at each concentration used. <sup>c</sup> Concentration producing a signal equal to twice the background standard deviation.

in Figure 5 do not deviate significantly from unity at the 95% confidence level. These data, like those in Figure 4, demonstrate good linearity over two orders of magnitude or more for all elements examined. Also, intercepts did not differ significantly from zero at the 95% confidence level. Sensitivities and detection limits are summarized in Table V.

**Discussion.** All comparisons made to this point between the silicon vidicon and image dissector systems apply for spectrometer configurations in which approximately the same spectral range was displayed on both detectors. Because of the different sizes of the active surfaces of the detectors, the output focal lengths and linear dispersions were different with the values for the image dissector being 20.0/13.5 or 1.48 times larger than corresponding values for the silicon vidicon.

If the silicon vidicon were used with the same optical configuration as the image dissector, then the spectral resolution reported earlier (1) for the vidicon should be improved by the factor of 1.5 and would approach more closely the values observed with the image dissector. However, this improved resolution with the vidicon would be achieved at the expense of some other characteristics. One of the most obvious tradeoffs would be spectral range; and this loss could be more serious than just a reduction of the number of orders that could be accommodated along the vertical axis. The increased dispersion would force regions at the ends of orders onto the edges of the active surface of the vidicon where performance is degraded. Thus, not only would the spectral

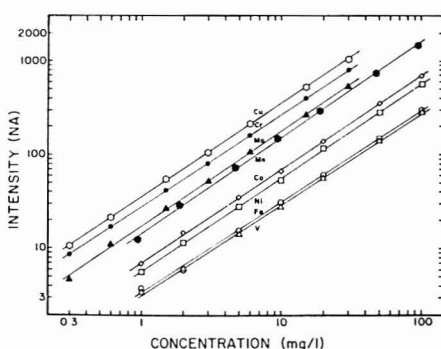


Figure 5. Linearity plots for the simultaneous determination of copper, chromium, molybdenum, manganese, cobalt, nickel, iron, and vanadium by atomic emission spectrometry. Cu (3247.54 Å); Cr (4254.35 Å); Mo (3798.25 Å); Mn (4030.76 Å); Co (3453.51 Å); Ni (3619.32 Å); Fe (3737.13 Å); V (4379.24 Å).

range be reduced, but some segments of the range would be lost. Another less obvious tradeoff would involve sensitivity and detection limits. The increased dispersion would concentrate less of the available energy on individual electronic



Table VI. Comparison of Detection Limits for Different Plasma Sources

Element	ID-DCP <sup>a</sup>	PMT-DCP <sup>b</sup>	ICP <sup>c</sup>
Li	0.029	0.001	—
Na	0.0015	0.02	0.0002
K	0.039	—	—
Mg	0.0038	0.002	0.0007
Ca	0.00072	0.002	0.00007
Sr	0.00099	0.01	0.00002
Ba	0.003	0.2	0.0001
Cu	0.004	0.02	0.001
Cr	0.005	0.009	0.001
Mn	0.012	0.02	0.0007
Mo	0.010	0.1	0.005
Co	0.027	0.8	0.003
V	0.034	0.01	0.006
Ni	0.043	0.01	0.006
Fe	0.073	0.02	0.005

<sup>a</sup> Image dissector-dc plasma, <sup>b</sup> dc plasma, other investigators (12, 18–20). <sup>c</sup> Inductively coupled plasma (21).

resolution elements, resulting in lower signals for the same total flux. Because the background imprecision of the vidicon camera system is fixed at about 40 pA, this would mean an increase in detection limits by a factor of about 1.5<sup>2</sup> or 2.3 over those reported in Table III for the vidicon.

The echelle image reduction factor of 3.9 used with the image dissector would require an entrance slit width of 150  $\mu$ m to match the 38- $\mu$ m aperture of the image dissector. Thus, the 200- $\mu$ m slit width available for this work likely degraded the ultimate resolution obtained with the image dissector by as much as 30% of that which could be achieved with the smaller slit.

It is more difficult to evaluate the effects of these projected changes, or differences in the deflection systems of the two detectors on the wavelength prediction errors. It is probable that these predictions could be improved somewhat by using more than the 12 calibration wavelengths utilized in this work, and including higher order terms in the DAC coordinate prediction model. However, the uncertainties reported in Table I are already well within the half widths of lines at all wavelengths, and we judge it is simpler and more reliable to locate peak maxima after the approximate positions of the lines have been located.

One important difference between these detectors that has not been represented by any data presented above, involves interactions among different electronic resolution elements. The vidicon and other integrating types of detectors are subject to charge migration or "blooming" effects. Preliminary data obtained for the optical configurations described above indicate that charge migration in the vidicon can cause significant signals in two to three orders on either side of the order for a moderately intense line. Similar data for the image dissector suggest interactions across no more than one order on either side of the order in which a line is observed, and this interaction could probably be reduced by working with a smaller slit height at the expense of some sensitivity. Although the "blooming" effect is absent for the image dissector, an analogous phenomenon may reduce the available linear dynamic range. If bright images are incident on the photocathode when a measurement of illumination at a low level is being made, the back-scattered flux from internal tube parts may limit the dynamic range to only 2 or 3 orders of magnitude, depending on the area, brightness, and location of the disturbing flux. Unlike storage camera tubes, the output signal from an image dissector is completely independent of scan rates or scan history and, therefore, there is no need to erase or prime the target between random access scans. This simplifies software control and permits more rapid acquisition

of spectral information. For the camera systems and modes of operation used in this work, the linear dynamic range for the silicon vidicon was about 10<sup>3</sup> while that for the image dissector was at least 10<sup>4</sup>.

Experiments were carried out to evaluate effects of compromise conditions on sensitivities of the elements in the two groups discussed earlier. Near-optimum conditions were established for each element determined individually, and the sensitivity of that element under the optimum conditions is compared with the sensitivity obtained with compromise conditions used for multielement determinations. Results are presented in Table IV for these comparisons.

The data show that single element sensitivities for the alkali and alkaline earth elements are about 30% higher than the multielement sensitivities. On the other hand, for the transition elements, there is little difference between single- and multielement sensitivities. The differences result because the alkali metals tend to emit most strongly in cooler regions of the plasma while the alkaline earth elements tend to emit most strongly in somewhat hotter regions of the plasma. In the case of the transition elements, optimum emission regions are in close proximity so that all elements are determined at near optimum conditions.

Data in Table VI provide a comparison of results obtained here with results reported by others with other systems. Our data in the second column are compared with single element results in the third column obtained with conventional optics, photomultiplier detectors, and a dc plasma (12, 18–20) similar to that used in this work and with results in the fourth column obtained with an inductively coupled plasma (21). Probably the most significant conclusion to be drawn from this comparison is that the echelle spectrometer/image dissector data compare very favorably with the conventional optics/photomultiplier data obtained with the same excitation source. Any advantages relative to the dc plasma offered by another excitation source such as the inductively coupled plasma with conventional optics/detectors should also be realizable with the echelle/image dissector system. Thus, with the image dissector, it is possible to realize the numerous advantages associated with electronic selection of all wavelengths of interest without significant compromises in performance characteristics. These data justify continued effort to exploit the full potential and establish the real limitations of the echelle spectrometer/imaging detector approach to simultaneous multielement determinations.

While these data show that the image dissector is superior to the silicon vidicon in several respects for atomic emission spectrometry, we believe the silicon vidicon and other integrating detectors retain significant advantages for molecular absorption (22) and fluorescence spectrometry (23) where resolution requirements are not so demanding and available radiant fluxes are higher.

#### LITERATURE CITED

- (1) H. L. Felkel, Jr., and H. L. Pardue, *Anal. Chem.*, **49**, 1112 (1977).
- (2) Y. Talmi, *Anal. Chem.*, **47**, 658A (1975).
- (3) Y. Talmi, *Anal. Chem.*, **47**, 697A (1975).
- (4) M. J. Milano, H. L. Pardue, T. E. Cook, R. E. Santini, D. W. Margerum, and J. M. T. Raycheba, *Anal. Chem.*, **46**, 374 (1974).
- (5) T. L. Chester, H. Haraguchi, D. O. Knapp, J. D. Messman, and J. D. Winefordner, *Appl. Spectrosc.*, **30**, 410 (1976).
- (6) G. Hornek, E. G. Codding, and S. T. Leung, *Appl. Spectrosc.*, **29**, 48 (1975).
- (7) K. M. Aldous, D. G. Mitchell, and K. W. Jackson, *Anal. Chem.*, **47**, 1034 (1975).
- (8) N. G. Howell and G. H. Morrison, *Anal. Chem.*, **49**, 106 (1977).
- (9) D. L. Wood, A. B. Dargis, and D. L. Nash, *Appl. Spectrosc.*, **27**, 310 (1975).
- (10) A. Danielsson, P. Lindblom, and E. Söderman, *Chem. Scr.*, **6**, 5 (1974).
- (11) A. Danielsson and P. Lindblom, *Appl. Spectrosc.*, **30**, 151 (1976).
- (12) R. K. Skogerboe, I. T. Urra, and G. N. Coleman, *Appl. Spectrosc.*, **30**, 500 (1976).
- (13) H. L. Pardue, T. E. Hewitt, and M. J. Milano, *Clin. Chem. (Winston-Salem, N.C.)*, **20**, 1028 (1974).
- (14) T. E. Cook, M. J. Milano, and H. L. Pardue, *Clin. Chem. (Winston-Salem, N.C.)*, **20**, 1422 (1974).

- (15) R. P. Cooney, G. D. Boutilier, and J. D. Winefordner, *Anal. Chem.*, **49**, 1048 (1977).
- (16) R. E. Dessy, W. D. Reynolds, W. G. Nunn, C. A. Titus, and G. F. Moler, *Clin. Chem. (Winston-Salem, N.C.)*, **22**, 1472 (1976).
- (17) G. F. Larson, V. A. Fassel, R. H. Scott, and R. N. Kniseley, *Anal. Chem.*, **47**, 236 (1975).
- (18) S. E. Valente and W. G. Schrenk, *Appl. Spectrosc.*, **24**, 197 (1970).
- (19) W. E. Rippetoe, E. R. Johnson, and T. J. Vickers, *Anal. Chem.*, **47**, 436 (1975).
- (20) J. F. Chapman, L. S. Dale, and R. N. Whittam, *Analyst (London)*, **98**, 529 (1973).
- (21) V. A. Fassel and R. N. Kniseley, *Anal. Chem.*, **46**, 1110A (1974).

- (22) A. E. McDowell and H. L. Pardue, *Anal. Chem.*, **49**, 1171 (1977).
- (23) I. M. Warner, J. B. Callis, E. R. Davidson, and G. D. Christian, *Clin. Chem. (Winston-Salem, N.C.)*, **22**, 1483 (1976).

RECEIVED for review September 10, 1977. Accepted January 9, 1978. This work was supported by Grant No. CHE75-13404 from the National Science Foundation. One of us (H.L.F.) expresses appreciation for an ACS Analytical Division Fellowship sponsored by Procter and Gamble Co.

## Room-Temperature Phosphorescence of the Phthalic Acid Isomers, *p*-Aminobenzoic Acid, and Terephthalamide Adsorbed on Silica Gel

Charles D. Ford and Robert J. Hurtubise\*

Chemistry Department, University of Wyoming, Laramie, Wyoming 82071

The phthalic acid isomers and other compounds exhibited room-temperature phosphorescence when adsorbed on dried silica gel. Compounds with structural similarities to terephthalic acid were studied to ascertain the mode of interaction between the adsorbed molecule and the silica gel surface. From the results of this study, it appears that the interaction is mainly hydrogen bonding. Also, the analytical potential of determining terephthalic acid by room-temperature phosphorescence is discussed.

Room-temperature phosphorescence (RTP) was first reported by Roth (1). He obtained RTP from aromatic compounds adsorbed on filter paper and cellulose. Schulman and Walling (2, 3) reported the RTP of ionic organic compounds adsorbed on solid supports such as silica, alumina, paper, and asbestos. Paynter et al. (4) developed quantitative methods employing RTP to determine many compounds of biological importance. Wellons et al. (5) further studied ionic compounds which exhibited RTP when adsorbed on filter paper. Seybold and White (6) used the external heavy atom effect to enhance the RTP of compounds adsorbed on filter paper. White and Seybold (7) further studied the effect of the external heavy atom effect on RTP. Vo-Dinh et al. (8, 9) reported the RTP of several polycyclic aromatic hydrocarbons and the use of NaI as an external heavy atom to enhance the RTP of several biologically important compounds. Jakovljevic (10) employed lead or thallium salts as external heavy atoms to enhance RTP of compounds adsorbed on filter paper. von Wandruszka and Hurtubise (11-13) developed a room-temperature phosphorimetric method for determining *p*-aminobenzoic acid adsorbed on sodium acetate, obtained analytically useful signals from several other organic compounds, and offered explanations for the mode of interaction of the compounds with sodium acetate. Recently, Schulman and Parker (14) studied the effects of moisture, O<sub>2</sub>, and the nature of the support-phosphor interaction on RTP.

In the present work, RTP was obtained from the phthalic acid isomers and other compounds adsorbed on dried silica gel.

### EXPERIMENTAL

**Apparatus.** Phosphorescence excitation and emission spectra and maximum excitation and emission wavelengths were obtained using the phosphoroscope accessory of the Perkin-Elmer MPF-2A fluorescence spectrophotometer with the excitation and emission

slits set at 16 nm. All relative emission intensities of adsorbed species were obtained with a Schoeffel SD3000 spectrodensitometer with the inlet slit at 2.0 mm and the exit slit at 3.0 mm. Experimental details have been previously described (11).

Low-temperature phosphorescence intensities were determined for several compounds by employing a cold stage with the spectrodensitometer. The cold stage was constructed by coiling 2-mm i.d. copper tubing into a circular copper box such that the maximum surface area of the box was in contact with the tubing. A copper top was fixed on the box and positioned to ensure contact with the copper tubing. The copper tubing exited the box on opposite sides. The dimensions of the cold stage are as follows: height, 0.9 cm; diameter, 6.0 cm; exit copper tubing length, 0.5 m; and entrance copper tubing length, 1.0 m. The cold stage was fitted into a styrofoam holder for insulation. Liquid nitrogen was forced through the cold stage and the stage approached approximately liquid nitrogen temperature in about 10 min.

**Reagents.** Ethanol was purified by distillation as described by Winefordner and Tin (15). SpectraAR grade dimethylformamide (Mallinckrodt, St. Louis, Mo.) was used without further purification. Terephthalic acid (TPA) and *p*-aminobenzoic acid (PABA) were purified by recrystallization from ethanol. The silica gel chromatoplates were aluminum backed (EM Laboratories Inc., Elmsford, N.Y.). Aluminum backed chromatoplates were used because of their heating and cooling characteristics. Plastic backed plates would not withstand high temperature and glass backed plates required longer heating and cooling times. Each chromatoplate was developed with distilled ethanol prior to use to concentrate any fluorescent impurities at one end of the plate. All other compounds were reagent grade and used without further purification.

**Procedure.** Standard solutions of TPA were prepared as follows. An appropriate weight of TPA was dissolved in ethanol:dimethylformamide (8:2) to give a concentration of 1 µg/µL (16). From this solution standards were prepared such that 5 µL of the solutions to be spotted contained 0.10 to 1.3 µg of TPA. After spotting the standards, the chromatoplate was then placed in an oven at 110 °C for 45 min and then allowed to cool to room temperature. The plate was then placed on the moving stage of the spectrodensitometer and each spot was scanned with the excitation monochromator set at 293 nm and the wedge emission monochromator set at 435 nm. The phosphorescence signal from each spot was maximized before measurements were recorded. All other compounds were dissolved in ethanol before spotting on silica gel chromatoplates.

### RESULTS AND DISCUSSION

**Excitation and Emission Spectra and Calibration Curve.** Phosphorescence excitation and emission spectra of TPA and the other compounds adsorbed on silica gel were

Table I. Room-Temperature and Low-Temperature Phosphorescence Properties of Compounds Adsorbed on Silica Gel<sup>a</sup>

	$\lambda_{ex}$ max, nm	$\lambda_{em}$ max, nm	Room-temperature relative intensity <sup>b</sup>	Room-temperature relative intensity <sup>c</sup>	Low-temperature relative intensity <sup>d</sup>
Terephthalic acid	292	418	100	223	1338
<i>p</i> -Aminobenzoic acid	287	432	50	78	411
Terephthalamide	283	410	none detected	25	275
Phthalic acid	289	432	11.5	12.5	123
Isophthalic acid	291	415	none detected	none detected	none detected

<sup>a</sup> Each sample at 0.40  $\mu$ g. <sup>b</sup> Dried for 10 min at 110 °C. <sup>c</sup> Dried for 10 min at 110 °C then an additional 10 min at 210 °C. <sup>d</sup> Dried for 10 min at 210 °C.

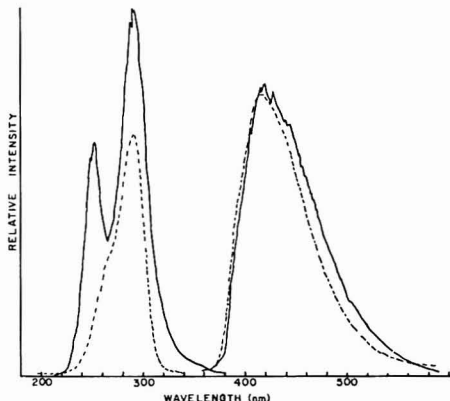


Figure 1. Room temperature (---) phosphorescence excitation and emission spectra of TPA adsorbed on silica gel and liquid nitrogen temperature (—) phosphorescence excitation and emission spectra of TPA in ethanol. Relative intensities were adjusted arbitrarily.

obtained using the phosphoroscope accessory of the fluorescence spectrophotometer. For TPA, spectra were obtained both at liquid nitrogen temperature in ethanol, and at room-temperature with TPA adsorbed on silica gel (Figure 1). The low-temperature phosphorescence excitation and emission maxima were 294 nm and 420 nm, respectively, whereas, the room-temperature phosphorescence excitation and emission maxima were 292 nm and 418 nm, respectively. The fluorescence excitation and emission spectra of TPA at 1  $\mu$ g/mL in ethanol were obtained with the fluorescence spectrophotometer. Weak fluorescent signals were obtained. The fluorescence excitation and emission maxima were 297 nm and 345 nm, respectively. The fluorescence of TPA on silica gel was assumed to be in the ultraviolet region. However, the fluorescence of TPA could not be distinguished on silica gel with either the fluorescence spectrophotometer or spectrodensitometer because of a scatter peak. Fluorescence is not expected to interfere with phosphorescence measurements when using the spectrodensitometer because the fluorescence of TPA is weak and the spectrodensitometer employs an ultraviolet cutoff filter.

The calibration curve for TPA adsorbed on silica gel was linear from 0 to 600 ng (Figure 2).

**Moisture Dependency.** The phosphorescence intensity of TPA and the other compounds adsorbed on silica gel proved to be moisture dependent (Table I). A 0.4- $\mu$ g sample of TPA adsorbed on a silica gel chromatoplate was placed in an oven at 110 °C and allowed to dry for 10 min. The relative intensity of the phosphorescence signal was measured and arbitrarily set at 100. The plate was then allowed to dry in an oven at 210 °C for an additional 10 min. The relative intensity of the

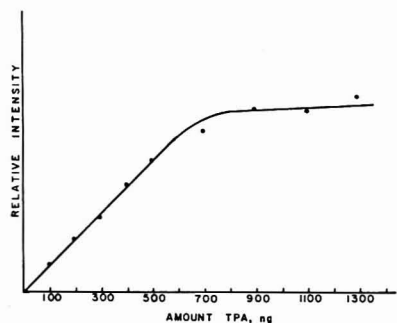
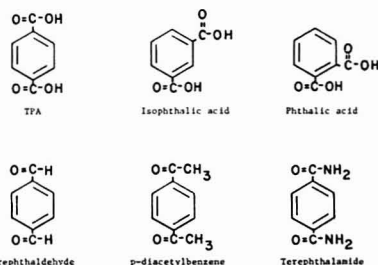


Figure 2. Calibration curve: phosphorescence intensity vs. amount of TPA.

phosphorescence was again measured and was found to be 223. It is assumed that the increase in phosphorescence is the result of less water absorbed on the silica gel surface. Schulman and Parker (14) have shown that the presence of moisture in several solid supports allows for collisional deactivation of the excited phosphor and increased penetration of O<sub>2</sub> into the sample matrix. Their results lend support to our conclusion. Also, Schulman and Parker discuss the effect of oxygen on quantitative reproducibility of the RTP method. No attempt was made in this work to exclude oxygen from our system because strong phosphorescent signals were obtained under the conditions employed. In preparing the calibration curves for TPA, the chromatoplates were dried for 45 min. at 110 °C (Figure 1). Further studies are needed to decide on the best conditions for maximum phosphorescent signals.

**Adsorption Mechanism.** For RTP to occur it seems necessary for the adsorbed molecule to be held rigidly to the adsorbent (4, 13, 14). To gain some insight into the mechanism of surface interaction between the adsorbate and silica gel, other compounds were studied which had structural similarities to terephthalic acid.



Terephthalaldehyde and *p*-diacetylbenzene exhibited no RTP on silica gel after drying; however, both of these compounds

exhibited moderate phosphorescence on silica gel at liquid nitrogen temperature. Terephthalamide gave a weak RTP signal when adsorbed on dried silica gel and a relatively weak signal at liquid nitrogen temperature (Table I).

Since terephthaldehyde and *p*-diacetylbenzene did not exhibit RTP and terephthalamide and TPA did, the interaction of the latter two compounds with silica gel is stronger compared to the interaction of the former two compounds with silica gel. Terephthalamide contains two primary amide nitrogens and amide hydrogens that are not found in terephthaldehyde or *p*-diacetylbenzene, whereas TPA contains two hydroxy groups which are absent in the dialdehyde and diacetyl compounds. The presence of primary amide nitrogens and amide hydrogens or hydroxyl groups allows for stronger interaction with the silica gel surface. It appears the main type of interaction with the silica gel surface is hydrogen bonding between the surface hydroxyl groups and the primary amide nitrogens and amide hydrogens or hydroxy groups on the molecules (14). The carbonyl groups in terephthalamide and TPA could also participate in hydrogen bonding (17-19).

PABA was spotted on a silica gel chromatoplate, dried, and excited with shortwave UV radiation from a hand lamp. The PABA exhibited a moderate RTP signal. When 4-chlorobenzoic acid was investigated under the same conditions, it exhibited phosphorescence only at liquid nitrogen temperature. A partial explanation for the difference is probably that the amino group forms stronger hydrogen bonds with surface hydroxyl groups compared to the chloro group.

TPA was placed on silica gel, dried, and then excited with shortwave UV radiation after the silica gel plate was submerged in *n*-hexane. It was assumed *n*-hexane would not disrupt hydrogen bonding between the adsorbate and adsorbent. The assumption was valid because RTP from the submerged plate was observed with little or no loss of intensity. However, when the same dried plate was placed in distilled water, the RTP was immediately quenched, presumably because of the disruption of the hydrogen bonds between TPA and silica gel surface. When the plate was removed from the water and dried, the RTP reappeared.

The other phthalic acid isomers were examined to determine what role para substitution played in the surface interaction. Phthalic acid on dried silica gel exhibited a moderate RTP signal when viewed under shortwave UV radiation. Isophthalic acid exhibited a very weak RTP signal under the same conditions which proved undetectable with the spectrophotometer (Table I). The RTP excitation and emission maxima and the relative phosphorescence intensities of the compounds studied are given in Table I. The data suggest that the strongest interaction with the silica gel surface is provided by para substitution, and meta substitution provides the weakest interaction.

Finally, no RTP signals were obtained by drying the chromatoplate first and then putting the sample on the dried plate. This suggests that water and ethanol are adsorbed very rapidly and occupy sites on silica gel that would otherwise be available to other molecules.

**Room-Temperature Phosphorescence vs. Low-Temperature Phosphorescence.** As Table I shows, the low-temperature phosphorescence signals obtained with the cold stage are enhanced compared to the signals obtained at room temperature. One would expect the compound which has the strongest interaction with silica gel to exhibit the least amount of signal enhancement at low temperature. PABA had a signal enhancement of 5.3 at low temperature compared to the signal obtained at room temperature for silica gel dried at 110 °C and 210 °C. A similar comparison showed that TPA had a

low-temperature signal enhancement of 6.0 indicating less interaction of TPA with the silica gel surface compared to PABA. Phthalic acid showed a low-temperature signal enhancement of 9.8. Finally, terephthalamide with a low-temperature signal enhancement of 11.0 has the weakest interaction with the surface.

**Analytical Potential.** A simple method of determining terephthalic acid in the presence of its isomers could be developed. The method would involve the separation of the dicarboxylic acids on a silica gel chromatoplate and a subsequent RTP measurement directly from the plate with a spectrophotometer. Braun and Geenen (20) have described the separation of aliphatic dicarboxylic acids on silica gel chromatoplates by employing an alcohol/water/ammonium hydroxide (100:12:16) eluting solvent. This solvent system proved useful in our work for the separation of the phthalic acid isomers. Following development, the chromatoplate was dried in an oven at 210 °C and then viewed under shortwave UV radiation. Three RTP signals were observed which corresponded to the phthalic acid isomers. The  $R_f$  values obtained for terephthalic acid, isophthalic acid, and phthalic acid were 0.42, 0.35, and 0.18, respectively. Mori and Takeuchi (21) separated the phthalic acid isomers on silica gel chromatoplates by employing a phenol/*n*-butanol/formic acid/water (5:2:1:2) eluting solvent or a phenol/formic acid/water (74:1:25) eluting solvent. These systems may prove useful. The calculated limit of detection at twice the background signal for TPA based on the data from the calibration curve in Figure 2 was 62 ng TPA. However, further enhancement of the phosphorescence signals and a lower limit of detection could be achieved for TPA adsorbed on dried silica gel by employing the cold stage described previously.

Other researchers (2-5, 8, 14) have employed alkaline solutions of compounds in their work with RTP. We found that a 1 M NaOH ethanol solution of TPA spotted on silica gel and dried gave no RTP. Also, TPA in ethanol:dimethylformamide(8:2) when added to 1 M NaOH ethanol solution gave a fine white precipitate. The method discussed for TPA does not require alkaline solutions and readily lends itself to thin-layer chromatography.

## LITERATURE CITED

- (1) M. Roth, *J. Chromatogr.*, **30**, 276 (1967).
- (2) E. M. Schulman and C. Walling, *Science*, **178**, 53 (1972).
- (3) E. M. Schulman and C. Walling, *J. Phys. Chem.*, **77**, 902 (1973).
- (4) R. A. Paynter, S. L. Wellons, and J. D. Winefordner, *Anal. Chem.*, **46**(6), 736 (1974).
- (5) S. L. Wellons, R. A. Paynter, and J. D. Winefordner, *Spectrochim. Acta, Part A*, **30**, 2133 (1974).
- (6) G. Seybold and W. White, *Anal. Chem.*, **47**, 1199 (1975).
- (7) W. White and P. G. Seybold, *J. Phys. Chem.*, **81**, 2035 (1977).
- (8) T. Vo-Dinh, E. L. Yen, and J. D. Winefordner, *Anal. Chem.*, **48**, 1186 (1976).
- (9) T. Vo-Dinh, E. Leu Yen, and J. D. Winefordner, *Talanta*, **24**, 146 (1977).
- (10) I. M. Jakovljevic, *Anal. Chem.*, **49**, 2048 (1977).
- (11) R. M. A. von Wandruszka and R. J. Hurtubise, *Anal. Chem.*, **48**, 1784 (1976).
- (12) R. M. A. von Wandruszka and R. J. Hurtubise, *Anal. Chim. Acta*, **83**, 331 (1977).
- (13) R. M. A. von Wandruszka and R. J. Hurtubise, *Anal. Chem.*, **49**, 2164 (1977).
- (14) E. M. Schulman and R. T. Parker, *J. Phys. Chem.*, **81**, 1932 (1977).
- (15) J. D. Winefordner and M. Tin, *Anal. Chim. Acta*, **31**, 239 (1964).
- (16) C. A. Lucchesi, *Anal. Chem.*, **48**, 433A (1974).
- (17) L. H. Little, "Infrared Spectra of Adsorbed Species", Academic Press, London, 1966, pp 228-272.
- (18) A. H. Sporer and K. N. Trueblood, *J. Chromatogr.*, **2**, 449 (1959).
- (19) R. Snyder and J. W. Ward, *J. Phys. Chem.*, **70**, 3941 (1966).
- (20) D. Braun and H. Geenen, *J. Chromatogr.*, **7**, 56 (1962).
- (21) S. Mori and T. Takeuchi, *J. Chromatogr.*, **47**, 224 (1970).

RECEIVED for review December 5, 1977. Accepted January 16, 1978.

# Solvent Enhancement Effects in Thin-Layer Phosphorimetry

J. N. Miller,\* D. L. Phillips, and D. Thorburn Burns<sup>1</sup>

*Department of Chemistry, Loughborough University, Loughborough, Leicestershire LE11 3TU, U.K.*

J. W. Bridges

*Department of Biochemistry, University of Surrey, Guildford, Surrey, GU2 5XH, U.K.*

The construction and use of an improved thin-layer phosphorimeter is described. The device permits flexible chromatography media to be scanned at 77 K, and also allows a complete characterization of the luminescence properties of the chromatographically-separated solutes. It is shown that the phosphorescence intensities of a variety of adsorbed materials are greatly increased by spraying the chromatography medium with a suitable solvent immediately before examination. The magnitude of the effect depends on the stationary phase, the structure of the adsorbed material, and the solvent sprayed. With the aid of the enhancement effect, nanogram quantities of separated solutes can be analyzed. The instrument is also suitable for examining the luminescence of adsorbed molecules at ambient temperatures.

Combinations of chromatographic methods and fluorescence spectrometry at room temperature have been repeatedly shown to be powerful analytical techniques which combine the selectivity of chromatographic separations with the sensitivity of fluorimetry. The use of fluorimetry to locate and quantitate the components of complex mixtures separated by thin-layer chromatography (TLC) is a particularly convenient approach (e.g., Ref. 1) which permits the simultaneous study of several very small samples, and instruments designed for the quantitative fluorimetric scanning of TLC plates are commercially available. Although recent studies have amply demonstrated the analytical value of phosphorimetry (2), a technique normally performed at 77 K, combinations of TLC and phosphorimetry have so far been little used. Winefordner and co-workers determined biphenyl in oranges (3), 4-nitrophenol in urine (4), and alkaloids in tobacco (5) by separating the samples on TLC plates, eluting the separated fractions with a suitable solvent, and determining them using conventional phosphorimetric sampling techniques. Studies have also been described in which the phosphorescence of samples separated by TLC have been detected visually by dipping the chromatography plates into liquid nitrogen and observing them under UV illumination. Sawicki et al. (6) investigated a series of aromatic atmospheric pollutants using this approach, and more recently de Silva and Strojny (7) have detected nanogram quantities of various drugs. In the authors' laboratory a thin layer phosphorimeter has been developed (8) as an accessory suitable for commercially-available spectrofluorimeters. This device permits the *in situ* quantitative determination and spectroscopic characterization, at 77 K, of solutes separated on flexible TLC media. The present paper describes the construction and evaluation of an improved thin-layer phosphorimeter. In particular it is demonstrated that the phosphorescence of solutes adsorbed on TLC plates can sometimes be greatly enhanced by spraying the plates with organic solvents before scanning, a procedure which permits the determination of nanogram quantities of such solutes.

## EXPERIMENTAL

**Construction of the Thin-Layer Phosphorimeter.** The thin-layer phosphorimeter is designed to fit the sample compartment of the Baird-Atomic (Baintree, Essex, U.K.) "Fluoriscord" spectrofluorimeter, and is illustrated in Figures 1 and 2. The TLC plate is affixed with elastic bands to the outside of a hollow copper sample drum (diameter 6.5 cm) which can be filled with liquid nitrogen through a narrower upper cylinder. The bottom of the drum is lipped to allow accurate positioning on the turntable in the holder compartment. This turntable is driven by a 12-V motor (Maxon 2125-912, Trident Engineering Ltd., Wokingham, U.K.) via a reduction gearbox and intermediate gear. The rate of rotation of the turntable is controlled by a variable output transformer and provides a scanning rate of 3–40 cm min<sup>-1</sup>. The outer cylinder of the sample holder compartment is pierced to permit two silica windows to be fitted. These windows allow incident light to reach the sample on the TLC plate at 45° to the normal, and the emitted light (observed at 45° to the normal) to reach the detector. Slots are provided on the cylinder which hold fixed slits. An annular space approximately 7 mm across separates the surface of the TLC plate from the inner surface of the cylinder and this space, and the outer surfaces of the silica windows, are continuously swept by a stream of dry oxygen-free nitrogen to prevent the formation of ice and to minimize luminescence quenching by oxygen. Phosphorescence and other long-lived luminescence phenomena are distinguished from prompt emissions and scattered light using a single disc phosphoscope (9). The disc, 65 mm in diameter, has three equally spaced slots 13 × 16 mm long cut in it and is driven at speeds of up to 10500 rpm by a 12-V electric motor (Paulhaber 26 PC.210, Portescap U.K. Ltd., Reading, U.K.). The phosphoscope assembly is painted matt black, and is fitted with a light baffle; it can be removed completely to permit observations of total luminescence. Small modifications to the sample chamber door on the spectrofluorimeter are necessary to accommodate the phosphorimeter assembly.

**Operation of the Thin-Layer Phosphorimeter.** Chromatographic separations were normally performed on silica gel TLC plates with aluminum foil backing (E. G. Merck, obtained through British Drug Houses, Poole, U.K.); the layer thickness was 250 µm and the plates supplied were cut into strips 20 cm long and 5 cm wide. (In a few experiments cellulose (Merck) or alumina plates prepared in this laboratory were used.) The luminescence background signal of the silica gel stationary phase was reduced by developing the plates in a chromatography tank with ethanol. Luminescent impurities were carried to one end of the thin layers and were removed by cutting the top 2 cm off the plates. The plates were then dried thoroughly before the chromatography proper began.

Samples, 5 µL in volume were applied to the TLC plates using an Arnold microapplicator (Burkard Instruments, Rickmansworth, U.K.). Test experiments showed that the relative standard deviation of the sample spot diameter obtained using this method was as low as 0.8%. The precision obtained using disposable micropipettes (Corning) was inferior (relative standard deviation 2.5%) but still adequate for many analyses. Chromatographic separations were carried out in a Shandon chromatographic tank lined with Whatman No. 1 filter paper; all experiments were carried out in the dark to minimize the possibility of photodecomposition. The drugs studied, their sources and luminescence characteristics and, where applicable, the solvent systems used and the *R<sub>f</sub>* values obtained, are shown in Table I. After development of a chromatogram, the plate was dried and wrapped

<sup>1</sup>Present address, Department of Chemistry, The Queen's University, Belfast, Northern Ireland.



Table I. Sources and Properties of Compounds Studied

Compound	Source	Excitation wavelength, nm	Phosphorescence wavelength, nm	Solvent system for TLC <sup>a</sup>	R <sub>f</sub> value
Benzophenone	B.D.H. Ltd.	350	445	-	-
4-Aminobenzoic acid	B.D.H. Ltd.	305	425	1	0.57
Phenobarbitone	May and Baker Ltd.	266	395	-	-
Phenobarbitone sodium	May and Baker Ltd.	266	395	-	-
N-Methylphenobarbitone	Winthrop Labs.	260	395	-	-
5-Phenyl-5-methylbarbituric acid	May and Baker Ltd.	266	395	-	-
Pericyazine	May and Baker Ltd.	315	540	-	-
Chlorpromazine-HCl	May and Baker Ltd.	310	490	-	-
Methotrimeprazine maleate	May and Baker Ltd.	305	485	-	-
Procaine-HCl	B.D.H. Ltd.	310	430	2	0.52
Sulfanilamide	May and Baker Ltd.	305	405	3	0.28
N-4-Acetylsulfanilamide	See Ref. 10	290	410	4	0.61
Sulfadiazine	May and Baker Ltd.	310	420	5	0.40
Sulfamerazine	May and Baker Ltd.	310	412	-	-
Sulfamethazine	May and Baker Ltd.	310	410	-	-
Sulfamethoxazole	May and Baker Ltd.	310	412	1	0.55

<sup>a</sup> Solvent systems: (1) Chloroform:butanol:acetic acid, 15:1:1, v/v/v. (2) Methanol. (3) Chloroform:methanol, 9:1, v/v. (4) Chloroform:butanol:ethanol:25% ammonia, 15:5:5:1 v/v/v/v. (5) Ethyl acetate:methanol:25% ammonia, 17:6:5, v/v/v.

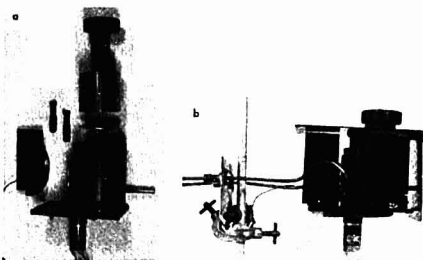


Figure 1. The thin-layer phosphorimeter attachment. (a) An exploded view of the sample drum (top), outer cylinder and turntable assembly (bottom), and single disc phosphoroscope (left). (b) Assembled, showing the fluorimeter sample compartment door and tubes for the dry nitrogen supply.

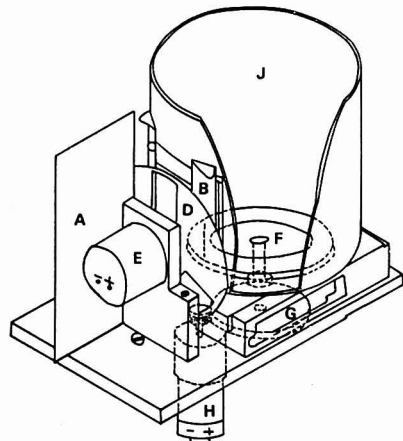


Figure 2. Sectional diagram of the thin-layer phosphorimeter attachment, showing the light baffle (A), slits (B, C), disc phosphoroscope (D), phosphoroscope motor (E), turntable (F), intermediate gear (G), turntable driving motor (H), and outer cylinder (J). The sample drum is omitted for the sake of clarity.

round the sample holder drum. It was then sprayed with ethanol or another solvent (see below) until just wet and the drum inserted into its compartment and filled with liquid nitrogen. After being allowed to cool for 2 min, the TLC plate was scanned at the rate of ca. 5 cm min<sup>-1</sup> and the results were displayed on the chart-recorder attached to the fluorimeter. The detection limit of a compound was taken to be that concentration giving a luminescence signal equal to twice the standard deviation of the background signal. Phosphorescence lifetimes were determined using a chart recorder as previously described (10).

In experiments to test the precision of thin-layer phosphorimetry, and in studies of the effects of spraying solvents on to phosphorescent spots, 5-μL samples of ethanolic solutions of various compounds were applied to TLC plates and studied directly, i.e., without a prior chromatographic step. All solvents and other chemicals were of AR or equivalent grade.

## RESULTS

When a single 5-μL sample of benzophenone on a silica gel layer was scanned repeatedly using the thin-layer phosphorimeter, the measured peak intensities showed a relative standard deviation of 4%. When samples that had been separated by TLC before scanning were studied, reproducible results were obtained only when the TLC plate was sprayed with a solvent (see below) and when an internal standard was used. In these circumstances the relative standard deviation for several solutes was ca. 8%.

Preliminary experiments showed that the phosphorescence intensity of adsorbed solutes was often dramatically enhanced by spraying the developed plate with a solvent before scanning; thus, the phosphorescence of chlorpromazine hydrochloride on silica gel was enhanced 100-fold by spraying the silica gel with ethanol from a distance of 20 cm for about 30 s. The background phosphorescence was enhanced only 10-fold. An extensive study of this phenomenon was undertaken, with the following results.

It was found that the measured phosphorescence intensity was maximized by spraying the plate until it had just acquired a wet appearance, i.e., there was a continuous film of solvent on the stationary phase. Spraying for longer periods produced no extra enhancement but sometimes caused the disruption of the stationary phase when the plate was subsequently cooled. In practice, no difficulty was experienced in assessing the optimal spraying time.

Table II shows the enhancement of phosphorescence of four drugs, adsorbed on silica gel layers, by a variety of solvents. The effects of a series of alcohols were investigated, to study the influence of hydrocarbon chain length on enhancement.

Table II. Enhancement of Phosphorescence on Silica Gel by Spraying with Various Solvents

Solvent	Dielectric constant (20 °C) <sup>a</sup>	Refractive Index (25 °C) <sup>a</sup>	Sulfadiazine	Sulfamethazine	Phenobarbitone	Methotrimprazine maleate
Methanol	32.8	1.326	65	251	15	96
Ethanol	24.3	1.359	91	240	20	80
1-Propanol	20.1	1.383	120	250	20	75
2-Propanol	18.3	1.375	112	270	34	100
1-Butanol	17.1	1.397	100	240	35	100
2-Methyl-2-propanol	10.9	1.383	30	60	-	-
1-Pentanol	13.9	1.408	45	136	16	66
1-Hexanol	13.3	1.416	21	70	9	50
Triethylamine	2.4	1.398	5	6	2	18
Dimethylformamide	37.6	1.427	108	152	9	53
Formamide	109.5	1.446	21	18	5	45
Diethylketone	17.0	1.392	4	12	-	32
Ethanol/potassium iodide	-	-	205	288	30	75
Methyl iodide	7.0	1.530	2	8	1	1
Dimethylsulfoxide	46.7	1.477	137	300	13	86
Hexane	1.89	1.372	11	31	11	12
Water	80.4	1.333	11	19	7	50

<sup>a</sup> From "Handbook of Chemistry and Physics," 55th ed., 1975.

Table III. Enhancing Effect of Ethanol on the Phosphorescence of Compounds Adsorbed onto Silica Gel

Compound	Enhancement factor
N-Methylphenobarbitone	16
Phenobarbitone	20
Phenobarbitone sodium	20
5-Phenyl-5-methyl barbituric acid	18
Sulfadiazine	91
Sulfamerazine	165
Sulfamethazine	240
Methotrimprazine maleate	80
Pericyazine	55
Chlorpromazine-HCl	52

Further solvents with diverse dielectric constants were examined, and methyl iodide and ethanol saturated with potassium iodide were used to ascertain whether a useful external heavy atom effect could be observed. In all cases ethanol, which was readily available in a state of high purity, produced a substantial enhancement of phosphorescence, and this solvent was used in subsequent studies involving other chromatographic media and samples. Phosphorescence enhancements were also observed on cellulose and alumina layers, but these effects were much smaller than those on silica gel layers; thus the enhancement factor for methotrimprazine maleate sprayed with ethanol was 80 on silica gel, 2.8 on alumina, and 2.2 on cellulose.

The effects of ethanol spraying on 10 drugs (including those listed in Table II) adsorbed on silica gel are shown in Table III — substantial enhancements were observed in all cases. The phosphorescence lifetimes at 77 K of sulfadiazine and sulfamethazine adsorbed on silica gel were determined, and compared with the values obtained in an ethanol glass. In all cases the values obtained were  $0.7 \pm 0.1$  s, in excellent agreement with previous determinations (10).

Table IV shows the limits of detection of six compounds determined using the thin-layer phosphorimeter at 77 K; the results are compared with recent estimates of the visual detection limits, also at 77 K, given by de Silva and Strojny (7).

## DISCUSSION

It is apparent from the results that thin-layer phosphorimetry, in conjunction with the solvent enhancement technique, offers a new and powerful approach to the analysis of complex mixtures of luminescent materials. Nanogram

Table IV. Detection Limits of Compounds on TLC Plates (ng/spot)

Compound	TLC phosphorimetry, 77K	Visual detection limits, native phosphorescence 77K (Ref. 7)
Sulfanilamide	0.5	100
Sulfadiazine	2	1000
Sulfamethoxazole	3	1000
N-4-Acetylsulfanilamide	7	-
4-Aminobenzoic acid	0.6	100
Procaine hydrochloride	2	100

quantities of phosphorescent compounds can be determined using a relatively simple accessory fitted to a fluorimeter, and the reproducibility, which is similar to that obtained in the fluorimetric scanning of TLC plates at room temperature (11), is quite adequate for most applications. The method will be expected to be of the greatest value in the analysis of mixtures of closely-similar materials such as a drug and its metabolites. Thus, nanogram quantities of thioridazine and five of its metabolites have been successfully separated and analyzed in recent experiments (12). The development of a thin-layer phosphorimeter also foreshadows the introduction of phosphorescent label molecules which, like the currently-used fluorescence labels, form strongly phosphorescent derivatives with specific functional groups of non- or feebly-luminescent molecules. Phosphorescent labels for phenols are under study in this laboratory (E. U. Akusoba and J. N. Miller, unpublished work). The apparatus described can also be used without liquid nitrogen for analyses by the newly-developed technique of room-temperature phosphorimetry (13).

The data cited may provide some evidence on the nature of the phosphorescence enhancement effect. Lawrence and Frei showed (14) that spraying dimethylamino-naphthalenesulfonyl ("dansyl") derivatives of primary amines on TLC plates with a triethanolamine-isopropanol mixture stabilized their fluorescence, and that other spray-reagents, including dioxan and various aqueous buffers, produced increases in the fluorescence signals. These effects were ascribed to the desorption of the sample molecules from the chromatographic medium into a thin surface layer of solvent. The enhancements of phosphorescence found in the present work, however, are far larger, and seem to depend on a number of factors, including the sprayed solvent, the chromatographic

stationary phase, and the type of compound under study. Consideration of Table II fails to reveal any obvious correlations between the observed magnitudes of the enhancement and the physical properties of the solvents; this is probably because the refractive index and dielectric constant data cited were mostly determined at room temperatures rather than 77 K. Among the eight alcohols used, 1-propanol and 2-propanol generally gave the best enhancements (although ethanol has been used in routine analysis, see above) and 1-pentanol and 1-hexanol gave poor results. The attempt to utilize the heavy atom effect by adding potassium iodide to the ethanol spray proved useful in the case of sulfadiazine but was of little value in the other cases: similarly uneven results have been observed in ethanol glasses at 77 K (15), and in room temperature phosphorimetry (16). Table III shows that different types of sample molecules will show widely different enhancement effects: the four oxybarbiturates showed similar but very moderate enhancements, the three sulfonamides all showed very substantial enhancements, and the three phenothiazines exhibited intermediate enhancement values. In contrast to the situation in room temperature phosphorescence (17), there is little evidence that the number of charged groups on the molecule has an appreciable effect on the observed enhancement; on the other hand the results in the case of sulfadiazine, sulfamerazine, and sulfamethazine indicate the possible importance of non-polar substituents.

It thus seems likely that no single factor can account for the enhancement phenomenon which is of such importance in thin-layer phosphorimetry.

## ACKNOWLEDGMENT

We thank L. A. Gifford and M. J. Jaycock for many valuable discussions, and A. Stevens for expert technical assistance.

## LITERATURE CITED

- (1) R. W. Frei, J. F. Lawrence, and P. E. Bellevue, *Fresenius Z. Anal. Chem.*, **254**, 271 (1971).
- (2) C. M. O'Donnell and J. D. Winefordner, *Clin. Chem. (Winston-Salem, N.C.)*, **21**, 285 (1975).
- (3) W. J. McCarthy and J. D. Winefordner, *J. Assoc. Off. Agric. Chem.*, **48**, 915 (1965).
- (4) W. J. McCarthy and J. D. Winefordner, *Anal. Chim. Acta*, **35**, 120 (1966).
- (5) J. D. Winefordner and H. A. Moye, *Anal. Chim. Acta*, **32**, 278 (1965).
- (6) E. Sawicki and H. Johnson, *Microchem. J.*, **8**, 85 (1964).
- (7) J. A. F. deSilva and N. Strojny, *Anal. Chem.*, **47**, 714 (1975).
- (8) L. A. Gifford, J. N. Miller, D. T. Burns, and J. W. Bridges, *J. Chromatogr.*, **103**, 15 (1975).
- (9) L. Langouet, *Appl. Opt.*, **11**, 2358 (1972).
- (10) J. W. Bridges, L. A. Gifford, W. P. Hayes, J. N. Miller, and D. T. Burns, *Anal. Chem.*, **468**, 1010 (1974).
- (11) D. E. Jänchen, in "Quantitative Paper and Thin Layer Chromatography", E. J. Sheiellard, Ed., Academic Press, London, 1968.
- (12) D. L. Phillips, J. N. Miller, and J. W. Bridges, in preparation.
- (13) R. A. Paynter, S. L. Wellons, and J. D. Winefordner, *Anal. Chem.*, **46**, 736 (1974).
- (14) J. F. Lawrence and R. W. Frei, *J. Chromatogr.*, **66**, 93 (1972).
- (15) W. J. McCarthy and J. D. Winefordner, *Talanta*, **78**, 305 (1970).
- (16) T. Vo Dinh, E. Lue Yen, and J. D. Winefordner, *Anal. Chem.*, **48**, 1186 (1976).
- (17) S. L. Wellons, R. A. Paynter, and J. D. Winefordner, *Spectrochem. Acta, Part A*, **30**, 2133 (1974).

RECEIVED for review November 29, 1977. Accepted December 23, 1977. We are grateful to the Medical Research Council for their continuing support of this work through the award of a Project Grant (G973/349/C).

# Comparison of Different Experimental Configurations in Pulsed Laser Induced Molecular Fluorescence

J. H. Richardson\* and S. M. George<sup>1</sup>

Lawrence Livermore Laboratory, General Chemistry Division, University of California, Livermore, California 94550

Three laser excitation sources (nitrogen pumped dye laser, cavity dumped argon ion laser, and externally pulse-picked mode-locked argon ion laser) are compared using rhodamine B as an ideal fluorophore. The major variable which was compared is peak power vs. repetition rate, complementary characteristics in current lasers. Boxcar detection is used with the first two sources, while photon counting techniques are used with the latter source. The limits of detection achieved were 1.0, 0.5 and 15 parts-per-trillion, respectively. For many analytical problems, the nitrogen pumped dye laser appears to be the most flexible and generally applicable laser excitation source.

The recent development of lasers has awakened a renaissance in many disciplines of chemistry. Analytical chemistry has been somewhat reluctant to embrace this new technology, but within the past several years there have been many reports of laser technology being applied advantageously to various analytical problems: (1) gas phase detection of atoms and molecules by absorption (1, 2), fluorescence (3-9),

electrical conductivity (10), and ionization (11); (2) optoacoustic techniques for gas (12) and condensed phases (13, 14); (3) detectors for thin-layer chromatography (15) and high pressure liquid chromatography (16, 17); (4) detection of trace contaminants in solids (18, 19); (5) detection of trace species in solution by fluorescence techniques (20-26).

The many capabilities offered by laser technology invariably give rise to confusion as to which laser is most appropriate for a given application. For example, for trace detection in solution, linewidth is obviously a minor consideration but tunability is just as obviously a major consideration. Less obvious are the relative merits of laser excitation pulse width. A narrow pulse width is desirable for temporal discrimination (23) against background fluorescence, but how significant the temporal resolution can be, will depend on the relative decay times of the laser excitation source, the background fluorescence, and the signal fluorescence. Other factors are repetition rate and peak power. With current laser technology, these two factors can be treated simultaneously, as they inevitably involve a trade-off: high peak powers entail low repetition rates, and high repetition rates entail low peak powers.

The relative merits of these latter two factors with respect to trace detection in solution have not been examined experimentally. There have been several theoretical papers

<sup>1</sup> Present address, University of California, Chemistry Department, Berkeley, Calif. 94720.

comparing pulsed vs. CW source excitation via signal/noise ratio calculations (27, 28). A pulsed nitrogen laser (337.1 nm) has been evaluated as an excitation source in various fluorimetric configurations (29). The effect of sufficiently high peak power is saturation of the absorber, and hence a limit to the fluorescence signal expected as a function of excitation power (30). However, even many high peak power lasers, unless very tightly focused, lack the power density necessary for saturation of a typical organic in solution (31, 32).

In this paper we compare the limit of detection obtainable for rhodamine B using boxcar detection with a high peak power, low repetition rate laser vs. a low peak power, high repetition rate laser. We then briefly compare these results with a slightly different low peak power, high repetition rate laser which uses photon counting. Similar limits of detection were obtained using boxcar detection with either laser source; however, the limit of detection using photon counting techniques was significantly higher. Secondary considerations make the high peak power, low repetition rate laser more useful for many analytical problems than the low peak power, high repetition rate laser.

### EXPERIMENTAL

**Chemicals.** Rhodamine B was obtained from Eastman Kodak and used without further purification. Previously distilled water was further purified using the Corning water still and demineralizer.

**Apparatus.** Figure 1a is a schematic of the experimental apparatus for determining the limit of detection using a high peak power, low repetition rate laser. A Moletron UV1000 was used to transversely pump a Moletron dye laser operated in the DL200 configuration. The dye laser pulse output (10 ns) was tuned to 514.5 nm (C485) and maximized for power at a 30-Hz repetition rate. The actual peak power delivered to the sample cell was 2 kW, measured with a Scientech 362 power meter (there are considerable losses going through the beam steering and shaping optics necessary to get the pulsed dye laser output into the sample cell).

The exact same sample chamber configuration was used in all three experimental arrangements (22–24). In addition, the same detection and signal processing equipment was used in comparing the high peak power, low repetition rate excitation source to the low peak power, high repetition rate source (compare Figures 1a and 1b).

Two lenses were used to image the fluorescence at right angles onto the photomultiplier tube (RCA 8850). Typically the PMT was operated at 1100 V. A Schott KV 555 long pass filter was used to eliminate Rayleigh scattering. A beam splitter was used to direct a small portion of the excitation radiation into a RCA 1P28 photomultiplier tube. This signal provided the trigger to the boxcar integrator (PAR 162). The 163 sampled integrator (S5 sampling head, 1-ns risetime) was used with the Moletron dye laser studies. Both the model 163 and the model 164 gated integrator (10 ns window) were used with the experimental configuration depicted in Figure 1b.

The maximum trigger rate for the 163/162 boxcar system was 10 kHz; for the 164/162 boxcar system, the maximum trigger rate was 5 MHz. Consequently there was no wasted excitation of the sample, as the excitation rate was always well below the maximum trigger rate and the excitation also provided the trigger. A nominal deadtime of 75 ns between the trigger pulse and the start of the signal processing by the boxcar was compensated for by additional delay line between the signal detector and boxcar.

Figure 1b is a schematic of the experimental apparatus for determining the limit of detection using a low peak power, high repetition rate laser. A Spectra-Physics 170-09 argon ion laser was used along with the Spectra-Physics acousto-optic output coupler (model 365/465). A Data Pulse 110B was used to generate the pulses for the rf driver. A symmetrically shaped 12-ns FWHM pulse was used at a repetition rate of 1 MHz. Lower frequencies were used to evaluate the effect of repetition rate on signal-to-noise at  $1 \times 10^{-11}$  M (vide infra). The peak power at 514.5 nm actually delivered to the sample was  $\sim 5$  W at 1 MHz (somewhat higher peak powers at lower repetition rates). The sample chamber,

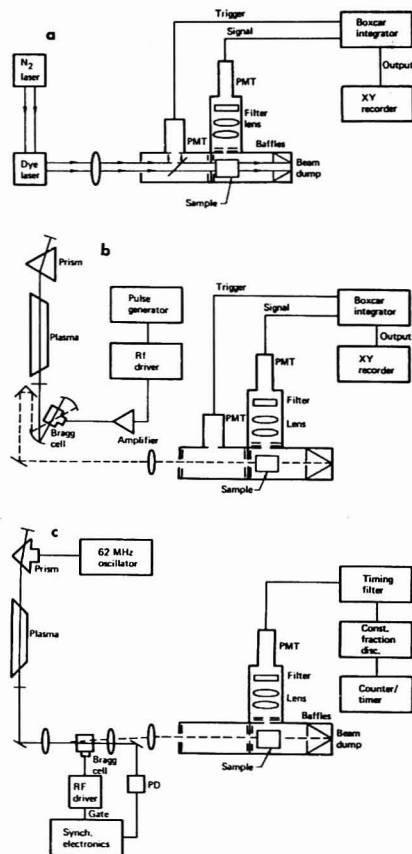


**Figure 1.** Schematic of the experimental apparatus: (a) nitrogen pumped dye laser/boxcar detection; (b) cavity dumped argon ion laser/boxcar detection; (c) pulse picked mode-locked argon ion laser/photon counting

detection, and signal processing were identical to that used with the Moletron laser. Typically the PMT was operated at 2000 V.

Figure 1c is a schematic of the experimental apparatus for determining the relative merits of photon counting to boxcar averaging using a short-lived fluorophore and a low peak power, high repetition rate laser. A Lextel 96 argon ion laser operating at 514.5 nm was used with a Spectra-Physics 361A mode locker. The laser was run at lower powers to obtain narrower pulses, typical pulse widths being 200–300 ps. A Spectra-Physics acousto-optic coupler identical to that used in cavity dumping (Figure 1b) was used to externally select a mode-locked pulse at a variable frequency. Typically the peak power of pulses directed into the sample chamber was 1 W.

The undeflected mode-locked train of pulses ( $\sim 120$  MHz) was directed into a TIXL56 avalanche photodiode to produce an electrical train of pulses of the same frequency but approximately 0.5 ns in width. These pulses are divided in frequency by a programmable counter (MECL logic) to produce a slower pulse train (33). A four-decade selectable switch allows repetition rate selection up to  $\sim 8$  MHz, although for these studies it was run at 1 MHz. Synchronizing logic then compares the divided pulsed

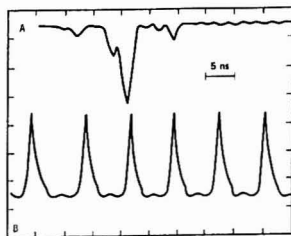


Figure 2. (A) Single pulse synchronously picked from (B) train of mode locked pulses

train with the original photodiode pulses to ensure coincidence between optical pulses and gate commands. A coaxial cable length provides gate pulse width control, thus allowing only as many optical pulses to be gated as desired. Under normal operation, the cable length is chosen to produce 10 ns wide gate pulses. These gate pulses in turn, control the Spectra-Physics rf driver, thereby creating in synchronization with the arrival of a mode-locked pulse the acoustic grating in the Bragg cell to deflect the mode-locked pulse into the sample chamber (Figure 2).

An EMI 9789 photomultiplier tube was operated at 1200 V for the photon counting detection because of its low dark current at room temperature ( $\sim 7$  counts per second). The bi-alkali spectral response of the EMI 9789 is similar to the 116 spectral response of the RCA 8850 for wavelengths greater than 550 nm. The PMT output was shaped by the Ortec 454 Timing Filter Amplifier, processed through the Ortec 473A Constant Fraction Discriminator, and counted by the Ortec 776 Counter-Timer (usually for 10-s intervals).

**Procedures.** Standard 1-cm Suprasil quartz fluorimeter cells were used. The cells are mounted in a rigid, rotatable cuvette holder which reproducibly determines their spatial position but permits rapid comparison with blanks.

Samples were made from several various stock solutions, not by progressive dilutions. The more dilute solutions were prepared just prior to measurement using freshly distilled water, standard volumetric flasks, and syringes. All glassware was thoroughly washed and rinsed with copious amounts of water. Glassware which came into contact with the more dilute solutions was investigated and eliminated as a possible contributor to the fluorescence signal. Each dilution was sampled several times; several different solutions of the same concentration were prepared and sampled. No other special precautions were taken in the sample handling (e.g., no attempt was made to remove oxygen from the solutions).

## RESULTS AND DISCUSSION

Rhodamine B was chosen as the fluorophor to compare the three experimental configurations for several reasons: a high extinction coefficient at 514 nm ( $2 \times 10^4 \text{ M}^{-1} \text{ cm}^{-1}$ ), a large Stokes shift ( $\lambda_{\text{em}}(\text{max}) = 572 \text{ nm}$ ), a high quantum yield ( $\sim 0.6$ ) (34) and a lifetime considerably less than 10 ns (34). Water is an admittedly poor solvent to use with rhodamine B if the goal is the ultimate in sensitivity. The Raman band at  $\sim 620 \text{ nm}$  does interfere in an experiment such as this one where temporal discrimination is not possible. However, in this particular wavelength region we have not noticed that water gave a particularly higher background signal than did other solvents and, in any event, water seems to be the most significant solvent from the standpoint of general purpose analytical relevance.

With the Moletron dye laser (Figure 1a) the limit of detection was  $2 \times 10^{-12} \text{ M}$  (1 part-per-trillion). For comparison, replacing the filter with a monochromator (a Jobin-Yvon H-20, 8-nm FWHM) resulted in a limit of detection of  $3 \times 10^{-11} \text{ M}$  (15 ppt). Figure 3 shows the dependence of fluorescence intensity on concentration; this curve was extended to  $1 \times 10^{-6} \text{ M}$ , and thus is linear for a dynamic range

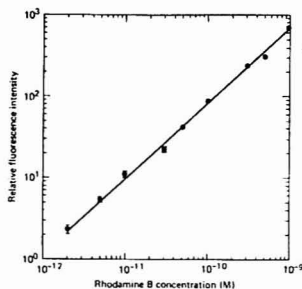


Figure 3. Rhodamine B fluorescence intensity vs. concentration using a nitrogen pumped dye laser as the excitation source

of over six orders of magnitude. A linear least-squares fit to the data in Figure 3 yields a slope of  $0.916 \pm 0.016$ . The individual error bars represent standard deviations in the several measurements taken at each concentration. Reproducibility was a greater deterrent than signal-to-noise in going to lower concentrations. Figure 4a shows representative data taken at  $1 \times 10^{-11} \text{ M}$ , with the PMT at 1100 V. All of the data with the nitrogen pumped dye laser was obtained using the sampled integrator with an effective time constant of 1.7 s. Increasing the effective time constant to 17 s greatly improved the S/N ratio at  $5 \times 10^{-12} \text{ M}$ , but long term drift associated with sample handling and laser power made it impossible to obtain reproducibly meaningful data.

The limit of detection for rhodamine B with the cavity dumped argon ion laser was  $1 \times 10^{-12} \text{ M}$  (0.5 ppt). This is an improvement in sensitivity of over two orders of magnitude compared to an earlier study which also used a cavity dumped argon ion laser (35), although some of this improvement is undoubtedly due to the wider bandpass used in the present experiments. A linear least-squares fit to the data yields a slope of  $0.84 \pm 0.03$ . Figure 4b shows representative data taken at  $1 \times 10^{-11} \text{ M}$  with the PMT at 2000 V. The signals were much smaller with the cavity dumped system, hence the need for much larger amplification. The limit of detection, 0.5 ppt, corresponded to a S/N ratio of approximately 2; i.e., reproducibility and sample handling were relatively less important than the slower pulsed nitrogen pumped dye laser. Decreasing the frequency to match the average power of the ion laser to that of the nitrogen pumped dye laser resulted in a slightly poorer S/N ratio and higher detection limit. Finally, at equal frequencies the fluorescence signal at  $1 \times 10^{-11} \text{ M}$  was not observed with the cavity dumped ion laser. Each instrumental system, therefore, had approximately the same absolute sensitivity in terms of ppt detected per unit energy delivered per second. A useful figure of merit is the detectability-power product, and these were approximately equal for the two systems ( $\sim 0.5 \text{ ppt-mW}$ ).

For comparison, Figure 4c shows representative data taken at  $1 \times 10^{-11} \text{ M}$  with the gated integrator and an effective time constant of 0.14 s. Considerable improvement in S/N is obtained at the expense of temporal resolution and overall signal intensity. It is evident that long term drift and sample handling, not S/N, would limit the sensitivity with the gated integrator and an effective time constant of 0.14 s. Considerable improvement in S/N is obtained at the expense of temporal resolution and overall signal intensity. It is evident that long term drift and sample handling, not S/N, would limit the sensitivity with the gated integrator. However, in this instance the detectability power product is poorer. The S/N was improved by an order of magnitude but the average power delivered went up by nearly two orders of magnitude, hence



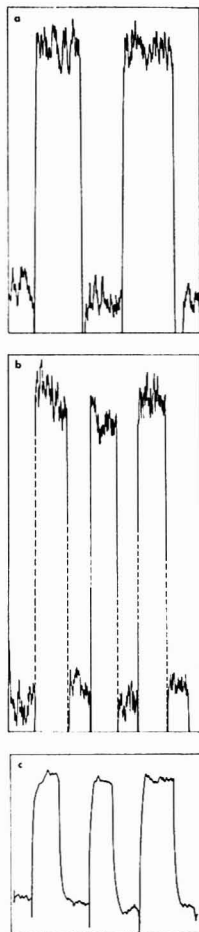


Figure 4. Representative data taken at  $1 \times 10^{-11}$  M with various laser excitation sources: (a) nitrogen pumped dye laser with 163 sampled integrator, PMT at 1100 V, effective TC = 1.7 s, 1 V/in, 1 V full scale; (b) cavity dumped argon ion laser with 163 sampled integrator, PMT at 2000 V, effective TC = 0.5 s, 1 V/in, 1 V full scale; (c) cavity dumped argon ion laser with 164 gated integrator, PMT at 2000 V, effective TC = 0.14 s, <1 V/in, 100 mV full scale

the detectability-power product is  $\sim 2.5$  ppt-mW.

Finally, data were obtained by photon counting with the pulse picked mode-locked argon ion laser (Figure 1c). The linear least-squares fit to these data yields a slope  $0.96 \pm 0.06$ . The limit of detection  $3 \times 10^{-11}$  M (15 ppt) is considerably higher than previously obtained, as is the scatter in the data. There was no temporal resolution in the current experiment, although with the narrow subnanosecond pulses afforded by the mode locked laser, temporal resolution vastly superior to the other two excitation sources could be achieved with a multichannel analyzer and time-to-amplitude converter. Longer counting times did not improve the sensitivity. Typical counting rates were 1300 counts/s at  $1 \times 10^{-10}$  M, with 600 counts/s from the blank.

Photon counting is, of course, best suited to low light levels, either due to low level sample absorption (high repetition flash lamps), wavelength resolution (laser Raman), or long lived species (36, 37). In summary, the poorer results obtained with the photon counting apparatus are not indicative of the general analytical utility of this technique, but instead reflect its particular disadvantages in this specific experiment.

## CONCLUSIONS

A nitrogen pumped dye laser and a cavity dumped argon ion laser have been shown to perform equally well under identical conditions for trace detection. However, other factors should be considered in choosing a laser system for analytical applications. Rhodamine B was specifically chosen as the test fluorophore so as not to unduly handicap the ion laser systems. The cavity dumped ion laser offers only a few select lines; the output can be used to pump a dye laser but at a considerable power loss and potential frequency spread (38). The smaller signal size associated with smaller peak powers leads to less flexibility in wavelength selection. For example, including a monochromator appears to decrease the sensitivity by about one order of magnitude with the nitrogen pumped dye laser system. This loss in signal can be mostly compensated for by increasing the amplifier gain (PMT); with the cavity dumped system, all the gain is needed with just the filter because of the low signal levels involved (the gain of the PMT for the cavity dumped system was higher than the nitrogen pumped dye laser system by more than a factor of  $5 \times 10^2$ ).

Tunability is much larger with the nitrogen pumped dye laser through a wider selection of both dyes and doubling techniques. Furthermore, the higher peak powers permit the application of nonlinear optical techniques to analytical problems (e.g., CARS (16)). Consequently, the nitrogen pumped dye laser offers greater flexibility in potential analytical applications. These results indicate that the synchronously pumped dye laser might prove to be another reasonable alternative, although it is more laser-technology oriented (39).

Digital detection doesn't appear to offer any improvement in sensitivity over gated analog detection. For on-line analysis of photostable, short-lived species, it appears to be even somewhat less sensitive, although its advantages in other types of analytical problems are undoubtedly significant.

## ACKNOWLEDGMENT

We thank L. Steinmetz and B. Wallin for technical assistance, and G. Haugen and R. Bystroff for assistance with the photon counting apparatus.

## LITERATURE CITED

- (1) M. Maeda, F. Ishitsuka, M. Matsumoto, and Y. Miyazoe, *Appl. Opt.*, **16**, 403 (1977).
- (2) T. W. Hänsch, A. C. Schawlow, and P. E. Toschek, *IEEE J. Quantum Electron.*, **8**, 802 (1972).
- (3) W. M. Fairbank, Jr., T. W. Hänsch, and A. C. Schawlow, *J. Opt. Soc. Am.*, **65**, 199 (1975).
- (4) J. A. Gellwachs, C. F. Klein, and J. E. Wessel, *Appl. Phys. Lett.*, **30**, 487 (1977).
- (5) G. M. Hietje, T. R. Copeland, and D. R. De Oliveira, *Anal. Chem.*, **48**, 142R (1976).
- (6) N. Omenetto, *Anal. Chem.*, **48**, 75A (1976).
- (7) R. B. Green, J. C. Travis, and R. A. Keller, *Anal. Chem.*, **48**, 195A (1976).
- (8) M. B. Denton and H. V. Malmstadt, *Appl. Phys. Lett.*, **18**, 465 (1971).
- (9) L. M. Frazer and J. D. Winefordner, *Anal. Chem.*, **43**, 1693 (1971).
- (10) R. B. Green, R. A. Keller, G. G. Luther, P. K. Schenck, and J. C. Travis, *Appl. Phys. Lett.*, **29**, 727 (1976).
- (11) G. S. Hurst, M. H. Nayfeh, and J. P. Young, *Phys. Rev. A*, **15**, 2283 (1977).
- (12) L. B. Kreuzer, *Anal. Chem.*, **48**, 237A (1974).
- (13) W. Labmann, H. J. Ludwig, and H. Welling, *Anal. Chem.*, **49**, 549 (1977).
- (14) M. Dixon, D. A. Hesser, and C. R. Webster, *Chem. Phys.*, **22**, 199 (1977).
- (15) M. R. Berman and R. N. Zare, *Anal. Chem.*, **47**, 1200 (1975).
- (16) L. B. Rogers, J. D. Stuart, L. P. Goss, T. B. Malloy, Jr., and L. A. Carreira, *Anal. Chem.*, **49**, 959 (1977).
- (17) M. J. Sepaniak and E. S. Yeung, *Anal. Chem.*, **49**, 1554 (1977).
- (18) J. C. Gustafson and J. C. Wright, *Anal. Chem.*, **49**, 1680 (1977).
- (19) F. J. Wright, *Anal. Chem.*, **49**, 1690 (1977).
- (20) T. Hirschfeld, *Appl. Opt.*, **15**, 2985 (1976).
- (21) A. B. Bradley and R. N. Zare, *J. Am. Chem. Soc.*, **98**, 620 (1976).

- (22) J. H. Richardson, B. W. Wallin, D. C. Johnson, and L. W. Hrubesh, *Anal. Chim. Acta*, **86**, 263 (1976).
- (23) J. H. Richardson and M. E. Ando, *Anal. Chem.*, **49**, 955 (1977).
- (24) J. H. Richardson, *Anal. Biochem.*, **83**, 754 (1977).
- (25) T. Imasaka, H. Kadone, T. Ogawa, and N. Ishibashi, *Anal. Chem.*, **49**, 667 (1977).
- (26) J. P. Hohlmer and P. J. Hargis, *Appl. Phys. Lett.*, **30**, 344 (1977).
- (27) G. D. Boutilier, J. D. Bradshaw, S. J. Weeks, and J. D. Winefordner, *Appl. Spectrosc.*, **31**, 307 (1977).
- (28) N. Omenetto, L. M. Frazer, and J. D. Winefordner, *Appl. Spectrosc. Rev.*, **7**, 147 (1973).
- (29) T. F. Van Geel and J. D. Winefordner, *Anal. Chem.*, **48**, 335 (1976).
- (30) N. Omenetto, P. Benetti, L. P. Hart, J. D. Winefordner, and C. Th. J. Alkemade, *Spectrochim. Acta, Part B*, **28**, 289 (1973).
- (31) L. Huff and L. G. De Shezer, *J. Opt. Soc. Am.*, **60**, 157 (1970).
- (32) G. R. Giuliano and L. D. Hess, *IEEE J. Quantum Electron.*, **3**, 358 (1967).
- (33) J. Breshers, L. L. Steinmetz, B. W. Wallin, and G. R. Haugen, *Rev. Sci. Instrum.*, manuscript in preparation.
- (34) M. J. Weber and M. Bass, *IEEE J. Quantum Electron.*, **5**, 175 (1969).
- (35) F. E. Lytle and M. S. Keltner, *Anal. Chem.*, **46**, 855 (1974).
- (36) R. S. Meltzer and R. M. Wood, *Appl. Opt.*, **16**, 1432 (1977).

- (37) As an example, trace uranium detection ( $r \sim 55 \mu\text{s}$  for  $\text{UO}_2^{2+}$ ) is extremely difficult without apparatus. F. B. Stephens, G. R. Haugen, and J. H. Richardson, our unpublished work (internal report UCID-17549 available from Technical Information Department, Lawrence Livermore Laboratory, University of California, Livermore, Calif. 94550).
- (38) J. H. Richardson, L. L. Steinmetz, and B. W. Wallin, *Appl. Opt.*, **16**, 1133 (1977).
- (39) J. M. Harris, L. M. Gray, M. J. Pelletier, and F. E. Lytle, *Mol. Photochem.*, **8**, 161 (1977).

RECEIVED November 7, 1977. Accepted January 13, 1978. Work performed under the auspices of the U.S. Department of Energy under contract No. W-7405-Eng-48. Reference to a company or product name does not imply approval or recommendation of the product by the University of California or the U.S. Energy Research & Development Administration to the exclusion of others that may be suitable.

## Automated Three-Dimensional Plotter for Fluorescence Measurements

Joon H. Rho\*

Clinical Pharmacology, Department of Medicine, Schools of Medicine and Pharmacy, University of Southern California, Los Angeles, California 90033

J. L. Stuart

J. Stuart Enterprises, Grass Valley, California 95945

The design and construction of an automated three-dimensional plotter for fluorescence measurements are described. The excitation and emission wavelengths form the abscissa and ordinate, respectively, and emission intensity is indicated by a series of isointensity contours similar to elevation levels on a topographic map. The device is used with a commercial spectrophotometer to rapidly record characteristic fluorographs of fluorescent substances in such a way that the spectral band contours at selected emission intensities are displayed to reveal all the spectral parameters at their peak intensities. Three-dimensional fluorescence properties of a wide variety of biological compounds were displayed by the contour plotter to show the characteristic spectral patterns of the compounds: photosynthetic pigments, proteins, polycyclic hydrocarbons, and crude oils. A stereofluorograph completely integrating all of the spectral characteristics can be constructed, and it is expected to be unique and quantitative for each substance.

The fluorescence property of a compound is conventionally studied by examination of both the activation spectrum and the emission spectrum. The fluorescence can be examined at one or more excitation wavelengths, or the excitation curve can be determined at a given fluorescence wavelength. There are many fluorescent compounds which yield almost identical excited electronic structure and their distinction at low concentration levels requires the examination of all details of the fluorescence spectra.

For complex spectra, the recording of a complete series of activation and fluorescence spectra is a rather tedious task. All permutations of emission intensity as a function of both

excitation and emission wavelengths will yield a three-dimensional response surface which can be visualized as a small mountain range. In an attempt to construct three-dimensional fluorescence spectral maxima, Schachter and Haenni (1963) developed a device for simultaneous recording of the activation and emission spectra, with the activation wavelengths on the vertical scale, and the emission wavelengths on the horizontal scale of a cathode ray oscilloscope graticule, the trace being recorded on Polaroid film (1). This yields a print with a raster of diagonal lines interrupted in wavelength regions of emitted radiation to produce a characteristic pattern of contour spots, ideally one for each maximum. The dimensions of each discrete spot are proportional to the width of the corresponding spectral band and the coordinates of the centroid for each discrete spot are the wavelengths of the activation and fluorescence maxima. To depict the three-dimensional fluorescence parameters, Fregard et al. obtained emission spectra at different excitation wavelengths and manually plotted contours of equal fluorescence intensity against excitation and emission wavenumbers to construct a "contour" map (2). In order to simplify this data processing task, Rho and Stuart (3) developed a device for the simultaneous recording of the activation and emission spectra, with fluorescence intensity levels plotted by a series of isointensity contours similar to elevation levels on a topographic map. Hornig et al. (4) pursued the contour plotting in which they repetitively scan with a spectrofluorometer to generate luminescence data which are taken directly into a minicomputer for correction and reduction to contour graphs. A computer-assisted structural interpretation of fluorescence spectra was also developed by Miller and Faulkner (5). A minicomputer was interfaced to an Aminco-Bowman spectro-

## PEN DROP CONTOUR PLOTTER DIAGRAM

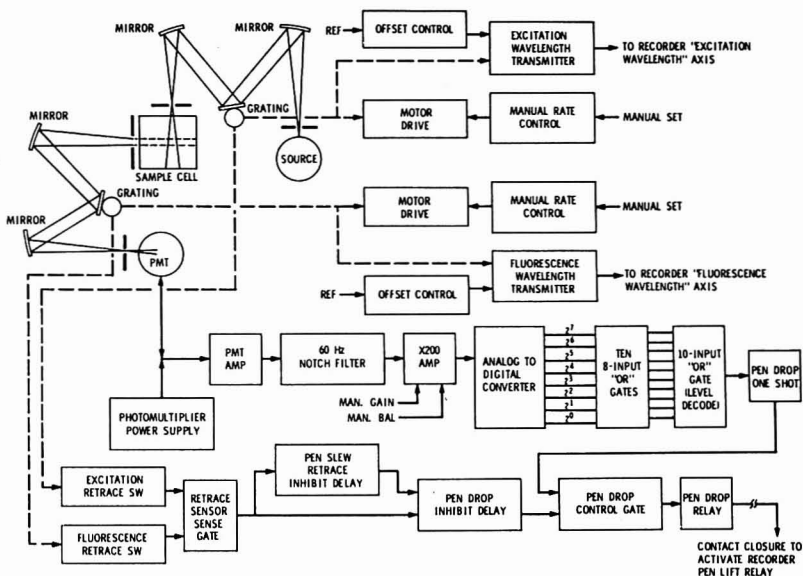


Figure 1. Schematic diagram of the electronics circuit designed to generate the isointensity contour plot. PMT: photomultiplier; Source: excitation light source

photofluorometer for the direct acquisition and comparisons of the most obvious spectral features such as the total number of peaks, peak locations, relative intensities, and the location of an excitation minimum. Recently, a method for displaying fluorescence spectra in a three-dimensional graphical format was developed by Warner et al. (6, 7) and Johnson et al. (8). They have used a polychromatic irradiation of the sample cuvette and a silicon-intensified target vidicon detector to measure all regions of the emission-excitation matrix simultaneously. In this paper, a simple noncomputerized method of obtaining a fluorescence contour map is described in detail. This method automatically records all the fluorescence spectral parameters of a given sample directly on a X-Y recorder in such a way that, in effect, a "stereofingerprint" of fluorescent mixture is presented in one plot. It delineates not only the activation and emission wavelengths, and emission intensities for each peak, but also the activation/emission spectral band stereo envelopes. Accordingly, this method permits unique characterization of even very closely related structures.

#### INSTRUMENT DESIGN AND DESCRIPTION

An Amino-Bowman Spectrophotofluorometer (Catalogue No. 4-8106) is used as a basic instrument. The light source used was a high-pressure xenon compact arc lamp (150 W) equipped with an off-axis ellipsoidal mirror. The light emitted by the sample was detected either with a highly sensitive trialkali photocathode tube or with a gallium-arsenide photocathode tube cooled to  $-20^{\circ}\text{C}$  to reduce noise. At the start of the measurement, the excitation monochromator is set at a lower end of the excitation wavelength and the emission monochromator is set to scan the entire region in 15 to 20 s. When a fluorescence scan is completed, the excitation monochromator advances automatically by a small increment (1 to 2 nm) to the next higher excitation wavelength point and the fluorescence is scanned again. Both the increment of the excitation wavelength and the scanning speed of the fluorescence are

manually adjustable. In this way, the entire excitation vs. fluorescence wavelength domain will be scanned within 10 to 15 min. The photomultiplier will sense the emission intensity level at every point in the scanned wavelength domain. If the detector output is quantized at discrete levels of intensity and these levels are plotted, then a three-dimensional representation of the fluorescent fingerprint will be generated. However, it is simpler to generate this information in the form of contours representing fixed levels of intensity. The block diagram of the electronics circuit designed to generate these isointensity plots is shown in Figure 1.

The wavelength transmitters position the recorder pen at the point representing the values of excitation and emission wavelength for each moment in time. The photomultiplier detector output will indicate the observed intensity for that point.

A binary-coded equivalent of the analog signal from the photomultiplier is generated through the use of a tracking analog to digital converter. This is a relatively simple system both in concept and in practice. Basic design requires the three major elements: an up/down counter, a current output digital to analog (D/A) converter, and a voltage comparator. The voltage at the comparator input will be the result of the analog input voltage minus the (D/A) comparator output sink current multiplied by the input resistance.

Assuming a perfect comparator, if the output voltage is above ground, the comparator output will be low causing the up/down counter to increase the D/A converter sink current by one least significant bit. The comparator will continue to examine the output voltage for polarity and will always drive the counter's code in the direction which causes the comparator output voltage to approach zero. Once a balance is achieved the loop is "locked" and tracks the analog input signal so long as the loop slow rate is not exceeded. When the loop is balanced, the converters' output is the binary-coded equivalent of the analog input. When encoding a dc signal the digital output will "dither" or alternate between the two adjacent states which bracket the theoretically correct output value. This is of little consequence as all A/D converters suffer an equivalent error known as the "Quantizing" error.

## Fluorograms of Benzo(a)pyrene Metabolites

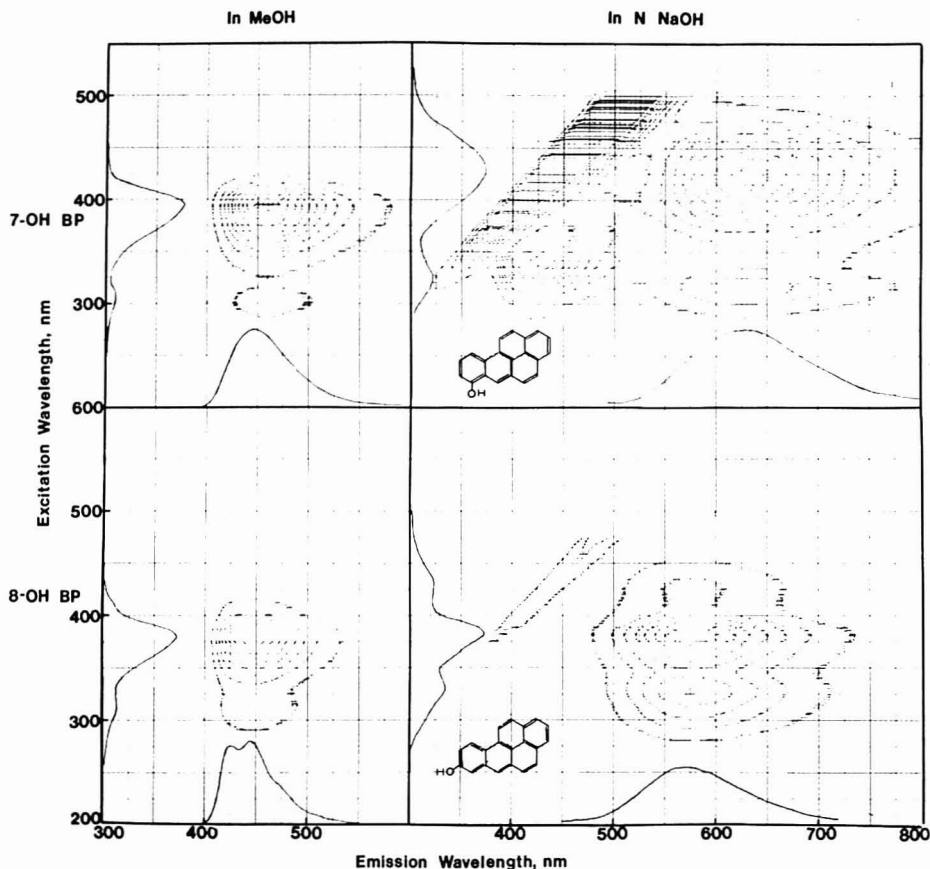


Figure 2. Fluorograms of 7-hydroxybenzo[a]pyrene (0.2 ng/mL), 7-OH BP and 8-hydroxybenzo[a]pyrene (0.2 ng/mL), 8-OH BP. Linear plots of the 7-OH BP and 8-OH BP both in methanol and in 1 N NaOH. The conventional fluorescence spectra are plotted, excitation spectra on the vertical axis and emission on the horizontal axis. The fluorescence intensity levels were plotted by the isointensity contours representing fixed linear levels of intensity; the outermost contour (level 1) represents 10% level of the full scale; level 2, 20%; level 3, 30%; etc.

The digital output of the up/down counter is a measure of the photometer signal. Since eight binary bits are presented to each of the level decode gates, it is obvious that the system has a resolution capacity of one part in 256. It was originally intended that ten contour lines be generated. Hence, the decoder or gates were set up to select the amplitude level corresponding to 25 counts out of 256 counts. Level 1 occurs at 25 counts, level 2 at 50 counts, level 3 at 75 counts, etc., and level 9 occurs at 225 counts. The output of each level decoder gate is "OR"ed in the decoder OR gate. The output of the decoder "OR" gate represents the command signals which will energize the pen drop one-shot. The one-shot generates a signal of approximately 9 ms and is combined with the pen drop inhibit delay gate signal. If the delay gate signal is present, the pen drop commands are inhibited. If the delay gate signal is not present, the pen drop commands will pass through the control gate and energize the pen drop relay, which in turn will energize the control relay and consequently the control switch. When the pen drop control switch closes, the X-Y recorder pen drop will be energized and dropped on the paper to make

a dot. As the two spectrometer gratings scan through their respective wavelengths, the wavelength position potentiometers transmit the information to the X-Y recorder which then drives the pen back and forth over the chart paper. Every time the photometer intensity level crosses any of the preset decode intensity levels, a signal is generated causing the pen to drop. Eventually all the points on the emission-excitation plot will have been covered and all of the isointensity points will appear to join together to form a contour line.

However, it is necessary to provide an additional pen drop inhibit in order to prevent the pen from marking the chart during those periods of time when the grating drives are resetting. This inhibit is generated by the mechanical switches located on the grating drive mechanism. The output of each switch controls an input to the retrace sensor gate. The output of this gate is low only when both switches are open circuited, indicating that both excitation and emission gratings are actually scanning the spectrum. At any other time the output of this gate is high and the pen drop is inhibited. The gate output transition from low

to high will trigger the pen slew retrace inhibit delay which lengthens the retrace sensor gate signal to inhibit the pen drop gate for a few milliseconds required to stabilize the grating drivers at the beginning of a scan. During this time, the pen drop control gate is also inhibited from allowing the pen drop one-shot command to pass and cause the pen to drop.

### EXPERIMENTAL

A number of synthetic benzo[a]pyrene phenols were obtained from the National Cancer Institute, NIH. Both histones and nonhistone chromosomal proteins were prepared from rat liver by the procedures described by Marushige and Bonner (9). All the organic solvents used were fluorometric grade and the chemicals were reagent grade.

### RESULTS AND DISCUSSION

Three-dimensional fluorescence properties of a wide variety of biological compounds have been examined by the contour plotter to illustrate the characteristic spectral patterns of the compounds: polycyclic hydrocarbons, proteins, nucleic acid bases, photosynthetic pigments, and other classes of biological compounds. The entire recording is made in about 20 min.

#### Fluorescence Spectra of Benzo[a]Pyrene Phenols.

Two benzo[a]pyrene phenols which have been hydroxylated at two different positions have been examined for their fluorescence properties by such a fluorescence measurement technique. Typical data of 7-hydroxybenzo[a]pyrene (7-OH BP) and 8-hydroxybenzo[a]pyrene (8-OH BP) are shown in Figure 2, both in methanol and in an alkaline media. The concentrations of both 7-OH BP and 8-OH BP were about 0.2 ng per mL. This represents the linear plots showing a typical benzo[a]pyrene phenol fluorescence in organic solvent, peaking around 450 nm with excitation in the range from 250 to 450 nm as well as those of the corresponding anions in an alkaline medium. An apparent fluorescence peak position generated by an uncorrected mode of fluorescence measurement is a function of both light source and the spectral response characteristics of photodetector. In the present study, we have used a xenon lamp as a light source and a gallium-arsenide photocathode tube as a photodetector which gives a rather flat response pattern from the 300 to 800 nm region. The conventional fluorescence spectra are also plotted, excitation spectra on the vertical axis and the emission on the horizontal axis. Although the structural difference is very small, the electronic spectra appear to be quite distinct from each other, particularly in the anionic species. In these fluorograms of BP metabolites, the fluorescence intensity levels were plotted in the form of isointensity contours representing fixed linear levels of intensity. The outermost contour (level 1) represents the 10% level of the full scale while level 2, the 20% level; level 3, the 30%, etc. The dimension of each discrete contour plot is proportional to the width of the corresponding spectral band at the respective fluorescence intensity level and the coordinates of the centroid for each discrete plot are the wavelengths of the activation and fluorescence maxima. Thus, the fluorogram of 7-OH BP in methanol shows two discrete contour plots indicating one fluorescence maximum at 450 nm with two excitation peaks, the higher one (100%) corresponding to 390 nm and the lower one (10%) 310 nm. The fluorogram of the anionic species of 7-OH BP in 1 N NaOH shows a much more complex spectrum. It not only shows a broad emission spectrum peaking at 635 nm with two excitation peaks, the one at 425 nm and the other at 320 nm but also presents another major emission peak at 420 nm with the two excitation peaks in the range from 315 to 350 nm. This fluorescence peak at the shorter wavelength may represent the fluorescence of any additional compound in the sample which fluoresces only in an alkaline medium. In any case, the three-dimensional plotting (3-D) method delineates not only the activation and emission

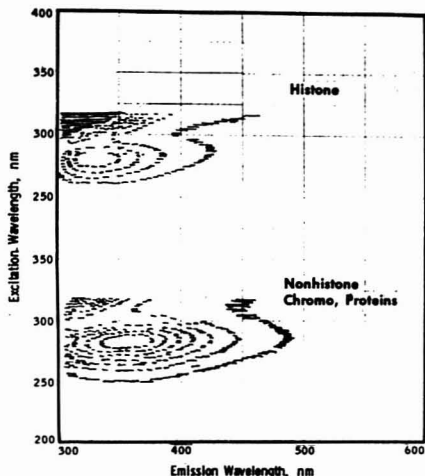


Figure 3. Fluorograms of histone and nonhistone chromosomal proteins. The proteins were isolated from rat liver and their fluorograms were recorded with about 10 ng of the proteins per mL of 10 mM Tris-HCl buffer, pH 7.5

wavelengths and emission intensities for each fluorophore, but also the activation/emission spectral band stereoenvelopes. The detectability limits of the method is about  $10^{-12}$  mol BP phenols per mL volume.

Scattered light appears as a narrow band diagonal to the abscissa and ordinate in this type of display, and the commonly observed Raman effect as a similar narrow band displaced toward the higher emission wavelength scale. The fluorogram of the anionic species of 8-OH BP also shows much more information about the electronic spectra. Both the excitation and the emission maxima of 8-OH BP are located at about 50 and 60 nm lower than the respective spectrum of 7-OH BP. The differences between the spectra of the closely related structures are more obvious in 3-D presentation than in the conventional presentation.

**Fluorescence Spectra of Chromosomal Proteins.** Most proteins contain tryptophan and almost all proteins contain tyrosine which strongly fluoresce even in intact proteins (10). Thus, nonhistone chromosomal proteins are known to contain both tryptophan and tyrosine while histones lack the tryptophan amino acid. We have isolated the histones and nonhistone chromosomal proteins from rat liver by the procedure described by Marushige and Bonner (9) and examined about a 10 ng per mL each of the proteins for their three-dimensional fluorescence properties. The fluorescence property of histone is easily distinguished from that of nonhistone proteins as shown in Figure 3. This graph illustrates a linear plot showing both the tyrosine-tryptophan fluorescence peak of the nonhistone proteins around 360 nm with excitation in the range from 260 to 300 nm and the tyrosine fluorescence peak of histone around 325 nm with excitation from 265 to 290 nm. The lack of tryptophan in histones shifted its fluorescence maximum from the 360 nm peak position of nonhistone to about the 325 nm region. Scattered light also shows as a band diagonal to the abscissa and ordinate above 300 nm.

**Fluorescence Spectra of Chlorophylls.** Chlorophylls are the highly fluorescent photopigments in plants and green algae. The two major types of chlorophylls found in green plants and green algae are chlorophyll a and chlorophyll b (11).



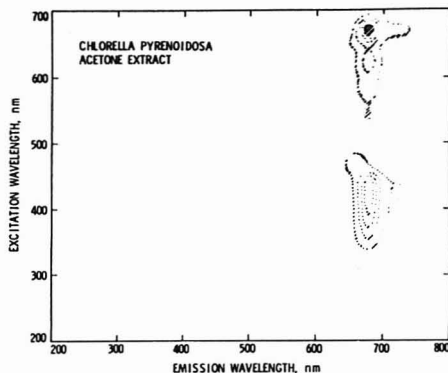


Figure 4. Fluorogram of the acetone extract of *Chlorella pyrenoidosa*. About  $10^6$  cells of *Chlorella* were extracted in 1 mL of acetone at 25 °C and the fluorescence spectrum obtained in acetone solvent.

We extracted about  $10^6$  cells of *Chlorella pyrenoidosa* into 1 mL of acetone and examined the fluorescence property of the extract by the 3-D plotter. As shown in Figure 4, the fluorogram of the algal extract presents a major emission band at 670 nm with two minor peaks, one around 650 nm and the other from 710 to 730 nm. The excitation is achieved most strongly in the spectral region from 660 to 670 nm, weakly around 620 nm, and moderately strong in the range from 400 to 450 nm. Chlorophyll *a* is known to absorb a broad spectrum of light peaking at 410, 429, 532, 576, 614, and 660 nm and fluorescing around 670 nm (12). Chlorophyll *b* also absorbs intensely both at 450 and 643 nm (13). The contour map presented in Figure 4 shows not only the emission peaks of chlorophyll *a* at 680 and 720 nm but also that of chlorophyll *b* at 650 nm in the respective excitation ranges. This acetone extract of the *Chlorella* presents, in effect, a "stereofingerprint" of the mixture of the photopigments in one plot.

**Fluorescence Spectra of Crude Oils.** Fluorescence spectroscopy, a powerful tool in fingerprinting oil spills, is extremely sensitive to the naturally fluorescing components of oil. Many approaches have been proposed to use fluorescence for quantitative oil measurements and characterization. Jadamec and Porro (14) examined a large variety of oils for their emission at excitation wavelength 254 nm and found that it gave more structured emission spectra than any other excitation wavelength. Frank (15) obtained the emission peak maxima from excitation at 15 different wavelengths between 220 and 500 nm and manually plotted them against excitation wavelengths as points. Freearge et al. (2) proposed a contour plot in which contours of equal fluorescence intensity are plotted against excitation and emission wavenumbers. Hornig and Brownrigg (4) pursued this procedure in which they repetitively scanned the spectrum with a spectrofluorometer to generate luminescence data which are taken directly into a minicomputer for correction and reduction to contour graphs.

We examined two types of crude oils with our 3-D fluorometry to obtain their "stereofingerprint" of the fluorescence mixture of the oils. A typical fluorogram of Eocene Oil is presented in Figure 5 and that of Miocene Oil in Figure 6. The 3-D map of diluted Eocene Oil ( $1$  to  $10^3$  in benzene) shows two emission peaks, the major one at 360 nm and the minor at 410 nm with excitation around 300 nm. In contrast, the fluorogram of Miocene Oil shows the emission at considerably longer wavelengths. In comparison to those of Eocene Oil,

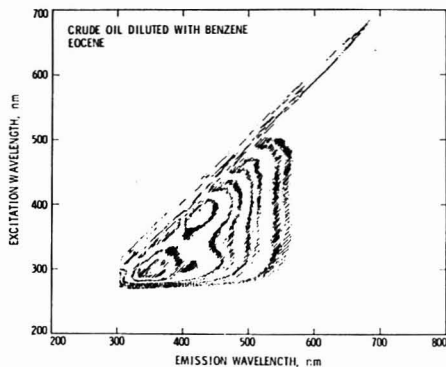


Figure 5. Fluorogram of crude oil of Eocene origin in benzene. The concentrated crude oil was diluted ( $1$  to  $10^3$ ) with benzene and the fluorescence spectrum was recorded in benzene solvent.

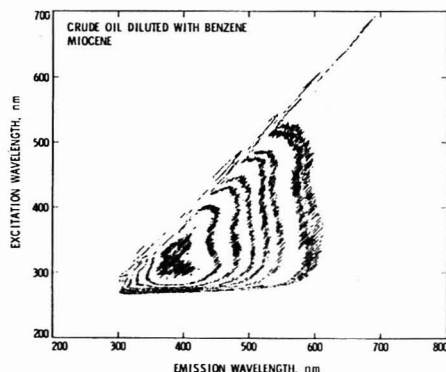


Figure 6. Fluorogram of crude oil of Miocene origin in benzene. The concentrated crude oil was diluted ( $1$  to  $10^3$ ) with benzene and the fluorescence spectrum was plotted in benzene solvent.

the two excitation peaks of the Miocene Oils (diluted  $1$  to  $10^3$  in benzene) also occur at a longer wavelength range. This may indicate that Miocene Oil contains more extensively conjugated polycyclic hydrocarbons than those of Eocene Oil. Since this fluorogram was obtained by an uncorrected mode of fluorescence measurement, the apparent fluorescence peaks are generated as a function of both light source and the spectral response characteristics of photomultiplier used.

## LITERATURE CITED

- (1) M. M. Schachter and E. P. Haenni, Pittsburgh Conference on Analytical Chemistry and Applied Spectroscopy, March 1963.
- (2) M. Freearge, C. G. Heitchard, and C. A. Parker, *Lab. Pract.*, **20**, 35 (1971).
- (3) J. H. Rho and J. L. Stuart, *Pacif. Conf. Chem. Spectrosc. Opt. Soc. Am. Abstr.*, **56** (1972).
- (4) A. W. Hornig and J. T. Brownrigg, Pittsburgh Conference on Analytical Chemistry and Applied Spectroscopy, Cleveland, Ohio, 1975.
- (5) T. C. Miller and L. R. Faulkner, *Anal. Chem.*, **48**, 2083 (1976).
- (6) I. M. Warner, J. B. Callis, E. R. Davidson, M. Gouterman, and G. D. Christian, *Anal. Lett.*, **8**, 665 (1975).
- (7) I. M. Warner, G. D. Christian, E. R. Davidson, and J. B. Callis, *Anal. Chem.*, **49**, 564 (1977).
- (8) D. W. Johnson, J. B. Callis, and G. D. Christian, *Anal. Chem.*, **49**, 747A (1977).
- (9) K. Marushige and J. Bonner, *Proc. Natl. Acad. Sci. U.S.A.*, **68**, 2941 (1971).
- (10) D. E. Duggan and S. Udenfriend, *J. Biol. Chem.*, **223**, 313 (1956).

- (11) C. S. French, J. H. C. Smith, H. I. Virgin, and R. L. Airth, *Plant Physiol.*, **31**, 369 (1956).  
 (12) R. Livingston, W. F. Watson, and J. McArdle, *J. Am. Chem. Soc.*, **71**, 1543 (1949).  
 (13) F. P. Zschelle and D. G. Harris, *J. Phys. Chem.*, **47**, 623 (1943).  
 (14) J. R. Jadamiec and T. J. Porro, Pittsburgh Conference on Analytical Chemistry and Applied Spectroscopy, 219 (1974).

- (15) U. Frank, *Proc. Joint Conf. Prevention Control Oil Pollut.*, **87** (1975).

RECEIVED for review September 22, 1977. Accepted January 6, 1978. This work was supported by the Michael J. Connell Foundation.

## Atomic Fluorescence Spectrometry with a Wavelength-Modulated Continuous Wave Dye Laser

David A. Goff and Edward S. Yeung\*

Ames Laboratory—U.S. Department of Energy and Department of Chemistry, Iowa State University Ames, Iowa 50011

One major problem in laser atomic fluorescence spectrometry is light scattering, which may ultimately determine the minimum detectable atomic concentration. Using a commercial electro-optical tuning element, we are able to provide wavelength modulation in a CW dye laser for excitation of atoms in a premixed flame. With proper lock-in detection, we not only can eliminate most of the background emission in the flame, but can also extend the minimum detectable concentration beyond that obtained using a mechanical chopper in the determination of barium.

The demonstration of the detection of 100 atoms/cm<sup>3</sup> of sodium by Fairbank et al. (1) shows the impressive limits of detection that can be achieved in laser atomic fluorescence spectrometry. In practical applications in analysis, however, one cannot expect to achieve similar limits of detection because of the far-from-ideal conditions associated with the necessity to atomize a real sample. Emission from the atomizer, particularly black body radiation and molecular emission by thermal excitation, gives a constant background signal in addition to the fluorescence from the atoms. Such emission background can be controlled by using filters or monochromators to limit the spectral width of observation, by using gated detection in conjunction with pulsed lasers (2-4), or by using lock-in detection together with mechanical chopping of the laser (5, 6). As one pushes for lower and lower limits of detection, and as one uses high laser powers to ensure saturation in excitation (7), light scattering from particulates, atomic and molecular species, as well as stray laser radiation, will eventually become a problem. The fact that these occur at the same time and at the same wavelength as the resonance fluorescence makes them difficult to eliminate. The use of direct-line (8) rather than resonance fluorescence is a solution, but requires the presence of appropriate atomic energy levels.

There are several ways to minimize the contributions of light scattering. Rayleigh scattering has a unique angular dependence on the orientation of the polarization vector and on the direction of propagation of the scattered light (9). By using linearly polarized light for excitation and by placing the detector at right angles to the direction of propagation of the exciting light in the same plane as the plane of polarization, one can minimize scattering while maintaining the fluorescence signal. The practical limitation of this scheme is that the cone defined by the collection optics contains light rays travelling in a range of directions rather than a unique direction. Also, scattering by larger particles cannot be similarly treated. One can also attempt to correct for the signal due to light scattering

by actually monitoring its intensity at a nonresonant wavelength. The scheme of Chester and Winefordner (10) using two electrodeless discharge lamps (EDL) seems readily adaptable to provide such corrected measurements, if the wavelength dependence of the scattered light is properly accounted for. Another possibility is to use a magnetically tuned EDL for excitation whenever the atom of interest shows a favorable Zeeman effect (11).

In what follows, we shall describe the use of a wavelength-modulated CW dye laser in atomic fluorescence spectrometry. This method preserves the advantages of amplitude modulation using a mechanical chopper in that background emission from the atomizer is minimized. In addition, since the signal from light scattering should be independent of the modulation, one effectively can extract a fluorescence signal much smaller than that from light scattering. The need for wavelength modulation has already been pointed out in earlier work (1). However, the modulation frequency of 1.5 Hz in that work is too slow to be useful in practical atomizers such as the flame. The recent availability of an electro-optical tuner for the CW dye laser (12) has made it possible to provide wavelength modulation to the MHz regime. The evaluation of such a scheme for atomic fluorescence spectrometry has been performed using a premixed burner for the determination of barium, and is reported here.

### EXPERIMENTAL

A schematic of the experimental arrangement for this work is shown in Figure 1. The individual components and the most important experimental conditions are listed in Table I. The argon ion laser is operated at 5-W all-lines output. Rhodamine 110 dye from Exciton Chemical Co., Dayton, Ohio, is used in the dye laser to give about 50 mW of tuned output. The laser bandwidth is estimated to be about 0.5 Å. Distilled water is deionized by passing through a mixed-bed ion-exchange resin and used for all solutions. The barium solutions are prepared from Certified ACS grade BaCl<sub>2</sub> and are stored in polyethylene bottles to be run the same day as prepared.

With no tuning element inside the cavity of the dye laser, it runs freely in a 50-100 Å band depending on the concentration of the dye. The addition of an etalon decreases this lasing range somewhat because of the losses introduced. What is more important is that the laser output is restricted to 0.5-Å bands separated by 10 Å each, corresponding to the free spectral range of the etalon. The electro-scan tuner further limits lasing in only one of these bands depending on the applied voltage. In this way, a square-wave modulation of the applied voltage results in alternate lasing between two wavelengths separated by a multiple of 10 Å. In practice, the laser is first tuned without the square-wave modulation to the atomic resonance by adjusting the etalon and a dc bias voltage on the electro-scan tuner. A 50-ppm

Table I. Components for Atomic Fluorescence Spectrometry Based on a Wavelength-Modulated CW Dye Laser

Item	Manufacturer
Ar ion laser	Model 553, Control Laser Corp., Orlando, Fla.
CW dye laser	Model 375, Spectra-Physics Inc., Mountain View, Calif.
Electro-scan tuner	Model LS-14, Ithaca Research Corp., Ithaca, N.Y.
Lens (source)	49-mm diameter, 94-mm focal length achromatic fused silica lens
Lens (detector)	67-mm diameter, 76-mm focal length achromatic fused silica lens
Filters	Model 7155 variable interference filter, Oriel Corp., Stamford, Conn. 600-nm short pass filter Corning glass filters 4-45, 3-67, 3-69, Corning Glass Works, Corning, N.Y.
Photomultiplier tube	56 TYP, Amperex Electronic Corp., Slatersville, R.I.
Photomultiplier housing	Model 3378, Pacific Photometric Instruments, Emeryville, Calif.
Photomultiplier power supply (set at -1600 V)	Model 242, Keithley Instruments Inc., Cleveland, Ohio
Lock-in amplifier	Model 9503/5002, Ortec Inc., Oakridge, Tenn. (10 <sup>-14</sup> A full-scale)
Wave generator	Model 162, Wavetek, San Diego, Calif.
H.V. op amp	Model PZ-70, Burleigh Instruments Inc., E. Rochester, N.Y.
Burner-nebulizer (C <sub>2</sub> H <sub>2</sub> , 0.8 L/min; air, 3.8 L/min; solution, 0.7 mL/min)	Premix slot burner with pneumatic nebulization, Varian Associates, San Carlos, Calif.
Power meter	Model 210, Coherent Radiation, Palo Alto, Calif.
Oscilloscope	Model 7904 with 7A16 plug-ins, Tektronix Inc., Beaverton, Ore.
Photodiode	Model PVS-010, Infrared Industries, Waltham, Mass.
Monochromator	Double Grating Monochromator, Bausch & Lomb, Rochester, N.Y.

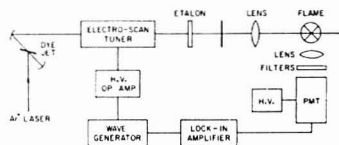


Figure 1. An atomic fluorescence spectrometer based on a wavelength-modulated CW dye laser

solution of Ba in the flame gives a clearly visible fluorescence output, and is used to optimize the laser wavelength. The modulation is then superimposed on the dc bias so that lasing alternates between two wavelengths 10 Å apart. This is found to be optimum since any larger separation of the two wavelengths will require larger applied voltages, which in turn demands a faster slew rate of the high voltage op amp. Also, for such small separations, the wavelength dependence of light scattering can be neglected. Finally, by readjusting the dc bias voltage, one can shift the dye laser gain curve to obtain equal intensities at the two wavelengths. This last step is necessary to ensure that light scattering is not modulated, so that it will not be detected.

In Figure 2, we can see the course of events as displayed on an oscilloscope. The top trace (ground = 2 divisions from top) represents the square-wave modulation applied to the electro-scan tuner. Slight curvatures in the vertical segments are results of the limited slew rate of the op amp. The second trace (ground = 2 divisions from top) is the negative-going signal from a photodiode monitoring the laser output through a monochromator set at the barium resonance frequency of 5535 Å. The third trace (ground = 4 divisions from top) is the same as the second trace,

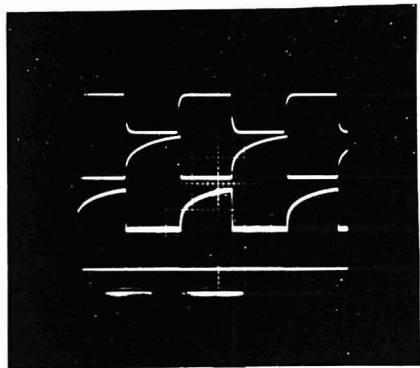


Figure 2. Oscilloscope display of modulation of the laser wavelength (for details, see text). The horizontal scale is 0.25 ms/div

except that the monochromator is set at 5545 Å. The curvature on the falling edges of the photodiode signals simply reflects the characteristic fall times of these photodiodes. In fact, the spectral output is quite close to being 100% modulated. The bottom trace (ground = 6 divisions from top) shows the total output of the laser, with no detectable modulation on the amplitude.

Electro-scan tuners that replace the function of the etalon are also commercially available. It seems at first sight that using such tuners will produce equivalent results. In practice, however, it

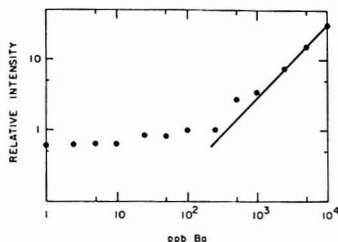


Figure 3. Analytical calibration curve for atomic fluorescence of barium using amplitude modulation

requires a very reliable wave generator and a very stable high voltage op amp to reproducibly center on the atomic resonance line using these other tuners. In contrast, our present scheme relies only on the etalon to properly center on the atomic line. Slight imperfections in the modulation electronics will lead only to incomplete modulation between the two fixed wavelengths, but will not change these two wavelengths.

### RESULTS AND DISCUSSION

The sensitivity and the ultimate limit of the detection for a given atomic fluorescence spectrometer depend on many experimental variables. The most obvious ones are the flow rate of the solution, flame stoichiometry, exciting photon flux, laser bandwidth, efficiency of the collection optics, and the stability of the detection electronics. For the purpose of demonstrating the usefulness of our scheme of wavelength modulation, it is most appropriate to compare it with an amplitude modulation scheme while fixing all of these other experimental variables. We have therefore performed two parallel sets of measurements on the atomic fluorometric determination of barium using the 5535-Å resonance line. The first set is based on amplitude modulation using a mechanical chopper for a fixed-frequency laser, and is shown in Figure 3. The second set is based on the wavelength-modulated laser described above, and is shown in Figure 4. The modulation frequency is 1 kHz in both cases. Data points for higher barium concentrations are not shown, but extrapolate quite well for at least two orders of magnitude.

We can see that for the case of amplitude modulation, contributions from light scattering set in at about 300 ppb Ba so that lower concentrations cannot be detected, even though the photomultiplier tube has no difficulties in registering much smaller signals. For the case of wavelength modulation, one can extend the limit of detection to the 10-ppb Ba range. The ultimate limit here is determined by the overload capability of the particular lock-in amplifier used. By using a monochromator rather than a set of filters, as is done in Ref. 6, one should be able to reduce the dc signal from flame background emission further, so that still lower limits of detection can be achieved. Increasing the laser power is another alternative. Furthermore, the modulation frequency in this work was chosen to coincide with the available mechanical chopper so that a proper comparison could be made. For actual applications, the modulation frequency should be

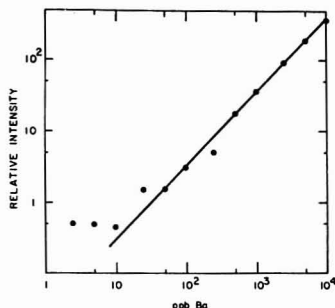


Figure 4. Analytical calibration curve for atomic fluorescence of barium using wavelength modulation

chosen to minimize the effects of fluctuations in the flame and other electronic noise in the system. These electro-scan tuners can be effectively used even in the MHz range. It is interesting to note that using a combination of electro-scan tuners, one can in principle step from one atomic line to another (within the gain curve of the dye) rapidly by properly controlling the voltage on the electro-scan tuner. This opens up the possibility of sequential multielement analysis using laser-excited atomic fluorescence spectrometry, free from the limitations of conventional mechanical scanning devices.

### CONCLUSIONS

The use of an electro-optically tuned CW dye laser in atomic fluorescence spectrometry offers several advantages. (1) Wavelength modulation becomes feasible so that problems associated with light scattering can be minimized and the limits of detection can be improved. (2) The frequency of modulation can be extended to the MHz range so that optimization of this frequency to eliminate inherent fluctuations is possible. (3) Reliable and rapid tuning can be accomplished, leading to the possibility of multielement analysis.

### LITERATURE CITED

- (1) W. M. Fairbank, T. W. Hänsch, and A. L. Schawlow, *J. Opt. Soc. Am.*, **65**, 199 (1975).
- (2) L. M. Fraser and J. D. Winefordner, *Anal. Chem.*, **43**, 1693 (1971).
- (3) L. M. Fraser and J. D. Winefordner, *Anal. Chem.*, **44**, 1444 (1972).
- (4) J. Kuhl and H. Spitschan, *Opt. Commun.*, **7**, 256 (1973).
- (5) B. Smith, J. D. Winefordner, and N. Ormenetto, *J. Appl. Phys.*, **48**, 2676 (1977).
- (6) R. B. Green, J. C. Travis, and R. A. Keller, *Anal. Chem.*, **48**, 1955 (1976).
- (7) E. H. Piepmeyer, *Spectrochim. Acta, Part B*, **27**, 431 (1972).
- (8) J. D. Winefordner, M. L. Parsons, J. M. Mansfield, and W. J. McCarthy, *Spectrochim. Acta, Part B*, **23**, 37 (1967).
- (9) M. Born and E. Wolf, "Principles of Optics", fifth ed., Pergamon Press, Elmsford, N.Y., 1975, p. 653.
- (10) T. L. Chester and J. D. Winefordner, *Spectrochim. Acta, Part B*, **31**, 21 (1976).
- (11) H. Kozumi and K. Yasuda, *Spectrochim. Acta, Part B*, **31**, 237 (1976).
- (12) J. M. Telle and C. L. Tang, *Appl. Phys. Lett.*, **15**, 85 (1974).

RECEIVED for review December 27, 1977. Accepted January 26, 1978. Research supported by the U. S. Department of Energy, Division of Basic Energy Sciences.

# Theory of Atom Vapor Transport from a Moving Point Source in Flame Spectrometry

Kuang-Pang Li

Department of Chemistry, University of Florida, Gainesville, Florida 32611

The atom distribution of an analyte in an analytical flame is evaluated by using a moving point source model. The point source chosen is a dry aerosol particle which gives out a small amount of atom vapor at a particular location. At another location, the particle will give out a different amount of vapor. These vapor increments diffuse away independently. Hence, the atom concentration observed at a particular point and at a particular moment will be the sum of the vapor increments diffused to that point at that moment from the moving particle. This model gives a more precise and more realistic description of the vapor transport in flames than the existing flame models.

Knowledge of atom distribution in plasma, e.g., a flame, an arc, etc., is of ultimate importance in atomic spectrometry. It provides not only the basis for plasma diagnostics and signal prediction, but also guidelines for systematic optimization and modification for sensitivity enhancement and interference reduction. There have been several theoretical treatments on atom vapor transport in high temperature gaseous media. The concise work of Wilson (1) on the diffusion of alkali atoms from a point source in a flame is of primary significance. Because of its mathematical simplicity and its adaptability to experimental verification, it has often been employed for diffusion coefficient determination in flames and arcs (2-4). Serious discrepancies from theoretical expectation have been found in arcs because of the negligence of the finite size of the source in the model. Boumans and co-workers (5) modified the model by taking the size of the electrode into consideration. Their disk source model gave a better description of vapor transport in dc arcs than the point source. However, the disk source can hardly be applied to flame spectrometry. L'vov and co-workers (6, 7) developed a horizontal thin thread source model for atom distribution in a slotted burner flame. All these treatments relate only to the transport of the analyte atoms in the plasma and invariably use a constant feeding approach.

Recently, Li (8) described, for the first time, the entire atomization process with a consistent theoretical approach. In his approach, the atomic concentration at the point of observation is evaluated stochastically. That is, the contribution from an arbitrarily selected droplet is treated rigorously. A statistical method is then applied to the result to yield the overall concentration for a large ensemble of droplets. He employed Wilson's result directly for the vaporization process. His treatment can actually be envisaged as for a vertical thin thread source model.

Li's model provides a novel way of treating the flame processes and is useful for flame diagnostic studies. Unfortunately, under the operational conditions of an analytical flame, the rate of droplet generation is far smaller than that required for the thread model. Every droplet in the flame is pretty much independent of other droplets. The vaporization of each salt particle is a transient phenomenon. Even though the ensemble average of atom distribution from a large number of such particles may be time-independent, treating

them as infinitive atom reservoirs is certainly unrealistic and erroneous.

In the present report, the atom vapor transport in flames will be treated with a more realistic moving point source model. The point source is a completely desolvated salt particle which continuously loses its mass via vaporization on its way up in the flame. The airborne droplet forming the salt particle of interest can be one of the thousands generated by a nebulizer or by other droplet generators. It can be introduced at any angle and at any place in the flame. Since the stochastic approach developed by Li can still be used for the atom concentration evaluation, only the vapor transport process will be discussed here.

In the dynamic study of desolvating droplet (9-11), it has been demonstrated that a droplet, no matter how it is introduced into the flame, will rapidly acquire the same velocity as the flame gases. If the particle at different locations is treated as different sources, and if a cylindrical coordinate system with its origin located at the center of mass of the source is employed, the atom vapor transport can be described with the following equation:

$$\frac{\partial n}{\partial t} = D \left[ \frac{1}{r} \frac{\partial}{\partial r} \left( r \frac{\partial n}{\partial r} \right) + \frac{\partial^2 n}{\partial z^2} \right] - v \frac{\partial n}{\partial z} \quad (1)$$

where  $v$ , in cm/s, is the flame gas velocity and  $n(r, z, t)$  is the instantaneous atom concentration observed at  $(r, z)$  and time  $t$ .  $D$  is the diffusion coefficient of the analyte atom in the flame. Because the atom vapor plume is symmetrical along the  $z$  axis, the function  $n$  is independent of the angle.

## THEORY

**Description of the Moving Point Source Model.** We will employ a circular, premixed, laminar flame of diameter 2L cm. The flame has a uniform temperature and composition in the region of interest. The flame is sheathed so it has no significant horizontal velocity. Edge effects are assumed to be minimized and will not be taken into consideration.

A droplet of initial diameter,  $d_i$ , cm, containing  $m_i$  g, of the analyte, is introduced into the flame at  $(R_i, 0, Z_i)$  referring to a set of spatially fixed coordinates,  $R$ - $\theta$ - $Z$ , originated at the center of the circular burner head. The point of introduction is not necessarily at the burner head. Desolvation before the droplet enters the flame is not considered. This ignorance of the pre-flame desolvation does not imply that the model is inapplicable in such cases. It is mainly because this desolvation process has not been described quantitatively. To include it in the model will require an introduction of empirical parameters which will only complicate the expressions. The angle of introduction is also not necessarily restricted to  $90^\circ$  to the burner surface, because the droplet will rapidly acquire the velocity of the flame gases (9-11).

Assuming that at the moment  $\tau = \tau_0$ , the droplet moves to a new location,  $(R_0, 0, Z_0)$  (See Figure 1) and is completely desolvated and starts vaporizing. The diameter of the particle is now  $d_0$ , cm, and the mass,  $m_0$ . The rate of vaporization is arbitrarily assumed to be controlled by the rate of mass transfer of the analyte from the salt particle. As one can see



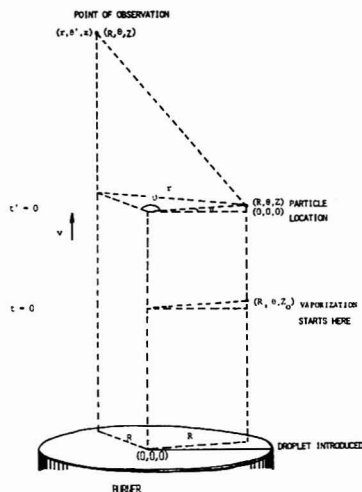


Figure 1. Coordinates of the vaporizing particle and the point of observation.  $R-\theta-Z$  are the spatially fixed coordinates located at the center of the burner head and  $r-\theta'-z$  are the coordinates located at the center of gravity of the particle

from the final results, the atom concentration depends mainly on the rate of vaporization. Furthermore, in analytical flame spectrometry, the solutions used are normally dilute solutions (in the ppm or ppb regions). The salt particles formed from these solutions are usually very small. The rate of mass transfer controlled vaporization for these particles can be expressed as (12):

$$-\frac{dm}{dt} = kd^2 \quad (2)$$

where  $m$  and  $d$  are the instantaneous mass and diameter of the particle at the time  $t = \tau - \tau_0$ . The constant  $k$  is the rate constant in  $\text{g cm}^{-2} \text{s}^{-1}$  of the vaporization process.

Now, if another set of coordinates,  $r-\theta'-z$ , is placed at the center of gravity of the spherical particle located at  $(R, \theta, Z)$  with respect to the spatially fixed coordinates, at the moment between  $t$  and  $t + dt$ , a small amount of the analyte,  $dm$ , will be diffusing away from the particle. At another moment, the particle will move to another location and give out a different amount of analyte vapor. The vaporization process continues until the whole particle is vaporized. The small increments of atom vapor leaving the particle at different locations diffuse away according to Fick's law given in Equation 1. The atom concentration at a given point in space due to each of these vapor increments depends on its time of diffusion. The longer it diffuses, the smaller the concentration will be. The instantaneous total concentration at the point of observation is the sum (or integral) of the concentration contributed by diffusion of the vapor increments from the particle at different locations. In other words, if the incremental concentration due to a source at  $(R, \theta, Z)$  is expressed as

$$\delta n(R, \theta, Z, t) = n(r, \theta', z, t') \quad (3)$$

where  $(R, \theta, Z)$  is the point of observation,  $z = Z - Z_0$  and  $r^2 = R^2 + R^2 - 2RR \cos(\theta - \theta')$ ,  $t'$  is the time required for the vapor increment to travel from the particle to the point of observation, i.e.,  $t' = t - (Z - Z_0)/v$ , then the total atom concentration at the point of observation is

$$N(R, \theta, Z, t) = \int_{Z_0}^Z \delta n(R, \theta, Z, t) dZ \quad (4)$$

**Derivation of  $n(r, \theta', z, t')$ .** Since the particle is moving very fast in the flame, it spends only a very short period of time,  $dt' = dZ/v$ , in the interval between  $Z$  and  $Z + dZ$ . During that time interval, the particle gives out via vaporization a tiny amount of analyte,  $dm$  in g, or  $(N/M)dm$  in number of atoms, where  $N$  is Avogadro's number and  $M$  the atomic weight of the analyte atom. The magnitude of  $dm$  depends on how long the particle has traveled in the flame. This time-dependence of  $dm$  is evaluated from Equation 2 and can be expressed as

$$\frac{dm}{dt} = \frac{Nk^3k_c^3}{9M} [\gamma - t]^2 \quad (5)$$

where  $\gamma = (3m_0^{1/3}/kk_c)$ ,  $k_c = [6/\rho\pi]^{2/3}$ , and  $\rho$  is the density of the salt particle at temperature  $T$ .

The initial and boundary conditions for Equation 1 for a point source at  $(R, \theta, Z)$  can be defined in terms of the coordinates  $r-\theta'-z$ :

$$n(r, \theta', z, t') = 0 \quad \text{at } t' = 0 \quad (6a)$$

$$n(r, \theta', z, t') = 0 \quad \text{at } r, z = \infty \quad (6b)$$

$$n(r, \theta', z, t') = 0 \quad \text{at } r = L - R \quad (6c)$$

and

$$\lim_{x \rightarrow d/2} 4\pi x^2 D \frac{\partial n}{\partial x} = \frac{dm}{dt'} \quad (6d)$$

where  $x^2 = r^2 + Z^2$ ,  $dm/dt'$  is the rate of mass transport from the particle in the time interval between  $t' = 0$  and  $t' + dt'$ . Outside this region the rate is zero because the particle is no longer at the location  $(R, \theta, Z)$ . The boundary condition (Equation 6c) states that the atom concentration is maintained at zero along the edge of the flame. Condition (6d) can be rearranged as follows by using Equation 2:

$$\lim_{x \rightarrow d/2} \frac{\partial n}{\partial x} = \lim_{x \rightarrow d/2} \frac{1}{4\pi x^2 D} \frac{dm}{dt'} = \frac{k}{\pi D} \quad 0 \leq t' \leq dt' \\ = 0 \quad t' > dt' \quad (6d')$$

From Equation 1 we see that the function  $n$  is not a function of  $\theta'$ , we will therefore drop the angular parameter from the expression.

Taking the Laplace transform of  $n$  and  $\partial n/\partial t'$  one obtains

$$L\{n\} = \int \exp(-st') n(r, z, t') dt' = \\ h(r, z, s) = u(r, s) w(z, s) \quad (7)$$

$$L\left\{\frac{\partial n}{\partial t'}\right\} = sh - n(r, z, 0) = sh \quad (8)$$

Substitution of these quantities into the Laplace transform of Equation 1 gives the following equations after separation of variables:

$$\frac{d^2 u}{dr^2} + \frac{1}{r} \frac{du}{dr} + \alpha^2 u = 0 \quad (9)$$

and

$$\frac{d^2 w}{dz^2} - \frac{v}{D} \frac{dw}{dz} - (\alpha^2 + \frac{s}{D}) w = 0 \quad (10)$$

where  $\alpha$  is a constant.

The solution of Equation 9 is

$$u(r, s) = A'(s) J_0(\alpha r) \quad (11)$$

where  $J_0$  is the Bessel function of the order zero. From the

boundary condition:  $u(L-R, s) = 0$ , it is seen that  $J_0[\alpha(L-R)] = 0$ .

The solution of Equation 10 is

$$w(z, s) = A''(s) \exp \left\{ \frac{vz}{2D} - \frac{z}{\sqrt{D}} \sqrt{\frac{v^2}{4D} + D\alpha^2 + s} \right\} \quad (12)$$

By combining Equations 11 and 12, we obtain

$$h(r, z, s) = u(r, s)w(z, s) \\ = A(s)J_0(\alpha r) \exp \left\{ \frac{vz}{2D} - \frac{z}{\sqrt{D}} \sqrt{\frac{v^2}{4D} + D\alpha^2 + s} \right\} \quad (13)$$

If the vaporization at the surface of the salt particle is assumed to be isotropic, then the Laplace transform of the initial condition (Equation 6d') can be expressed as,

$$\lim_{x \rightarrow d/2} \frac{\partial h}{\partial x} = \lim_{r \rightarrow d/2} \frac{dh}{dr} = \frac{k}{\pi D} \left[ \frac{1 - \exp(-sd')}{s} \right] = \\ \frac{kdt'}{\pi D} = \frac{k dZ}{\pi D} \quad (14)$$

Substitution of the differential of Equation 13 with respect to  $r$  into Equation 14 gives Equation 15 after rearrangement:

$$A(s) = \frac{k dZ}{\pi D v J_1(\frac{\alpha d}{2})} \exp \left[ \frac{v d}{4D} - \frac{d}{2\sqrt{D}} \sqrt{s + a} \right] \quad (15)$$

where  $a = (v^2/4D) + D\alpha^2$ .  $J_1$  is the Bessel function of the first order. The atom concentration at the point of observation is given in the Laplace coordinates as:

$$h(r, z, s) = \frac{k dZ J_0(\alpha r)}{\pi D v \alpha J_1(\frac{\alpha d}{2})} \times \\ \exp \left[ \frac{v(2z-d)}{4D} - \frac{(2z-d)}{2\sqrt{D}} \sqrt{s+a} \right] \quad (16)$$

which is reversed to give

$$n(r, z, t') = \frac{k dZ J_0(\alpha r)(2z-d)}{4(\pi D)^{3/2} v \alpha J_1(\frac{\alpha d}{2})} \times \\ \exp \left[ \frac{v(2z-d)}{4D} - \frac{(2z-d)^2}{4Dt'} - at' \right] \\ t'^{3/2} \quad (17)$$

Since  $\alpha$  represents a series of numbers,  $\alpha_p$ , which satisfy the equation

$$J_0[\alpha(L-R)] = 0 \quad (18)$$

the solution can be expressed as

$$n(r, z, t') = \sum_{p=1}^{\infty} \frac{\Delta(d) k dZ J_0(\alpha_p r)(2z-d)}{4(\pi D)^{3/2} v \alpha_p J_1(\frac{\alpha_p d}{2})} \times \\ \exp \left[ \frac{v(2z-d)}{4D} - \frac{(2z-d)^2}{4Dt'} - \alpha_p^2 t' \right] \\ t'^{3/2} \quad (19)$$

where  $\alpha_p = (v^2/4D) + D\alpha_p^2$ , and  $\Delta(d)$  is a step function having unit magnitude when  $d$  is greater than 0 and zero when  $d$  is zero.  $\Delta(d)$  is introduced to take into consideration the

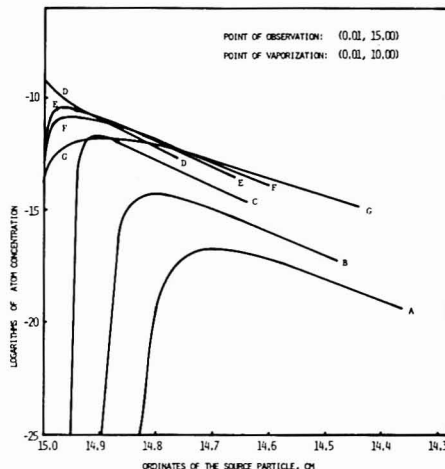


**Figure 2.** Total atom concentration  $N(R, Z, t)$  at the point of observation at different observation times. Data used for simulation are:  $D$ :  $30.0 \text{ cm}^2/\text{s}$ ;  $k$ :  $10^{-3} \text{ g/s cm}^2$ ;  $D_1$ :  $10^{-3} \text{ cm}$ ; solution concentration,  $C_0$ :  $10^{-6} \text{ g/cm}^3$ ; density of the salt particle,  $\rho$ :  $2.0 \text{ g/cm}^3$ ;  $v$ :  $1000 \text{ cm/s}$ ; particle vaporization initiates at  $(0.01, 10.00)$ ; time of observation measured from vaporization starting point: curve A: 4.85 ms; curve B: 4.90 ms; curve C: 4.95 ms; curve D: 5.00 ms; curve E: 5.05 ms; curve F: 5.10 ms; and curve G: 5.30 ms

possibility that the salt particle may be completely vaporized before it reaches the level where  $Z = Z_0$ .

Substitution of the relations:  $t' = t - (Z - Z_0/v)$ ,  $z = Z - Z$  and  $r = R - R$  into Equation 19 and integration with respect to  $Z$  from  $Z_0$  to  $Z$  gives  $N(R, Z, t)$ .

## DISCUSSION

Although the numerical values of the function  $N(R, Z, t)$  will have to be evaluated with the aid of a computer, its general feature can be visualized by the examination of the functional form of  $n(r, z, t')$ .

Both functions  $n$  and  $N$  at the point of observation are zero when the salt particle just starts to vaporize, i.e.,  $Z = Z_0$ , and  $t = t' = 0$ . They are zero again when  $t$  and  $t'$  become infinitely large. This indicates that the atom concentration at the point of observation must have a maximum with respect to time. If the observation point is close to the course of flight of the airborne particle, the occurrence of the maximum is right at the moment the particle reaches the same altitude as the observation point. This is because the gas velocity, thus, the particle velocity, is much higher than the velocity of atom diffusion under the operative conditions of an analytical flame. The mass of the atom vapor travels with the particle up in the flame. However, because of the friction of the gaseous medium, the vapor cloud is not spherical. As a matter of fact, it has a sharp leading front and a diffused tail with most of the vapor surrounding the particle. The asymmetry of the atom distribution is shown in Figure 2. In this simulation, the particle is assumed to start vaporization at the point  $(0.0, 10.0)$  on the flame axis. The observation point is at  $(0.1, 15.0)$ . The flame gas is moving upward with a speed of  $1000 \text{ cm/s}$ . Therefore, it will take  $5.0 \text{ ms}$  for the vaporizing particle to reach the altitude of the observation point. If measurement is made before the particle reaches the same altitude, the concentration observed is attributed entirely to the atoms diffusing ahead of the gas flow. The number of such atoms is, of course, very small and depends very much on how far

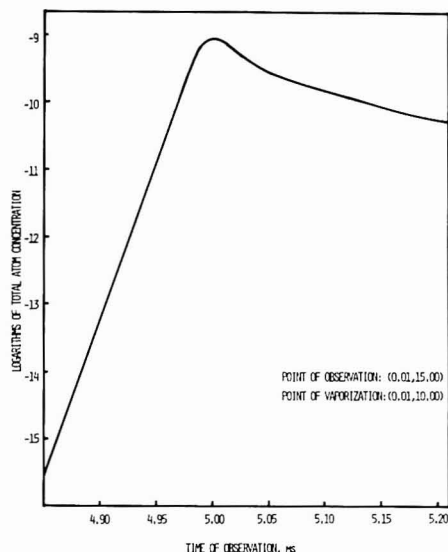


Figure 3. Atom distribution,  $n(r, z, t)$ , at the point of observation due to vaporization of the source particle at different locations. Data used for simulation are identical to those used in Figure 2.

the particle is below the observation point. As a result, the leading edge of the plot is very steep. However, the change in concentration is rather slow after the particle has passed the observation point. This is probably due to the arrival of the atoms which are vaporized far below the observation point and lag behind the gas flow because of backward diffusion.

Figure 3 was simulated under the same conditions as Figure 2. It shows the dependence of the function  $n$  upon the coordinates of the source particle at different observation times. It is seen that, at a certain observation time, there is an optimal position where the particle contributes most. The optimal altitude approaches the observation point as  $t$  approaches 5.0 ms, but moves away slowly from the observation point when  $t$  is greater than 5.0 ms.

The function  $n$  also shows maximum with respect to  $z$ , so does  $N$  with respect to  $Z$ . The position of the maximum depends on  $k$ . As a result, a salt with higher boiling point, i.e., smaller  $k$ , will be better observed at a higher position in the flame.

Since the Bessel function  $J_0(ar)$ , has a maximum at  $r = 0$  but approaches zero periodically as  $r$  increases, it is very likely

that  $N$  is also maximized at  $r = R - R = 0$ . For a flame with negligibly small edge effects, a droplet introduced at the center of the flame will, therefore, give symmetrical distribution of atom vapor with maximum concentration along the flame axis. However, if edge effects are significant, the distribution may have several maxima due to the reflection of the atom vapor at the flame edge.

The solution (Equation 19) predicts that the function  $n$  be related inversely to  $D^{3/2}$ . However, in flame spectrometry, convection due to flame gas flow is usually large as compared to the diffusion, the exponential of the factor  $uz/2D$  may be more significant in determining the residence time of the atom vapor in the flame. In other words, elements with different diffusion coefficients are likely to spend approximately the same length of time in the flame. This fact has been observed by Malykh and Serd in 1964 (13) and later by others. Malykh and Serd reported that the mean transit times of elements, Li, Na, and Tl, are almost identical in air-acetylene flames, whereas, their transit times are significantly different in dc arcs.

Experimental verification is possible with setups similar to that developed by Hieftje and Malmstadt (11). For measurements of atom concentrations, the two-line atomic fluorescence method (14-17) or laser-excitation luminescence technique should be appropriate. In these methods, modulated high intensity sources are focused sharply at a particular point of observation in the flame, and the transient fluorescence signal from a particular droplet is traced. If the droplet generation is highly reproducible, the profile of the entire vapor plume may be traced. When such information is available, comparison of the theoretical expectation with experimental findings will help in establishing much better understanding of the atomization phenomenon.

#### LITERATURE CITED

- (1) H. A. Wilson, *Phil. Mag.*, **24**, (6), 118 (1912).
- (2) L. A. Giesel and L. S. Ornstein, *Z. Phys.*, **84**, 278 (1933).
- (3) R. E. Walker and A. A. Westenberg, *J. Chem. Phys.*, **29**, 1139 (1958).
- (4) G. Ember, J. R. Ferron, and K. Wohl, *J. Chem. Phys.*, **37**, 891 (1962).
- (5) P. W. J. M. Boumans and L. DeGalan, *Anal. Chem.*, **38**, 674 (1966).
- (6) B. V. L'vov, L. P. Kruglikova, L. K. Polzik, and D. A. Katskov, *J. Anal. Chem., USSR*, **30**, 545 (1975).
- (7) B. V. L'vov, L. P. Kruglikova, L. K. Polzik, and D. A. Katskov, *J. Anal. Chem., USSR*, **30**, 551 (1975).
- (8) K. P. Li, *Anal. Chem.*, **48**, 2050 (1976).
- (9) K. P. Li, *Anal. Chem.*, **49**, 2086 (1977).
- (10) C. B. Boss and G. M. Hieftje, *Anal. Chem.*, **49**, 2112 (1977).
- (11) G. M. Hieftje and H. V. Malmstadt, *Anal. Chem.*, **40**, 1860 (1968).
- (12) G. J. Bastiaans and G. M. Hieftje, *Anal. Chem.*, **48**, 901 (1974).
- (13) V. D. Malykh and M. A. Serd, *Opt. Spectrosc. (USSR)*, **16**, 203 (1964).
- (14) H. Haraguchi, B. Smith, S. Weeks, D. J. Johnson, and J. D. Winefordner, *Appl. Spectrosc.*, **31**, 156 (1977).
- (15) H. Haraguchi and J. D. Winefordner, *Appl. Spectrosc.*, **31**, 195 (1977).
- (16) H. Haraguchi and J. D. Winefordner, *Appl. Spectrosc.*, **31**, 330 (1977).
- (17) H. Haraguchi, S. Weeks, and J. D. Winefordner, *Can. J. Spectrosc.*, **22**, 61 (1977).

RECEIVED for review August 8, 1977. Accepted January 13, 1978.

# Band-Broadening Phenomena in Microcapillary Tubes under the Conditions of Liquid Chromatography

Takao Tsuda<sup>1</sup> and Milos Novotny\*

Department of Chemistry, Indiana University, Bloomington, Indiana 47401

Chromatographic measurements are described in which band-broadening phenomena were studied under different conditions in glass thick-walled, micron-size capillaries. These experiments were conducted to investigate basic processes involved in (possibly feasible) capillary LC. Measurements carried out with a nonretained solute in microcapillaries of various diameters indicate that the plate height values are considerably better than predicted from the theory. Geometrical characteristics of the inner surface seem to play only a minor role in reducing band-broadening. The "coil effect" and secondary flow phenomena may be important in future attempts to develop capillary LC.

While assessing the theoretical limit of separating ability of gas and liquid chromatography, Giddings (1) calculated that the theoretical limit to the number of plates is roughly 1000 times higher in liquid than in gas chromatography (LC and GC, respectively). Such numbers are roughly of the same proportion as the products of viscosity and solute diffusivity in the respective phases. He also suggested that the open tubular (capillary) columns in liquid chromatography are worth considering. Although wall-coated capillary columns in gas chromatography are now well-established means to achieve theoretical plate numbers typically between  $10^5$  and  $10^6$ , best reported separations in modern liquid chromatography are currently obtained with small-particle packed columns.

Mobile-phase viscosity (roughly two orders of magnitude different) and solute diffusivity in mass-transfer processes (typically, five orders of magnitude smaller in LC than in GC) are two basic properties that govern column efficiency. Thus, while the "openness" of GC columns has long been recognized as their beneficial attribute (2), the packing tightness is characteristically sought in high-performance LC separations.

When considering a translation of Golay's considerations (3) into the conditions of LC, capillary columns would hardly seem to be worthy of investigation because of the limited radial diffusion possibilities. However, certain additional circumstances must be taken into account. Under the conditions of laminar flow, Taylor (4) established that the only means of lowering the plate height,  $H$ , is a decrease of column diameter:

$$\frac{H}{v} = \frac{r^2}{24 D_M}$$

where  $v$  = flow velocity,  $r$  = column radius, and  $D_M$  = solute diffusivity in the mobile phase. Thus, a decrease of column diameter in LC by approximately one order of magnitude compared to the currently used GC capillary columns may lead to appreciable gains in column efficiency. While limited practical value of this approach with currently available LC technology is apparent, the same may not hold true for future

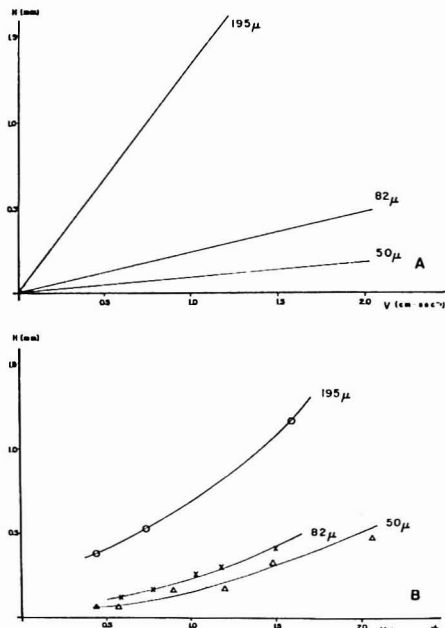


Figure 1. Comparison of plate heights at different mobile-phase velocities for microcapillaries of different internal diameters. (A) plots derived from the Taylor equation; (B) experimental curves. ( $\Delta$ ) column length ( $L$ ) = 11 m; ( $\times$ )  $L$  = 7.5 m; ( $\circ$ )  $L$  = 102 m

separations. Such directions were recently advocated by Golay (5).

If solute transport by a process other than diffusion can be achieved in the radial direction, separating conditions may be arrived at. Thus, under the conditions of turbulent flow, where the radial component of the total flow is considerably increased and the flow profiles are significantly altered, the plate height should decrease with increasing flow rate, as calculated by Pretorius and Smuts (6). Experiments of Giddings et al. (7) in gas-adsorption capillary chromatography actually demonstrated this phenomenon; an impressive efficiency figure of 3800 plates per second was obtained at a very high Reynolds number. Enormous inlet pressures would be required for turbulent flow capillary LC (6).

Perhaps, a more attractive route to higher column efficiencies in capillary LC lies in the utilization of secondary flow phenomena induced in helical columns by centrifugal forces. As discussed by Koutsky and Adler (8), this phenomenon has been known for over a hundred years. In both laminar and turbulent flow regions, the secondary flow inhibits axial dispersion by displacing molecules into perpendicular position.

<sup>1</sup> On leave from the Department of Applied Chemistry, Faculty of Engineering, Nagoya University, Nagoya, Japan.

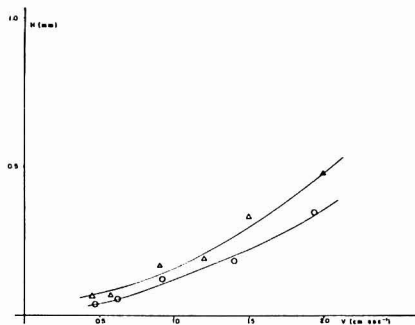


Figure 2. Effect of surface treatment on the plate height vs. velocity curves. Both columns are 11 m long, with 50- $\mu$ m i.d. ( $\Delta$ ) smooth (untreated) wall. (O) capillary lined with "whiskers".

The extent of action of the centrifugal forces is dependent on both column inner diameter and the radius of coil.

Although the possible existence of the "coil effect" was not considered by Golay (3), calculations by Tijssen (9), Tijssen and Wittebrood (10), and more recently Wong et al. (11) strongly indicate that such phenomenon is existent in GC capillary columns. With higher density of liquids than gases, the centrifugal effect will also be greater in LC.

While too low theoretical plate numbers were encountered in the earlier work of Horvath et al. (12) conducted with wide-bore capillary columns under the conditions of high-speed LC, the present study was undertaken to measure the extent of chromatographic band-broadening in the range of column diameters with potential utilization. Since Horvath's work (12) indicated possible beneficial departures from the values predicted by Taylor (4), it has been of some interest to know their magnitude with column diameters approximately an order of magnitude smaller. As the surface factor is likely to play some role in the solute transport phenomena in the micron-size tubes, we have also studied band-broadening phenomena in capillary columns down to 50- $\mu$ m diameters, provided with silica "whiskers" of micron sizes (13). In addition, the "coil effect" was investigated with glass capillary columns of various diameters.

### EXPERIMENTAL

Thick-walled glass capillaries of various lengths and diameters were drawn from glass tubes of appropriate dimensions by means of a commercial glass drawing machine (Hupe and Busch, Grotzingen, West Germany). Columns with internal diameters

down to about 20  $\mu$ m are readily feasible; for example, common polarographic capillaries make convenient starting materials for glass drawing. Column diameter is occasionally checked under the microscope. If a proper control of drawing parameters is maintained, fluctuations in capillary diameter should be no more than 10% (14) with the micron-size capillaries.

The LC apparatus for measuring the extent of band-broadening has been basically described in our recent publication on packed microcapillary columns (15). The system included a splitting injector and an assembly for additional liquid purge at the column exit, to overcome detector volume problems. A restrictor was added beyond the detector cell to prevent formation of bubbles within the detector.

At the present time, investigations were performed only with benzene (a nonretained solute). Injected amounts were kept constant and near the sensitivity limit of the UV monitor. Splitting ratios between 1:1000 and 1:2500 were typically used.

Whereas some measurements were performed with untreated glass capillaries, we also investigated the effects of surface modification. For the latter case, silica "whiskers" were formed inside the columns according to the method of Onuska et al. (13). The "whisker" structures of adequate density were observed microscopically after a double treatment of glass wall with 0.5% solution of  $\text{NH}_4\text{F} \cdot \text{HF}$  in methanol. Observations of the "whisker" density after LC experiments demonstrated no substantial changes, attesting to good mechanical stability of this surface treatment.

In order to investigate an effect of column coiling on plate height values at different velocities, the glass drawing machine was modified with home-made coiling tubes to prepare columns with smaller- or greater-than-usual coil radii.

Mobile-phase velocities were evaluated from the retention times of benzene. Hexane was used exclusively as a mobile phase. To estimate plate height values from the Taylor equation (4), the value of diffusion coefficient for benzene in hexane at 23  $^{\circ}\text{C}$  ( $3.0 \times 10^{-5} \text{ cm}^2 \text{ s}^{-1}$ ) was calculated from viscosity, molar volume, and heat of vaporization data according to the procedure of Othmer and Thakar (16).

### RESULTS AND DISCUSSION

Comparisons of theoretical and experimental data, concerning plate height ( $H$ ) vs. flow velocity ( $v$ ) curves, are included in Figure 1 for three different capillary inner diameters. Similarly to the earlier observations of Horvath et al. (12) with wider columns,  $H$  values are significantly lower than predicted through the Taylor equation. Although the difference between theoretical and experimental curves appears less pronounced for capillaries of smaller radii, it is of practical importance that this beneficial effect occurs in the range of column diameters of potential use.

Whereas the presented results were obtained with non-retained solute only and a possible development of capillary LC as an analytical method may still be only a remote

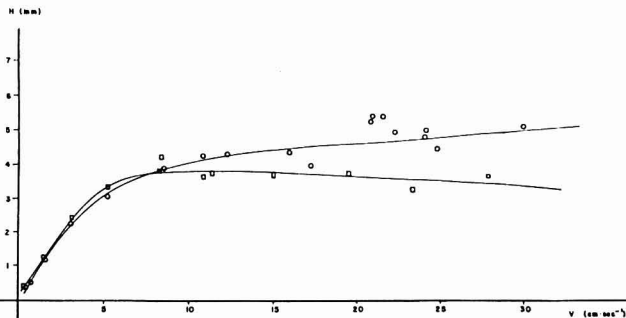


Figure 3. Plate height vs. velocity curves obtained with glass capillaries of identical internal diameters (195  $\mu$ m), but different coil diameters. (O)  $L = 102$  m, coil diameter = 23.5 cm. ( $\square$ )  $L = 87$  m, coil diameter = 5.7 cm.



possibility, these experimental values give rise to certain expectations.

In order to investigate surface effects as possible contributors to the significant plate height reduction observed above, several columns with different radii were compared in untreated and "whisker" forms. Only minor differences were observed, and these were frequently within the measurement precision of the conducted experiments. This situation is exemplified by Figure 2, where 50- $\mu$ m columns with two different surface characteristics are compared. The observed difference is indeed small.

The "coil effect" and possible utilization of the secondary flow present some interesting alternatives. If the earlier theoretical assumptions (8-11) are correct, a decrease of coil diameter can lead to a significant reduction of chromatographic band-broadening. Rather than coil diameter alone, the ratio of such quantity to the column internal diameter must be considered. While reducing the column inner radius, the plate height will decrease. However, the "coil effect" is also likely to be less beneficial. We have made this observation in the previously reported work on packed microcapillaries (15), and the results on open tubes studied in this work show similar trends. Thus,  $H$  vs.  $v$  curves obtained with different coil radii for both packed (15) and open microcapillaries (of approximately 100  $\mu$ m and smaller internal diameters) demonstrated no appreciable differences. However, a diameter increase to 190  $\mu$ m shows a significant departure of the corresponding curves from each other at high flow rates, suggesting that the "coil effect" is operational here (see Figure 3).

Although the plate heights obtained with larger diameters are, regrettably, too high, the flatness of both curves at high velocity values is commendable. Alternatively, the coil radius could be further reduced. However, we find technical difficulties in drawing glass columns with coil diameter smaller than about 4 cm.

Whereas coiling and surface treatment could result in minor plate-height reductions in a more or less additive fashion, they still fail to explain the differences between predicted and measured values. While potentially significant for the future of capillary LC, this discrepancy remains to be an interesting theoretical problem.

Whether considering achievement of high plate numbers through reduction of column radius, or utilizing secondary flow phenomena in very long columns of somewhat larger diameters, there will be many technical difficulties involved with any future attempts to make capillary LC viable. In fact, it is entirely possible that the columns are considerably better

than our presently crude sampling and detection techniques reveal. Developments of smaller and more sensitive detectors and the high-pressure capabilities beyond the present state, are indeed a challenge.

While the presented results are limited to a nonretained solute, suitable column technology is likely to require much additional work. With the limited capacity of small-bore open tubular columns, the recently developed packed microcapillary columns (15) may be a better alternative. In spite of the disadvantages of microcapillary columns named above, these columns also possess some unique features: (a) the overall miniaturization of separation processes can be accomplished; and, (b) because of the very low flow rates through such columns, a new relationship between the column and detectors or ancillary tools is now available. These considerations appear to provide incentive for further theoretical and experimental studies of capillary LC.

**Note Added in Proof.** During the 12th International Symposium Advances in Chromatography, held in Amsterdam on November 7-10, 1977, we became aware that research along somewhat similar lines has been underway in the Research Laboratories of Shell Oil Company, Amsterdam, by R. Tijssen, the author of the earlier published theoretical papers (ref. 9 and 10).

#### LITERATURE CITED

- (1) J. C. Giddings, *Anal. Chem.*, **36**, 1890 (1964).
- (2) L. S. Ettre, "Open Tubular Columns in Gas Chromatography", Plenum Press, New York, N.Y., 1965.
- (3) M. J. E. Golay, in "Gas Chromatography 1958", D. H. Desty, Ed., Academic Press, New York, N.Y., 1958, p. 36.
- (4) G. Taylor, *Proc. R. Soc. (London)*, **219A**, 186 (1953).
- (5) M. J. E. Golay, *Chromatographia*, **6**, 242 (1973).
- (6) V. Pretorius and T. W. Smuts, *Anal. Chem.*, **38**, 274 (1966).
- (7) J. C. Giddings, W. A. Manwaring, and M. N. Myers, *Science*, **154**, 146 (1966).
- (8) J. A. Koutsky and R. J. Adler, *Can. J. Chem. Eng.*, **43**, 239 (1964).
- (9) R. Tijssen, *Chromatographia*, **3**, 525 (1970).
- (10) R. Tijssen and R. T. Wittebrood, *Chromatographia*, **5**, 286 (1972).
- (11) A. K. Wong, B. J. McCoy, and R. G. Carbonell, *J. Chromatogr.*, **129**, 1 (1976).
- (12) C. G. Horvath, B. A. Preiss, and S. R. Lipsky, *Anal. Chem.*, **39**, 1422 (1967).
- (13) F. I. Onuska, P. D. Goulden, M. E. Comba, and R. J. Wilkinson, *J. Chromatogr.*, **142**, 117 (1977).
- (14) K. Tesarik and M. Novotny, *Chem. Listy*, **62**, 1111 (1968).
- (15) T. Tsuda and M. Novotny, *Anal. Chem.*, **50**, 271 (1978).
- (16) D. F. Othmer and M. S. Thakar, *Ind. Eng. Chem.*, **45**, 569 (1953).

RECEIVED for review November 9, 1977. Accepted December 27, 1977. This work was supported by Grant No. MPS 75-04932 from the National Science Foundation.

# Improved Detectability of Barbiturates in High Performance Liquid Chromatography by Post-Column Ionization

C. Randall Clark\* and Jen-Lee Chan

School of Pharmacy, Auburn University, Auburn, Alabama 36830

The post-column ionization of 5,5-dialkylbarbituric acid derivatives is shown to enhance their UV detectability. The simple ionization of a weak acid substance such as the barbiturates is perhaps the most fundamental method of producing an "in line" chromophoric species. The kinetics of the process is rapid with ionization occurring immediately upon addition of the basic medium. The ionization is achieved by the post-column infusion of a pH 10 borate buffer solution. The  $pK_a$  values of the common barbiturates used in therapy are from 7 to 8; therefore, at a pH of 10, these weak acids exist almost exclusively in the anionic thus chromophoric form. An HPLC procedure is described for the separation of the free acid barbiturates, their post-column ionization, and detection as the anionic chromophore. The ionization process allows for a 20-fold increase in peak area over the same concentration of un-ionized barbiturate.

High performance liquid chromatography (HPLC) has become a very valuable technique in the analysis of drugs from pharmaceutical formulations (1-3) and biological samples (4, 5). The highly efficient separation powers of HPLC have been demonstrated in many areas of analytical chemistry. The nondestructive spectrophotometric method of detection is an additional advantage of HPLC in the analysis of samples of limited quantity. This allows for sample collection following analysis for the generation of additional analytical data. However, the limits of spectrophotometric detection vary with the absorptivity of individual compounds. Molecules having high natural absorptivity can be detected in low concentrations but trace amounts of compounds having low absorptivity values cannot be determined directly. The use of derivatization procedures to enhance the absorptivity, and thus the detectability, of these compounds is well documented (6, 7).

The use of derivatizing reagents to produce molecules of high absorptivity has been applied to many classes of compounds (8-10). These derivatization procedures generally link chromophore to substrate through a covalent bond. These procedures are often referred to as pre-column techniques. The reaction times required in these procedures range from 30 min up to several hours. The covalently linked derivatives generally display chromatographic properties different from the parent molecule and all further analytical data obtained on the sample must be generated on the derivatized sample.

Post-column derivatization techniques offer several advantages over the pre-column methods. One important advantage is the separation process can be carried out on the parent molecule without extra sample preparation or the development of additional chromatographic conditions. However, the use of post-column derivatization requires a reaction which is complete within a few seconds, a mobile phase which is a suitable reaction medium, and a derivatization reagent which is not detected under the same conditions as the derivative. Furthermore, a derivative which could be easily converted back to the original molecule following

detection would represent a further advancement in derivatization techniques.

The UV absorption properties of the weak acid barbiturates are such that the free acid form (un-ionized) has very weak absorbing properties; however, the anionic form is a strong chromophore. The reverse phase chromatographic properties of the barbiturates have been studied extensively (11) showing the free acid form of these drugs to be easily separated, but little separation was observed when the pH of the mobile phase produced the anion as the dominant barbiturate species. Thus, for barbiturates, good chromatographic properties are observed in the free acid form and good chromophoric properties are observed only in the anionic species. This paper reports the results of our initial efforts at combining both these advantages into a single analytical technique. The barbiturates are separated as the free acids by reversed phase chromatography, the pH of the mobile phase is changed by a post-column technique, and the molecules are detected as the chromophoric anion.

## EXPERIMENTAL

**Apparatus.** The liquid chromatograph consisted of a Waters model 6000A solvent pump, model U6K injector equipped with a 2-mL loop, a model 440 UV detector, and a Hitachi recorder. A second solvent pump (Waters model 6000) was connected to the HPLC system by means of a 1/4-inch Swagelok union tee (part no. SS-100-3) installed in the line between the column and the UV detector. This pump is used to introduce the reagent solution for the "in-line" formation of the chromophores. Ultraviolet absorption spectra were measured using a Hitachi model 60 or a Perkin-Elmer model 200 spectrophotometer.

**Reagents.** All reagents were of ACS reagent-grade quality and were used as purchased without further purification. Spectrophotometric grade methanol was obtained from Fisher Scientific Company, Atlanta, Ga. The barbiturates were purchased from Sigma Chemical Company, St. Louis, Mo. All barbiturate salts were converted to the free acid form for chromatography and solutions were prepared in spectrophotometric grade methanol. The pH 10 borate buffer was prepared by mixing 250 mL of 0.2 M  $H_2BO_3$ , 250 mL of 0.2 M KCl, 220 mL of 0.2 M NaOH and diluting to 1 L. All aqueous solutions were prepared in double distilled water.

**Chromatographic Procedure.** Separation by HPLC was accomplished using a 1/4-in. o.d. by 30-cm micro-bond  $C_{18}$  column (Waters Associates, Milford, Mass.). The mobile phase consisted of a mixture of 65% water (double distilled, pH 7) and 35% methanol. The mobile phase flow rate was 1.5 mL/min, and the UV detector was operated at 254 nm (0.01 AUFS). In each analysis, 5  $\mu$ L of a methanol solution of the barbiturates (free acid, 50  $\mu$ g/mL) was injected using a 25- $\mu$ L syringe. The separations were carried out at ambient temperature without thermostating. The pH 10 borate buffer was pumped into the system at a rate of 0.2 mL/min. In all runs not requiring the addition of buffer, the union tee was plugged and remained in the line.

## RESULTS AND DISCUSSION

The chromatographic behavior of a wide variety of drugs on an octadecylsilane stationary phase has been examined by Twitchett and Moffat (11). This work illustrated the profound effects of the  $pK_a$  of the drug and the pH of the eluent upon retention characteristics, pointing out that only the un-ionized

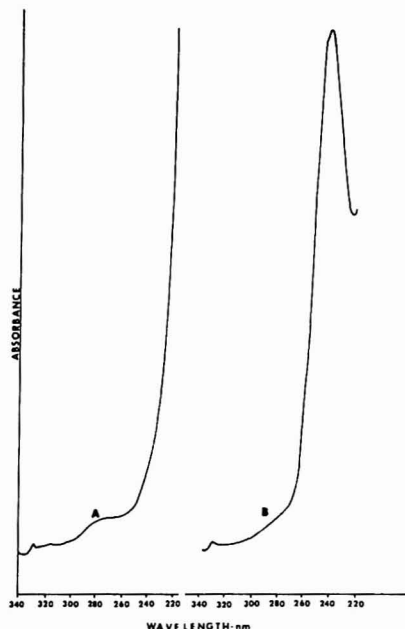
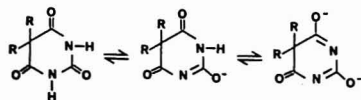


Figure 1. Ultraviolet absorption spectrum of butabarbital. (A) Methanol-water solvent, pH 7. (B) Methanol-water solvent adjusted to pH 10 with borate buffer (0.2 mL buffer/1.5 mL of barbiturate solution)

form of weak acid drugs will partition into the stationary phase. The retention of the un-ionized form of the weak acids was shown to parallel the *n*-octanol-water partition coefficient ( $\log P$ ).

The UV absorption characteristics of barbiturates are well documented (12) and the absorption spectrum of an example compound, butabarbital, is shown in Figure 1. The 5,5-dialkylbarbiturates are very weak absorbers in the free acid form; however, the species present in basic solution is a strong absorber. The kinetics of the conversion of the free acid barbiturates to the conjugate base is rapid with maximum absorption achieved immediately upon addition of the borate buffer. The 5,5-disubstituted barbiturates are diprotic weak acids showing two  $pK_a$  values. The initial ionization has a  $pK_a$  between 7 and 8, and the second ionization occurs in the pH 12 to 13 range. The UV absorption properties of the monoanion shows an intense band with a maximum in the 245 nm range, the dianion has a less intense absorption maximum at 260–270 nm. Thus, by buffering the pH at 10 the desired monoanionic chromophore is the dominate species present in solution.



For maximum effectiveness, the HPLC method should combine the excellent chromatographic properties of the un-ionized barbiturates and the chromophoric properties of the monoanionic species. A pH of 10 is outside of pH range recommended for eluents in bonded octadecylsilane stationary phases. These bonded phases are reported to be slowly cleaved

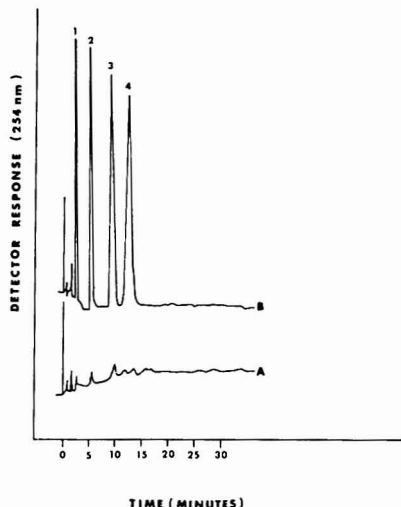


Figure 2. Water-methanol isocratic elution HPLC of some 5,5-di-alkylbarbiturates. (A) Barbiturate mixture without post-column ionization. (B) Barbiturate mixture with the post-column addition of pH 10 borate buffer (0.2 mL/min). Peaks: (1) barbital, (2) butabarbital, (3) amobarbital, (4) secobarbital

under basic conditions (13). Our approach to this problem is to attempt to generate the chromophore at a point in the HPLC system between the column and the detector. This post-column technique would allow for maximum HPLC effectiveness in the analysis of barbiturates.

The separation of a representative group of barbiturates is shown in Figure 2. The elution of the barbiturates from the octadecylsilane stationary phase is in order of decreasing water solubility or increasing  $\log P$ . Thus, the long acting barbiturate barbital elutes from the column before butabarbital and amobarbital (intermediate acting) and before secobarbital (short acting). Figure 2 shows the results obtained by injecting 5  $\mu$ L of a solution of a barbiturate mixture both in the absence of buffer and in the presence of 0.2 mL/min borate buffer. The significant increase in peak areas produced by the ionization process should be noted. Since the chromatography is achieved with the free acid and ionized in this post-column procedure, the retention time is the same for both free acid and anion. A plot of peak area vs. concentration for butabarbital both with and without the addition of buffer showed an approximate 20-fold increase in peak area in the presence of buffer. An injection of 244 ng of butabarbital produced a peak of approximately 5:1 signal-to-noise ratio without buffer infusion and an injection of 12.2 ng produced a peak of approximately equal size in the presence of pH 10 buffer.

Since the chromophoric species is produced by a simple pH change, it is not necessary to add additional UV absorbing reagents for the post-column derivatization. Therefore, the addition of the pH 10 borate buffer solution does not produce the excess background absorbance sometimes encountered in post-column techniques. A slight increase in baseline noise was noted but can be attributed to the pulsed flow produced by adding the buffer solution with the piston type pump. Frei (14) has pointed out the necessity of completely pulse-free addition of the post-column reagent to minimize the background. Since the buffer solution is completely transparent

at 254 nm, the pulsing does not produce significant baseline noise.

It has been noted in other work (15) that the constant infusion of a relatively large volume of a second solution following the chromatography column produces peak broadening. Although the buffer delivery system has no effect on the chromatographic process, the addition of the post-column reagent at relatively high flow rates can produce effects similar to chromatographic band spreading. The addition of the union tee itself at a post-column position might be expected to produce some band broadening, since the volume of the tee would represent a potential mixing chamber. The effects of the additional equipment necessary to carry out post-column derivatization were investigated. A sample of butabarbital was injected to produce a peak of approximately the same height into (A) the standard HPLC system (no union tee in the system), (B) the HPLC system plus the post-column union tee (third inlet plugged), (C) the HPLC system plus the union tee and 0.2 mL/min of pH 10 borate buffer. The peak widths were quite similar for the three situations, pointing out that post-column derivatization procedures can be accomplished without serious detrimental effects on the separation process.

One drawback to conventional pre-column derivatization procedures is the additional problems produced by permanently bonding a chromophoric group to the compound of interest. This requires additional sample preparation and, if the sample is to be collected from the HPLC effluent for other analytical tests, these additional procedures must be performed on the derivatized sample. The post-column

technique described in this paper requires no additional sample workup, the chromophore is generated by a simple pH change, and the original molecule can be easily regenerated by a second pH change to neutralize the borate buffer.

#### ACKNOWLEDGMENT

We gratefully acknowledge the technical assistance by Kay F. Wamble in this investigation.

#### LITERATURE CITED

- (1) E. Heftmann, Ed., "Chromatography, Third Edition," Van Nostrand Reinhold Company, New York, N.Y., 1975, pp 675-714.
- (2) C. K. Wong, D. M. Cohen, and K. P. Munnely, *J. Pharm. Sci.*, **65**, 1090 (1976).
- (3) D. C. Chatterji and J. F. Gaskelli, *J. Pharm. Sci.*, **66**, 1219 (1977).
- (4) M. J. Cooper, A. R. Sinak, M. W. Anders, and B. L. Mirkin, *Anal. Chem.*, **48**, 1110 (1976).
- (5) L. C. Francini, G. L. Hawk, B. J. Sandmann, and W. G. Haney, *Anal. Chem.*, **48**, 372 (1976).
- (6) J. F. Lawrence and R. W. Frei, "Chemical Derivatization in Liquid Chromatography," Elsevier North-Holland, New York, N.Y., 1977.
- (7) H. Jupille, *Ann. Lab.*, **8**, 85 (1976).
- (8) F. A. Fitzpatrick, M. A. Wynakke, and D. G. Kaiser, *Anal. Chem.*, **49**, 1032 (1977).
- (9) N. E. Hoffman and J. C. Liao, *Anal. Chem.*, **48**, 1104 (1976).
- (10) F. Nachtmann, H. Spitz, and R. W. Frei, *Anal. Chem.*, **48**, 1576 (1976).
- (11) P. J. Twitcheit and A. C. Moffat, *J. Chromatogr.*, **111**, 149 (1975).
- (12) K. A. Corners, "A Textbook of Pharmaceutical Analysis, Second Edition," John Wiley and Sons, New York, N.Y., 1975, pp 204-205.
- (13) C. Horvath, W. Melander, and I. Molnar, *Anal. Chem.*, **49**, 142 (1977).
- (14) R. W. Frei, *Res./Dev.*, **28**, 42 (1977).
- (15) C. R. Clark, C. M. Darling, J. L. Chan, and A. C. Nichols, *Anal. Chem.*, **49**, 2080 (1977).

RECEIVED for review December 15, 1977. Accepted January 23, 1978.

## Quantitative Determination of D- and L-Amino Acids by Reaction with *tert*-Butyloxycarbonyl-L-leucine *N*-Hydroxysuccinimide Ester and Chromatographic Separation as L,D and L,L Dipeptides

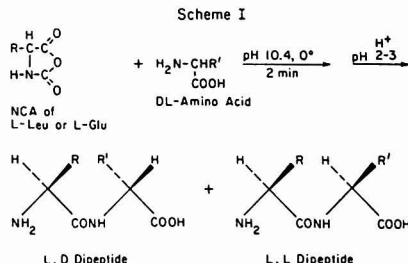
A. R. Mitchell,<sup>1</sup> S. B. H. Kent, I. C. Chu, and R. B. Merrifield\*

The Rockefeller University, New York, New York 10021

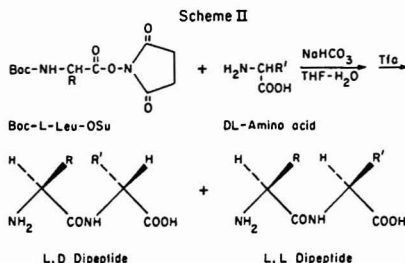
Free D- and L-amino acids have been reacted with Boc-L-leucine *N*-hydroxysuccinimide ester to form, after acidolytic cleavage of the Boc group, the diastereomeric dipeptides L-Leu-D-amino acid and L-Leu-L-amino acid in high yield (> 95%) and without detectable racemization (<0.1%). A convenient general protocol for the reaction is described. Conditions are described for the separation of the [L-Leu]<sup>1</sup>-dipeptide diastereomers of each common amino acid on the standard amino acid analyzer. Shorter ion exchange columns and/or more basic buffers were used for the [L-Leu]<sup>1</sup>-dipeptides containing the aromatic or basic D- and L-amino acids. This modification of the Manning-Moore procedure allows the detection and quantitation of less than one part D-amino acid in the presence of 1000 parts L-amino acid.

The rapid, accurate determination of the optical purity of amino acids is a subject of some importance (1-3). In par-

<sup>1</sup> Present address, Lawrence Livermore Laboratory, Livermore, Calif. 94550.



ticular, chemical synthesis of optically pure peptides requires starting materials that have high stereochemical purity. We have employed the Manning-Moore procedure (4) extensively to establish the stereochemical purity of D- and L-amino acids from various sources. In addition we have used this procedure to determine the purity of derivatives prepared from these



amino acids. Feinberg and Merrifield (5), for example, established the optical purity of a complete set of protected amino acids before using them in solid phase peptide synthesis. In each case the synthesis, isolation, and deprotection of the derivative proceeded without detectable racemization (< 0.05%).

The widely used method of Manning and Moore (4) combines a rapid procedure (6, 7) for converting the D- and L-isomers of amino acids into diastereomers with an ion exchange chromatographic procedure for their separation and quantitation (Scheme I). In their method L-leucine *N*-carboxyanhydride (L-Leu NCA) is used to prepare, without racemization (7), the [L-Leu]<sup>1</sup>dipeptides of the acidic and neutral amino acids which are separated on an amino acid analyzer. The [L-Leu]<sup>1</sup>dipeptides of the aromatic and basic amino acids are severely retarded on this column, and L-glutamic acid NCA is used to prepare resolvable dipeptides of these amino acids. Under the proper conditions as little as 0.01% of the opposite enantiomer can be detected in an amino acid.

The success of the Manning-Moore procedure for the determination of D- and L-amino acids is contingent upon the availability of L-Leu NCA and L-Glu NCA. The synthesis of L-Leu NCA is straightforward but that of L-Glu NCA is difficult and gives variable yields. In addition, the commercial availability of these labile compounds has been erratic (8). Furthermore, L-Glu NCA and L-Leu NCA deteriorate at room temperature and must be stored dry at -20 °C to retard decomposition and polymerization.

The present paper describes a convenient procedure for the conversion of D- and L-amino acids to the corresponding [L-Leu]<sup>1</sup>dipeptides using the *N*-hydroxysuccinimide ester of Boc-L-leucine. The use of *N*-hydroxysuccinimide (HOSu) esters of benzyloxycarbonyl (Z) and *tert*-butoxycarbonyl (Boc) amino acids in peptide synthesis is well known (9, 10). They react with amino acids and peptides without detectable racemization. Further, they are crystalline solids which exhibit good stability at room temperature and are readily accessible by synthesis (9) or from commercial sources. We have reacted Boc-L-leucine *N*-hydroxysuccinimide ester (Boc-L-Leu-OSu) with D- and L-amino acids. The resulting Boc-[L-Leu]<sup>1</sup>dipeptides were deprotected in trifluoroacetic acid to give the free diastereomeric dipeptides which could then be separated by ion exchange chromatography (Scheme II). The use of Z-L-Leu-OSu in a similar procedure to estimate the optical purity of a nonprotein amino acid has been described (11).

We have also derived conditions for the separation of the [L-Leu]<sup>1</sup>dipeptide diastereomers of each common amino acid by ion exchange chromatography. As the separation of the [L-Leu]<sup>1</sup>dipeptides containing acidic or neutral D- and L-amino acids has already been reported (4, 5), it was necessary only to derive conditions for the separation of the [L-Leu]<sup>1</sup>dipeptides containing the aromatic or basic D- and L-amino acids. We have achieved this by the use of shorter ion exchange

columns and/or more basic buffers.

## EXPERIMENTAL

**Materials.** All solvents and bulk chemicals were reagent grade and were used without further purification. The amino acids used in this study were obtained from a variety of sources: D-Tyr (Fluka), L-Tyr (Cyclo, Ajinomoto), L-Phe and DL-Phe (Sigma), L-His and DL-His (Mann), L-Arg-HCl (Merck), DL-Lys-HCl (Sigma), L-Lys (Merck).

DL-Arg-HCl was prepared by racemization of L-Arg with acetic anhydride (12). *N*<sup>α</sup>-Z-L-Lys was purchased from Schwarz/Mann, while *N*<sup>α</sup>-Z-L-Lys was prepared according to Bezas and Zervas (13).

**Boc-L-Leu-OSu.** Boc-L-Leu-OSu was prepared from Boc-L-Leu (Chemalco) as described by Anderson et al. (9). Boc-L-leucine (4.62 g, 20 mmol) and *N*-hydroxysuccinimide (2.76 g, 24 mmol) were dissolved in 60 mL THF and chilled to 0 °C. Dicyclohexylcarbodiimide (4.12 g, 20 mmol) was added with stirring and the solution kept at 0–5 °C for 18 h. Acetic acid (0.23 mL, 4 mmol) was added. After 15 min the insoluble urea was removed by filtration and the solvent removed at 35–40 °C under reduced pressure. Recrystallization of the residual oil from diisopropyl ether (650 mL) gave crystals, 2.70 g, mp. 111–112 °C.

Anal. Calcd. for C<sub>12</sub>H<sub>21</sub>N<sub>2</sub>O<sub>5</sub>: C, 54.86; H, 7.37; N, 8.53. Found: C, 54.94; H, 7.41; N, 8.59. Boc-L-Leu-OSu is also available from suppliers of amino acid and peptide derivatives (Bachem, Chemalco, Fluka, Peninsula, Vega-Fox).

Stock solutions of sodium bicarbonate (0.333 M) in water and Boc-L-Leu-OSu (0.333 M) in tetrahydrofuran were used in the derivatization reactions. The Boc-L-Leu-OSu solution was stable for at least 1 week at room temperature, and at least 1 month if stored at 4 °C.

**Procedure. A. Reaction of Tyr, Phe, His, and Arg with Boc-L-Leu-OSu.** Sodium bicarbonate stock solution (0.12 mL, 40 μmol) was added to a 1-mL reaction vial (Wheaton Vitro "200" Vial, SGA-5050, with a Teflon-lined cap) containing free amino acid (20 μmol) and a 4-mm Teflon coated magnetic stirring bar. The solution was stirred for 1 min on a stirring plate and Boc-L-Leu-OSu stock solution (0.12 mL, 40 μmol) in THF was added. The reaction mixture was stirred at room temperature for 1 h, washed with THF into a 50-mL round bottom flask, and evaporated to dryness using a rotary evaporator at 45–50 °C. The residue was dissolved in trifluoroacetic acid (1 mL) and allowed to stand in a stoppered flask for 1 h at room temperature to remove the Boc group. The trifluoroacetic acid was evaporated in vacuo with the aid of dichloromethane on the rotary evaporator. The residue was dissolved in pH 2.2 sodium citrate buffer (20 mL), filtered through a Millipore filter (0.22 μm, No. GSWP 01300) in a Swinny adaptor (No. XX 3001200), and an aliquot (1 mL) was injected onto the appropriate column of the amino acid analyzer. Elution conditions and peak widths for the [L-Leu]<sup>1</sup>dipeptides prepared by this procedure are given in Table I. The reactions went to over 94% completion in 1 h as judged by the amount of free amino acid remaining.

**B. Reaction of Acidic and Neutral Amino Acids with Boc-L-Leu-OSu.** The procedure described above was applied to all the neutral amino acids. For glutamic and aspartic acids, an additional two equivalents of sodium bicarbonate was added to ensure neutralization of the acid side chains. Yields of all dipeptides were greater than 95% based on the residual free amino acid.

**C. Reaction of Lys, *N*<sup>α</sup>-Z-Lys, and *N*<sup>α</sup>-Z-Lys with Boc-L-Leu-OSu.** Sodium bicarbonate (40 μmol), L-Lys (20 μmol), and Boc-L-Leu-OSu (200 μmol) were reacted and worked up as described for A. The reaction went to 97% completion as judged by depletion of amino acid and the presence of only trace amounts of the monoacylated products *N*<sup>α</sup>-L-Leu-L-Lys and *N*<sup>α</sup>-L-Leu-L-Lys.

The above procedure was repeated with *N*<sup>α</sup>-Z-L-Lys and *N*<sup>α</sup>-Z-L-Lys in place of L-Lys and DL-Lys. Anhydrous HBr (32%) in acetic acid (Eastman) was used to remove both the Boc and Z groups after the coupling reactions. In this manner, *N*<sup>α</sup>-Z-L-Lys gave rise to *N*<sup>α</sup>-L-Leu-L-Lys and *N*<sup>α</sup>-Z-L-Lys afforded *N*<sup>α</sup>-L-Leu-L-Lys. Elution conditions and peak widths for the L-leucyl derivatives of lysine are given in Table II.

**D. Protected Amino Acids.** After removal of the protecting groups, the protocols described above can be used on the free



Table I. Elution Conditions for L-Leucyl Derivatives of Tyr, Phe, His, and Arg

DL-AA	pH	Column, <sup>a</sup> cm	L-Leu	Elution time, min <sup>b</sup>			NH <sub>4</sub> <sup>+</sup>
				Unreacted DL-AA	LD Dipeptide	LL Dipeptide	
Tyr	4.25 <sup>c</sup>	58	58 (<4)	71 (3)	140 (10.5)	217 (11)	300
Phe	5.26	58	39 (<4)	63 (3)	104 (7.5)	86 (6)	>130
His	4.66	10.5	20	95 (4.5)	148 (8)	198 (11.5)	101
Arg	5.26	10.5	17	105 (5)	200 (13.5)	161 (11)	71

<sup>a</sup> The 0.9 × 58 cm column contained Beckman AA-15 resin, while the 0.9 × 10.5 cm column contained Beckman PA-35 resin. Both columns were operated at 61 mL/h, 57 °C. <sup>b</sup> Figures in parentheses are peak widths given in minutes. <sup>c</sup> Containing 1.5% (v/v) benzyl alcohol and 2% (v/v) 1-propanol.

Table II. Elution Conditions for L-Leucyl Derivatives of Lys<sup>a</sup>

Derivative	Elution time, min	Peak width, min
L-Leu	38	<4
N <sup>α</sup> -L-Leu-L-Lys	112	4.5
N <sup>α,ε</sup> -(di-L-Leu)-L-Lys	128	7.5
DL-Lys	164	4
N <sup>ε</sup> -L-Leu-L-Lys	208	7.5
N <sup>α,ε</sup> -(di-L-Leu)-D-Lys	240	14
NH <sub>4</sub> <sup>+</sup>	258	6

<sup>a</sup> 0.9 × 58 cm Beckman AA-15 column, pH 7.00, 61 mL/h, 57 °C.

amino acids. The reaction mixture must be kept at about pH 9 for the reaction with Boc-L-Leu-OSu. Where strong acid conditions were used to remove protecting groups, it is important to thoroughly remove traces of acid and to check and adjust, if necessary, the pH of the amino acid solution prior to the addition of Boc-L-Leu-OSu.

**Chromatography.** Ion exchange chromatography was performed with a Beckman Model 120B amino acid analyzer based on the design of Spackman, Stein, and Moore (14). Conditions for the analysis of the [L-Leu]<sup>1</sup>dipeptides of the acidic and neutral amino acids have been reported (4, 5). A long column (0.9 × 58 cm; Beckman AA-15 sulfonated polystyrene) was used for the chromatography of [L-Leu]<sup>1</sup>dipeptides containing Tyr (pH 4.25), Phe (pH 5.26), and Lys (pH 7.00), while a short column (0.9 × 10.5 cm; Beckman PA-35 sulfonated polystyrene) sufficed to resolve [L-Leu]<sup>1</sup>dipeptides containing His (pH 4.66) and Arg (pH 5.26). Both columns were operated at a flow rate of 61 mL/h and 57 °C. Samples (1.0 mL) were applied with an Altex rotary-valve sample injector.

The pH 2.2 sodium citrate buffer (0.2 N in sodium) was used for samples applied to the analyzer column (14). The pH 4.25 (0.2 N in sodium) and pH 5.26 (0.35 N in sodium) citrate buffers were prepared from Beckman concentrates. The pH 4.25 buffer used in the resolution of L-Leu-DL-Tyr diastereomers also contained 1.5% benzyl alcohol (v/v) and 2% 1-propanol (v/v). The pH 4.66 buffer was prepared by mixing three parts pH 4.25 buffer with one part of pH 5.26 buffer. The pH 7.00 buffer was prepared by titration of the pH 5.26 buffer with 50% NaOH. A Corning Digital Research pH meter was used to measure the pH of the buffer solutions.

**Check for Racemization.** Boc-L-Leu was deprotected with trifluoroacetic acid for 1 h at room temperature and converted to the [L-Leu]<sup>1</sup>dipeptide according to the above procedures. The Boc-L-Leu-OSu used had been prepared from this same lot of Boc-L-Leu. The product was chromatographed as previously described (5) at a 5-μmol loading.

## RESULTS AND DISCUSSION

Boc-L-leucine *N*-hydroxysuccinimide ester reacts with amino acids to give diastereomeric [L-Leu]<sup>1</sup>dipeptides which are suitable, after deprotection, for chromatographic separation. The standard protocol involves the reaction of amino acid (1 equiv) with Boc-L-Leu-OSu (2 equiv) and sodium bicarbonate (2 equiv) in tetrahydrofuran-water (1:1) at room

Table III. Elution Conditions for Diastereomeric Dipeptides

Dipeptide	pH	Column length, cm	Elution time, min
L-Leu-D-Tyr	4.25 <sup>a</sup>	58	140
L-Leu-L-Tyr	4.25 <sup>a</sup>	58	217
L-Leu-D-Phe	5.26	58	104
L-Leu-L-Phe	5.26	58	86
N <sup>α,ε</sup> -(di-L-Leu)-D-Lys	7.00	58	240
N <sup>α,ε</sup> -(di-L-Leu)-L-Lys	7.00	58	128
L-Leu-D-His	4.66	10.5	148
L-Leu-L-His	4.66	10.5	198
L-Leu-D-Arg	5.26	10.5	200
L-Leu-L-Arg	5.26	10.5	161

<sup>a</sup> Containing 1.5% (v/v) benzyl alcohol and 2% (v/v) 1-propanol.

temperature for 1 h, followed by trifluoroacetic acid deprotection. The stock solution of Boc-L-Leu-OSu in tetrahydrofuran is stable at room temperature for at least 1 week. Coupling yields, as measured by the disappearance of amino acid, have varied from 94.5 to 99.8%. A larger excess of Boc-L-Leu-OSu (10 equiv) was employed in the conversion of DL-lysine to N<sup>α,ε</sup>-(di-L-Leu)-DL-Lys, which gave a coupling yield of 97%.

DL-Amino acids reacted essentially quantitatively under the chosen conditions ruling out the possibility of stereoselective reaction. The Boc-L-Leu-OSu was optically pure and reacted without racemization. This was shown by self-calibration of the reagent by deprotection of Boc-L-Leu and reaction with Boc-L-Leu-OSu made from the same lot of Boc-L-Leu. Since the enantiomers D-Leu-L-Leu and L-Leu-D-Leu coelute, any D-amino acid containing dipeptide would represent the sum of contributions from: racemization in the synthesis of the Boc-L-Leu-OSu, racemization in the peptide bond forming step, and twice the level of any Boc-D-Leu present in the starting material. No D-amino acid containing dipeptide was detected (<0.1%). It is important to note that the formation of [Leu]<sup>1</sup>[Leu]<sup>2</sup>tripeptides is not observed with this procedure. The presence of varying amounts of L-Leu-L-Leu-DL-amino acid tripeptides is sometimes observed when L-Leu NCA reacts with DL-amino acids and can give rise to extraneous peaks during ion exchange chromatography (8).

The resolution of diastereomeric dipeptides, as well as unreacted amino acids and ammonia, obtained from the reaction of basic and aromatic D- and L-amino acids with Boc-L-Leu-OSu, has been achieved (Tables I and II). A summary of elution conditions and times for only the diastereomeric [L-Leu]<sup>1</sup>dipeptides of these amino acids is given in Table III. We have typically chromatographed 1-μmol samples and have been able to detect less than one part (0.1%) of D-amino acid in the presence of 1000 parts of L-amino acid. This level of sensitivity is sufficient for almost all cases of practical interest. A larger sample (20 μmol) has been used with the detection of as little as 0.01% D-amino acid in the

presence of the L-isomer. Naturally, the accuracy of such a determination will be dependent on the optical purity of the Boc-L-Leu-OSu used.

It has been our experience that commercial L-amino acids are generally free of D-amino acids (<0.1%). Most of the D-amino acids are of comparable optical purity, although commercial samples of D-threonine and D-isoleucine often contain substantial (up to 10%) amounts of the diastereomeric L-allo-amino acids. Boc-L-amino acid derivatives are also usually optically pure (>99.9%). However, Boc-L-Ser (OBzl) may contain substantial amounts of Boc-D-Ser(OBzl) depending on the method of synthesis.

The procedures described are not intended to determine all DL-amino acids simultaneously. In general, the diastereomeric dipeptides from different amino acids may interfere with one another, although certain pairs can be separated. In particular, the enantiomeric purity of a basic or aromatic amino acid can be determined in the presence of acidic and neutral amino acids. Under the appropriate chromatographic conditions the acidic and neutral amino acids and their [L-Leu]<sup>1</sup>dipeptides elute at or near the column void volume and do not interfere with the determination of the diastereomers of the basic or aromatic amino acid. This is of great use in the determination of the optical purity of these residues in peptides (15, 16).

In summary, we have prepared diastereomeric dipeptides by the reaction of D- and L-amino acids with Boc-L-Leu-OSu followed by treatment with trifluoroacetic acid. Conditions for the separation of the resulting [L-Leu]<sup>1</sup>dipeptide diastereomers have been derived, which can allow the detection of less than one part D-amino acid in the presence of 1000 parts

L-amino acid. This modification of the Manning-Moore procedure should find general application in amino acid and peptide chemistry.

## LITERATURE CITED

- (1) P. Sieber, B. Finkler, M. Brugger, B. Kamber, and W. Rittel, *Helv. Chim. Acta*, **53**, 2135 (1970).
- (2) P. M. Helfman and J. L. Bada, *Proc. Natl. Acad. Sci. U.S.A.*, **72**, 2891 (1975).
- (3) J. M. Chalovich, C. T. Burt, S. M. Cohen, T. Gionek, and M. Barany, *Arch. Biochem. Biophys.*, **182**, 683 (1977).
- (4) J. M. Manning and S. Moore, *J. Biol. Chem.*, **243**, 5591 (1968).
- (5) R. S. Feinberg and R. B. Merrifield, *Tetrahedron*, **28**, 5865 (1972).
- (6) R. Hirschmann, R. G. Strachan, H. Schwam, E. F. Schoenewaldt, H. Joshua, B. Barkemeyer, D. F. Veber, W. J. Paleveda, Jr., T. A. Jacob, T. E. Beesley, and R. G. Denkwaller, *J. Org. Chem.*, **32**, 3415 (1967).
- (7) R. G. Denkwaller, H. Schwam, R. G. Strachan, T. E. Beesley, D. F. Veber, E. F. Schoenewaldt, H. Barkemeyer, W. J. Paleveda, Jr., T. A. Jacob, and R. Hirschmann, *J. Am. Chem. Soc.*, **88**, 3163 (1966).
- (8) Observations of this laboratory.
- (9) G. W. Anderson, J. E. Zimmerman, and F. M. Callahan, *J. Am. Chem. Soc.*, **86**, 1839 (1964).
- (10) F. M. Finn and K. Hofman, in "The Proteins", 3rd ed., Vol. 2, H. Neurath and R. L. Hill, Eds., Academic Press, New York, N.Y., 1976, pp 105-253.
- (11) Y. Shimohigashi, S. Lee, and N. Izumiya, *Bull. Chem. Soc. Jpn.*, **49**, 3280 (1976).
- (12) V. du Vigneaud and C. E. Meyer, *J. Biol. Chem.*, **98**, 295 (1932).
- (13) B. Bezaz and D. Zervas, *J. Am. Chem. Soc.*, **83**, 719 (1961).
- (14) D. H. Spackman, W. H. Stein, and S. Moore, *Anal. Chem.*, **30**, 1190 (1958).
- (15) J. M. Manning, *J. Am. Chem. Soc.*, **92**, 7449 (1970).
- (16) J. M. Manning, A. Marglin, and S. Moore in "Progress in Peptide Research", Vol. 2, S. Lander, Ed., Gordon and Breach, London, 1972, p 173-183.

RECEIVED for review November 28, 1977. Accepted January 3, 1978. Supported in part by Grant AM 01260 from the U.S. Public Health Service and by a grant from the Hoffmann-La Roche Foundation.

# Cyanuric Chloride as a General Linking Agent for Modified Electrodes: Attachment of Redox Groups to Pyrolytic Graphite

Alexander M. Yacynych and Theodore Kuwana\*

Department of Chemistry, The Ohio State University, Columbus, Ohio 43210

Cyanuric chloride was used as a linking agent for the attachment of hydroxymethylferrocene to a pyrolytic graphite electrode. The cyanuric chloride was attached to hydroxyl functional groups on the surface of the graphite electrode. These hydroxyl groups were maximized on the electrode surface by radiofrequency oxygen plasma treatment and subsequent lithium hydride reduction. The pyrolytic graphite modified by cyanuric chloride and subsequent linkage of hydroxymethylferrocene exhibited electrochemical activity and was characterized by cyclic voltammetry and differential pulse polarography at pH 3 and pH 7. The effect of various treatment steps to the pyrolytic graphite surface including the reactions of cyanuric chloride and hydroxymethyl ferrocene was monitored by x-ray photoelectron spectroscopy (ESCA).

There has recently been considerable interest and research activity in the area of "chemically modified electrodes" (1-16). Applications of chemically modified electrodes have included asymmetric synthesis (1-3) and electrocatalysis (9). Miller has attached optically active amino acids to carbon (1, 2) and metal oxide electrodes (3) to produce a chiral surface. This

chiral surface, although electroinactive, has been used to produce optically active products. Murray has attached a variety of electroactive materials to carbon (4, 5) and metal oxide electrodes (6-8). These surface groups were then monitored electrochemically and with x-ray photoelectron spectroscopy (ESCA). The oxidation of ascorbic acid has been electrocatalyzed with benzidine attached to a pyrolytic graphite electrode in our laboratory (9).

A variety of reaction schemes have been used to chemically modify electrodes (1-16). In this paper we demonstrate a different type of reaction scheme employing cyanuric chloride (trichloro-s-triazine) as a general linking agent. We will also discuss the electrode pretreatments which optimize the attachment of cyanuric chloride (CC).

CC has been used to covalently attach enzymes (immobilized enzymes) to water-insoluble supports for affinity chromatography (17-21). One of the advantages of using CC as a linking agent is the variety of reactions that it can undergo. It can react with hydroxyl and amino compounds (22). By using surface hydroxyl groups, CC can be attached to both carbon and metal oxide electrodes (16). CC can also react with alkyl and aryl Grignard reagents (22) and with organic hydrazine derivatives (23). A general reaction scheme employing

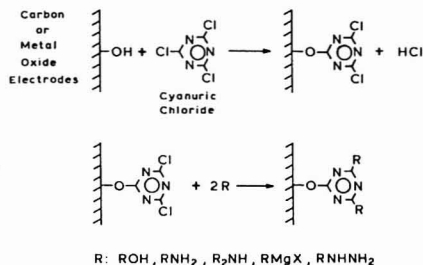


Figure 1. General reaction scheme employing cyanuric chloride as a linking agent for carbon or metal oxide electrodes

CC as a linking agent for carbon or metal oxide electrodes is illustrated in Figure 1.

CC produces a linkage that is stable to electrolysis. This is of paramount importance in employing a chemically modified electrode for electrocatalysis or asymmetric synthesis. Also, the distance between the graphite matrix and the aromatic framework of the CC molecule is very short (less than 10 Å), and it is expected that electron transfer can readily take place over such short distances. By using a short bond connecting the aromatic CC molecules, the steric problems requiring the close approach of the electroactive center to the electrode surface for electron transfer may be minimized (7). Another advantage of using CC is that it is electroinactive in the potential region employed with the pyrolytic graphite electrodes. Therefore, the electroactive center can be monitored electrochemically without interference from the linkage that binds it to the electrode.

CC was bound to the pyrolytic graphite electrode via surface hydroxyl groups. This reaction was optimized by employing oxidative and reductive electrode pretreatments. Both chemical oxidation and radiofrequency oxygen plasma treatment (15) were used to maximize oxygen-containing functional groups on the electrode surface. Carbon that has been oxidized is reported to have a variety of surface functional groups, such as carboxylic acids, quinones, ketones, hydroxyls, aldehydes, and lactones (24). If attachment is made through one type of functional group, only a small percentage of the available bonding sites will be utilized. However, by reducing the electrode surface with lithium aluminum hydride, most of the oxygen-containing functional groups may be converted to their respective hydroxyl analogues, which are then available for binding with CC.

Hydroxymethylferrocene (HMF) was attached to the pyrolytic graphite as an example of an electroactive terminal group. This compound has been previously used as an electron mediator for biological molecules that have kinetically limited electron transfer rates at ordinary electrodes (25). Characterization of these chemically modified electrodes was done by cyclic voltammetry and differential pulse polarography, and electrode surface analysis was done by ESCA.

### EXPERIMENTAL

**Electrode Pretreatment.** The pyrolytic graphite electrodes were obtained from Ultra Carbon Corporation (Bay City, Mich.). They are machined disks of pressed microcrystalline graphite on which a 1000-μm thick layer of pyrolytic graphite was vapor deposited. The electrodes were extracted with anhydrous methanol in a Soxhlet apparatus for 24 h prior to use to remove any organic contaminants.

Radiofrequency (RF) oxygen plasma treatments were performed in an electrodeless discharge plasma generator (Harrick Scientific, Inc., Ossining, N.Y.). The plasma generator was differentially pumped while anhydrous oxygen was admitted to the plasma chamber via a needle valve. The pressure was

maintained at 150 mTorr and was monitored by a thermocouple vacuum gauge. The electrodes were treated with the RF oxygen plasma for 1 h. The pumping and plasma treatment were stopped and the oxygen was increased to atmospheric pressure for an additional hour.

The electrode surface was chemically reduced by refluxing with 2 g of lithium aluminum hydride (Alfa Ventron Corp., Danvers, Mass.) in 100 mL of anhydrous ether for 4 h. The electrodes were rinsed in ether, 1 M nitric acid, and triply distilled water to remove any contaminants.

**Attachment of Cyanuric Chloride.** The cyanuric chloride (99%, Aldrich Chemical Co., Milwaukee, Wis.) was recrystallized from carbon tetrachloride. The anhydrous reagent grade benzene was distilled over molecular sieves (4 Å).

The chemically reduced electrodes were heated in an oven at 120 °C for 14 h to remove adsorbed water. They were then quickly transferred from the oven to the reaction flask to avoid readorption of water from the atmosphere. The electrodes were reacted with 5 g of CC in 100 mL of benzene for 14 h with mechanical shaking at room temperature. The electrodes were then extracted with anhydrous benzene in a Soxhlet apparatus for 24 h to remove any adsorbed CC.

**Attachment of Hydroxymethylferrocene.** The HMF (Strem Chemicals Inc., Danvers, Mass.) was recrystallized from triply distilled water. The sodium hydride was used as received (50% mineral oil mull, Alfa Ventron Corp., Danvers, Mass.).

The CC chemically modified electrodes were reacted with 0.370 g of HMF and 0.1 g of sodium hydride in 100 mL of benzene for 14 h with mechanical shaking at room temperature. These electrodes were then rinsed in distilled water and were subsequently extracted with anhydrous benzene in a Soxhlet apparatus for 24 h to remove any adsorbed reactants.

**ESCA.** ESCA analyses of surfaces were performed using a Physical Electronics Industries (Eden Prairie, Minn.) model 548 electron spectrometer equipped with a Mg Kα (1253.6 eV) x-ray excitation source. All spectra were run at pressures less than 5 × 10<sup>-9</sup> Torr. ESCA spectra signal averaging was performed using a Nova 800 minicomputer (Data General Co.) equipped with 32 K of memory and 2 Diablo disks (1.2 M words). Binding energies were normalized to the pyrolytic graphite carbon (C 1s) which was assigned a BE value of 284.4 eV.

**Electrochemistry.** Cyclic voltammetry was conducted using a conventional three-electrode potentiostat. A Princeton Applied Research model 174 polarograph was employed for differential pulse polarography. The electrochemical cell was machined from a 1.5-inch diameter Lucite rod and was 1 inch in length. A 0.5-inch hole was drilled in the center of the Lucite rod and the graphite disk working electrode was attached at one end with a rubber O-ring and brass coverplate. The other end of the cell consisted of a Lucite coverplate with holes drilled for the counter and reference electrodes and a tube for nitrogen degassing. All electrode potentials were measured vs. a Ag/AgCl (saturated KCl) reference electrode.

### RESULTS AND DISCUSSION

**Electrode Pretreatment.** Initially, oxidative chemical pretreatments were attempted in order to increase the amount of oxygen-containing functional groups on the electrode surface. Oxidation treatments with potassium permanganate and sodium dichromate showed a significant increase in oxygen content, but trace contamination of the electrodes by the reactants, as shown by ESCA analysis, could not be removed even with extensive washing. As this trace contamination would interfere with the interpretation of any results, chemical oxidative pretreatments were discontinued.

Because of these surface contaminations when chemical oxidants were used and the low oxygen-to-carbon ratios with potassium monopersulfate and Fenton's reagent, the RF oxygen plasma method developed by Evans and Kuwana (15) was used. This method is rapid, produces no contaminants, and gives reproducible results, as will be further discussed.

The modification procedures conducted on the pyrolytic graphite electrodes are summarized in Table I. The pretreatment steps (1-3) were performed to remove surface

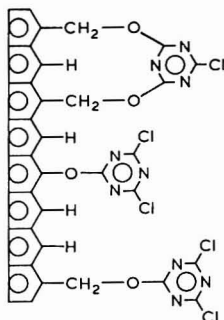
**Table I. Modification Procedures Conducted on Pyrolytic Graphite Electrodes**

Step	Procedure
1	Extraction with anhydrous methanol
2	Radiofrequency oxygen plasma treatment
3	LiAlH <sub>4</sub> reduction
4	Attachment of cyanuric chloride
5	Attachment of hydroxymethylferrocene

impurities, to introduce oxygen functional groups, and then to convert groups, such as carboxylic acids, quinones, etc., to hydroxyls.

**ESCA Results.** Elemental atomic ratios were determined from the peak heights of low resolution spectra after these peaks were corrected by normalization to the theoretical cross sections (26). Although greater accuracy could result from comparison of peak areas rather than peak heights, these ratios were judged sufficient for monitoring the relative effects of the various modification steps as listed in Table I. As may be seen from the elemental atomic ratios given in Table II, the radiofrequency oxygen plasma treatment (steps 1 and 2) increased the oxygen content on the PG surface by a factor of ca. 3 over electrodes which had been methanol extracted (step 1). The lithium aluminum hydride reduction (step 3) would not be expected to increase the oxygen content. Whether the small increase in the O/C ratio (from 0.154 to 0.174 for steps 1, 2 and 1, 2, 3, respectively) is significant is presently unknown. The decrease in the O/C ratio with the attachment of CC (steps 1-4) and HMF (steps 1-5) is partially explained by the attenuation of the graphitic carbon by these attached molecules. Some surface oxygen groups may also have been lost in the heat treatment immediately preceding the attachment of CC.

The introduction of CC on the surface was clearly evidenced by the appearance of the N(1s) ESCA peak. The increase in the attachment of CC after various pretreatment steps are reflected in the N/C ratios of 0.029, 0.043, and 0.094 which correspond to CC after steps 1 and 4; 1, 2 and 4; and 1-4, respectively. The Cl/C ratio also followed a similar increasing trend for these same steps. However, the amount of CC attachment could not be ascertained from the Cl/C ratio because of the difficulty in judging the extent of attenuation of the graphitic carbon by the attached CC. On the other hand, the average Cl/N ratio of 0.21 for surfaces which had been reacted through steps 1-4; 1 and 4; and 1, 2, and 4, was considerably below the maximum of 0.67 expected for CC attachment as shown in Figure 1. Part of the reason for the

**Figure 2.** Various possibilities of binding cyanuric chloride to the surface of a graphite electrode

lower Cl/N ratio may be rationalized by examining the various possible modes of CC attachment as seen in Figure 2. By using CPK space filling models, it can be demonstrated that CC can bind through the reaction of two chlorine atoms of CC with two aliphatic hydroxyl groups on the surface. The CC molecule in each of the different attachments shown in Figure 2 is actually quite close to the electrode surface because of the oxygen bond angle as confirmed by CPK space filling models. This close proximity of the CC to the electrode surface may be an important consideration in the rate of electron transfer. The aliphatic hydroxyl groups can be formed as the reduction products of carboxylic acid, aldehyde, and lactone groups on the surface. Therefore, the exact nature of the CC binding to the surface cannot be determined from the N/O ratio because the distribution of different types of binding is unknown. There are two possibilities for the remaining chlorine atoms. They can be hydrolyzed or HMF can be attached. Hydrolysis by trace amounts of water can occur during the attachment of CC or the terminal group, but it is minimized by using a large excess of reactant. For the case of a single ether linkage to CC, there are three possibilities for attachment of terminal groups (2 hydroxyls, 1 hydroxyl and 1 HMF, or 2 HMF's). For two ether linkages per CC, there are two possibilities (1 hydroxyl or 1 HMF). Taking into account the two different types of ether linkages, there are eight different possibilities for surface groups. In some cases, the graphitic carbon skeleton may be disordered, which would allow longer aliphatic hydroxyl chains for binding CC.

**Table II. Elemental Atomic Ratios<sup>a</sup> Determined from ESCA Data for Various Steps in the Modification of Pyrolytic Graphite Electrodes**

Reaction steps	No. of samples	O/C	N/C	Cl/C	Fe/C	N/O	Cl/N <sup>c</sup>	Cl/O <sup>c</sup>	Fe/N
1 <sup>b</sup>	3	0.052 ±0.012							
1, 2	3	0.154 ±0.022							
1, 2, 3	3	0.174 ±0.016							
1, 2, 3, 4	6	0.115 ±0.021	0.094 ±0.017	0.018 ±0.004	...	0.82 ±0.13	0.19	0.16	
1, 2, 3, 4, 5	2	0.117 ±0.013	0.064 ±0.007	0.012 ±0.004	0.011 ±0.003	0.56 ±0.13	0.19	0.10	0.17 ±0.03
<b>Controls</b>									
1, 4	1	0.033	0.029	0.004		0.88	0.14	0.12	
1, 2, 4	1	0.094	0.043	0.013		0.46	0.30	0.14	
1, 2, 3, 5	1	0.0137			...				...

<sup>a</sup> Average atomic ratio and the average deviation reported when 2 or more samples run. Theoretical photoionization cross-section corrections (26): C(1s) = 1.00, O(1s) = 2.85, N(1s) = 1.77, Cl(2p<sub>3/2</sub> and 2p<sub>1/2</sub>) = 2.36, and Fe(2p<sub>3/2</sub>) = 10.54. <sup>b</sup> Steps listed in Table I. <sup>c</sup> Calculated from the N/C and Cl/C, the O/C and Cl/C ratios, respectively.

Also, cross polymerization between CC groups could occur. This would further increase the possibilities for different surface groups.

Thus, it is not surprising to find that the Cl/N ratio was considerably below 0.67. The N/O and Cl/O ratios are also correspondingly lower than expected from the model of attachment as shown in Figure 1. These ratios suggest that all of the oxygen functionalities present on the surface do not participate in the reaction with CC.

When HMF was attached (steps 1-5), the Fe peak appeared on the ESCA spectrum. It was absent on the control sample when step 4 was omitted indicating no reaction or observable adsorption of HMF. The HMF reaction with bound CC is relatively complete assuming the Cl/N and Fe/N ratios are meaningful. However, the presence of Cl on the HMF/CC reacted electrodes is bothersome. The Cl may be present on the surface as adsorbed chloride and not as Cl which remained unreacted on CC. Such chloride has been observed on modified tin oxide electrodes which had been reacted with HMF after CC attachment. Further high resolution ESCA studies are necessary to resolve this problem.

**Surface Coverage.** A general idea of surface coverage can be obtained from the atomic ratios in Table II. ESCA signals when corrected for cross section should approximate the atomic ratios. The escape depth of electrons from graphite determined by Penn (27) is 13.5 Å. For graphite, the number of carbon atoms in the volume element,  $1 \text{ cm} \times 1 \text{ cm} \times 13.5 \text{ Å}$ , can be calculated. This value multiplied by the atomic ratio, N/C for example, gives the number of nitrogen atoms, and dividing by three gives a rough estimate of the number of CC molecules on the surface of this volume element. The average CC surface concentration for samples taken through steps 1-4 was  $1.0 \times 10^{-9} \text{ mol/cm}^2$ . If the same calculation is performed using the Fe/C ratio, the surface concentration of HMF can be determined. For samples taken through steps 1-5, the average surface concentration of HMF was calculated to be  $3.5 \times 10^{-10} \text{ mol/cm}^2$ . Some of the reasons for a lower surface concentration of HMF as compared to CC could be hydrolysis, cross polymerization, and incomplete reaction. The surface concentration as calculated from the ESCA atomic ratios assumes that the signal for the carbon atoms in the graphite is not attenuated by the presence of CC. Also, the carbon atoms in CC have not been included in the calculation. Thus, the surface concentration calculations are then, at best, an order of magnitude estimate which confirms the presence of CC and HMF when correlated with other experimental data.

If a model of the graphite electrode with no surface roughness and free rotation of the attached CC is assumed, an area of  $55 \text{ Å}^2$  is occupied by each molecule as determined from CPK space filling models. The surface concentration of CC using this model is  $3 \times 10^{-10} \text{ mol/cm}^2$ . This concentration is lower than that obtained from the ESCA data, but can be accounted for by assuming a surface roughness factor of four. Double layer capacitance measurements (15) of pyrolytic graphite before and after RF plasma treatment indicated that the surface roughness increased (by a factor of ca. 2). However, the roughness of pyrolytic graphite with respect to a perfectly smooth surface is not known.

**High Resolution ESCA Results.** Figure 3 shows the high resolution carbon (1s) peaks for the various reaction steps. All high resolution ESCA spectra are 50 scans that have been computer time averaged. After the radiofrequency oxygen plasma treatment (reaction step 1 and 2), a shoulder can be noticed at 286.7 eV. This is due to an increased amount of carbon that is bound to the oxygen functional groups. A shift to higher binding energies for this type of carbon atom is expected from binding energy shift data (28).

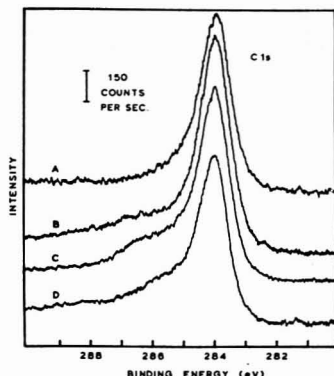


Figure 3. High resolution ESCA spectra of carbon (1s) peaks for the various reaction steps. Each spectrum has been computer time averaged for 50 scans. (A) reaction step 1, (B) reaction steps 1 and 2, (C) reaction steps 1-3, (D) reaction steps 1-4

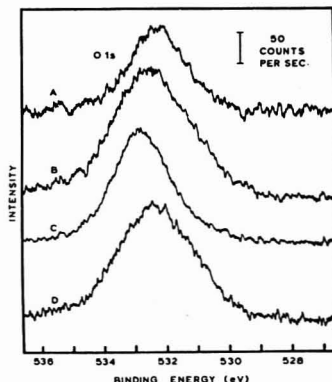


Figure 4. High resolution ESCA spectra of oxygen (1s) peaks for the various reaction steps. Each spectrum has been computer time averaged for 50 scans. (A) reaction step 1, (B) reaction steps 1 and 2, (C) reaction steps 1-3, (D) reaction steps 1-4

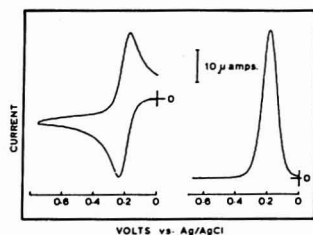
Figure 4 shows the high resolution oxygen (1s) peaks for the various reaction steps. It is interesting to note that the FWHM for reaction steps 1 and 2 is 3 eV. After reduction (reaction steps 1, 2, and 3), it decreased to 2 eV, indicating a greater uniformity in the types of oxygen functionality. This would be expected where a variety of oxygen functional groups are all reduced to a hydroxyl functionality.

The high resolution nitrogen 1s peak for reaction steps 1-4 was asymmetric, indicating nitrogen atoms that are in different environments, consistent with a heterogeneous surface.

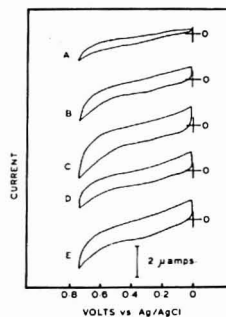
**Electrochemical Results.** A cyclic voltammogram and differential pulse polarogram of 1 mM HMF in pH 7 phosphate buffer are shown in Figure 5. The electrode was a pyrolytic graphite disk on which pretreatment steps 1 and 2 were performed. The anodic peak potential separation was 63 mV. The ratio of the anodic to cathodic peak currents was unity. The solution redox of HMF satisfies the conditions for electrochemical reversibility.

Figure 6 shows the cyclic voltammograms of the pyrolytic graphite electrodes in pH 7 phosphate buffer after each of the various treatment steps have been performed. The increase





**Figure 5.** Cyclic voltammogram and differential pulse polarogram of 1 nM hydroxymethylferrocene in pH 7 phosphate buffer. The electrode was a pyrolytic graphite disk on which pretreatment steps 1 and 2 were performed. The potential scale is volts vs. a Ag/AgCl (satd. KCl) reference electrode. The scan rate was 50 mV/s for the cyclic voltammogram and 2 mV/s for the differential pulse polarogram.

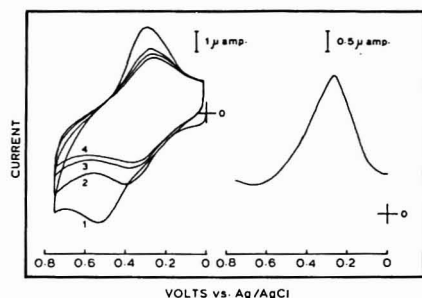


**Figure 6.** Cyclic voltammograms of the pyrolytic graphite electrodes in pH 7 phosphate buffer after the various reaction steps have been performed. The potential scale is volts vs. a Ag/AgCl (satd. KCl) reference electrode. The scan rate was 50 mV/s. (A) reaction step 1, (B) reaction steps 1 and 2, (C) reaction steps 1, 2, and 3, (D) reaction steps 1, 2, 3, and 4, (E) reaction steps 1, 2, 3, and 5.

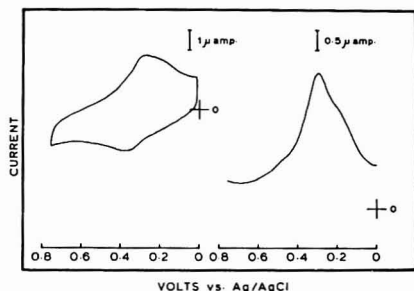
in charging current with treatment steps 1 and 2 is due to surface roughening and a corresponding increase in surface area. The cyclic voltammogram for reaction steps 1, 2, 3, and 5 was conducted as a control to check for adsorption of HMF, and no current indicative of adsorption was observed.

Figure 7 shows the cyclic voltammogram and the differential pulse polarogram of HMF attached to the electrode surface in pH 7 phosphate buffer. Figure 8 shows the same electrode in pH 3 Clark-Lubs buffer. When the modified electrode was immersed in 0.1 N HCl there was no electrochemical evidence for the presence of any attached HMF. Apparently, the HMF linkage was hydrolyzed at this low pH. Evidence exists in the literature for the hydrolysis of the ether linkage at both low and high pH (22). The first cyclic voltammogram scan in Figure 7 is apparently due to adsorbed HMF. This type of adsorption of HMF was typical for several electrodes. The reason for adsorbed HMF in this case, and not for reaction steps 1, 2, 3, and 5 is not clear. In succeeding scans, the peak potential shifted cathodically and the current decreased, becoming constant after about four scans. The anodic peak potential was 0.37 V and the peak potential separation, 100 mV. The attached HMF was more difficult to oxidize and more irreversible than the solution species. Also, the cyclic voltammogram wave was broader which could partly be due to the heterogeneity of the CC/HMF attachment as discussed previously.

The cyclic voltammogram of the surface bound HMF in pH 3 Clark-Lubs buffer was quite similar to that in pH 7



**Figure 7.** Cyclic voltammogram and differential pulse polarogram of hydroxymethylferrocene attached to a pyrolytic graphite electrode in pH 7 phosphate buffer. The potential scale is volts vs. a Ag/AgCl (satd. KCl) reference electrode. The scan rate was 50 mV/s for the cyclic voltammogram and 2 mV/s for the differential pulse polarogram. (1), (2), (3), and (4) are the first through fourth scans.



**Figure 8.** Cyclic voltammogram and differential pulse polarogram of hydroxymethylferrocene attached to a pyrolytic graphite electrode in pH 3 Clark-Lubs buffer. The potential scale is volts vs. a Ag/AgCl (satd. KCl) reference electrode. The scan rate was 50 mV/s for the cyclic voltammogram and 2 mV/s for the differential pulse polarogram.

phosphate buffer. This would be expected when there is no proton participation in redox reaction. The differential pulse polarograms were also similar in each case, but they were broad and asymmetric, indicating varied environments and linkages for redox couples on the electrode surface.

The surface concentration of HMF can be determined from the cyclic voltammogram using Faraday's law. The charge was determined by integrating the area under the peaks (after desorption of HMF) and correcting for background charge. Assuming a one-electron redox process, the number of moles of HMF on surface divided by the geometric electrode area ( $0.387 \text{ cm}^2$ ) gave a surface concentration of  $2.1 \times 10^{-10} \text{ mol/cm}^2$ . This value agrees well with the estimated surface concentration determined by ESCA.

The same electrode, used in the pH 7 and pH 3 buffer solutions, remained unchanged for 20 scans at 50 mV/s from 0 to +0.6 V. The activity of the HMF electrode slowly degrades, however, due to the instability of the ferrocenium ion in aqueous solutions. This problem can be avoided by the judicious choice of terminal group and/or solvent conditions.

## CONCLUSION

Cyanuric chloride is an attractive reagent for the attachment of terminal groups to graphite and metal oxide (ref. 16) electrodes. It is commercially available in relatively high purity at low cost. It reacts readily through a predictable chemical route to form ether linkages with surface hydroxyl

groups both in nonaqueous solution and in the gas phase (16). The ether linkage formed is chemically and electrochemically quite stable. This linkage can offer a much shorter bonding distance between the electrode and the aromatic framework compared to the more common amide or silane linkages and, as such, is expected to facilitate electron transfer between the electrode and terminal groups. The reactive chlorides in the "bound" CC offers the possibility to attach a wide variety of terminal groups which may contain hydroxy, amine, or other nucleophilic groups. The versatility of CC still remains to be fully explored and tested, but preliminary experiments have shown promising results with attachment of redox reactants such as *o*-toluidine and bis(hydroxymethyl)ferrocene to PG and to tin and indium oxide electrodes.

#### ACKNOWLEDGMENT

The authors express their gratitude to J. F. Evans for suggestions and helpful discussions during the course of this work.

#### LITERATURE CITED

- (1) B. F. Watkins, J. R. Behling, E. Kariv, and L. L. Miller, *J. Am. Chem. Soc.*, **97**, 3549 (1975).
- (2) B. E. Firth, L. L. Miller, M. Mitani, T. Rogers, J. Lennox, and R. W. Murray, *J. Am. Chem. Soc.*, **98**, 8271 (1976).
- (3) B. E. Firth and L. L. Miller, *J. Am. Chem. Soc.*, **98**, 8272 (1976).
- (4) C. M. Elliot and R. W. Murray, *Anal. Chem.*, **48**, 1247 (1976).
- (5) D. F. Ustereker, J. C. Lennox, L. M. Wier, P. R. Moses, and R. W. Murray, *J. Electroanal. Chem.*, **81**, 309 (1977).
- (6) P. R. Moses, L. Wier, and R. W. Murray, *Anal. Chem.*, **47**, 1882 (1975).
- (7) P. R. Moses and R. W. Murray, *J. Am. Chem. Soc.*, **98**, 7435 (1976).
- (8) P. R. Moses and R. W. Murray, *J. Electroanal. Chem.*, in press.
- (9) J. F. Evans, T. Kuwana, M. T. Henne, and G. P. Royer, *J. Electroanal. Chem.*, **80**, 409 (1977).
- (10) N. R. Armstrong, A. W. C. Lin, M. Fujihira, and T. Kuwana, *Anal. Chem.*, **48**, 741 (1976).
- (11) M. Fujihira, T. Matsue, and T. Osa, *Chem. Lett.*, 875 (1976).
- (12) R. J. Burt, G. J. Leigh, and C. J. Pickett, *J. Chem. Soc., Chem. Commun.*, 940 (1976).
- (13) S. Mayer, T. Matusinovic, and K. Cammann, *J. Am. Chem. Soc.*, **99**, 3888 (1977).
- (14) M. Fujihira and T. Osa, *Nature (London)*, **284**, 349 (1976).
- (15) J. F. Evans and T. Kuwana, *Anal. Chem.*, **49**, 1632 (1977).
- (16) A. W. C. Lin, P. Yeh, and T. Kuwana, unpublished data.
- (17) G. Kay and E. M. Crook, *Nature (London)*, **218**, 514 (1967).
- (18) G. Kay, M. D. Lilly, A. K. Sharp, and R. J. H. Wilson, *Nature (London)*, **217**, 641 (1968).
- (19) R. J. H. Wilson, G. Kay, and M. D. Lilly, *Biochem. J.*, **108**, 845 (1968).
- (20) R. J. H. Wilson and M. D. Lilly, *Biotech. Bioeng.*, **11**, 349 (1969).
- (21) A. K. Sharp, G. Kay, and M. D. Lilly, *Biotech. Bioeng.*, **11**, 363 (1969).
- (22) E. M. Smolin and L. Rapoport, "N-Triazines and Derivatives", Interscience Publishers, New York, N.Y., 1959, pp 48-82 and 68-80.
- (23) P. Leow and C. D. Weis, *J. Heterocyclic Chem.*, **13**, 829 (1976).
- (24) S. S. Barton and B. H. Harrison, *Carbon*, **13**, 283 (1975).
- (25) W. M. Clark, "Oxidation-Reduction Potentials of Organic Systems", The Williams and Wilkins Co., Baltimore, Md., 1960, p 464.
- (26) J. H. Scofield, *J. Electron Spectrosc. Relat. Phenom.*, **8**, 129 (1976).
- (27) D. R. Penn, *J. Electron Spectrosc. Relat. Phenom.*, **9**, 29 (1976).
- (28) S. Evans and J. M. Thomas, *Proc. R. Soc. London, Ser. A*, **353**, 103 (1975).

RECEIVED for review July 8, 1977. Accepted January 19, 1978. This work was supported by funds from NSF Grant Numbers CHE 73-04882, CHE 76-04911 and US PHS Grant Number 19181.

## Simultaneous Determination of Reversible Potential and Rate Constant for a First-Order EC Reaction by Potential Dependent Chronoamperometry

Hung-Yuan Cheng and Richard L. McCreery\*

Department of Chemistry, The Ohio State University, Columbus, Ohio 43210

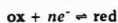
When potential step experiments are performed at potentials in the region of the reversible  $E_{1/2}$  for EC type systems, the current vs. time decay is dependent both on the applied potential and the rate constant for the homogeneous reaction subsequent to charge transfer. Provided charge transfer equilibrium is established rapidly relative to the chemical reaction, both the reversible  $E_{1/2}$  and the rate constant may be determined by applying curve fitting procedures to the current vs. time transient. A simplex optimization procedure was evaluated using the benzidine rearrangement as a test system, and the accuracies of the determinations of  $E_{1/2}$  and  $k$  compare well with other electrochemical techniques. The advantage of the present approach, in addition to the ability to determine  $E_{1/2}$  and  $k$  simultaneously, is a large expansion in experimental time frame over other methods. Experiments lasting many times longer than the homogeneous reaction half life can be used to evaluate  $E_{1/2}$  and  $k$ .

The study of homogeneous chemical reactions associated with oxidation reduction processes at electrode surfaces has

been a major endeavor of electrochemistry during the past several decades. In particular, the examination of the mechanisms and kinetics of the reactions of electrogenerated reactive species has been carried out with both electrochemical techniques and electrochemistry coupled with optical spectroscopy and other analytical probes. In general, three types of chemical information are desired in the study of homogeneous reactions accompanying charge transfer. First, the mechanism of the reaction of the oxidized or reduced form of the starting material may be determined with electrochemistry and ancillary analytical techniques. Second, the rate constant for reactions subsequent to charge transfer may be determined, along with pH and temperature effects and any other relevant kinetic information. Third, the reversible half wave potential,  $E_{1/2}$ , for the original redox system may be determined, an often nontrivial task given the distortion of the electrochemical response by the ensuing chemical reactions.

While mechanism diagnosis is an important and useful aspect of electrochemically initiated reactions, it is not the subject of the present work. Once the mechanism is known, the kinetics of the process may be examined by a variety of

techniques; discussed here for the so-called EC case, an irreversible pseudo first-order chemical reaction following reversible charge transfer:



The numerous methods for examining such systems are discussed elsewhere (1-3) but two techniques of relevance to this work are double step chronoamperometry (4) and cyclic voltammetry (5). In the double step approach, the reactive form (red) is generated electrochemically and, after allowing the irreversible reaction to proceed, the potential is switched to where the remaining reactive form is re-oxidized, and the rate constant is determined from the current resulting from oxidation of the reactive form. With cyclic voltammetry, the rate constant may be determined either from the ratio of the anodic to cathodic peak currents (5, 6) or the shift in peak potential caused by the homogeneous reaction (5, 7). For an accurate determination of the rate constant with these and other electrochemical techniques, the time frame of the experiment must be on the same order as the half-life of the homogeneous reaction. This constraint limits the methods to reactions slow enough to be accurately monitored with these techniques, i.e., reactions with half-lives of greater than a few hundred microseconds.

The problem of determining the reversible  $E_{1/2}^{\circ}$  for reactive systems has been addressed since at least the 1930's, when flowing streams were combined with potentiometric methods. Contemporary electrochemical approaches to the problem are based on two distinct methods. In the first, the time frame of the experiment is decreased to a point where the  $E_{1/2}^{\circ}$  measurement may be made before the ensuing homogeneous reaction distorts the electrochemical response. An example is a cyclic voltammetric experiment at sufficiently high scan rate so an EC type reaction does not distort the current-potential curve (5). The theory for ac polarographic determination of  $E_{1/2}^{\circ}$  of reactive systems has been developed and tested (8, 9) and has been used to determine the redox potentials of electrogenerated free radicals (10). Again, these methods rely on the experimental probe being significantly faster than the reaction subsequent to charge transfer. The second approach to determining  $E_{1/2}^{\circ}$  involves comparison of electrochemical data with theoretical curves for situations where the follow-up reaction has distorted the ideal response. The effect of EC reactions on voltammetric data has been calculated, (5) and a simple method for determining  $E_{1/2}^{\circ}$  and rate constants from these curves has been described (11). Because of the relative insensitivity of single-sweep voltammetric results to EC reactions, this method yielded rate constants accurate to about 20-50%, and the accuracy of the  $E_{1/2}^{\circ}$  value was not assessed.

Marcoux and O'Brien (3) have presented the theory for a method for determining EC rate constants termed "potential dependent chronoamperometry", and its experimental applicability has been verified in our laboratory (12). Consider a chronoamperometry experiment performed under potentiostatic conditions at potentials near  $E_{1/2}^{\circ}$ . The ox/red ratio is therefore held constant at the electrode surface, assuming charge transfer equilibrium. In the absence of a homogeneous reaction, the current will have the usual  $t^{-1/2}$  dependence, although its magnitude will depend upon the difference between the applied potential ( $E_{\text{app}}$ ) and  $E_{1/2}^{\circ}$ . If the reduced form undergoes an irreversible homogeneous reaction, however, additional current will flow to maintain a constant Nernstian ratio. The current decay for an EC case will not have a  $t^{-1/2}$  dependence, but will depend on both the applied potential and the rate constant for the homogeneous reaction. Given a knowledge of  $E_{1/2}^{\circ}$ , the homogeneous rate

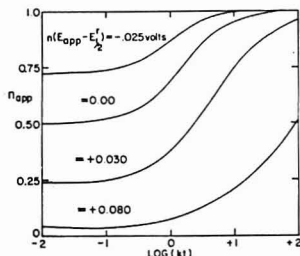


Figure 1. Working curves for potential dependent chronoamperometry derived by Marcoux and O'Brien (3).  $n_{\text{app}}$  is the current at a particular  $kt$  value divided by the diffusion limited current at the same  $kt$  value

constant can be determined from the current vs. time transient. Note that at potentials significantly negative of  $E_{1/2}^{\circ}$ , where the ox/red ratio is virtually zero at the electrode surface, the reaction has no effect on the current, and the current time transient has its usual diffusion limited  $t^{-1/2}$  decay.

Marcoux and O'Brien (3, 13) solved the appropriate equations for this technique for several homogeneous reaction mechanisms, and the working curves for the EC case are shown in Figure 1.  $n_{\text{app}}$  is the ratio of the current at a particular time and applied potential to the current for the diffusion limited case ( $E_{\text{app}} \ll E_{1/2}^{\circ}$ ). Marcoux showed that the shape of the working curves differed substantially for different follow-up mechanisms (13), and used the approach for mechanism diagnosis of a single system (14). During our experimental verification of the theory (12), it was apparent that a major advantage of potential dependent chronoamperometry is an expansion of the time frame of the experiment to values much greater than the half-life of the reaction. At potentials positive of  $E_{1/2}^{\circ}$ , only a fraction of the total electroactive species is in the reactive form (red), so the reaction proceeds at a much slower rate than if total conversion to red had occurred. For example, a reaction having a half-life of 9 ms was monitored with an experiment lasting 2 s, and a rate constant accurate to 10% was determined. At the final time of 2 s,  $n_{\text{app}}$  had increased to a value midway between its initial and diffusion controlled values, so the experiment could have lasted much longer, and still allowed an accurate estimate of  $k$ . This expansion in time frame is limited only by the requirement that the charge transfer process be fast relative to the homogeneous reaction, and the usual constraints on diffusion processes.

A severe limitation of this approach is the requirement for an accurate knowledge of  $E_{1/2}^{\circ}$ . As shown in our original report (12), errors of a few millivolts in  $E_{1/2}^{\circ}$  can cause 10-100% errors in the determination of  $k$ . For pseudo first-order reactions involving an attacking species,  $E_{1/2}^{\circ}$  may be accurately determined in the absence of the second reactant. But for cases where the homogeneous reaction cannot be suppressed,  $E_{1/2}^{\circ}$  must be determined by extrapolation of current time transients to short times, as suggested by Marcoux (3). This requirement for fast experiments eliminates the advantage of expansion of the experimental time frame.

In the present work, the requirement for an accurate knowledge of  $E_{1/2}^{\circ}$  is alleviated by simultaneous determination of  $E_{1/2}^{\circ}$  and  $k$  from potential dependent chronoamperometric data. It is apparent from Figure 1 that the shapes of the  $n_{\text{app}}$  vs.  $\log(kt)$  curves differ with applied potential. Therefore curve fitting of experimental data to the working curves by adjustment of  $k$  and  $n(E_{\text{app}} - E_{1/2}^{\circ})$  will allow determination of both  $k$  and  $E_{1/2}^{\circ}$  from a single current vs. time transient. As demonstrated below,  $k$  and  $E_{1/2}^{\circ}$  may be determined with

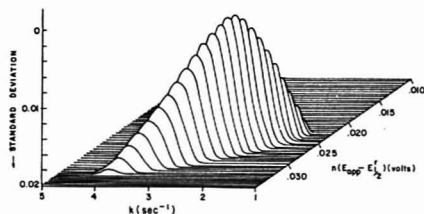


Figure 2. Standard deviation of experimental points vs. theoretical values as a function of  $k$  and  $n(E_{app} - E_{1/2}')$ . Note that standard deviation increases in the negative  $z$  direction, and that all values above 0.02 are considered equal to 0.02. Experimental data was acquired at an applied potential of 0.0891 V;  $\text{HClO}_4$  concentration equaled 1.037 M. Given a knowledge of  $n$  and  $E_{app}$ ,  $k$  and  $E_{1/2}'$  can be determined from the optimum values on the surface.

good accuracy, and the expansion in experimental time frame is retained.

### EXPERIMENTAL

The computer controlled potentiostat, cell, and hanging mercury drop electrode have been described previously (12) and were used without further modification. The test system employed was the familiar benzidine rearrangement, wherein the reduction product of the reversible azobenzene reduction undergoes an irreversible pseudo first-order rearrangement to benzidine (4). The reaction is second-order in hydronium ion, and the rate constant can be varied over a wide range by varying the acidity. The solvent was 50% ethanol in water, with perchloric acid as the electrolyte. Calculations and plotting were carried out on the same Hewlett-Packard 21MX computer used for data acquisition.

### RESULTS AND DISCUSSION

The feasibility of using a curve fitting procedure to extract both  $E_{1/2}'$  and  $k$  from potential dependent chronoamperometric data was established by constructing the plot shown in Figure 2. At a particular applied potential, the current vs. time transient was recorded and converted to  $n_{app}$  vs. time by dividing by the diffusion limited current. Then for all combinations of  $k$  and  $n(E_{app} - E_{1/2}')$  within appropriate ranges, the theoretical  $n_{app}$  vs. time curves were calculated from the equation derived by Marcoux (Equation 1).

$$n_{app} = \frac{R}{1-R^2} \left\{ e^{-kt} - R + \frac{2kte^{-kt}}{(1-R^2)} \sum_{n=0}^{\infty} \frac{2^n}{(2n+1)!} \left( \frac{kt}{1-R^2} \right)^n - \frac{2Rkt}{(1-R^2)} \sum_{n=0}^{\infty} \frac{2^n}{(2n+1)!} \left( \frac{R^2 kt}{1-R^2} \right)^n \right\} \quad (1)$$

$$R = \exp \left[ \frac{nF}{RT} (E_{app} - E_{1/2}') \right]$$

For each  $k$  and  $n(E_{app} - E_{1/2}')$  pair, the standard deviation of the experimental points from the theoretical points was calculated according to Equation 2

$$\text{standard deviation} = \left[ \frac{\sum [n_{app}(\text{theo}) - n_{app}(\text{exp})]^2}{N_T - 1} \right]^{1/2} \quad (2)$$

where  $N_T$  ( $10 < N_T < 50$ ) points were taken along the  $n_{app}$  vs. time curves. The standard deviation is plotted vs.  $k$  and  $n(E_{app} - E_{1/2}')$  in Figure 2. Notice that the standard deviation increases in the negative  $z$  direction, for purposes of clarity. In addition, standard deviations greater than 0.02 are all considered equal to 0.02, to provide an easily visualized background for the surface.

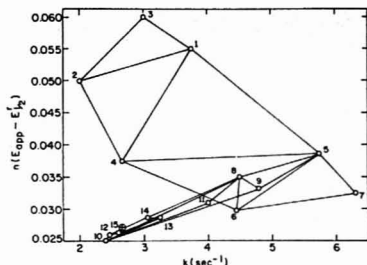


Figure 3. Progress of modified simplex optimization program for the same experimental data used in Figure 2. Cross indicates optimum value reached after 27 simplex steps, where the standard deviation of  $n_{app}$  equaled 0.004. Note that simplex steps 16-26 are not shown for purposes of clarity.

Table I. Rate Constants for the Benzidine Rearrangement

$\text{HClO}_4$ Concn, M	$E_{app}$ , V	$E_{1/2}'$ , V <sup>a</sup>	$k$ , s <sup>-1a</sup>	$E_{1/2}'$ , V <sup>b</sup>	$k$ , s <sup>-1c</sup>
1.037	0.0696	0.0754	2.77	0.0754	2.51
	0.0891	0.0756	2.63		
1.414	0.0915	0.0833	9.29	0.0845	8.60
	0.0964	0.0836	9.18		
1.885	0.1050	0.1017	30.4	0.1020	28.5
	0.1099	0.1013	29.6		
	0.1148	0.1013	29.1		
2.395	0.1295	0.1147	57.0	0.1134	73.0
	0.1440	0.1125	82.5		
	0.1599	0.1127	80.5		

<sup>a</sup> Determined from simplex approach. <sup>b</sup> Determined by extrapolation of current/time curves to short times.

<sup>c</sup> Determined by conventional double-step chronoamperometry.

Figure 2 indicates a single optimum value for  $k$  and  $n(E_{app} - E_{1/2}')$ , with a standard deviation of 0.004, and also provides an indication of the accuracy of the method. The range of  $k$  values along the  $x$  axis is large, implying that  $k$  may not be determined with great accuracy; in contrast, the value  $n(E_{app} - E_{1/2}')$  and therefore  $E_{1/2}'$  may be determined more accurately, since the range of values along the potential axis is small. While both  $E_{1/2}'$  and  $k$  could be determined by visual inspection of Figure 2, a more sophisticated approach provides a faster and more accurate means.

The modified simplex optimization procedure described by others (15-17) was used to analyze the same experimental data used to construct Figure 2. The method starts with three arbitrarily chosen  $n(E_{app} - E_{1/2}')$  and  $k$  pairs, then adjusts these values to minimize the standard deviation as calculated from Equation 2. Expansion and contraction factors for the simplex program were arbitrarily chosen at 2.0 and 0.5, respectively.

The progress of such an analysis is shown in Figure 3, for an acid concentration of 1.037 M and  $E_{app}$  of 0.0891 V vs. SCE. After 27 simplex steps, optimum values of  $k = 2.63 \text{ s}^{-1}$  and  $n(E_{app} - E_{1/2}') = 0.0271 \text{ V}$  were obtained, with the final standard deviation of  $n_{app}$  being 0.004. These results yield a value for  $E_{1/2}'$  of 0.0756 V vs. SCE.

The results of similar simultaneous determinations of  $E_{1/2}'$  and  $k$  for several acidities and applied potentials are shown in Table I. The simplex determinations of  $k$  are compared with values from conventional double-step methods. The accuracy of the  $E_{1/2}'$  values derived from the simplex analysis was assessed by independently determining  $E_{1/2}'$  as recommended by Marcoux. The current vs. time transients were extrapolated to short times at a series of potentials, and  $E_{1/2}'$

was determined from the Nernst equation, as described elsewhere (12). This extrapolation method becomes much less accurate as the rate constant increases, and the aberrations of fast electrochemical experiments appear. The approximately 10% disagreement in  $k$  between the double-step and simplex derived results is comparable to the error observed in the double step approach.

It is apparent from Table I that the values of  $k$  and  $E_{1/2}'$  compare favorably with those from other methods in the reaction considered here. The accuracy of  $k$  (~10%) is substantially better than that derived from line shape analysis of voltammograms (20–50%), (11), while the  $E_{1/2}'$  values agree with the extrapolated values to better than 1 mV. While this approach is an accurate method to determine  $k$  and  $E_{1/2}'$  for EC reactions with reversible charge transfer, many other methods exist to determine these parameters individually. The only advantage of the present method as discussed thus far is the ability to determine both values from a single experiment.

When examining fast reactions, however, an additional advantage may be derived from the expansion of the time frame of the experiment relative to the half-life of the reaction. For example, the last two determinations of  $k$  and  $E_{1/2}'$  at the highest acidity were obtained from data acquired in the time range of 0.18 to 1.0 s. Since the reaction half-life calculated from the rate constant is 9 ms, data acquisition did not even begin until after 20 reaction half-lives had elapsed. This extension of time frame is a direct consequence of the high value of  $\alpha_{\text{red}}$  at potentials positive of  $E_{1/2}'$ , such that a relatively small fraction of starting material is in the reactive form (red). It was observed empirically that better accuracy for fast reactions was obtained if the  $n_{\text{app}}$  points chosen for analysis were equally spaced along the  $\log(k/t)$  axis.

The accuracy of both the  $E_{1/2}'$  and  $k$  values is poorer for very fast reactions, but may be improved substantially by averaging determinations at several different potentials, as is apparent from the data in 2.395 M acid. Monitoring of faster reactions was not attempted here, because the azobenzene reduction process is accompanied by adsorption which interferes with very fast experiments. The theoretical limit on the maximum rate constants which may be determined is the requirement that the Nernstian ratio be established rapidly relative to the homogeneous reactions. Extensions to potentials much more positive than those used here is possible, although a sacrifice in accuracy will result. Reasonable estimates for the upper limit of the expansion of experimental time frame, i.e. the ratio of the meaningful duration of the experiment to the nominal half-life of the reaction, are  $10^4$  if  $E_{1/2}'$  is known and  $10^2$  if it is not.

The present method is very similar in concept to the line shape analysis of single sweep voltammetric data presented by Mohammed (11). Potential dependent chronoamperometric data is much more sensitive to ensuing reactions than voltammetric data, however, so the present method allows more accurate determination of  $k$ . The expansion in time frame discussed above negates the need for fast voltammetric sweep rates to monitor fast reactions. In addition, the

chronoamperometry experiment is not accompanied by the constant charging current associated with linear sweep voltammetry, although charging current can be observed for potentiostatic experiments in certain circumstances (18). The ac polarographic approach of Smith, while experimentally more complex, appears an excellent technique for determining  $E_{1/2}'$  of electrochemically reversible systems with a reactive component (8). The ac approach is conceptually distinct from potential dependent chronoamperometry in that the time frame of the experiment is decreased to values below the half-life of the reaction. Second harmonic ac polarography was shown theoretically to allow determination of  $E_{1/2}'$  for couples involving follow-up reactions with half-lives in the submillisecond range (9). The method presented here is unlikely to produce a more accurate value of  $E_{1/2}'$ , but will provide the additional value of  $k$ , and allow the use of the comparatively simple chronoamperometric technique.

## CONCLUSION

With careful curve fitting procedures, potential dependent chronoamperometry allows determination of both  $E_{1/2}'$  and  $k$  for a first-order EC reaction from a single potential step experiment. For reactions with rate constants below  $30 \text{ s}^{-1}$ , the accuracy of the method compares well with that of other techniques such as double-step chronoamperometry.  $E_{1/2}'$  and  $k$  for much faster reactions may be determined, with some sacrifice in accuracy. By proper choice of the applied potential, the experimental time frame of the method may be extended to values many times longer than the half-life of the homogeneous reaction. When both thermodynamic and kinetic information are desired from experiments on EC type reactions, potential dependent chronoamperometry is a viable approach when compared to existing methods.

## ACKNOWLEDGMENT

The authors thank Robert Szentirmay for assistance with constructing Figure 2.

## LITERATURE CITED

- (1) R. N. Adams, "Electrochemistry at Solid Electrodes", Marcel Dekker, New York, N.Y., 1969.
- (2) Z. Galus, "Fundamentals of Electrochemical Analysis", John Wiley, New York, N.Y., 1976.
- (3) L. Marcoux and T. J. P. O'Brien, *J. Phys. Chem.*, **76**, 1666 (1972).
- (4) W. M. Schwarz and I. Shain, *J. Phys. Chem.*, **69**, 30 (1965).
- (5) R. S. Nicholson and I. Shain, *Anal. Chem.*, **38**, 706 (1964).
- (6) S. P. Perone and W. J. Kretlow, *Anal. Chem.*, **38**, 1760 (1966).
- (7) M. Mohammad, *Anal. Chem.*, **47**, 958 (1975).
- (8) T. G. McCord and D. E. Smith, *Anal. Chem.*, **41**, 1423 (1969).
- (9) A. M. Bond and D. E. Smith, *Anal. Chem.*, **46**, 1946 (1974).
- (10) M. R. Wasielewski and R. Breslow, *J. Am. Chem. Soc.*, **98**, 4222 (1976).
- (11) M. Mohammad, *Anal. Chem.*, **49**, 60 (1977).
- (12) H. Y. Cheng and R. L. McCreery, *J. Electroanal. Chem.*, **85**, 361 (1977).
- (13) L. Marcoux, *J. Phys. Chem.*, **76**, 3254 (1972).
- (14) L. Marcoux and R. N. Adams, *J. Electroanal. Chem.*, **49**, 111 (1974).
- (15) M. K. Harsley, R. L. Scott, T. H. Ridgway, and C. N. Reilly, *Anal. Chem.*, **50**, 116 (1978).
- (16) S. N. Deming and S. L. Morgan, *Anal. Chem.*, **45**, 278A (1973).
- (17) S. L. Morgan and S. N. Deming, *Anal. Chem.*, **46**, 1170 (1974).
- (18) S. S. Fraton, Jr. and S. P. Perone, *Anal. Chem.*, **48**, 287 (1976).

RECEIVED November 10, 1977. Accepted January 19, 1978. This work was supported by NIMH through grant MH 28412-01.



# Volatilization of Arsenic(III, V), Antimony(III, V), and Selenium(IV, VI) from Mixtures of Hydrogen Fluoride and Perchloric Acid Solution: Application to Silicate Analysis

Sixto Jabo

Swiss Federal Institute for Reactor Research, 5303 Würenlingen, Switzerland

The possible volatilization of As(III, V), Sb(III, V), and Se(IV, VI) from mixtures of  $\text{HClO}_4/\text{HF}$  is investigated. It is shown that there are no losses with Sb and Se irrespective of the initial oxidation state, and with As(V). As(III) is partially or totally lost by volatilization; this can be avoided by oxidizing As with  $\text{HClO}_4$ . The oxidation state of all three elements after the  $\text{HClO}_4/\text{HF}$  treatment is determined. These results lead to a recommended procedure for the dissolution of siliceous materials in which As, Sb, or Se are to be determined.

Silicates are often dissolved for analytical purposes by a mixture of HF and  $\text{HClO}_4$  (1, 2). However, it is not clear from the literature (3, 4) if in the course of this operation, which comprises partial or total evaporation of the solution, there are losses of traces of As, Sb, and Se. The usefulness of some existing literature data is restricted, because (a) the oxidation state and the weight of the elements used in an experiment are not stated (5), (b) the possibility of absorption by platinum vessels—which was demonstrated for Se (6)—is often not taken into account (5, 7, 8), (c) it is often not possible to decide if the observed losses are really due to volatilization and not to some other step in the procedure used.

The volatilization of Se from different solutions was studied by Bock and Jacob (9), but the system  $\text{HF}/\text{HClO}_4$  has received little attention. The determination of As after dissolution of silicates with HF,  $\text{HClO}_4$ ,  $\text{HNO}_3$ , and  $\text{KMnO}_4$  was described by Terashima (10), and after vapor phase attack by HF and  $\text{HNO}_3$  by Feldman (11).

It was the purpose of the present investigation to establish reliable data on the volatilization of As, Sb, and Se from a mixture of HF and  $\text{HClO}_4$  under conditions that are representative for the dissolution of silicates. The elements were studied in the range of 1  $\mu\text{g}$  to 1 mg, and great care was taken to use them in well defined oxidation states. The experiments were done in the presence of silicates (as granite) and without silicates. Losses were determined by the radiotracer method, and the oxidation state was determined again after the experiment.

## EXPERIMENTAL

**Reagents and Apparatus.** The acids used were  $\text{HNO}_3$  (65%),  $\text{HClO}_4$  (60%), and HF (40%). The solution of zinc bis(dithiodithiocarbamate) ( $\text{Zn}(\text{DDC})_2$ ) was  $1.7 \times 10^{-3}$  M in  $\text{CHCl}_3$  (12). The grain size of the granite used was  $<180 \mu\text{m}$ .

All the evaporations were made in 150-mL Teflon beakers. A glass recovery vessel (250 mL) equipped with a finger fitting into the borehole of the NaI(Tl) crystal of a  $\gamma$ -spectrometer was used for the recovery measurements (Figure 1).

The liquid-liquid extractions were made in 250-mL separatory funnels similar to the recovery vessel (Figure 1), except that they had a stopcock at the end of the finger. A shaking machine with a frequency of 6  $\text{s}^{-1}$  and an amplitude of 6 cm was employed for the extractions.

**Preparation of the Radioactive Tracers.** Solutions of  $^{76}\text{As}$ ,  $^{121,123}\text{Sb}$ , and  $^{76}\text{Se}$  were prepared from neutron irradiated high

purity metals (10–20 mg) by the following procedures.

**As(III), Sb(III).** Dissolution with hot concentrated (95–97%)  $\text{H}_2\text{SO}_4$  and dilution with  $\text{H}_2\text{O}$  to an acidity of 4 M.

**Se(IV).** Dissolution with hot  $\text{HNO}_3$ , evaporation at 125  $^\circ\text{C}$ , and redissolution with 0.1 M  $\text{HNO}_3$ .

**As(V), Se(VI).** Dissolution with hot  $\text{HNO}_3$ , evaporation at 125  $^\circ\text{C}$ , redissolution with 4 mL 2 M KOH. The resulting solution is boiled for 5 min with 2 mL  $\text{NaClO}$  (13%) and taken to dryness after the addition of 2 mL  $\text{H}_2\text{O}_2$  (30%). The residue is taken up by  $\text{H}_2\text{O}$ .

**Sb(V).** Dissolution with  $\text{HNO}_3$  (100%), evaporation (water bath) and redissolution with 4 mL 2 M KOH and 2 mL  $\text{H}_2\text{O}_2$  (30%). The resulting solution is boiled for 5 min and taken to dryness at 125  $^\circ\text{C}$ . The residue is taken up by  $\text{H}_2\text{O}$ .

The stock solutions resulting from the above procedures had a metal concentration of 1 mg/mL. They were used directly or diluted 10- or 100-fold while keeping their acidity constant (As(III), Sb(III), and Se(IV)) or by dilution with water (As(V), Sb(V), and Se(VI)).

**Preparation of Carrier Solutions.** Carrier solutions containing a metal concentration of 5 mg/mL were prepared by the following procedures.

**As(III).**  $\text{As}_2\text{O}_3$  was dissolved with warm NaOH and brought to pH 1 with  $\text{HClO}_4$ .

**As(V).** 3  $\text{As}_2\text{O}_3 \cdot 5 \text{H}_2\text{O}$  was dissolved with 0.1 M NaOH.

**Sb(V).**  $\text{K}(\text{Sb}(\text{OH})_6)$  was dissolved with 0.1 M KOH.

**Se(IV).**  $\text{H}_2\text{SeO}_3$  was dissolved with 0.1 M  $\text{HNO}_3$ .

**Sb(III) and Se(VI)** were prepared by the same method as the tracer solutions.

**Checking of the Oxidation States.** The purity of the tracer solutions with respect to the specified oxidation state was checked by extraction with  $\text{Zn}(\text{DDC})_2$ , taking advantage of the fact that As(III), Sb(III), and Se(IV) are quantitatively extracted under the conditions used, whereas As(V), Sb(V), and Se(VI) do not extract (13). Aliquots of the solutions to be tested were made up to 100 mL with 0.5 M  $\text{H}_2\text{SO}_4$  and extracted twice with 30 mL  $\text{Zn}(\text{DDC})_2$  for 2 min; the activity of aliquots of the organic and the aqueous phases was measured with the  $\gamma$ -spectrometer. It was found that the purity of the As(III) tracer solution was  $\geq 99.5\%$  and that of all other tracer solutions  $\geq 99.9\%$ .

The solutions resulting from the volatilization experiments were diluted with water to 100 mL and extracted with  $\text{Zn}(\text{DDC})_2$  as in the case of the tracer solutions. The acidity of these solutions was 0.2–0.4 M in  $\text{HClO}_4$ .

**Volatilization Experiments. Procedure A.** One gram of granite, 100  $\mu\text{L}$  of tracer solution, 200  $\mu\text{L}$  of carrier solution (only in the experiments with 1 mg of the element), 500  $\mu\text{L}$   $\text{H}_2\text{O}$ , 10 mL  $\text{HClO}_4$ , and 10 mL HF were placed in this order into the Teflon beaker. The beaker was placed on a hot plate, whose surface temperature was raised from 150 to 225  $^\circ\text{C}$  in 60–90 min and kept at this temperature for 10 to 15 min. The beaker was removed and cooled; the final solution was 2 to 3 mL.

**Procedure B** is identical to procedure A, but after evaporation to 2–3 mL, the solution was diluted with 5 mL  $\text{HClO}_4$  and 10 mL HF and again heated and evaporated to 2–3 mL.

**Procedure C** is identical to procedure B except that the first addition of HF was replaced by 10 mL  $\text{HNO}_3$ .

The final volume in all three procedures was 2 to 3 mL, to which 20 mL  $\text{H}_2\text{O}$  was added. The beaker was covered with a watch glass and the solution boiled for 10 min, then cooled; in some cases it contained a slight precipitate. The solution with the precipitate

Table I. Recoveries in Volatilization Experiments<sup>a</sup>

Ion added	Procedure	Granite	Weight of the ion added, $\mu\text{g}$			
			1000	100	10	1
As (III)	A	no	0.8 $\pm$ 0.6 (4)	0.3 $\pm$ 0.1 (4)	0.2 $\pm$ 0.1 (4)	0.6 $\pm$ 0.03 (4)
	A	yes	16.0 $\pm$ 2.2 (4)	23.6 $\pm$ 1.2 (4)	63.6 $\pm$ 5.9 (4)	72.5 $\pm$ 7.3 (4)
	C	no	100.6 $\pm$ 1.1 (4)	N.I. <sup>b</sup>	100.3 $\pm$ 1.0 (4)	101.1 $\pm$ 1.1 (4)
	C	yes	100.7 $\pm$ 1.0 (4)	102.6 $\pm$ 0.7 (4)	101.5 $\pm$ 1.9 (4)	101.5 $\pm$ 2.1 (4)
As (V)	A	no	97.7 $\pm$ 4.4 (4)	100.7 $\pm$ 2.1 (4)	101.8 $\pm$ 2.2 (3)	101.1 $\pm$ 0.8 (4)
	A	yes	101.4 $\pm$ 1.6 (7)	101.5 $\pm$ 1.7 (7)	103.0 $\pm$ 1.4 (3)	99.6 $\pm$ 0.9 (4)
	B	no	99.5 $\pm$ 1.1 (4)	101.0 $\pm$ 2.0 (4)	101.6 $\pm$ 0.8 (4)	100.9 $\pm$ 0.4 (4)
	B	yes	101.5 $\pm$ 1.8 (4)	100.0 $\pm$ 2.0 (4)	99.2 $\pm$ 1.0 (4)	100.0 $\pm$ 0.9 (4)
Sb (III)	A	no	101.1 $\pm$ 1.5 (4)	101.8 $\pm$ 0.7 (3)	103.4 $\pm$ 2.2 (3)	102.3 $\pm$ 1.2 (3)
	A	yes	102.0 $\pm$ 0.9 (3)	101.4 $\pm$ 0.8 (3)	101.4 $\pm$ 0.4 (3)	102.5 $\pm$ 1.8 (3)
Sb (V)	A	no	102.1 $\pm$ 2.6 (3)	100.2 $\pm$ 1.0 (3)	102.2 $\pm$ 0.5 (4)	102.0 $\pm$ 1.3 (4)
	A	yes	98.0 $\pm$ 4.7 (3)	101.1 $\pm$ 1.0 (3)	102.0 $\pm$ 0.6 (4)	101.4 $\pm$ 0.2 (4)
	B	no	101.4 $\pm$ 0.9 (4)	101.8 $\pm$ 0.8 (4)	102.4 $\pm$ 1.0 (4)	100.8 $\pm$ 0.7 (4)
	B	yes	100.8 $\pm$ 0.8 (4)	100.6 $\pm$ 0.6 (4)	101.3 $\pm$ 0.5 (4)	101.6 $\pm$ 0.8 (4)
Se (IV)	A	no	100.6 $\pm$ 1.8 (3)	101.0 $\pm$ 2.0 (3)	101.5 $\pm$ 0.4 (3)	102.0 $\pm$ 2.3 (3)
	A	yes	100.0 $\pm$ 0.5 (4)	101.0 $\pm$ 1.5 (15)	99.7 $\pm$ 0.6 (4)	99.3 $\pm$ 1.7 (13)
	B	no	100.6 $\pm$ 1.6 (4)	N.I.	N.I.	99.0 $\pm$ 0.6 (4)
	B	yes	100.5 $\pm$ 0.9 (6)	99.7 $\pm$ 0.8 (3)	99.0 $\pm$ 0.8 (3)	98.4 $\pm$ 2.7 (7)
Se (VI)	A	no	100.3 $\pm$ 1.0 (4)	100.0 $\pm$ 1.1 (3)	N.I.	98.4 $\pm$ 1.2 (3)
	A	yes	100.0 $\pm$ 1.2 (4)	100.2 $\pm$ 0.9 (4)	N.I.	100.8 $\pm$ 1.7 (4)
	B	no	100.6 $\pm$ 0.9 (4)	100.1 $\pm$ 0.9 (4)	N.I.	99.2 $\pm$ 1.1 (4)
	B	yes	99.9 $\pm$ 0.5 (4)	100.7 $\pm$ 0.7 (6)	N.I.	100.3 $\pm$ 1.4 (4)

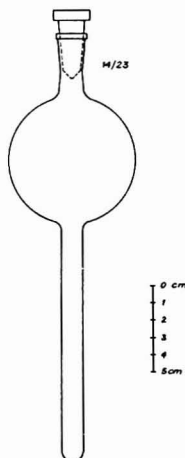
<sup>a</sup> Recovery is given as percentage; also indicated is the standard deviation. The number of replicates is given in brackets.<sup>b</sup> N.I. = Not investigated.

Figure 1. Recovery vessel

was transferred to the recovery vessel through a 32-mm Whatman GF/B filter. The filter was washed with water to get a total volume of about 40 mL.

**Determination of Losses.** The losses occurring during the volatilization experiments were evaluated by the determination of the percentage  $R$  of the activity that survived the experiments. The following procedure was used: The activity ( $A_1$ ) of the filtered solution from above was measured in the NaI borehole detector. Then another 100  $\mu\text{L}$  of tracer solution was added to the system and the activity determined again ( $A_2$ ). The recovery  $R$  is then given by  $R = 100 \times A_1 / (A_2 - A_1)$ .

The accuracy of this procedure was checked by separate experiments (10 for each isotope used), in which the isotopes (100  $\mu\text{L}$ ) were added to about 40 mL of water and measured directly. The resulting mean values of  $R$  were found to be in the interval

100.2–100.8% with a standard deviation of 1 to 2%, which is in accord with the standard deviation expected from counting statistics.

## RESULTS

**Solid Residue after Dissolution.** While dissolution of granite according to method B (with two additions of HF) always yielded a clear solution, methods A and C (with one addition of HF only) sometimes gave solutions containing a fine white residue, the weight of which amounted up to 3% of the granite used. This residue was found to be practically pure  $\text{SiO}_2$  and to retain only very small quantities of the added tracers ( $\leq 0.5\%$  for 10  $\mu\text{g}$  Sb(III),  $< 0.1\%$  in all other cases).

**Losses Due to Volatilization.** The recoveries found in the volatilization experiments are given in Table I. The following can be seen.

*As(V), Sb(III), Sb(V), Se(IV), and Se(VI).* These ions show no losses due to volatilization, irrespective of the quantity of metal used (1  $\mu\text{g}$  to 1 mg), of the method used for dissolution (A or B) and of the presence or absence of granite. These results are in contrast to other findings (3–5) and invalidate the reasonings advanced there for the explanation of apparent losses. It is interesting to note that the final temperature used here (225 °C) exceeds the boiling point of all binary fluorides involved except  $\text{SbF}_3$  (14).

*As(III)* is almost quantitatively lost if method A is used in the absence of granite. In the presence of granite, losses are still substantial and they increase with the amount of As present in the system. With method C, total recovery is obtained.

**Oxidation State after Dissolution.** In the final solution, As and Sb were always found in the (V) state irrespective of the oxidation state and the weight of the element added, indicating complete oxidation during dissolution.

If Se was originally added as Se(IV), more than 95% retained this oxidation state in the experiments with or without granite, except the experiments made with 1  $\mu\text{g}$  of Se by method B in the presence of granite, where 20 to 90% were found as Se(VI). If Se was added as Se(VI), more than 95% was found in the same oxidation state in the experiments

without granite. In the presence of granite, only 20–90% was found as Se(VI). It therefore seems that the oxidation state of Se varies in an unpredictable manner.

### DISCUSSION

Se. Neither dissolution method yields a well defined oxidation state. Since recovery of Se was quantitative in all cases, it seems that neither Se(IV) nor Se(VI) is volatile under the specified conditions. However, it must be strongly stressed that taking the solutions to complete dryness has to be avoided, since we found losses of Se in preliminary experiments without granite. This is in accord with the findings by Bock and Jacob (9) and is probably due to volatilization of oxides of selenium. It might be added that the use of Teflon beakers is an advantage here since the formation of dry spots of residue next to a small volume of liquid is greatly reduced if compared to platinum vessels.

Sb. Since Sb is always found as Sb(V) after dissolution, even if it has been added as Sb(III), it is concluded that Sb(III) is oxidized by  $\text{HClO}_4$ . The recovery of Sb is always quantitative, which either means that neither Sb(III) nor Sb(V) are volatilized, or—if Sb(III) is volatile—that the oxidation of Sb(III) to the nonvolatile Sb(V) is much faster than the volatilization of Sb.

As. If As is added as As(V), it retains this oxidation state and shows quantitative recovery, indicating that As(V) is not volatile under the conditions used. However, with As(III), there are substantial losses if the starting solution contains HF, indicating that volatilization of As(III) is much more rapid than its oxidation by  $\text{HClO}_4$  to the nonvolatile As(V). Since losses are smaller in solutions containing granite than in solutions without granite, it is suspected that the granite used contained very small amounts of a substance that oxidizes As(III) to As(V); this explanation is sustained by the observation that losses are smaller when only very small quantities of As(III) are used.

Advantage could be taken from the fact that As(III) can be volatilized with HF—probably as  $\text{AsF}_3$ —but not As(V); a selective volatilization of As(III) seems to be possible by attacking siliceous materials with HF vapor in a nonoxidizing atmosphere. Such a procedure would be valuable, since there seems to be no reliable method for the separate determination of As(III) and As(V) in silicates (15).

**Recommended Procedure for Dissolution of Siliceous Materials.** As has been shown, dissolution methods A and B yield quantitative recoveries of Sb and Se, whereas for As only method C works satisfactory. Method C is therefore recommended for all three elements; it comprises the following steps.

(1) To 1 g of the sample 10 mL  $\text{HNO}_3$  and 10 mL  $\text{HClO}_4$  are placed in a Teflon beaker. The beaker is placed on a hot plate, whose surface temperature is raised from 150 to 225 °C in 60–90 min and kept at this temperature until the volume is reduced to 2 to 3 mL. The beaker is then removed and cooled.

(2) Add 5 mL  $\text{HClO}_4$  and 10 mL HF, and repeat the temperature cycle used in step 1, again keeping the final volume to 2 to 3 mL. Add 20 mL water, cover with a watch glass, and boil for 10 min; if there is a precipitate, filter through a Whatman GF/B filter. The solution will contain As and Sb as (V), Se as (IV) and (VI).

Step 1 in the recommended procedure allows for the destruction of any organic material that might be present in samples of soil or sediments. It has been shown repeatedly that the treatment by  $\text{HNO}_3/\text{HClO}_4$  entails no losses of As, Sb, or Se (16, 17) and that most organic products are destroyed (18). Concurrently this treatment oxidizes the sulfides and the chalcogenides, which are a likely source of As, Sb, and Se (19).

Step 2 attacks the silicates and removes the silicium from the system as  $\text{SiF}_4$ . If the attack of the silicate matrix sets free any As, Sb, or Se, there is no danger of subsequent volatilization loss (see Table I, Methods A and B) with the possible exception of As(III). This last point could not be covered by the present experiments, in which the elements tested were always added separately and not as a component of the granite matrix. Pending further experiments, the addition of an oxidizing agent like  $\text{KMnO}_4$  in this step (10) will oxidize As(III) to As(V) and thus prevent its volatilization.

Boiling the final solution of  $\text{HClO}_4$  after dilution with water releases any As, Sb, or Se that was sorbed on the postprecipitated  $\text{SiO}_2$  during the last strong dehydrating step. Concurrently, rehydrating of Sb(V)-oxides will bring this ion in a reactive form.

### LITERATURE CITED

- (1) F. J. Langmyhr and S. Sveen, *Anal. Chim. Acta*, **32**, 1 (1965).
- (2) F. J. Langmyhr, *Anal. Chim. Acta*, **39**, 516 (1967).
- (3) J. Dolezal, P. Povondra, and Z. Sulzec, "Decomposition Techniques in Inorganic Analysis", Int. Books Ltd.-American Elsevier Publishing Company Inc., London-New York, 1968.
- (4) R. Bock, "Aufschlussmethoden der anorganischen und organischen Chemie", Verlag Chemie, Weinheim/Bergstr., 1972.
- (5) F. W. Chapman, Jr., G. W. Martin, and J. Tyree, Jr., *Anal. Chem.*, **21**, 700 (1949).
- (6) M. M. Schneple, *J. Res. U.S. Geol. Survey*, **2**, 631 (1974).
- (7) I. I. Nazarenko and I. V. Kislova, *Ind. Lab.*, (Engl. transl.) **37**, 525 (1971).
- (8) G. Tölg, *Fresenius' Z. Anal. Chem.*, **190**, 161 (1962).
- (9) R. Bock and D. Jacob, *Fresenius' Z. Anal. Chem.*, **200**, 81 (1964).
- (10) S. Terashima, *Anal. Chim. Acta*, **86**, 43 (1976).
- (11) C. Feldman, *Anal. Chem.*, **49**, 825 (1977).
- (12) A. Wittenbach and S. Bajo, *Anal. Chem.*, **47**, 1613 (1975).
- (13) S. Bajo and A. Wittenbach, unpublished results.
- (14) Reference 4, p. 45.
- (15) H. Onishi, Arsenic, in "Handbook of Geochemistry", Vol. II/3, K. H. Wedepohl, Ed., Springer Verlag, Berlin-Heidelberg-New York, 1972.
- (16) T. T. Gorsuch, "The destruction of organic matter", Pergamon Press, Oxford, 1970.
- (17) B. Bistberg, "Studies on Selenium in Plant and Soils", Danish Atomic Energy Commission, Risø Report Nr. 200, 1972.
- (18) G. D. Martinie and A. A. Schitt, *Anal. Chem.*, **48**, 70 (1976).
- (19) L. Ahrens, "Distribution of the Elements in our Planet", McGraw-Hill, New York, N.Y., 1965.

RECEIVED for review November 7, 1977. Accepted January 27, 1978.

# Comparison of Three Techniques for the Measurement of Depleted Uranium in Soils

Ernest S. Gladney,\* Walter K. Hensley, and Michael M. Minor

University of California, Los Alamos Scientific Laboratory, P. O. Box 1663, Los Alamos, New Mexico 87545

**Instrumental Epithermal Neutron Activation Analysis** has been shown to be an effective method for measuring depleted uranium in environmental samples. Good agreement was obtained with total U determinations by fluorometric technique, but poor correlation was observed with analyses done by delayed neutron assay technique. The ratio of U concentrations determined by delayed neutron assay and epithermal activation may be used to indicate isotopic deviation from natural abundance.

Rapid analysis for uranium in soils and water has recently become a more important and more sophisticated business. The call for numerous new reactors to help relieve the energy shortage has focused on the need for vast quantities of U to feed the new facilities. Several hydrogeochemical uranium search programs are underway worldwide to locate surface and subsurface ore bodies (1).

A concern within the nuclear community is the clean-up of presently contaminated areas. Depleted uranium ( $^{235}\text{U}/^{238}\text{U} < 0.0072$ ), as well as other radioactive materials, is of interest in the clean-up activities. Two techniques are presently widely used for measuring U in these programs: delayed neutron assay (DNA) and fluorescence analysis (FA). Both of these techniques have certain limitations when dealing with the unusual nature of depleted uranium (DU). Fluorescence analysis requires the sample to be in solution. It is also very sensitive to quenching interferences and to the exact conditions during pellet fusion, and may exhibit poor precision on occasion (2). The delayed neutron assay technique operates on the principle of a fixed U isotopic ratio ( $^{235}\text{U}/^{238}\text{U}$ ) because  $^{238}\text{U}$  does not fission with thermal neutrons. If the ratio departs from 0.0072 (crustal abundance), large errors in determination of total U can be made. Direct measurement of ppm levels of  $^{238}\text{U}$  in soil has been reported (3) but this procedure requires long counting times.

Depleted uranium comes up in another context, that of environmental studies of its movement in contaminated areas.

Table I. U Concentrations by Three Techniques (ppm unless stated otherwise)

Sample No.	IENNA	Delayed neutron	Fluorescence	IENNA/fluorescence
1651	1.45%	5050	1.40%	1.04
1652	1.88%	6130	2.15%	0.87
1660	1500	654	1680	0.89
1707	3.2	3.9	4.5	0.71
1708	62	59	63	0.98
1731	4600	2180	5500	0.84
1733	2200	774	2400	0.92
1734	3100	1050	3900	0.79
1739	600	375	620	0.97
1740	1440	712	1700	0.85
1747	3.4	3.7	2.6	1.31
1748	29	20	23	1.27
1771	3400	1480	3500	0.97
1772	5300	2110	6800	0.78
1773	2000	678	2000	1.00
1774	2200	726	2200	1.00
1779	440	255	500	0.88
1780	1000	484	1400	0.71
1787	2.2	4.0	2.7	0.81
1788	26	19	22	1.18
1811	3100	1280	3000	1.03
1812	3600	1200	4200	0.86
1813	2700	930	3300	0.82
1814	2900	790	2600	1.11
1819	330	225	360	0.92
1827	1.8	3.9	3.1	0.58
1828	9.0	7.5	6.6	1.36
1851	2200	866	2000	1.10
1852	8200	5350	8850	0.93
1853	2200	823	2400	0.92
1854	2200	701	2000	1.10
1867	1.1	3.7	2.4	0.46
1868	1.1	6.1	1.0	1.10
				Av 0.94
				$\sigma$ 0.19
NBS FA	10.6 $\pm$ 0.6	11.3 $\pm$ 0.3	8.6 $\pm$ 1.0	(Certified value = 11.6 $\pm$ 0.2)
IAEA	118 $\pm$ 5	129 $\pm$ 2	112 $\pm$ 7	(Certified value = 119 ppm)

Such a study was the impetus behind the present investigation. Sizeable numbers of soil, atmospheric particulate, vegetation, and small rodent samples containing highly variable amounts of added  $^{235}\text{U}$ , needed to be rapidly analyzed. Instrumental Epithermal Neutron Activation Analysis (IENAA) was selected as a promising method for comparison to DNA and FA.

### EXPERIMENTAL

A set of soil samples was collected in an area of known DU use. Thirty-three of these were subjected to IENAA (4) DNA (5) and finally FA (2, 6). Since the first two techniques are nondestructive, the same aliquot of the original sample could be examined by each analyst.

The samples were first irradiated with epithermal neutrons for 2 min in the Los Alamos Omega West Reactor's pneumatic epithermal neutron facility. After 2 to 4 days decay, the  $\gamma$  spectra of the samples were recorded for 5 min each with a large Ge(Li) detector (FWHM = 1.9 KeV at 1332 KeV). The 228- and 278-KeV transitions from the decay of  $^{239}\text{Np}$  ( $t_{1/2} = 2.35$  d) were observed and used for quantitative analysis. The spectra were accumulated on a 4000-channel analyzer, the regions of interest punched on paper tape, and the data reduced by computer. International Atomic Energy Agency (IAEA) soils with certified U concentrations were used to standardize the analysis.

Delayed neutron measurements were performed on each sample by first irradiating the sample for 20 s in a thermal neutron flux. Irradiations were made at different reactor power levels, but in all cases the thermal neutron flux was monitored during the irradiation using a fission ion chamber. After irradiation, the sample was pneumatically transferred to a neutron detector (7) of 27% efficiency and counted for 20 s following a 10-s delay. The neutron data were normalized to a constant flux and the system was calibrated using samples of NBS SRM-1633. Uranium concentrations were calculated assuming natural isotopic abundance of  $^{235}\text{U}$ .

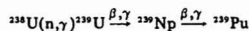
For fluorometric analysis, soil samples were dissolved in a mixture of  $\text{HNO}_3$  and HF, small volumes pipetted onto 50 mg NaF/LiF pellets, the pellets dried under an IR lamp, and fused for 2 min at approximately 1200 °C using a burner similar to that of Price et al. (6). The pellets were allowed to cool for 15 min and then the fluorescence at 245 nm was "read" on a Fischer Mod 26-000 fluorometer. The resulting data were reduced by computer to U concentrations.

### RESULTS AND DISCUSSION

Table I displays the data accumulated from the three different methods of U analysis. The results of determinations on National Bureau of Standards Reference Materials and IAEA soil standards attest to the relative accuracy of the procedures. The table quickly reveals that most of the samples have much more U than the crustal abundance of about 3 ppm (8). The added U is nearly all depleted to some extent in  $^{235}\text{U}$ . This has disturbed the normal U isotopic ratio and thus DNA yields a low result in almost every case (as expected). The IENAA technique is, however, insensitive to  $^{235}\text{U}$ , so if the

added U in the soil has been enriched ( $^{235}\text{U}/^{238}\text{U} > 0.0072$ ), the IENAA would have yielded low results for total U concentration. A ratio of DNA/INEAA uranium determination that is less than 1 implies that the sample is in fact depleted in  $^{235}\text{U}$ ; while a ratio of greater than 1 implies enrichment. Thus, where the history of a sample is unknown, the surest approach is to use both methods and simply sum the absolute amounts of  $^{235}\text{U}$  and  $^{238}\text{U}$ . Note that when the soil has been removed from a "background" site (e.g., 1707, 1787, 1827, 1867), the data from all three techniques are comparable and the U concentration is near the crustal abundance.

The last column of the table is the ratio of IENAA/FA. On a sample by sample basis, the U values agree reasonably well, the mean ratio and standard deviation being  $0.94 \pm 0.19$ . Our determination of U by the reaction



using epithermal neutrons, is not original (4), however, the application of the method to DU samples is new. Epithermal neutron activation is ideal for rapid determination of U at ppm levels and, as shown in Table I, compares well with the more classical FA. While IENAA is completely instrumental and nondestructive, samples for FA must be in solution. As residues from dissolution may contain U, it is possible for the yield to be underestimated by FA. Furthermore, quenching from common cations (e.g., Fe, Ni, Cu) sometimes interferes with the FA measurements, whereas in the IENAA technique, measurements are made on two relatively interference-free, intense  $\gamma$  rays. Both methods have detection limits of about 10 ng total U.

### ACKNOWLEDGMENT

We thank the staff of the Omega West Reactor for their assistance with the irradiations and Priscilla Jose for her fluorometric analyses.

### LITERATURE CITED

- (1) U.S. Energy Research and Development Administration, "A National Plan for Energy Research, Development, and Demonstration: Creating Energy Choices for the Future", USERDA Report ERDA-48, June 1975.
- (2) J. W. Owens, Los Alamos Informal Report LA-6338-MS, April 1976.
- (3) D. G. Coles, J. W. T. Meadows, and C. L. Lindeken, *Sci. Total Environ.*, **5**, 171 (1976).
- (4) E. Steinnes, "Epithermal Neutron Activation Analysis of Geological Material", in "Activation Analysis in Geochemistry and Cosmochemistry", A. O. Brunfelt and E. Steinnes, Ed., Oslo, Universitets Forlaget, 1971, pp 113-128.
- (5) S. Amiel, *Anal. Chem.*, **34**, 1683 (1962).
- (6) G. R. Price, R. J. Ferretti, and S. Schwartz, *Anal. Chem.*, **25**, 322 (1953).
- (7) S. J. Balestrini, J. P. Bagnia, and H. O. Menlove, *Nucl. Instrum. Methods*, **136**, 521 (1976).
- (8) S. R. Taylor, *Geochim. Cosmochim. Acta*, **28**, 1273 (1964).

RECEIVED for review October 11, 1977. Accepted January 16, 1978. Work performed under the auspices of the Department of Energy.



## CORRESPONDENCE

## Construction of pH Gradients in Flow-Injection Analysis and Their Potential Use for Multielement Analysis in a Single Sample Bolus

**Sir:** We are carrying out a long term investigation into the possibility of performing multielement trace analysis by nonsegmented continuous flow analysis, which is more concisely known as flow-injection analysis (FIA) (1). The rationale and some preliminary results are reported here.

**Basic Idea.** The distinctive feature of FIA, compared to conventional automatic analysis, is the direct injection of a sample into the carrier solution. It follows that there is an interfacial region between the sample plug and the carrier and that, during the course of mixing, concentration gradients are established across the interface if the initial concentrations in the carrier and sample are different. Thus, if we have a system in which the sample solution is a mixture of metal ions and the carrier is a solution of a reagent which reacts with the metal ions, the sample and carrier being of different pH, then we would expect a well defined sequence of color-forming reactions to take place across the interfacial region as the reagent and metal ions reacted and the pH changed.

Under static conditions, pH-absorbance curves (Figure 1) can be readily established and are known to be characteristic for any given metal ion-reagent combination. They are additive, and of such a shape that if the curve for a mixture of ions were mathematically differentiated, it would give rise to a well defined series of peaks, whose relative areas reflected the composition of the original mixture.

Under the dynamic conditions of FIA, the chemistry becomes complicated, but Figure 1 suggests the crucial experiment to test whether concentration changes across the interface can be used for analytical purposes. If the carrier is a solution of 4-(2-pyridylazo)resorcinol, PAR, at pH 9 and the sample bolus is a solution of lead(II) and vanadium(V) at pH 2, the pH across the bolus-carrier interface will vary between 9 and 2. At pH 9, only the lead will react with the PAR whereas at pH 2 only vanadium forms a color. Hence, the peak obtained by measuring the absorbance downstream from the injection point will not have the Gaussian shape which is obtained when the sample solution contains only a single metal ion, and it might contain enough information for the two ions to be determined.

## EXPERIMENTAL

**Reagent.** 4-(2-Pyridylazo)resorcinol. Reagent streams are prepared freshly from reagent grade PAR diluted to  $10^{-3}$  M.

**Ammonia-Ammonium Chloride Buffer.** The reagent stream is buffered at pH 9.9 by dissolving 12.2 g of ammonium chloride and 50 mL of 35% ammonia solution in each liter of reagent solution.

**Samples.** Samples were prepared for stock solutions of AnalA<sup>R</sup> ammonium metavanadate in dilute hydrochloric acid (0.025 M) and AnalA<sup>R</sup> lead nitrate. Each sample was prepared as a solution of 0.025 M hydrochloric acid.

**Apparatus.** Constant Head. The stream was motivated by a constant head of reagent at a flow rate of 2.5 mL/min.

**Sample Injection.** Samples were injected from a disposable plastic syringe through a septum valve into the reagent stream.

**Mixing Coils.** Since a large sample volume is used, a coil of 100 cm is required before the injection block to accommodate any backflow of sample on injection. The reaction coil was 215 cm in length and both coils were 0.086 cm i.d.

Table I. Effect of Vanadium Concentration on Lead Peaks

Concn Pb(II), $10^{-5}$ M	Concn V(V), $10^{-5}$ M	Peak height of lead peak, cm
5.4	6.7	17
5.4	13.3	16
5.4	20.0	16
5.4	26.7	16.5

**Spectrophotometer.** The peaks were detected using a 1-mm Perspex cell in a Unicam SP600 spectrophotometer set at 530 nm, the flow direction being normal to the light path.

**Procedure.** In view of the known solution chemistry of vanadium and lead and the need to establish an optimal pH gradient across the bolus-carrier interfaces, it is important to maintain close control of the hydrochloric acid and ammonia-ammonium chloride buffer constituents and to use recently prepared solutions of vanadium(V) and buffered reagent solution. Each sample solution was prepared as a solution of 0.025 M hydrochloric acid. The vanadium solutions were used within 24 h of their preparation.

Sample volumes of 1.25 mL were used in all experiments. Sample batches were prepared to establish the effect on the peak height for an analyte when its concentration was varied in the presence of (a) a constant concentration of the second analyte, (b) a varying concentration of the second analyte, and (c) when its concentration was held constant while the second analyte concentration was varied.

## RESULTS AND DISCUSSION

Typical peak profiles are shown in Figure 2. The outer peaks arise from the reaction of PAR with lead while the inner peak is due to vanadium.

A straight line calibration is obtained for lead in the presence of a constant concentration of vanadium (Figure 3a).

No effect is detected in the lead peak obtained with a constant concentration of lead when varying the concentration of vanadium, the peak heights all being within the expected precision limits of a single sample, viz. standard deviation (1-2%) (Table I).

A straight line calibration is obtained for the lead peaks of varying concentration in the presence of varying vanadium concentrations (Figure 3b). Clearly lead can be determined selectively in the presence of vanadium.

The resolution of the lead and vanadium peaks as shown in Figure 2 is greatest when the vanadium concentration is reasonably high. This puts the range of concentration of vanadium over which determinations can be made out of the linear range obtainable with the PAR concentration. Hence the determination of concentration is much less precise. The calibration curves which can be obtained (Figure 4) are in the region of the break point similar to that which is obtained in conventional mole ratio plots. (See Theoretical discussion.) In this case the lead concentration has been kept constant.

When the lead concentration is varied, the peaks for lead and vanadium overlap, significantly at high lead concentration. It is no longer possible simply to measure the peak height of the vanadium peak from the baseline. Since the calibration curve for vanadium is very shallow locating the "base" of the

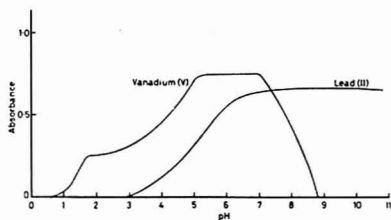


Figure 1. pH-absorbance curves for lead(II) and vanadium(V) with 4-(2-pyridylazo)resorcinol.  $Pb^{2+} = V^{5+} = 2 \times 10^{-5} M$ ; PAR =  $2 \times 10^{-4} M$ ; wavelength, 530 nm

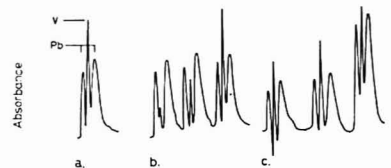


Figure 2. Peaks obtained from one sample containing a mixture of Pb(II) and V(V) injected into a solution of PAR. (a) General shape of curve. (b) Increasing concentration of V(V) while that of Pb(II) is held constant. (c) Increasing concentration of Pb(II) while that of V(V) is held constant

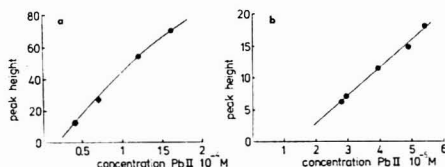


Figure 3. (a) Peak height of lead peak vs. Pb(II) concentration with V(V) concentration constant at  $5.0 \times 10^{-5} M$ . (b) Peak height of lead peaks vs. Pb(II) concentration with V(V) concentration varying randomly. For points from left to right, the V(V) concentration is 7.1, 11.1, 2.5, 2.9, 8.9,  $6.7 \times 10^{-5} M$

vanadium peak must be very precise. It is for this reason that the calibration curves obtained for vanadium in the presence of varying lead have not been useful.

We believe, however, that these results demonstrate the feasibility of using unsegmented continuous flow systems to obtain a range of conditions (pH gradient, masking gradient, etc.) over a single sample bolus so that resolution of absorbing species in multielement determination may be achieved. It would seem certain from the results presented and difficulties high-lighted that some modicum of computing power will be required for peak resolution and more precise determination of peak characteristics.

**Theoretical Consideration.** The basic assumption made is that when there is a difference in the initial concentrations of a species in the carrier and sample solution, a concentration gradient is established in the interfacial region. The reasonableness of this assumption is suggested by Taylor's theory on the dispersion of a plug of sample injected into a flowing solvent (2). In essence, the theory is that at low flow rates and within specified dimensions of tubing, the dispersion of the sample into the carrier is mainly by diffusion and that the concentration profile of the sample bolus downstream is Gaussian. Thus, the concentration gradient, although non-linear is mathematically predictable and, more important, is reproducible. In other studies in this laboratory, we have

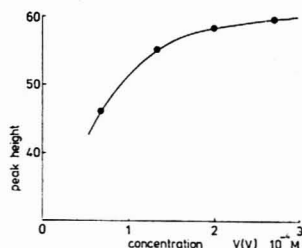


Figure 4. Peak height of vanadium peak vs. V(V) concentration with Pb(II) concentration constant at  $5.4 \times 10^{-5} M$

found that Taylor's theory fits the experimental results very well. It is a good first approximation even when, as in this instance, the flow rate is slightly greater than allowed for in the theory.

This theory based on laminar flow seemed more suitable than one which assumed turbulent flow, since the flow rate which corresponds to a Reynolds number of 2000, usually set as the onset of turbulence, is  $81.3 mL min^{-1}$ . Ruzicka and Hansen, at first recommended turbulent flow, but soon abandoned that viewpoint and have recently proved that it is inessential to FIA (3). It is not even certain that a change to turbulent flow would upset the argument greatly since Taylor has shown that diffusion is important under these conditions and that peak shapes are predictable (4). However the experimental arguments overwhelmingly favor slow flow rates, and the discussion about turbulence is a little academic.

We have checked the possibility that some of the peak spreading arises from chromatographic processes, by performing the experiment at different flow rates. The results clearly indicate that the effective partition coefficient approximates to zero and that diffusion is the major cause of peak spreading.

In general, the identification and determination of elements in a mixture may be made easier by a "substoichiometric sharpening effect". It seems probable that a substoichiometric amount of reagent presents itself to the metal ion at any given point across the interface. Thus the reaction which is favored at that point, is the one with the greatest conditional equilibrium constant. Hence, in general, one would expect metal ions to be complexed sequentially, not simultaneously. As the pH varies, so do the conditional constants, and, in those instances where the relative magnitude of the constants is reversed (as here at approximately pH 7), one would expect the effect observed.

This argument may seem a little farfetched since in the system there is clearly an excess of reagent overall. However, three kinetic factors govern the amount of reagent which can react with the sample by the time the plug reaches the point of measurement: (i) the rate of flow of carrier, (ii) the rate of mixing of sample and carrier, (iii) the rate of chemical reaction between reagent and metal ion. We have performed experiments equivalent to those used to determine the mole ratio in spectrophotometry, i.e., we have injected a given volume of increasingly concentrated solution of lead(II) into a carrier solution of PAR at fixed concentration. Plots of peak height vs. lead concentration are identical to those obtained in conventional mole ratio experiments (Figure 5). Thus, it is possible to think of an "available amount" of reagent and also of substoichiometry since that amount is not available all at once.

The successful extension of the method to more complex systems depends on the ability to choose suitable combinations of reagents, pH, masking agents, and metal ions, on the ability

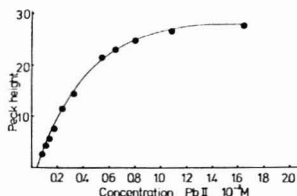
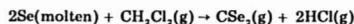


Figure 5. Peak height vs. Pb(II) concentration showing the region of limiting reagent concentration. The PAR concentration was  $10^{-3}$  M. (The chelate stoichiometry is  $Pb(PAR)_2$ )

to process the results rapidly, and on the development of a satisfactory theory of FIA. However, we believe these results show that it is possible to create suitable conditions for multielement determinations along a single sample plug.

## Gas Chromatographic Determination and Purification of Carbon Diselenide

Sir: We have recently had occasion to look into the purity of commercially prepared carbon diselenide in conjunction with our study of its high temperature pyrolysis (1). Since carbon diselenide is highly noxious and poisonous, it must be handled with considerable caution. It is not surprising that there are few commercial suppliers, that neither the nature nor amounts of impurities in commercial samples is well known, and that no suitable means of purification have been described. The major commercial supplier (Strem Chemicals, Inc., Danvers, Mass.) reports (2) preparation of carbon diselenide by the method of Ives, Pittman, and Wardlaw (3), i.e., by passing methylene chloride vapor over molten selenium metal:



The carbon diselenide is distilled at 13 Torr (boiling point 45 °C) with a packed column, quick-frozen in a dry ice bath, and stored at -20 °C in the dark to prevent decomposition. Even when kept in this manner,  $CSe_2$  turns from a clear, lemon-yellow color to orange within a couple of weeks and finally to black as solid  $CSe_2$  polymers form (4). When  $CSe_2$  is vaporized at ambient temperature and recondensed, it is again lemon-yellow, the polymeric forms remaining behind.

Wagner suggests that methylene chloride is the main contaminant at the 1 to 5% level (2), possibly due to the formation of an azeotrope as is found in the  $CS_2$ -methylene chloride system (5). Apparently a serious search for other impurities had not been conducted.

Marquart, Belford, and Fraenkel (1) worked out a convenient procedure to determine the concentration of  $CSe_2$  in a vapor phase by ultraviolet absorption spectrometry in the region of an intense electronic band (2150–2500 Å). (NOTE: The instability of  $CSe_2$  in UV light necessitates rapid handling.)

**Elemental Analysis.** Our elemental analysis (performed by the University of Illinois Microanalytical Laboratory under the direction of Josef Nemeth) on a sample of  $CSe_2$ (I) showed 7.63% C, 0.21% H, and 2.61% Cl indicating that the commercial sample is about 95% pure and that chlorinated species are prevalent impurities.

## ACKNOWLEDGMENT

We are grateful to J. Ruzicka and E. H. Hansen for the gift of a sample injection block and to J. H. Purnell for discussions on the theory of dispersion.

## LITERATURE CITED

- (1) J. Ruzicka and E. H. Hansen, *Anal. Chim. Acta*, **78**, 145 (1975).
- (2) G. Taylor, *Proc. R. Soc. (London) Ser. A*, **219**, 188 (1953).
- (3) E. H. Hansen, J. Ruzicka, and B. Rietz, *Anal. Chim. Acta*, **89**, 241 (1977).
- (4) G. Taylor, *Proc. R. Soc. (London) Ser. A*, **227**, 446 (1953).

D. Betteridge\*  
Bernard Fields

Chemistry Department  
University College of Swansea  
Swansea SA2 8PP, U.K.

RECEIVED for review August 9, 1977. Accepted December 27, 1977. The Science Research Council provided a Studentship for B.F.

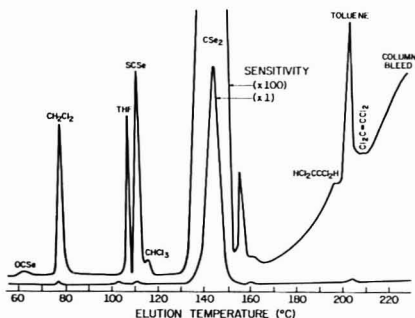
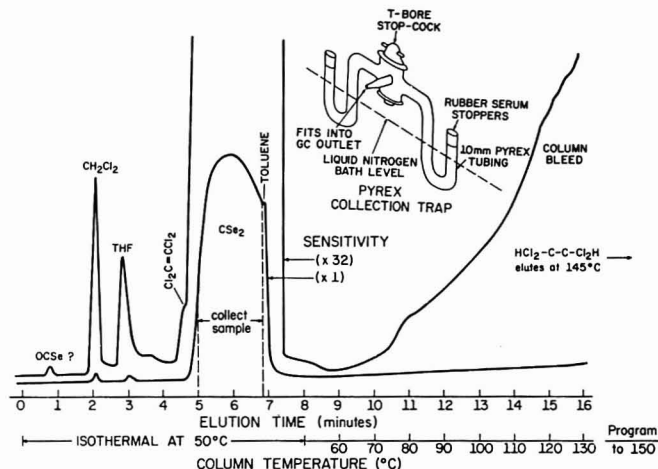


Figure 1. Gas chromatogram with flame ionization detection of commercially prepared  $CSe_2$ . Chromatographic conditions: sample injection, neat liquid  $CSe_2$ , 0.1  $\mu$ L; column, 6-foot Pyrex (1/2-in. by 2-mm i.d.); packing, 0.4% Carbowax 1500 on 60/80 mesh Carbowax A (Supelco, Inc.); inlet temperature, 150 °C; column temperature, 50 to 175 °C at 10 °C/min; carrier gas (helium), 30 mL/min; detector temperature, 150 °C.

**Gas Chromatographic Analysis.** The gas chromatographic analyses of  $CSe_2$  required only very little sample, which was burned in the flame ionization detector. Only small amounts of selenium were released into the atmosphere, no longer in the form of the volatile and noxious  $CSe_2$ . Accordingly, no special handling techniques were needed.

By gas chromatographic-mass spectrometry, we have isolated and identified four chlorinated hydrocarbons: methylene chloride, chloroform, 1,1,2,2-tetrachloroethane, and tetrachloroethylene (1). The last three are probably produced by side reactions during preparation. Tetrahydrofuran (THF), toluene,  $OCSe$ , and  $SCSe$  are also present. A typical mass spectrum is shown in Ref. 1.

Once peaks had been identified, flame ionization detection gave a simpler and generally adequate means of monitoring  $CSe_2$  purity. Figure 1 shows typical results with a Varian



**Figure 2.** Preparative gas chromatogram of commercially prepared  $\text{CSe}_2$ . Chromatographic conditions: sample injection, neat liquid  $\text{CSe}_2$ , 10 to 50  $\mu\text{L}$ ; column, 6-ft aluminum ( $1/8$ -in. o.d. by 5-mm i.d.); packing, 20% DEGS (Applied Science Lab., Inc.) on 60/80 mesh Chromosorb P (Johns-Manville) DMCS-treated and acid-washed; inlet and detector temperatures, 150  $^\circ\text{C}$ ; collection trap stopcock and line temperature, 125  $^\circ\text{C}$  (with heating tape); carrier gas (helium), 30 mL/min; column programmed 50 to 150  $^\circ\text{C}$  as shown

Aerograph Model 2700 gas chromatograph. Flame ionization detectors are relatively less sensitive to the sulfur and selenium compounds than is the total ion collector used in the mass spectrometric detection system. Also, column bleed interferes more with the detection of peaks eluting at higher temperatures.

**Preparative Gas Chromatographic Purification.** Having first attempted to purify  $\text{CSe}_2$  by crystallization, sublimation, and simple redistillation methods with little gain, we then turned to preparative gas chromatographic methods (Figure 2). The noxiousness of the samples required extreme precautions during purification.

A Varian Aerograph series 90P gas chromatograph was used with a thermal conductivity detector for actual collection runs. The  $\text{CSe}_2$  eluent was detected by an in-line thermal conductivity detector and trapped in a liquid-nitrogen-cooled collector (Figure 2 inset). The T-bore stopcock was lightly lubricated with Dow-Corning silicone high vacuum grease. Effluent gas from the collection trap was vented by inserting an 18-gauge syringe needle into each serum cap. One-eighth-inch vinyl tubing carried effluent to a solid KOH bed to remove  $\text{CSe}_2$  (WARNING: very toxic and foul smelling). The gas chromatograph was set up in a hood.

Although 0.4% Carbowax 1500 on Carbowax A support is suitable for analysis, a heavily loaded column was needed to allow injections of up to 50  $\mu\text{L}$  for practical preparative gas-chromatographic separation. Carbowax A has a small surface area and will not hold heavy loadings. Also, it is quite expensive for extensive preparative use. Chromosorb P is designed for heavy loadings but would not hold 20% Carbowax 1500 without excessive column bleed at 110  $^\circ\text{C}$ . Twenty percent poly(diethylene) glycol succinate (DEGS) on Chro-

mosorb P gave adequate separation for 50- $\mu\text{L}$  injections.

The gas chromatogram shown in Figure 2 was obtained by use of a more sensitive flame ionization detector to show better where each component elutes. Note that toluene and tetrachloroethylene do not resolve well from the huge  $\text{CSe}_2$  peak. Even so, samples accumulated over the "collect sample" range shown in Figure 2 contained only about 20% and 7%, respectively, of the original proportions of toluene and tetrachloroethylene. Methylene chloride was reduced fifty-fold and other impurities below detectable limits. Total sample purity is estimated to exceed 99.5%.

#### LITERATURE CITED

- (1) J. R. Marquart, R. L. Belford, and H. A. Fraenkel, *Int. J. Chem. Kinet.*, **9**, 671 (1977).
- (2) Frank Wagner, Strem Chemicals, Inc. Danvers, Mass., private telephone conversation August 1976.
- (3) D. J. G. Ives, R. W. Pittmann, and W. Wardlaw, *J. Chem. Soc. (London)*, 1080 (1947).
- (4) A. J. Brown and E. Whalley, *Inorg. Chem.*, **7**, 1254 (1968).
- (5) T. Wentink, *J. Chem. Phys.*, **29**, 188 (1958).

J. R. Marquart

Department of Chemistry  
Mercer University  
Macon, Georgia 31207

R. L. Belford\*

School of Chemical Sciences  
University of Illinois  
Urbana, Illinois 61801

RECEIVED for review September 7, 1977. Accepted December 1, 1977. Supported by a grant from the National Science Foundation.

## Autoclave Digestion Procedure for the Determination of Total Iron Content of Waters

**Sir:** As colorimetric procedures for ferrous iron have been automated, solubilization of iron has been the rate determining step. Wilson (1) evaluated iron digestion procedures for small amounts of particulate matter in large volumes. "Standard Methods" (2) recommends concentrating the sample to one third of its original volume in hydrochloric acid-hydroxylamine media. The latter procedure is time consuming, rather dangerous, and the resultant acid fumes produce extremely corrosive conditions in the fume hoods. Digestion by autoclaving samples under similar acid-reducing conditions markedly reduces these drawbacks. The use of an autoclave has been described by Armstrong (3), but the technique is so uncommon that a detailed evaluation with respect to recovery was undertaken.

A number of accepted colorimetric procedures for soluble or reactive iron are described in the literature, but the use of the chromophore 2,4,6-tri(2-pyridyl)-1,3,5-triazine (TPTZ) is particularly attractive as such systems are highly sensitive and very stable. This reagent was introduced by Diehl and Smith (4), and has been adapted by a number of authors to both manual (5, 6) and automated (7, 8) systems. The violet ferrous-TPTZ complex has a molar absorptivity (4) of approximately  $2.23 \times 10^4$  at 595 nm and thus the interference due to the natural color of samples can usually be eliminated by in-line dilution. The intensity of the colored complex does not change appreciably over the pH range 3.4 to 5.8 permitting stabilization of the system by incorporating a sodium acetate-acetic acid buffer. Accordingly, the manual TPTZ procedure described by Dougan and Wilson (6) was automated for the range 0 to 2.0 mg/L Fe.

### EXPERIMENTAL

**Apparatus.** The autoclave was equipped with an automatic slow exhaust and capable of being operated at 121 °C. Culture tubes (25 × 150 mm) with Teflon lined screw caps were the sample containers, and racks to hold these tubes were utilized for the autoclave step. The digestant was added via an Oxford Pipettor. The TPTZ colorimetry utilized a single channel Technicon AAI AutoAnalyzer system and a single pen recorder. The drum of the Technicon sampler (large industrial model) was modified to accept the tall culture tubes.

**Reagents.** The Digestion Acid contained 640 mL of concentrated hydrochloric acid plus 30 g of hydroxylammonium chloride per liter. Hydrochloric acid was the active or solubilizing agent but the hydroxylammonium chloride was included to prevent loss of iron by reduction to the divalent state, and to reduce any oxidizing agents which might be present in the sample.

An Acid Wash was required for the AutoAnalyzer system to maintain an acceptable baseline. The concentration of hydrochloric acid (4% by volume) in this wash equaled that in the digested sample.

Reagents associated with the TPTZ colorimetric phase were also required.

**Procedure.** After thoroughly shaking the sample, a 30.0-mL aliquot was transferred to a culture tube via a wide mouth pipet, and 2.0 mL of the digestant acid was added, with an Oxford Pipettor. The Teflon-lined cap was screwed on tight, the vial placed in a rack, and the rack set on an enamel tray to protect the autoclave in case of breakage or leaking. The culture tubes (as many as 250) were autoclaved at 121 °C for 60 min. After the pressure in the autoclave had been discharged, the door was left ajar for 15 min to protect the operator against an exploding tube. To date approximately 15,000 tubes have been autoclaved without breakage. Moreover, iron losses are minimal; after 200 tubes had been autoclaved, the trace of condensate in the enamel trays contained 0.12 mg/L Fe and had a pH value of 6.8. The samples were allowed to cool to room temperature before pro-

ceeding with the colorimetric phase. The use of the same vials in the colorimetric step avoided errors associated with transferring the samples.

### RESULTS AND DISCUSSION

In selecting the experimental conditions for solubilizing the iron, the autoclave temperature was not varied; it remained 121 °C throughout. To select the volume of digestant, 30.0-mL aliquots of ten routine samples were autoclaved for 40 min in the presence of 1.0 mL and 2.0 mL of digestant; the same samples were also digested according to "Standard Methods" (2); using the latter data as reference, the average recovery of iron was 93% for 1 mL of digestant and 100% for 2 mL of digestant. To select the required period of autoclaving, 20 routine samples were autoclaved for 20, 40, and 60 min (2.0 mL of digestant per 30.0 mL of sample); again the same samples were digested according to "Standard Methods" (2), and the latter data were used as reference. As the digestion period increased from 20 to 60 min, the average recovery increased only from 99 to 101%. Although 40 min appeared sufficient, the 60-min digestion period was selected to provide a safety margin. To confirm the overall procedure, solutions of ferrous sulfate, ferric chloride, potassium ferrocyanide, and potassium ferricyanide were analyzed. The measured and theoretical iron concentrations differed by less than 1%.

A linear calibration was obtained for the autoclave-TPTZ procedure for total iron. The precision of the method was estimated by analyzing routine water samples in duplicate on different days, and determining the mean standard deviation of the differences for two concentration ranges. For the concentration range 0 to 0.4 mg/L Fe, the mean standard deviation was 0.017 mg/L Fe ( $n = 48$ ), and for the range 0.4 to 1.0 mg/L Fe, the mean standard deviation was 0.037 mg/L Fe ( $n = 28$ ). These levels of between-run precision also reflect the sampling difficulties associated with particulate matter, and are considered satisfactory for routine analyses.

The interference study showed that iron was recovered with 2% of the theoretical value in the presence of common ions; ten cations and six anions were tested at concentration levels in excess of those normally encountered in water samples. Neither the disodium dihydrogen salt of adenosine-5'-triphosphoric acid nor pyrophosphate anions affected the recovery of iron at the 5 mg/L P level. Sulfide, linear alkylate sulfonate, humic acid, and tannic acid were also tolerated at the 5 mg/L concentration levels.

To complete the evaluation of the autoclave-TPTZ procedure, the iron contents of 610 routine water samples from Central and Southern Ontario were determined by the subject method and by the acid digestion-phenanthroline procedure recommended by "Standard Methods" (2). The samples were divided into three groups; (a) domestic water supplies and landfill leachates, (b) river, lake, and snow samples collected in the winter months, and (c) river and lake samples submitted during the spring runoff. With the exception of the leachates (about 10%), group (a) were the "cleanest" samples. The linear regression analyses for the three sets of data (Table I) indicate that the two procedures give comparable results; the slopes for the comparisons were within 1% of 1.00. The mean differences and standard deviations for the three groups were (a) 0.003 mg/L Fe ( $\sigma = 0.024$ ), (b) 0.000 mg/L Fe ( $\sigma = 0.037$ ), and (c) 0.003 mg/L Fe ( $\sigma = 0.073$ ). The lowest standard deviation was obtained for group (a) which normally contain little or no particulate matter while the largest standard deviation was associated with spring runoff samples which



Table I. Comparison of Autoclave-TPTZ and Standard Methods Procedures by Linear Regression Analysis

Statistical Parameter	Type of water sample		
	Domestic water supplies and leachates	Rivers and lakes, Winter months	Rivers and lakes, Spring runoff
No. of Samples	251	194	165
Correlation	0.9973	0.9948	0.9893
Y on X regression <sup>a</sup>			
Slope	1.0097	0.9982	1.0024
Intercept (mg/L Fe)	-0.0044	0.0025	0.0038
Std dev (mg/L Fe)	0.024	0.0369	0.0726
X on Y regression			
Slope	1.0043	0.9879	0.9811
Intercept (mg/L Fe)	-0.0032	0.0057	0.0163
Std dev (mg/L Fe)	0.024	0.0366	0.0720

<sup>a</sup> X refers to the data obtained using the procedure from "Standard Methods" (2).

contain so much silt that it is extremely difficult to select a representative sample. Winter samples contain small amounts of particulate matter and the standard deviation was intermediate (0.037 mg/L Fe). If the autoclave digestion technique was inadequate, the measured iron content would tend to be

lower than that determined by the "Standard Method" procedure (2). Such a bias (5 to 10% lower) was found when creek and snow samples from two locations were analyzed. Although this weakness can be tolerated in view of its infrequent occurrence and the size of error involved, analysts should evaluate the autoclave digestion procedure for their particular waters before adopting the technique.

## LITERATURE CITED

- (1) A. L. Wilson, *Analyst*, (London), **89**, 402 (1964).
- (2) American Public Health Association, "Standard Methods for the Examination of Water and Wastewater", 14th ed., APHA, Washington, D.C., 1976, p. 208.
- (3) F. A. J. Armstrong, *J. Mar. Biol. Assoc. U.K.*, **36**, 509 (1957).
- (4) H. Diehl and G. F. Smith, "The Iron Reagents: Bathophenanthroline, Bathophenanthroline-Disulfonic Acid, 2,4,6-Triphenyl-5-triazine, Phenyl-2-pyridyl ketoxime", 2nd ed., G. Frederick Smith Chemical Company, Columbus, Ohio, 1965.
- (5) P. F. Collins, H. Diehl, and G. F. Smith, *Anal. Chem.*, **31**, 1862 (1959).
- (6) W. K. Dougan and A. L. Wilson, *Water Treat. Exam.*, **22**, 100 (1973).
- (7) R. D. Britt, Jr., *Anal. Chem.*, **34**, 1728 (1962).
- (8) A. Henriksen, *Vattenhygien*, **22**, 2 (1968).

Joan Crowther

Ontario Ministry of the Environment  
Laboratory Services Branch  
Water Quality Section  
Box 213  
Rexdale, Ontario  
Canada M9W 6L1

RECEIVED for review October 17, 1977. Accepted January 3, 1978.

## On-Line Coupling of a Micro Liquid Chromatograph and Mass Spectrometer through a Jet Separator

**Sir:** High performance liquid chromatography (HPLC) has become almost comparable to gas chromatography (GC) in separation capability and analysis time. The former, however, still has some disadvantages in its versatile detection system. Therefore, on-line coupling of HPLC to the mass spectrometer (MS) has been studied as one of the most promising approaches to develop a universal detection system: using a moving wire (1), a silicon membrane separator (2), direct introduction of a portion of the column effluent into the chemical ionization source through a fine glass capillary (3-5) or atmospheric pressure ionization (6). The first commercial LC/MS interface was produced by Finnigan Ltd., where the moving wire was replaced with a continuous belt to enable efficient sample loading.

Recently, Ishii has developed a micro LC (7, 8), which requires a flow rate of only a few microliters per minute and has separation ability almost comparable to the conventional LC.

In our study, an ordinary one-stage jet separator for GC/MS was used as an interface for coupling of the micro LC with MS. The total LC effluent solution was continuously introduced into the heated separator through a stainless steel capillary tubing and evaporated. The sample-enriched vapor is transferred to the chemical ionization source in MS where the solvent acts as the reagent gas. With this method, it is possible to maintain a constant pressure of the ionization chamber even under various LC flow rates by adjusting the evacuation rate at the jet separator, and the solute concen-

tration is enriched since the solute molecule is usually larger than the solvent molecule.

## EXPERIMENTAL

**Apparatus.** A schematic diagram of the micro LC/MS system is shown in Figure 1. The micro LC is a FAMILIC-100 from Japan Spectroscopic Co., Ltd. (JASCO, Tokyo, Japan) equipped with a gas-tight micro syringe (250  $\mu$ L in volume). Flow rates of 2, 4, 8, and 16  $\mu$ L/min can be selected. The UV spectrophotometer is a UVIDE-100 from JASCO and the flow cell (8  $\mu$ L in volume) attached to the spectrophotometer was replaced by a quartz capillary cell (ca. 0.5  $\mu$ L in volume). One end of the cell was directly connected to the outlet of a micro LC column of polytetrafluoroethylene (PTFE) tubing. The other end was combined with a PTFE tubing (0.1-mm i.d.) to a stainless steel capillary (30 cm in length, ca. 4  $\mu$ L in volume). The capillary was directly connected to the separator through a silicon septum. The total eluent from LC was introduced into the separator, which is evacuated by a rotary pump at the maximum pumping speed of 80 L/min. The separator orifices are 0.1 and 0.3 mm, respectively, with a distance of 0.4 mm used at a temperature of 150 °C to enable the rapid vaporization of the column effluent.

The mass spectrometer used is a JMS-Q10A quadrupole mass spectrometer from Japan Electron Optics Laboratory Co., Ltd., equipped with an EI/CI ion source and an oil diffusion pump (1000 L/s pumping speed).

**Column.** A micro column used for separation is a PTFE tubing (0.5-mm i.d., 7 cm in length) packed with Silica ODS SC-01 from JASCO.

**MS Detection.** MS detection was carried out using the CI source under the following conditions: ionizing voltage of 250 eV,

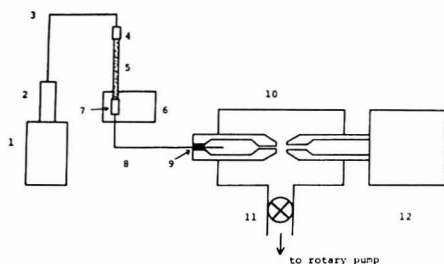


**Figure 1.** Schematic diagram of the micro LC/MS system: (1) pump (microfeeder), (2) gas-tight microsyringe, (3) PTFE tubing, (4) sample inlet, (5) micro column, (6) UV spectrophotometer, (7) micro flow cell, (8) stainless steel capillary, (9) silicon septum, (10) heated jet separator, (11) control valve, (12) mass spectrometer

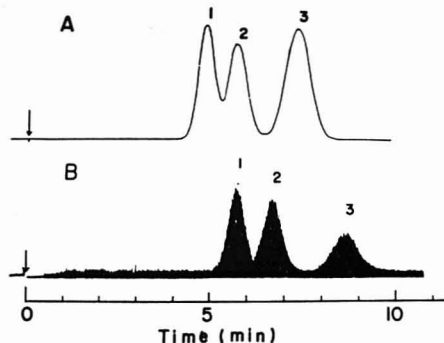


**Figure 2.** Comparison of (A) UV detector and (B) MS detection chromatograms for aromatic hydrocarbons. Peaks: (1) biphenyl, (2) fluorene, (3) anthracene. Mobile phase: 70% acetonitrile in water. Flow rate: 8  $\mu$ L/min

filament current of 400 mA, and ionizing current of 100  $\mu$ A. The pressure in the ion source was maintained at ca. 1 Torr at 8  $\mu$ L/min of flow rate.

### RESULTS AND DISCUSSION

When methanol was used as a carrier, the flow rate to yield an ion source pressure of 1 Torr was 1  $\mu$ L/min without any evacuation at the separator and 8  $\mu$ L/min with full evacuation, respectively. Under each of these conditions, 10 ng biphenyl in methanol solution was injected and the peak of  $MH^+$  ( $m/e$  155) was monitored. From the results, a yield of about 80% and subsequently an enrichment of sample to solvent of 6 were attained at a flow rate of 8  $\mu$ L/min with full evacuation. Furthermore, in the range from 1  $\mu$ g to 1 ng of biphenyl, a good linearity of ion current at  $m/e$  155 to sample quantity was obtained.

Figure 2 shows the chromatograms of an aromatic hydrocarbon mixture monitored simultaneously by an UV spectrophotometer and mass spectrometer using the system (Figure 1). MS detection was carried out by repetitive scanning (1 s/scan) in the mass range of  $m/e$  150–180 to cover only the  $(M+1)^+$  peaks. In the chromatogram by MS de-

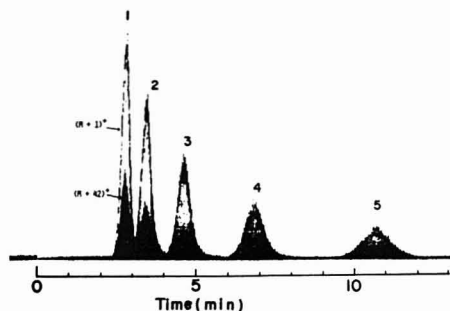


**Figure 3.** Separation of fatty acid methyl esters. Peaks: (1) capric, (2) lauric, (3) myristic, (4) palmitic, (5) stearic. Mobile phase: 100% acetonitrile. Flow rate: 8  $\mu$ L/min

tection, ca. 30-s time delay is observed because of additional dead volume. But the relative positions of the peaks in (B) are in good agreement with those in (A). Here, it is very interesting to notice that on the chromatogram by MS detection, the overlapping peaks, 1 and 2, can be discriminately detected to yield independent peaks.

As another example, Figure 3 shows a MS detection chromatogram of fatty acid methyl esters, which was obtained by repetitive scanning in the mass range of  $m/e$  180–350. The most abundant peak is  $(M+1)^+$  and the second is attributed to  $(M+42)^+$ . It is evident that MS detection is very useful for these compounds which have a weak or no absorption in the UV region.

This LC/MS system can also be applicable to ordinary HPLC using appropriate splitter. Further fundamental and application work is in progress.

### ACKNOWLEDGMENT

The authors are grateful to D. Ishii for instrumentation and technique of the micro LC.

### LITERATURE CITED

- (1) R. P. W. Scott, C. G. Scott, M. Munroe, and J. Hess, Jr., *J. Chromatogr.*, **99**, 395 (1974).
- (2) P. R. Jones and S. K. Yang, *Anal. Chem.*, **47**, 1000 (1975).
- (3) P. Arpino, M. A. Baldwin, and F. W. McLafferty, *Biomed. Mass Spectrom.*, **1**, 80 (1974).
- (4) P. J. Arpino, B. G. Dawkins, and F. W. McLafferty, *J. Chromatogr. Sci.*, **12**, 574 (1974).
- (5) F. W. McLafferty, R. Knüttel, R. Venkataraghavan, P. J. Arpino, and B. G. Dawkins, *Anal. Chem.*, **47**, 1503 (1975).
- (6) E. C. Horning, D. I. Carroll, I. Dzidic, K. D. Haegle, M. G. Horning, and R. N. Stillwell, *J. Chromatogr. Sci.*, **12**, 725 (1974).
- (7) D. Ishii, K. Asai, K. Hibi, T. Jonokuchi, and M. Nagaya, *J. Chromatogr.*, **144**, 157 (1977).
- (8) F. W. Karasek, *Res. Dev.*, **28** (1), 42 (1977).

Tsugio Takeuchi\*  
Yukio Hirata  
Yoshio Okumura

Department of Synthetic Chemistry  
Faculty of Engineering  
Nagoya University  
Nagoya, Japan

RECEIVED for review November 3, 1977. Accepted December 28, 1977. Part of this work was supported by a grant from the Ministry of Education.

# AIDS FOR ANALYTICAL CHEMISTS

## Separation of Perfluorinated Hydrocarbons by Gas-Solid Chromatography

Ronald R. Shields\*

IBM Systems Products Division, East Fishkill Facility, Hopewell Junction, New York 12533

John A. Nieman

IBM System Products Division, Poughkeepsie, New York 12602

Perfluorinated hydrocarbons are of considerable interest to investigators in fields as diverse as medicine and electrical engineering. However, for those investigators working with these compounds, the separation and identification of multicomponent isomeric mixtures have been a difficult matter. Reed (1) studied the gas-liquid chromatographic separation of  $C_5$ ,  $C_7$ , and  $C_9$  fluorocarbons on six stationary phase liquids. He reported that fluorocarbon and chlorofluorocarbon stationary liquid phases gave better resolution of fluorocarbon mixtures than hydrocarbon phases, but that they could not separate closely boiling isomers as effectively. Reed then reported the separation of the  $C_6F_{14}$  isomers (2) and later the separation of  $C_7F_{16}$  isomers (3) by use of *n*-hexadecane on Chromosorb-P. However, it was necessary to use a column that was 17 meters in length to accomplish the separation. The use of this column for the separation of higher molecular weight fluorocarbon isomers is limited by the fact the *n*-hexadecane has a narrow operating range (20–50 °C).

Green and Wachi (4) reported the separation of certain low molecular weight perfluorocarbons ( $C_3$ – $C_4$ ) by use of gas-solid chromatography on a temperature programmed silica gel column. Later, Wright and Askew (5) showed that the use of silica gel could be extended to separate the perfluoroalkanes into molecular weight classes from  $CF_4$  to  $C_8F_{18}$ , but the separation of isomers was not realized.

Certain tests performed in our laboratory required the use of a column for analyzing perfluorocarbon isomeric mixtures ranging from  $C_4$  to  $C_9$ . Therefore, a column other than those found in the literature was necessary. The use of graphitized carbon black has been reported by various investigators (6–10) as an efficient method for separating hydrocarbon isomers. The objective of this study was to compare the general separation characteristics of selected hydrocarbons and perfluorocarbons on this adsorbent.

### EXPERIMENTAL

The graphitized carbon black (GCB) used in this study was 80/100 mesh Carbowax C (Supelco, Inc., Bellefonte, Pa.), which has a surface area of 12 m<sup>2</sup>/g. A moderately polar stationary phase, SP-1000 (0.1% w/w), prepared from Carbowax 20M and a derivative of terephthalic acid, was used to modify the surface of the Carbowax C. The columns used were 6 ft × 1/4 in. o.d. × 4 mm i.d. and made of glass. They were purchased from Supelco, Inc., prepacked with the above GCB and modifier. The columns were conditioned before use for 14 h at 175 °C.

The gas chromatograph on which retention data were measured was a Hewlett-Packard series 700. Thermal conductivity, with helium as the carrier gas, was used for detection. The carrier flow rate was measured with a soap-bubble flowmeter at the column exit. Oven temperature was measurable to ±0.5 °C by the use of an external thermocouple system more sensitive than the one on the HP-700.

The sample size used for GC analysis was, in each case, 0.5 µL. Each sample was approximately a 2:1 mixture of perfluorocarbon (or hydrocarbon) to *n*-hexane.

The hydrocarbons used were reagent grade chemicals obtained from Aldrich Chemical Co., Milwaukee, Wis. Commercial samples of *n*-perfluoropentane and *n*-perfluorohexane were obtained from the 3M Co. Other perfluorocarbons were obtained from Pierce Chemical Co., Rockford, Ill., with the exception of perfluoro-2-methylpentane, which was a gift from Farbwerke Hoechst, Germany.

Commercial samples of  $C_2F_{10}$ ,  $C_3F_{14}$ , and  $C_7F_{16}$ , when analyzed, produced many impurity peaks. Subsequently, these samples were analyzed by gas chromatography-mass spectrometry (Hewlett-Packard 5982A) to confirm the elution order of the compounds of interest. Chemical ionization with methane and electron impact ionization modes were used to assign empirical formulas to eluting components. Structural assignments were made by spiking mixtures with the known compound whenever possible. A separate 6 ft × 1/4 in. o.d. × 4 mm i.d. glass column, with 0.1% SP-1000 on Carbowax C, was used for the GC/MS work. Sample spiking with known compounds was employed to confirm that the elution order of compounds on both columns reported in this study was the same.

### RESULTS AND DISCUSSION

A preliminary evaluation of unmodified graphitized carbon black columns showed that the elution order of components was not affected by the presence of the modifier described in the Experimental section. Rather, retention times were considerably longer and peak shape was poorer because of tailing. Increasing the percentage of the liquid modifier had the effect of decreasing retention time and eventually resulted in a loss of separation. Because of the above behavior, only a column with a low level of modifier was employed in this study.

The retention behavior of selected hydrocarbons and perfluorocarbons is tabulated in Table I, which gives the values for adjusted retention time and for retention time relative to an internal standard (*n*-hexane) at 120 °C. When homologous compounds are being separated, retention time increases with increasing molecular weight. Spherical molecules elute with shorter retention times than straight chain molecules having the same molecular weight, and the isomer having the greatest spherical geometry has the shortest retention time. Additionally, it was observed that for all compounds tested, the fluorocarbon has a shorter retention time than the corresponding hydrocarbon, indicating a weaker interaction with the adsorbent surface.

The similarity of the elution sequence observed for the hydrocarbons and perfluorocarbons in Table I indicates that the nature of the basic interaction with the adsorbent surface is the same for both classes of molecules. Likewise, the slopes of the lines obtained from plots of the log of the capacity ratio  $k'$  vs. the inverse temperature indicate that for both classes of compounds, the temperature dependency of the interaction between the sample and the adsorbent decreases in the order alkenes ≥ alkanes ≥ cyclic structures.

Since the fluorine atom is larger than the hydrogen atom,



## Removal of Soluble Organic Matter from Rock Samples with a Flow-Through Extraction Cell

Matthias Radke, Hans G. Siltardt, and Dietrich H. Wette\*

Programmgruppe für Erdöl und Organische Geochemie der Kernforschungsanlage Jülich GmbH, D-5170 Jülich, West Germany

Research in Organic Geochemistry frequently deals with organic matter extracted from sedimentary rock samples using organic solvents such as methylene chloride, chloroform, and benzene-methanol mixtures. Extract yield values are used as indicators for evaluating the degree of diagenesis and the oil-generating potential of source rocks. In Environmental Sciences, extraction yields are of interest in many respects, e.g., to discover pollution of recent sediments. High precision of extract yields has to be considered as a primary condition for proper interpretation of results. High-speed extraction of samples is desirable whenever organic geochemical methods are used during petroleum exploration.

Of the several extraction devices which have appeared in the literature, the Soxhlet apparatus is most widely used (1) although it has the disadvantage of poor reproducibility (2) and long extraction times (3-5). Exhaustive pre-extraction of extraction thimbles is also required (6-8) which is considered too time consuming for routine work. The use of solvent mixtures is generally restricted to azeotropic mixtures (9). Attempts have been made to achieve better reproducibility using special extraction apparatus (2, 10), or to cut down extraction time by application of ultrasonics (11, 12) or mechanical shredding (13).

The "flow-blending" method described in this article provides both good precision and short extraction time. Solvent mixtures other than azeotropes may be used. In contrast to conventional techniques, blending is carried out in a small cell through which the solvent-solid slurry is continuously recirculated.

Elemental sulfur is often present in sedimentary rock samples, either indigenous or artificially produced during field handling and laboratory preparation of the samples (14). Because of its solubility in organic solvents, free sulfur is removed from the rock matrix in procedures used for solvent extraction of rock samples (15). As the extracted organic matter is determined by weight, sulfur has to be removed from the extraction mixture prior to sample recovery. In the flow-blending method, copper powder which is capable of quantitative removal of free sulfur is used for this purpose.

Different methods for removal of elemental sulfur from extracts are known from the literature. The use of copper was first described by Blumer (15) and is now the reagent most widely used for this purpose. Precipitated copper powder, prepared using the Blumer method, is obtained in a highly active form, while products available from commercial sources need to be activated before use, i.e., copper oxide has to be removed from the surface by treatment with nitric or hydrochloric acid (16). Problems arise from handling and storage of activated copper as it is readily deactivated by exposure to air, especially if copper powder (15), gauze (16), wool (17) or granule (18) is used.

The flow-blending method differs from conventional procedures in that commercial copper powder is used without further treatment, activation being due to the abrasive action of the blender blades and the rock powder during the extraction procedure.

### EXPERIMENTAL

**Apparatus.** Extractions were carried out in an apparatus of special design (Figure 1). The basic principle of this pump/blender is that a tight fitting cylinder incorporating two blades

(the rotor) revolves in a slitted cylinder (the stator). The relative movement of the stator and rotor serves both to pump the slurry and to grind the entrained particles.

An ILAD rotor-stator system Model 21/G with driving motor Model X 10/20, speed regulating device Model T 600, and flow-through cell Model 22/Z (Internationale Laboratoriums—Apparate GmbH, D-7801 Ballrechten-Dottingen, Germany) was modified by replacing the nozzles of the original cell by stainless steel cones. FIVAC Teflon bellows adaptor Model FVB/2 (Fisons Scientific Apparatus, Loughborough, Leicestershire) provided a flexible connection with small dead volume. All other parts were manufactured from standard glassware. A set of four flow-through vessels (0.5 L, 1.0 L, 2.5 L, 5.0 L) and corresponding circulation pipes were used throughout this study. The apparatus may easily be adapted for use with larger volumes if required. The length of the flow-through vessel should be increased rather than its diameter, in order to maintain good flow-through characteristics. The shape of the circulation pipe is critical for proper action. The inner diameter must be 18 mm and the bends rectangular. Teflon spray was applied to the glass-to-glass and the glass-to-metal joints before they were fixed by clamps or springs. In order to achieve complete discharge of the extraction mixture, the apparatus was mounted in a position differing from Figure 1 in that it was rotated ca. 20° clockwise about the horizontal axis.

Soxhlet apparatus heated by six-place water baths were used to make comparative extractions. Water was kept circulating through pairs of baths by centrifugal pumps keeping temperature gradients at a minimum. Spectrophotometric measurements were made with a Perkin-Elmer Model 551 UV-VIS spectrophotometer.

**Samples.** Pulverized outcrop rock samples from West Germany (No. 1-15, Table III) and oil shales from Brazil (No. 16, 17, Table III) and Austria (No. 18, Table III) were used for extraction experiments. Initial particle size is not critical for the flow-blending technique but should be less than 150 µm to prevent the rotor-stator system from clogging. Initial particle size distribution determined from samples used in this study was: 52% less than 63 µm, 30% 63-125 µm, 17% 125-200 µm, and 1% greater than 200 µm. Grain size distribution of the residual sediment after 10 min extraction (which is critical for extraction efficiency): 70% less than 63 µm, 24% 63-125 µm, 6% 125-200 µm, and no particles greater than 200 µm.

**Reagents.** Analytical reagent grade methylene chloride (E. Merck, Darmstadt, Germany) was dried over anhydrous calcium chloride and distilled. Next 0.1% v/v anhydrous methanol was added as stabilizer. The solvent was checked to contain less than 0.3 mg/L of impurities which were not volatile under the conditions employed for sample recovery (19).

Analytical reagent grade fine copper powder was obtained from E. Merck. Coils made from 0.5 × 5 cm strips of copper foil (thickness 0.1 mm, E. Merck) were activated immediately before use by treatment with hot hydrochloric acid and washed successively with water, acetone, and methylene chloride (16).

Neutral Aluminum Oxide 90, active for column chromatography (E. Merck), was partially deactivated by adding 2.5% distilled water. Flowers of sulfur were heated for several hours to 100 °C before use to ensure complete conversion of any amorphous sulfur into the soluble crystalline form (16, 20).

**Extraction Procedures.** "Flow-Blending" Method. The flow-through vessel was charged with 0.5 L of methylene chloride, the speed regulation device set to position 4, and the motor started. At this setting the quantity of solvent delivered by the rotor-stator system was found to be 14.8 L/min at 19600 rpm. One hundred grams of pulverized rock sample and 1 g of copper powder were added to the stream of circulating solvent. After 10 min, the mixture was discharged into centrifuge tubes and centrifuged 5 min at 5000 rpm. The extract was decanted and most of the



Table I. Precision Data of "Flow-Blending" and Soxhlet Method

Run No.	Extraction yield, ppm		
	Flow-Blending method	Soxhlet method	
	a	a	b
1	5059	6177	6682
2	5409	5497	6954
3	5315	5556	5652
4	5442	4653	5706
5	5119	6333	5426
6	5181	5426	6410
7	5431		
8	5328		
9	5402		
10	5549		
Mean, ppm	5324	5607	6138
Std dev	157	602	626
Rel std dev, %	3.0	10.7	10.2

<sup>a</sup> From 100 g rock sample No. 14. <sup>b</sup> From 50 g rock sample No. 14.

Table II. Linearity of Extraction Yield vs. Sample Weight

Sample weight, g	No. of expts	Average extraction yield	
		mg	ppm
1	2	5.75	5750
10	2	53.75	5375
20	4	113.4	5670
40	2	229.4	5735
50	4	259.0	5180
60	2	352.5	5875
80	2	431.4	5393
100	4	546.6	5466
1000	2	5502.0	5502

solvent was evaporated under reduced pressure on a rotary evaporator. The concentrate was then transferred to a 5-mL vial, placed in the hole of an aluminum heating block (40 °C) and the solvent removed completely by a slow stream of nitrogen.

**Soxhlet Method.** One hundred grams of pulverized rock sample were placed into a pre-extracted thimble and extracted with 400 mL of boiling methylene chloride for 20 h. Solvent removal from the extract was performed as described above.

**Sulfur Removal.** To measure the effectiveness of copper powder as a reagent for removing elemental sulfur, increasing amounts of copper powder ranging from 100 mg to 1.5 g were added to solutions of 100 mg of sulfur in 0.5 L methylene chloride.

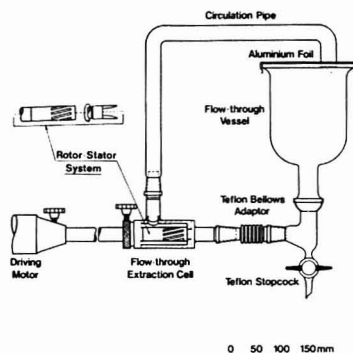


Figure 1. "Flow-blending" extraction apparatus

Then 20 g of alumina or 20 g of pre-extracted pulverized carbonaceous rock were introduced prior to copper powder in successive experiments. The mixtures were circulated for 10 min each under the conditions given for the extraction procedure. Aliquots of the mixtures were filtered and 0.5 mL of the filtrates diluted to 10 mL by addition of methylene chloride. The absorbance of the resulting solutions were measured at 260 nm (20, 21) vs. a blank of the same solvent. The measured absorbance was then compared with that given by the calibration plot. Blanks were run on sulfur solutions showing that the absorbance was not influenced by the addition of alumina or pre-extracted rock samples.

Elemental sulfur was removed from Soxhlet extracts by a coil of activated copper foil located in the extraction flask throughout the extraction procedure (22). If the surface of the copper foil was covered completely by black sulfide, more strips were added until the surface of the last strip added remained unchanged.

## RESULTS AND DISCUSSION

The yield of extract as a function of extraction time was determined. The results are shown in Figure 2. The end point of extraction, taken as the point where a doubling of the extraction time gives less than a 5% increase in yield, was reached after 10 min. Precision was evaluated for the flow-blending and the Soxhlet method as shown in Table I. Poor precision of the Soxhlet method is at least partly due to the fact that constant boiling of the solvent generally is not achieved (9). Furthermore, the Soxhlet method was found

Table III. Comparison of Extract Data, Soxhlet Method vs. "Flow-Blending" Method

Sample No.	Era	Lithology	Extraction yield, ppm	
			Flow-Blending method	Soxhlet method
1	Up. Permian	Limestone	25	37
2	Md. Jurassic	Shale	42	43
3	Lw. Cretaceous	Shale	58	42
4	Up. Devonian	Limestone	72	69
5	Up./Md. Jurassic	Marl	92	80
6	Lw. Jurassic	Marl	126	118
7	Md. Jurassic	Shale	150	170
8	Up. Permian	Marl	282	288
9	Md./Lw. Jurassic	Marl	658	636
10	Lw. Cretaceous	Shale	704	550
11	Lw. Cretaceous	Shale	3040	2960
12	Up. Permian	Marl	3638	2302
13	Lw. Cretaceous	Shale/Coal	4812	4220
14	Lw. Jurassic	Marl	5324	5607
15	Md. Eocene	Shale	9308	7613
16	Up. Permian	Shale	16472	11998
17	Up. Permian	Shale	18618	16655
18	Up. Triassic	Shale	28649	26597

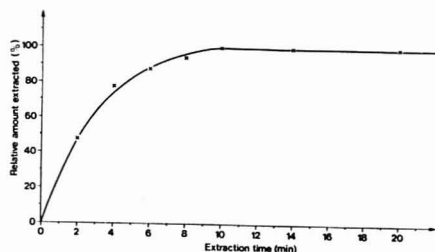


Figure 2. Influence of extraction time upon extraction yield

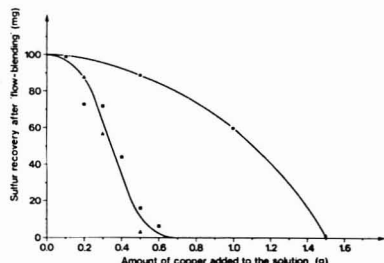


Figure 3. Sulfur removal by copper powder. (●) Copper only, (▲) copper and alumina, (■) copper and carbonaceous rock

lacking in that the surface area of sediment particles efficiently washed by percolating solvent may decrease markedly during extractions due to the compaction of the sample or the channeling of the solvent (2).

Problems arising from insufficient contact between particles and solvent have been overcome by application of the flow-blending method. The sample is finely dispersed in the circulating solvent by the action of the rotor-stator system. Particle surface area is increased rather than decreased by the impact of shear forces and cavitation as particles pass the blending cell. Kerogen degradation which may occur during extractions using high energy ultrasonics (11) and which can blur the determination of the extraction end point, was not observed using the flow-blending method.

The yield of extract as a function of sample weight was determined. A least-squares fit of data from Table II gave a regression equation  $y = 5.501 \times 10^{-3}x + 0.793 \times 10^{-3}$  g with

a correlation coefficient  $r^2 = 0.99996$ .

Extraction yields obtained by the flow-blending and the Soxhlet method are closely correlated as shown in Table III. Regression of Soxhlet (y) vs. flow-blending (x) values yielded  $y = 0.885x - 84.65$  ppm. The correlation coefficient  $r^2$  of the data was 0.9886.

As shown in Figure 3, efficiency of copper powder as a reagent for removing elemental sulfur was markedly increased as alumina or carbonaceous rock was added. One gram of copper powder added to the extraction mixture will remove up to 150 mg of free sulfur.

#### ACKNOWLEDGMENT

We express our appreciation to W. Seemann for providing the samples and C. Cornford for reading the manuscript and proposing the name "flow-blending" method.

#### LITERATURE CITED

- (1) L. C. Craig and D. Craig in "Technique of Organic Chemistry", Vol. III, Part 1, "Separation and Purification", A. Weissberger, Ed., Interscience Publishers, New York, N.Y., 1956, p. 149.
- (2) W. S. Ferguson, *Bull. Am. Assoc. Pet. Geol.*, **46**, 1613 (1962).
- (3) J. L. Oudin, *Rev. Inst. Fr. Pet.*, **25**, (1), 3 (1970).
- (4) V. T. Vuchev, W. G. Howells, and A. L. Burlingame in "Advances in Organic Geochemistry 1971", H. R. v. Gertner and H. Wehner, Ed., Pergamon Press, New York, N.Y., 1972, p. 365.
- (5) H. Dembrick, Jr., W. G. Meinschein, and D. E. Hattin, *Geochim. Cosmochim. Acta*, **40**, 203 (1976).
- (6) J. M. Hunt in "Advances in Organic Geochemistry 1973", B. Tissot and F. Blenner, Ed., Editions Technip, Paris, 1974, p. 593.
- (7) J. W. Farrington, S. M. Henrichs, and R. Anderson, *Geochim. Cosmochim. Acta*, **41**, 289 (1977).
- (8) E. D. John and G. Nickless, *J. Chromatogr.*, **138**, 399 (1977).
- (9) D. G. Peters, J. M. Hayes, and G. M. Hietfle in "Chemical Separations and Measurements: The Theory and Practice of Analytical Chemistry", W. B. Saunders Company, Philadelphia, Pa., 1974, p. 504.
- (10) M. Vandenbroucke, *Ref. A*, p. 547.
- (11) R. D. McIver, *Geochim. Cosmochim. Acta*, **26**, 343 (1962).
- (12) M. T. J. Murphy in "Organic Geochemistry", G. Eglington and M. T. J. Murphy, Ed., Springer Verlag, New York, N.Y., 1969, p. 74.
- (13) C. Golden and E. Sawicki, *Anal. Lett.*, **9**, 957 (1976).
- (14) J. G. Palacas and A. H. Love, *U.S. Geol. Survey Prof. Pap.*, **800-D**, D67 (1972).
- (15) M. Blumer, *Anal. Chem.*, **29**, 1039 (1957).
- (16) W. N. Tuller in "The Analytical Chemistry of Sulfur and Its Compounds", Part I, J. H. Karchmer, Ed., Interscience Publishers, New York, N.Y., 1970, p. 1.
- (17) P. Gearing, J. N. Gearing, T. F. Lytle, and J. S. Lytle, *Geochim. Cosmochim. Acta*, **40**, 1005 (1976).
- (18) D. H. Welte, *Geol. Rundsch.*, **55**, (1), 131 (1965).
- (19) E. D. Evans, G. S. Kenny, W. G. Meinschein, and E. E. Bray, *Anal. Chem.*, **29**, 1858 (1957).
- (20) R. M. Cassidy, *J. Chromatogr.*, **117**, 71, (1976).
- (21) J. E. Baer and M. Carmack, *J. Am. Chem. Soc.*, **71**, 1215 (1949).
- (22) D. Leythaeuser, *Geochim. Cosmochim. Acta*, **37**, 113 (1973).

RECEIVED for review July 26, 1977. Accepted November 4, 1977. Work supported by the Government of the Federal Republic of Germany, Energy Research and Development Program No. 3.2.1.

## Computer Interfaceable Potentiostat

Basil H. Vassos\* and Guillermo Martinez

Chemistry Department, University of Puerto Rico, Rio Piedras, Puerto Rico 00931

The present design is of a potentiostat suitable for use in automated environments, for example in computer-controlled electrochemistry. The requirements for such an instrument are: stability in operating with a variety of cell configurations, absence of manual adjustments, and a balanced correction of various errors. This last feature is important in a general purpose instrument, since various error corrections tend to

operate at the expense of each other. The features we considered in this design were the following.

(a) **Uncompensated Resistance Correction.** There is a long history (1-5) of preoccupation with this correction. Although complete computer correction of this fault is possible (6), most potentiostats use positive feedback for this purpose, which brings the system just short of self-oscillation. We

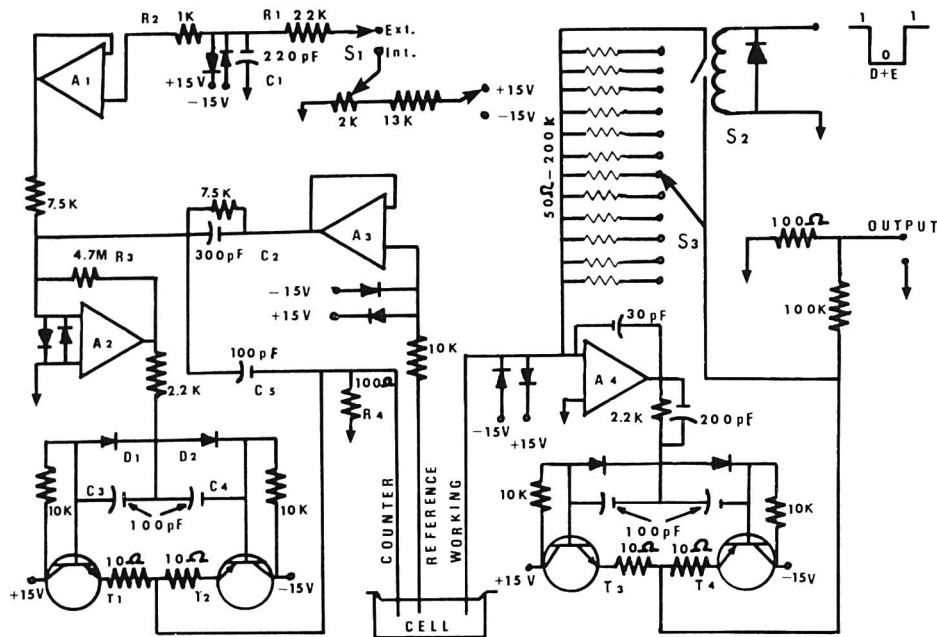


Figure 1. Schematic of the potentiostat. All diodes are type 1N 4448.  $T_1$ ,  $T_2$  are TIP 29, while  $T_3$  and  $T_4$  are TIP-30 transistor (Texas Instruments). All capacitors are ceramic disk.  $A_1$  is a 741, all the other operational amplifiers are 40J (Analog Devices). The 2-k $\Omega$  variable resistor is a Helipot. The power supply used is a model giving 350 mA at  $\pm 15$  V. The relay  $S_2$  is a model SIGMA 191TE 1 A 1-55.

eliminated this feature for the sake of automatic use under changing conditions, but the feature can be added later. Note also that many recent application of potentiostats (1-9) still use the classical three-amplifier system (10) and no particular correction, with acceptable results.

(b) **Matching of Load and Controller.** Another procedure that was considered and discarded is the electrical matching of potentiostat and cell. While this can result in spectacular performance (2, 11) we preferred to have a system that behaves satisfactorily under a wide range of conditions rather than optimally for only a particular load.

(c) **E/I Gain Switching.** A rather serious limitation in the response time of the system is the current limitation caused by the current-measuring resistor.

For example, at the 1- $\mu$ A range, a 100-k $\Omega$  current measuring resistor is needed for a 100-mV output. With this resistor, the slewing rate on charging a 1- $\mu$ F cell capacitance is of 1 V in 10 ms which is too slow for many purposes.

In order to improve the rise time, one can use one of three methods: (1) Decrease the value of the current-measuring resistor. This means a lower output of, for example, 1 mV full scale, which causes a degradation in the S/N ratio. (2) Use of a Zener diode or a similar nonlinear device in parallel with the current-measuring resistor. The approach is acceptable except for some noise generated in the Zener region and for the reverse leakage of the diode. (3) Use of a switching system (the approach we took), to substitute a short circuit during the periods when actual current measurements are not made.

In our system, the I/E function is done by amplifier  $A_4$  in Figure 1, the switching system (clamp) is done by the relay controlled by a logic signal. Upon receiving a logic "0" input,

the instrument operates normally, while a "1" input shorts out the I/E resistor. The major utility of such clamps is when the signal applied involves large transitions, at high sensitivity settings. In such cases, the "rise time" can become very large in the sense that the system saturates for a long period while pumping slowly the charging current through the current measuring resistor. In Figure 2b is shown, such a case where the output of the I/E amplifier stayed at the saturation (10 V) for the whole rise time. Note that during this time, the summing point lifts off-zero and gives a false cell potential for the whole saturation period. In contrast, when the signal (c) was applied to the cell, which was switched to a high current mode (clamp) for a few milliseconds, the faradaic current emerged clearly with practically no charging current left (d). Note that the clamp need not be as long as the one used above, usually one millisecond or less will suffice. Note also the elimination of the saturation when using the clamp. This logic controlled system is useful if the potentiostat is driven by a controller such as a digital computer. More modest setups, as for instance using square wave generators to drive the potentiostat, can also be coped with. A single integrated circuit, a monostable, can provide a short clamping pulse at each transition for momentary gain switching and accommodate the steep rise times of the square wave without any difficulty.

(d) **Use of a Pre-Filter.** Due to various limitations, for a general purpose instrument, a rise time of 10  $\mu$ s and a frequency band up to 50 kHz are both a realistic and an adequate design target. This allows for over 1000 V/s cyclic voltammetry rate (12). Note also that general purpose cells will have uncompensated RC time constants of several micro-seconds, indicating no real need for speeds beyond the 10

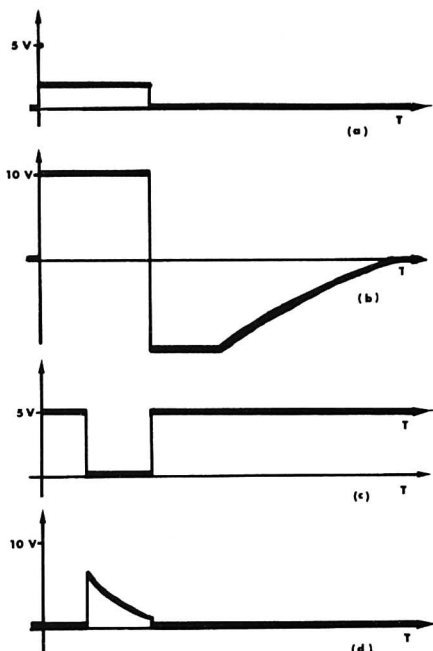


Figure 2. Example of clamp. (a) Applied pulse, (b) Output of I/E showing saturation during the entire pulse and for some time afterwards, (c) clamp: a "window" type clamp, that opens to read during the time of interest and keeps the output clamped otherwise, (d) Resulting output

$\mu$ s rise time mentioned above (13). This being the case, it is very advantageous to limit the frequency response of the signal before it is applied to the potentiostat. The reason is that the operational amplifiers, when submitted to rise times faster than they can accommodate, enter in a special form of saturation caused by the absence of the negative feedback. During this time, the amplifier simply does not respond to the input wave-form, but sails instead on the same course regardless of the input. This is followed by oscillation on reaching the top of the transition, and eventually the system settles. This type of misbehavior has been long recognized in audio engineering as transient intermodulation distortion, TIM. A large feedback capacitor does not resolve the problem too well, even though it removes some of the nonlinear behavior present by acting as an active filter.

The solution we adopted is to design the system, not only the potentiostating amplifier, for the desired response. For this purpose the amplifier  $A_1$ , in input follower, was given the wave-shaping function by means of the  $R_1C_1$  circuit. It limits the waveforms to a rise time of about 5  $\mu$ s. Once this wave shaping burden is removed from the potentiostating amplifier  $A_2$ , the latter can be easily designed for optimal stability. At no time now is  $A_2$  limited by its slow rate; consequently the transient distortion disappears. In its place appears some frequency band limitation, but this is now done by smooth linear elements  $R_1C_1$ , and not by a saturated amplifier. Another consequence is that it is now possible to use more freely phase-lead compensation, in order to correct the crossover distortion (see section e below). Since phase lead increases with frequency, it is difficult to avoid instability or

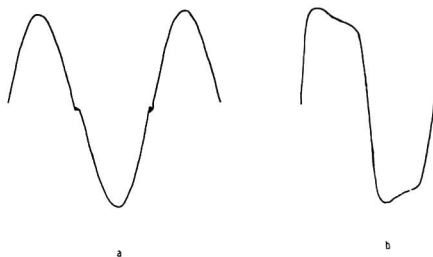


Figure 3. (a) Example of crossover distortion. (b) The square wave response at minimum sensitivity  $E/I$  mode. The amplitude is 1.2 V and the repetition rate is 5 kHz. Most of the rounding off of the square wave comes from double layer charging. A purely resistive dummy cell gives a very clean practically square output

oscillations if steep waveforms are encountered; as it is, the system is stable with only 100 pF of phase lag compensation, capacitor  $C_5$ , and the phase lead discussed below.

Additional stability elements are provided by  $R_3$  and  $R_4$ . It has been shown (14, 15) that instability occurs in some systems at high frequency and high load resistance. Consequently we provided for a minimum load of 100  $\Omega$ , which was found to improve the transient behavior, even though it is a bit wasteful of power. It can be left out without ill effects.

The resistor  $R_3$  serves to limit the effective open loop gain of  $A_2$  to about 500. It might appear unwise to cut so low the gain (of 200000) of the amplifier used (40J). In reality, because of gain-bandwidth considerations, this amplifier maintains the full gain only up to about 10 Hz, after which it drops continuously. By the addition of  $R_3$ , the response becomes flat (at a lower level) from dc into the kilohertz region. This smooth frequency response makes for a much cleaner transient behavior. Of course an error is introduced, proportional to the reciprocal of the new gain, but  $1/500$  is quite an acceptable precision (16).

It must be also mentioned that, for really stable operation, one must select very carefully the amplifier types used. We found the ubiquitous 741 and the Analog Devices type 40J to be very satisfactory. Many other amplifiers showed various dynamic idiosyncrasies. In any case it is very advisable to always use the same type of amplifier for  $A_2$ ,  $A_3$ , and  $A_4$ .

(e) **Crossover Distortion.** This type of error is produced by the finite time needed to switch back and forth from the NPN to the PNP transistors in the power stage, and generates a hesitation on a sine wave on crossing zero, visible as a bright dot on the scope. At higher frequencies and very small amplitudes, around zero, the effect can be so strong as to make the response unrecognizable. This form of distortion did not receive too much attention in potentiostat design, since it is visible only in the particular conditions mentioned above (Figure 3a).

The crossover distortion is best fought by some phase-lead compensation. In our case,  $C_3$  and  $C_4$  prove to be adequate. An alternate approach would be to increase the current into diodes D1 and D2 which will ensure a continuous biasing on of the transistors  $T_1$  and  $T_2$ , and to decrease the value of their emitter resistor. This approach though, we found out, could lead into self-destruction of  $T_1$  and  $T_2$ . Some potentiostat designs used one single power transistor, with elimination of the cross over between PNP and NPN (17), at the expense of versatility.

**Use and Performance.** The potentiostat can be used manually at a fixed voltage by selecting with switch  $S_1$ , the internal voltage source, the 2-K helipot. In the same time switch  $S_2$  must be connected to "0V" to remove the clamp.

For automatic use, the control of the relay is done remotely, and a control voltage is introduced through  $S_1$ . The data at the output is attenuated to 1 mV for recording purposes; this can be changed to suit. The potentiostat was used under various conditions and showed exemplary behavior at small amplitude around zero. For larger transitions, the clamp could cope easily with 1-V steps on 5- $\mu$ A scale. An example of transient behavior, in the absence of clamping, is shown in Figure 3b where the response of the system is shown at the highest current range. The cell solution used was 0.01 M  $K_2SO_4$  and 0.01 M  $H_2SO_4$  and the working electrode was of platinum wire. At 1.2-V square wave produces about 10  $\mu$ s of rise time with moderate overshoot and no instability. Large transitions at low current setting are accommodated by clamping. The relay used allows about 1 ms of reliable operation which is satisfactory for most applications.

In conclusion, the present design, at low signal amplitude and with small current measuring resistors is able to operate within about 3% dynamic error to about 30 kHz sine and 50- $\mu$ s rise times. Useful response extends to 60 kHz sine waves and 10- $\mu$ s rise times. Low frequency operation is error free.

When using large voltage steps in dilute solutions and a high current measuring resistor, the effective rise time is maintained to about a millisecond by clamping. The speed of the clamping relay (0.2 ms) is here the limiting factor. FET switching was experimented with and shown to give faster response, but we prefer the relay for reasons of simplicity and reliability.

The authors have more detailed construction details available for persons interested in duplicating the construction, as well as some details about preliminary work to program completely automatically the gain of the  $I/E$  section.

## LITERATURE CITED

- (1) F. Haber, *Z. Phys. Chem.*, **32**, 193 (1900).
- (2) G. L. Booman and W. B. Holbrook, *Anal. Chem.*, **37**, 795 (1965).
- (3) R. R. Schoeder and I. Shain, *Chem. Instrum.*, **1**, 233 (1969).
- (4) J. E. Mumby and S. P. Perone, *Chem. Instrum.*, **3**, 191 (1971).
- (5) C. Lamy and C. C. Herrmann, *J. Electroanal. Chem.*, **59**, 113 (1975).
- (6) C. Yanitzki and Y. Friedman, *Anal. Chem.*, **47**, 880 (1975).
- (7) K. S. Stulick and V. Hora, *J. Electroanal. Chem.*, **70**, 253 (1976).
- (8) J. P. Van Dieren, B. G. W. Kaars, J. M. Los, and B. J. C. Wetsema, *J. Electroanal. Chem.*, **68**, 129 (1976).
- (9) J. Deroo, J. P. Diard, J. Guitton, and B. Le Gorrec, *J. Electroanal. Chem.*, **67**, 263 (1976).
- (10) M. T. Kelley, H. C. Jones, and D. J. Fisher, *Anal. Chem.*, **32**, 1263 (1960).
- (11) See ref. 4.
- (12) J. L. Anderson, *Chem. Instrum.*, **7**, 25 (1976).
- (13) K. B. Oldham, *J. Electroanal. Chem.*, **11**, 171 (1966).
- (14) D. K. Roe, *Chem. Instrum.*, **4**, 15 (1972).
- (15) J. E. Davis and E. C. Toren, *Anal. Chem.*, **46**, 647 (1974).
- (16) B. H. Vassos and G. W. Ewing, "Analog and Digital Electronics for Scientists", J. Wiley, New York, N.Y., 1972, p. 163.
- (17) T. S. Randhawa and R. L. Sotherwell, *Analyst (London)*, **100**, 726 (1975).

RECEIVED for review September 7, 1977. Accepted December 7, 1977. Acknowledgement is made to the Office of Coordination of Research and to the Center for Energy and Environmental Research of the University of Puerto Rico for financial support.

## Technique for the Prevention of Column Contamination in Pyrolysis Gas-Liquid Chromatography

Annabel Mitchell and Manuel Needleman\*

Victorian College of Pharmacy, 381 Royal Parade, Parkville, Victoria, Australia, 3052

There has been an increasing interest in the past decade in the application of pyrolysis gas-liquid chromatography to the identification of microorganisms. It is surprising, therefore, to observe that the problem of column contamination has been mentioned only recently (1, 2). The contamination, which evidences itself as a tarry deposit on the column after approximately 100 h of column use, results in a loss of resolution, with a concomitant decrease in long-term reproducibility (2), and is most marked when capillary columns are used.

Attempts have been made to solve the problem by repacking (3) or removing (1) the first section of the column. Alternative proposals have been to use long precolumns (1) and backflushing of the column after each chromatographic run (2). Experiments using the latter idea showed that high boiling contaminants still built up insidiously on the column, and a significant fraction, once deposited, was resistant to backflushing. Therefore, the final successful arrangement, shown in Figure 1, incorporated a short disposable precolumn and effectively amalgamated the above-mentioned proposals.

## EXPERIMENTAL

All apparatus and procedures, except for those detailed below, have been previously described (2).

The glass precolumn shown in Figure 1 was obtained by cutting a 1-m length from a column similar to the main SCOT column. The columns were connected with glass-lined steel tubing, which was also used for the ancillary plumbing.

The diagram shows how closing the valve (MNVV needle valve, Scientific Glass Engineering, Melbourne) changes the gas flow

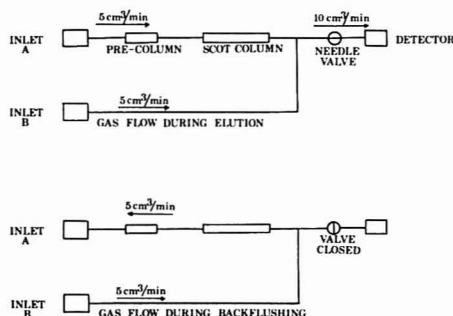


Figure 1. Backflush plumbing arrangement

pattern from the elution to the backflush mode. The sequence adopted was to raise the temperature to 180 °C, after elution was complete, then to remove the pyroprobe from inlet A, leaving it open, and to backflush for 1 h.

## RESULTS AND DISCUSSION

This technique has been in operation for over 500 h of column use and no contamination of the main column has been observed. After about 200 h of use, the first 5 cm of precolumn showed some discoloration but, because of the disposable nature of the precolumn, this has not proved to



be a serious problem. The efficacy of the backflush procedure has been shown by the significant deposition of contaminants, similar to those previously observed, on the glass injection sleeve, which is replaced each time the pyroprobe is removed prior to backflushing.

Our experience has shown the advantages of using a precolumn, together with backflushing, as the main column has been kept free of contamination and the replacement frequency of the precolumn has been minimized, thus avoiding the regular replumbing involved in a precolumn system that does not incorporate backflushing. The relatively low cost

of the valve, allied to the advantages outlined above, makes this system an attractive alternative to an automatic backflush arrangement.

### LITERATURE CITED

- (1) P. A. Quinn, *J. Chromatogr. Sci.*, **12**, 796 (1974).
- (2) M. Needelman and P. Suchter, "Analytical Pyrolysis", C. E. R. Jones and C. A. Cramers, Ed., Elsevier, Amsterdam, 1976, p. 77.
- (3) M. V. Stack, H. D. Donoghue, J. E. Tyler, and M. Marshall, ref. 2, p. 57.

RECEIVED for review September 19, 1977. Accepted December 19, 1977.

## Gas Chromatographic Determination of Dissolved Hydrogen and Oxygen in Photolysis of Water

Steven J. Valenty

General Electric Corporate Research and Development, Schenectady, New York 12301

The use of visible light energy to decompose water into hydrogen and oxygen is a subject of current interest (1-3). The principal analytical tool used to detect the small amounts of gaseous products produced in these studies has been mass spectrometry. In an attempt to observe trace quantities of  $H_2$  and  $O_2$  which might be evolved during the photolysis of glass supported monolayer assemblies of surfactant derivatives of tris(2,2'-bipyridine)ruthenium(II) (2), a simple chromatographic method has been utilized and is reported here. Determination of traces of  $H_2$ ,  $N_2$ , and  $O_2$  in aqueous solutions by vapor phase chromatography has been reviewed by Tolk and co-workers (4). In the present method, the aqueous solution is injected directly onto a chromatographic column filled with molecular sieves and the eluting  $H_2$  and  $O_2$  monitored by a standard thermal conductivity detector. The validity of the hydrogen analysis was tested by using the acidic ferrocyanide/isopropanol system as a reference actinometer (5, 6).

### EXPERIMENTAL

**Materials.** Linde purified He and Ar were used as carrier gases. The argon was passed through a 20-in.  $\times$  0.375-in. stainless steel tube filled with activated "Ridox" (Fisher Scientific) to minimize the oxygen concentration. Molecular sieve 5A (60/80 mesh) was obtained from Supelco. Potassium ferrocyanide (Baker Analyzed), isopropanol (MCB Spectro), and perchloric acid (Baker Analyzed) were used for the hydrogen actinometry experiments as received with triply distilled water as solvent.

**Apparatus.** A Hewlett-Packard F & M Model 5750 Chromatograph equipped with a thermal conductivity detector and 0.125-in. sleeves in the injector block was utilized. The column (stainless steel, 0.125-in. o.d., 0.010-in. wall) is composed of two shorter columns coupled in series; both filled with 60/80 mesh molecular sieve 5A. The "water adsorbing" precolumn (0.5-m length) is attached to the injector followed by the longer (2.1 m) "gas separating" column. The column was activated by heating in a He stream at 300 °C for 4 h before use. Conditions for the gas analyses are given in Table I. The aqueous solutions are sampled by a 100  $\mu$ L "Pressure-Lok" series A-2 syringe which has a valve behind the needle such that samples can be transferred (and stored) in the syringe barrel without gas loss.

A 4-W germicidal lamp (General Electric G4T4-1, output >210 nm) in a convection cooled housing was attached to a thermostated brass photolysis cell holder such that the plane of the "U" shaped lamp was parallel to and 5 cm distant from the cell's front window. The light intensity was attenuated with fine copper mesh screen. Of the light incident on the cell face, 88% had a wavelength of 253.7 nm with the remainder not photochemically active.

Table I. Experimental Conditions

Condition	$O_2$ analysis	$H_2$ analysis
Carrier gas	He	Ar
Carrier gas flow, mL/min	60	40
Injector temp., °C	100	100
Column temp., °C	60	60
Detector temp., °C	100	100
TC filament current, mA	240	150
TC attenuator setting	1X	1X

Table II. Observed Analytical Data for Dissolved Gas Detection

Observation	$H_2$	$O_2$
Instrument calibration factor, mol/mm peak height	$8.4 \times 10^{-11}$	$1.3 \times 10^{-9}$
Minimum amount detectable, mol, S/N = 4	$1.7 \times 10^{-10}$	$2.5 \times 10^{-9}$
Maximum injection volume, $\mu$ L	50	100
Minimum concentration detectable, mol, S/N = 4	$3.4 \times 10^{-6}$	$2.5 \times 10^{-5}$
Precision, %	$\pm 10$	$\pm 10$
Linearity, % gas saturation	2-100	2-100
Retention time, min <sup>a</sup>	$0.9 \pm 0.1$	$1.1 \pm 0.1$

<sup>a</sup> See Table I for carrier gas and flow rate used.

The photolysis cell, constructed of either Teflon or Al alloy, is demountable and is assembled from four side pieces and two quartz windows using Teflon tape as gasket material around the perimeters of the windows. For these experiments, the light path through the cell is either 0.5 cm (ferrioxalate actinometry) or 0.1 cm (hydrogen actinometry) and the cell's contents accessed through a septum seal in the top. The cell front window was masked to provide a 2.3 cm  $\times$  2.6 cm opening.

A Perkin-Elmer Model 575 was used to record all ultraviolet and visible absorption spectra.

**Procedure.** Ferrioxalate actinometry was used for the light intensity determination at 254 nm (7). The light intensities used in this study are  $5.0 \pm 0.1 \times 10^{-9}$  einstein/s/cm<sup>2</sup> (bare lamp output) and  $4.5 \pm 0.1 \times 10^{-10}$  einstein/s/cm<sup>2</sup> (Cu mesh attenuated output).

Routine calibration was done by injecting known volumes of a  $H_2$  or  $O_2$  saturated aqueous solution ( $25 \pm 1$  °C, under 1 atm of pure gas) into the chromatograph. In another method, standard solutions containing less than saturation concentrations of  $H_2$  were prepared by 254 nm photolysis ( $I = 0.1$  cm, 25 °C) of a  $N_2$  purged aqueous solution (1.0 mL) containing:  $1.0 \times 10^{-3}$  M  $K_4[Fe(CN)_6]$ .

**Table III.** Comparison of  $H_2$  Actinometer and VPC Results

% Reaction <sup>a</sup> (No. of samples)	VPC % $H_2$ , satd $H_2O$ ( $\pm$ Err) <sup>b</sup>	Calcd % $H_2$ , satd $H_2O$ ( $\pm$ Err) <sup>c</sup>
0	0	0
7 (3)	6 (8)	5 (10)
14 (3)	10 (4)	10 (10)
28 (5)	15 (6)	19 (10)

<sup>a</sup> Calculated from the absorbance at 420 nm for  $[Fe^{III}(CN)_6]^{3-}$ ,  $\epsilon_{max} = 1.00 \times 10^3 M^{-1} cm^{-1}$ . <sup>b</sup> VPC %  $H_2$ , satd  $H_2O = (\text{Peak Height } H_2 \text{ at } t) / (\text{Peak Height } H_2 \text{ satd } H_2O) \times 100$ , where  $t$  is the photolysis time. <sup>c</sup> Calcd %  $H_2$ , satd  $H_2O = (\text{No. Moles } H_2 \text{ at } t) / (\text{No. Moles } H_2 \text{ in satd } H_2O) \times 100 = [(I_0/I_t)(\Phi_{H_2}^{21}) (t) / (7.6 \times 10^{-7} \text{ mL})] \times 100$ , where  $I_0 = 0.55$ ,  $I_t = 3.0 \times 10^{-4}$  einstein  $s^{-1}$ ,  $\Phi_{H_2}^{21} = 0.43$ ,  $t$  is the photolysis time.

$1.0 \times 10^{-3} M HClO_4$  and  $0.10 M$  isopropanol. The solutions were analyzed for  $H_2$  assuming  $\Phi_{H_2} = 0.43$  (5). Peak heights were measured with a millimeter ruler.

### RESULTS AND DISCUSSION

The analytical data observed for the detection of dissolved  $H_2$  and  $O_2$  are presented in Table II. While the maximum volume that can be injected directly on column is limited, this method has proved more sensitive and reproducible than two systems tested in this laboratory based on stripping the gases from a larger volume of solution (1–3 mL) by passing a finely dispersed carrier gas stream through the liquid before the drying and analyzing columns (8). The long term, transient (5–10 min) decrease in carrier gas flow following liquid injection results in an irreproducible baseline which effectively limits the size of injection. The use of larger diameter precolumns resulted in peak broadening and consequent decrease in sensitivity. Currently, the "water-absorbing" precolumn is changed after a total of ca. 1 mL liquid has been

injected. The reported procedure, while utilizing standard and readily available equipment, approaches the sensitivity for dissolved  $H_2$  detection ( $\sim 1 \times 10^{-6} M$ ) of the best published chromatography method (4) which requires specialized apparatus.

The photolysis of acidic aqueous ferrocyanide solutions containing the hydrogen atom donor isopropanol, was found to provide a useful calibrated source of  $H_2$  in subsaturation concentrations under conditions nearly identical to those employed for the monolayer experiments. As noted in Table III, the results of the two methods are the same at low conversions to ferricyanide. At conversions  $>15\%$ , deviations occur and become increasingly larger at higher conversions.

### ACKNOWLEDGMENT

I am indebted to P. Behnken, D. A. Bolon, G. L. Gaines, Jr., and J. E. Girard for loan of equipment and helpful discussions in the course of this work.

### LITERATURE CITED

- (1) K. R. Mann, N. S. Lewis, V. M. Miskowski, D. K. Erwin, G. S. Hammond, and H. B. Gray, *J. Am. Chem. Soc.*, **99**, 5525 (1977).
- (2) G. Spritschnick, H. W. Spritschnick, P. P. Kirsch, and D. G. Whitten, *J. Am. Chem. Soc.*, **99**, 4947 (1977); *ibid.*, **98**, 2337 (1976).
- (3) P. A. Jacobs, J. B. Vetterhoeven, and H. K. Beyer, *J. Chem. Soc., Chem. Commun.*, **1977**, 128.
- (4) A. Tok, W. A. Lingerak, A. Kout, and D. Börger, *Anal. Chim. Acta*, **45**, 137 (1969).
- (5) P. L. Airey and F. S. Dainton, *Proc. R. Soc. London, Ser. A*, **291**, 340, 478 (1966).
- (6) R. E. Hintze and P. C. Ford, *J. Am. Chem. Soc.*, **97**, 2664 (1975).
- (7) C. A. Parker, "Photoluminescence of Solutions", Elsevier, New York, N.Y., 1968.
- (8) J. W. Swinnerton, V. J. Linnenborn, and C. H. Cheek, *Anal. Chem.*, **34**, 483 (1962).

RECEIVED for review October 21, 1977. Accepted December 7, 1977. This research was partially supported by the Division of Basic Energy Sciences, Department of Energy (EG-77-C-02-4395).

## Separation of Rhodium-103m from Ruthenium-103 by Solvent Extraction

Jih-Hung Chlu, Robert R. Landolt,\* and Wayne V. Kessler

Bionucleonics Department, Purdue University, West Lafayette, Indiana 47907

A previous paper (1) reported a procedure for the separation of  $^{103m}Ru$  from  $^{103}Ru$ . The yield of  $^{103m}Ru$  was  $94 \pm 0.6\%$ , and the amount of  $^{103}Ru$  contamination was  $3.8 \pm 0.7\%$ .

Continued work to improve the separation procedure has resulted in one that is considerably better. The procedure of Meadows and Matlack (2), developed for the separation of radioruthenium from fission product waste, was modified and used in the initial steps. The yield of  $^{103m}Ru$  was quantitative and there was no measurable  $^{103}Ru$  contamination.

### EXPERIMENTAL

**Reagents.** A ruthenium carrier solution containing 3 g of ruthenium chloride (Alpha Products) in 500 mL of distilled water was prepared. The solution was filtered through Whatman 41 paper. SpectraAR grade carbon tetrachloride (Mallinckrodt) was used without further purification. Ruthenium-103 in equilibrium with  $^{103m}Ru$  was obtained from Amersham/Searle as ruthenium chloride in 4 N HCl. A stock solution containing  $1 \mu Ci$  of  $^{103}Ru/mL$  in 6 N HCl was prepared.

**Separation Procedure.** The procedure of Meadows and Matlack (2) was followed with modifications. A 0.5-mL aliquot

of the  $^{103}Ru/^{103m}Ru$  stock solution was placed in a 60-mL separatory funnel containing 2 mL of concentrated HCl and 2 mL of ruthenium carrier solution. With frequent swirling, 12 N NaOH was added dropwise until black ruthenium hydroxide precipitated. Ten more drops of NaOH was added, followed by 1 mL of 5% sodium hypochlorite with thorough mixing. The ruthenium hydroxide dissolved and the solution turned green. After 1 h, 10 mL of carbon tetrachloride was added, followed by dropwise addition of 6 N HCl, with swirling, until the color suddenly turned light yellowish green. Four more drops of HCl was added. The contents of the funnel were mixed for 1 min, and the carbon tetrachloride layer containing  $^{103}RuO_4$  was drained, leaving the  $^{103m}Ru$  in the aqueous layer. The aqueous layer was extracted with an additional 10 mL of carbon tetrachloride and was then drained into a graduated 50-mL centrifuge tube.

**Purification of  $^{103m}Ru$ .** The aqueous solution in the tube was gently boiled over a flame for 3 to 5 min until the volume was reduced to less than 10 mL. Suspended carbon tetrachloride, residual  $^{103}RuO_4$ , and residual chlorine evaporated. The solution was cooled and diluted to 10 mL. A 5.0-mL aliquot was placed in a polypropylene counting tube. The  $^{103m}Ru$  and  $^{103}Ru$  activities were measured immediately by  $\gamma$ -ray spectrometry in the manner previously reported (1).

## RESULTS AND DISCUSSION

The  $^{103}\text{mRh}$  yield of the extraction and the  $^{103}\text{Ru}$  contamination of the  $^{103}\text{mRh}$  solution were calculated (1). The results for eight replications of the extraction and purification procedures were:  $^{103}\text{mRh}$  yield,  $100.9 \pm 2.1\%$  and  $^{103}\text{Ru}$  contamination,  $0.0\%$ .

The use of sodium hypochlorite as the oxidizing agent was an improvement over the previously reported (1) use of ceric sulfate. The oxidizing capacity of sodium hypochlorite was not affected by the presence of chloride ions. Consequently, in addition to giving quantitative yields of  $^{103}\text{mRh}$ , the use of sodium hypochlorite eliminated the need for fuming with  $1:1 \text{ H}_2\text{SO}_4$  to eliminate chlorides as was required in the ceric sulfate method.

Meadows and Matlack (2) reported that a pH of 4 in the aqueous phase was optimum for extraction of  $\text{RuO}_4$  into carbon tetrachloride. In the present study, it was found that the optimum pH was in the range of 6.5 to 7.5. Preliminary studies also showed that considerable contamination of the aqueous solution with  $^{103}\text{Ru}$  occurred when the pH was lower than 4. Two carbon tetrachloride extractions were sufficient to quantitatively remove  $^{103}\text{RuO}_4$ .

The boiling procedure used to purify the extracted aqueous solution of  $^{103}\text{mRh}$  was efficient. In preliminary studies of the extraction procedure, when boiling was not used, the  $^{103}\text{Ru}$  contamination in the aqueous phase was  $0.9 \pm 0.8\%$  for six replications. This contamination was believed to result from visible suspended droplets of carbon tetrachloride containing

$^{103}\text{RuO}_4$  and possibly some nonextracted  $^{103}\text{RuO}_4$ . After boiling, the solution was clear and free of  $^{103}\text{Ru}$  because of evaporation of both carbon tetrachloride (bp  $76.7^\circ\text{C}$ ) and the very volatile (3)  $^{103}\text{RuO}_4$ .

The boiling procedure also eliminated any chlorine present as a result of the excess sodium hypochlorite. However, it was found, using potassium iodide and the starch test, that some hypochlorite remained in solution. The addition of 1 drop of 1 M sodium bisulfite solution after boiling resulted in a negative starch test.

In conclusion, this method for separating  $^{103}\text{mRh}$  from  $^{103}\text{Ru}$  is simple, fast, and efficient. The reagents used are common and only a small number are necessary. The time interval from the first carbon tetrachloride extraction to the counting of the  $^{103}\text{mRh}$  is only about 16 min, thus making possible a high concentration of the short lived  $^{103}\text{mRh}$ . The  $^{103}\text{mRh}$  concentration can be further increased by boiling because the chloride form of  $^{103}\text{mRh}$  is not volatile. The final pH is near neutral and sodium chloride is the only major contaminant.

## LITERATURE CITED

- (1) C. E. Epperson, R. R. Landolt, and W. V. Kessler, *Anal. Chem.*, **48**, 979-981 (1976).
- (2) J. W. T. Meadows and G. M. Matlack, *Anal. Chem.*, **34**, 89-91 (1962).
- (3) "The Merck Index," 9th ed., Merck & Co., Inc., Rahway, N.J., 1976, p. 1075.

RECEIVED for review October 27, 1977. Accepted December 22, 1977.

## Serial Dilution Pipet for Generating Instrument Calibration Standards

Daniel S. Berry

Searle Diagnostics, Inc., 2000 Nuclear Drive, Des Plaines, Illinois 60018

Many analytical chemical determinations require the construction of a standard curve from a serial dilution of a concentrated standard solution. Although numerous commercial devices exist for pipetting and diluting individual samples, equipment for semiautomatic multiple dilutions of a standard is not readily available. The device described below is based on repeated addition and withdrawal of constant volumes of diluent and diluted standard from a concentrated standard solution. This simple apparatus can save considerable time in generating standard curves for calibrating instruments.

## EXPERIMENTAL

A 20-mL glass hypodermic syringe was fitted with an upper and lower mechanical stop. In the model shown in Figure 1, the upper stop is an adjustable screw and the lower stop is a length of metal tubing cemented onto the syringe piston. The syringe was fitted with a three-way valve (Hamilton) and reservoir of diluent solution with appropriate tubing. A small magnetic stirring bar was inserted into the active volume of the syringe, to mix the standard with diluent. This apparatus, in addition to a small magnetic stirrer, was clamped to a ring stand, as shown in Figure 1.

In operation, a concentrated standard solution is drawn into the clean, dry apparatus by unclamping the syringe from the ring stand and pumping it into an inverted bottle fitted with a rubber septum cap until all air bubbles are removed and the syringe is filled to its maximum stop. It is then resealed, needled down, and allowed to drain into an appropriate receiver to its bottom stop. The quantity of residual solution fixed by the length of the

Table I. Gravimetric Calibration of Serial Dilution Apparatus

Run	Total grams of NaCl delivered	Expected dilution factor	Ratio of successive weights of NaCl	Average ratio and RSD
1	1.4123	0	2.015	2.03 $\pm 1\%$
	0.7009	1/2	2.012	
	0.3484	1/4	2.056	
	0.1695	1/8	2.02	
	0.0839	1/16		
2	1.4072	0	2.004	2.01 $\pm 2\%$
	0.7003	1/2	2.071	
	0.3382	1/4	1.993	
	0.1697	1/8	1.97	
	0.0860	1/16		
3	1.3949	0	2.011	2.00 $\pm 1\%$
	0.6936	1/2	2.034	
	0.3410	1/4	1.984	
	0.1719	1/8	1.99	
	0.0863	1/16		

bottom stop is now diluted by turning the three-way valve to admit diluent, and pulling the syringe piston to the upper stop. The magnetic stirrer is activated to mix the standard with diluent. The three-way valve is turned to let the syringe drain the diluted standard, plus the undiluted material in the needle, into the next receiver. The valve is then turned to admit fresh diluent to the upper stop and, following a few seconds mixing, turned again to drain into the next receiver. This process is repeated until the

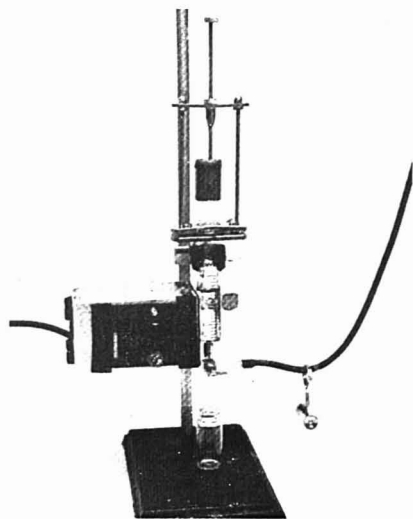


Figure 1. Diluter with piston at upper stop

required number of dilutions is obtained. The apparatus is taken apart for cleaning by removing the bar which holds the adjustable upper stop.

Calibration of the apparatus can be accomplished by successive fine adjustments, once a dilution factor is chosen and approxi-

mately set by fixing the upper and lower stops. The volume of the stir bar must be subtracted from the residual concentrated standard volume in fixing the bottom stop, and the unmixed solution in the needle must be considered in setting the volume of diluent added by fixing the top stop. These approximate settings can be made using the calibration marks on the syringe or by weighing the apparatus empty and filled to the top and bottom stop. Fine adjustments are made by turning the upper stop screw and measuring the resultant change. Dyes or salt solutions can be used to determine the dilution factor optically or gravimetrically.

## RESULTS AND DISCUSSION

Table I gives the results of a series of dilutions determined gravimetrically using a solution of sodium chloride as the standard. The solutions, including the most concentrated, were received directly into pre-weighed pans, dried in an oven and weighed again. The dilution apparatus had been previously adjusted using a dye and fluorometer to fix it at a dilution of 1 to 1. Ten repetitive weighings of pure water indicated that 7.51 mL were delivered for each dilution; the volumetric error was less than 0.1%. The diluent reservoir was placed on top of a cabinet giving about a 2-m water head which was sufficient to force the piston to rise to its upper stop when the three-way valve was turned to admit diluent. Since this apparatus does not require the complete rinseout of the solution being diluted, as is the case in most sampler dilutors, it is possible to make dilutions with small additions of diluent to a larger volume of concentrated standard. Since the syringe and stops are not particularly expensive, a given dilution factor may be permanently fixed by cementing the adjustment screw in place.

RECEIVED for review November 21, 1977. Accepted December 12, 1977.

## Preparation and Characterization of Glass Beads for Use in Thermionic Gas Chromatographic Detectors

J. A. Lubkowitz,<sup>1</sup> B. P. Semonian,<sup>2</sup> Javier Galobardes, and L. B. Rogers\*

Department of Chemistry, University of Georgia, Athens, Georgia 30602

Alkali thermionic detectors have been used for many years in gas chromatography but they have been notoriously difficult to work with because careful control of all detector parameters is necessary to obtain reproducibility. The use of ceramic elements for halogen detection has been previously described (1). Recently, a new version of this detector has appeared (2, 3) which utilizes a small glass bead containing rubidium (oxide or silicate). This bead is positioned within 0.5–1.5 mm of the flame tip and is maintained at a negative potential. The detector can be operated in a nitrogen-phosphorus (N-P) mode or in a phosphorus (P) mode by changing the flow rates of hydrogen and air as well as the potential applied to the flame tip. The bead is heated electrically and, thus, careful control of the volatility of alkali atoms in the glass can be achieved. Our recent studies of the response of this detector have shown that, if the bead current is carefully controlled, the detector is very reproducible (4).

During our studies aimed at characterizing the detector, these beads were found to have lifetimes of only about 3–4

months, so numerous beads were utilized. As a result, an effort was made to produce these beads in the laboratory. Unfortunately, a description of the glass composition and the procedure of the beads was not available. Hence, we examined the behavior of several different compositions. Furthermore, we wanted to see if the sensitivities and specificities could be modified by changing bead composition.

This paper describes a simple procedure for preparing the beads using materials having a cost of about \$1.00 per bead. The most important characteristics of the beads are also given.

## EXPERIMENTAL

**Chemicals.** Amorphous silica (Illinois, Mineral Co., Cairo, Ill.), grade 200, was used in preparing beads 5–8. Beads 1–3 were prepared from finely ground Corning glass 7740 (Pyrex). Sodium carbonate (Baker Analyzed reagent) was added as a flux to beads 1 and 6–8. Boric acid (Baker Analyzed reagent) was also used as a flux in beads 6–8. Sodium borate decahydrate (Baker Analyzed reagent) was used in making bead 5 and thus the sodium-to-boron ratio was fixed. Rubidium nitrate (Fairmount Chemical Co., Newark, N.J.) was used in beads 1–3 and 5–7. In the case of bead 8, cesium fluoride (Peninsula Chemical Research, Gainesville, Fla.) was used instead of rubidium nitrate. All beads were fused to a platinum wire (Fisher Scientific, Atlanta, Ga.) having a diameter of 0.020 cm whereas the commercial bead was mounted on 0.025-mm wire.

<sup>1</sup> On leave for the academic year 1976–1977 from Instituto Venezolano de Investigaciones Científicas, Apartado 1827, Caracas, Venezuela.

<sup>2</sup> Present address, Union Carbide Corporation, Box 8361, South Charleston, W.Va. 25303.

Table I. Characteristics of Glass Beads

Property	Operating Mode	Bead No.							
		1	2	3	4	5	6	7	8
Composition									
%SiO <sub>2</sub>		61.1	69.1	69.1	- <sup>d</sup>	60.0	94.1	68.2	69.5
%B <sub>2</sub> O <sub>3</sub>		9.79	11.1	11.1	-	24.5	1.14	2.80	1.95
%Na <sub>2</sub> O		14.4	3.30	3.30	-	10.9	-	7.90	8.65
%K <sub>2</sub> O		0.30	0.33	0.33	-	-	-	-	-
%Al <sub>2</sub> O <sub>3</sub>		1.70	1.90	1.90	-	-	-	-	-
%Rb <sub>2</sub> O		12.7	14.4	14.4	-	4.53	4.73	21.1	-
%Cs <sub>2</sub> O		-	-	-	-	-	-	-	20.0
Current range									
Heating, A	N-P	3.98-4.13	3.90-4.30	4.10-4.40	2.70-3.50	2.80-3.50	3.99-4.30	3.90-4.11	3.40-3.90
Bead, pA	N-P	0.40-9.0	0.50-7.00	0.50-7.00	0.50-10.0	0.50-7.00	0.10-1.00	0.20-10.0	2.5-10.0
Sensitivity									
Azobenzene, C/g × 10 <sup>-3</sup>	N-P	2.41	1.91	2.30	1.06	5.40	0.184	4.50	2.85
Malathion, C/g × 10 <sup>-1</sup>	N-P	4.91	1.89	1.96	0.960	-	0.330	6.55	2.45
Ratio <sup>a</sup>	N-P	20.4	9.92	8.52	9.06	-	17.9	14.6	8.60
Ratio <sup>b</sup>	N-P	24.5	15.9	13.4	9.06	-	26.6	15.6	17.7
n-Hexane, C/g × 10 <sup>-4</sup>	N-P	2.1	1.3	-	2.8	1.3	0.66	4.3	3.8
Azobenzene, C/g × 10 <sup>-3</sup>	P	3.35	0.933	0.179	3.10	-	0.0672	42.5	-
Malathion, C/g × 10 <sup>-1</sup>	P	1.14	1.48	0.132	2.01	-	0.120	6.91	0.102
Ratio <sup>c</sup>	P	34.0	159	73.7	64.8	-	179	16.3	-
n-Hexane, C/g × 10 <sup>-4</sup>	P	9.3	-	-	21	-	-	12	19
Detectability, g/s × 10 <sup>-13</sup>									
Azobenzene	N-P	75	86	52	110	-	330	22	49
Malathion	N-P	3.7	8.7	6.1	12	-	18	1.5	5.7
Azobenzene	P	180	880	-	130	-	8900	19	-
Malathion	P	5.3	5.5	-	2.0	-	50	1.1	118
Linearity, × 10 <sup>3</sup>	N-P	4.1	-	-	3.0	-	-	11.0	3.2
Loss of bead current, %/h	N-P	6.2	5.3	5.8	5.1	~12	3.0	4.0	5.2

<sup>a</sup> Sensitivity ratio: malathion/azobenzene at 7.8 pA. <sup>b</sup> Sensitivity ratio: malathion to azobenzene at 3.0 pA.

<sup>c</sup> Sensitivity ratio: malathion to azobenzene. <sup>d</sup> A dash indicates that a particular measurement was not made.

Malathion and azobenzene were used as model compounds for characterization of the beads. Malathion, S(1,2-dicarboxyethyl)-O,O-dimethylthiophosphate (American Cyanamid Co., Princeton, N.J.) having a purity of 99.3% was dissolved in n-hexane (Nanograde, Mallinckrodt, St. Louis, Mo.). The concentration of the solution was 5 ng/μL. Solutions of azobenzene (Eastman, Rochester, N.Y.) in n-hexane were prepared containing 0.05, 0.5, 5, 50, 500 and 5000 ng/μL.

A glass column, 183 cm × 2 mm i.d., containing 3% OV-1 on 90-100 mesh Gas-Chrom Q (Applied Science Labs., State College, Pa.) was used. Nitrogen (Selox) was purified by passage through molecular sieve and silica gel. Air and hydrogen (Selox), purified by passage through molecular sieve and silica gel, were used as auxiliary gases for the flame ionization detector and the nitrogen-phosphorus detector.

**Apparatus.** A Perkin-Elmer nitrogen-phosphorus detector was used on their Model 3920 gas chromatograph. All of our beads were mounted in the Perkin-Elmer bead assembly. The heating current was measured by placing a 0-10A ammeter (Weston, Newark, N.J.) in series with the bead. A flame ionization detector mounted in parallel with the nitrogen-phosphorus detector received 48.5% of the injected sample. The output of the electrometer was fed to a Linear Instruments Co. dual-pen recorder (Irvine, Calif.).

**Procedures. Bead Construction.** The glass mixture was prepared by weighing the silica, the fluxes, and either the rubidium nitrate or cesium fluoride. The weight of the total mixture was kept at about 2 g. The percentage composition of each bead prepared is given in Table I. Beads 1-3 were made by using ground Corning glass 7740 and subsequently adding sodium carbonate (bead 1) and rubidium nitrate (beads 1-3). Again, the total weight was kept at about 2 g. To calculate the final composition of the latter beads, the original composition of Corning 7740, as reported in the literature, was used (5). The weights of all components in the mixture are reported in Table I as the oxide, a common practice in reporting glass composition (5).

The weighed mixture was transferred to a 15-mL Coors porcelain crucible. Using a natural gas-oxygen rich mixture and a blow pipe torch (National 3A, Atlanta, Ga.), the powder mixture

was melted and stirred with a quartz rod. At this point, a thin strand of glass was pulled from the melt. The strand was later used to make the bead. The fused glass mixture could be left in the crucible and reheated at a later time to obtain additional strands. The mixture for making bead 6 was melted using an oxyacetylene "Rose-bud" heating tip (Meco-Wg-1) because its low sodium content resulted in a very high melting material.

A 1.5-cm section of the 0.020-mm diameter platinum wire was shaped in the form of an arch and secured in a vise. A 7 cm × 0.159 cm piece of stainless steel tubing was inserted into the tip of the torch. The torch was lit and the natural gas-oxygen mixture was adjusted so that the flame was no longer than 0.5 cm. The tip of the strand of glass was brought to the flame and held there long enough to form a bead no larger than 1.5 mm in diameter. The platinum and bead were heated again and brought together to attach the bead to the wire. By reheating the bead and the strand of glass, they could be reunited to adjust the size of the bead. The bead was then reheated and the heat maintained long enough for the wire to reach the center of the bead. The bead always assumed a nearly spherical shape with a slightly shorter transverse axis. All beads had dimensions of 1.4 × 1.6 mm and weighed about 4 mg. However, bead 3 was made by adding additional glass to bead 2 until the bead was 1.8 × 2.0 mm. A magnifying glass provided with a mm scale was used to measure bead size. The entire step of attachment and centering of the bead on the wire required only about 5 min.

The wire-bead assembly was then spot-welded to the Perkin-Elmer bead assembly holder. After installation, the beads were conditioned by passing sufficient current to cause the bead to glow with a medium red color. The conditioning period for beads 1-7 lasted from 1-24 h. During the conditioning period, the bead current (background current) reached values of about 200 pA. The sensitivity toward either malathion or azobenzene was quite low and the detector was almost useless. However, after the bead had been conditioned, the bead current usually reached about 1 pA and gave sensitivities typified by those in Table I. One exception to that behavior was bead 8 for which details will be discussed later.

**Bead Current.** All beads were tested in the range of 0.50-10.0 pA because we have previously shown (4) that a 10-pA bead



current was the best compromise between sensitivity and bead lifetime. All beads, except bead 6, were capable of delivering currents greater than 100 pA. Bead 6, which had a high silica concentration, low boron and low rubidium concentration, showed a short range of bead current.

**Heating Current.** The heating current was dependent, among other variables, upon the cross-sectional area of the wire. The wire used in this study was slightly smaller than that used in the commercially available bead. Thus, the heating currents were higher due to the increased heat-loss. The heating current was also a function of the bead composition since, in the molten state, the bead conducted electricity. Thus, it was observed that a high boron content and the presence of cesium led to low bead currents at lower heating currents. The importance of achieving a low heating current lies in the fact that the power supply was current-limited so it would shut off at currents of about 4.6 A.

**Gas Chromatography.** Each bead was characterized in the N-P mode and in the P mode. In the N-P mode, hydrogen flow was kept constant at 2.60 mL/min while air was maintained at 83.5 mL/min. In the P-mode, hydrogen flow was 23.1 mL/min and air was kept at 240 mL/min. The heating current in the N-P mode was adjusted as shown in Table I so as to obtain a bead current in the range of 0.1–10 pA. However, since the beads did differ substantially in the P mode, a heating current was selected so as to obtain a sensitivity of about 0.1 C/g. A more detailed description of these two modes of operation has been recently prepared (6).

The detectors were maintained at 260 °C, the column at 190 °C, and the injector at 260 °C. The carrier gas flow rate was 80 mL/min. The samples were injected using a Hamilton 75N-5  $\mu$ L syringe (Supelco Inc., Bellefonte, Pa.). The injection volume was kept constant at 3.2  $\mu$ L. The areas were obtained from the mean of two injections except when measuring the reproducibility of response when larger numbers of replicates were used.

**Calculations.** None of the column or operating parameters were changed during the study. The peak shapes for azobenzene and malathion were very symmetrical. Thus, the peak areas were obtained by the product of height and width at half height. The peak areas were expressed in terms of coulombs (C) and divided by the mass injected. Thus, the sensitivity as defined by Hartmann (7) was used as one of the criteria for characterization. Ratios of sensitivities at bead currents of 3.0 and 7.8 pA were also calculated. This ratio indicated the specificity of the detector (7).

Noise measurements were made with the recorder and expressed in amperes. The detectabilities were calculated as twice the noise divided by the sensitivity (7).

Linearity ranges were determined by a semilogarithmic plot of sensitivity vs. logarithm of the mass injected. The slope of this plot should be zero. The upper limit was the mass that yielded a response which deviated from linearity by an arbitrarily defined 5%; the lower limit was the mass where the signal was equal to twice the size of the noise. The linearity range was the ratio of the upper limit to the lower limit.

Stability of the detector with different beads was calculated by measuring the bead current for 12–14 h. The loss in bead current per hour was expressed as a percentage of the original bead current. All beads were subjected to a reproducibility test by injecting azobenzene and malathion over a 5–6 h period. During that time, the bead current was maintained constant by increasing the electrical heating.

## RESULTS

In the early part of our preliminary studies, we fashioned several batches of Borax beads after those used in classical "bead tests". We soon found that the size of the bead influenced both the sensitivity and the selectivity, as will be documented later. However, when the size of the bead was carefully controlled, as described in the Experimental section of this paper, the characteristics for beads made from three replicate batches were found to disagree a maximum of 10%, even though the bead composition was that which was later found to have the least stable response (No. 5, Table I). Hence, we felt confident that when beads of the same size were compared under the same operating conditions (4, 6), large

differences in their operating characteristics could be assigned, with a high degree of confidence, to differences in the compositions of the beads.

**Sensitivity Studies in the N-P Mode.** The plots of sensitivity vs. bead current for the commercial beads were linear for azobenzene in the range of 1–150 pA and for malathion in the range of 1–50 pA (4, 6). However, the beads made in our laboratory showed linear plots of sensitivity vs. bead current for azobenzene only in the range of 1–10 pA, and for malathion, in the region of 1–4 pA. Thus, when the sensitivities are compared in Table I at bead currents of 3.0 and 7.8 pA, one expects to find a higher sensitivity ratio of malathion to azobenzene at 3.0 pA than at 7.8 pA. This characteristic is not necessarily a disadvantage because it permits one to control to a certain extent the specificity by means of the bead current. At present, we do not have an explanation for this difference except that it is related to the composition of the beads.

Bead 7 which contained the highest rubidium content, showed the closest behavior to the commercially available bead. This is reflected by the fact that ratio of sensitivities at the two currents differed by less than 7%.

Bead 5, which had the highest percentages of boron oxide and sodium oxide, showed the greatest sensitivity for azobenzene. However, this bead was not extensively studied since it suffered drastically from losses in bead current over short periods of time. Sensitivity toward azobenzene did not show a trend with increasing boron oxide concentration alone. However, it is significant that the three most sensitive beads 1, 8, and 7 all had a ratio of  $\text{Na}_2\text{O}$  to  $\text{B}_2\text{O}_3$  greater than unity. Hence, sodium in conjunction with boron appears to lead to high nitrogen sensitivity. Bead 7, which had a high concentration of rubidium, also had a high sensitivity toward azobenzene. Replacing rubidium by cesium also yielded a nitrogen sensitivity. However, the azobenzene sensitivity did not necessarily increase with rubidium concentration as can be seen from beads 1 and 2.

Bead 6, which had a high silica content but no sodium, showed the lowest sensitivity for azobenzene. That result is not surprising considering that this bead was capable of generating only very low bead currents. This bead also had one of the lowest rubidium contents.

The sensitivities of the beads toward malathion followed the same order as that for azobenzene. An exception was the reversal in which bead 1, a Pyrex glass with added sodium, showed higher sensitivity than bead 8, which contained a high cesium content. The opposite was true for azobenzene. Thus, the sensitivity toward both azobenzene and malathion increased with the ratio of sodium to boron and with rubidium concentration and, possibly, cesium concentration. In addition, a comparison of beads 2 and 3 showed that the larger bead had a somewhat greater sensitivity and improved detectability for both compounds.

The ratio of the sensitivities under conditions of equal noise is defined as the specificity (7). With the exception of the larger size Pyrex bead 3 and the cesium bead 8, the sensitivity ratio for malathion to azobenzene was always higher than that of the commercially available bead. This indicates that the beads were better phosphorus detectors than nitrogen detectors. Nevertheless, the sensitivities of our beads toward nitrogen were higher than that of the commercial bead except for bead 6 which contained no sodium. Hence, our beads were generally more specific toward phosphorus while, at the same time, more sensitive toward nitrogen than the commercial bead. However, the departures from linearity in the plots of sensitivity vs. bead currents for malathion were greater for our stabilized beads. A marked exception was noted in the freshly prepared high cesium oxide bead which showed low

malathion-azobenzene ratios, from 2.4–4.6 which means that the sensitivity toward azobenzene was 80 times greater than usual, especially when first used. However, after aging for 3 weeks, the behavior resembled that of the other beads.

For some beads, the sensitivity toward the solvent *n*-hexane was measured. The sensitivity for azobenzene and malathion was  $10^6$  and  $10^7$  larger than that for *n*-hexane. Thus, the beads had large specificities for nitrogen and phosphorus relative to hydrocarbons. The values were not significantly different, especially when one considers that they were not measured at the same bead current.

**Sensitivity Studies in the P Mode.** The use of the term, P mode, is deceptive in that azobenzene could usually be determined with reasonable sensitivity. The only exception was the high cesium bead, 8, which showed no sensitivity toward nitrogen in this mode. The sensitivities for azobenzene and malathion were less, except for the high rubidium bead, 7, than those obtained in the N-P mode, an observation consistent with what we have previously reported for the commercial bead 4 (6). However, the orders of sensitivity toward azobenzene and malathion were not the same in this mode. As indicated above, the cesium bead, 8, showed a low sensitivity for malathion, and it was not possible to detect azobenzene in this mode. At the other extreme the high rubidium bead, 7, showed sensitivities toward both compounds which were nearly the same in both modes.

In the P mode, the larger bead, 3, showed similar, rather low, sensitivities for both compounds whereas the smaller bead showed a higher sensitivity (and selectivity) toward malathion. When the larger bead was removed and examined under magnification, it appeared that only half of the bead had been heated by the flame because a crater appeared in the bead directly above the flame. This confirms our previous study (6) and indicates that the flame profile is important in this mode.

The data suggest that sensitivity toward nitrogen was related to the sodium content. The bead having no sodium showed low azobenzene sensitivity relative to that of malathion. Beads 2 and 6 that had the highest sensitivity ratio had the lowest amount of sodium oxide. Among the rubidium beads, those having the highest sensitivities toward both compounds had the highest rubidium concentration. Thus, in the P-mode just as in the N-P mode, high sodium and high rubidium led to high sensitivity for both compounds.

The sensitivity towards *n*-hexane, although low, was about 150–50 000 times greater in this mode. Thus, one should chromatograph under conditions where solvent tailing will not interfere with the component in question.

**Detectability Studies in the N-P Mode.** The beads usually fell in the same order with respect to detectability as they did for the sensitivity. The only exceptions were the reversals of beads 1 and 3 with respect to azobenzene. Bead 1, the Pyrex with sodium added, had lower detectability. There was no obvious explanation for the lower noise of the larger size Pyrex bead 3. It is worthwhile noting that, when comparing bead 4 with 6, and bead 1 with 3, the sensitivities for beads 6 and 3 were lower but their detectabilities were either higher (bead 3) or comparable (bead 6). This is a direct result of the lower noise of beads 3 and 6. Hence, larger bead size and low sodium content led to lower noise values.

**Detectability Studies in the P Mode.** Similar trends in sensitivities and detectabilities were observed in this mode. However, a reversal was obtained with beads 4 and 1 in their responses toward azobenzene. Although bead 1 had a higher sensitivity, bead 4 showed a higher detectability. Since the composition of the commercial bead, 4, is not known, one cannot make any correlations with composition.

**Linearity.** Although our method for determining the linear range was more rigorous than the conventional method, the four beads for which linearity ranges were calculated had values comparable to those reported for older versions of thermionic detectors (8, 9). The highest linear range was found for bead 7 which had the highest rubidium concentration. However, the linearity values must be used with caution because they will undoubtedly depend on the nitrogen or phosphorus compound used.

**Loss of Bead Current.** This is one of the most important aspects of the thermionic detector. We have previously shown how the very small changes in bead current drastically altered the reproducibility of the detector (4). If the bead current vs. heating current shifted too rapidly toward higher heating currents, continuous readjustments by the operator were required in order to achieve the best reproducibility of response. We obtained relative standard deviations of 3–6% in a 6-h period by maintaining the bead current constant.

Bead 6, the sodium-free bead, showed the highest stability, while bead 5, which had high boron and sodium contents, showed the least stability.

## DISCUSSION

A high rubidium oxide concentration (10–20%), a high sodium oxide content (4–10%), and a low boron oxide content (2–3%) yielded beads having good sensitivities and detectabilities. However, a reasonably good bead could be made without sodium in contrast to what has been stated (3). While bead 6 showed very good stability and low noise, it did have lower sensitivities. It would be desirable to study beads having no sodium but a higher rubidium concentration. Those beads should have much higher sensitivities and detectabilities, the latter because of their low noise.

The presence of  $Al_2O_3$  and  $K_2O$  was not deleterious to bead performance. In fact, bead 7 was an exceptional bead which showed larger sensitivities than the commercially available bead in both modes for azobenzene and malathion. Furthermore, its N-P and P modes did not show significant differences in behavior.

Cesium bromide and chloride have been previously used as an alkali source in thermionic detectors (8). Our bead 8 showed good sensitivity and detectability in the N-P mode but very low sensitivities in the P mode. It would be worthwhile to investigate compositions that might stabilize the bead current at 600–800 pA because, at those high bead currents, the bead showed the best azobenzene sensitivity (approximately 1.2 C/g) for azobenzene relative to malathion, a commendable property. The need for detection of phosphorus is less acute because it can also be performed using the flame photometric detector (9).

The beads were easily made in the laboratory, and they showed good sensitivities and detectabilities for nitrogen and phosphorus compounds. In addition, a new bead could easily be fused to the wire of the commercially available bead holder. The easiest beads to prepare were beads 1 and 2 because it was necessary only to add either rubidium nitrate or a mixture of the rubidium nitrate and sodium carbonate to powdered glass.

A word of caution is necessary. Our conclusions were reached using different heating currents but with otherwise identical operating conditions. From earlier studies (6), we know that operating conditions can drastically change both the sensitivity and the selectivity of a bead. Hence, one should recognize the limitations of our conclusions until detailed studies have been made under optimal conditions for each bead.

Finally, after this study had been completed, we learned that Aue and his co-workers (10) had also been successful in making beads. They confined their study to rubidium-doped

beads of quartz. Unfortunately, their results cannot be compared with ours because they studied different volatile species, and they did not characterize their beads in terms of bead current nor standardize the conditions under which they made comparative measurements. However, both their study and ours showed a higher sensitivity toward both nitrogen and phosphorus compounds for higher concentrations of rubidium in the beads.

#### LITERATURE CITED

- (1) C. W. Rice, German Patent 907223 (1947).
- (2) B. Kolb and J. Bischoff, *J. Chromatogr. Sci.*, **12**, 625 (1974).
- (3) B. Kolb and J. Bischoff, U.S. Patent 3852037 (1974).
- (4) J. A. Lubkowitz, J. L. Glajch, B. P. Semonian, and L. B. Rogers, *J. Chromatogr.*, **133**, 37 (1977).
- (5) E. L. Wheeler, "Scientific Glass Blowing", Interscience Publishers, New York, N.Y., 1966, p. 12.
- (6) B. P. Semonian, J. A. Lubkowitz, and L. B. Rogers, submitted to *J. Chromatogr.*
- (7) C. H. Hartmann, *Anal. Chem.*, **43** (2), 113A (1971).
- (8) D. J. Davy, "Gas Chromatographic Detectors", John Wiley and Sons, New York, N.Y., 1974, p. 131.
- (9) J. Sevcik, "Detectors in Gas Chromatography", Elsevier Scientific Publishing Co., Amsterdam, 1976, p. 115.
- (10) R. Greenhalgh, J. Müller, and W. A. Aue, Private communication, June 1976.

RECEIVED for review June 9, 1977. Accepted January 9, 1978.  
This work was partially supported by the U.S. Energy Research and Development Administration through Contract No. E(38-1)-854.

## Microprocessor-Based, Linear Response Time Low-Pass Filter

T. C. O'Haver

Department of Chemistry, University of Maryland, College Park, Maryland 20742

One of the most widely cited applications of microprocessors in scientific instrumentation is an alternative to hard-wired digital and analog circuitry. In addition to the advantages of exceptional versatility and the potential for standardization of hardware, the microprocessor approach often allows the ready implementation of functions which would be difficult to implement in hard-wired electronics. This paper describes the use of a microprocessor to implement a particularly useful type of low-pass filter, a function normally performed by analog circuitry. Although a few years ago such an application would have been quite impractical from an economic point of view, the continuing reduction in the complexity and cost of microprocessor systems and support hardware will make such an application increasingly practical in the future. More significantly for the present application, however, is that a microprocessor-based low pass filter can be designed to have uniquely desirable properties which would be difficult or impossible to achieve using conventional analog hardware. Consider for example the low-pass filter used to smooth the output signal of a flame atomic absorption spectrometer. The output signal of such an instrument (for flame atomization) is essentially a series of rectangular pulses of varying height and duration depending on the concentration and aspiration time of each sample, standard, and blank solution. Superimposed on this signal is a certain amount of random noise of white or  $1/f$  spectral distribution. The objective of measurement is to determine the average height of each rectangular pulse. Low-pass filtering is commonly applied to the output signal to aid in this determination; although unnecessary if the signal is recorded on a strip-chart recorder (as then the signal may be averaged or integrated manually in various ways), low-pass filtering is often essential if a panel meter or numerical digital readout is employed. It is clearly desirable in this application to obtain the greatest noise filtering capability with the minimum response time. Long time constants, although possibly improving the signal-to-noise ratio, naturally result in long analysis times, increased sample consumption, and increased problems from long-term drift. Moreover, with graphite furnace atomization, excessively long time constants result in reduced sensitivity and greater analytical curve nonlinearity. Thus, it would seem reasonable that, if one were to compare two low-pass filters of equal

noise-filtering capability, the one with the shortest effective response time would be the best for atomic absorption applications and indeed for many other applications as well.

The most commonly used type of low-pass filter in analytical instrumentation is an active or passive single-stage RC filter, which has an exponential response to a step input. A variety of more elaborate filter types, such as Butterworth, Bessel, etc., are occasionally used for special purposes. These have different, and in some cases more efficient, response behaviors, but in many respects the ideal filter would have a linear response to a step input which would not "slow down at the end" like the RC and most other filter types. This is the response behavior of an integrator, now a standard feature on atomic absorption instruments, and in fact it is this linear response behavior which is the essential advantage of integration compared to low-pass filtering. However, the conventional integrator produces a discontinuous output signal which is unsuitable for recording spectral scans. A low-pass filter giving a continuous output signal but with the linear response of an integrator would be ideal. The closest analog approach to this ideal is the *Paynter* filter (1), a complex, third-order, linear-phase-shift active filter design employing 14 critically matched resistors and capacitors. This filter is especially useful for averaging nonstationary random variables, since its transient-response time is minimum for a given averaging time. Such a filter might be designed for any one time constant, but to make it variable would entail considerable difficulty. The microprocessor-based low-pass filter described here is an ideal linear-response time filter. It is based on a real-time modification of the sliding window algorithm widely used to smooth data arrays. Essentially, the system samples the input analog signal repetitively at some constant rate, computes the average of the last  $2^n$  data points (where  $0 \leq n \leq 8$ ) and outputs the average to a digital-to-analog converter. The response time of the filter, which depends upon the number of data points averaged, is theoretically expected to be one half that of a simple RC filter with the same noise filtering capability (2).

#### EXPERIMENTAL

The filter algorithm was coded for a MOS-Technology 6502 microprocessor and run on an Ebka 6502 Familiarizer (Ebka

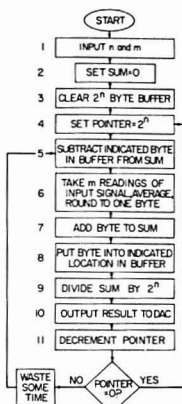


Figure 1. Flow chart for the sliding-average low-pass filter algorithm

Industries, Inc., Oklahoma City, Okla.). The Ebka system has 1 K RAM, sockets for 1 K EPROM (1702A type), a hex keyboard, hex LED readout, and one each 8-bit input and latched output port. To this was added one more latched output port (a pair of 74175 quad latches), an 8-bit ADC (DATEL E8HB1), a 12-bit DAC (DATEL DAC 69), and a power supply (+5 V, -9,  $\pm 15$  V). The additional output port is necessary to allow the use of the 12-bit DAC. Since the purpose of the filter is signal-to-noise enhancement, it is reasonable to employ a more precise converter on the output than on the input. The 8-bit ADC is a convenient choice. Since the signal-to-noise ratio (SNR) of the input signal is likely to be much less than 256 in most applications, its quantization errors will be randomized, as Horlick has explained (3). With a 12-bit DAC, the output quantization noise will probably be insignificant compared to the residual random noise-in-signal in most cases. (However, if the output signal of the filter will be scale-expanded, for example as is sometimes done by manipulation of recorder zero and range controls, then a more precise DAC may be useful. A 16-bit DAC is available from Datel, Model DAC-169-16B, for \$109.00.) Naturally, if the random noise in the input signal is less than one quantization level of the ADC, the overall resolution of the filter will be only 8 bits, regardless of the resolution of the output DAC.

Because the Ebka microprocessor board by itself does not decode any extra address for future expansion, additional address decoding was added to decode eight new address strobes, one of which is used for the new output port, another to strobe the ADC, and the rest are left for future expansion. The decoding circuitry required four TTL packages and was modeled after that on the processor board.

The flow chart for the filter algorithm is shown in Figure 1. The effective time constant is controlled by the number of points averaged. This number is determined by entering the appropriate power of two (0 to 8, for 1 to 256 points) via the hex keyboard. There are, therefore, eight time constants available, each one differing by a factor of two from the next. This results in a selection rather like that of the conventional switched analog filters found on commercial instruments. Limiting the number of points to a power of 2 also allows a simple (and fast)  $n$ -bit shift routine to be used to divide the sum by  $2^n$  (9th block in the flowchart). This division, which is necessary to ensure unity gain at all time constants, must be done in such a way as not to lose the least significant bits. In an 8-bit processor, both sum and the resulting average (sum/ $2^n$ ) are kept in double precision, the sum being a 16-bit integer and the average being a 16-bit binary fraction with the assumed binary point between the two halves. In the present system, only the 12 most significant bits of the average are converted by the DAC.

The actual response time of the filter is also influenced by the processor clock frequency, since the sampling frequency is de-

Table I. Response Times of Sliding-Average Low-Pass Filter

n	No. of points averaged	No. of significant bits in average	Response time	
			Low range (m = 1)	High range (m = 256)
1	2	9	1 ms	37 ms
2	4	10	2 ms	75 ms
3	8	11	4 ms	0.15 s
4	16	12	8 ms	0.3 s
5	32	13	16 ms	0.6 s
6	64	14	32 ms	1.2 s
7	128	15	64 ms	2.5 s
8	256	16	128 ms	5 s

termined by software rather than by a real-time clock. Care must therefore be taken that the code for the double-precision addition and subtraction (required for an 8-bit processor) is written so that the execution time is the same whether or not a carry or borrow occurs. Otherwise, a signal amplitude dependent timing jitter will result. Similarly, in the fork at the bottom of the flow chart, some time-wasting "dummy" instructions must be included when the "NO" branch is taken (i.e., when the pointer is not equal to zero) to account for the time required to set the pointer equal to  $2^n$  when the "YES" branch is taken. These precautions require a few extra bytes of code and slow down the operation slightly, but are necessary for smooth operation. Alternatively, the program can be written as an interrupt service routine and driven by interrupts from a real-time clock. This relaxes the restrictions on code timing but requires additional hardware.

The 6th block of the flow chart is the analog input routine. For the faster time constants, this will simply amount to taking a single (8-bit) reading of the input voltage (i.e.,  $m = 1$ ). In this case, the DAC outputs are updated once each ADC sample. For long time constants we can average 256 readings (i.e.,  $m = 256$ ), discard all but the most significant bits and pass this on as one byte of data. In this case the rate of DAC output updates will be reduced because of the time required to acquire 256 points. Thus this option should only be used for response times above the  $m = 1$  range.

The 6502 machine code for the sliding average filter occupies 146 bytes of PROM in the low ( $m = 1$ ) range and 180 bytes in the high ( $m = 256$ ) range. A maximum of nine additional bytes of "scratch pad" RAM is required, in addition to the 256-byte data buffer. The slow-rate limiter (discussed below) requires 67 bytes of PROM and 3 bytes of RAM.

The analog input and output voltage ranges are  $\pm 5$  V for the ADC and DAC specified. The filter has unity gain. Analog pre-filtering with a cut-off frequency of about 500 Hz is necessary to reduce the possibility of aliasing of high-frequency components in the input signal.

The program code is easily modified for other 6502-based systems simply by changing the addresses references to I/O ports. No PROM monitor routines are used in operation. Of course, the code is not directly transportable to other processors (e.g., 8080, etc.).

## RESULTS AND DISCUSSION

Table I lists the response times for each value of  $n$  in the low range ( $m = 1$ ) and in the high range ( $m = 256$ ). These data were measured at a 500-KHz processor clock frequency and with an ADC fast enough to require no additional conversion delay. (Other clock frequencies or ADC speeds may change these results correspondingly.) The output update rate (i.e., the rate at which averages are output to the DAC) is 1.6 KHz in the high range and 55 Hz in the low range. The available response times range from 1 ms to 5 s, which is sufficient for many applications. However, if even longer response times are required, these can be easily produced by including a time delay in the analog input routine. (This may be required in any case if a slow ADC is used.) If this is done, the output update will of course be reduced. For example, using a simple 8-byte delay routine in the high ( $m = 256$ ) range yields response times up to 256 s at an update rate of 1 Hz.

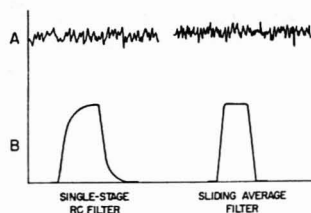


Figure 2. Comparison of the step response of an RC filter and the proposed sliding-average filter

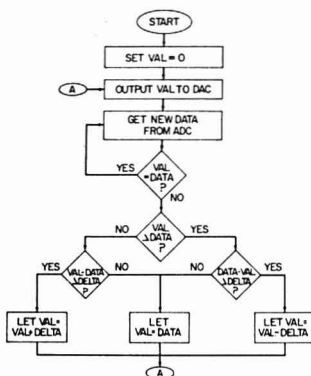


Figure 3. A slow-rate limiting algorithm which can be used for a spike (impulse noise) filter

One could also increase the response time by employing a larger data buffer.

The advantage of the sliding-average filter over a conventional RC filter is that the response time is faster for a given degree of noise reduction. This is illustrated in Figure 2. The tracings in the top half of this figure are strip-chart recordings of the output signals obtained when the same noisy DC signal is applied to each filter. The gain of both filters is unity and their time constants have been adjusted so that the average amplitudes of their output noises are equal. The response of the same two filters to a noiseless step input, shown in the bottom half of Figure 2, demonstrates the expected linear response and twofold faster response time of the sliding average filter. Although the sliding average filter clearly has an advantage for the rectangular signal shape and random noise characteristics of the signals of interest to us, we do not claim that this filter will be optimum for other signal shapes or noise characteristics.

The sine wave frequency response of the sliding average filter is the same as that of an integrator with the same averaging time (2). The phase characteristics were not investigated as they were not of interest in our application.

Another algorithm which acts under some conditions like a linear response low-pass filter is shown in Figure 3. This is essentially a software emulation of a feedback servo-mechanism with an adjustable slow-rate limit. Each new input sample (DATA) is compared to the previous DAC output (VAL), and if the difference is less than DELTA, the new DATA is transferred unchanged to the DAC. But if the new DATA differs from VAL by more than DELTA, then DELTA is either added to or subtracted from DATA, as appropriate, and then output to DAC. Thus, this filter will follow slow

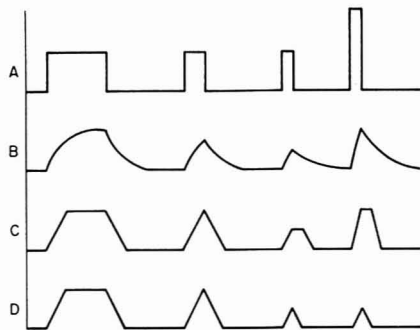


Figure 4. Comparison of the response of all three filter types to rectangular pulses of various durations. Note the radically different response to short input pulses

changes in input signal without effect, while limiting the maximum rate (slow rate) at which the output can change in response to fast changes in input signal. By selecting DELTA from 1 to 255, the maximum slow-rate limit may be controlled. This type of filter is especially useful for attenuating short "spikes" (impulse noise), but it is less effective than the sliding-average filter for conventional random noise.

The response behavior of both filter algorithms is compared to that of an RC filter in Figure 4. The input signal is shown in A, and the outputs of the RC, sliding-average, and slow-rate limit filters are shown in B, C, and D, respectively. The averaging time of the RC and sliding-average filters are approximately equal. Note that if the duration of the signal peak approaches the averaging time, the RC filter does not respond completely, while the sliding-average filter does, a consequence of its shorter response time. If the duration of the signal peak is shorter than the averaging time, the peak heights of both the RC and sliding-average filters are too low, although the peak heights are proportional to the input peak heights and in both cases the area under the output peaks is equal to that of the input peak. The output peak height of the slow-rate limit filter, on the other hand, is independent of the peak input amplitude under these conditions and is related only to the duration of the peak. Its effectiveness for rejecting sharp spikes is thus clear.

It is possible to combine both filters by replacing the data acquisition routine in the sliding-average program (block 6) with a subroutine call to data acquisition routine in the slow-rate limit filter and by replacing the back branches in the latter with returns to the sliding-average program. This allows independent adjustment of the averaging time and the slow-rate limit. It would also be quite possible to add an amplitude limiter routine ("clipper") if desirable for some particular application. The significant point here is that such additions can be made with no additional hardware simply by modifying the software.

The cost of the hardware required to implement the above filter algorithms is less than the cost of a typical pH meter or strip chart recorder. However, the total cost in energy and time which would have to be expended by the laboratory investigator inexperienced in such matters to get this system up and running from scratch will probably be unjustified for this one application alone. The reader must carefully judge whether the practical advantages of the proposed approach are essential for his application or whether the experience gained will be valuable in other applications. In spite of the considerable advances in the field of digital microelectronics in the last few years, it would be unwise to pretend that the



design, construction, and operation of any microprocessor-based real-time signal processing system is without pitfalls.

### LITERATURE CITED

- (1) Philbrick Researches, Inc., "Applications Manual for Computing Amplifiers", Nirmor Press, N.Y., 1966, p. 75.
- (2) H. V. Malmstadt, C. G. Enke, and S. R. Crouch, "Electronic Measurements for Scientists", Benjamin, Menlo Park, Calif., 1974, p. 822.

## Metaborate Digestion Procedure for Inductively Coupled Plasma-Optical Emission Spectrometry

Jan-Ola Burman, Christer Pontér, and Kurt Boström\*

Department of Economic Geology, University of Luleå, 951 87 Luleå, Sweden

Microwave plasmas (MWP) and Inductively coupled plasmas (ICP) have proved to be good-to-excellent excitation sources in optical emission spectrometry for the analysis of geological materials (Govindaraju et al. (1); Burman et al. (2)).

The analysis of silica rich geological materials requires awkward digestion procedures involving, for instance, lithium metaborate or sodium carbonate fusion as a critical step. The complete dissolution of silicate rocks usually demands a large excess of fusing agent, commonly in the proportions 10:1 to 7:1, but even proportions as low as 4:1 have been successfully used (Suh et al. (3); Ingamells (4); Govindaraju et al. (1); Joensuu (5)). In our MWP spectroscopic work, the preferred ratio has been 7 parts of  $\text{LiBO}_2$  (350 mg) to 1 part sample (50 mg). Our preparation of the metaborate is essentially identical to that in references (3, 4).

In the fall of 1977, the MWP source in our sequence reading emission spectrometer (ARL 33 000) was replaced by an ICP unit, see Table I. Samples dissolved in  $\text{HF-HClO}_4$  can easily be analyzed by means of this setup, but metaborate fused samples always cause a continuous drift in the readings, and usually the nebulizer clogs and becomes inoperable within 15–20 min after it is turned on. Inspection of the tip of a clogged nebulizer reveals that a deposit is the culprit. This deposit changes the gas flows to a fatal extent, including the sample flow.

This clogging can be avoided by additional dilution of the solutions, but this is objectionable, since it decreases the sensitivity of the procedure. We have therefore experimented with less metaborate in the fusing step.

### EXPERIMENTAL

The instrumental system is described in Table I. The selected wavelengths are those listed in (2). Various observation heights are selected to optimize the signal-to-noise ratio for each element. This observation height is 26 mm for all elements, except for Mg, Ba, and Si which are observed at a height of 18 mm over the induction coil. It should be pointed out, however, that future studies in our laboratory may lead to better experimental conditions than those reported in Table I.

All chemicals used are of reagent or analytical reagent grade.

### RESULTS AND DISCUSSION

In our experiments we found that as little as 50 mg of  $\text{LiBO}_2$  can fuse 50 mg of silicate rock in a graphite crucible at 1000 °C under 30 min. As was noticed previously (2) there is no tendency for the formed borate beads to stick to the crucible walls, but they can be dissolved in toto in dilute nitric acid (8% v/v). The total dissolution time is 3–4 h, and after this the solutions are diluted to 100 mL before the analysis. Solid residues were never observed after this step. This observation is well supported by our analyses for Cr. Cr is present to a large extent as refractory oxides (e.g.,  $\text{FeCr}_2\text{O}_4$ ) in our rock

(3) Gary Horlick, *Anal. Chem.*, **47**, 352 (1975).

RECEIVED August 26, 1977. Accepted January 12, 1978. Presented in part at the 28th Pittsburgh Conference on Analytical Chemistry and Applied Spectroscopy, Cleveland, Ohio, March 2, 1977.

Table I. Instrumental System

The ARL 33000 CA sequential reading spectrometer is described in (2)

Plasma conditions: RF-Generator model Henry; 3 kW;  
27.12 MHz, Crystal controlled.  
Forward RF power: 1200 W  
Argon coolant gas flow rate: 10 L/min  
Argon plasma gas flow rate: 0.8 L/min  
Argon sample transport gas flow rate: 1.0 L/min  
Nebulizer: type J. E. Meinhard concentric glass nebulizer.  
Sample uptake rate: 0.8 mL/min

Table II. Standard Deviations and Relative Errors for Certified Rock Analyses<sup>a</sup>

A	B	C	D	E	F
$\text{SiO}_2$ (in %)	0-76 38-76	0.45 0.54	1.2 0.95	...	...
$\text{Al}_2\text{O}_3$ (in %)	0-18	0.19	2.1	1.5	4.4
$\text{TiO}_2$ (in %)	0-2.6	0.032	2.5	10	22
$\text{CaO}$ (in %)	0-14	0.090	1.3	3.6	8.1
	0-2.5	0.043	3.4	...	...
$\text{MgO}$ (in %)	0-35	0.103	0.60	3.6	6.9
	0-4.5	0.031	1.4	...	...
$\text{Na}_2\text{O}$ (in %)	0-3.9	0.055	2.8	...	6.6
	2.9-3.9	0.048	1.4	3.6	...
$\text{Fe}_2\text{O}_3$ (in %)	0-13	0.046	0.70	3.1	6.8
$\text{MnO}$ (in ppm)	0-2100	32	3.1	13	17
$\text{Cr}$ (in ppm)	0-420	15	7.1	...	...
$\text{Ba}$ (in ppm)	0-850	22	5.2	10	35
$\text{Zr}$ (in ppm)	0-240	28	23	...	...
$\text{Cu}$ (in ppm)	0-1000	7.7	1.5	...	...

<sup>a</sup> A. Analyzed component and concentration units. B. Studied concentration interval. Units as in A. C. Standard error,  $\text{Sy}\cdot\text{x}$  (this work). This represents the standard error of estimate of y on x in a linear regression fit for the data, where y = concentration and x = intensity of readings. All results based on one set of readings. D. Relative error (in %) for the ICP analyses reported in column C, defined as  $100 \text{ Sy}\cdot\text{x}$ , divided by the mean concentration for the studied concentration interval. E. Relative errors (in %), obtained by MWP-analyses (2). Defined as for D. All results based on one set of readings, except the data for  $\text{SiO}_2$ , which is based on four readings of each sample. F. Average relative errors (in %) reported in (6-8). NOTE: Ba and Cr have been studied only for the concentration interval near the detection limit; higher concentrations cause no problems in the analytical work. Artificial solutions have been used for Cu, since the range of Cu values in the standard rocks is very limited, 12–70 ppm.

samples. Such oxides are not completely decomposed by HF, but are easily put into solution by our procedure. Clogging and drift were not noticed during the analyses. The fusion procedure described here has now (Dec. 1977) been in routine

use in our laboratory for 3 months without complications. During this period we have made more than 100 rock analyses with the reproducibilities indicated in Table II, columns C and D.

The usefulness and reliability of the method was tested on the standard rocks BR, GA, GH, GS-N, DR-N, and UB-N; the composition of these rocks has been discussed by de la Roche et al. (6, 7) and Roubault et al. (8). The results of this test are shown in Table II. These standard rocks are extensively used in our analytical work, fresh standard solutions being prepared every week.

The results demonstrate that the borate fusion advocated here is excellent for the analysis by ICP spectrometry of silicate rocks. The fusion and dissolution brings all material in solution, and the ICP-excitation leads to a marked improvement in the reproducibility and to lower detection limits than are possible with MWP excitation (2).

As to the success of our digestion procedure, we can only speculate, but possibly the use of only a little metaborate leads to an incomplete destruction of the silicates. The silica and alumina may therefore exist as dissolved large complexes in the final acid solutions. These complexes cannot be broken down in a cold atomic absorption flame (3, 4), but are completely decomposed in a hot plasma.

The data for  $\text{SiO}_2$  in Table II superficially suggest that the data here are somewhat inferior to the results by MWP spectrometry. However, the MWP-data in Table II for  $\text{SiO}_2$  were obtained by four repeated readings in order to reduce the drift in the MWP system; this drift is particularly annoying for  $\text{SiO}_2$  (2). The ICP data in Table II for  $\text{SiO}_2$  on the other hand are based on only one set of readings. The spread in the data for  $\text{TiO}_2$ ,  $\text{MgO}$ ,  $\text{Fe}_2\text{O}_3$ ,  $\text{MnO}$ , and  $\text{BaO}$  is considerably smaller than that reported in the literature for certified rocks, see last column in Table II. The geochemical literature is rich in rock analyses that have poor Ti, Ba, and Mn determinations. The method presented here therefore represents a considerable improvement in rock analytical procedure.

Our results demonstrate that several minor and trace elements can be determined in a satisfactory way by the

procedure outlined here. Studies in progress suggest that this conclusion is correct also for many trace constituents not reported here, such as Ni, Co, Sr, La, and Y. For traces present in low concentrations, however, (at the 1 ppm level or less) one will have to use  $\text{HF-HClO}_4$  dissolution of larger quantities of sample to be able to measure low element concentrations.

Other advantages with the present method are the small amounts of contaminants that are added by reagents, the reduced costs for high purity (or purification of)  $\text{LiBO}_2$ , and the reduced work in preparing it. The method is well suited for the analysis of very small geological samples (15–50 mg), which frequently are the only ones available, for instance when thin layers from sediment cores are studied.

Comparisons of our MWP results (2) with the present ICP results suggest that the MWP method is very sensitive to interelement effects; compare for instance the spread in  $\text{TiO}_2$  and Ba in this work and in (2). These observations will be discussed elsewhere.

## ACKNOWLEDGMENT

We thank K. Govindaraju, who cordially sent us the standard rocks GA, GH, UB-N, BR, DR-N, and GS-N.

## LITERATURE CITED

- (1) K. Govindaraju, G. Mevello, and C. Chouard, *Anal. Chem.*, **48**, 1325–1331 (1976).
- (2) J. O. Burman, B. Boström, and K. Boström, *Geol. Foeren. Stockholm Foehr.*, **99**, 102–110 (1977).
- (3) N. H. Suhr, and C. O. Ingamells, *Anal. Chem.*, **38**, 730–734 (1966).
- (4) C. O. Ingamells, *Anal. Chem.*, **38**, 1228–1234 (1966).
- (5) C. Joensuu, Rosenstiel School, University of Miami, Coral Gables, Fla., personal communication, 1976.
- (6) H. de la Roche, and K. Govindaraju, Rapport (1972) sur quatre standards géochimiques (DR-N, UB-N, BX-N and DT-N), *Bull. Soc. Fr. Géom.*, **100**, 49–75 (1973).
- (7) H. de la Roche, and K. Govindaraju, Rapport préliminaire (1974) sur deux nouveaux standards géochimiques de l'A.N.R.T. (GS-N, FK-H), (1975).
- (8) M. Roubault, H. de la Roche, and K. Govindaraju, Etat actuel (1970) des études coopératives géochimiques, *Sci. Terre*, **15**, 351–393 (1970).

RECEIVED for review November 4, 1977. Accepted December 27, 1977. This work was supported by the Swedish Board of Technical Development (STU) under a grant to K. Boström.

## Size, Shape, and Position of a Spectrophotometer Light Beam

Stephen D. Rains

Bausch & Lomb Incorporated, Analytical Systems Division, 820 Linden Avenue, Rochester, New York 14625

Among the users of spectrophotometers, there is a great interest in testing instrument performance. Determining the size, shape, and position of the light beam as it passes through the cuvette location is a useful part of such testing, since it informs the user of the size and position requirements for the optical free aperture of the cuvette. This information may be photographically recorded by trimming a small piece of light sensitive material comprising a diazonium compound (for example, blueprint paper) to fit in the cuvette holder just ahead of the cuvette itself. That is, the incident light should, for the purpose of the test, strike the photosensitive surface of the blueprint paper rather than the optical window of the cuvette.

After an exposure at approximately 425 nm of from 1 to 24 hours (depending on the light level used in the particular

instrument), a photographic image will be obtained of the size, shape and position of the cross-section of the light beam as it enters that location.

The chief advantages of using blueprint paper are that it can be cut and mounted in room light if this is done without undue delay, and the development process (exposure to ammonia) is fast, simple, and dry.

Although they may not be as convenient as blueprint paper, other photosensitive materials such as photographic emulsions could be used to test at other wavelengths or to decrease the exposure time needed.

All of the above variations share the advantages of creating a lasting record and of being usable in locations that are not accessible for direct visual observation.

Interested users could improvise many simple types of film holders to photograph the cross-section of the energy beam at other locations in a spectrophotometer or in other optical instruments. In some cases it is beneficial to devise a template (which could be as simple as a cardboard cutout) to exactly locate the photosensitive material with reference to some

mechanical reference point in the instrument. This would enable comparison of the beam location observations taken at different times in the life of the instrument.

RECEIVED for review September 16, 1977. Accepted December 27, 1977.

## Evaluation of the Dynamic Performance of Selected Ion Monitoring Mass Spectrometers

D. E. Matthews,<sup>1</sup> K. B. Denson, and J. M. Hayes\*

Departments of Chemistry and Geology, Indiana University, Bloomington, Indiana 47401

Since the first reported use of selected ion monitoring with gas chromatography-mass spectrometry (1), the technique has become an important tool in biomedical research, environmental trace analysis, and other fields of research. Mass selection is commonly accomplished by control of a voltage level—rod voltage in the case of a quadrupole mass filter, or ion-accelerating voltage in the case of a magnetic deflection mass spectrometer. Such voltage changes can be carried out rapidly, and the rate of "ion beam switching" is, accordingly, quite high, with the "dwell time" (time allowed for a single ion current measurement at a single mass) in some systems being much less than 1 second. There is a trend toward the use of increasingly higher beam switching frequencies, not only because electronic technical developments allow it, but also because it then becomes possible to follow more rapidly varying ion-current signals while retaining accuracy in ratio measurements (2) or to select a wider variety of masses for observation. As these developments proceed, it becomes increasingly important to understand the dynamic characteristics of the mass spectrometer systems. Most importantly, once the spectrometer-control system has commanded a change in the selected mass, how much time must elapse before accurate ion-current measurements can begin? Not only does knowledge of such ion-current settling characteristics allow avoidance of outright errors in measurement, it also allows optimization of the pattern and rate of mass selection, thus increasing both the accuracy and efficiency with which analytical information can be extracted from the system.

It has long been recognized (3) that the stability of an accelerating voltage power supply can be conveniently tested by monitoring the ion current at some mass setting at which the ion current is strongly dependent on the accelerating voltage. This requirement is easily met by selecting a voltage which allows about half the maximum ion current for a given mass to reach the collector, i.e., by selecting a voltage on the "side" of a mass peak. In these circumstances, any subsequent drift in the accelerating voltage modulates the ion current, and knowledge of the slope of the ion current vs. voltage curve allows quantitative evaluation of the stability of the voltage source. To make a similar observation of ion-current settling characteristics important in beam switching, it is necessary only to use such a half maximum point as the target to which the mass spectrometer is directed by the selected ion monitoring control system. The time required to reach the target, crucial details of the final approach to the selected mass, and the required settling time can all then be deduced from a recording of detector output vs. time.

## EXPERIMENTAL

**Mass Spectrometers.** Results have been obtained using two different instruments. The first, a Varian CH-7 single-focusing magnetic deflection instrument, has been described in detail elsewhere (4). The accelerating voltage power supply of this instrument has a maximum output of 3000 V and can be externally programmed in the range 2700–3000 V. The second mass spectrometer is a CEC 21-110B double-focusing instrument (Mattauch-Herzog geometry) in which both the accelerating voltage and electric sector voltage power supplies have been replaced (5). These supplies have maximum outputs of 10 000 and 500 volts, respectively, and can be externally programmed in any arbitrarily selected voltage range. Both instruments are controlled via a Varian 6201 minicomputer. The computer communicates with the power supplies by means of digital-to-analog converters having 12-bit resolution.

**Ion-Current Measurements.** Ion counting was used for measurements on the single-focusing instrument. The amplifier-discriminator-counter system, which has been described in detail elsewhere (6), has an effective deadtime of less than 50 ns. An electron multiplier-analog amplifier system was used on the double focusing instrument, the original amplifier having been replaced by a feedback electrometer based on an Analog Devices 43J operational amplifier. The electrometer employs a  $10^7 \Omega$  feedback resistor, and has a bandpass, taking account of the effects of stray capacitance, of better than 3 kHz. A Teleadyne Philbrick 470501 voltage-to-frequency converter (0–10 V input, 0–1 MHz output) was used to interface the amplifier with the same counting system used in ion-counting measurements.

**Procedure.** Programs have been written allowing the entire experiment to proceed under software control, with the computer both controlling the power supplies and recording the ion-current signals. In a typical measurement, argon ( $m/e = 40$ ) is introduced to provide a single, prominent resolved ion-current signal, the magnetic field is adjusted to place the peak at either the high or the low end of the accessible selected mass range, and software control is initiated. Information required for effective control and data interpretation is acquired in the first steps, which vary the power supply voltages in order to locate the half maximum point on one side of the mass peak, measure the signal at that point, and then "map" the voltage vs. ion-current function on the side of the peak by systematically varying the voltages and recording observed ion currents. Data allowing determination of the settling characteristics are obtained by stepping to some voltage well removed from the half maximum point, allowing an adequate time for the system to stabilize, and commanding a step back to the half maximum point while recording the ion current at a function of time. This process is repeated under do-loop control for a systematically varying sequence of voltage steps in order to determine the relationship between settling time and the magnitude of the commanded voltage change.

## RESULTS AND DISCUSSION

Figure 1 shows the ion-current settling profile for an 8.5% increase in the accelerating voltage of the single-focusing

<sup>1</sup> Present address, Department of Medicine, Washington University School of Medicine, St. Louis, Mo. 63110.

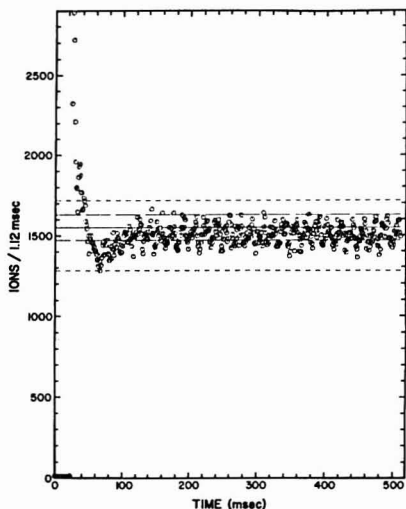


**Figure 1.** Ion current settling profile for an increase in the accelerating voltage of the single focusing mass spectrometer. The figure plots ion current vs. time after a step change in the accelerating voltage from 2700 to 2950 V (corresponds to an 8.5% decrease in mass) ending at the half-maximum point of  $m/e = 40$  (expected signal level indicated by the solid line). The long broken lines indicate signal levels  $\pm 2$  standard deviations from the half-maximum signal intensity. The short broken lines indicate the signal levels at points 2 voltage increments (49 ppm) on either side of the half-maximum point.

instrument. Prior to jumping to the target, the half-maximum on the high mass side of mass 40 (from argon), the computer determined the ion current at the target location (the solid line at 1550 counts) and at two voltage increments ( $\pm 49$  ppm) above and below the target (the short-broken lines at 1710 and 1270 counts). For the first 25 ms after the command to jump to the target was made, the accelerating voltage was still slewing toward the mass peak half-height and no ion current was observed. At 30 ms the signal suddenly appeared and surpassed its expected value (the solid line), indicating that the voltage had overshot the target. At 70 ms the signal dropped below the solid line, indicating that the voltage was ringing slightly as it finally stabilized after 130 ms had elapsed.

Several strengths of the technique become apparent through consideration of Figure 1. First, unlike an oscilloscopic recording of the power supply output waveform, the ion-current monitoring technique provides its most detailed information in the range of greatest mass spectrometric interest, namely the small voltage range closest to the target point. Oscilloscopic testing allows convenient visualization of the gross features of the voltage vs. time output of the power supply; ion-current monitoring allows the last few ppm of voltage settling to be observed in detail. Second, while the ion-current monitoring technique undoubtedly acts primarily to test the power supply performance, the results will alert the experimenter to any other problems in the mass spectrometer system, since the measurement involves all system components from the ion source to the ion-current-readout system. Of course, for this same reason, it is not possible instantly to be sure that an observed instability is due to the accelerating or deflecting power supplies. Instabilities in ion-source-filament or detector power supplies would, however, modulate not only the signal observed at the side of a peak but also the signal at the top of the peak. By applying this simple test, the origins

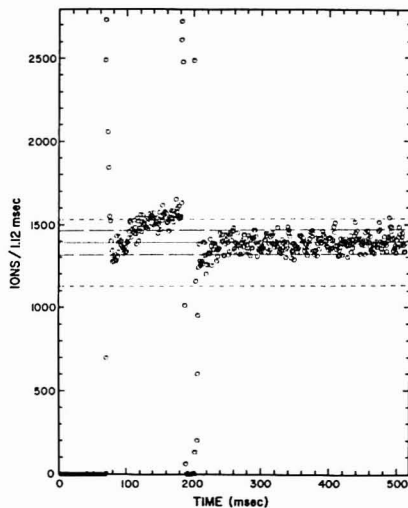


**Figure 2.** Ion current settling profile for a decrease in the accelerating voltage of the single focusing mass spectrometer. The figure plots ion current vs. time after a step change in the accelerating voltage from 3000 to 2740 V (corresponds to an 8.5% increase in mass) ending at the half-maximum point of  $m/e = 40$  (expected signal level indicated by the solid line). The long broken lines indicate signal levels  $\pm 2$  standard deviations from the half-maximum signal intensity. The short broken lines indicate the signal levels at points 2 voltage increments (49 ppm) on either side of the half-maximum point.

of observed instabilities can usually be adequately defined. Third, the use of a computer-based ion-current-recording system is superior to oscilloscopic recording of the ion current. The system becomes "self-testing," and many uncertainties associated with other diagnostic procedures are removed. There can be no fear that the observed results are due to some inadequacy in the test equipment, cables, or connections. There can be no uncertainty about the relationship between triggering of the test device and the command to the power supply. The procedure is much more convenient, and the plotter output displays excellent resolution and is highly readable, with the signal output scale being automatically marked in terms of the expected target signal and related levels.

The practical utility and quantitative interpretation of test results depends largely on the experimental context. In the present case, for example, the spectrometer was being operated with ion source and collector slits which produced peaks with flat tops more than 975 ppm in width in the mass range of interest. Because the voltage targets during actual analytical measurements lie at the centers of these broad, flat tops, it is evident that complete, or perfect, settling to the target voltage is not required, and that collection of data could begin within 40–50 ms of any mass selection command like that shown in Figure 1. If, on the other hand, narrow peaks with widths of approximately 50 ppm were being monitored, data collection would have to be delayed for 100 ms after any mass selection command as large as that employed in Figure 1.

Figure 2 shows the ion-current settling profile for an 8.5% decrease in the accelerating voltage of the single-focusing instrument. Prior to commanding mass selection, the computer supervised determination of the expected signal level at the target location (the solid line at 1400 counts) and at points 49 ppm above and below the target voltage (the short

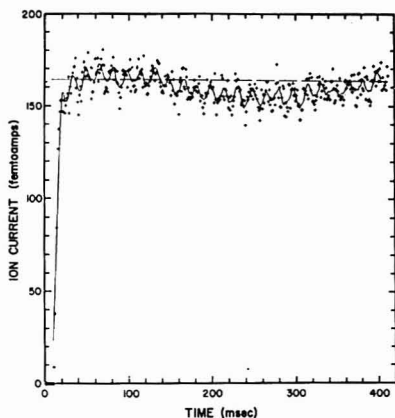


Figure 3. Ion current settling profile for a decrease in the accelerating and electric sector voltages of the double focusing mass spectrometer. The figure plots ion current vs. time after a step change in the accelerating voltage from 8000 to 3920 V and a step change in the electric sector voltage from 400 to 196 V ending at the half-maximum point of  $m/e = 40$  (the broken line).

broken lines at 1530 and 1130 counts). Study of Figure 2 shows that, in this case, the slewing time required to reach the "neighborhood" of the target was approximately 75 ms, a very substantial increase over the 25 ms required for a voltage increase of equal magnitude. When the ion-current signal did appear, it climbed very steeply and quickly exceeded its expected value, indicating that the voltage had overshoot the target by at least several hundred ppm. The ion current then stabilized at the unexpected value of 1550 counts, indicating that the power supply had "falsely settled" 50 ppm above the target point. Suddenly, more than 180 ms after the mass selection command, the ion current oscillated abruptly, indicating large changes in the accelerating voltage, and finally settled at the expected value more than 230 ms after the initial mass selection command!

The ion-current record shown in Figure 2 is only one representative of a family of such curves obtained by varying the mass interval traversed in order to reach the selected target. When other curves from this family are studied, it can be observed that the delayed oscillation decreases in magnitude as the mass interval traversed is reduced from 8.5% (the value in Figure 2) to 2.0%. If, for example, the effect of a step change in the mass from  $m/e$  101 to  $m/e$  103 were to be considered, it would be found that the delayed oscillation was completely absent and that data acquisition could begin 40 ms after the mass selection command.

The double-focusing instrument employs electric sector and accelerating voltage power supplies of more recent design, and Figure 3 indicates that they are capable of much more rapid response. Figure 3 represents a 51% decrease in the electric sector and accelerating voltages, corresponding approximately

to a doubling of the selected mass. Given the relatively wide mass range and the higher resolution of this instrument, the division of the accessible mass range into 4096 increments results in peaks only a few "voltage bits" in width (each bit corresponds to 122 ppm of the maximum voltage). Thus, the solid line represents the expected signal at the target point near the peak of  $m/e$  40, but the short dashed lines representing signal levels at voltages two increments above and below the target are absent because no signal is present at these points. Analysis of the ion current recording indicates that the voltages settle within 100 ppm of the target in less than 20 ms, and that overshoot and ringing are absent.

Further analysis of the recording beyond 50 ms reveals two residual noise sources not recognized in the preceding figures. Two small amplitude oscillations, one with a period of 400 ms (2.5 Hz), and the other with a period of 17 ms (60 Hz) can be seen. The 2.5-Hz noise is apparent from visual inspection of the record, but the 60-Hz noise can be noted only after the data have been processed by the 17-point Savitsky-Golay smoothing routine (7) used to generate the unbroken curve in Figure 3. When the collector slit was opened in order to generate a flat-topped peak and allow a stable measurement of resolved beam current, (a) the 60-Hz modulation vanished, indicating that it was due to an instability in beam location rather than signal level (this oscillation was traced to an electric motor placed near the magnetic sector); and (b) the 2.5-Hz modulation was not found to be constantly present in either the top or the side of the peak, indicating that it was somehow associated with the voltage jumping process itself. Installing a new filament and cleaning the ion source removed this feature, leading us to suggest that it represented an interaction between leakage currents, sudden ion source voltage changes, and the time constant of the emission current regulator circuit.

It should be apparent that this very simple technique provides an extremely useful tool for examining the dynamic performance of selected ion monitoring mass spectrometers, and that the data can have great diagnostic value.

#### ACKNOWLEDGMENT

The ion current measurement system used on the double-focusing mass spectrometer was constructed by D. W. Peterson.

#### LITERATURE CITED

- (1) C. C. Sweeley, W. H. Elliott, I. Fries, and R. Ryhage, *Anal. Chem.*, **38**, 1549 (1966).
- (2) D. E. Matthews and J. M. Hayes, *Anal. Chem.*, **48**, 1375 (1976).
- (3) A. C. Nier in "Mass Spectrometry in Physics Research", *Natl. Bur. Stand. (U.S.) Cir.*, **522**, 29-37 (1953).
- (4) D. A. Schoeller and J. M. Hayes, *Anal. Chem.*, **47**, 408 (1975).
- (5) K. B. Denson, S. P. Taylor, and J. M. Hayes, *Proc. 24th Ann. Conf. Mass Spectrom. Allied Topics*, 548 (1976).
- (6) J. M. Hayes, D. E. Matthews, and D. A. Schoeller, *Anal. Chem.*, **50**, 25 (1978).
- (7) A. Savitsky and M. J. E. Golay, *Anal. Chem.*, **38**, 1627 (1964).

RECEIVED for review October 24, 1977. Accepted December 23, 1977. We appreciate the support of the National Aeronautics and Space Administration (NGR 15-003-118) and The National Institutes of Health (GM-18979).



## Photometric Detection of Oxygen

Zbigniew Mielniczuk,<sup>1</sup> Christopher G. Flinn, and Walter A. Aue\*

5637 Life Sciences Building, Dalhousie University, Halifax, N. S., Canada

The determination of molecular oxygen is a frequent but often difficult task in analytical chemistry. A wide variety of methods can be employed depending on the type of sample and analytical requirements. Often gas chromatography (1-3) is used prior to detection by thermal conductivity (4). Further detection approaches include coulometry (5), ionization by metastable helium atoms (6), capacitance (7), quenching of flame emission (8), flame ionization (9, 10) and others.

In this study we are exploring a different approach: the selective and highly sensitive detection of oxygen via its chemiluminescent reaction with phosphorus vapor.

The emission of light in the oxidation of phosphorus has aroused the interest of scientists for more than a century (11) and the literature on the subject, especially the early literature, is voluminous (12). The greenish glow (the "cool flame") can be observed when phosphorus vapor reacts with oxygen of a pressure within sharply defined upper and lower limits. The glow is generated by a complex isothermal branched-chain type reaction (13) and formulas are available for the calculation of critical oxygen pressures in relation to phosphorus and inert gas pressures as well as to reactor dimensions (14). Gilbert comments: "The glow of white phosphorus has been much studied but is still poorly understood." (15).

### EXPERIMENTAL

"Prepurified" grade nitrogen or helium was further purified (a necessary procedure) by passage through a heated scavenger cartridge (Supelco, Bellefonte, Pa.) and used as carrier for both reagent and sample. One fraction of the carrier (10 mL/min) was bubbled through molten white phosphorus at ca. 50 °C; the other (10 to 30 mL/min, usually ca. 20 mL/min) was used to transport gaseous samples (from a six-port valve, or a gas chromatographic injection port) to a quartz tube situated in the viewing area of a photomultiplier, where the two gas streams met. Residual phosphorus vapor and any volatile reaction products were disposed of by connecting the detector exhaust tube directly to the exhaust duct of a fume hood; nonvolatile products were removed about once a week. The detector was kept at 100 °C (for chromatographic experience); the chemiluminescence can be equally well observed at room temperature.

Figure 1 shows a schematic of the simple arrangement of the phosphorus doping vessel and chemiluminescence detector (drawn approximately to size; the tubes in view of the PM tube are  $\frac{1}{4}$  in. and  $\frac{1}{16}$  in. o.d. The luminescent area, visually, is a few mm<sup>2</sup>). Parts of a Bendix photometric detector system (SPED electrometer, photomultiplier unit with EMI 9524 B tube, and random, epoxy-potted glass fiber light guide; but without interference filter) were used for the optical channel. An aperture of fixed size (ca. 0.2-mm diameter) was used when attenuation (~200:1) of the light became desirable. The detector assembly was carefully shielded from room light. The sampling valve was a Valco 6-port model, with various lab-made loops. The detector, and the sampling arrangement with sample reservoir and appropriate valves, were mounted on opposite sides of a Varian 1200 GC column bath. A gas chromatographic column (Linde 5A molecular sieve) could thus be used, but was by-passed in most experiments. Sample mixtures were prepared from purified nitrogen (or helium) either in a 400-mL reservoir equipped with a septum for injection of small volumes of atmosphere with a gas-tight syringe, or by adding a constant, very small stream of "high purity" grade nitrogen—whose oxygen content was determined as 14 ppm—to a larger carrier stream. The combined stream, as well as the reservoir, were under slight overpressure

and could be sampled by the six-port valve. Sampling valve loops ranged from 0.05 to 5 mL.

In separate experiments, the spectra emitted by the cold flame of phosphorus were scanned by a grating monochromator (part of the Varian AA-5 unit), using an appropriately modified detector version, and good exhaust facilities (considerable amounts of O<sub>3</sub> are formed in this reaction in addition to various phosphorus compounds).

### RESULTS AND DISCUSSION

The spectra emitted by the reaction of phosphorus with excess oxygen in the gas phase are shown in Figure 2; using both dry and humid oxygen. The spectra contain nothing new (15) but are interesting in the present context. The band system in the UV is the  $\gamma$  system of PO. The origin of the continuum has not been established. The bands superimposed on the continuum in the presence of water are those of HPO. The light as seen by the PM tube in the detector proper will, of course, have a somewhat different spectral distribution. For one, the type of glass fiber light guide used in this study is known to attenuate somewhat S<sub>2</sub> emission at 394 nm but pass HPO emission at 526 nm. It is, of course, opaque to the PO bands in the UV. However, the dominant continuum fits well into the spectral range of both light guide and photomultiplier and, is, without much doubt, responsible for the detector's response.

Figure 3 shows a calibration curve for peak heights resulting from valve injections, without a GC column, of O<sub>2</sub> as measured on the analytical setup over a period of one month, using different loops, sample streams, etc., as indicated by different data point representation. The line through the points was deliberately drawn at exactly 45°. The deviations, in our opinion, are primarily due to difficulties associated with the preparation and manipulation of samples rather than to the reaction in the detector itself. (Typical GC peaks showed similar linearity, both in peak height and area, but were tested only over a much more restricted range.) The upper part of the linear range can be extended by increasing the phosphorus supply as was shown in separate experiments. The lower limit of response is given essentially by photomultiplier noise; it could most likely be lowered considerably by using a geometrically optimized reaction chamber immediately bordering the photocathode of a cooled PM tube; and by a further decrease in the oxygen content of the carrier gas, e.g., by a preliminary reaction with a separate phosphorus source. Furthermore, an even supply of P<sub>4</sub> vapor (no fluctuations due to bubbling N<sub>2</sub> through liquid phosphorus) may be helpful. Even with the rather simple arrangement used, however, the minimum detectable amount of O<sub>2</sub> was ca.  $2 \times 10^{-11}$  g (extrapolated from the response of  $9 \times 10^{-11}$  g to S:N = 2:1). The minimum detectable concentration depends, obviously, on flow conditions and sample size. We had little trouble detecting 0.1 ppm O<sub>2</sub> and, with proper instrumental change and optimization (and calibration standards available), analysis in the lower ppb ranges should be possible.

It must be noted in this context, however, that many studies in the literature show chemiluminescence to occur only within a certain range of O<sub>2</sub> pressure. Even though most of these reports concern reactions involving phosphorus in solid rather than in vapor form, it would need to be experimentally proved that the minimum detectable amounts or concentrations can be lowered by appropriate instrumental changes. Our own

<sup>1</sup> Present address, Institute of Food and Nutrition, Warsaw, Poland.

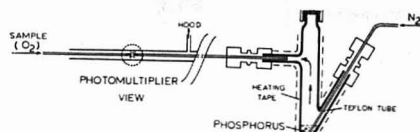


Figure 1. Schematic of phosphorus-doping tube and chemiluminescent reaction zone

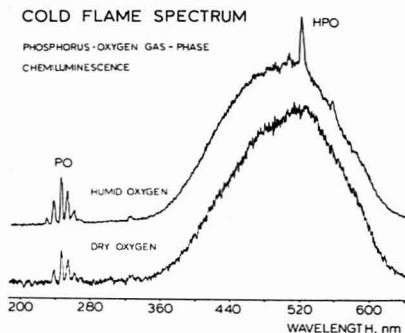


Figure 2. Spectra emitted by the reaction of phosphorus vapor with excess dry and humid oxygen. Upper spectrum offset

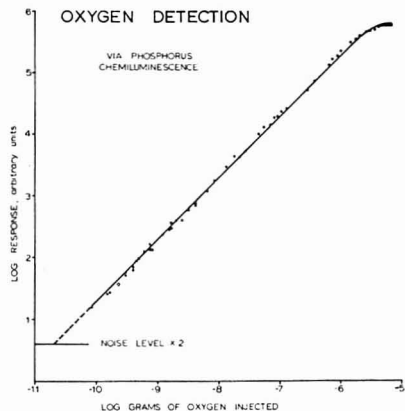


Figure 3. Calibration curve for oxygen (in nitrogen) as supplied by valve sampling of static samples as well as flowing stream mixtures of (purified) carrier and small amounts of "high purity" nitrogen (14 ppm  $O_2$ ). No GC column. Carrier from sampling valve to detector: ca. 30 mL/min (purified)  $N_2$ . Sampling loops ranged from 0.05 to 5.0 mL. Values above  $3 \times 10^{-7}$  g  $O_2$ . Direct injection of atmosphere by gas-tight syringe

opinion is that this should be possible without major difficulties.

Figure 4 shows six successive (valve) injections in two regions of the calibration curve three orders of magnitude apart. The deviations are not greater than those to be expected from parts of the instrument other than the detector, e.g., recorder overshoot, PM tube noise, inconsistencies in turning of the sampling valve, etc.

It is obvious from the way this device was tested that it could be used either as a gas chromatographic detector or as a gas stream monitor. Response was well reproducible and no significant interferences were noticed. Various changes

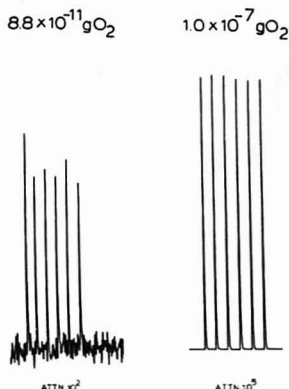


Figure 4. Repeated valve injections at two oxygen levels as indicated. 0.125-mL sampling loop, static samples

in experimental conditions (temperature,  $N_2$  or He as carrier, excess of phosphorus) appeared to have little, if any, effect on detector performance.

Judging from what is known about phosphorus chemiluminescence, the reaction could be assumed to be specific for the elemental forms of oxygen (including, perhaps, some peroxides). In our study, a few gases and a wide variety of volatile organics (hydrogen chloride, ammonia, carbon dioxide, methanol, acetic acid, ethyl acetate, nitroethane, acetone, *n*-propylamine, chloroform, carbon tetrachloride, 1-bromobutane, chlorobenzene, pyridine, 2-heptene, diallyl ether, hexane, acetylacetone, diacetyl, thiophene, *p*-quinone and piazselenole) were injected without eliciting any significant response. However, the question of selectivity was not further investigated.

#### ACKNOWLEDGMENT

We are most grateful to Shubhender Kapila for putting together the first prototype.

#### LITERATURE CITED

- (1) J. Janák, "Chromatography of Nonhydrocarbon Gases", in "Chromatography", 3rd ed., E. Heftmann, Ed., Van Nostrand Reinhold, New York, N.Y., 1975, p. 882-914.
- (2) H. Hachenberg, "Industrial Gas Chromatographic Trace Analysis", Heyden & Son Ltd., London, 1973.
- (3) P. G. Jeffery and P. J. Kipping, "Gas Analysis by Gas Chromatography", Int. Ser. Monogr. Anal. Chem., Vol. 17, 2nd ed., Pergamon Press, Oxford, 1972.
- (4) H. Kern and M. Elser, International Symposium on Microchemical Techniques 1977, Davos, Switzerland.
- (5) G. Barton, A. Littlewood, and W. A. Wiseman, in "Gas Chromatography 1968", A. B. Littlewood, Ed., Elsevier, Amsterdam, 1967.
- (6) C. H. Hartmann and K. P. Dimick, J. Gas Chromatogr., 4 (5), 163 (1966).
- (7) J. D. Winefordner, H. P. Williams, and C. D. Miller, Anal. Chem., 37, 163 (1965).
- (8) C. V. Overfield and J. D. Winefordner, J. Chromatogr., 30, 339 (1967).
- (9) B. A. Schaefer, J. Chromatogr. Sci., 10, 110 (1972).
- (10) P. Russev, T. A. Gough, and C. J. Woolam, J. Chromatogr., 119, 461 (1976).
- (11) E. Newton Harvey, "A History of Luminescence", The American Philosophical Society, Philadelphia, Pa., 1957.
- (12) Grmelin "Phosphorus" Teil B (16), 1964; Teil C (16), 1965.
- (13) N. Semenov, "Chemical Kinetics and Chain Reactions", Clarendon Press, Oxford, 1935, p. 163.
- (14) F. S. Dainton and H. M. Kimberley, Trans. Faraday Soc., 46, 629 (1950).
- (15) P. T. Gilbert, in "Analytical Flame Spectroscopy", R. Mavrodineanu, Ed., Macmillan, Toronto, 1970, p. 253.

RECEIVED for review November 9, 1977. Accepted January 3, 1978. This study was supported by NRC grant 9604, AC grant 6099, and a grant by the Faculty of Graduate Studies, Dalhousie University.

## Modified Nebulizer for Inductively Coupled Plasma Spectrometry

D. L. Donohue\* and J. A. Carter

Oak Ridge National Laboratory, Oak Ridge, Tennessee 37830

A number of papers have appeared recently dealing with the problem of liquid sample nebulization in Inductively Coupled Plasma Atomic Emission Spectrometry (1-4). Many authors agree that precise, reproducible sample introduction into the argon plasma is the most pressing problem in this field. The major types of nebulizer in use are the concentric glass pneumatic type, the so-called "Iowa State" crossed-flow type, and the ultrasonic nebulizer. This paper will describe a modified design of the crossed-flow type which has certain desirable characteristics. In addition, a novel application will be described which involves the use of two or more sample inlets to produce a mixed aerosol.

The "Iowa State" crossed-flow nebulizer (1) is capable of moderately good precision even at low Ar flow rates, and is less expensive than the ultrasonic nebulizer. Its efficiency at low gas flow rates is between that of the two other major types, with the ultrasonic type being the most efficient at producing the proper droplet size. The disadvantages of the crossed-flow nebulizer have been the expense of the machine work required to produce one, and the tendency to break the rather fragile glass needles. Proper alignment of the needles is essential, but this is sometimes difficult for laboratory personnel to accomplish. In addition, the various metal parts are subject to corrosion by acidic samples.

The nebulizer described here overcomes many of the above problems and utilizes all plastic and glass construction to minimize corrosion damage. It is easily fabricated and allows for quick and precise alignment of the needles to produce an aerosol with the desired properties. An additional feature is that several sample introduction ports can be included, which may be advantageous for certain applications.

A cross-sectional view is shown in Figure 1. The glass needles are capillary tubing drawn to approximately 2 mm in diameter and inserted snugly into holes in the Teflon inserts which are undersized by  $\sim 0.002$  inch. This provides sufficient pressure so that the aspiration needle will not move at Ar pressures of up to 50 psi. The needles are drawn down at the end and polished to a tapered tip using a silicon carbide saw. Sample uptake is by  $1/8$ -inch Tygon tubing slipped over the end of the sample needle. The needle fittings consist of  $1/4$ -inch i.d. nylon Swagelok unions which have been cut in half and machined to a flat surface. They are held against  $1/4$ -inch i.d. neoprene "O" rings by means of a rigid plastic flange and four 6-32 nylon screws. The main body of the nebulizer is Teflon with a 35-mm opening to accommodate commercially available spray chambers (Plasma Therm, Inc., Kresson, N.J.). The aerosol Ar gas enters through  $1/4$ -inch polyethylene tubing which can be heated and bent to shape.

Adjusting the position of the needles is a simple matter of tightening the appropriate screw which holds the swaged assembly in place. This compresses the O ring slightly and moves the needle tip accordingly. Movement in and out is accomplished first by proper placement of the needle in the Teflon insert and then by tightening or loosening all of the retaining screws by the same amount. The advantage of this design is that no force is exerted which could break the needles. All adjustments made in this way will remain unchanged for long periods, even with routine handling of the nebulizer assembly.

If another sample needle is introduced through an auxiliary port, with its tip in close proximity to the first sample needle, it becomes possible to aspirate two separate solutions. This

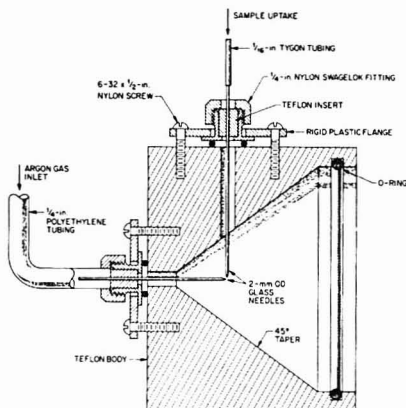


Figure 1. Modified cross flow nebulizer design utilizing all plastic and glass construction

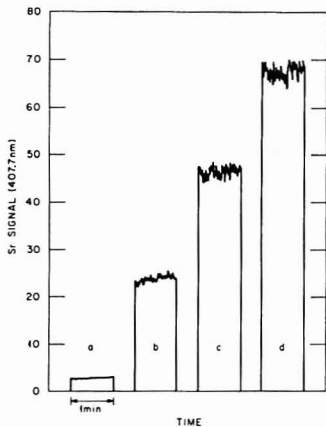


Figure 2. Signal vs. time for dual sample nebulizer

has been accomplished using kerosene and water in an experiment to produce a mixed aerosol of the two. The uptake rate of each liquid was controlled by valves as well as by the size of the opening in the glass needle used for each sample. Nebulization ratios of from 1:1 to 10:1 were obtained at aspiration rates of from 0.3 to 3 mL/min for each liquid.

This multiple-sampling ability is of interest in work with organic solvents, where the properties of the inductively coupled plasma vary with the type of sample injected. In particular, the more volatile organic liquids such as acetone or gasoline may be analyzed, using water as the second liquid to initially stabilize the plasma by forming the axial channel. This would be followed by gradual introduction of the organic sample and subsequent reduction of the water uptake rate. Another area of application might be in the selection of

analytical emission lines for an unknown sample. With the sample being aspirated, the auxiliary needle may be used to introduce a standard solution of the desired element(s). In this way, spectral interference effects at a particular wavelength can be studied. This scheme would also be helpful in organic sample analysis where cheaper and more convenient aqueous standards could be introduced through the auxiliary needle to locate and evaluate spectral lines. One disadvantage of the dual sampling scheme is that the precision is degraded by a factor of 2 compared to single sample aspiration.

In a study to show the additivity of the signals from each of two sample needles, a 1 µg/mL solution of Sr was used. The results are shown in Figure 2. It can be seen that the nebulization ratio for needles A and B is approximately 1:2. The composite signal, *d*, is equal to the sum of the individual signals corrected for the background (blank) level. The peak-to-peak noise seen on the signals also appears to be additive, with the relative noise being essentially constant at 2-3% RSD.

In conclusion, this design has been shown to offer simple and rugged operation, with the capability for precise positioning of the glass needles. The nebulizer requires less machine work than other designs and should be less expensive to manufacture. The absence of metals provides a measure of safety from corrosion by highly acidic samples. Finally, the multiple sampling capability may prove useful in specialized areas of analysis.

### LITERATURE CITED

- (1) R. N. Kniseley, H. Amenson, C. C. Butler, and V. A. Fassel, *Appl. Spectrosc.*, **28**, 285 (1974).
- (2) K. W. Olson, W. J. Haas, Jr., and V. A. Fassel, *Anal. Chem.*, **49**, 632 (1977).
- (3) K. Ohts, *ICP Inform. Newsl.*, **2**, 357 (1977).
- (4) C. C. Wohlers, *ICP Inform. Newsl.*, **3**, 37 (1977).

RECEIVED November 14, 1977. Accepted January 13, 1978.  
Research sponsored by the Department of Energy under contract with the Union Carbide Corporation.

## Dropping Mercury Electrode for Polarography in Glass-Corroding Media

Hugues Menard\* and Francine LeBlond-Routhier

Department of Chemistry, University of Sherbrooke, Sherbrooke, Quebec, Canada J1K 2R1

During the past few years, a section of analytical chemistry dealing with polarography in glass-corroding media seems to have attracted many workers. This is due to the construction of capillaries protected by polychlorotrifluoroethylene (KEL-F) or polytetrafluoroethylene (Teflon). With these capillaries, polarographic measurements can be made directly in hydrofluoric acid or concentrated sodium hydroxide solutions that are used as solvents for metallic samples containing silicates, thus eliminating stages of evaporation and redissolution which were previously necessary to protect the glass capillaries but could also lead to systematic errors.

Techniques of constructing those capillaries inert to corrosive solvents have been summarized by Bond and co-workers (1, 2), who also add that all the techniques are extremely hard to put into practice and that the chances of success are few. It must also be said that enormous work has been accomplished by Raen (3-11) eight to fifteen years ago and by Clifford and Balog (12) concerning the construction and use of a capillary inert in hydrofluoric acid which made possible the study of some redox, reactions especially of metal ions in glass-corroding media. Devynck (13) recently studied the polarography of antimony in hydrofluoric acid. But, up to now, it seems that all techniques for the construction of capillaries require a certain dexterity and could be said to be almost an art. From the analytical point of view, the availability of a simple technique in making such capillaries would be of great concern for all interested laboratories. We present here a method of constructing a polyethylene capillary for use in solutions extremely corrosive to glass.

### EXPERIMENTAL

**Construction of a Capillary.** A "Sargent-Welch Scientific Company" capillary C 2-5 s No drop-time S-29419 is cut into 5-cm lengths. One end of the 5-cm long capillary is immersed in a melted polyethylene bath (for example, in a beaker filled with granulated polyethylene heated at 200 °C). Then, when it is removed slowly, a mass (Figure 1a) of polyethylene adheres very well to the glass but does not penetrate into the glass capillary.

Just before the polyethylene chills, a mild pressure of nitrogen is applied at the other end of the capillary so as to form a 1- to 2-mm diam. bubble (Figure 1b). When the polyethylene is well chilled, it is tooled to get a more adequate form so that it can be inserted into a polarographic cell (Figure 1c). The polyethylene on the glass capillary must be at least 2-mm thick so as to maintain a good mechanical resistance. Then, with a No. 80 drill (0.0343-cm diam.) revolving at 17000 turns/min (Dumore Hi Speed sensitive drill No. 8226), a hole is drilled into the bubble (Figure 1d).

The minimum length between the bubble and the end of the polyethylene capillary is 0.5 to 1 cm. The drop time of the mercury drop will depend on the length of the glass capillary and also the orifice diameter of the polyethylene capillary. The glass capillary should be kept as short as possible, that is, 5 cm. Also, the form of the orifice of the polyethylene capillary should be modified; this can be done by using a needle point. The main purpose of the use and construction of the capillary is to eliminate any defect from dead volume that could trap air bubbles in the portion between the two capillaries.

**Reagents.** Stock solutions of bismuth trioxide,  $10^{-3}$  M, (Fisher Scientific Co.) are prepared from commercial HF 48% by volume (Allied Chemical). Bismuth trichloride,  $10^{-3}$  M, (J. T. Baker Chemical Co.) is prepared from sodium hydroxide (Anachemia Chemicals Ltd.) with twice-distilled water.

**Apparatus.** A model 174 A polarograph (Princeton Applied Research) was used with a three-electrode system. The saturated calomel reference electrode was separated from the test solution by a porous Teflon junction.

### RESULTS AND DISCUSSION

We selected polyethylene for several reasons. Polyethylene is known (14) to be inert to hydrofluoric acid at room temperature and to have mechanical properties comparable with those of Teflon. Also, it is not toxic and can be manipulated without any danger. We noticed that it sticks to glass but does not penetrate into the capillary; this was not the case when we tried other polyolefins such as polypropylene for example.

Figure 2 is an x-ray photograph of two capillaries filled with mercury. We note that the mercury completely fills the junction of the two capillaries and that the capillaries work well even though the bubble is spherical. The drill doesn't

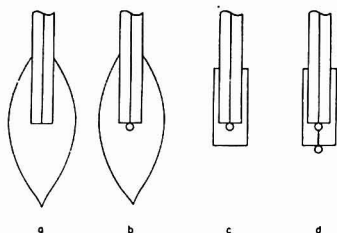


Figure 1. Sketches of the capillary-fabrication steps after: (a) it is taken out slowly of the polyethylene bath; (b) a mild pressure of nitrogen has been applied; (c) being worked up for the polarographic cell; (d) having been bored with a drill



Figure 2. X-ray of two capillaries filled with mercury

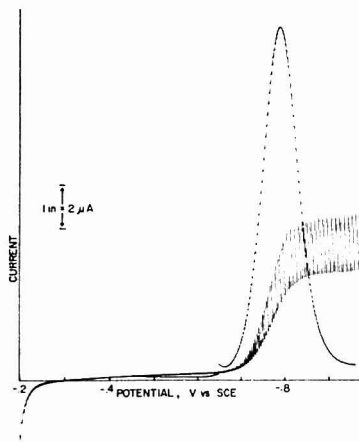


Figure 3. (a) Classical polarogram of  $10^{-3} m \text{Bi}^{3+}$  in  $\text{NaOH } 10 \text{ M}$ ; (b) differential pulse polarogram, same conditions

reach the inferior part of the bubble due to the fact that there is no air in this cavity.

Figure 3 shows the classical polarogram of  $10^{-3} m \text{Bi}^{3+}$  in a  $10 m \text{NaOH}$  solution. To demonstrate the good performance of the polyethylene capillary, a differential pulse polarogram is superposed, which indicates adequately the reproducibility of the mercury drops.

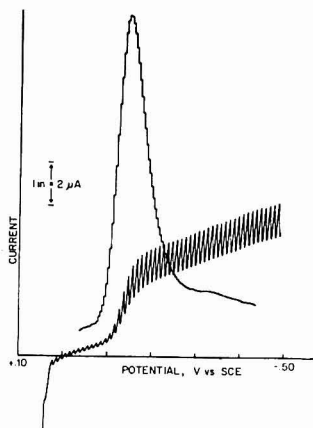


Figure 4. (a) Classical polarogram of  $10^{-3} m \text{Bi}^{3+}$  in  $48\% \text{ commercial HF}$ ; (b) differential pulse polarogram, same conditions

Figure 4 gives the classical and the differential pulse polarograms of  $10^{-3} m \text{Bi}^{3+}$  in  $48\% \text{ commercial HF}$ . The shapes of the two curves demonstrate that this capillary can be used in media extremely corrosive to glass.

A polarogram of acetonitrile in anhydrous  $\text{HF}$  recorded in the laboratories of the National Institute of Science and Nuclear Techniques in Saclay (15) confirms the efficiency of the capillary.

#### ACKNOWLEDGMENT

The authors thank Miss Charest for her technical assistance in radiology. And, most of all, sincere thanks to F. Kimmerle for his interest and good discussions.

#### LITERATURE CITED

- (1) A. M. Bond, T. A. O'Donnell, and A. B. Waugh, *J. Electroanal. Chem.*, **39**, 137 (1972).
- (2) A. M. Bond and T. A. O'Donnell, *Anal. Chem.*, **44**, 590 (1972).
- (3) H. P. Raean, *Anal. Chem.*, **34**, 1714 (1962).
- (4) H. P. Raean, *Anal. Chem.*, **36**, 2420 (1964).
- (5) H. P. Raean, *Anal. Chem.*, **37**, 677 (1965).
- (6) H. P. Raean, *Anal. Chem.*, **37**, 1355 (1965).
- (7) H. P. Raean, "Analysis Instrumentation 1965", Plenum Press, New York, N.Y., 1966, p 219.
- (8) H. P. Raean, *Chem. Instrum.*, **1**, 287 (1969).
- (9) H. P. Raean, *Anal. Chim. Acta*, **44**, 205 (1969).
- (10) H. P. Raean, *Anal. Chim. Acta*, **46**, 427 (1969).
- (11) W. L. Belev and H. P. Raean, *J. Electroanal. Chem.*, **8**, 475 (1964).
- (12) A. F. Clifford and G. Balog, *Nucl. Sci. Abstr.*, **5**, 694 (1951).
- (13) J. Devynck, H. Ménard, G. Comarmond, and B. Trémillon, *Can. J. Chem.*, in press.
- (14) P. P. Coppola and R. C. Hughes, *Anal. Chem.*, **24**, 768 (1952).
- (15) J. Devynck, personal communication, May 1977.

RECEIVED for review November 29, 1977. Accepted January 27, 1978. Support of this work by the National Research Council of Canada is gratefully acknowledged.



Altschuler, S. J.	564	Flinn, C. G.	684
Anders, O. U.	564	Ford, C. D.	610
Aue, W. A.	684		
		Galobardes, J.	672
Bajo, S.	649	George, S. M.	616
Bartel, J. F.	564	Gladney, E. S.	652
Belford, R. L.	656	Goff, D. A.	625
Berry, D. S.	671	Guiochon, G.	549
Betteridge, D.	654		
Boström, K.	679	Hagel, L.	569
Bridges, J. W.	613	Hajibrahim, S. K.	549
Burman, J.-O.	679	Haukka, M. T.	592
Burns, D. T.	613	Hayes, J. M.	681
		Hensley, W. K.	652
Carter, J. A.	686	Hirata, Y.	659
Chan, J.-L.	635	Hurtubise, R. J.	610
Cheng, H.-Y.	645		
Cheng, K.-H.	601	Janjić, T. J.	597
Chiu, J.-H.	670		
Chu, I. C.	637	Kent, S. B. H.	637
Clark, C. R.	635	Kessler, W. V.	670
Colin, H.	549	Kuksis, A.	557
Cox, J. A.	601	Kuwana, T.	640
Crowther, J.	658		
		Landolt, R. R.	670
Deming, S. N.	546	LeBlond-Routhier, F.	687
Denson, K. B.	681	Lenhard, J. R.	576
Donohue, D. L.	686	Lennox, J. C.	576
		Li, K.-P.	628
Eaton, H. E.	587	Lubkowitz, J. A.	672
Eglinton, G.	549		
		McCreery, R. L.	645
Felkel, H. L., Jr.	602	Marai, L.	557
Fields, B.	654	Marquart, J. R.	656
Finklea, H. O.	576	Martinez, G.	665

## Author Index

Matthews, D. E.	681	Rho, J. H.	620
Maxwell, J. R.	549	Richardson, J. H.	616
Menard, H.	687	Risby, T. H.	562
Merrifield, R. B.	637	Rogers, L. B.	672
Mielniczuk, Z.	684		
Miller, J. N.	613	Semonian, B. P.	672
Milosavljević, E. B.	597	Shields, R. R.	661
Minor, M. M.	652	Sittard, H. G.	663
Mitchell, A.	668	Sojka, S. A.	585
Mitchell, A. R.	637	Stuart, J. D.	587
Moses, P. R.	576	Stuart, J. L.	620
Murray, R. W.	576		
Myher, J. J.	557	Takeuchi, T.	659
		Thomas, I. L.	592
Needleman, M.	668	Tibbetts, P. J. C.	549
Nieman, J. A.	661	Tsuda, T.	632
Novotny, M.	632	Turoff, M. L. H.	546
O'Haver, T. C.	676	Valenty, S. J.	669
Okumura, Y.	659	Vassos, B. H.	665
Pardue, H. L.	602	Watts, C. D.	549
Perchalski, R. J.	554	Welte, D. H.	663
Phillips, D. L.	613	Wier, L. M.	576
Ponté, C.	679	Wilder, B. J.	554
Prescott, S. R.	562	Wolfe, R. A.	585
Radke, M.	663	Yacynych, A. M.	640
Rains, S. D.	680	Yeung, E. S.	625
		Yeung, S. K. F.	557

### Liquid-Liquid Extraction of Zinc from Aqueous Iodide Solutions with 4-(5-Nonyl)pyridine in Benzene

S. Ud-Zuha and M. Ejaz

### Double Enzymatic Assay for Determination of Glutamine and Glutamic Acids in Cerebrospinal Fluid and Plasma

I. F. Pye, C. Stonier, and E. H. F. McGale

### Separation of Aromatic Compounds in Lubricant Base Oils by High Performance Liquid Chromatography

A. Matsunaga and M. Yagi

### Change in Resolution of Reverse Phase Liquid Chromatographic Columns with Temperature

W. A. Saner, J. R. Jadamec, and R. W. Sager

### Gas Chromatographic Determination of 2,3,7,8-Tetrachlorodibenzodioxin in the Experimental Decontamination of Severo Soil by Ultraviolet Radiation

G. Bertoni, D. Brocco, V. Di Palo, A. Liberti, M. Possanzini, and F. Bruner

### Elution Behavior of Some Solutes on a Porous Polystyrene Gel in High Performance Liquid Chromatography

S. Mori

## Future Articles

### Determination of Chlorinated Dibenzo-*p*-dioxins in Purified Pentachlorophenol by Liquid Chromatography

C. D. Pfeiffer, T. J. Nestruck, and C. W. Kocher

### Effects of Surface Heterogeneity on the Sensitivity of Sulfide Ion-Selective Electrodes

J. Gulens and B. Ikeda

### Determination of Trace Level Hydrocarbons in Marine Biota

S. N. Chesler, B. H. Gump, H. S. Hertz, W. E. May, and S. A. Wise

### Determination of Rhodium in Platinum-Rhodium Loaded Automotive Catalyst Material by Graphite Furnace Atomic Absorption Spectrometry

N. M. Potter

### Trapping and Determination of Labile Compounds in the Gas Phase of Cigarette Smoke

S. G. Zeldes and A. D. Horton

### Auger Electron Spectra and Chemical Shifts of the Chloromethanes

M. Thompson, P. A. Hewitt, and D. S. Wooliscroft

### Adsorption Preconcentration for the Direct Analytical Determination of Heme

C. F. Kolpin and H. S. Swofford, Jr.

# Calculating the mean weight or net weight of 48 weighed samples takes time.

## On a Sartorius, it takes 1 second.

On other scales or balances, determining the average weight of 48 individually-weighed samples takes time. It may also take a pad and pencil, an adding machine or a calculator.

On a new Sartorius MP Balance, the same determination takes only seconds. After each sample weighing, simply press a single key on the Sartorius data keyboard. When all samples have been weighed, press the recall keys for instant display of the mean weight or the number of samples weighed. If printed results are required, simply connect the balance to Sartorius peripheral equipment.

The storage capability of the new Sartorius MP Balances permits the determination of net or fill weights by automatically deducting tare or container weights. Automatic mean weight and net weight determinations make these balances ideally suited for the weighing of pharmaceuticals, cosmetics, packaged foods, electronic components,

industrial parts, routine packaging and filling, and numerous other applications.

Utilizing Texas Instruments microprocessors, Sartorius MP Balances with optional plug-in data keyboards are today's most advanced and versatile electronic weighing instruments. They are available in single and dual range models with a weighing range/readability from 0-160g/0.001g to 0-16000g/0.1g. Prices begin at only \$1,295.

For literature, just write: Sartorius Balances Division, Brinkmann Instruments, Inc., Cantiague Road, Westbury, N.Y. 11590.

### New Sartorius MP Electronic Balances with plug-in data keyboards.



CIRCLE 23 ON READER SERVICE CARD

26 APR 1981